Ontario Geological Survey
Miscellaneous Paper 127

Geoscience Research Grant Program
Summary of Research 1984–1985

edited by
V.G. Milne

1985

Ontario

Ministry of
Northern Development
and Mines

René Fontaine
Minister
George Tough
Deputy Minister

©1985 Government of Ontario
Printed in Ontario, Canada

ISSN 0704-2752 (Series)
ISBN 0225-5316 (Sub-series)

The illustrations in this report were author prepared.

Publications of the Ontario Geological Survey, Ministry of Northern Affairs and Mines, are available from the following sources. Orders for publications should be accompanied by cheque or money order payable to the *Treasurer of Ontario.*

Reports, maps, and price lists (personal shopping or mail order):

Public Information Centre, Ministry of Natural Resources
Room 1640, Whitney Block, Queen's Park
Toronto, Ontario M7A 1W3

Reports and accompanying maps only (personal shopping):

Main Floor, 880 Bay Street
Toronto, Ontario

Reports and accompanying maps (mail order or telephone orders):

Publications Services Section, Ministry of Government Services
5th Floor, 880 Bay Street
Toronto, Ontario M7A 1N8
Telephone (local calls) 965-6015
Toll-free long distance 1-800-268-7540
Toll-free from Area Code 807 0-ZENITH-67200

Every possible effort is made to ensure the accuracy of the information contained in this report, but the Ministry of Natural Resources and the Ministry of Northern Affairs and Mines do not assume any liability for errors that may occur. Source references are included in the report and users may wish to verify critical information.

Parts of this publication may be quoted if credit is given. It is recommended that reference be made in the following form:

Farvolden, R.N., Greenhouse, J.P., and Karrow, P.F.
1985: Subsurface Quarternary Stratigraphy using Borehole Geophysics: Grant 128, p.4-9 *in* Geoscience Research Grant Program, Summary of Research 1984-1985, edited by V.G. Milne, Ontario Geological Survey, Miscellaneous Paper 127, 246p.

Scientific Editor: M.L.T. Stuart

1500-85-Maracle

Contents

Introductory Remarks, *V.G. Milne,* 2

Grant 128 Subsurface Quaternary Stratigraphy using Borehole Geophysics, *R.N. Farvolden, J.P. Greenhouse, and P.F. Karrow* 4

Grant 132 Rare Earth Element Properties of Archean Iron Formations and their Host Rocks—Some Results from the Temagami and Boston Iron Formations, *J.H. Crocket and R.J. Bowins* 10

Grant 134 Geochemistry and Petrography of the Mattagami Formation Lignites (Northern Ontario), *C.G. Winder, J.R. Brown, B.I. Kronberg, W.S. Fyfe, and F.H. Murray* 15

Grant 138 Mineralogy and Geochemistry of the Chrysotile Asbestos Deposits of Ontario: A Progress Report on the Stable Isotope and Boron Survey, *J. Ozoray, F.J. Wicks, and M.D. Higgins* 25

Grant 146 Major and Trace Element and Isotopic Studies at Sudbury—A Model for the Structure and its Ores, *Anthony J. Naldrett, B.V. Rao, Norman M. Evensen, and Burkhard O. Dressler* 30

Grant 148 Geochemical Study of the Salina Group of Southern Ontario—Isotopes, and Major and Minor Elements, *M.C. Miles, E.C. Appleyard, K. O'Shea, P. Lapcevic, S.K. Frape, and P. Fritz* 45

GRANT 149 Structural Signature and Tectonic History of Deformed Gold-bearing Rocks in Northwestern Ontario, *Hervé Hugon and W.M. Schwerdtner* 62

Grant 168 Petrogenesis of Mineralized Horizons in Uchi Lake Metavolcanic Rocks, *S.R. Noble, N.M. Evensen, and T.E. Krogh* 73

Grant 173 Sedimentary Rocks and Strata-Bound Mineralization in the Cobalt Region, *J.A. Donaldson, F.A. Michel, P.S. Mustard, R. Rainbird, B.R. Rust, D.H. Watkinson, and B. Wilson* 87

Grant 179 The Petrogenesis and Metallogenesis of the Atikwa-Lawrence Volcanic-Plutonic Terrain, *D.W. Davis and G.R. Edwards* 101

Grant 187 Sedimentology of the Cambro-Ordovician Sandstones of Eastern Ontario, *Rainer R. Wolf and Robert W. Dalrymple* 112

Grant 189 Preliminary Report on the Stratigraphy and Sedimentology of the Bar River Formation, *D.J. Wright and B.R. Rust* 119

Grant 192 Geochemical Exploration For Gold, *Ian Nichol and Gene S. Shelp* 124

Grant 193 The Geological Setting and Genesis of the Cameron Lake Gold Deposit, *D.R. Melling, D.H. Watkinson, K.H. Poulsen, and L.B. Chorlton* 136

Grant 202 Sulphur Isotope Studies of Archean Gold Deposits, *H.P. Schwarcz and C.E. Rees* 151

Grant 205 Clay Mineralogy of Two Selected Carbonate Reservoirs in Southwestern Ontario, *P.L. Churcher and M.B. Dusseault* 157

Grant 216 Sedimentology of the Long Rapids Formation, Preliminary Results, *R.K.A. Bezys and M.J. Risk* 165

Grant 221 The Significance and Genesis of Chloritoid Alteration in Volcanic Rocks of the Michipicoten Belt, Ontario, *M.B. Lockwood, J.M. Franklin, J.M. Moore* 175

Grant 225 Genesis of Pegmatites in the Quetico Gneiss Belt of Northwestern Ontario—Rare-Element Pegmatites and Associated Granitoids of the Georgia Lake Pegmatite Field, *S.A. Kissin and B. Zayachkivsky* 186

Grant 227 A Structural Investigation between the Kirkland Lake and Larder Lake Gold Camps, *D.J. Toogood and C.J. Hodgson* 200

Grant 230 Petrology, Geochemistry, Isotopic Studies, and Platinum Group Element Potential of the Nipissing Diabase, *D.M. Conrod and A.J. Naldrett* 206

Grant 233 The Dating of Ontario's Gold Deposits, *A. Masliwec, Derek York, P. Kuybida, and C.M. Hall* 223

Grant 236 Geological, Fluid Inclusion, and Isotopic (Carbon and Sulphur) Studies of Au-Quartz-Carbonate-Pyrite-Scheelite Vein Mineralization and Intrusion-Hosted Cu-(Au-Mo) Mineralization in the Hollinger-McIntyre System, Timmins, Ontario, *E.T.C. Spooner, P.C. Wood, D.R. Burrows, A.V. Thomas, and S.R. Noble* 229

Conversion Factors for Measurements in Ontario Geological Survey Publications

If the reader wishes to convert imperial units to SI (metric) units or SI units to imperial units the following multipliers should be used:

CONVERSION FROM SI TO IMPERIAL — **CONVERSION FROM IMPERIAL TO SI**

SI Unit	*Multiplied by*	*Gives*	*Imperial Unit*	*Multiplied by*	*Gives*
			LENGTH		
1 mm	0.039 37	inches	1 inch	**25.4**	mm
1 cm	0.393 70	inches	1 inch	**2.54**	cm
1 m	3.280 84	feet	1 foot	**0.304 8**	m
1 m	0.049 709 7	chains	1 chain	20.116 8	m
1 km	0.621 371	miles (statute)	1 mile (statute)	**1.609 344**	km
			AREA		
1 cm²	0.155 0	square inches	1 square inch	**6.451 6**	cm²
1 m²	1[illegible]763 9	square feet	1 square foot	**0.092 903 04**	m²
1 km²	0.386 10	square miles	1 square mile	2.589 988	km²
1 ha	2.471 054	acres	1 acre	0.404 685 6	ha
			VOLUME		
1 cm³	0.061 02	cubic inches	1 cubic inch	**16.387 064**	cm³
1 m³	35.314 7	cubic feet	1 cubic foot	0.028 316 85	m³
1 m³	1.308 0	cubic yards	1 cubic yard	0.764 555	m³
			CAPACITY		
1 L	1.759 755	pints	1 pint	0.568 261	L
1 L	0.879 877	quarts	1 quart	1.136 522	L
1 L	0.219 969	gallons	1 gallon	**4.546 090**	L
			MASS		
1 g	0.035 273 96	ounces (avdp)	1 ounce (avdp)	28.349 523	g
1 g	0.032 150 75	ounces (troy)	1 ounce (troy)	**31.103 476 8**	g
1 kg	2.204 62	pounds (avdp)	1 pound (avdp)	**0.453 592 37**	kg
1 kg	0.001 102 3	tons (short)	1 ton (short)	**907.184 74**	kg
1 t	1.102 311	tons (short)	1 ton (short)	**0.907 184 74**	t
1 kg	0.000 984 21	tons (long)	1 ton (long)	**1016.046 908 8**	kg
1 t	0.984 206 5	tons (long)	1 ton (long)	**1.016 046 908 8**	t
			CONCENTRATION		
1 g/t	0.029 166 6	ounce (troy)/ ton (short)	1 ounce (troy)/ ton (short)	34.285 714 2	g/t
1 g/t	0.583 333 33	pennyweights/ ton (short)	1 pennyweight/ ton (short)	1.714 285 7	g/t

OTHER USEFUL CONVERSION FACTORS

1 ounce (troy)/ton (short)	20.0	pennyweights/ton (short)
1 pennyweight/ton (short)	0.05	ounce (troy)/ton (short)

NOTE—Conversion factors which are in bold type are exact. The conversion factors have been taken from or have been derived from factors given in the Metric Practice Guide for the Canadian Mining and Metallurgical Industries published by The Mining Association of Canada in cooperation with the Coal Association of Canada.

Geoscience Research Grant Program
Summary of Research 1984-1985

---

edited by
V.G. Milne

Director, Ontario Geological Survey

Introductory Remarks

The Ontario Geoscience Research Grants Program was initiated in 1978 to encourage geoscience research at Ontario universities. By supporting mission-oriented geologically related projects, a program of research was established which would complement the work of the Ontario Geological Survey through its mandate:

> To stimulate exploration for, and facilitate sound planning in all matters related to, mineral and other earth resources by providing an inventory and analysis of the geology and mineral deposits of Ontario.

The program supports applied studies of up to 3 years duration towards: mineral deposit characterization involving studies of specific occurrences or groups of occurrences within Ontario; petrology, rock geochemistry, structural geology, stratigraphy, and geochronology studies; field and laboratory studies leading to the development of new geophysical or geochemical concepts and techniques; engineering and environmental geology studies, and methods for improving automated or mineral processing, and facilitating the interpretation of geoscience data.

In order to receive funding, applications should be forwarded to the Ontario Geological Survey prior to November 15. Project proposals are subject to review by a committee which reports to the Director of the Ontario Geological Survey. This committee consists of 3 representatives of the mineral industry, 3 representatives of the university community, 4 representatives of the Survey, and a chairperson. Members review proposals based on scientific merit and relevance of the research to Ontario Geological Survey activities, concentrating on those projects which will stimulate and benefit exploration in the Province. Members of the 1984-85 committee included:

S.N. Charteris, Chairman; S.N. Charteris and Associates

Dr. A.C. Colvine; Ontario Geological Survey

Dr. J.A. Donaldson; Carleton University

Dr. J.A.C. Fortescue; Ontario Geological Survey

Dr. R. Hodder; University of Western Ontario

Dr. C.J. Hodgson; Queen's University

Dr. J. Misener; Paterson, Grant & Watson Ltd.

E.V. Sado; Ontario Geological Survey

Dr. H. Seigel; Scintrex Ltd.

Dr. J. Stewart; Selco Division-BP Resources Canada Limited

J. Wood; Ontario Geological Survey

Successful grant recipients are expected to submit reports for publication in the annual *Summary of Research* and participate in an annual OGS Geoscience Research Seminar held annually in December.

Publication in other scientific journals is encouraged and a final report summarizing the project objective is required to be submitted to the Ontario Geological Survey within 6 months of termination of funding.

The following research projects partially or wholly funded by this program during 1984-85 will be published as Ontario Geological Survey, Open File Reports:

Grant 128: Subsurface Quaternary Stratigraphy Using Borehole Geophysics: R.N. Farvolden, University of Waterloo.

Grant 132: Genesis of Precambrian Iron Formations—Links with Base and Precious Metal Mineralization; J.H. Crocket, McMaster University.

Grant 134: Stratigraphy and Geochemistry of Northern Ontario Carbonaceous Deposits: Onakawana Lignites and James Bay Peats; W.S. Fyfe, University of Western Ontario.

Grant 138: Mineralogy and Geochemistry of the Chrysotile Asbestos Deposits of Ontario; F.J. Wicks, University of Toronto.

Grant 146: Contamination and the Genesis of the Sudbury Ores; A.J. Naldrett, University of Toronto.

Grant 148: Geochemical and Isotopic Studies of the Salina Formation; P. Fritz, University of Waterloo.

Grant 179: The Petrogenesis and Metallogenesis of the Atikwa-Lawrence Volcanic-Plutonic Terrane; G.R. Edwards, York University.

Grant 202: Sulphur Isotope Studies of Archean Gold Deposits; H.P. Schwarcz, McMaster University.

During 1984-85, 23 projects were funded under the Program. Of these, 11 were renewal projects:

University	Value of Grants	No. of Grants
Carleton	$ 61,500**	3
Lakehead	9,325	1
McMaster	59,400	3
Ottawa	6,000	1
Queen's	73,625	3
Toronto	173,400	7
Waterloo	44,450	3
Western	34,300*	1
York	18,350	1
TOTAL	$480,350	

*A grant of $34,300 to the University of Western Ontario involved staff from Laurentian University.

**A grant of $24,800 to Carleton University involved staff of the University of Ottawa.

The undersigned would like to thank Mr. S.N. Charteris, who acted as Committee Chairman, and the rest of the Review Committee Members who gave freely of their time. The efforts of the researchers are acknowledged and Mr. R.B. Watson, who served as Grants Administrator and Secretary to the Committee, deserves thanks.

V.G. Milne
Director
Ontario Geological Survey

Grant 128 Subsurface Quaternary Stratigraphy using Borehole Geophysics

R.N. Farvolden, J.P. Greenhouse, and P.F. Karrow

Department of Earth Sciences, University of Waterloo

This project began in the fall of 1982. It had as its dual objectives obtaining information on the Quaternary stratigraphy of the Kitchener-Waterloo region, and improving techniques of recording and interpreting geophysical logs for this purpose. Original plans called for 3 traverses. Each traverse was to consist of 3 rotary drilled holes for logging and 1 continuously-cored hole for calibration. The logging holes were to be spaced by about 1.5 km, and the traverses were to extend roughly north, and west from the central Greenbrook well field. The core was to be acquired immediately adjacent to 1 of the logged holes and used to calibrate the geophysical responses, which in turn could be used to interpret the stratigraphy at the remaining 2 holes on each section. This information was to be incorporated with existing data to complete detailed geological sections along the 3 traverses.

Two previous reports (Farvolden *et al.* 1984; Greenhouse *et al.* 1983) have described the approach taken and the progress achieved. Summarized briefly in the first year (1982-1983), 3 rotary drilled boreholes were completed to bedrock (typically at 65 m) along a transect extending north from the Grand River at Homer Watson Park to the Greenbrook well field. Following electric and caliper logging, each hole was lined with a 7.5 cm ID PVC casing and filled with fresh water, providing a "standard" environment for gamma, neutron, and density logging. A continuous core was obtained immediately adjacent to one of these standard boreholes. In 1983-1984, a fourth standard hole was installed on a planned traverse from Greenbrook well field to the University of Waterloo Campus, and continuous core recovered from an adjacent borehole. Continuous core was also obtained to a depth of about 20 m beside one of the standard holes of the previous year. In addition, 2 shallow holes which intersected the 2 prominent tills of the area were installed at a North Waterloo site, and geophysical logs and core obtained. Furthermore, a calibration site was established for the logging tools on the North Campus of the University of Waterloo (UW).

The UW geophysical logging equipment was modified in the first year of the project to allow full digital logging. Each log was run a minimum of 3 times and the responses averaged over 15-cm sections of the hole for comparison with the core. All the logs obtained in this project are stored in digital form. The cores were described by P.F. Karrow, and selected sections subjected to grain size analysis by P. Pehme. The geophysical logs and core data collectively form the data base for a detailed comparison of these two means of lithologic description.

In 1984-1985, our efforts have been spent on analyzing this data base. After an unsuccessful attempt to use regression techniques to link core description to geophysical responses, we decided to concentrate on establishing response spaces for only the broadest lithologic and stratigraphic units: gravel, sand, silt, clay, till, non-till, Catfish Creek Till, and Maryhill Till. From the data base, the responses in neutron-gamma and neutron-density spaces were plotted for each category. Pehme (1984) and Leask (1985) have quantitatively analyzed these cross-plot spaces. Pehme developed a method of contouring the density distribution of the responses in each of these categories. Leask has digitized these contours and written a computer code to scan a new suite of logs and analyze each 15-cm segment in terms of the probability that it lies within one or more of the categories. Examples of the contoured cross-plots are given in Figures 128.1, 128.2, 128.3, and 128.4. Table 128.1 compares the output of Leask's program with the geologic core description at one of the boreholes.

This "expert system" has to date been applied only to logs which were used to describe the various response spaces in the first place, so it is too early to say how useful this attempt at an automatic interpretation really is. Until new data can be acquired, however, this program represents the end product of our work on log/core correlation. The core data from this project are being added to existing data for the region by Linda Ross as part of her M.Sc. project, and new sections will be produced to partially meet the second objective of our program. We are satisified that a good start has been made toward our original goals, and that future work can easily build on the base established. An unanticipated benefit of the program is the availability of 4 well documented and secure boreholes that are being used by a number of public and private organizations to test and calibrate equipment. The boreholes also form valuable teaching resources for this University.

We intend to complete the project as soon as funding can be obtained for more borehole data. At the moment, a catalogue of geophysical logs for the Waterloo region is being prepared. A second related project, currently being pursued by F. El Buras as part of his M.Sc. program, is using the methodology developed to analyze several suites of logs through a thick sand section below the Woolwich landfill site in terms of hydrological parameters such as permeability and porosity.

REFERENCES

Farvolden, R.N., Greenhouse, J.P., and Karrow, P.F.
1984: Subsurface Quaternary Stratigraphy using Borehole Geophysics; Grant 128, p.59-64 *in* Geoscience Research Grant Program, Summary of Research 1983-1984, edited by V.G. Milne, Ontario Geological Survey, Miscellaneous Paper 121, 252p.

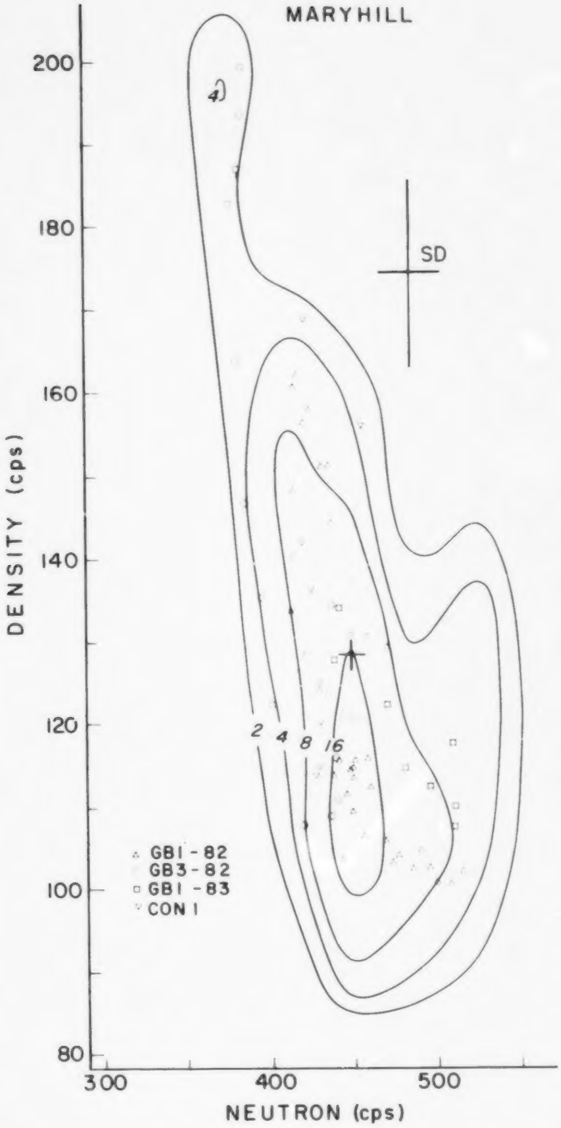

SD = STANDARD DEVIATIONS

Figure 128.1. *Distribution of log responses for the Maryhill Till on a neutron-density cross-plot. The contours describe the density of data points, using a method proposed by Pehme (1984). Data from all available core-log comparisons are included.*

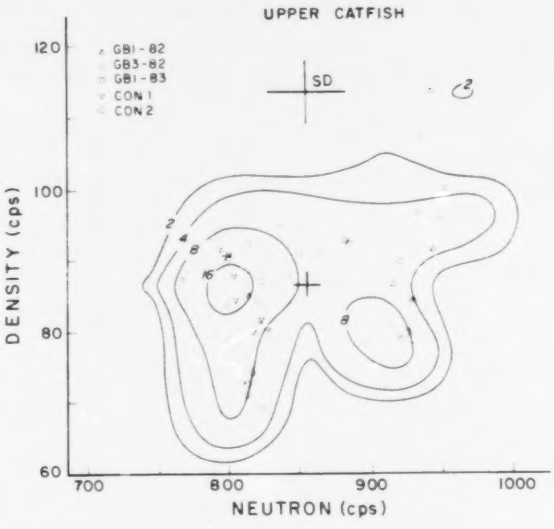

SD = STANDARD DEVIATIONS

Figure 128.2. *Distribution of log responses for the upper Catfish Creek Till on a neutron-density cross-plot. The contours describe the density of data points, using a method proposed by Pehme (1984). Data from all available core-log comparisons are included.*

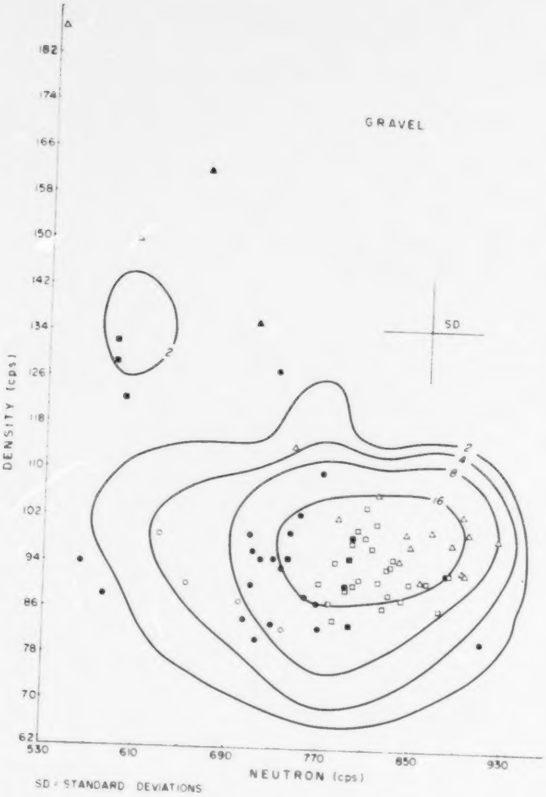

Figure 128.3. Neutron-density cross-plot for materials described as gravels in the core analysis.

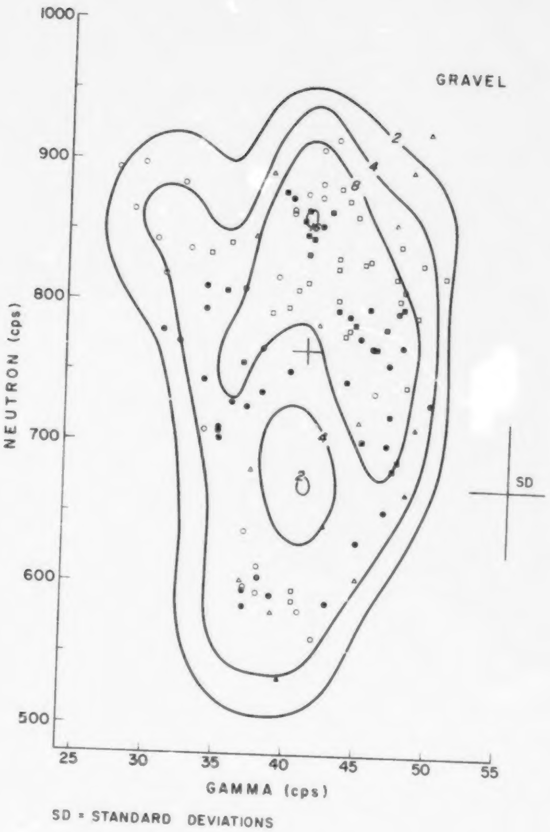

Figure 128.4. Neutron-gamma cross-plot for materials described as gravels in the core analysis.

TABLE 128.1. A COMPARISON OF THE COMPUTER-GENERATED CORE DESCRIPTION BASED ON THE GEOPHYSICAL LOG RESPONSES (LEFT) AND THE DETAILED CORE DESCRIPTION, AT BOREHOLE GB1-83.*

GEOPHYSICAL CORE LOG	CONTINUOUS CORE LOG	
	1'-3.5'	disturbed dirty buff medium sand and soil
	3.5'-4.5'	stony sandy topsoil
	4.5'-8.5'	dirty gravely sand
	8.5'-9.0'	fine silty sand
silty-clay 11.3' - 12.3'	9.0'-12.0'	dark pink grey stratified silt & clay, some fine sand
	12.0'-12.5'	fine olive sand
	12.5'-13.0'	stratified silt & clay some fine sand, dark pink grey
	13.0'-14.5'	fine grey buff sand
	14.5'-14.7'	3" sand, silt & clay
	14.75'-15'	3" band sand
	15'-18.5'	dark grey brown, disturbed clay & silt, sheared contorted bedding
	18.5'-23.5'	same sheared dark grey clay stratification, only evident intermittently. Only slightly moist, quite crumbly
silty - sand 26.3'-40.3'	23.5'-28.5'	stratified wet fine to medium sand, some silt
	28.5'-33.5'	(note only 1 ½ ft. sample) grey buff stratified fine sand silt
	33.5'-34'	silt & sand
	34'-36'	crumbly sheared clay & silt
	36.5'-40.5'	wet med. to coarse sand, white chert grains common
sand 40.3'-41.3'	40.5'-41.5'	fine wet sand with black streaks, possibly contamination, oily smell
silty - sand 41.3'-64.8'	41.5'-46.5'	wet med.to coarse sand, white chert grains common
	46.5'-47.5'	grey stratified silt with some fine sand, bedding 45^{0}
	47.5'-52.5'	grey buff stratified med. to fine sand w/silty bands & some clay in lower part
	52.5'-55.75'	grey buff, fine stratified sand with silty zones
	55.75'-58'	stratified silt, 2 pebbles near base
	58'-59.5'	olive med. stratified sand, clay ball inclusions
	59.5' -61.0'	stratified silt & clay with sand bands
	61'-62'	olive mixed sand & gravel with till-like balls
	62'-63'	poorly sorted sand & gravel
	63'-64.5'	olive to grey dirty med. sand, some fine gravel
	64.5'-65.5'	breccia like & till like gravelly sand, partly cemented
gravel 66.3'-70.3'	65.5'-66.5'	stratified dirty medium sand
	66.5'-67.5'	dirty sand & gravel, many pebbles rounded
	67.5'-68.5'	pebbly med. to fine sand
	1 ft. missing	
sand; 71.8'-72.3'	69.5'-73'	dirty med. sandy gravel
silt; 73.8'-74.8'	73' - 76'	rounded to angular sandy med. to fine gravel
	76'-77'	dirty olive similar gravel
	77'-78'	very dirty, sandy gravel with 2 clay bands near top and bottom

TABLE 128.1 CONT'D

	GEOPHYSICAL CORE LOG	CONTINUOUS CORE LOG	
Maryhill Till 82.8'-90.3'	silty-clay 73.3'-91.3'	78'-78.5'	grey silty clay till, few pebbles
		SAMPLE A	
		78.5'-83'	variable, mostly, some stratification, often disturbed blocky silty clay with silty zones - Maryhill complex
		83'-88'	massive to slightly stratified Maryhill Drift, silty clay, few pebbles
		SAMPLE B AT 85'	
		88'-90'	massive silty clay till - Maryhill
		SAMPLE C AT 89'	
		90'-92.5'	decreasingly sheared varved clay
		92.5'-93'	undisturbed varved clay, brownish to dark grey varves 2 cm thick, rapidly gradational into olive stony silt till
Catfish Creek Till: Upper - 92.3'-110.3' ; Lower - 99.8'-112.3'		93'-93.5'	separate bag - grey sandy stony till
		93'-94.5'	olive stony sandy till - Catfish
		SAMPLE D AT 93.5'	
	gravel/ silty-gravel 93.8'-125.8'	1 ft. missing	
		95.5'-96.5'	olive stony sandy till
		96.5'-97.25'	olive stony sandy till
		97.25'-98'	olive stony sandy till
		SAMPLE E AT 98'	
		98'-99'	same till
		99'-99.5'	crumbly same till
		100'-101'	olive gravely sandy till
		101'-102'	same
		102'-102.5'	same till
		1 ft. missing	
		103.5'-104.5'	same till
		SAMPLE F AT 104'	
		104.5'-105.25'	same till
		105.5'-106'	same till
		1 ft. missing	
		107'-107.5'	stony silty sandy till, disturbed
		107.5'-108.5'	olive gravelly sandy till
		108.5'-109.25'	olive stony sandy till
		109.5'-110.25'	stony sandy till
		SAMPLE G AT 110'	
		110.25'-111'	gravelly sandy till, crumbly
		111'-111.33'	stony sandy till
		111.33'-111.75'	same
		112'-112.5'	olive stony sandy till
		SAMPLE H AT 112.5'	
	small core	113.5'-114.0'	same

---

*Core data were available to 114 feet, whereas geophysical logs were recorded to bedrock at 200 feet. The bracketed sections immediately left of the dividing line are intervals where the automatic interpretations could be made. In other intervals the log responses were judged to be transitional and no attempt to categorize them was made. Each 15-cm section of core was further characterized by the automatic procedure as to whether it was, or was not, a till. Those that were judged to be till were further categorized as Maryhill, or upper or lower Catfish. These results are shown on the extreme left of the table.

Greenhouse, J.P., Karrow, P.F., and Farvolden, R.N.
1983: Subsurface Quaternary Stratigraphy using Borehole Geophysics; Grant 128, p.93-95 *in* Geoscience Research Grant Program, Summary of Research 1982-1983, edited by E.G. Pye, Ontario Geological Survey, Miscellaneous Paper 113, 199p.

Leask, N.E.
1985: An Expert System to Interpret Lithology and Stratigraphy from Geophysical Logs in Waterloo Region; Unpublished B.Sc. Thesis, The Department of Earth Sciences, University of Waterloo, Waterloo, Ontario, 38p.

Pehme, P.E.
1984: Identification of Quaternary Deposits with Borehole Geophysics in the Waterloo Region; Unpublished M.Sc. Thesis, The Department of Earth Sciences, University of Waterloo, Waterloo, Ontario, 124p.

Grant 132 Rare Earth Element Properties of Archean Iron Formations and their Host Rocks—Some Results from the Temagami and Boston Iron Formations

J.H. Crocket and R.J. Bowins

Department of Geology, McMaster University

ABSTRACT

Iron formations and host rocks from the Adams Mine (Boston Township) and the Sherman Mine near Temagami were analyzed for rare earth elements by neutron activation analysis. The purpose of the study was to evaluate whether the rare earth element properties of these iron formations might aid in better understanding the role of volcanism in the generation of Archean banded iron formation. The rare earth element signatures of these 2 iron formations and associated cherts were found to be very similar. Positive europium anomalies and weakly fractionated chondrite normalized patterns characterize all iron formation and chert samples. Differences in absolute rare earth content from sample to sample were small but significant in that Adams Mine iron formation was characterized by higher rare earth content than Temagami iron formation. Felsic volcaniclastic host rocks from Temagami were characterized by rare earth patterns without europium anomalies, greater light-to-heavy rare earth fractionation, and much higher rare earth concentrations than the iron formations. It was concluded that the rare earth complement of these iron formations was derived from a well mixed homogeneous reservoir of wide geographic distribution, probably seawater. The data do not support the concept that iron formations are precipitated from hydrothermal discharge near source vents or that they necessarily form in proximal volcanic environments.

INTRODUCTION AND GEOLOGICAL BACKGROUND

This report discusses the results of a study of rare earth elements (REE) in Archean banded iron formation (BIF) and some of their host rocks. It is part of a project to evaluate the possible significance of the banded iron formation environment as an indicator of the economic potential of the associated volcanic and sedimentary rocks. The iron formations under study include the Temagami iron formation in Strathy, Strathcona, and Briggs Townships (District of Nipissing), and the Boston iron formation in Boston Township (District of Timiskaming). Previous reports (Crocket *et al.* 1983, 1984) have dealt with the preliminary findings of isotopic (sulphur, oxygen), lithogeochemistry and geological mapping studies of the iron formations and their host rocks.

This study considers the implications of REE data on the genesis of the iron formations. It is widely acknowledged that the Archean BIF (Algoman type) is an integral component of greenstone belts, and in this sense is related to volcanism (Goodwin 1973). However, it is not clear whether Archean iron formations are precipitates of volcanogenic fluids exhaled in a proximal volcanic setting (near an eruptive volcanic centre), or whether precipitation can occur in a marine basin in which hydrothermal activity is absent.

If the REE complement of BIF is derived from a well mixed, large-volume reservoir, then consistent REE properties (fractionation pattern, Eu anomaly characteristics) may be expected. However, if BIF involves localized emission of volcanogenic fluids in near-vent settings, then variable REE properties might be expected from one iron formation to another. To test this hypothesis and to improve the REE data base for Archean BIF, which currently is poorly documented (Fryer 1977a, 1978b), BIF and associated host rocks from the Temagami and Boston iron formations were analyzed for REE by neutron activation analysis.

METHODOLOGY

SAMPLING

The general geology and distribution of iron formations in the Adams and Sherman Mine areas is shown in Figures 132.1a and 132.1b respectively. At the Adams Mine, oxide facies BIF samples were collected from the Peria, Central, and North Central pits. This sampling represents at least 2 different beds of iron formation. Two main bands of iron formation make up the Sherman Mine at Temagami. Samples of the northern band were taken from the West and North pits. The southern band was sampled from the South pit and from the Turtle Lake area where drill core provided both iron formation samples and felsic volcaniclastic host rocks interbedded with the iron formation. The chert samples were also taken from Turtle Lake core.

Analytical

The REE were determined by instrumental neutron activation using the McMaster nuclear reactor as an irradiation source. The procedure follows that described by Jacobs *et al.* (1977) except that 2 irradiations were used. The first was a 15 minute irradiation in an epithermal (cadmium shielded) flux. Samples were counted for La and Sm after a decay period of approximately 2 days. After 2 weeks samples were re-irradiated for 3 hours in a thermal flux of 10^{13} neutrons/cm^2/sec. Following the second irradiation, samples were counted after 10 days decay, and finally, after 60 days decay for the remainder of the REE. The procedure is more time consuming than that usually employed for activation analysis of REE, but allows for determination of heavy metals including Au, As, Sb, and W in the first count period, and in addition to the REE, a further 10 elements in the final count.

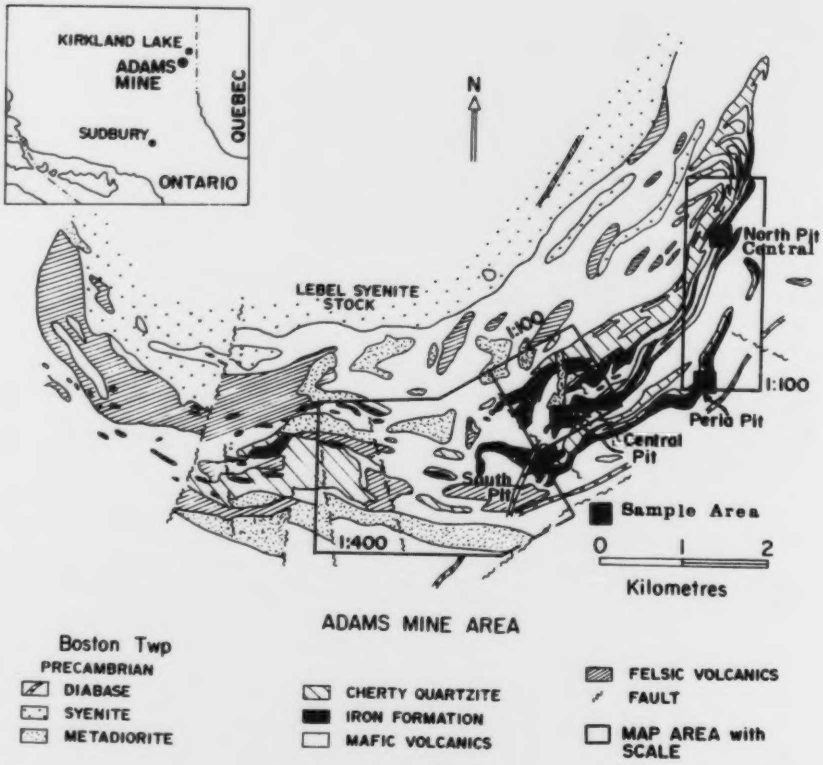
KIRKLAND LAKE
ADAMS MINE
SUDBURY
QUEBEC
ONTARIO
N
LEBEL SYENITE STOCK
1:100
North Pit
Central
1:100
Peria Pit
Central Pit
South Pit
1:400
Sample Area
0
1
2
Kilometres
ADAMS MINE AREA
Boston Twp
PRECAMBRIAN
DIABASE
SYENITE
METADIORITE
CHERTY QUARTZITE
IRON FORMATION
MAFIC VOLCANICS
FELSIC VOLCANICS
FAULT
MAP AREA with SCALE

Figure 132.1a. *Sample location map for the Adams Mine area, Boston Township.*

DISCUSSION

REE CHARACTERISTICS OF IRON FORMATION

Oxide Facies Rocks

Chondrite normalized REE profiles for oxide facies BIF are summarized in Figure 132.2. The thick and thin lined envelopes encompass a suite of 7 samples from the Adams Mine and 9 samples from the Sherman Mine areas respectively. The suites include iron formation made up dominantly of magnetite, jasper, and chert mesobands. Minor amounts (5%) of silicate, carbonate, and sulphide minerals are present in some samples. The general REE properties of both suites are very similar. All samples have strong positive Eu anomalies and a weakly fractionated REE pattern (shallow chondrite normalized slope). On average the La/Lu ratio is ~ 2. The significant difference between the 2 suites is that the Adams Mine rocks are usually higher in total REE abundance, particularly with respect to the light REE.

Cherts

Chondrite normalized REE profiles for 11 cherts from the Sherman Mine BIF are summarized in Figure 132.3. Most samples were taken from core drilled through the southern iron formation band under Turtle Lake. Very siliceous rocks were classified as chert on textural and compositional grounds. The characteristic textural properties were aphanitic granularity and the presence of microbands (bands of ≤ 1 mm thickness). The compositional screen used was $SiO_2 + Fe_2O_3 \geq 90\%$ and $Al_2O_3 \leq 2\%$. The colour of cherts varied widely from jet black, when fine-grained graphite was present, to white. The thick line envelope in Figure 132.3 encompasses 9 REE patterns for Sherman Mine cherts. The thin line is the average for 2 very pure cherts with SiO_2 ~ 98%.

Characteristic REE properties are a distinct positive Eu anomaly and a weakly fractionated pattern with average La/Lu ~ 3. The 2 samples of nearly pure silica also show positive Eu anomalies and weak fractionation of light to heavy REE, but are distinguished by very low total REE content. The REE properties of Sherman Mine cherts and oxide facies BIF are very similar. They differ only in that the cherts are slightly higher in light REE. The similar and distinctive REE patterns, particularly the strong positive Eu anomalies, shown by both the iron formations and the cherts, suggest that both rocks derive their REE complement from a common source.

REE CHARACTERISTICS OF HOST ROCKS

Host rocks to the south band of iron formation at Sherman Mine, sampled from the Turtle Lake core, consist mainly of felsic volcaniclastic rocks. Generally these rocks are fine grained and occur as beds of a few centimetres in thickness. Some units, however, are made up of 10 cm and thicker beds consisting of medium-grained material. Quartz, feldspar, and lithic fragments are the most abundant constituents. The SiO_2 contents range from 60% to 73% and, pending completion of whole-rock analysis, the suite is regarded as mainly dacitic in composition.

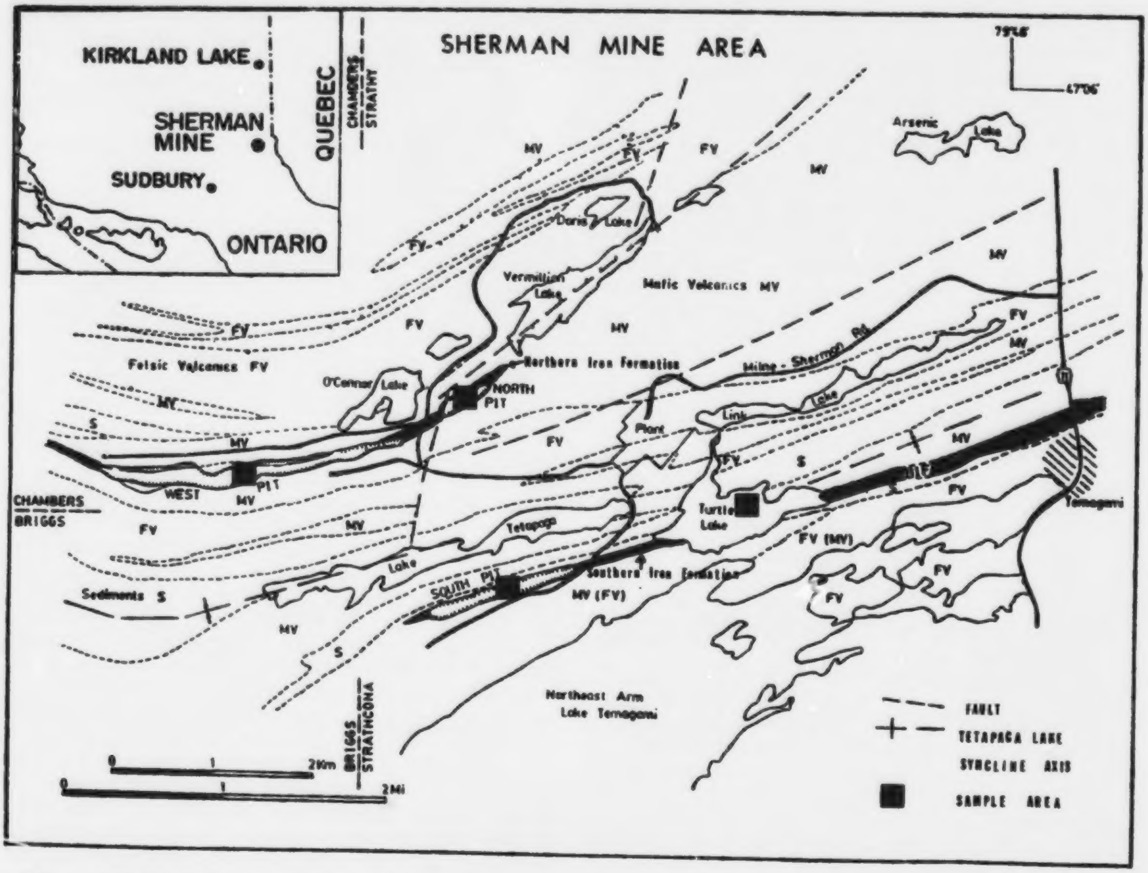
SHERMAN MINE AREA
KIRKLAND LAKE
SHERMAN MINE
SUDBURY
QUEBEC
ONTARIO
CHAMBERS
STRATHY
79°46'
47°06'
Arsenic Lake
MV
FV
Doris Lake
Vermillion Lake
Mafic Volcanics MV
Felsic Volcanics FV
O'Connor Lake
Northern Iron Formation
NORTH PIT
Milne - Sherman Rd.
Link Lake
Plant
S
WEST PIT
CHAMBERS
BRIGGS
Tetapaga Lake
Turtle Lake
FV (MV)
Temagami
SOUTH PIT
Southern Iron Formation
MV (FV)
Sediments S
Northeast Arm Lake Temagami
BRIGGS
STRATHCONA
0
1
2Km
0
1
2Mi
FAULT
TETAPAGA LAKE SYNCLINE AXIS
SAMPLE AREA

Figure 132.1b. Sample location map for the Sherman Mine area, Temagami.

The REE envelope for 14 felsic volcaniclastic rocks shown in Figure 132.4 is seen to encompass a relatively narrow range of total REE contents. La is 50 to 100 times chondritic while Lu is 5 to 10 times chondritic. There is a distinct break in slope at the middle rare earths but few samples are characterized by a distinct Eu anomaly. The light REE slope (La/Eu) averages 5, whereas the heavy REE slope (Eu/Lu) is about 2. These patterns are comparable to those reported by Condie (1976) for Archean felsic volcanic rocks.

SOURCES OF REE IN IRON FORMATION

Archean BIF is commonly interpreted as a chemical sediment (Goodwin 1973; Maynard 1983) in which volcanogenic fluids are important contributors of metals. The most distinctive aspect of the REE signature of the oxide facies BIF is the similarity of REE properties in a suite of samples representing 2 different areas and several different iron formations in each area. The consistent Eu anomaly and weak REE fractionation shown by all samples suggest that the REE source was one characterized by a homogeneous, uniform, and well mixed REE pool of wide geographic distribution. It is suggested that the immediate REE source to the iron formations was the marine water of the individual basins in which iron formation was deposited.

Ultimately, volcanic activity and the resultant rock column can be regarded as the source of many constituents to the hydrosphere. The REE have some bearing on whether local, proximal volcanogenic sources were involved, or whether iron precipitation occurred in well mixed marine waters in geological terrain remote from centres of eruptive volcanic activity. The Temagami felsic volcaniclastic host rocks are mainly fine grained and thinly bedded. Felsic flows and intrusives are rare, particularly in the vicinity of the south band iron formation. Tentatively, the volcaniclastics are interpreted as of distal character with respect to proximity to a vent or volcanic centre. The distal character of these host rocks and the uniform REE signatures in all Temagami BIF suggest an absence of proximal sources of volcanogenic fluids, and is more compatible with the concept of low intensity water-rock exchange and/or chemical weathering as a source of REE to the marine environment.

The Adams Mine BIF suite differs in one significant aspect of its REE signature from the Temagami suite. This difference is a higher total REE content in the Adams samples. If the idea that large-scale

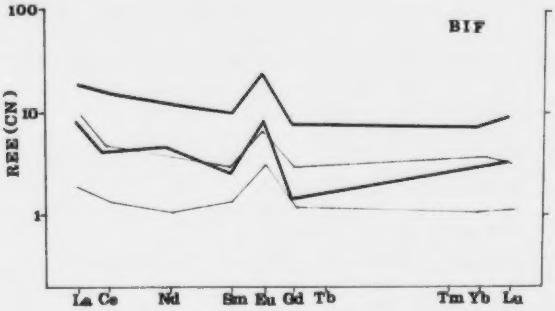

Figure 132.2. *Envelopes for chondrite normalized REE patterns for oxide facies BIF from the Adams Mine area (thick lines) and the Sherman Mine area (thin lines). The Adams Mine suite includes samples from the Peria, Central, and North Central pits. The Sherman Mine suite includes samples from the West and North pits on the northern band of iron formation, and the South pit and Turtle Lake area on the southern iron formation band. In this and succeeding figures, REE(CN) refers to chondrite normalized REE content.*

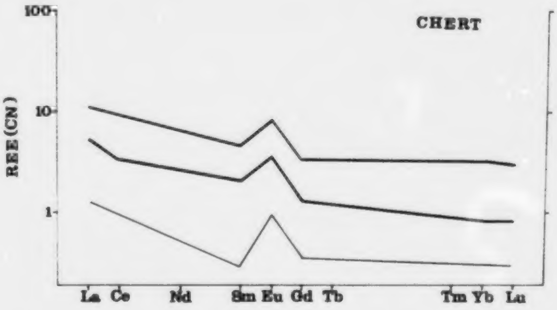

Figure 132.3. *Envelope for chondrite normalized REE patterns for cherts from the Turtle Lake area, southern iron formation band, Sherman Mine (thick lines). The average pattern for 2 very pure cherts (SiO_2 ~ 98%) from the Turtle Lake area is shown as the thin line profile.*

water-rock exchange is an important process in establishing the REE characteristics of marine waters is valid, then such differences may reflect different lithic proportions in the relevant rock columns. It was noted in a previous report (Crocket *et al.* 1983) that mafic-ultramafic rocks are more voluminous in the Adams Mine area. A source with high abundance of mafic rocks might be expected to yield lower absolute REE content than one with a high proportion of felsic rocks. However, the relative lack of mineral phases to host light REE (e.g., potash feldspars) may be of more importance with respect to ease of exchange of REE with fluids than absolute content of REE. Thus, leaching of REE, particularly light REE, may have been more effective in the Adams Mine environment, and a higher REE complement may have resulted in relevant depositional basins. Differences in REE content in the Adams and Sherman suites are most pronounced for the light REE.

SIGNIFICANCE OF REE PATTERNS OF CHERTS

Chert macrobands are perhaps the most common lithology interbedded with magnetite- and hematite-bearing layers in oxide facies BIF. Cherty rocks, often with graphite and pyrite, are also common in wallrocks to both the Adams and Sherman Mine BIF. The REE signature of cherts is nearly identical to that of magnetite- and hematite-rich iron formation rocks. The distinctive positive Eu anomaly and similar fractionation patterns are present in both rock types. Furthermore, very pure microbanded cherts (SiO_2, 98%) have similar Eu anomaly and REE fractionation patterns. They differ only in their lower content of total REE. The similar REE signatures of cherts and oxide facies BIF, and the common interbedding of magnetite-rich and quartz-rich bands in iron formation suggests that both rock types inherit their REE complement from the same source. This source is probably the seawater of the depositional basin in that the same arguments supporting a seawater source for REE in the iron-rich rocks are also applicable to the source of REE for the cherts.

SIGNIFICANCE OF BIF FOR REE IN ARCHEAN SEAWATER

It is suggested that some of the REE properties of BIF are inherited directly from seawater. Specifically, the positive Eu anomaly and weak fractionation pattern are probably a direct reflection of the REE properties of Archean seawater. Many models of Archean BIF as a chemical sediment envisage some type of silica and ferric hydroxide gels as the primary precipitates and precursors to magnetite, hematite, and quartz (*see* Maynard 1983, Chapter 2). In a low temperature marine environment it is unlikely that the crystallographic structure of the solid phase will be as important a factor contributing to REE fractionation as in high temperture igneous melts. The nearly identical REE properties of chert and BIF suggest that the primary precipitates did not significantly differentiate between individual REE. Consequently, the Eu anomaly is probably inherited from the seawater medium rather than produced by selective exchange at the precipitate-seawater interface.

Fryer (1977b) argued that Archean seawater was characterized by a positive Eu anomaly due to enhanced solubility of the divalent species which was suggsted to be stable at the redox potential of Archean seawater. Graf (1978), however, found positive Eu anomalies in Ordovician age Algoma-like iron formation from the Bathurst, New Brunswick, sulphide district, and argued that the nature of water-rock reactions in seawater hydrothermal systems were responsible for the Eu anomalies, rather than seawater chemistry. There is little evidence from our data of host rocks with positive Eu anomalies which tentatively favours Fryer's point of view.

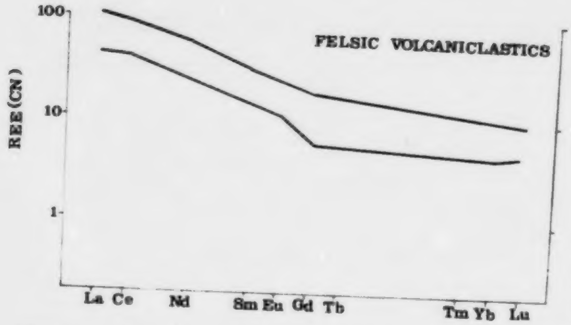

Figure 132.4. *Envelope for chondrite normalized REE patterns for felsic volcaniclastic rocks which host BIF in the Turtle Lake area, southern iron formation band, Sherman Mine.*

CONCLUSIONS

The main conclusion from this study is that the REE complement of BIF is drawn from a well mixed, homogeneous source of wide geographic distribution. Seawater from sedimentary basins with somewhat restricted circulation to open oceans is a viable REE source. The concept that BIF is precipitated from a hot, well focused hydrothermal discharge emanating from near-source volcanic vents and fissures or other proximal settings, is considered less probable. A speculative implication is that BIF would not be expected to show enrichment in those heavy metals which tend to concentrate in precipitates from high temperature, evolved seawater-hydrothermal fluids.

ACKNOWLEDGMENTS

Access to the open pits of the Adams and Sherman Mines, through the cooperation of Mr. Keith Oliver and Mr. Bob Garrett respectively, is sincerely appreciated.

REFERENCES

Condie, K.C.
1976: Trace-Element Geochemistry of Archean Greenstone Belts; Earth-Science Reviews, Volume 12, p.393-417.

Crocket, J.H., McNutt, R.H., Schwarcz, H.P., Rees, C.E., Blum, N., Hurley, T.D., Bowins, R.J., and Kabir, A.
1983: Isotopic and Geochemical Characterization of Archean Iron Formation and Associated Volcanic Rocks—Some Preliminary Results from the Temagami and Boston Iron Formations; Grant 132, p.29-40 *in* Geoscience Grants Research Program, Summary of Research 1982-1983, edited by E.G. Pye, Ontario Geological Survey, Miscellaneous Paper 113, 199p.

Crocket, J.H., Blum, N., Hurley, T.D., Bowins, R.J., McRoberts, G., Fyon, J.A., McNutt, R.H., Schwarcz, H.P., and Rees, C.E.
1984: Geological and Geochemical Studies of the Boston and Temagami Iron Formations and Their Contiguous Volcanosedimentary Piles; Grant 132, p.72-83 *in* Geoscience Grants Research Program, Summary of Research 1983-1984, edited by V.G. Milne, Ontario Geological Survey, Miscellaneous Paper 121, 252p.

Fryer, B.J.
1977a: Trace Element Geochemistry of the Sokoman Iron Formation; Canadian Journal of Earth Sciences, Volume 14, p.1598-1610.
1977b: Rare Earth Evidence in Iron-Formations for Changing Precambrian Oxidation States; Geochimica et Cosmochimica Acta, Volume 41, p.361-367.

Goodwin, A.M.
1973: Archean Iron-Formation and Tectonic Basins of the Canadian Shield; Economic Geology, Volume 68, p.915-933.

Graf, J.L.
1978: Rare Earth Elements, Iron Formations and Seawater; Geochimica et Cosmochimica Acta, Volume 42, p.1845-1850.

Jacobs, J.W., Korotev, R.L., Blanchard, D.P., and Haskin, L.A.
1977: A Well-Tested Procedure for Instrumental Neutron Activation Analysis of Silcate Rocks and Minerals; Journal of Radioanalytical Chemistry, Volume 40, p.93-114.

Maynard, J.B.
1983: Geochemistry of Sedimentary Ore Deposits; Springer-Verlag, New York, 305p.

Grant 134 Geochemistry and Petrography of the Mattagami Formation Lignites (Northern Ontario)

C.G. Winder[1], J.R. Brown[2], B.I. Kronberg[1], W.S. Fyfe[1], and F.H. Murray[1]

[1]Geology Department, University of Western Ontario

[2]Catalysis Research Section, Energy Research Laboratory, CANMET, Canada Energy, Mines, and Resources,
555 Booth Street, Ottawa, Ontario, Canada K1A 0G1

ABSTRACT

A multi-technique approach has been used to characterize lignites from the Mattagami Formation of northern Ontario. This report focuses on the petrographic information and surface studies by X-ray photoelectron spectroscopy (XPS).

The petrographic studies demonstrate the low rank of these coals despite their deposition during the Cretaceous. The petrography reveals a low degree of compaction during diagenesis. Surface studies by XPS corroborate previously reported geochemical data that demonstrated the chemically clean nature of the Mattagami Formation coals. Integration of the petrographic and surface information with the geochemical data leads to a picture of an intensely weathered depositional environment. Lack of burial and compaction maintained large porosities, which permitted intense leaching, presumably during glacial retreats. These factors would account for the formation of these clean coals.

INTRODUCTION

In designing suitable strategies for coal use, detailed chemical and petrographic studies are of fundamental importance. In the work described here and in two previous reports (Fyfe *et al.* 1983; Murray *et al.* 1984), a multi-technique approach has been successful in characterizing lignites from the Mattagami Formation located in northern Ontario. Several lines of information have been integrated in our studies. Petrographic studies were important in demonstrating the immature nature of these coals and the low degree of compaction during diagenesis. Geochemical fingerprinting of the ashes of these coals showed that background levels of minor and trace elements are low in comparison with other coals. Major and trace element and mineral compositions were consistent with original deposition in a highly weathered environment and subsequent preservation in the upper crust. Surface studies of fossil woody materials and their ashes provided further evidence of the chemically clean nature of these coals and the apparent lack of contamination by saline waters of either deep continental or marine origin.

This paper describes the petrographical studies and surface analyses by X-ray photoelectron spectroscopy (XPS).

GEOLOGICAL SETTING

The Mattagami Formation is a sequence of Cretaceous sediments located in the Moose River Basin in the James Bay Lowlands of northern Ontario (*see* Figure 1 *in* Murray *et al.* 1984). The Cretaceous sediments form a semi-elliptical lens (170 km by 80 km) consisting of quartz sands, gravels, clays, and lignites. In the modern stratigraphic setting, the observed maximum thickness of the formation is 160 m, but with considerable local variation which may have been controlled by factors relating to the glacial episodes of the Pleistocene and topography on the top of the underlying Devonian. There are few outcrops of the Mattagami Formation and the proposed stratigraphic model (Try *et al.* 1984) was constructed from drill core findings (Try *et al.* 1984). It appears that the lignite accumulated in paleovalleys such as at Onakawana, where lignite was first observed in outcrops along the Abitibi River. Palynological evidence suggests a Lower Cretaceous age for the Mattagami Formation (Norris 1977; Legault and Norris 1982), and the palynomorphs are typical of freshwater and upland environments (Norris *et al.* 1976).

THE MATTAGAMI FORMATION LIGNITES

The most extensive accumulation of these lignites is in the Onakawana coal field where the 2 main seams have a combined thickness averaging 11 m. Several years ago the Onakawana field was stripped open and several thousand tonnes of lignite were removed for thermal power feasibility studies. Recoverable reserves are estimated to be 189 million tons. Exploration of the Moose River Basin included an extensive drilling program carried out under the auspices of the Ontario Geological Survey (Telford and Sawicki 1983), the Ontario Energy Corporation (Try *et al.* 1984) and Lignasco Resources (Try *et al.* 1984).

In hand specimen, the lignites appear unaltered physically. Pieces of wood, tree roots, twigs, etc., are easily identified. One tree stump was observed on Adam Creek and an upright tree trunk was observed in the sediments. The samples discussed here include 2 types of lignite, distinguished by Tasker (1933): peaty (high ash content) and woody (low ash content). In lignite "boulders" found along Adam Creek 2 lignite textures could be distinguished:

1. mattes of flattened twigs and stems including fragments of coalified wood (in which the grain could still be identified) and in 1 sample, a flattened branch 10 cm by 1 cm. The "boulders" of compressed twigs appear to have high porosity and from the petrographic work, it is evident that the macerals, texinite, and fusinite are especially porous.
2. a solid mass of detrital material with scattered angular nuggets of fusinite up to 2 cm across.

In the stock pile at Onakawana and in the lignite "boulders" along Adam Creek there is evidence for rapid disintegration after contact with the surface environment.

The estimated average composition of these lignites is: 46% moisture, 8% ash, 22% volatiles, and 23% fixed carbon. By North American standards these coals are low in sulphur (0.51%, corresponding to 1.12% on a dry ash-free basis) and are classified as low rank coals (2739 kcal/kg). Although the Mattagami Formation lignites are considered part of the carbonaceous fuel reserves of Ontario, there are no current plans for their use as a source of energy.

PETROGRAPHY

SAMPLE PREPARATION

Preliminary studies were started by selecting identifiable material such as twigs, branches, wood, etc., and crushing and sieving to between 20 and 200 mesh (0.074 to 0.814 mm particles). Pellets were made by mixing with epoxy resin using the standard procedure. Problems arose at this stage because the Mattagami Formation lignites are particularly soft and friable. For example, crushing and sieving produced a notable amount of dust. Realistically, loss of this material could skew the distribution of particles in the pellet. In addition, producing a pellet using the standard pressure technique was impossible with some samples and the pellets were prepared by stirring a few drops of epoxy into a gram or two of crushed material. Because the resulting pellet is unsatisfactory for point counting, a procedure was developed using a 400 point rectangular grid with summation and statistical analysis (percentage, standard deviation) processed on a Zeiss Zonax microcomputer.

Polishing the pellets with water also produced unsatisfactory results, and all cutting, grinding, and polishing were done with isopropyl alcohol. After smoothing the surface with 600-grit silicon paper, final polishing was done exclusively with isopropyl alcohol. Experience revealed that hand holding rather than multiple processing with Automet provided a better result. Polishing on silk at high speed for 2 minutes with 0.3 μm alumina (the matted polishing discs seem to tear out the particles) was followed by polishing with 0.05 μm alumina on silk at high speed. The slurry ratio is 5 g of powder to 200 ml of isopropyl alcohol. The final polish was 20 seconds on the same lap with isopropyl alcohol only (blow dry). The specimens were examined within 24 hours, as the quality of polish appears to deteriorate although repeating the final step does restore the polish.

MACERALS

Given the scope of this paper only a brief summary of the petrographic studies carried out by one of the authors (C.G. Winder) is presented. The exceptionally low rank of these lignites has allowed the preservation of a great variety of distinctive types of material. Selected examples are shown in Photos 134.1, 134.2. Complete organic entities are numerous as illustrated by the cutinite shown in (Photo 134.1, 2-16). In the huminite category, 12 types were identified. The corpohuminite masses show a great variety of shape, texture, orientation, and presence of vacuoles. Some have a distinctive "olive" colour and shape. Cutinite could be identified under ordinary light, but other liptinites such as spores and algae could be seen only with ultraviolet light.

The most abundant inertinites are various types of fusinites. One variety of telocollinite (Photo 134.1, 3-27) could be compared to a charred specimen (Photo 134.2, 8-24) because of characteristic cell walls. Several varieties of sclerotinite are present. A maceral identified as micrinite is abundant (not illustrated here). Fusinite "dust" is very abundant and adheres to the surface of the crushed particles.

Detrinite is abundant but highly variable as a percentage of constituents, i.e., huminite and inertinite. One combination is particularly noteworthy—Photo 134.2 (2-10) shows an organic structure, possibly with a thin cuticle surrounded by fine humino-detrinite. Similar material occurs between the cuticles in Photo 134.1 (2-16). Some pellets consist of over 20% of this material, which may represent layers of leaves and other organic structures separated by a layer of detritus with a significant component of fusinite fragments.

Pyrite occurs in 3 forms: masses filling pores of fusinite, isolated masses commonly in detrinite, and single and composite framboids in detrinite. A content of up to 3.5%, based on point counting, indicates a sulphur content higher than determined by trace element geochemistry.

MACERAL COMPOSITION

Standard point counting was inadequate because all liptinites could not be observed. Insufficient data have been collected using the grid count system but maceral distribution is approximately: huminites - 75%; liptinites - 6%; inertinites - 14%; and minerals, mainly pyrite - 2%. The most striking feature of the Mattagami Formation lignites is that even though the age is Lower Cretaceous, the rank is remarkably low. Reflectance determinations are of little use because values range from 0.15 to 0.38. Generally the uncompressed woody fragments, textinite, have low reflectance and the flattened gelified ones have high values.

ANALYSIS BY X–RAY PHOTOELECTRON SPECTROSCOPY

INTRODUCTION

Chemical analysis of the Mattagami Formation lignites by X-ray photoelectron spectroscopy (XPS, also known as ESCA) provided information complementary to the petrographic information discussed above and the geochemical data reported previously. XPS is a surface-sensitive, non-destructive technique providing quantitative information on all elements (except H and He) in the outermost 1 to 5 nanometres of a solid and with an ultimate sensitivity approaching 10^{-9}g cm^{-2}. The parameter of interest is the change in binding energy, E_b, or the "chemical shift", which represents the change in energy level of core electrons; thus XPS may be used both to identify elements and to obtain information on chemical structure, such as oxidation state, coordination number, etc. Several good reviews of XPS theory and instrumentation are available (Winograd and Gaarenstroom 1980; Duke 1982; Seah and Briggs 1983).

The application of XPS in Earth and Life Sciences for studying complex organic materials (e.g., poly-

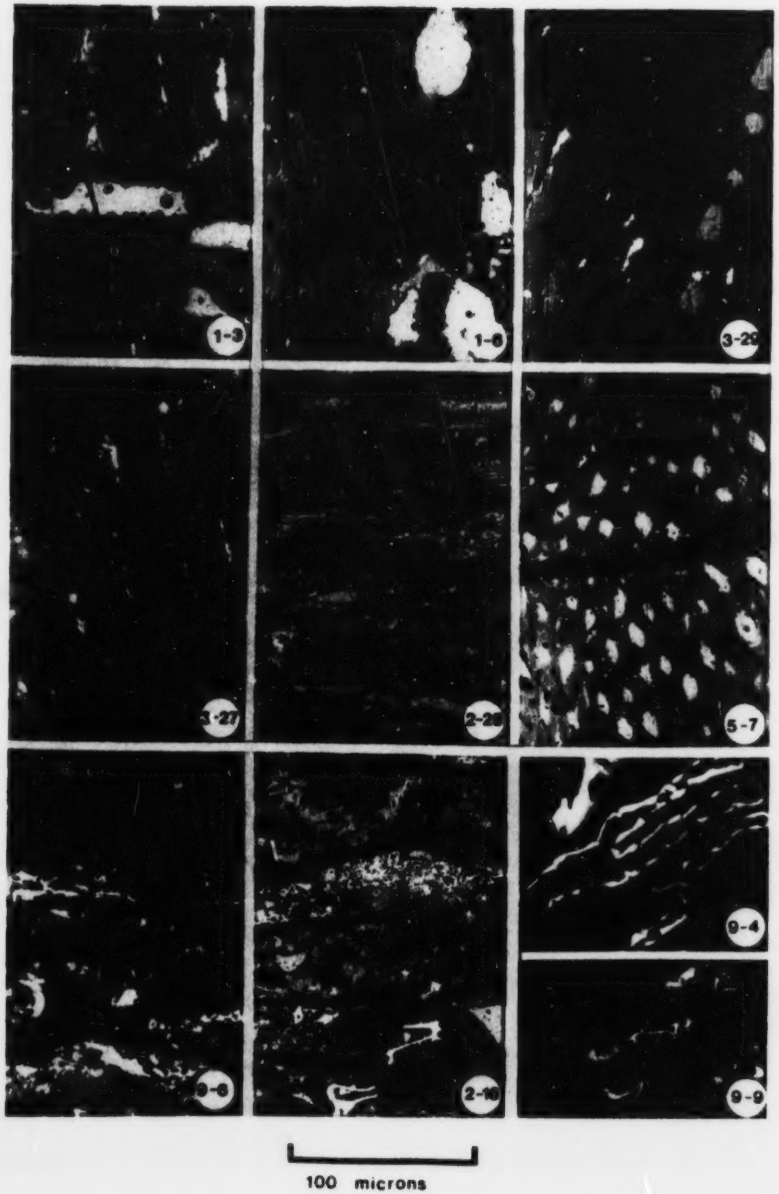

Photo 134.1

1-3*	Textinite, sample from uncompressed wood with porosity, corpohuminite bodies trending perpendicular to trend of cells, mosaic texture and porous.
1-6	Texto-ulminite with partially gelified cell walls, some porosity, corpohuminite has a coarse mosaic texture.
3-29	Eu-ulminite with associated corpohuminite concentrated along one boundary.
3-27	Telocollinite with "dinosaur" porosity.
3-38	Telinite, porous, with cell walls showing ribs.
5-7	Telocollinite, distinctive spotted pattern without obvious cell walls may be root structures.
9-6	Phlobaphinite, and cutinite separated by zones of huminodetrinite.
2-16	Layered cutinite showing internal zones with epidermal cells, second cuticle from top has pore near right margin, separated by huminodetrinite, corpohuminite at lower right margin.
9-4	cutinite under ultraviolet light
9-9	sporinite under ultraviolet light

* First number refers to negative roll Number, second number refers to frame number

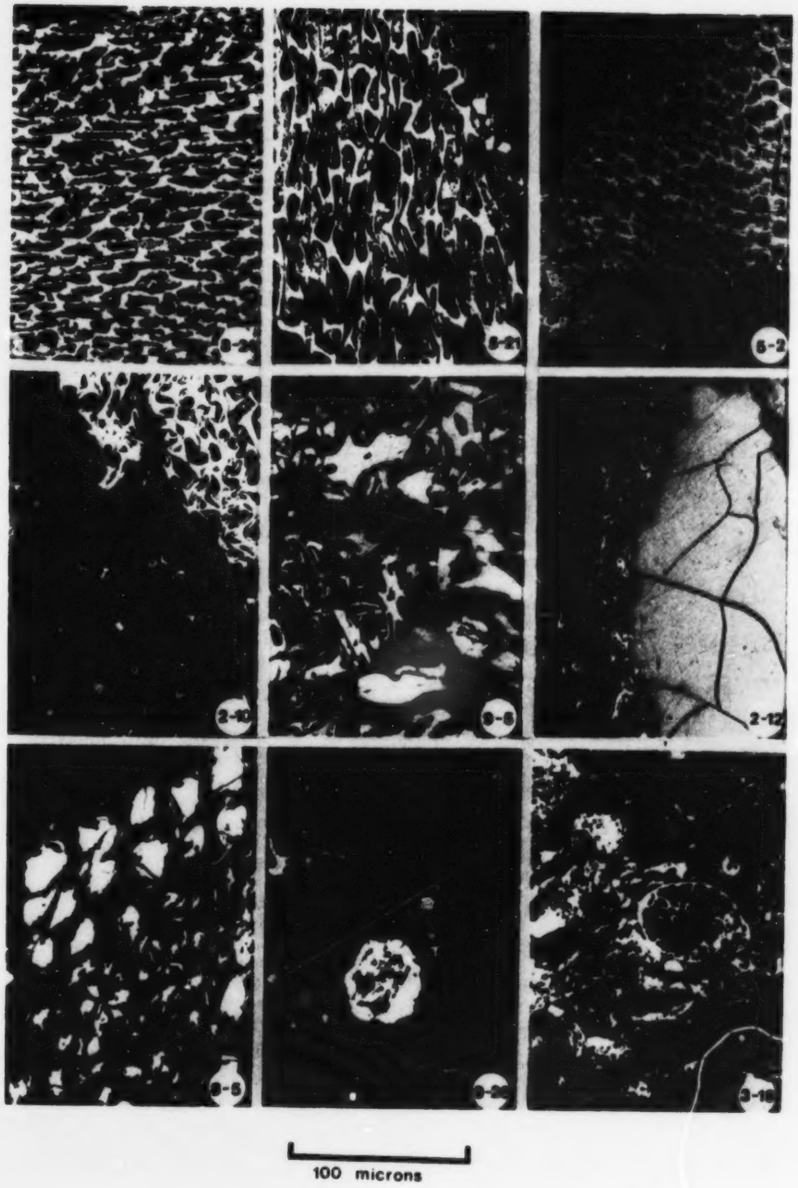

Photo 134.2

8-24*	Fusinite with cell walls suggesting "dinosaur" porosity (as in 3-27, Photo 134.1).
5-21	Fusinite with thin cell walls (similar to 1-6, Photo 134.1)
5-2	Fusinite "dark" shows morphology of fusinite but lower reflectance, collinite in pores.
2-10	Organic structure possibly with thin cuticle (left) with huminodetrinite and patch of fusinite bogen structure.
9-5	Inertodetrinite
2-12	Macrinite in huminodetrinite with very small sclerotinite.
8-5	Fusinite with pores filled with massive pyrite.
9-28	Pyrite ball (not framboid) in huminodetrinite.
3-18	Sclerotinite in huminodetrinite.

* First number refers to negative roll number, second number refers to frame number.

Photo 134.3. Woody lignite sample.

mers, coal, etc.) has increased rapidly over the past several years. For example, in the case of coal, carbon and oxygen functional groups, along with nitrogen, chlorine and organic/inorganic sulphur components may be monitored, and in many cases, common minerals such as alumino-silicates, silica, sulphides, sulphates, phosphates, and carbonates may be fingerprinted (Brown *et al.* 1981; Perry and Grint 1983; McIntyre *et al.* in press; Hirokawa and Danzaki 1984; Clark and Wilson 1983).

The XPS spectrometer used was a Physical Electronics Industries (PHI) model 548. This instrument is computer controlled and employs a dual anode X-ray source (Mg and Al K_α). The energy scale is calibrated using gold (Au $4f_{7/2}$= 83.8 eV) and copper (Cu $2p_{3/2}$= 932.6 eV, Cu 3p = 75.0 eV) and peak positions are considered accurate to ±0.2 eV. The base pressure of the vacuum console is 2 x 10^{-10} torr. Lignite and lignite ash are routinely analyzed at vacuum pressures of 10^{-8} torr.

METHOD AND RESULTS

Relatively smooth flat chunks of lignite (10 by 10 by 2 mm) were selected and dried at circa 100°C overnight prior to analysis. Ash was analyzed after it was pressed in pellet form. Following analysis, semiquantitative XPS data were derived by equating each elemental major photoelectron line intensity with its sensitivity factor. In addition, some photoelectron lines, which clearly exhibited several different chemical structures, were resolved using an iterative nonlinear least squares curve-fitting computer program.

Two types of lignites from the Mattagami Formation were examined:

1. woody lignite with well preserved, hard lignite wood (WL-1 and WL-2), in which the grain and texture of the original wood was visible, and
2. featureless lignite with chunks of soft lignite (FL-1 and FL-2) having no distinctive physical features and a tendency to crumble easily.

A comparison of surface and bulk chemical analysis of the woody lignite is given in Table 134.1. A photograph (Photo 134.3) of this material shows the preserved wood grain. Hydrogen cannot be detected by XPS and thus the surface is calibrated on a hydrogen-free basis. Generally, the XPS results for the major and minor elements agree well with classical chemical techniques. XPS is useful in identifying and measuring semi-quantitatively the inorganic phases incorporated into coals. Actually in these particular lignite samples there is very little mineral matter, as shown by the wide energy scan XPS spectra in Figure 134.1a. The carbon content (75%) can be classified into 4 distinct groups using the C 1s spectra (Figure 134.1b). These 4 species are (i) O-C=O, 289 eV (peak 1), (ii) C=O, 287.8 eV (peak 2), (iii) C-O, 286.6 eV (peak 3), and (iv) $(CH_2)_n$, 284.6 eV (peak 4), and occur in a ratio of circa 1:1:5:30 respectively. The O 1s region (Figure 134.1c) can be resolved into 2 peaks. These 2 peaks are actually composed of several smaller peaks closely separated in binding energies that arise from the presence of oxygen species in the coal having similar chemical environments. The large peak at circa 533 eV (peak 1) is assigned to oxygen singly bonded to carbon as well as oxygen from silica, sulphate, and water, while the smaller peak at circa 531 eV (peak 2) is assigned to oxygen doubly bonded to carbon and oxygen from other minerals. Since lignite samples WL-1 and WL-2 contain small amounts of oxides, silicates and sulphates (Table 134.1), nearly half the larger peak arises from structural water. Note, the measured oxygen peak intensity ratios are circa 11 (large/small peak) while the C-O/C=O peak ratios measured from the C 1s spectra are circa 5 (Figure 134.1b).

TABLE 134.1. XPS CHEMICAL ANALYSIS OF WOODY LIGNITE SAMPLES WL-1 AND WL-2. COMPOSITION IN WT %.

	WL-1		WL-2	
	bulk	XPS	bulk	XPS
C-volatile	37.4	75.6	35.9	73.7
C-fixed	43.7		42.4	
O	16.9[c]	22.8	19.8[c]	24.9
S	0.47	0.4	0.53	0.5
Si	bd[a]	0.7	bd	0.5
Al	0.2	0.7	0.2	0.3
N	bd	0.1	bd	<0.1
Ca	0.64	0.2	0.55	0.3
Ash	1.95	ND[c]	1.86	ND

[a]bd = below detection
[b]ND = not detectable
[c] by difference

TABLE 134.2. XRF CHEMICAL ANALYSIS OF LIGNITE ASH WL-1 AND WL-2. COMPOSITION IN WT %.

	WL-1	WL-2
SiO_2	bd*	3.6
Al_2O_3	9.5	10.0
Fe_2O_3	8.3	9.1
TiO_2	0.02	0.02
CaO	35.3	35.3
MgO	16.9	12.3
SO_3-	21.5	23.0
Na_2O	2.7	2.4
K_2O	0.2	0.3
BaO	3.6	1.9
SrO	0.9	0.8
P_2O_5	1.3	1.2

*bd = below detection

TABLE 134.3. XPS CHEMICAL ANALYSIS OF FEATURELESS LIGNITE SAMPLES FL-1 AND FL-2. COMPOSITION IN WEIGHT %.

	FL-1	FL-1	FL-2
	bulk	XPS	XPS
C	55.1	61.4	74.1
O	23.6[d]	26.3[c]	23.3[c]
S	0.13	bd[a]	0.8
N	0.51	2.1	1.0
Al	5.53	3.3	0.2
Si		4.3	0.2
Ca		1.7	0.2
Fe		0.8	0.9
Moisture	12.1	ND[b]	ND
H	3.0	ND	ND
Total	100.0	99.3	100.1

[a]bd = below detection
[b]ND = not detectable
[c]includes moisture
[d]by difference

TABLE 134.4. XPS CHEMICAL ANALYSIS OF FL-1 ASH. COMPOSITION IN WEIGHT %.

	XPS	XRF
C	27.8	14.4(a)
O	27.6	35.5(b)
Si	3.4	4.9
Al	9.6	6.0
Fe	3.7	5.0
Ca	12.7	23.7
Mg	9.7	5.3
S	4.4	4.9
Na	1.1	0.7
K	bd*	0.3
Total	100	100

(a) loss on fusion
(b) oxygen calculated by difference
*bd = below detection

The XPS data also indicate high Ca and S contents in these samples and an Al/Si ratio which exceeds that of alumino-silicate minerals. These results are supported by the chemical analysis of the ash from the woody lignite specimens by X-ray fluorescence spectroscopy (XRF) (Table 134.2) which shows an abundance of alkaline earths, sulphur, and iron, and a high Al/Si ratio. The latter would be consistent with the presence of an aluminum-rich phase such as gibbsite. The source of the detected alkaline earths could be Pleistocene waters, draining carbonate-rich glacial debris. High levels of Fe and S are consistent with the numerous observations of pyrite by other methods.

The 2 pieces of featureless lignite (FL-1 and FL-2) have quite different XPS spectra (Figure 134.2a). Specimen FL-1 contains much more Ca, Si, Al, Fe, and N than FL-2. The C and O contents are similar however and agree very well with the bulk determinations (Table 134.3). For example, the C 1s spectra shown in Figure 134.2b indicate similar amounts in both samples of C=O, C-O, and $(CH_2)_n$ species in a ratio of 1:3:15. No O-C=O was detected.

The O 1s spectra, Figure 134.2c, indicates a larger mineral component in sample FL-1. Both samples also contain 2 chemical forms of nitrogen (Figure 134.2d): pyrrole-type, 400.8 eV (peak 1), and pyridine-type 399.5 eV (peak 2) found in a ratio of 2:1. Sulphur was detected in FL-2 (Figure 134.2e) and occurs in 3 environments: sulphate (peak 1), sulphite (peak 2), and sulphide (peak 3). Iron was also measured in FL-2 and it can be postulated to be present as pyrite. The pyrite surfaces are oxidized due to air exposure.

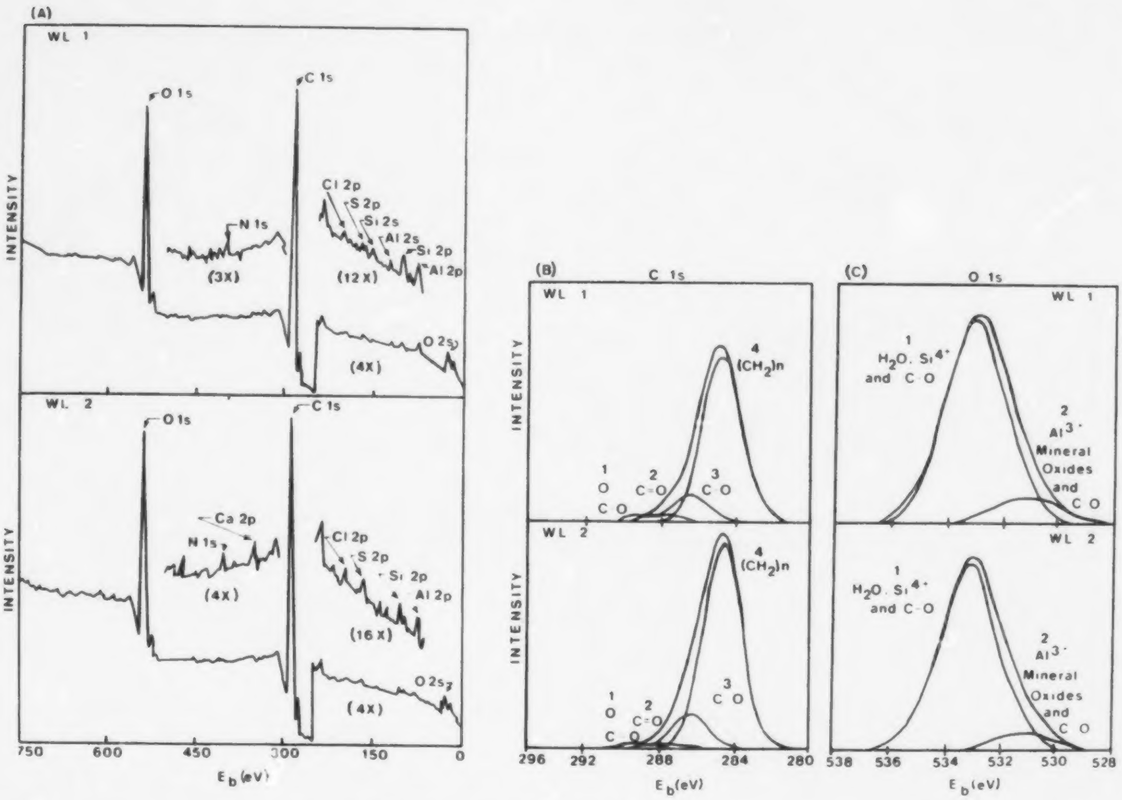

Figure 134.1. *XPS spectra of woody lignites WL-1 and WL-2*
(a) survey spectra,
(b,c) high resolution C 1s and O 1s energy regions.

The ash of FL-1, containing the larger mineral fraction, was analyzed by XPS (Figure 134.3a) and XRF techniques, and the results compared in Table 134.4. Combustion has greatly reduced the nitrogen and carbon contents. The Al/Si XPS ratio indicates the presence of an aluminum-rich mineral such as gibbsite. Gibbsite was also detected by scanning electron microscopy in the sediments associated with the Mattagami Formation lignites (E. van der Flier, personal communication). Again, high Ca and Mg concentrations are evident.

The C 1s spectrum of FL-1 ash shown in Figure 134.3b indicates the removal of $(CH_2)_n$ (species 4). Note that the C-O/$(CH_2)_n$ ratio is now much larger after combustion (compare Figures 134.2b and 134.3b). Most of the oxygen in the ash is sited in mineral matter specifically as sulphate species and Al and Si oxides (Figure 134.3c). The high sulphur content in the ash occurs mostly as sulphate (Figure 134.3d) in 2 environments, possibly $CaSO_4$ and $MgSO_4$ at 170 eV (peak 1), and $FeSO_4$ (peak 2). The small peak (peak 3) is indicative of sulphide.

CONCLUSIONS

One of the problems in using coal as a source of energy is that in order to burn coal efficiently and to reduce environmental hazards, it is necessary to have very detailed knowledge of the coal being used. This information is often very difficult to obtain due to the chemical and physical complexity of coal. For example, minor and trace element levels in coals are very important both in combustion (as catalysts and as catalyst poisons) and in assessing the environmental impact of burning a particular coal.

In the case of the Mattagami Formation lignites, our multidisciplinary approach was useful in showing not only how clean these coals are, but also in shedding light on the depostional and post-depositional environments. The explanation appears to lie in the lack of burial and compaction and therefore the preservation of large porosity, permitting intense leaching. It is also interesting that detailed studies, such as presented here, have led to paleoenvironmental information. The petrographical and all the detailed chemical data lead to a picture of an intensely weathered depositional environment. Following deposition, these coals were preserved at high crustal levels in a heavy-metal-poor environment. The few metal anomalies which exist (Zr, Au) may be due to periodic deposition of finely suspended particulates. Continuous and rapid flushing by rain water and an accelerated leaching event during the retreat of the great ice sheets has possibly led to the creation of this metal-poor coal.

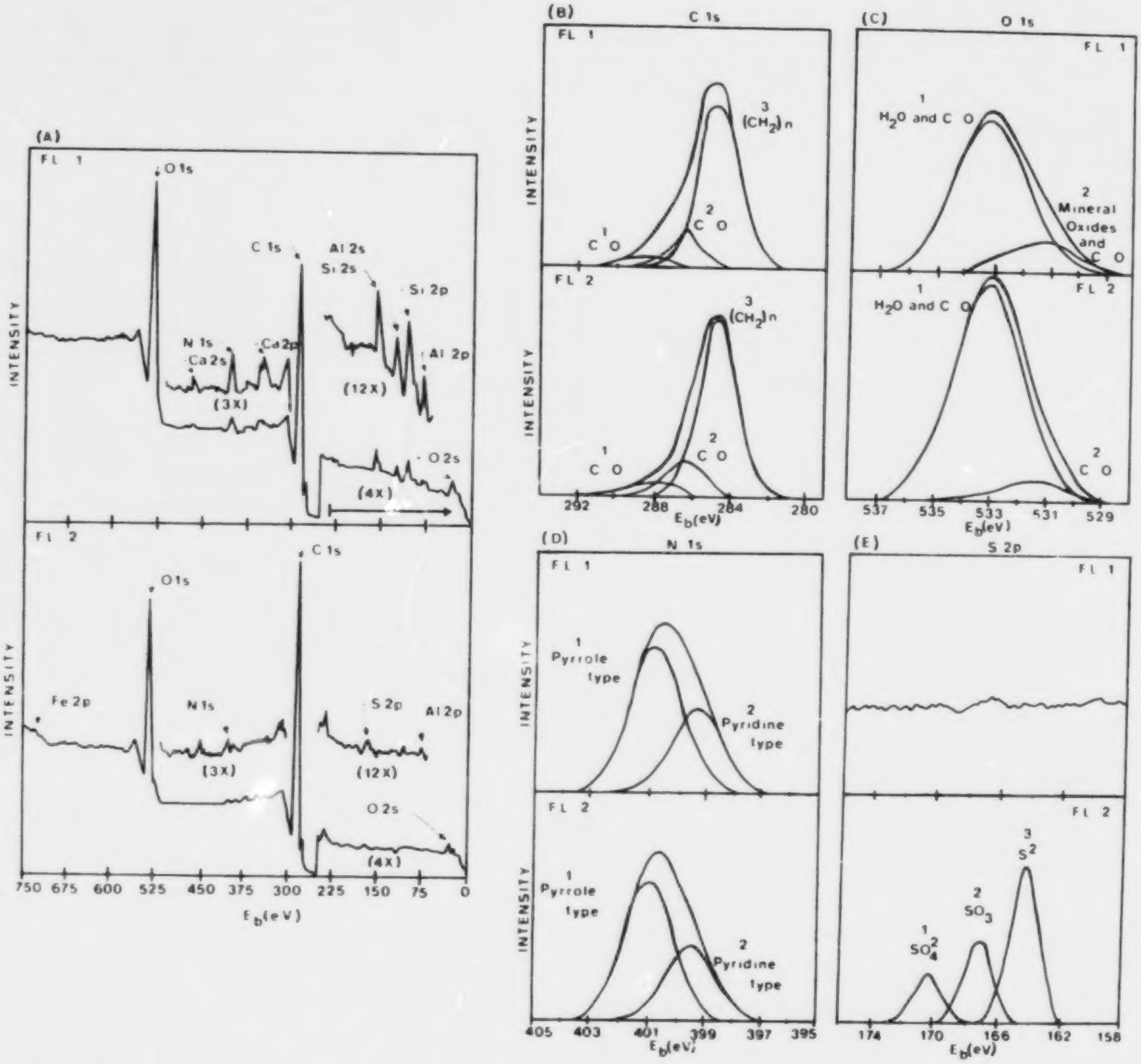

Figure 134.2. *XPS spectra of featureless lignites FL-1 and FL-2*
(a) survey spectra,
(b,c,d,e) high resolution C 1s, O 1s, N 1s, and S 2p energy regions.

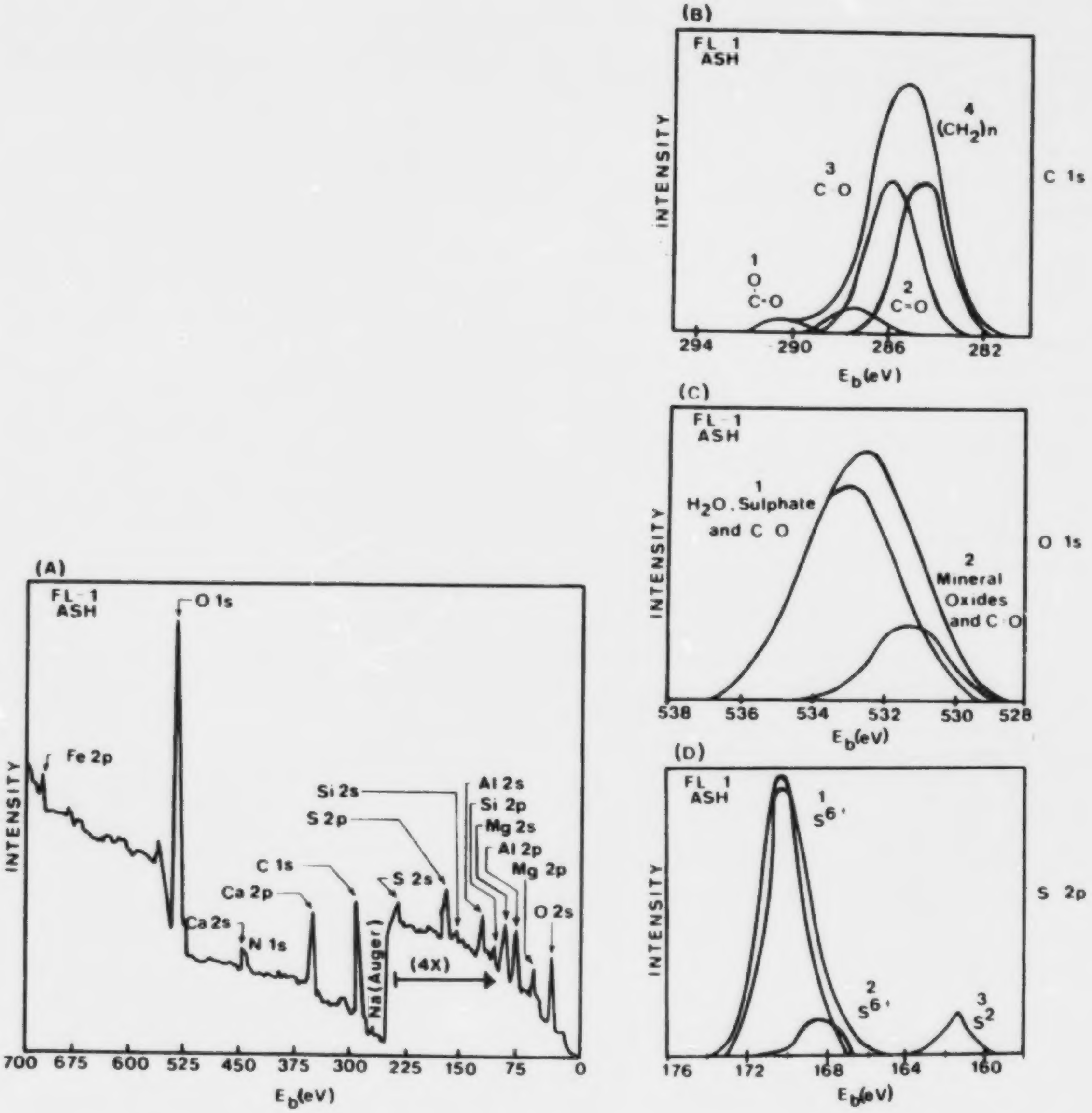

Figure 134.3. *XPS spectra of featureless FL-1 lignite ash*
(a) survey spectrum,
(b,c,d) high resolution C 1s, O 1s, and S 2p energy regions.

ACKNOWLEDGMENTS

C.G. Winder wishes to thank Alex Cameron of Geological Survey of Canada, Calgary, and Alan Hampson of DOFASCO, Hamilton, for an introduction to coal petrography and the reflecting microscope. Mohamed Khan and Bob Lamour of Algoma, Sault Ste. Marie provided invaluable assistance with developing sample preparation procedures. James VanDenbosseche was most helpful with writing computer programs as well as in developing sample preparation procedures. C.G. Winder claims sole responsibility for maceral identification. All the authors are grateful to Dr. N.S. McIntyre, Director of Surface Science Western, for constructive comments.

REFERENCES

Brown, J.R., Kronberg, B.I., and Fyfe, W.S.
1981: Semiquantitative ESCA Examination of Coal and Coal Ash Surfaces; Fuel, Volume 60, p.439-446.

Clark, D.T., and Wilson, R.
1983: ESCA Applied To Aspects of Coal Surface Chemistry; Fuel, Volume 62, p.1034-1040.

Duke, C.B.

1982: Surface Analysis: Prologue and Perspective; p.1-12 *in* Industrial Applications of Surface Analysis, edited by L.A. Casper and C.J. Powell; ACS Symposium Series, Number 199, ACS. Washington.

Fyfe, W.S., Kronberg, B.I., Long, D.F., Murray, F.H., Powell, M., Try, C., van der Flier, E., Winder, C.G., and Brown, J.R.

1983: Stratigraphy and Geochemistry of Northern Ontario Carbonaceous Deposits: Onakawana Lignites; Grant 134, p.63-81 *in* Geoscience Research Grant Program, Summary of Research 1982-1983, edited by E.G. Pye, Ontario Geological Survey, Miscellaneous Paper 113, 199p.

Hirokawa, K., and Danzaki, Y.

1984: Analytical Application of XPS for Surface Characterization of Coal Fly Ash and Coal; Surface and Interface Analysis, Volume 6, Number 4, p.193-195.

Legault, J.A., and Norris, G.

1982: Palynological Evidence for Recycling of Upper Devonian into Lower Cretaceous of the Moose River Basin, James Bay Lowland, Ontario; Canadian Journal of Earth Sciences, Volume 19, Number 1, p.1-7.

McIntyre, N.S., Martin, R.R., Chauvin, W.J., Winder, C.G., Brown, J.R., and McPhee, T.A.

In Press: Studies of Elemental Distributions within Discrete Coal Macerals Using Secondary Ion Mass Spectrometry and X-ray Photoelectron Spectroscopy; Fuel.

Murray, F.H., van der Flier, E., Fyfe, W.S., Kronberg, B.I., Long, D.F., Try, C., and Winder, C.G.

1984: Stratigraphy and Geochemistry of Northern Ontario Carbonaceous Deposits: Onakawana Lignites; Grant 134, p.84-98 *in* Geoscience Research Grant Program, Summary of Research 1983-1984, edited by E.G. Pye, Ontario Geological Survey, Miscellaneous Paper 121, 252p.

Norris, G.

1977: Palynofloral Evidence for Terrestrial Middle Jurassic in the Moose River Basin, Ontario; Canadian Journal of Earth Sciences, Volume 14, p.153-158.

Norris, G., Telford, P.G., and Vos, M.A.

1976: An Albian Microflora from the Mattagami Formation, James Bay Lowlands, Ontario; Canadian Journal of Earth Sciences, Volume 13, p.400-403.

Perry, D.L., and Grint, A.

1983: Application of XPS to Coal Characterization; Fuel, Volume 62, p.1024-1033.

Seah, M.P., and Briggs, D.

1983: A Perspective on the Analyses of Surfaces and Interfaces; p.1-16 *in* Practical Surface Analyses by Auger and X-ray Photoelectron Spectroscopy, edited by D. Briggs and M.P. Seah, J. Wiley and Sons, New York.

Tasker, C.

1933: A Technical Investigation of Northern Ontario Lignite; Canadian Institute of Mining and Metallurgy, Bulletin, April.

Telford, P.G., and Sawicki, D.W.

1983: Lignite Assessment Project, Moose River Basin, James Bay Lowlands; p.126-127 *in* Summary of Field Work, 1983, by the Ontario Geological Survey, edited by John Wood, Owen L. White, R.B. Barlow, and A.C. Colvine, Ontario Geological Survey Miscellaneous Paper 116, 313p.

Try, C.F., Long, D.G.F., and Winder, C.G.

1984: Sedimentology of Lower Cretaceous Mattagami Formation, Moose River Basin, James Bay Lowlands, Ontario, Canada: p.345-359 *in* The Mesozoic of Middle North America; edited by D.F. Stott and D.V. Glass; Canadian Society of Petroleum Geologists, Memoir 9.

Winograd, N., and Gaarenstroom, S.W.

1980: X-ray Photoelectron Spectroscopy; p.115-169 *in* Physical Methods in Modern Chemical Analysis, Volume 2, Edited by T. Kuwana, Academic Press, New York.

Grant 138 Mineralogy and Geochemistry of the Chrysotile Asbestos Deposits of Ontario: A Progress Report on the Stable Isotope and Boron Survey

J. Ozoray[1], F.J. Wicks[2], and M.D. Higgins[3]

[1]Department of Mineralogy and Geology, Royal Ontario Museum

[2]Department of Geology, University of Toronto

[3]Department of Geology, McMaster University

ABSTRACT

Thirteen serpentine separates from four serpentinized komatiites have been analyzed for oxygen isotopes and boron abundances. In samples that have undergone only retrograde serpentinization , δ^{18}O values vary from +3.7 to +6.3. In samples that have undergone both retrograde and prograde serpentinization , δ^{18}O values have a wider range from +3.9 to +8.8, with a clustering of samples at the higher end. Values do not vary systematically with sample location. Boron abundances vary from 13 ppm to 356 ppm. There is no correlation between B and δ^{18}O values. Deuterium/Hydrogen (D/H) ratios of these samples will be determined shortly.

INTRODUCTION

This study is a continuation of work carried out on the mineralogy and geochemistry of the asbestos deposits of Ontario (Wicks *et al.* 1983, 1984). The chrysotile asbestos deposits have already been characterized and the same suites of samples have been used for a preliminary stable isotope survey.

The range of ^{18}O/^{16}O and D/H ratios of substances of geological interest were established early (*see* Hoefs 1973). Later, in a specific study of serpentinites, ocean dredge samples of serpentinized ultramafic rocks were compared with ophiolites and Precambrian serpentinized ultramafic rocks, to determine the source of the fluids that produced the alteration (Wenner and Taylor 1971, 1973, 1974). Unless otherwise stated, the following information comes from the above works.

Both δD and δ^{18}O values of serpentinized ophiolite complexes were found to show a wider variation than oceanic serpentinites, demonstrating that different types of waters were involved during recrystallization. The source of metamorphic fluids for oceanic serpentinites was found to be ocean water, with possibly up to $\leq$25% magmatic water, or isotopically exchanged, deeply circulating ocean water. Serpentinization of ophiolite complexes was achieved by hot, exchanged meteoric groundwater, mixed meteoric-magmatic water, and/or mixed meteoric-connate water. This would indicate that ophiolites were largely unserpentinized prior to emplacement on land. Generally, δ^{18}O values reflect the highest temperature achieved during the metamorphism and show resistance to retrograde effects, although partial D/H exchange may take place later at lower temperatures.

Beaty and Taylor (1982) have determined the serpentinized whole-rock stable isotope composition of komatiite samples from Munro Township. The serpentinite samples were chosen on the basis of igneous textural variation. They considered that the source of the metamorphic fluid was deeply circulating Archean ocean water.

GEOLOGY

Four serpentinized ultramafic komatiites in the Abitibi greenstone belt were chosen for a stable isotope survey to study the conditions of serpentinization and chrysotile asbestos vein development. Three of these, Munro, Garrison, and Reeves, are chrysotile asbestos deposits, the general geoloy of which has been described by Vos (1971). A more detailed mineralogical study has been reported in Wicks *et al.* (1983, 1985). The fourth serpentinized komatiite at the Alexo Mine (Barnes *et al.* 1983) was chosen because it is an example of a single stage of retrograde serpentinization with no significant chrysotile asbestos development.

All 3 chrysotile asbestos deposits examined have experienced 2 stages of serpentinization. The first stage is an early retrograde event, characterized by pseudomorphic replacement of olivine and pyroxene by lizardite 1T ±magnetite mesh textures and lizardite 1T bastites, respectively. The serpentinite at Alexo has only experienced this retrograde serpentinization. This stage is related to prehnite-pumpellyite facies metamorphism (Jolly 1982). The degree of alteration is usually advanced but highly variable. Primary igneous minerals, particularly clinopyroxene, may be observed in some areas.

The second stage is a complex prograde event, producing variable mineralogy from deposit to deposit, resulting in nonpseudomorphic serpentine textures. Development of chrysotile asbestos veins is generally associated with this prograde event. The prograde serpentinization is related to greenschist or, occasionally, lower amphibolite facies metamorphism (Jolly 1982).

The 4 study areas can be arranged according to their serpentine mineralogy, in terms of increasing metamorphic grade: Alexo, Garrison, Munro, and Reeves.

SAMPLING AND EXPERIMENTAL TECHNIQUES

Specimens were selected on the basis of field observation and thin section examination to reflect all the different metamorphic phases. With the exception of the Alexo deposit, from which only 1 sample has been analyzed, samples from the chrysotile asbestos deposits were chosen to represent the chrysotile asbestos ore, the highly recrystallized prograde zone associated with the ore, and the earlier retrograde

TABLE 138.1. GEOCHEMICAL AND MINERALOGICAL DATA OF THE SAMPLES ANALYZED.

Sample Number	Mineralogy	$\delta^{18}O$ (per mil)	B(ppm)
Alexo			
W83-33	Lizardite 1T	6.336	17.3
Munro			
W82-175	Lizardite 1T	3.659	54.8
W82-186	Chrysotile $2M_{c1}$ + minor $2Or_{c1}$	7.891	62.6
W82-187	Lizardite 1T	3.884	183.4
W83-131	Chrysotile $2M_{c1}$ + minor $2Or_{c1}$	4.83	83.2
Garrison			
W70-570a	Lizardite 1T	6.697	
W70-570b	Chrysotile $2M_{c1}$	8.792	36.1
W71-280a	Lizardite 1T + Brucite	3.862	18.4
W71-280b	Lizardite 1T + Brucite	8.017	13.7
W71-280c	Lizardite 1T + Brucite	7.526	44.9
Reeves			
W70-410	Antigorite	7.349	98.4
W70-415	Olivine + very minor Antigorite + Lizardite	5.302	229.3
W70-417	Antigorite	3.868	374.8

serpentinization where it was still preserved. Attention was given where possible to choose representative samples from different textural zones as well.

Samples were crushed and sieved to -70 mesh. Mineral separates were obtained by free fall magnetic separation for magnetite, and by heavy liquids for the separation of the serpentine fraction. Olivine and pyroxene separates will be prepared at a later date. The light serpentine fraction was examined by Guinier X-ray camera for species identification and purity (Table 138.1).

Oxygen was liberated by reaction of serpentines with BrF_5 at 650°C overnight, using the technique described by Clayton and Mayeda (1963). The released oxygen was converted to CO_2 and analyzed on a Micromass 602D mass spectrometer at McMaster University. The results are given in δ notation in parts per mil, relative to SMOW, where:

$$\delta^{18}O_{\text{sample}} = \left[\frac{(^{18}O : {}^{16}O)_{\text{sample}}}{(^{18}O : {}^{16}O)_{\text{std}}} - 1\right] \times 1000$$

- NBS #28 was used for calibration, giving ^{18}O = +9.58 with a precision of ±0.3.

Water was liberated from the serpentine separates for later analysis of hydrogen isotopes. Samples were degassed at 200°C for up to 2 hours, then heated at 750°C for 2 hours. The structural water obtained was then frozen out in dry ice and sealed in glass tubes.

Boron concentrations were determined using prompt-gamma neutron activation analysis at the McMaster University nuclear reactor. Details of the analytical method are given in Higgins *et al.* (1984a).

RESULTS

OXYGEN ISOTOPES

The $\delta^{18}O$ values obtained show a wide variation, from +3.7 to +8.8 (Figure 138.1). The rocks that have undergone a single retrograde serpentinization have a narrower range, +3.7 to +6.3, than rocks that have undergone later prograde serpentinization, +3.9 to +8.8. The second group has a concentration of samples at the higher end of the scale. Rocks that show evidence of both serpentinization events have isotope ratios midway between these groups. Generally, late stage veins are richer in ^{18}O than the host rocks, indicating a higher water/rock ratio in the vein, or declining temperature with time (Wenner and Taylor 1973). The above results are in good agreement with published analyses.

The range of $^{18}O/^{16}O$ ratios for unaltered komatiites has been found, by Beaty and Taylor (1982) and Hoefs and Binns (1978), to be the same as present day fresh ultramafic rocks, that is, $\delta^{18}O$ = +5 to +6. The least altered rock from the present study shows a $\delta^{18}O$ value of +5.3, remarkably similar

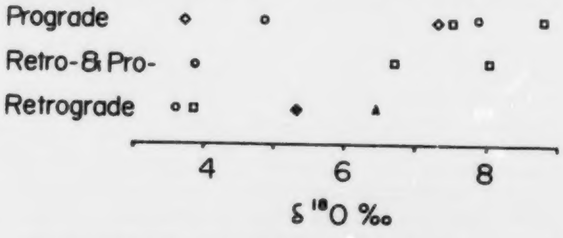

***Figure 138.1** Plot of $\delta^{18}O$ values of analyzed serpentinites. △ -Alexo, □ -Garrison, ○ -Munro, ◇ -Reeves, ◆ -sample of least altered komatiite.*

to other published values of unaltered ultramafic rocks. This is a composite separate, consisting predominantly of the primary minerals, olivine and pyroxene, with only magnetic minerals removed.

BORON ANALYSIS

Bergeron and Shaw (1984) have shown qualitatively that the boron (B) content of serpentinites has a strong negative correlation with temperature. Bonatti *et al.* (1984) quantified this correlation using whole-rock isotope and B data of bulk ocean dredge serpentinite samples. In this relatively simple system, serpentinization has occurred in a single stage at low temperatures. The B content of the whole rock increases with an increase in $\delta^{18}O$ values, and hence with decreasing temperature.

The present study, carried out on mineral separates, shows no such correlation (Figure 138.2). The data is essentially random. The observed bulk B content is probably a function of variable water/rock ratios as well as temperatures of mineralization. This has been the conclusion of previous work carried out by Higgins *et al.* (1984b) on serpentine and serpentinite samples. Several of the samples examined were from the present study area. Therefore, analysis of bulk samples for B in complex metamorphic terrains, whether whole rock or mineral separates, is meaningless. A number of samples have also been analyzed using alpha-track mapping. This is a technique whereby B abundances may be imaged (Carpenter 1972; Ozoray *et al.*, in preparation). Photos 138.1 and 138.2 show such alpha-track maps, where dark areas are high in B and pale areas are low in B. Magnetite has very low B content, as expected, but serpentine varies widely in B abundance. Veins are usually homogeneous in B content, with late veins having the highest B abundances. This probably reflects the greater affinity of serpentinites for B at lower temperatures. Therefore these alpha-track maps of thin sections may be used to indicate the sequence of mineralization (Higgins *et al.* 1984b). The complex variation in B abundances revealed by this method may be the reason for the lack of correlation between B and $\delta^{18}O$.

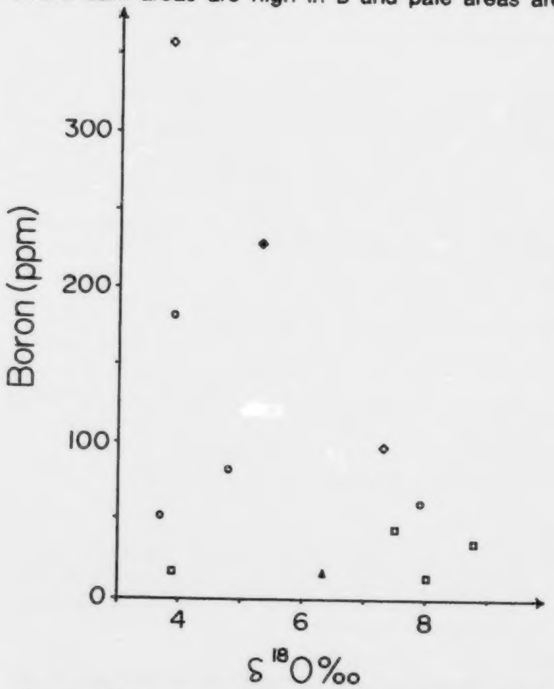

Figure 138.2 Plot of $\delta^{18}O$ against boron. Symbols as in Figure 138.1.

CONCLUSION

The temptation to over interpret data from work only partly completed should be avoided. However, it is clear that the $\delta^{18}O$ values can be correlated with the degree and intensity of alteration. No such correlation exists between B content and the degree of alteration. Boron is very easily mobilized, whereas $\delta^{18}O$ values are not. Hence, in these deposits their complex post metamorphic history is reflected in their variable B content. We hope to get a clearer understanding of these processes when the D/H ratios are obtained. D/H re-equilibration takes place more readily under conditions of falling temperatures than ^{18}O exchange. Partial D/H exchange is thus likely with recent meteoric waters. Another piece of information we hope to glean from δD values is whether the different serpentine textures represent non-equilibrium conditions or equilibrium crystallization under different temperatures.

A further aim of this study is to calculate the isotopic composition of waters that may have been in equilibrium with the serpentine minerals. For this, an accurate estimate of the temperature of serpentinization must be made. This can be based petrographically on mineral associations or based on measured $^{18}O/^{16}O$ fractionation between coexisting serpentine and magnetite (Wenner and Taylor 1971). The latter will be attempted when magnetite $\delta^{18}O$ values are obtained.

$^{18}O/^{16}O$ fractionation is independent of pressure. Assuming constant fluid composition (a reasonable assumption to make, since most of these deposits show evidence of sub-aqueous extrusion or near surface subvolcanic intrusion), with the additional data, we will be able to examine the question of the different amounts of, and types of, recrystallization in the various chrysotile asbestos deposits of the Abitibi greenstone belt of Ontario.

ACKNOWLEDGMENTS

We would like to thank Professor H.P. Schwarcz of McMaster University for the use of the isotope equipment. Boron analyses were obtained at McMaster University nuclear reactor, supported by Natural Sciences and Engineering Research Council (NSERC) grants to Professor D.M. Shaw.

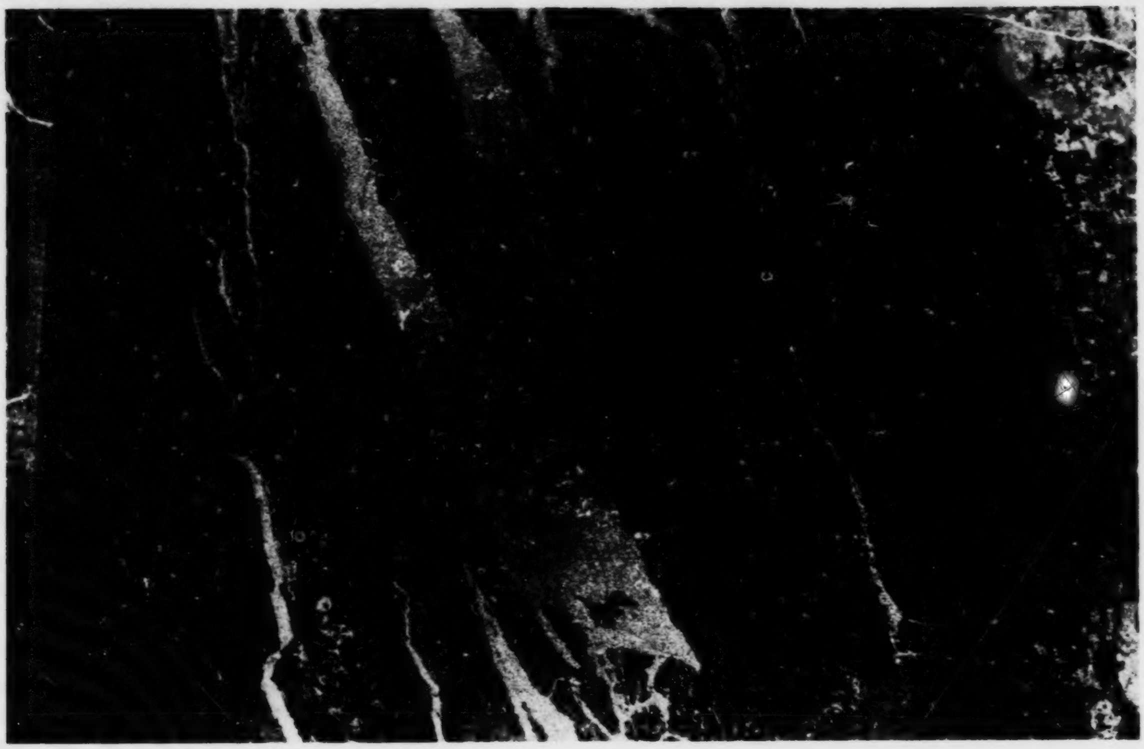

***Photo 138.1** Alpha-track map of serpentinite from Munro. Dark areas show high B abundance. White grains are magnetite. Wide picrolite vein at bottom is richer in B than the cross-fiber chrysotile vein at the top, which is rimmed by a very thin B-rich vein, demonstrating different episodes of formation.*

REFERENCES

Barnes, S.J., Gorton, M.P., and Naldrett, A.J.
1983: A Comparative Study of Olivine and Clinopyroxene Spinifex Flows from Alexo, Abitibi Greenstone Belt, Ontario, Canada; Contributions to Mineralogy and Petrology, Volume 83, p.293-308.

Beaty, D.W., and Taylor, H.P., Jr.
1982: The Oxygen Isotope Geochemistry of Komatiites: Evidence for Water-Rock Interaction; *in* Komatiites, edited by N.T. Arndt and E.G. Nisbet, Allen and Unwin, London.

Bergeron, M., and Shaw, D.M.
1984: The Behaviour of Boron in the Oceanic Lithosphere; GAC-MAC Program with Abstracts, Volume 9, p.46.

Bonatti, E., Laurence, J.R., and Morandi, N.
1984: Serpentinization of Oceanic Peridotites: Temperature Dependence of Mineralogy and Boron Content; Earth and Planetary Science Letters, Volume 70, p.88-94.

Carpenter, B.S.
1972: Determination of Trace Concentrations of Boron and Uranium in Glass by the Nuclear Track Technique; Analytical Chemistry, Volume 44, p.600-602.

Clayton, R.N., and Mayeda, T.K.
1963: The Use of Bromine Pentafluoride in the Extraction of Oxygen from Oxides and Silicates for Isotopic Analysis; Geochimica et Cosmochimica Acta, Volume 27, p.43-52.

Higgins, M.D., Truscott, M.G., Shaw, D.M., Bergeron, M., Buffet, G.H., Copley, J.R.D., and Prestwich, W.V.
1984: Prompt-gamma Neutron Activation Analysis at McMaster Nuclear Reactor; p.690-697 *in* Use and Development of Low and Medium Flux Research Reactors, Proceedings of an International Symposium, edited by O.K. Harling, L. Clark, and P. van der Hardt, Supplement to Volume 44, Atomkernenergie Kerntechnik.

Higgins, M.D., Ozoray, J., and Wicks, F.J.
1984: Boron in Serpentine Minerals; GAC-MAC Program with Abstracts, Volume 9, 73p.

Hoefs, J.
1973: Stable Isotope Geochemistry; Minerals, Rocks and Inorganic Materials and Experimental Studies 9. Subseries: Isotopes in Geochemistry, Springer-Verlag, First Edition.

Hoefs, J., and Binns, R.A.
1978: Oxygen Isotope Composition in Archean Rocks from Western Australia, with Special Reference to Komatiites; United States Geological Survey, Open File Report 78-701, p.180-182.

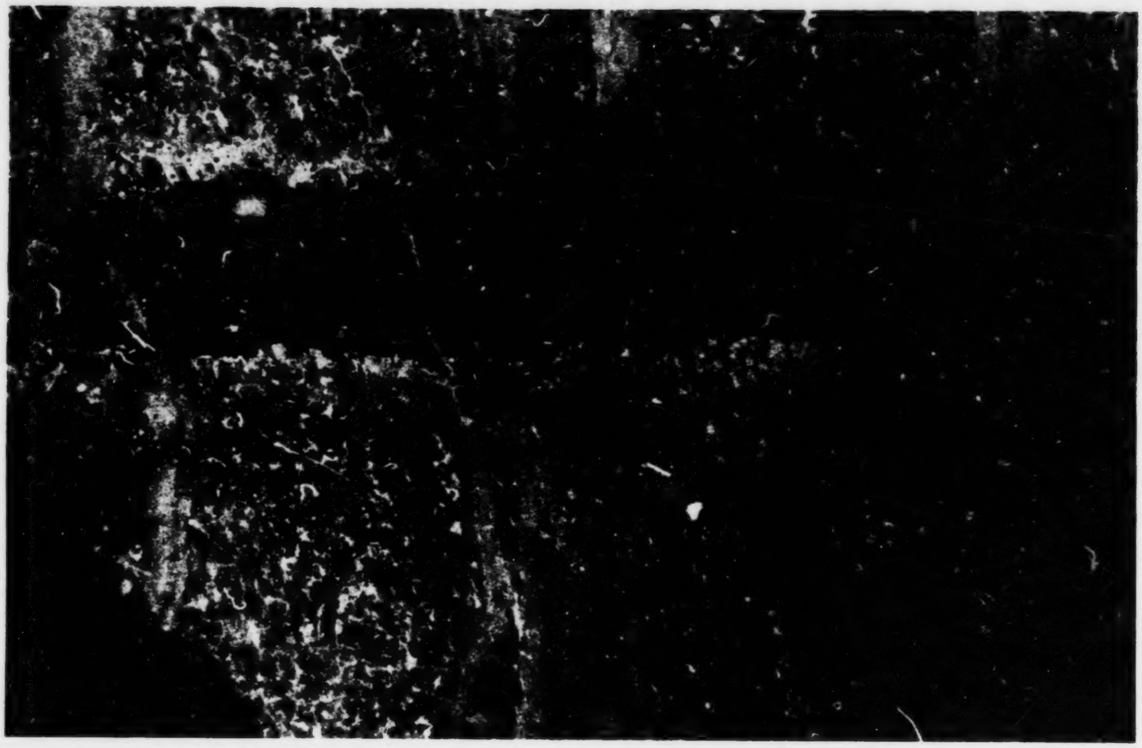

***Photo 138.2** Alpha-track map of serpentinite from Munro, showing complex structure within the cross-fiber chrysotile veins.*

Jolly, W.T.

1982: Progressive Metamorphism of Komatiites and Related Archean Lavas of the Abitibi Area, Canada; *in* Komatiites, edited by N.T. Arndt, and E.G. Nisbet, Allen and Unwin, London.

Ozorary, J., Wicks, F.J., and Higgins, M.D.

In Preparation: Boron Content and Metamorphism of the Cape Smith Foldbelt Serpentinites.

Vos, M.A.

1971: Asbestos in Ontario; Ontario Department of Mines and Northern Affairs, Industrial Mineral Report 36, 69p.

Wenner, D.B., and Taylor, H.P., Jr.

1971: Temperatures of Serpentinization of Ultramafic Rocks Based on $^{18}O/^{16}O$ Fractionation Between Coexisting Serpentine and Magnetite; Contributions to Mineralogy and Petrology, Volume 32, p.165-186.

1973: Oxygen and Hydrogen Isotope Studies of the Serpentinization of Ultramafic Rocks in Oceanic Environments and Continental Ophiolite Complexes; American Journal of Science, Volume 273, p.207-239.

1974: D/H and $^{18}O/^{16}O$ Studies of Serpentinization of Ultramafic Rocks; Geochimica et Cosmochimica Acta, Volume 38, p.1255-1286.

Wicks, F.J., Schandl, E.S., Ozoray, J., and Wan, Pu

1983: Mineralogy and Geochemistry of the Chrysotile Asbestos Deposits of Ontario; Grant 138, p.177-182 *in* Geoscience Research Grant Program, Summary of Research 1982-1983, edited by E.G. Pye, Ontario Geological Survey, Miscellaneous Paper 113, 199p.

Wicks, F.J., Wan, Pu, and Hedjran, K.

1984: Mineralogy and Geochemistry of the Chrysotile Asbestos Deposits of Ontario, Munro Mine and Garrison Deposit; Grant 138, p.99-110 *in* Geoscience Research Grant Program, Summary of Research 1983-1984, edited by V.G. Milne, Ontario Geological Survey, Miscellaneous Paper 121, 252p.

Grant 146 Major and Trace Element and Isotopic Studies at Sudbury—A Model for the Structure and its Ores

Anthony J. Naldrett[1], B.V. Rao[1], Norman M. Evensen[1], and Burkhard O. Dressler[2]

[1]Department of Geology, University of Toronto

[2]Ontario Geological Survey

ABSTRACT

The Sudbury Igneous Complex was intruded 1.85 x 10^9 years ago into the site of a large crater that was itself the result of a catastrophic explosion. The Complex lies at the centre of one of a chain of gravity anomalies. The Sudbury anomaly is interpreted as the consequence of a 4 km thick, subhorizontal, mafic to ultramafic sill lying 5 to 8 km below the present surface and extending well beyond the Complex.

The Main Mass of the Complex consists of a lower zone of norite, overlain by gabbro and granophyre. The Sublayer consists of distinctive, diabasic-textured intrusions that occur intermittently around the perimeter of the Main Mass. All carry inclusions of local country rocks; some also carry inclusions of a suite of ultramafic to mafic cumulates. The ore deposits are associated with only the latter type of Sublayer, which is itself sulphide-rich.

All rocks of the Complex are unusually salic and rich in incompatible elements. The major and trace element contents (including Rare Earths Elements (REE)) can be modelled in terms of a Continental Flood Basalt assimilating typical Archaen tonalite and quartz monzonite (50% for the Main Mass, 25% to 75% for the Sublayer). The Main Mass and South Rim Sublayer have ϵ_{Sr} ϵ_{Nd} values of +60 to +80 and -5 to -9 respectively; North Rim Mineralized Sublayer has similar ϵ_{Nd} but ϵ_{Sr} of from +13 to $+3^4$. Isotopic data thus support crustal contamination. Sublayer to the north is in contact with granulitic gneisses (ϵ_{Sr} = -11 to +11; ϵ_{Nd} = -3 to -11), and the ϵ_{Sr} values appear to reflect contamination by these.

The extensive assimilation of salic material is believed responsible for the segregation of major quantities of sulphide. It is suggested that the Sublayer magmas, sulphides, and inclusions have been derived from a series of hidden intrusions, related to the Complex, that formed at depth (thus accounting for the gravity anomaly), and which were disrupted as magma from lower bodies rose through upper ones to intrude the site of the main Complex.

INTRODUCTION

The Ni-Cu ores of the Sudbury district are associated with the Sudbury Igneous Complex (SIC), a layered intrusion ranging from quartz norite at the base, through gabbro, to a granophyric cap. The purpose of this paper is to describe the geological setting at Sudbury, present new data relating to the composition of the Complex and the rocks within which it is emplaced, show how the composition can account for the profusion of concentrations of magmatic sulphide ore, and propose a model to account for the geology of the Complex and some aspects of its setting.

REGIONAL GEOLOGICAL SETTING

The Complex is located at the contact between tonalitic gneisses and intrusive quartz monzonites all of Archean age to the north, and rocks of the Proterozoic Southern Province, which overlie the Archean basement unconformably and thicken to the south. The gneisses were subjected to amphibolite to granulite facies metamorphism and extend around much of the northern and western margins of the Complex (Figure 146.1). The Proterozoic rocks belong to the Huronian Supergroup; in the Sudbury area; they consist of local accumulations of mafic and felsic volcanic rocks, overlain by greywackes, conglomerates, siltstones, and arenites. Where clastic units occur at the base of the Huronian, they may contain high concentrations of detrital U- and Th-rich minerals. These reach their maximum developement 100 km to the west of Sudbury in the uranium ores of the Elliot Lake area.

Card *et al.* (1984) have drawn attention to a dominant linear gravity anomaly extending 350 km from Elliot Lake eastward to Englehart. The Sudbury Igneous Complex straddles this feature and coincides with one of 3 highpoints along it (Figure 146.1). Gupta *et al.* (1984) have analyzed the combined residual gravity and magnetic anomaly that marks the Sudbury region itself. After subtracting large-scale "super regional" gravity trends, they conclude that the broad +20 to +30 mGal anomaly at Sudbury cannot be explained by the rocks of the Complex itself. Their modelling indicates that a large (60 by 40 km) mass of mafic rock, with a density similar to gabbro or gabbro-anorthosite (3.02 ± 0.03 g/cc) underlies the Complex at a depth of at least 5 km, and extends beyond it, as is indicated in Figure 146.2. Their analysis of the regional magnetic data indicates that this can be explained if some of the rocks of this body are partially serpentinized.

LOCAL GEOLOGICAL SETTING

The SIC has intruded beneath the Onaping Formation of the Whitewater Group (Figure 146.3), a breccia composed of fragments of country rocks and recrystallized glassy material set in a matrix of glassy shards, and variably interpreted as an ignimbrite or the "fall-back" breccia resulting from the impact of a meteorite. The SIC and strata of the Whitewater Group overlying it are exposed as a series of concentric, crudely elliptical rings and dip towards the centre, giving rise to the interpretation of the structure as a basin.

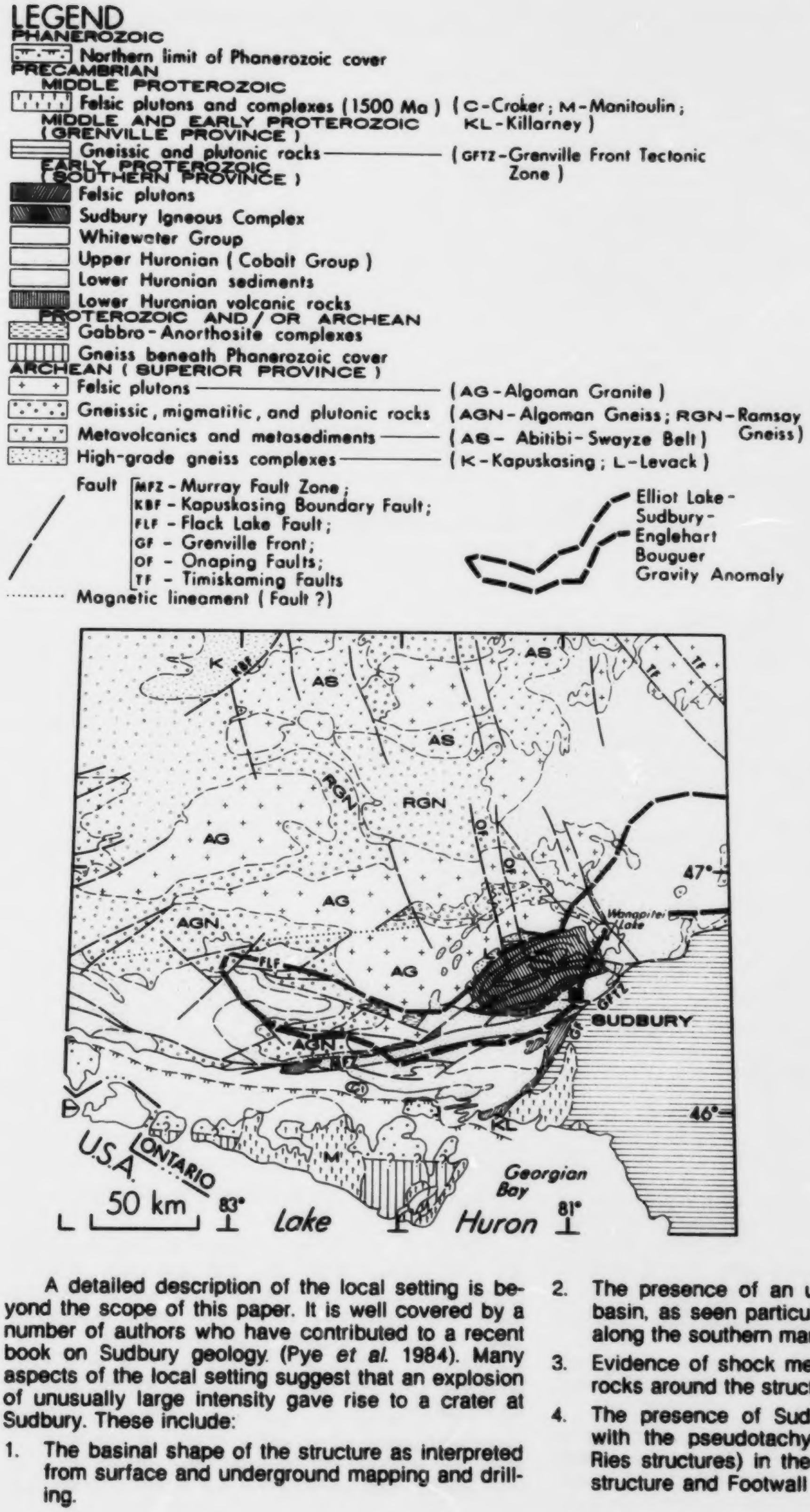
LEGEND
PHANEROZOIC
Northern limit of Phanerozoic cover
PRECAMBRIAN
MIDDLE PROTEROZOIC
Felsic plutons and complexes (1500 Ma) (C-Croker; M-Manitoulin; KL-Killarney)
MIDDLE AND EARLY PROTEROZOIC (GRENVILLE PROVINCE)
Gneissic and plutonic rocks (GFTZ-Grenville Front Tectonic Zone)
EARLY PROTEROZOIC (SOUTHERN PROVINCE)
Felsic plutons
Sudbury Igneous Complex
Whitewater Group
Upper Huronian (Cobalt Group)
Lower Huronian sediments
Lower Huronian volcanic rocks
PROTEROZOIC AND / OR ARCHEAN
Gabbro-Anorthosite complexes
Gneiss beneath Phanerozoic cover
ARCHEAN (SUPERIOR PROVINCE)
Felsic plutons (AG-Algoman Granite)
Gneissic, migmatitic, and plutonic rocks (AGN-Algoman Gneiss; RGN-Ramsay Gneiss)
Metavolcanics and metasediments (AS- Abitibi-Swayze Belt)
High-grade gneiss complexes (K-Kapuskasing; L-Levack)
Fault
MFZ - Murray Fault Zone;
KBF - Kapuskasing Boundary Fault;
FLF - Flack Lake Fault;
GF - Grenville Front;
OF - Onaping Faults;
TF - Timiskaming Faults
Magnetic lineament (Fault ?)
Elliot Lake - Sudbury - Englehart Bouguer Gravity Anomaly
K
KBF
AS
AS
AS
TF
TF
RGN
RGN
AG
AG
AG
AGN.
AGN
OF
OF
47°
Wanapitei Lake
FLF
GFTZ
SUDBURY
MFZ
GF
C
KL
M
46°
U.S.A.
ONTARIO
50 km
83°
Lake Huron
81°
Georgian Bay

Figure 146.1. Regional geological map in the vicinity of Sudbury. The Elliot Lake-Englehart regional gravity anomaly is shown by the stippling (after Card et al. 1984).

A detailed description of the local setting is beyond the scope of this paper. It is well covered by a number of authors who have contributed to a recent book on Sudbury geology. (Pye *et al.* 1984). Many aspects of the local setting suggest that an explosion of unusually large intensity gave rise to a crater at Sudbury. These include:

1. The basinal shape of the structure as interpreted from surface and underground mapping and drilling.
2. The presence of an upturned collar around the basin, as seen particularly in the Huronian rocks along the southern margin (Dressler 1984).
3. Evidence of shock metamorphism in the country rocks around the structure (Dressler 1984).
4. The presence of Sudbury Breccia (comparable with the pseudotachylite of the Vredefort and Ries structures) in the country rocks around the structure and Footwall Breccia beneath the Com-

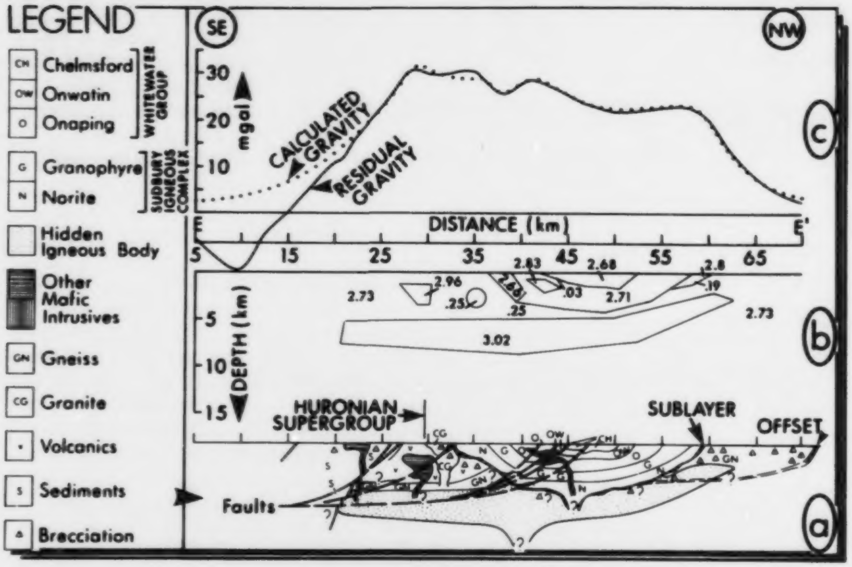
LEGEND
CH Chelmsford
OW Onwatin
O Onaping
WHITEWATER GROUP
G Granophyre
N Norite
SUDBURY IGNEOUS COMPLEX
Hidden Igneous Body
Other Mafic Intrusives
GN Gneiss
CG Granite
Volcanics
S Sediments
Brecciation
SE
NW
30
20
10
mgal
CALCULATED GRAVITY
RESIDUAL GRAVITY
c
E
DISTANCE (km)
E'
5
15
25
35
45
55
65
2.83
2.68
2.8
2.96
2.73
.25
.03
2.71
.19
2.73
3.02
5
10
15
DEPTH (km)
b
HURONIAN SUPERGROUP
SUBLAYER
OFFSET
Faults
a

Figure 146.2. A northwest-southeast section across the Sudbury District, showing the residual and calculated gravity profiles, a 2-dimensional reconstruction of the model used to calculate the gravity profile, and a geological interpretation consistent with the reconstruction (after Gupta et al. 1984).

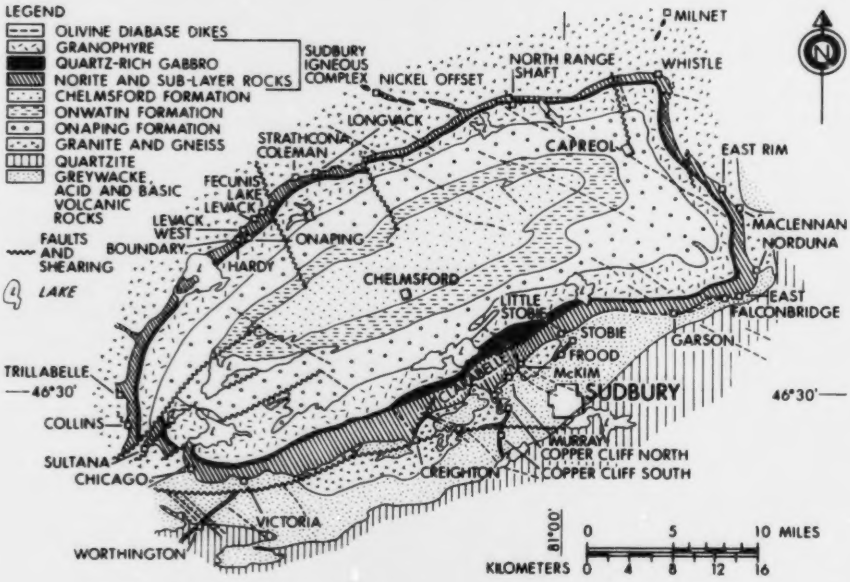
LEGEND
OLIVINE DIABASE DIKES
GRANOPHYRE
QUARTZ-RICH GABBRO
NORITE AND SUB-LAYER ROCKS
SUDBURY IGNEOUS COMPLEX
CHELMSFORD FORMATION
ONWATIN FORMATION
ONAPING FORMATION
GRANITE AND GNEISS
QUARTZITE
GREYWACKE, ACID AND BASIC VOLCANIC ROCKS
FAULTS AND SHEARING
LAKE
MILNET
NORTH RANGE SHAFT
WHISTLE
NICKEL OFFSET
LONGVACK
STRATHCONA COLEMAN
CAPREOL
EAST RIM
FECUNIS LAKE
LEVACK
LEVACK WEST
BOUNDARY
ONAPING
HARDY
MACLENNAN
NORDUNA
CHELMSFORD
LITTLE STOBIE
EAST FALCONBRIDGE
GARSON
STOBIE
FROOD
McKIM
SUDBURY
TRILLABELLE
46°30'
46°30'
COLLINS
SULTANA
CHICAGO
CLARABELLE
MURRAY
COPPER CLIFF NORTH
COPPER CLIFF SOUTH
CREIGHTON
VICTORIA
WORTHINGTON
81°00'
0
5
10 MILES
KILOMETERS
0
4
8
12
16
N

Figure 146.3. Geological map of the Sudbury Structure.

plex. Sudbury Breccia occurs as irregular masses and also as dikes that are radial and concentric to the structure. It occurs intermittently as much as 50 km away from the structure; a zone in which the breccia is common extends from 20 to 25 km north of the northern perimeter (Dressler 1984).

5. Evidence of shock metamorphism in country rock inclusions in the Onaping Formation (Muir and Peredery 1984).
6. The 1800 m of Onaping Formation itself, part of which is variably interpreted as a meteorite fallback breccia or a pyroclastic flow (Peredery and Morrison 1984; Muir 1984).

Opinions are divided between an extra-terrestrial and endogenic origin for the structure. Naldrett (1984) concluded that meteorite impact is the more likely origin, primarily because so many of the features observed at Sudbury are also found at known impact sites. There are, however, many difficulties with such an origin and these are summarized by Muir (1984).

PETROLOGY OF THE SUDBURY IGNEOUS COMPLEX

The main units of the Complex include (i) the Sublayer, (ii) the marginal Quartz-rich Norite of the South Range and Mafic Norite of the North Range, (iii) the South Range Norite and Felsic Norite, (iv) the Quartz Gabbro, and (v) the Granophyre and Plagioclase-rich Granophyre. All except the Sublayer are included within the Main Mass of the Complex.

MAIN MASS

The marginal unit of the Main Mass on the South Range is the Quartz-rich Norite. In this, the quartz content increases progressively towards the contact over the outer 300 m (Naldrett *et al.* 1970). This is unlikely to be due to contamination since the increase in quartz occurs as much where the footwall is composed of SiO_2-deficient greenstone as it does where it is composed of granite. This indicates that if contamination is involved, it is not *in situ*. The increase in quartz is accompanied by an equally progressive decrease in the average Mg/(Mg + Fe) ratio of the pyroxenes (Naldrett *et al.* 1970). This decrease is due to the pyroxenes becoming progressively more strongly zoned, with Mg/(Mg + Fe) decreasing towards the edges of grains while the cores retain a constant composition. These observations, coupled with a decrease in grain size towards the margins (Naldrett *et al.* 1970), indicate that the outer part of the Quartz-rich Norite is a non-cumulate rock that crystallized essentially *in situ*.

SUBLAYER

The Sublayer occurs discontinuously around the Complex. It can be divided logically into those variants which occur close to the outer contact and those which occupy dikes (known locally as offsets) that either radiate outwards from or are concentric to the Complex.

The Contact Sublayer consists of a suite of fine- to medium-grained norites and gabbros that can be distinguished from the Main Mass Felsic Norite and Quartz Gabbro by their lower quartz content in relation to pyroxene (Naldrett *et al.* 1972). Sublayer rocks occurring within the offsets generally have the composition of quartz diorite and are referred to as such. Some of the Sublayer has a high (> 5 modal percent) sulphide content and, in many cases, has deposits of Ni-Cu sulphide associated with it; this is referred to here as Mineralized Sublayer. Other Sublayer has a lower sulphide content and no associated orebodies. The sulphide content of the Mineralized Sublayer is greater than that which can be dissolved in basaltic magma (maximum approximately 1 wt. % sulphide). This Sublayer has therefore been enriched in sulphide at some stage before it reached its present position.

Geological relationships between the Sublayer and the Main Mass that bear on the relative ages of the two are conflicting. Inclusions of marginal, Quartz-rich Norite have been observed in the Sublayer and inclusions of Sublayer have been observed in norite of the Main Mass of the Complex. Contacts are never marked by fine-grained chill zones, suggesting that whichever was the older at any particular location, it was still warm at the time of intrusion of the younger. On the North Range, the distinction between Main Mass and Sublayer is always clear with the Sublayer having the finer grain size and lower quartz content. This is not always the case on the South Range, where a number of researchers have commented on gradations that are visible between the two (Slaught 1951; Cochrane 1984). It would seem, therefore, that the introduction of the Sublayer and Main Mass was a complicated process with one preceding the other and *vice versa* in different localities.

In some areas the Sublayer is characterized by inclusions. These can be divided into 2 groups, those of obviously local derivation, and those composed of mafic and ultramafic rocks, few of which outcrop in the Sudbury area. Scribbins *et al.* (1984) have described the latter group as ranging from peridotite, through clino- and orthopyroxenites, to olivine gabbro and norite. Most of this group of inclusions display either cataclastic or cumulate textures. Olivine within them ranges in composition from Fo_{86} to Fo_{72}, with the Fo content decreasing with plagioclase content. Scribbins *et al.* (1984) conclude that the inclusions are derived from layered intrusions that have fractionated at moderate depths in the crust.

MAJOR AND TRACE ELEMENT GEOCHEMISTRY

The average compositions of the Quartz-rich Norite, Mineralized Sublayer from Levack West, Strathcona and Little Stobie, and North and South Range Unmineralized Sublayer are given in Table 146.1.

MAJOR ELEMENTS

Since the SIC is a tholeiitic body emplaced into a cratonic environment, it is reasonable to compare it chemically with continental flood basalts (CFB). Naldrett (1984) pointed out that, judging from field and petrographic criteria, the Quartz-rich Norite is likely to be the rock type closest in composition to that of the magma giving rise to the Complex as it was emplaced along the South Range. He compared it on the basis of MgNo [MgO/(MgO + FeO) atomic ratio] to a series of Keweenawan and Columbia River flood basalts and showed it to be significantly richer in SiO_2 (SIC = 57; CFB = 49 wt.% SiO_2) and K_2O (SIC = 1.5; CFB = 0.249 wt.% K_2O) and poorer in CaO (SIC = 7; CFB = 11 wt.% CaO) and Na_2O/K_2O (SIC = 1.8; CFB = 6 to 12). In Table 146.2 it is shown that the result of mixing relatively unfractionated CFB (the average of 5 Keweenawan olivine tholeiitic basalts KEW, reported by the Basaltic Volcanism Project, 1981) with 45% of a 1:2 mixture respectively of quartz monzonite and tonalitic gneiss (QMT), which are the 2 principal rock types in the basement beneath the Complex and the Huronian, gives rise to a composition that is very similar to that of the Quartz-rich Norite (model QRN).

The SiO_2, K_2O, and CaO contents and Na_2O/K_2O of Mineralized and Unmineralized Sublayer are compared on the basis of MgNo in Figure 146.4 with the same CFB analyses as used by Naldrett (1984). Considering Unmineralized Sublayer, this is also distinct-

TABLE 146.1. AVERAGE COMPOSITIONS OF TYPICAL ROCKS OF THE SIC

Main Mass		Mineralized Sublayer			Unmineralized Sublayer	
	QRN	Lev. W.	Strath.	Litt. Stobie	North Range	South Range
SiO_2	57.0	54.9	54.23	56.0	58.74	57.43
TiO_2	1.34	0.55	0.44	0.60	1.01	0.99
Al_2O_3	16.4	14.80	11.91	17.19	14.63	15.93
FeO_T	7.33	9.15	10.71	8.96	9.51	9.13
MnO	0.13	0.15	0.18	0.12	0.15	0.13
MgO	6.40	7.97	11.81	4.72	5.08	5.28
CaO	7.28	7.93	7.92	7.26	5.96	6.48
Na_2O	2.41	2.77	2.01	2.88	2.83	2.95
K_2O	1.55	0.90	0.72	1.08	2.03	1.67
Trace Elements in ppm						
Ba	492	453	287	582	800	638
Pb	46	22	21	39.5	54	61
Th	5.5	2.4	1.647	5.8	4.3	3.8
K	14600	7500		9000	16900	14000
Ta	0.43	0.25	0.12	0.56	0.31	0.46
Sr	422	447	367	409	419	402
P	870	870		1050		
Zr	96	74	60	82	134	134
Hf	2.6	1.6	1.77	1.99	3.4	3.32
Ti	2880	3300		3600	6050	5930
Y	16	13	12	19	19	23.4
La	21.3	16.2	17.7	24.7	32.4	19.5
Ce	44.7	33.9	33.3	54.1	73.8	71.5
Nd	17.4	15.8	10.9	22.0	28.6	28.7
Sm	3.36	3.07	2.60	4.39	5.49	5.32
Eu	1.02	0.81	0.84	1.27	1.57	1.58
Tb	0.42	0.41	0.37	0.78	0.64	0.73
Yb	1.51	1.14	1.29	1.87	1.8	2.26

ly richer in SiO_2 and K_2O and lower in CaO and Na_2O/K_2O than CFB. There is relatively little difference between the North and South Range samples. With the exception of 1 sample with very high MgNo, the Mineralized Sublayer spans a similar range in MgNo and has a similar CaO content to the Unmineralized. However, the SiO_2 and K_2O contents of the Mineralized are distinctly lower and the Na_2O/K_2O distinctly higher than those of the Unmineralized Sublayer. There is no systematic variation within either group between these elements and MgNo. On the other hand, it can be seen from Figure 146.5 that SiO_2 is correlated positively with K_2O and negatively with CaO.

TRACE ELEMENTS

A spectrum of incompatible trace elements representing different units of the SIC are illustrated on a "spidergram" (constructed after Thompson 1982) in Figure 146.6. A number of distinctive characteristics are apparent:

1. All rocks are characterized by enrichment at the Ba end of the spectrum, and by Ta and Ti depletion.
2. The North Range Mineralized Sublayer is distinctly lower in Ba, Rb, and Th than other rock types. It shows a weak to distinct negative Th anomaly.
3. The South Range Mineralized Sublayer is similar to that of the North Range, except that it is higher in Ba, Rb, and Th and shows a positive Th anomaly. It also shows a weak negative Sr anomaly.
4. The unmineralized Sublayer is distinctly richer in trace elements ranging in the spectrum from La to Yb than the other rock units and shows pronounced negative Th and Sr anomalies.

Representative REE diagrams for different units of the Complex are illustrated in Figure 146.7. Slopes for all units are similar despite variation in the absolute levels of the REE. The Sublayer and Quartz-rich Norite show no Eu anomalies while the Felsic Norite is marked by a positive and the Granophyre by a negative Eu anomaly. Patterns for ultramafic inclusions from the Sublayer show the same steep slopes as other units of the Complex.

DISCUSSION

The lack of correlation shown in Figure 146.4 between MgNo and SiO_2, K_2O, and CaO indicates that fractionation is not directly responsible for the wide variation in the concentration of these oxides. The

TABLE 146.2. STARTING COMPOSITIONS AND END PRODUCTS OF MIXING MODELS.

	KEW	QMT	McK	LG	Model QRN	Model NR Min Sub	Model SR Min Sub	Model Unmin Sub
Ba	55	878	600	-	467	-	-	-
Rb	7.3	121	124^1	8	64	26.5	53.6	64.8
Th	0.54	11^3	14.6	0.2	5.77	2.17	5.44	6.59
K	2490	27100	23000	8100	14800	8550	11500	15300
Ta	0.267	0.4^3	1.20	0.17	0.3334	0.257	0.48	0.509
Sr	275	554	100	585	415	425	296	379
P	480	1300^2	-	990	890	790	-	-
Zr	69	193^3	109	147	131	116	102	130
Hf	1.5	4.9^3	3.7	2.83	3.2	2.51	2.62	3.23
Ti	5280	2580	4500	3420	3930	4210	4580	3950
Y	-	-	21.2	3.25	-	-	-	-
La	5.13	32	50.6	18.3	18.6	34.0	19.6	26.5
Ce	11.7	68	108	50.5	39.9	42.5	42.2	59.6
Nd	9.45	28.8	40.8	11.6	19.1	13.4	19.6	22.7
Sm	2.11	5.06	7.6	2.18	3.59	2.63	3.80	4.24
Tb	0.54	0.617	0.75	0.23	0.579	0.45	0.598	0.445
Yb	1.50	0.97	1.92	0.53	1.24	1.09	1.48	1.23

Data are as follows:

KEW Basaltic Volcanism Project (1981)
QMT Arth and Hanson (1975)
McK P. Fralick, Lakehead University, Thunder Bay, personal communication (1984)
LG This study - Except as indicated
1. From Sr coupled with Sr/Rb ratio of Fairbairn *et al.* (1969)
2. Sims *et al.* (1984)
3. Figure for Laxfordian gneiss (Wood 1980)

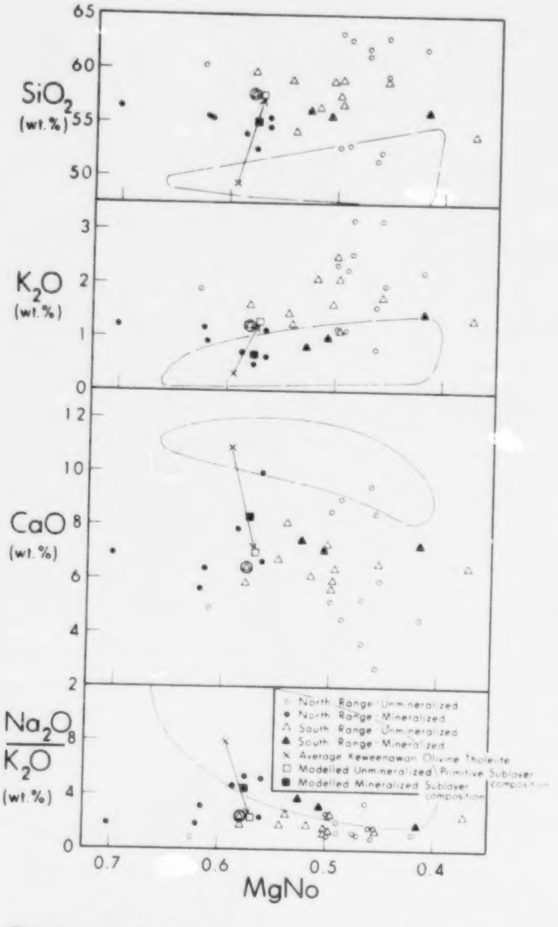

Figure 146.4. *Comparison of some major element concentrations in the Sublayer with those in typical continental flood basalts. Sample BVR 12 (referred to in text) is circled. Composition of KEW is shown by the start of the arrow; the model composition of BVR 12 by the cross at the end of the arrow. The model composition of the average North Range Mineralized Sublayer is shown by the solid square.*

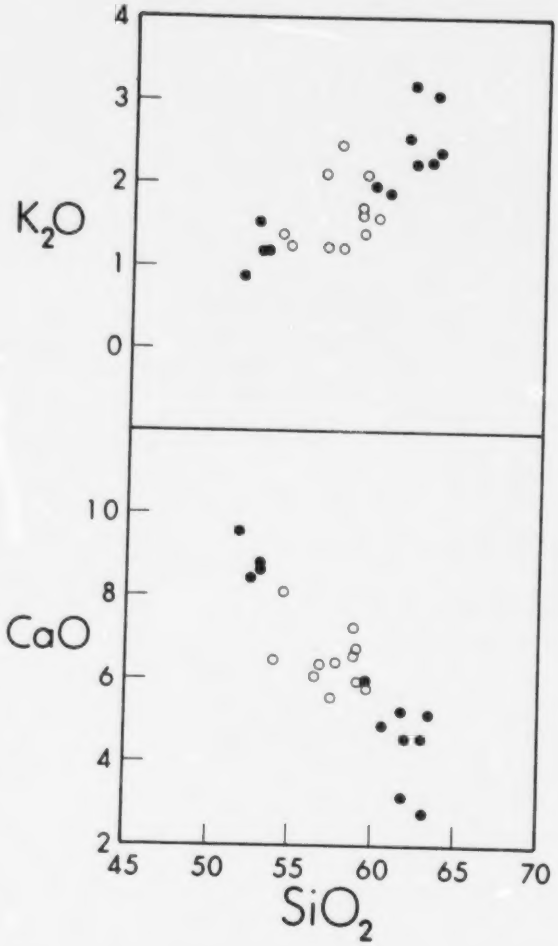

Figure 146.5. *Variation of K_2O and CaO with SiO_2 for samples of Mineralized and Unmineralized Sublayer.*

unusual major element composition of the SIC has long been explained as the consequence of contamination (Irvine 1975; Naldrett and Macdonald 1980). Kuo and Crocket (1979) interpreted the enrichment in LREE exhibited by all rocks at Sudbury to the same cause.

In Figure 146.4, an attempt has been made to model one of the most primitive of the Unmineralized Sublayer samples (BVR 12, circled in Figure 146.4) as the consequence of the mixing of the average of 5 Keweenawan olivine tholeiites (point at start of arrow in Figure 146.4) with 50 wt. % of the same 1:2 mixture of quartz monzonite and tonalite (referred to henceforth as QMT) as used for the Quartz-rich Norite. The result (shown by the cross at the end of the arrow) is close to BVR 12.

The correlation shown between SiO_2 and each of K_2O and CaO in Figure 146.5 is consistent with the premise that the variation shown by these oxides is the result of a variable degree of mixing of basaltic magma with a contaminant rich in SiO_2 and K_2O and poor in CaO. The range in MgNos shown by the rocks indicates that the magma has undergone fractional crystallization. Much of the contamination may have accompanied this fractionation, although, as pointed out above, the evidence of the major elements is against the degree of assimilation having been directly proportional to the degree of fractionation.

Figure 146.8 illustrates the trace element contents of some of the possible contaminants. An average upper crustal contaminant in the vicinity of Sudbury is taken to be QMT. In this, while the major element composition is based on rocks collected at Sudbury, the trace element concentrations are those of Arth and Hanson (1975) for rocks in Minnesota with the same major element compositions as those at Sudbury, coupled, for elements for which Arth and

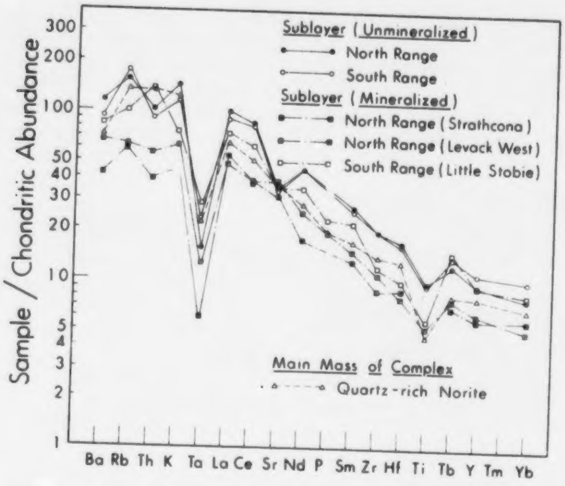

Figure 146.6. *"Spidergram" showing trace element concentrations in selected units of the Sudbury Igneous Complex. The elements are normalized by their chondritic abundances, except for K and Ti. Abundances used for the normalization in this and succeeding similar diagrams are (in ppm): Ba, 6.9; Rb, 0.35; Th, 0.042; K, 120; Ta, 0.02; La, 0.328; Ce, 0.815; Sr, 11.8; Nd, 0.63; P, 46; Sm, 0.203; Zr, 6.84; Hf, 0.2; Ti, 620; Tb, 0.052; Y, 2; Tm, 0.034; Yb, 0.22 (values from Thompson 1982).*

Hanson had no data, with data from Wood (1980) on the upper crustal Laxfordian amphibolite. The similarity between the REE profile of QMT and Shaw's *et al.* (1976) profile for the average Canadian Shield is illustrated in Figure 146.9; this is supportive of the use of QMT as a facsimile for the upper crust. As outlined above, granulite and amphibolite facies gneisses (Levack Gneiss) form the immediate Footwall to the Complex along the North Range and are a possible contaminant for the rocks emplaced there. McKim Formation pelites are common rocks south of the SIC and are a possible contaminant there. Data for the average of 5 Keweenawan olivine tholeiites are again used as a starting point from which to model the effect of contamination in reproducing the composition of the SIC.

Points worthy of note in Figure 146.8 are the low Rb and Th of the Levack Gneisses, which is a characteristic of most lower crustal granulites; the high Ba, Rb, Th, and K and negative Ta and Ti anomalies of both QMT and the McKim pelite; and the marked negative Sr anomaly of the McKim. This last characteristic is also present in the Matinenda arenite which underlies the McKim in the Elliot Lake area (P. Fralick, Lakehead University, Thunder Bay, personal communication, 1984). The negative Ta and Ti anomalies are a well established feature for continental shields and also for many volcanic rocks developed within island arcs (Nakamura *et al.* 1985). The reason for them is not understood.

The relatively high concentration of Rb and Th in all rocks of the SIC indicate that the Levack Gneiss alone cannot account for the contamination of even the immediately adjacent North Range Mineralized Sublayer. However, contaminating the Keweenawan basalt (KEW) with 50% of a 2:1 mixture of Levack Gneiss and QMT produces a reasonable match for the average trace element profile of the North Range Mineralized Sublayer, including the negative Th anomaly (Figure 146.10). The Zr and Hf contents of the model composition appear to be somewhat high, perhaps due to their being compatible in some minerals common in felsic rocks and thus difficult to judge when making estimates of the composition of mega sections of the crust. The major element composition of this mixture is also represented in Figure 146.4, in which it is seen to fall near the centre of the points representing the North Range Mineralized Sublayer.

The higher Rb and Th and slight negative Sr anomaly of the South Range Mineralized Sublayer can be explained as the consequence of contaminating KEW with 40% of a 1:1 mixture of McKim pelite and QMT (Figure 146.11). The positive Th anomaly present in the South Range Mineralized Sublayer is not reproduced by this model composition, but, as discussed above, the basal Huronian is characterized by localized concentrations of U and Th-bearing minerals, and assimilation of a small amount of this material would cause a very marked increase in the Th content of a magma.

The Quartz-rich Norite, representing the Main Mass of the SIC, has high Ba, Rb, Th, and K and can be modelled well (Figure 146.12) as the consequence of contaminating KEW with the same proportion of QMT as used to model the major elements (45%), except for the ubiquitous high Zr and Hf of the model curve.

In Figure 146.13, it is seen that the Unmineralized Sublayer, with its overall high concentrations of incompatible trace elements yet relatively (in comparison with other SIC units) low Rb/La ratio, and marked negative Sr anomaly, is best modelled as the consequence of mixing equal proportions of KEW, QMT, Levack Gneiss, and McKim pelite. The modelling attempted here for the trace elements differs from that for the major elements, in that, for the latter, one of the more primitive samples was modelled, while, for the former, modelling is attempted for the averages of the North and South Ranges. The similarity in the major and trace element contents of both the North and South Range representatives of this unit lends no support to models involving localized contamination, but is suggestive that this magma type had access to both sides of the Complex.

The Th-Hf-Ta diagram (Figure 146.14) illustrates some of the mechanisms discussed above from a different perspective. The model proposed for the North Range Mineralized Sublayer involves contamination of 75% of KEW with 25% of QMT to give composition 1, coupled with contamination of this with 33% of Levack Gneiss (LG) to give composition 2. That for the South Range Mineralized Sublayer involves contamination of KEW also with 25% QMT (composition 1) followed by contamination of this with 20% of McKim pelite (McK) to give composition 2. Small inaccuracies in the compositions of the start-

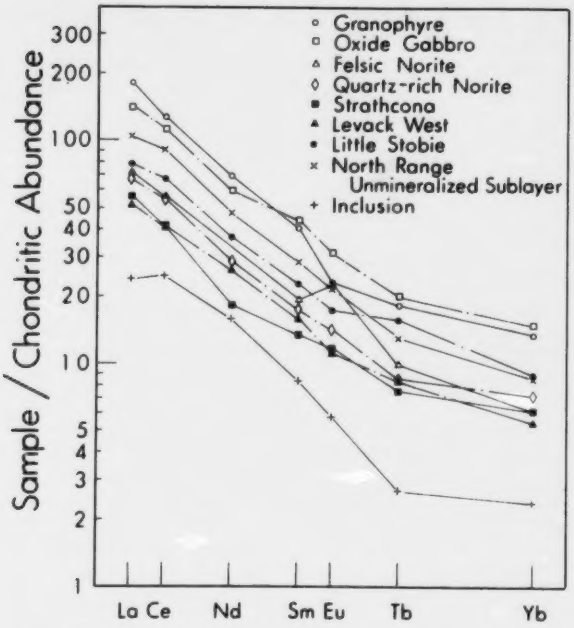

Figure 146.7. *REE chondrite normalized diagram for selected units of the Sudbury Igneous Complex, including one sample of ultramafic inclusions from the Strathcona Deposit.*

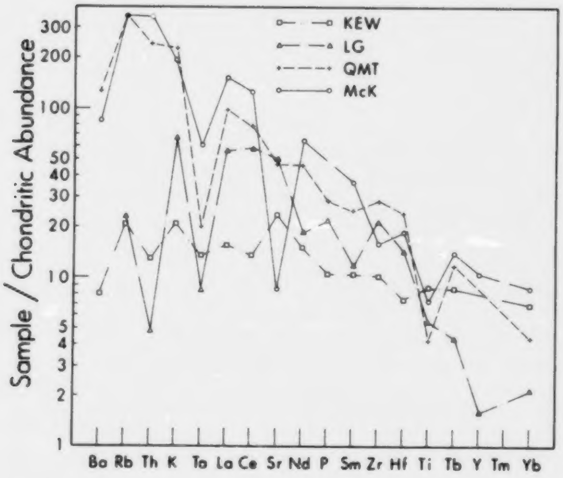

Figure 146.8. *Trace element variation in some possible contaminants for the Sudbury Igneous Complex. See legend for Figure 146.6 for further explanation.*

ing point or contaminants may be the cause of the less than perfect match between the modelled and actual compositions on this diagram. The diagram nevertheless illustrates the principle by which contamination by the country rocks can account for the difference in compositions of the North and South Range Mineralized Sublayer, the North Range rocks being deflected towards Hf through assimilation of Levack Gneiss, and the South Range rocks away from Hf through assimilation of McKim and other Th-rich material. The model composition for the Quartz-rich Norite, involving a 1:1 mix of KEW and QMT, also plots close to the actual position for this rock type.

SUMMARY OF CONCLUSIONS

1. Rocks of the SIC are highly contaminated, major and trace element modelling indicating that 33% to 75% contamination is involved.
2. The Main Mass of the Complex appears to have been contaminated largely by typical upper crustal rocks.
3. The Mineralized Sublayer has also been affected by typical upper crustal contamination, but a component of more localized contamination appears to be present as well. The North Range Mineralized Sublayer bears evidence of contamination by the lower crustal granulites which form the Footwall rocks immediately along the North Range. Contamination with a component from the McKim Formation can account for some of the characteristics of the South Range Mineralized Sublayer.
4. The Unmineralized Sublayer has an almost identical profile on both the North and South Ranges, which can be modelled as the consequence of contamination by a mixture of many of the country rocks at Sudbury.

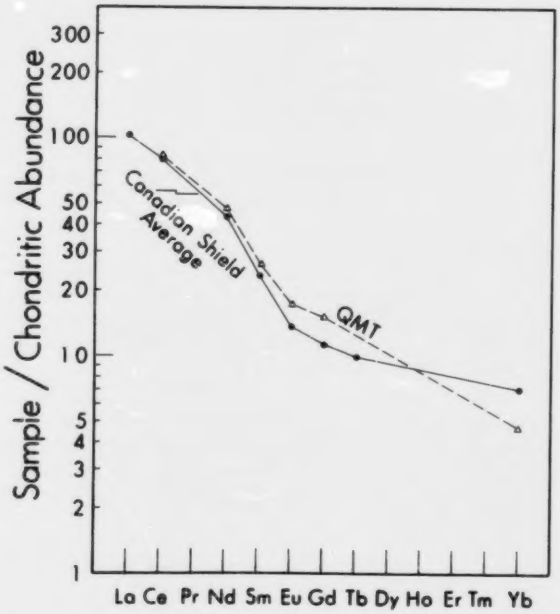

Figure 146.9. *REE data for the Quartz Monzonite-Tonalite mixture (QMT) used as a contaminant compared with Shaw's et al. (1976) data for the "average" Canadian Shield.*

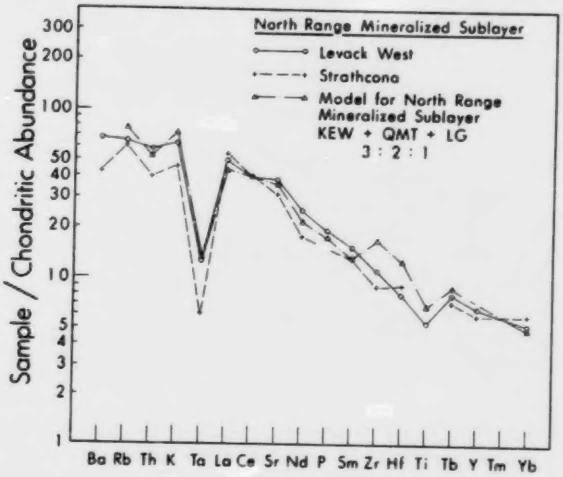

Figure 146.10. *Model trace element pattern for the North Range Mineralized Sublayer compared with observed patterns. See legend for Figure 146.6 for further explanation.*

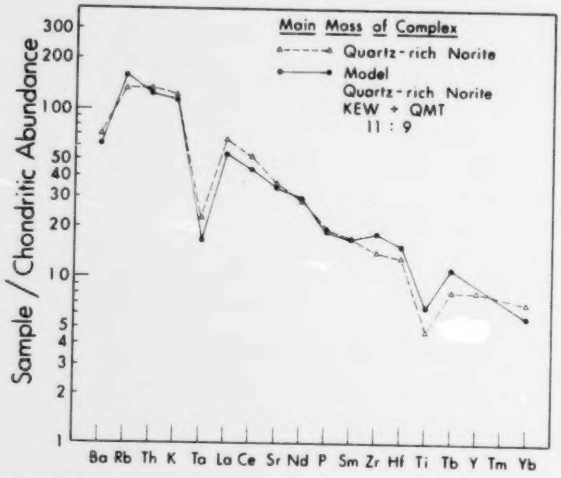

Figure 146.12. *Model trace element pattern for the Quartz-rich Norite compared to the observed pattern. See legend for Figure 146.6 for further explanation.*

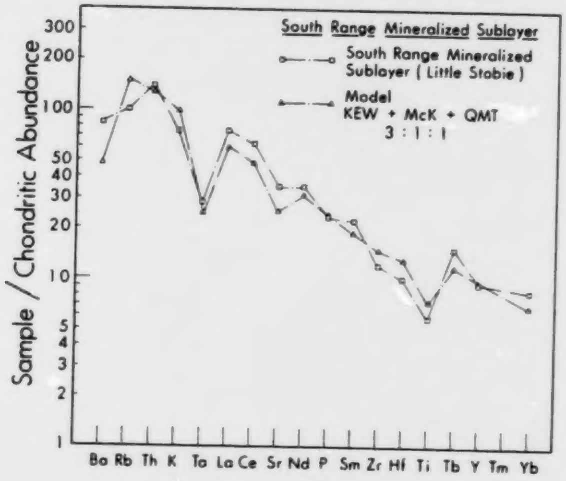

Figure 146.11. *Model trace element pattern for the South Range Mineralized Sublayer compared with the observed pattern. See legend for Figure 146.6 for further explanation.*

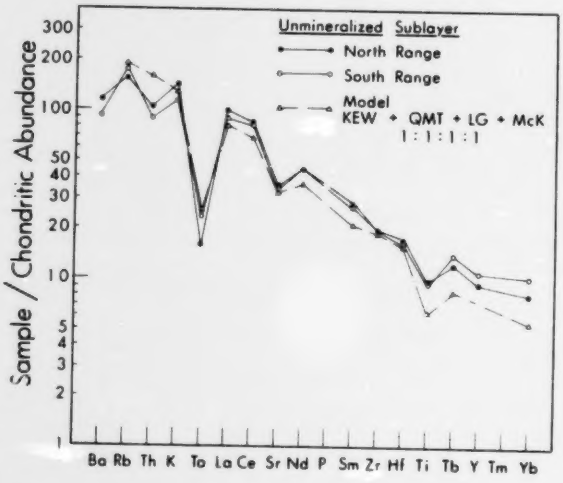

Figure 146.13 *Model trace element pattern for the Unmineralized Sublayer compared to observed patterns. See legend for Figure 146.6 for further explanation.*

ISOTOPE GEOCHEMISTRY

Isotope data for Sr and Nd (Rao *et al.* 1984, Rao *et al.* in preparation) are presented in Figure 146.15a,b. All rocks are characterized by negative values of ϵ_{Nd}. Most samples from the Main Mass of the Complex (Figure 146.15a) have ϵ_{Sr} values between +40 and +70, although a few samples, largely Granophyre, extend to +100 and beyond. The Main Mass samples lie close to a model line representing the mixing of a magma with an isotopic composition between bulk earth (1.849 Ga ago) and somewhat depleted mantle, with material believed to be typical of upper crust (*see* legend to Figure 146.15). The estimated degree of contamination varies with the degree of depletion of the primary magma, but is of the order of 40% to 60%.

Samples of Mineralized Sublayer from Little Stobie on the South Range lie close to the mixing line with upper crust (Figure 146.15b). Those for the North Range Mineralized Sublayer (Levack West and Strathcona) are displaced from this line, having much lower ϵ_{Sr} values. As might be expected from their mineralogical and trace element composition, the Levack Gneisses resemble other lower crustal granulites isotopically (Carter *et al.* 1978) in having both negative ϵ_{Sr} and ϵ_{Nd}. The isotopic composition of

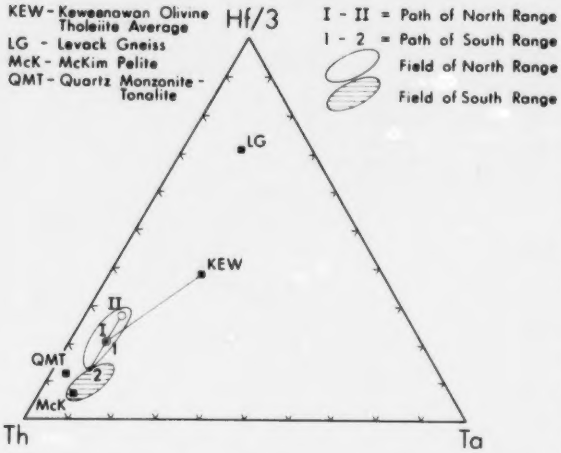
KEW - Keweenawan Olivine Tholeiite Average
LG - Levack Gneiss
McK - McKim Pelite
QMT - Quartz Monzonite - Tonalite
I - II = Path of North Range
1 - 2 = Path of South Range
Field of North Range
Field of South Range
Hf/3
LG
KEW
II
I
1
2
QMT
McK
Th
Ta

Figure 146.14. *Th-Hf-Ta diagram illustrating variations accompanying the contamination believed to have been experienced by the Mineralized Sublayer magmas. KEW = Average of 5 Keweenawan Olivine Tholeiites, LG = Levack Gneiss, QMT = Quartz Monzonite-Tonalite contaminant, McK = pelitic rock from the McKim formation, QRN = Quartz-rich Norite.*

the North Range Mineralized Sublayer is consistent with the trace element model suggesting contamination by both upper and lower crustal rocks. The present proximity of the North Range Sublayer to the Levack granulites, and the lack of evidence indicating that the Main Mass or South Range Sublayer magmas have interacted with granulites, is strongly indicative that granulite contamination of the North Range Mineralized Sublayer took place locally, that is in the upper rather than in the lower crust. This implies that it post-dated the component of contamination from typical upper crustal rocks.

Turning to the isotopic composition of the ultramafic inclusions, it is argued in the following section that these are related genetically to Sublayer magmas. However, the isotopes indicate that they have crystallized from magmas that had not experienced the same degree of upper crustal contamination as the Sublayer in which they occur.

RELATIONSHIP OF ORE DEPOSITS TO THE ROCKS OF THE COMPLEX

Although there is considerable variation in the characteristics of different ore deposits (Pye *et al.* 1984), there are a number of features common to all of them. These include:

1. *Embayments or other irregularities at the base of the SIC.* An increase in sulphide content is usually observed at the lower contact throughout the Complex, but it is where irregularities exist that the zone of sulphide thickens and increases in intensity sufficiently to form ore.

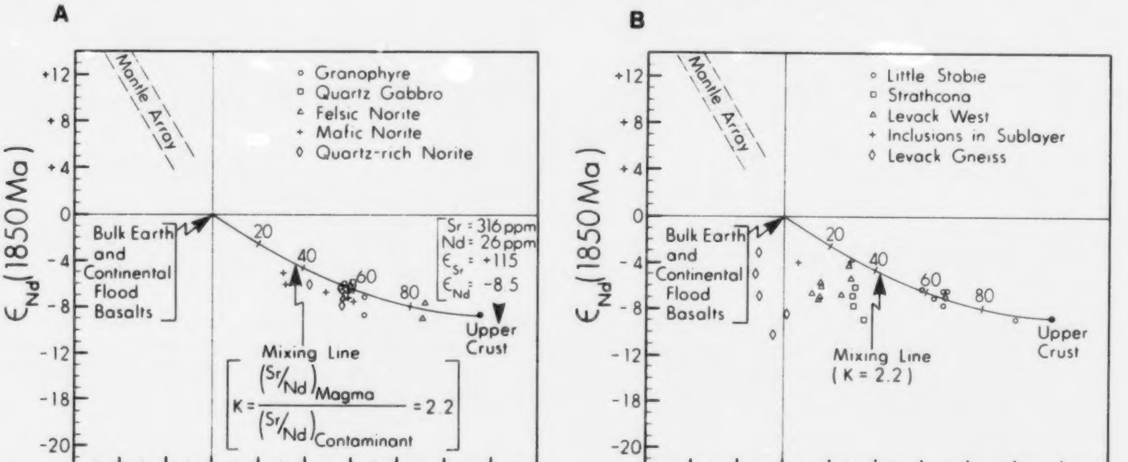

Figure 146.15. ϵ_{Nd} *vs* ϵ_{Sr} *diagram for units of the Main Mass of the SIC (a) and samples of Mineralized Sublayer (b). The measured values were recalculated to 1.850 Ga, the age of the Sudbury Igneous Complex (Krogh et al. 1984). Mixing curves calculated between the bulk earth and upper crust are shown in both diagrams. The upper crustal composition (at 1.85 Ga) was calculated using the data from McCulloch and Wasserburg (1978) and Taylor (1964). The Sr and Nd contents of the initial magma were assumed to be 400 and 15 ppm respectively. The tick marks on the mixing curves indicate the proportion of contaminant in the mixture. Note that the curvature of the mixing arrays on these diagrams is controlled by the value of K.*

2. *The presence of Sublayer.* The spatial relationship of ore to Sublayer is such that the sulphides constituting the orebodies appear to have settled out of bodies of Sublayer. Minor amounts (up to 5 modal percent) of sulphides also occur within border norites to the SIC, but, except where faulting obscures the original relationship of orebodies to units of the SIC, the ore deposits are invariably associated with Sublayer.
3. *Ultramafic inclusions within Sublayer.* Both in the contact and the offset environments, the mineralization is associated only with Sublayer that carries members of the suite of mafic and ultramafic inclusions described above. Scribbins *et al.* (1984) conclude that these inclusions are derived from 1 or more hidden layered intrusions.

RELATIONSHIP BETWEEN INCLUSIONS, SUBLAYER, AND MAIN MASS OF THE SIC

As discussed above, the trace element profiles of the Sudbury rocks differ from those of most mafic magmas and indicate that contamination by country rocks has occurred on a large scale. The similarity in the profiles of the Sublayer and the Main Mass rocks is suggestive that the magmas responsible for them have a common heritage. REE profiles for inclusions have the same steep slopes (Figure 146.7), although the abundances are lower. Thus there is some evidence that the inclusions were derived from a magma that had suffered similar contamination to the remainder of the SIC rocks.

The MgNos of samples of Sublayer are illustrated in Figure 146.16 (contrary to the previous representation of MgNos, in this figure only 90% of the total Fe has been included in calculating them, to allow for Fe in the magma in the ferric state). Using Roeder and Emslie's (1970) relationship between the Mg/Fe ratio of olivine and of the basaltic liquid that is in equilibrium with it, MgNos of liquids in equilibrium with the olivine of the inclusions have been calculated. It can be seen that these hypothetical liquids span essentially the same range of MgNos as that exhibited by the Sublayer samples. This indicates that the Mg/Fe ratio of the Sublayer samples is consistent with their being liquids derived from a chamber(s) in which the material from which the inclusions were derived was crystallizing as a cumulate(s). Many of the Sublayer samples are rich in SiO_2, and olivine would no be stable in equilibrium with a liquid this siliceous. However, Pattison (1979) has reported olivine present in Sublayer at Whistle (northeast corner of the structure) and G.A. Morrison (Inco Limited, Copper Cliff, Ontario, personal communication, 1984) has observed it at a number of locations. The Sublayer in these localities is not obviously different in composition to that elsewhere, which suggests that olivine may have played a role in the fractionation of much of the Sublayer, and only have disappeared from the liquidus shortly before it was emplaced.

It would be highly coincidental for the inclusions to be derived from a magma that had suffered the same extreme contamination as the SIC, in the same place, and yet be unrelated to it. The association between the inclusions and their host Sublayer is further evidence of a linkage between them. In the model presented at the end of this paper, it is proposed that the cumulates giving rise to the inclusions formed from Sublayer magma as it fractionated. As pointed out above, olivine compositions are consistent with this hypothesis.

SEGREGATION OF SULPHIDES

The SIC differs from other layered complexes in a number of significant ways, including:

1. Evidence that the area into which it was intruded had been involved in a catastrophic explosion, possibly the consequence of the impact of a meteorite.
2. Rocks of the Complex are very siliceous when compared with other intrusions on the basis of the Mg/(Mg + Fe) ratios of their pyroxenes, implying that the magma responsible was unusually siliceous for its state of fractionation.
3. Major and trace elements and isotopic analyses that indicate that the high SiO_2 content is the consequence of country rock assimilation.
4. An unusually large number of occurrences of very concentrated sulphide.

Irvine (1975) pointed out that assimilation of SiO_2-rich material by a mafic magma could lower the solubility of sulphur within it, and suggested that this had occurred at Sudbury. Naldrett and Macdonald (1980) pointed out that the SiO_2-rich nature of the SIC leant support to this hypothesis. The evidence presented in this paper, that extensive country rock assimilation has occurred, points to how the SiO_2-rich composition has been achieved.

It could be argued that assimilation of an equal mass or more of country rock by a mafic magma is impossible unless the magma was intruded with an unrealistically high degree of superheat. The problem of the heat budget would be helped if the assimilation accompanied fractional crystallization, so that the latent heat of crystallization was available for melting the country rocks. However, even if no heat whatsoever was lost to the surroundings during the assimilation and crystallization process, 50% con-

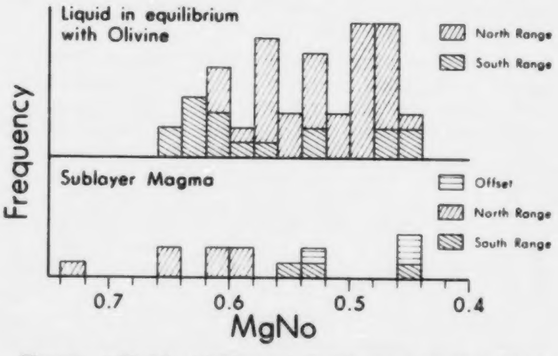

Figure 146.16. *MgNos of Sublayer samples that are believed to approximate the compositions of liquids, compared with the calculated MgNos of liquids in equilibrium with olivines of the inclusions of the Sublayer.*

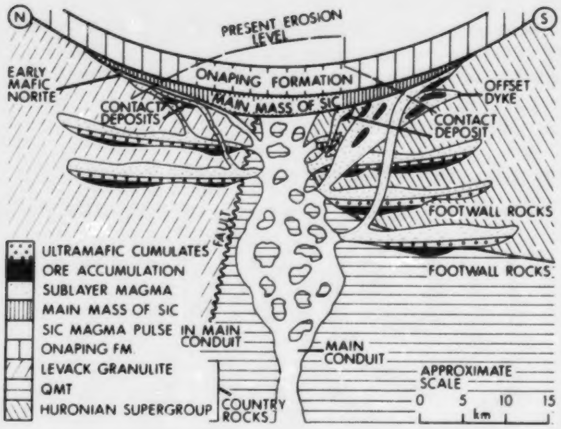

Figure 146.17. *Schematic cross-section illustrating the emplacement of the SIC. Magma rises up a vertical conduit into a highly fractured zone beneath an explosion (possibly impact) crater. The central body of magma cools somewhat slowly, assimilating much of the fractured country rocks. Subsequently it is emplaced into the crater, beneath the low density Onaping Formation, in response to structural readjustments in the area. It is probable that this is a multi-stage process. Magma has also spread out as a series of sills peripheral to the central conduit. Assimilation also occurs within these, giving rise to an imprint of localized contamination. The magma of the sills deposits sulphide and fractionates, giving rise to olivine and pyroxene-rich cumulates. Fractionated magma from the flanking sills also works its way up to the crater floor, intruding to form the Sublayer of the contact and offsets. Where magma from a lower sill has cut and disrupted an overlying one, it has picked up sulphides and inclusions, intruding with these in suspension within itself.*

tamination could not be achieved, since some heat would be used in heating the country rocks up to the temperature of the mafic magma.

It has been pointed out above that the contamination at Sudbury is rather unusual in that it is not particularly selective, but that major and trace element contents and isotope ratios can be modelled reasonably well by calling upon bulk assimilation of country rocks. A process such as this is much easier to envisage if it involves mainly the mixing of magmas, rather than the melting of and mixing with country rocks by a single magma. While Sudbury is unusual in the degree of bulk assimilation that appears to have occurred, it is also unusual in its geologic setting. It is suggested in this paper that preheating and extensive melting of the country rocks accompanied the catastrophic explosion that initiated the Sudbury event, thus providing the ideal environment for extensive contamination.

A MODEL FOR THE FORMATION OF THE SUDBURY IGNEOUS COMPLEX

It is proposed that the catastrophic explosion that occurred in the Sudbury region 1.85 Ga ago gave rise to the Onaping Formation, fractured and in part melted the underlying crust, and triggered ascent of a magma similar in its initial composition to continental flood basalt. Magma probably first rose up through the lower crust via a centralized plumbing system. After its initial ascent, the magma halted temporarily within the upper crust, fractionated to some degree, and became contaminated by surrounding rocks and zones of shock-melted material within them. The highly fractured, even pulverized (judging from the Sudbury and Footwall Breccias), nature of the country rocks at Sudbury would have greatly facilitated the assimilation, providing a large surface area for contact between the magma and its contaminant. At this stage, some magma spread out laterally through numerous subsidiary channels within the highly fractured ground beneath the crater (Figure 146.17). It is possible that these hidden, flanking intrusions account for the buried mass of mafic and ultramafic rock which underlies and extends beyond the present Sudbury structure, as indicated by the analysis of gravity and magnetic data by Gupta *et al.* (1984).

The batches of magma that infiltrated the flanking subsidiary channels cooled, fractionated further, giving rise to olivine and pyroxene-rich cumulates, and became contaminated through reaction with their surroundings. The contamination, coupled with the cooling, caused sulphides to precipitate at an early stage; these collected as massive bodies beneath the cumulates. It is at this stage that the distinctive local trace element and isotopic characteristics that have been documented in this paper started to be impressed on the Sublayer magmas.

Because of its greater dimensions, the main body of magma lost heat less quickly than that in the flanking chambers, and thus fractionated less rapidly. Successive injections of this magma occurred along the unconformity between the crater floor and the overlying, relatively unconsolidated and thus low density, Onaping Formation to give rise to the Main Mass of the Complex.

The faster cooling, and therefore more fractionated (consistent with the MgNos), magma of the flanking bodies was also squeezed up to intersect the crater floor, where it spread out, exploiting "troughs" and "embayments" in the floor and also infiltrating fractures in the basement rocks to form the offset dikes. This magma is responsible for the Mineralized Sublayer. It is likely that further contamination occurred during these events as the magma intruded into fractured, pulverized, and probably molten material on the crater floor. In some instances (Figure 146.17), as it rose up through the basement, it intersected and disrupted overlying bodies, picking up sulphides and ultramafic cumulates in the process, and giving rise to the enrichment in sulphides referred to above and to the very important association between the mineralization and the xenoliths. The offset dikes may represent, in part, channel-ways up which magma flowed to reach the overlying crater floor; erosion has stripped away the floor, leaving only the underlying feeder dikes. The face that the Sublayer intrusions were derived from a number of bodies following parallel, but distinct, evolutionary trends accounts for the greater variability of the Sublayer in MgNo and Sr initial ratio in comparison with the Main Mass.

The Unmineralized Sublayer is more problematical. Naldrett (1984) interpreted it as batches of magma from the flanking intrusions that reached the crater floor without intersecting overlying bodies. They were emplaced, therefore, without additional sulphides and carrying only country rock inclusions. The uniformity in trace element composition of this type of Sublayer all around the Complex, in contrast to the differences observed between the Mineralized Sublayer of the North and South Ranges, and the marked compositional differences between the unmineralized and mineralized variants of Sublayer, were unknown to Naldrett at the time he made his suggestion and cast doubt on the hypothesis. It is possible that the Unmineralized Sublayer represents hybrids produced as Main Mass magma rose up and mixed with debris and molten material on the crater floor.

ACKNOWLEDGMENTS

Dr. W.V. Peredery and Mr. L. Cochrane of Inco Limited and Mr. P. Snajdr of Falconbridge Limited made possible the sampling at Sudbury. Professor M.P. Gorton and Dr. R. Hancock of the University of Toronto were most helpful with the chemical analyses. Dr. T.E. Krogh of the Royal Ontario Museum kindly made his laboratory available at a crucial time for the isotopic analysis.

REFERENCES

Arth, J.F., and Hanson, G.N.
1975: Geochemistry and Origin of the Early Precambrian Crust of Northeastern Minnesota; Geochimica et Cosmochimica Acta, Volume 39, p.325-362.

Basaltic Volcanism Study Project
1981: Pre-Tertiary Continental Flood Basalts; p.30-77 *in* Basaltic Volcanism on the Terrestrial Planets, Pergamon Press, Incorporated, New York.

Card, K.D., Gupta, V.K., McGrath, P.H., and Grant, F.S.
1984: The Sudbury Structure: Its Regional Geological and Geophysical Setting; p.25-44 *in* The Geology and Ore Deposits of the Sudbury Structure, edited by E.G. Pye, A.J. Naldrett, and P.E. Giblin, Ontario Geological Survey, Special Volume 1, 603p.

Carter, S.R., Evensen, N.M., Hamilton, P.J., and O'Nions, R.K.
1978: Neodymium and Strontium Isotopic Evidence for Crustal Contamination of Continental Volcanics; Science, Volume 202, p.743-747.

Cochrane, L.B.
1984: Ore Deposits of the Copper Cliff Offset; p.347-360 *in* The Geology and Ore Deposits of the Sudbury Structure, edited by E.G. Pye, A.J. Naldrett, and P.E. Giblin, Ontario Geological Survey, Special Volume 1, 603p.

Dressler, B.O.
1984: The Effects of the Sudbury Event and the Intrusion of the Sudbury Igneous Complex on the Footwall of the Sudbury Structure; p.97-138 *in* The Geology and Ore Deposits of the Sudbury Structure, edited by E.G. Pye, A.J. Naldrett, and P.E. Giblin, Ontario Geological Survey, Special Volume 1, 603p.

Fairbairn, H.W. Faure, G., Pinson, W.H., and Hurley, P.M.
1968: Rb-Sr Whole-Rock Age of the Sudbury Lopolith and Basin Sediments; Canadian Journal of Earth Sciences, Volume 5, p.707-714.

Gupta, V.K., Grant, F.S., and Card, K.D.
1984: Gravity and Magnetic Characteristics of the Sudbury Structure; p.381-410 *in* The Geology and Ore Deposits of the Sudbury Structure, edited by E.G. Pye, A.J. Naldrett, and P.E. Giblin, Ontario Geological Survey, Special Volume 1, 603p.

Irvine, T.N.
1975: Crystallization Sequences of the Muskox Intrusion and Other Layered Intrusions—II; Origin of Chromitite Layers and Similar Deposits of Other Magmatic Ores; Geochimica et Cosmochimica Acta, Volume 3, p.991-1020.

Krogh, T.E., Davis, D.W., and Corfu, F.
1984: Precise U-Pb Zircon and Baddelyite Ages for the Sudbury Area; p.431-446 *in* The Geology and Ore Deposits of the Sudbury Structure, edited by E.G. Pye, A.J. Naldrett, and P.E. Giblin, Ontario Geological Survey, Special Volume 1, 603p.

Kuo, H.Y., and Crocket, J.H.
1979: Rare Earth Elements in the Sudbury Nickel Irruptive: Comparison with Layered Gabbros and Implications of Nickel Irruptive Petrogenesis; Economic Geology, Volume 79, p.590-605.

McKulloch M.R., and Wasserburg, G.J.
1978: Sn-Nd and Rb-Sr Chronology of Continental Crust Formation; Science, Volume 200, Number 4345, p.1003-1011.

Muir, T.E.
1984: The Sudbury Structure; Consideration for Models of an Endogenic Origin; p.449-490 *in* The Geology and Ore Deposits of the Sudbury Structure, edited by E.G. Pye, A.J. Naldrett, and P.E. Giblin, Ontario Geological Survey, Special Volume 1, 603p.

Muir, T.E., and Peredery, W.V.
1984: The Onaping Formation; p.139-210 *in* The Geology and Ore Deposits of the Sudbury Structure, edited by E.G. Pye, A.J. Naldrett, and P.E. Giblin, Ontario Geological Survey, Special Volume 1, 603p.

Nakamura, E., Campbell, I.H., and Sun, Shon-su
1985: The Influence of Subduction Processes on the Geochemistry of Japanese Alkaline Basalts; Nature, Volume 316, p.55-58.

Naldrett, A.J.
1984: Summary, Discussion and Synthesis; p.533-570 *in* The Geology and Ore Deposits of the Sudbury Structure, edited by E.G. Pye, A.J. Naldrett, and P.E. Giblin, Ontario Geological Survey, Special Volume 1, 603p.

Naldrett, A.J., Bray, J.G., Gasparrini, E.C., Pololsky, T., and Rucklidge, J.G.
1970: Cryptic Variation and the Petrology of the Sudbury Nickel Irruptive; Economic Geology, Volume 65, p.122-155.

Naldrett, A.J., Greenman, L., and Hewins, R.H.
1972: The Main Irruptive and the Sublayer at Sudbury Ontario; 24th International Geological Congress, Montreal, Proceedings, Section 4, p.206-214.

Naldrett, A.J., and Macdonald, A.J.
1980: Tectonic Settings of Some Ni-Cu Sulfide Ores: Importance in Genesis and Exploration; Geological Association of Canada, Special Paper 20, p.633-657.

Pattison, E.F.
1979: The Sudbury Sublayers: Its Characteristics and Relationships with the Main Mass of the Sudbury Irruptive; Canadian Mineralogist, Volume 17, p.257-274.

Peredery, W.V., and Morrison, G.G.
1984: Discussion of the Origin of the Sudbury Structure; p.491-512 *in* The Geology and Ore Deposits of the Sudbury Structure, edited by E.G. Pye, A.J. Naldrett, and P.E. Giblin, Ontario Geological Survey, Special Volume 1, 603p.

Pye, E.G., Naldrett, A.J., and Giblin, P. (Editors)
1984: The Geology and Ore Deposits of the Sudbury Structure; Ontario Geological Survey, Special Volume 1, 603p.

Rao, B.V., Naldrett, A.J., and Evensen, N.M.
1984: Crustal Signature in the Sublayer, Sudbury Igneous Complex: A Strontium and Neodymium Isotope Study (Abstract); *in* Geoscience Research Seminar and Open House '84, December 4-5, 1984, Abstracts, Ontario Geological Survey 1984, 23p.

Rao, B.V., Naldrett, A.J., Evensen, N.M., and B.O. Dressler
In Preparation: Crustal Contamination in the Sublayer, Sudbury Igneous Complex: An Evaluation by Major, Trace Element, and Sr, Nd-Isotope Study.

Roeder, P.L., and Emslie, R.F.
1970: Olivine-Liquid Equilibrium; Contributions to Mineralogy and Petrology, Volume 29, p.275-289.

Scribbins, B., Rae, D.R., and Naldrett, A.J.
1984: Mafic and Ultramafic Inclusions in the Sublayer of the Sudbury Igneous Complex; Canadian Mineralogist, Volume 22, Part 1, p.67-75.

Shaw, D.M., Dostal, J., and Keays, R.R.
1976: Additional Estimates of Continental Surface Precambrian Shield Composition; Geochimica et Cosmochimica Acta, Volume 40, p.73-83.

Sims, P.K., Peterman, Z.E., Prinz, W.C., and Benedict, F.C.
1984: Geology, Geochemistry, and Age of Archean and Early Proterozoic Rocks in the Marenisco-Watersmeet Area, Northern Michigan; United States Geological Survey, Professional Paper 1292-A, p.A1-A41.

Slaught, W.H.
1951: A Petrographic Study of the Copper Cliff Offset in the Sudbury District; Unpublished M.Sc. Thesis, McGill University.

Taylor, S.R.
1964: Abundances of Chemical Elements in the Continental Crust: A New Table; Geochimica et Cosmochimica Acta, Volume 28, p.1273-1285.

Thompson, R.N.
1982: Magmatism of the British Tertiary Volcanic Province; Scottish Journal of Geology, Volume 18, p.1-108.

Wood, D.A.
1980: The Application of a Th-Hf-Ta Diagram to Problems of Tectonomagmatic Classification and to Establishing the Nature of Crustal Contamination of Basaltic Lavas of the British Tertiary Volcanic Province; Earth and Planetary Science Letters, Volume 50, p.11-30.

Grant 148 Geochemical Study of the Salina Group of Southern Ontario—Isotopes, and Major and Minor Elements

M.C. Miles, E.C. Appleyard, K. O'Shea, P. Lapcevic, S.K. Frape, and P. Fritz

Department of Earth Sciences, University of Waterloo

ABSTRACT

In the second year of this project, the isotopic and geochemical data has expanded to include 2 more cores. Material sampled to date now includes 2 complete vertical sections in addition to other material from various stratigraphic horizons in the Salina. The sampled material represents all lithofacies zones present in the Salina.

A trend to negative ^{13}C values in the units above the B-Unit has been shown to be present in Lambton County as well as at the Fletcher Field, signifying a change in basin depositional environments that occurred after deposition of the B-Unit. Carbon-13 relative fluctuations have been tentatively correlated in the A-2 Unit and the C-D-E-F-G Units over large distances. Oxygen-18 values from the carbonates have been interpreted to be responsive to evaporative cycles but are generally depleted due to Silurian seawater ^{18}O depletion.

Major element chemistry of the Salina "shales" has outlined 2 trends. Both trends lack a magnesium-enriched clay fraction, unlike that of the evaporative Keuper Marl of England. The major element chemistry of the "shales" display strong evaporative signatures. However, differentiation of various facies or zones of differing paleosalinities, using major and minor element chemistry, is still very tentative. An absence of sepiolite, smectites, and other hypersaline indicator clays is tentatively ascribed to post-depositional alteration.

INTRODUCTION

This is the second summary of the geochemical study of the Salina Formation of Southern Ontario. The purpose of the study as a whole was to establish geochemical and isotopic evidence in support of paleoenvironmental interpretations and to provide modern analogue chemical data for Precambrian evaporite investigations.

In last year's summary (Miles *et al.* 1984), it was shown that carbon-13 compositions of the carbonates within the Salina were representative of primary depositional compositions, therefore allowing certain paleoenvironmental interpretations. Oxygen-18 compositions of the carbonate were also believed to be very close to primary values due to the process of penecontemporaneous dolomitization.

It was seen that on the margin of the Michigan Basin during Cayugan time a sabkha-shallow water environment prevailed. A dramatic trend to very negative carbon-13 values that occurred in the B-Unit at Caledonia, Ontario, was also observed in the B-Unit at the Fletcher Field, near Tilbury, Ontario. Both areas are situated in this marginal area although they are separated by 250 km. Since few environments are capable of producing such negative ^{13}C values, a subaerial or soil zone type of environment was interpreted to be present during the deposition of the B-Unit on the margins of the basin (Miles *et al.* 1984).

Another trend in ^{13}C that was observed at Fletcher Field was that the A-Units possessed generally positive δ^{13}C values, whereas the succeeding Salina units possessed generally negative δ^{13}C values (Miles *et al.* 1984). A basin evolution scheme similar to that of Matthews and Elgeson (1974) was proposed to explain this positive to negative cycle at Fletcher.

It was hoped that a link between the carbon and sulphur systems would allow comparisons between trends in carbon isotopic compositions and sulphur isotopic compositions. Such trends would help establish that basinal carbon budget changes were responsible for the observed carbon isotopic fluctuations.

The depleted nature of the ^{18}O values of the carbonate suggested that Silurian seawater was depleted in ^{18}O with respect to modern ocean water (Miles *et al.* 1984). The fact that carbonate within the halite units was more depleted with respect to contemporaneous carbonate further substantiated this theory.

It was thought that if primary ^{18}O compositions were to be preserved in an ancient carbonate, it would be from the carbonate within the halite. Unless it is accepted that the halite units are not impermeable to siginificant fluid flow or that meteoric water participated in the halite deposition then the ^{18}O values from the halite must be accepted as primary. Therefore, Silurian seawater must have been depleted in ^{18}O with respect to modern seawater. This corresponds to what was found by Brand and Veizer (1981) for the Silurian.

Minor cycles in ^{18}O at Fletcher were seen but were difficult to assess. However, they may be related to evaporative enrichment cycles. The generally enriched ^{18}O values of the carbonate at Fletcher with respect to the carbonate at Goderich was thought to be the result of evaporative enrichment in the sabkha zone at Fletcher.

The discovery of authigenic idiomorphic quartz crystals within the the halite beds at Goderich and Windsor was also an area of further study within the second year of this project. Their unusual isotopic composition and fluid inclusion temperatures suggested crystallization from a ^{18}O depleted fluid of a $CaCl_2$ chemistry.

Lithogeochemical studies had been initiated on the argillaceous, marly, and carbonaceous units of the Salina to establish what geochemical changes, if any, mark the various lithofacies domains of the basin. The study was to be extended to include specimens from the interpinnacle shelf and basin centre zones and a reconnaissance study of clay

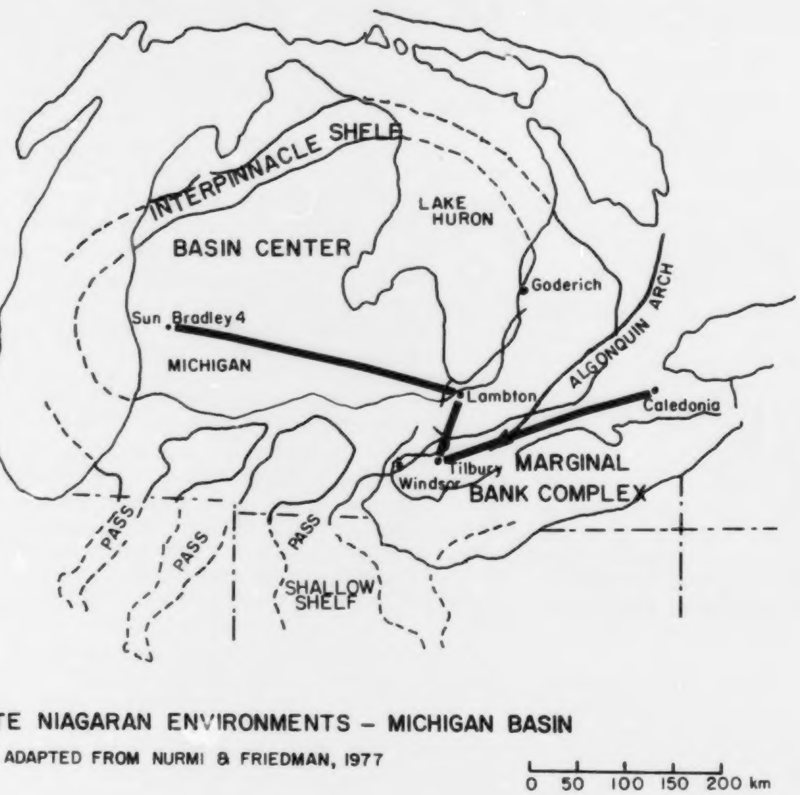

Figure 148.1. *Map showing core locations, lithofacies zones and line of cross-section depicted in Figure 148.5.*

mineral assemblages in all units was to be undertaken. In addition, data on sulphur-34 and oxygen-18 in sulphate from the various sample sites was to be obtained.

SAMPLE COVERAGE

Previous sample material was obtained from drill core at Domtar's gypsum mine in Caledonia, Ontario, 2 cores from Consumer's Gas at the Fletcher Field near Tilbury, Ontario, and sampled mine sections at Domtar's salt mine at Goderich, Ontario and the Canadian Rock Salt Company's salt mine at Windsor, Ontario. Samples now include material from the Lambton County Ontario Geological Survey (OGS) deep hole, and the Sun Bradley #4 hole at Newaygo County, Michigan (Figure 148.1).

The Caledonia material represents part of the A-2 Unit and most of the B-Unit. The sequence at Caledonia was interpreted to be a sabkha deposit occupying a marginal shelf or bank facies of the Michigan Basin (Miles 1982). Core from the Fletcher Field represents all Salina units of the marginal basin zone, and is interpreted to represent a sabkha deposit. All Salina units were sampled at the Fletcher Field. Material from the Goderich salt mine represents the A-2 Evaporite Unit. The environment of deposition is somewhat unknown and a subject of controversy. Material from the Windsor salt mine represents a F-Unit evaporite. Again, the environment of deposition is somewhat uncertain, however, a more shallow water origin is likely (Dellwig 1972; Matthews and Egeson 1974).

The core from Lambton County was sampled in every Salina unit except the B-Unit. Lambton is located in an interpinnacle reef-shelf facies of presumed variable water depth. Evidence of shallow water and deep water facies has been noted by O'Shea (1985). The core from Newaygo County was sampled only in the A-Carbonate Units due to poor core recovery and preservation. This core is situated in a basin centre facies of presumed deep water environment (Nurmi and Friedman 1977).

Therefore material sampled to date represents, all the various facies zones as outlined by Nurmi and Friedman (1977). As well, 2 rather complete vertical sections through the Salina have been sampled. The other material, described above, from isolated stratigraphic horizons in the Salina in different parts of the basin tie in to these complete vertical sections.

RESULTS

The analytical results are represented in the following figures. Carbon-13 and oxygen-18 compositions from carbonate at the OGS Lambton hole and from the Sun Bradley #4 hole, Newaygo County, are shown in Figures 148.2 and 148.3. A schematic diagram depicting a compilation of ^{13}C and ^{18}O results across the Michigan Basin is given in Figure 148.5 following the line of cross-section in Figure 148.1. Carbon-13 data from the C-D-E-F-G Units at Fletcher and Lamb-

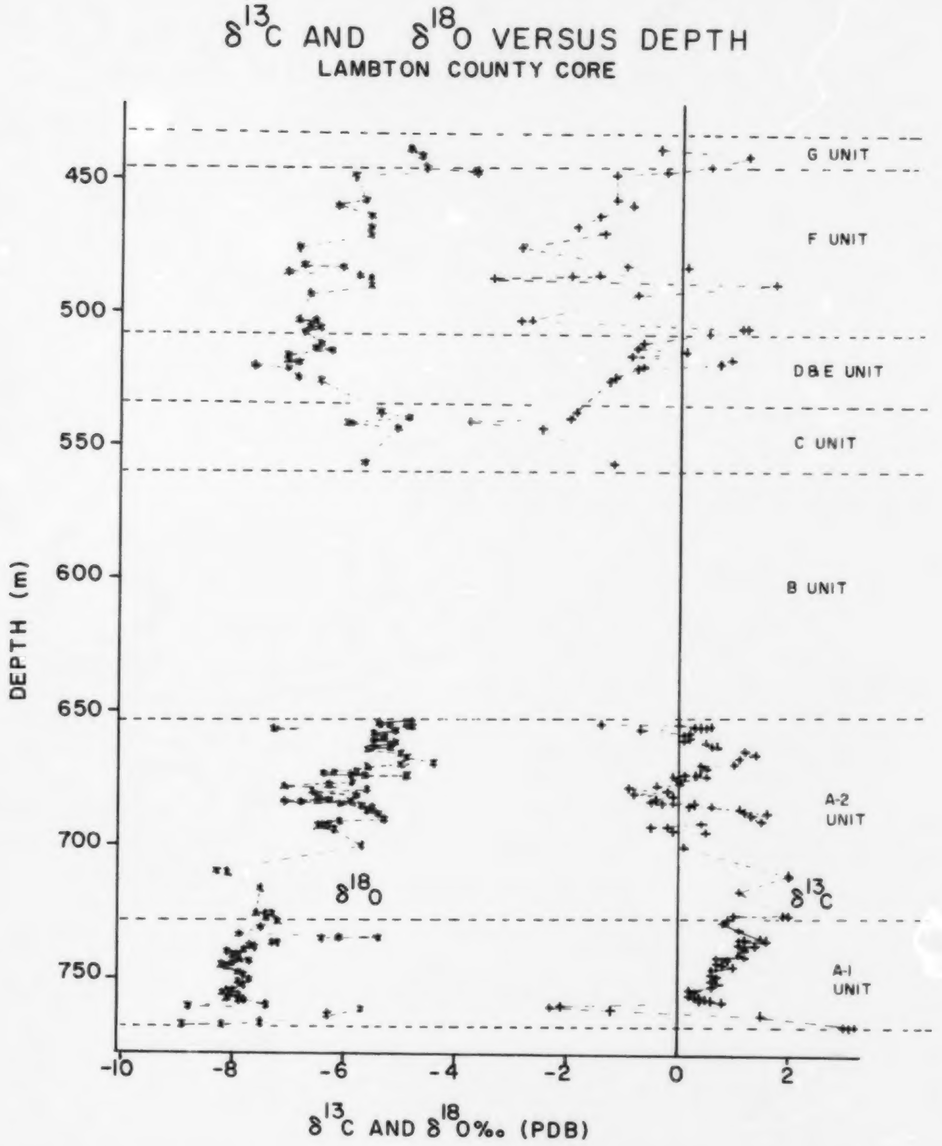

Figure 148.2. *Carbon and oxygen isotope results from carbonate at the Ontario Geological Survey core at Lambton County.*

ton County are compared in Figure 148.6. Carbon-13 data from the A-2 Units of Fletcher, Lambton County, and Newaygo County are compared in Figure 148.7. Sulphur-34 and oxygen-18 data from the OGS Lambton County hole are summarized in Figure 148.4.

DISCUSSION

ISOTOPIC RESULTS

Figure 148.5 shows that on the margin of the basin, as represented by the core from Fletcher and Caledonia, a ^{13}C negative event occurs in the B-Unit. Note from Figure 148.2 and Figure 148.5 that the same trend from generally positive ^{13}C values in the A-Units to generally negative ^{13}C values in the succeeding Salina units is also present at Lambton County.

It is believed that a change in lithology of the carbonate units from below the B-Unit to above, parallels the ^{13}C trend. In addition, sedimentological observation and measurement of total organic carbon contents (TOC) qualitatively support the assumption that the A-Units were originally organic rich and have preserved to some extent this organic carbon, whereas the B-C-D-E-F-G Units may have been organic rich but have not preserved their organic carbon.

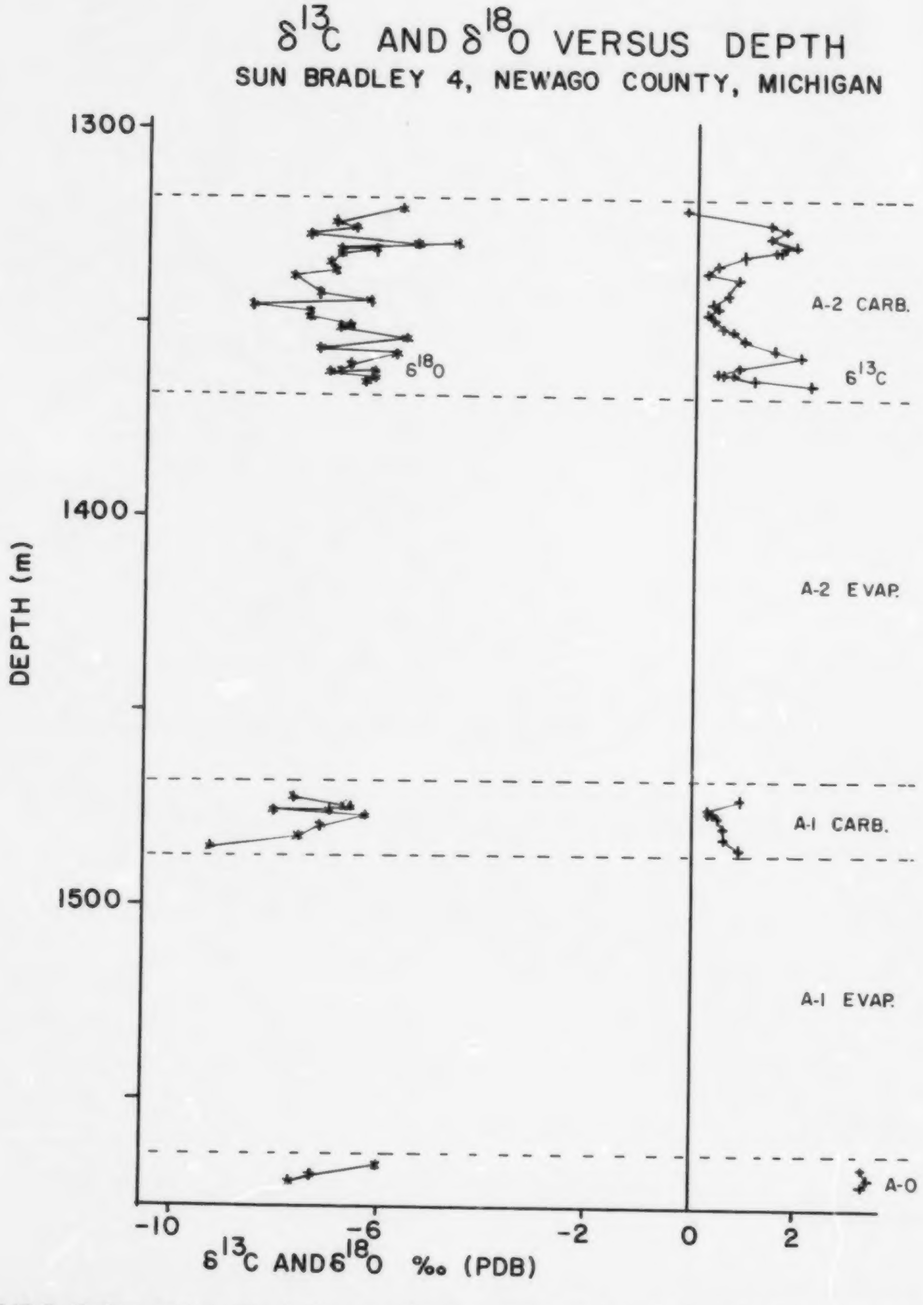

Figure 148.3. *Carbon and oxygen isotope results from carbonate at the Sun Bradley #4 core at Newaygo County, Michigan.*

Tentative correlation of relative ^{13}C fluctuations in the units above the B-Unit (Figure 148.6), in addition to lithologic, gamma ray log (Rickard 1969), and section thickness similarities in the units above the B-Unit, suggest that environments of deposition were very similar between the Fletcher Field and Lambton County after the deposition of the B-Unit. Such similarity in depositional environment perhaps can be extended throughout the Michigan basin during deposition of the Salina units above the B-Unit.

In the A-Units, similarity in ^{13}C fluctuations, lithologic character and section thickness are less well demonstrated. However, in Figure 148.7 some favourable comparisons between relative ^{13}C fluctuations in the A-2 Unit can be made between the Fletcher Field, Lambton County, and Newaygo Coun-

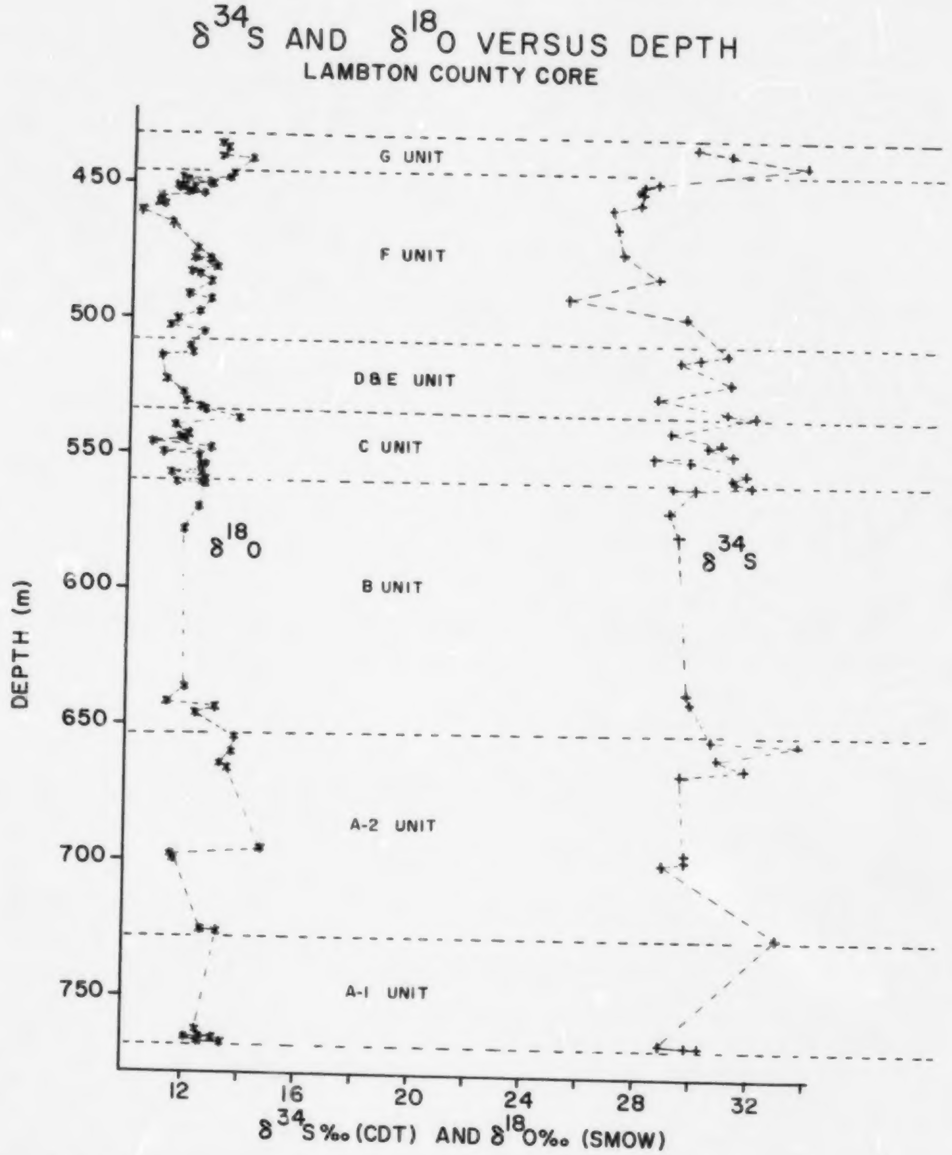

Figure 148.4. *Sulphur and oxygen isotope results from sulphate at the Ontario Geological Survey core at Lambton County (from Lapcevic 1985).*

ty. The absolute ^{13}C values are seen to be different in the A-2 Unit but similar trends can be identified. Such comparisons in the A-1 Unit are not observed.

Therefore, carbon isotopic compositional change parallels other changes within the Salina, reflecting a basinal change during or immediately after the deposition of the B-Unit. This change apparently results in environments throughout the basin becoming quite similar over wide areas as shown by correlation of ^{13}C fluctuations, lithologic character, and section thickness. Nurmi (1974) has suggested that little basinal relief existed during deposition of the B and C Units. The concept of a shallower more homogenously sedimented basin after deposition of the B-Unit would be supported by Nurmi and Friedman (1977) and Matthews and Elgeson (1974). Such a similarity in environments may have begun as early as the deposition of the A-2 Carbonate, although there is less evidence for this occurrence. It is possible that shallowing occurred as early as the A-2 Unit near the margins, and is recorded as the preserved isotopic signature of subaerial exposure on the margins during the deposition of the B-Unit.

Just what type of basinal change indicated by the carbon-13 compositions is uncertain. The absolute values of ^{13}C in the Units above the B-Unit suggest a continental type of environment where ^{13}C depleted continental type carbonate is deposited.

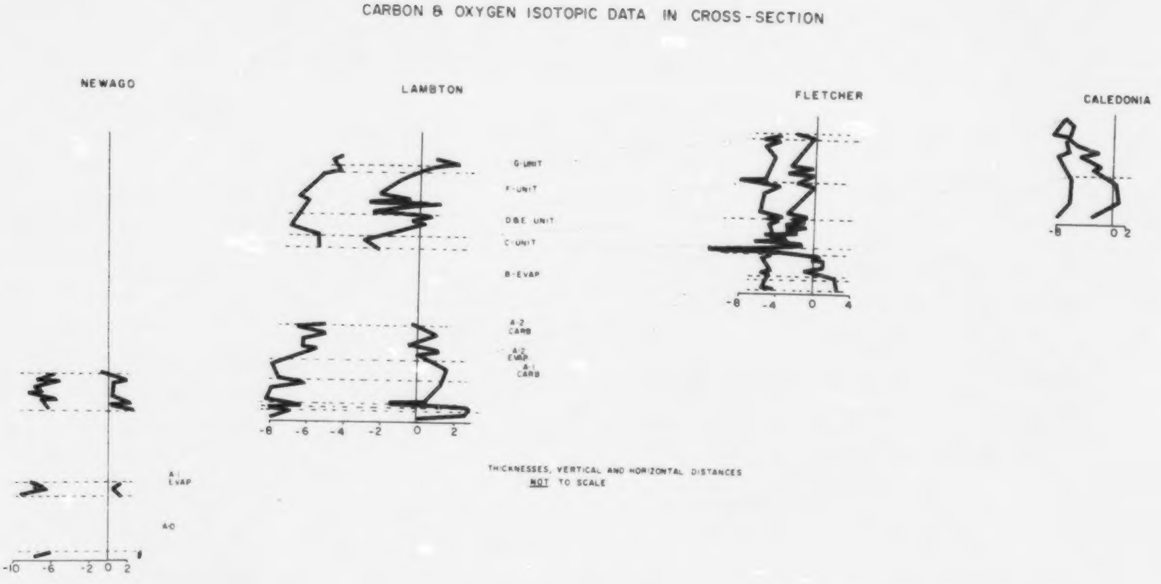

Figure 148.5. *Schematic cross-section along line shown in Figure 148.1 showing the carbon and isotopic data compiled in this study.*

Similar ^{13}C values are characteristic of continentally deposited or influenced carbonate (Pierre 1981; Deuser *et al.* 1978; Pierre and Fontes 1978; Allen and Keith 1965; Keith *et al.* 1964). The more argillaceous content of the units above the B-Unit would support the argument of an increased influence of a continental source. However, the halite sequences in the units above the B-Unit are definitely of marine origin (Holser 1966). Perhaps periodic marine incursions created the halite.

The change in ^{13}C composition from the A-Units to the units above the B-Unit may have been the result of changing water depth relationships in the Michigan basin in response to the filling of an originally deep basin. A deeper basin would be more conducive to the preservation of organic matter in deep anoxic waters as well as saline lagoons on the margin. However, when the basin became shallower oxidation of organic carbon was better accomplished allowing organically depleted ^{13}C to participate in the carbonate equilibria.

Unfortunately a carbon budget change cannot be substantiated using the isotopic composition of sulphate. A link between the carbon and sulphur system has been theorised to exist on a global scale by Veizer *et al.* 1980). Sulphur-34 and oxygen-18 of sulphate (Figure 148.4) show large variations at Lambton County. Such large variations are indicative of a shallow water or sabkha-like deposits where variable sources of sulphate are possible and bacterial reduction-oxidation processes can take place (Olson 1975). The large variations in ^{34}S do not show any correlation to ^{13}C variations at the Lambton County or the Fletcher Field. Since no correlation trends between ^{13}C and ^{34}S were seen on a local or regional scale it must be concluded that the link between the carbon and sulphur systems is either non-existent or

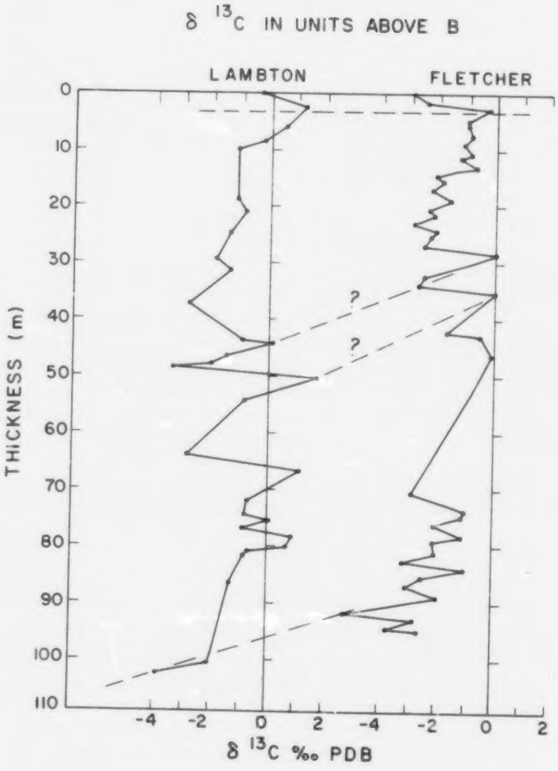

Figure 148.6. *Tentative correlation of relative carbon-13 fluctuations in the C-D-E-F-G Units between Lambton and Fletcher.*

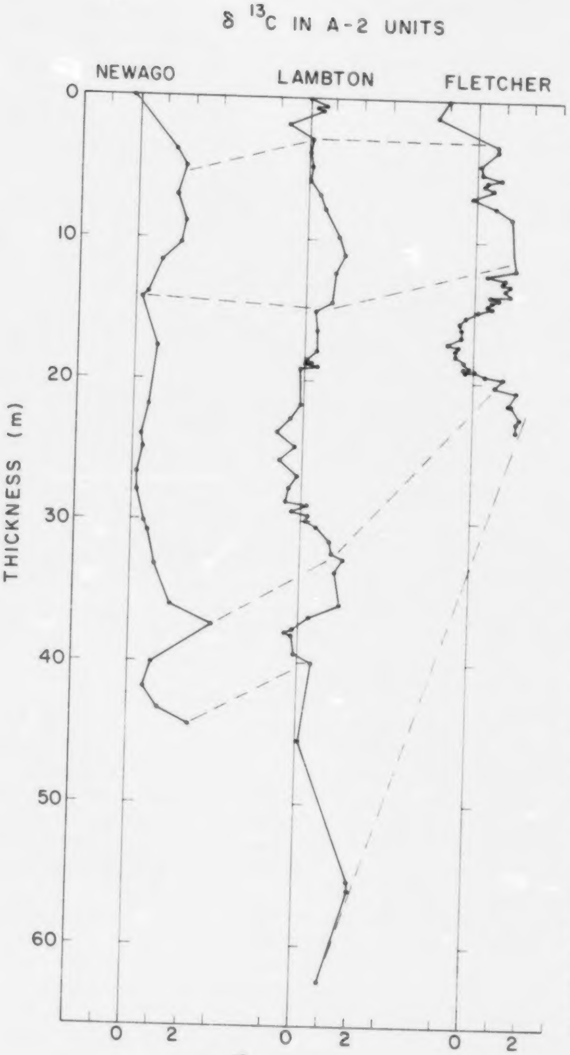

***Figure 148.7.** Tentative correlation of relative carbon-13 fluctuations in the A-2 Units between Lambton, Newaygo, and Fletcher.*

too complex to be observed on a local or regional scale.

Comment on carbon budget control of ^{13}C within the Michigan basin must therefore be withheld. It is believed that ^{13}C is more reflective of local conditions within the basin which are in turn affected by the evolution of environments during deposition of the Salina.

The ^{18}O compositions of the carbonate at Lambton display an interesting trend (Figure 148.2). In the A-1 Unit the carbonates are depleted but become more enriched as one goes higher in the column, whereupon in the A-2 Unit they remain more or less constant.

The ^{18}O enrichment of the carbonate may be due to evaporative enrichment of the water in equilibrium with the carbonate. It is believed that this signifies a shallowing of environment at Lambton County as early as the deposition of the A-2 Carbonate. Other ^{18}O cycles to enriched values in the A-1 Carbonate Unit at Lambton and Newaygo Counties may also show shallow environments developing where deeper water prevailed during deposition of the A-1 Unit. These minor cycles may indicate desiccation episodes within the originally deep Michigan basin.

The overall trend to enriched ^{18}O compositions at Lambton parallels the ^{13}C trend which was interpreted to be the establishment of a shallower more widespread carbonate depositing environment after the deposition of the B-Unit. The ^{18}O values from Lambton are in support of this theory.

QUARTZ

The isotopic and fluid inclusion data from the quartz has been augmented. It appears that the fluid inclusions are a $CaCl_2$ brine with a homogenization temperature of approximately 25°C. Two ranges of isotopic values have now been established for the quartz at Goderich. Very anomalously low values (+4‰ Standard Mean Ocean Water (SMOW)) for 1 bed were found last year (Miles *et al.* 1984). This year, values for another bed averaged 22‰ SMOW. At Windsor, 2 beds that possessed quartz crystals produced crystals with a $\delta^{18}O$ of 6.8, 8.7, and 10.8‰ SMOW. Again, very low ^{18}O values from quartz within a salt bed have been found.

Although the quartz with an ^{18}O of 22‰ can be classified as recrystallized detrital quartz, there still remains the quartz with the low ^{18}O values. Perhaps 2 generations of quartz crystals have been observed. One population of quartz dominantly formed from detrital quartz, the other population from primary SiO_2 within the halite. The low values still remain unexplained. However, speculation on biological factors and intrusions of depleted ^{18}O, $CaCl_2$ brines into the sedimenatry sequence are being entertained.

LITHOGEOCHEMICAL AND CLAY MINERAL STUDIES

The broad objective of this part of the Salina study was the acquisition of reference information on the whole-rock, major-, and trace-element geochemistry of the Salina shales, marls, and carbonate rocks and to integrate this information with a reconnaissance study of clay mineral assemblages. The principal goal was to determine whether such information could be used in characterizing the various environments of deposition of the formation. An ancillary goal was to collect a reference set of data pertaining to the geochemistry of evaporite-related sediments for application to studies of possible metamorphosed saliferous sediments.

Samples averaging 300 to 600 g in size and representing the so-called shale, marl, and carbonate units were selected for analysis. All analyses were performed by X-Ray Assay Laboratories, Don Mills, Ontario, from whom information on analytical procedures, precision, and accuracy can be obtained. Of

TABLE 148.1. MEAN COMPOSITIONS OF ARGILLACEOUS/DOLOMITIC SALINA SEDIMENTS.

	Dolomitic argillite	Dolomitic marl	Argillaceous dolomite	Carbonate rocks
n	6	29	26	7
SiO_2 (wt.%)	43.8	33.1	10.6	2.56
TiO_2	0.52	0.40	0.12	0.027
Al_2O_3	9.40	8.19	2.86	0.86
FeO (total)	2.93	2.69	1.00	0.43
MnO	0.027	0.025	0.013	0.005
MgO	8.30	11.7	14.8	11.6
CaO	9.16	14.6	25.5	36.1
Na_2O	1.85	0.29	0.77	0.03
K_2O	3.35	3.27	1.11	0.05
P_2O_5	0.123	0.091	0.042	0.017
F	0.177	0.172	0.118	0.215
Cl	3.12	0.334	1.97	0.224
SO_3	1.04	2.98	14.2	23.4
Li (ppm)	152	151	72	13
B	167	156	88	70
Sc	7.6	8.5	2.9	0.9
V	59	55	23	14
Cr	63	57	20	14
Co	15	14	7.1	6.1
Ni	34	37	19	16
Cu	9.0	14	7.7	3.7
Zn	24	28	14	5.1
Br	13	14	6.6	3.9
Rb	82	73	26	12
Sr	150	704	1385	1312
Y	25	18	9.4	7.9
Zr	172	101	15	5.0
Nb	49	14	9.4	7.9
Sb	0.50	0.48	0.33	0.14
Cs	9.7	2.4	1.0	0.16
Ba	308	218	33	5.0
Pb	27	29	30	5.0
Th	4.4	4.5	1.7	0.3
U	2.7	2.9	2.0	1.4

the 68 analyses obtained (*see* Table 148.5), there were 15 from the Caledonia site, 25 from the Tilbury (Fletcher Field) site, 24 from the Lambton borehole, and 4 from the Sun Oil hole in Newaygo County, Michigan. All samples can be broadly classified as part of a calcilutite-calcareous dolomite series. The classification adopted here is a simple, arbitrary system used by Moine *et al.* (1981) in which samples with 5% to 10% CaO are termed dolomitic argillite, 10% to 20% CaO as dolomitic marl, 20% to 30% CaO as arillaceous dolomites and > 30% CaO as carbonate (dolomite) rocks. The collection of analyses contains 6 dolomitic argillites, 29 dolomitic marls, 26 argillaceous dolomites, and 7 carbonate rocks. Average analyses for these 4 rock-types are given in Table 148.1.

GEOCHEMICAL CHARACTERISTICS

Clastic and carbonate sediments deposited in evaporitic depositional environments tend to differ compositionally from similar types of sediments deposited in normal marine and freshwater environments (Moine *et al.* 1981). The principal mineralogical effects of equilibration of the depositional assemblages with brines appear to be the stabilization of dolomite as the characteristic carbonate phase and a tendency to form syngenetic or diagenetic Mg-enriched clays, chlorite, and possibly talc (Jeans 1978). The unique geochemistry of evaporative sediments is due to the major and trace elements characteristics of these minerals, the nature of the influx of terrestrially-derived clastics, and the occurrence of the evaporative minerals themselves, gypsum, anhydrite, halite, and sylvite.

The major element diagram that best illustrates the effect of the above mineralogical relationships is the Ca-Mg-Al (molar ratio) diagram (Figure 148.8). The Salina sediments fall on 2 clear trajectories: (1) a trend from the Al-corner, representing the aluminous clay minerals and possibly minor clastic aluminosilicates, to the composition point of dolomite, and (2) a trend from the clay-dolomite axis toward the Ca-corner representing calcite, gypsum, and anhydrite.

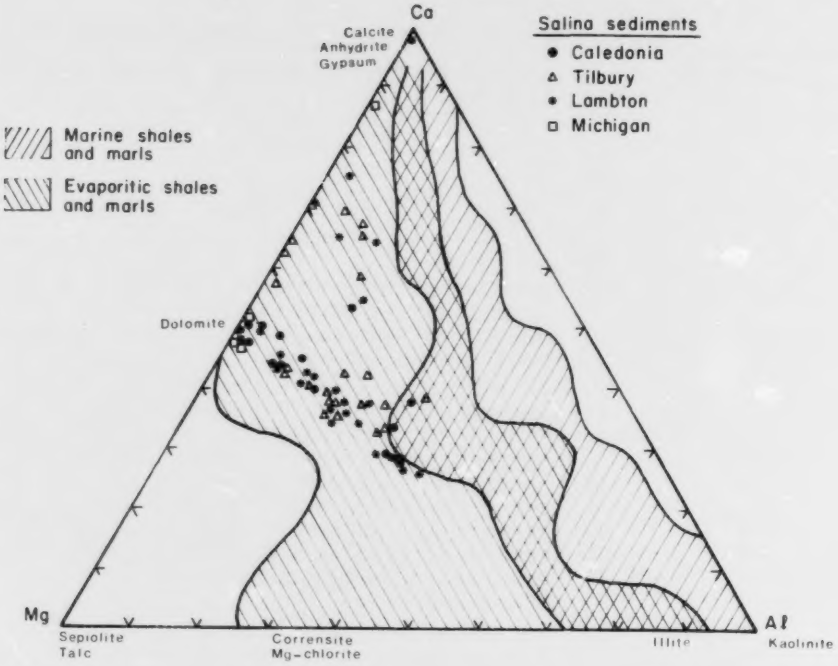

Figure 148.8. *Ca-Mg-Al molar ratio diagram for Salina sediments (after Moine et al. 1981). Note the concentration of sample points along the illite-dolomite join. Most samples plotting towards the Ca-corner are sulphate-bearing.*

Most of the Salina specimens that fall on the latter trend have high SO_3 values indicating that the Ca enrichment is the result of the presence of sulphates. There is a striking restriction of the Salina samples to the Al-dolomite axis with virtually no indication of compositions lying on the Mg-enriched side of this line. This relationship implies the absence of the Mg-enriched clay fraction found by Jeans (1978) to be characteristic of the Keuper Marl, a relationship that is confirmed in the clay mineral studies. The Salina sediments confirm the validity of the field of evaporative sediments indicated by Moine *et al.* (1981), showing even less overlap with the field of normal marine sediments than their data set. They explained the breadth of the overlap as due to the presence of data from marginal settings around evaporite basins.

Other compositional features are derived from the mineralogy of these rocks. Fe/Mg molar ratios are commonly very low. Moine *et al.* (1981) quote values of 0.9 for normal marine dolomite-free samples and values of 0.3 for evaporative equivalents. The most Fe-rich Salina specimen has a value of 0.27. Na/Al molar ratios are usually extremely low in halite-free rocks inasmuch as halite is virtually the only Na-rich mineral to be found in these rocks. The mean Na/Al ratio for Salina sediments is 0.074 (standard deviation (st. dev.) 0.065). This parameter is, however, not a good discriminant for evaporative sediments because normal marine equivalents have values < 0.10 (Moine *et al.* 1981). K/Al molar ratios, on the other hand, mainly reflect the presence of K-rich illites with possibly some contribution from detrital and/or diagenetic K-feldspars. Normal marine sediments have mean values of approximately 0.24, whereas evaporative sediments are usually much higher, reflecting the K-rich nature of brines in the gypsum and halite saturation range. The Salina sediments have a mean K/Al ratio of 0.39 (st. dev. 0.18).

Lithium geochemistry is controlled by the high Li values common in the Mg-rich clays and chlorites, and the very low tolerance for Li by the dolomite structure. Mean values of 152, 151, and 72 parts per million (ppm) Li in the dolomitic argillites, dolomitic marls, and the argillaceous dolomites of the Salina Formation (Table 148.1) are characteristic of evaporative rocks. Li/Mg ratios therefore depend on the relative proportions of clay minerals and carbonates. High absolute levels of Li (> 100 ppm) and high Li/Mg ratios are diagnostic of evaporative clay-rich sediments. In the Salina data set the maximum Li value is 310 ppm and the highest Li/Mg ratio is 0.0048.

Boron in clay sediments has long been regarded as being a paleosalinity indicator, although the indication may be rendered invalid if there is significant detrital tourmaline in the sediments (Degens *et al.* 1957). More recently a salinity scale based on B/Al molar ratios has been proposed by Porthault (1978, quoted by Moine *et al.* 1981) in which B/Al values < 0.004 are identified as characterizing hyposaline conditions, values between 0.004 and 0.006 are characteristic of normal marine conditions, and values > 0.006 are associated with hypersaline deposits. Saline values range from 0.0063 to 0.0997 (with 1 anomalously higher value), and with a mean of 0.0172 (st. dev. 0.0183), well within the evaporative range.

The halogens are highly characteristic of evaporative rocks. In the Salina collection chlorine reaches maximum values of 199 000 ppm and bromine 170 ppm. The mean Br/Cl (weight) ratio of all 68 specimens is 0.0152, substantially higher than

TABLE 148.2. CORRELATION COEFFICIENTS OF DETRITAL INDICATOR ELEMENTS IN SALINA SEDIMENTS.

Cation	Si	Al	Fe(total)
Ti	+0.957	+0.947	+0.906
K	+0.919	+0.928	+0.880
Sc	+0.861	+0.917	+0.888
V	+0.898	+0.973	+0.952
Cr	+0.850	+0.897	+0.900
Ni	+0.775	+0.834	+0.877
Cu	+0.294	+0.346	+0.388
Zn	+0.530	+0.563	+0.528
Br	+0.398	+0.410	+0.421
Rb	+0.830	+0.889	+0.855
Zr	+0.764	+0.620	+0.546
Ba	+0.915	+0.910	+0.892
U	+0.496	+0.543	+0.498

that of modern seawater, i.e. 0.00347 (Brehler and Fuge 1974), suggesting that a partitioning process was operative. Strong correlations with organic carbon have been noted elsewhere (Cosgrove 1970; Price *et al.* 1970), but such an explanation does not appear to be a factor here. On the other hand, bromine has moderate, positive correlation coefficients with Si and Al, (+0.398 and +0.410 respectively). It may be that the bromine is adsorbed on the surface of clay minerals or other detrital particles as suggested by Walters and Winchester (1971). Average fluorine values for the dolomitic marls exceed 1700 ppm (Table 148.1), much in excess of normal shales (500 ppm, Wedepohl 1979), and are even higher in the carbonate rocks.

GEOCHEMICAL INDICATORS OF DEPOSITIONAL ENVIRONMENTS

The Caledonia and Tilbury sites lie within the "marginal bank" environment of Nurmi and Friedman (1977), with the Lambton site situated within the "interpinnacle shelf", and the Michigan borehole within the "basin centre" areas. One of the goals of the study was to determine whether there are geochemical parameters that change from one lithofacies to the next and reflect differences in the influx of detritus, evaporite mineral deposition, or adsorptive characteristics of the clay minerals. The limited number of samples from Michigan, and the bias of their lithological types to the 2 most calcareous rock types severely limit the extent to which generalizations about basin margin to centre changes can be made. We present the data as they exist and emphasize the tentativeness of our interpretations.

Detrital indicators include the generally lithophile elements and those trace elements that are characteristic of silicates. Correlation coefficients of a group of elements believed to fall into this category with Si, Al, and Fe, are given in Table 148.2. Most of these elements decrease gradually from the marginal bank complex to the basin centre. Some irregularities in the data such as a slight peak in the Cr data from the interpinnacle shelf zone and a low peak in the Zr data in the Tilbury site may not be statistically valid, or may reflect variations of the sediment source and dispersal patterns across the region. The very limited data from Michigan suggest a reduction of the clastic load in the basin centre.

TABLE 148.3. CORRELATION COEFFICIENTS AMONG ILLITE INDICATOR ELEMENTS AND Li, B, AND Ba.

	Si	Al	K
Li	+0.695	+0.673	+0.791
B	+0.572	+0.714	+0.592
Ba	+0.937	+0.910	+0.829

Amongst the elements that reflect the evaporative process are Br, Cl, F, Na, and Sr. Superficially, Nb has a distribution pattern very similar to that of Na with an apparent peak in the Lambton hole but this is an artifact of one anomalous value. Nb correlates very weakly positive with Na and negatively with Cl. Its strongest positive correlations are with the lithophile elements. Cs is in an identical relationship; it has a strong positive correlation with Nb and other lithophile elements.

Na and Cl are not very reliable indicators in this data set inasmuch as they principally reflect the presence and abundance of halite in the sample. Nevertheless, the samples show marked increases of both elements in the interpinnnacle shelf and basin centre areas, as would be expected from the known distribution of halite in each lithofacies. As noted previously, bromine does not follow the same pattern. Br/Cl ratios decrease markedly from the margin to the centre, the values being 0.0370 at Caledonia, 0.0125 at Tilbury, 0.0062 at Lambton, and 0.0033 in the basin centre. Furthermore, the Br/Cl correlation coefficient is -0.133, while the Br/Si value is +0.494, Br/K is +0.437, etc. It is clear that in the present samples, bromine correlates much more closely with silicate minerals, possibly illite, than it does with halite. Fluorine shows a distinct tendency to be concentrated at Caledonia but it shows no strong correlations with any other element.

Elements that appear to be associated with clay minerals include Li, B, and Ba. Table 148.3 illustrates strong correlations between the illite indicator elements, Si, Al, and K and these elements. It is interesting to note that the B/Al ratio as an indicator of paleosalinity increases continuously from Caledonia to the basin centre, the value at Caledonia being 0.0108, at Tilbury it is 0.0121, at Lambton 0.0201, and at the Michigan site it is 0.0550. From the available data it appears that this ratio may be one of the most promising parameters to outline the paleosaline characteristics of the depositional basin.

CLAY MINERAL STUDIES

Insoluble residues from the more siliceous samples were analyzed using the X-Ray Diffractometry facilities of the University of Guelph. Specific sample preparation and analytical techniques are available from the authors. The results of this study are contained in Table 148.4. Illite and quartz are almost

TABLE 148.4. SUMMARY OF CLAY MINERAL DETERMINATIONS.

Sample	Illite	Kaolinite	Chlorite	Vermiculite	Quartz	Albite	Microcline	Other	Unknown
Caledonia									
3	X	?	?		X	M		Dol.	
5	X	?	X	X	M				
7	X		X		M	?			
9	X	X			X				4.67-4.87A
Tilbury									
32	X		X		X			Dol.	
37	X	X		?	M	M			
Lambton									
41	X	?	?		M	M			
42	X				X		M	Dol.	7.08A
44	X		M						
45	X		X		M				
46	X		X		M	M			
48	X		X		M				
49	X		X		X				
50	X	X		?	X	X		Dol.	
51	X	M	?		M	M			
52	X		X		X	M			
53	X		X		X	M			
54	X		X		M	M			
56	X						?	Anh.	
58	X				X				5.75A
59	X							Dol. Anh.	
60	X				M				3.55A
63	X				M				4.67-4.92A
64	X				M	M			4.67-4.92A
Michigan									
65					X			Dol.	
66	M	?	X		X			Dol.	4.76A
67						X		Anh. Dol.	

ubiquitous with chlorite and albite next in abundance. Despite careful scrutiny of the X-ray diffractometer traces, no evidence of smectite or sepiolitic clays was found, a relationship that conforms with the previous lithogeochemical evidence that such clays are not present. Minor indications of vermiculite constitute the only evidence of a highly magnesian clay phase. Kaolinite was definitely identified in 3 samples and was a minor or dubious phase in 5 additional samples; it was found at all 4 sample sites.

The Lambton Core provided the most complete set of results. Illite and quartz are present throughout the B and F units, however, kaolinite was identified in sample 50 within the F unit. In this sample a 7 angstrom unit (Å) peak, which is common to both chlorite and kaolinite, is present, thus the identification of kaolinite must be taken with caution.

Unidentified peaks were present in a number of the traces as indicated in Table 148.4, notably a broad peak from 4.67 to 4.92 Å, and sharper peaks at 3.55, 4.75, and 7.08 Å. Although illite does have a peak at 4.95 Å, it is thought that the broad peak might be due to zeolites such as stilbite (4.68 Å), brewsterite (4.66 Å), or edingtonite (4.80 Å). The 3.55 Å peak may be due to anatase (3.51 Å), anhydrite (3.50 Å), or septechlorite (3.58 Å). The 7.08 Å peak may represent septechlorite (7.19 Å) or chlorite (7.07 Å). In none of these cases was it considered justifiable to identify the mineral on the basis of 1 peak.

The prevalence of illite and chlorite as the principal layer silicates in the Salina sediments is evidently typical of Paleozoic evaporitic rocks (Droste 1963; Mossman *et al.* 1982). The absence of magnesian-rich phases such as sepiolite and the smectites, regarded by Jeans (1978) as forming diagenetically in hypersaline conditions is more noteworthy. Only vermiculite has been identified in these rocks and only with certainty in 1 specimen. Bartholome (1966) observed that sepiolite appears to be absent in pre-Mesozoic sediments and speculated that the cause may be related to compositional differences in seawater before that time. Mossman *et al.* (1982), however, report sepiolite from the Devonian Prairie Evaporite and suggest it is the oldest such assemblage recorded. Grim (1968) futhermore states that

TABLE 148.5 ANALYSES OF SALINA SEDIMENTS

SAMPLE	LOCATION	HOLE	DEPTH (m)	UNIT
1	Caledonia	80-170	21.0	B
2	Caledonia	80-170	31.7	B
3	Caledonia	80-171	21.9	B
4	Caledonia	80-171	28.3	B
5	Caledonia	80-172	27.7	B
6	Caledonia	80-172	33.2	B
7	Caledonia	80-173	23.8	B
8	Caledonia	80-173	29.5	B
9	Caledonia	80-174	23.2	B
10	Caledonia	80-174	29.9	B
11	Caledonia	80-176	21.0	B
12	Caledonia	80-176	28.0	B
13	Caledonia	80-176	31.1	B
14	Caledonia	80-177	20.9	B
15	Caledonia	80-177	28.3	B
16	Fletcher F.	33411	270.0	G

SAMPLE	SiO2	TiO2	Al2O3	FeO	MnO	MgO	CaO	Na2O	K2O	P2O5	LOI	CO2	TOC	F	Cl	S
1	13.6	0.17	4.63	1.46	0.022	17.9	23.5	0.18	1.59	0.04	37.4	n.d.	0.22	0.170	0.050	0.60
2	17.0	0.19	5.30	1.37	0.014	8.99	21.3	0.14	2.12	0.06	25.5	n.d.	0.09	0.200	0.005	11.3
3	42.9	0.52	11.2	3.32	0.028	9.60	9.67	0.21	4.53	0.09	17.8	n.d.	0.06	0.340	0.010	0.460
4	5.03	0.03	0.68	0.66	0.018	18.9	27.1	0.06	0.24	0.03	41.2	n.d.	0.16	0.620	0.015	2.93
5	42.5	0.52	10.8	3.17	0.025	9.57	9.95	0.29	4.21	0.09	18.2	n.d.	0.08	0.270	0.025	0.420
6	6.28	0.06	1.55	0.74	0.017	20.6	27.6	0.10	0.54	0.04	42.6	44.2	0.05	0.076	0.040	0.330
7	41.8	0.51	10.4	3.09	0.031	9.96	10.5	0.31	4.06	0.08	8.8	n.d.	0.06	0.300	0.020	0.450
8	8.90	0.07	1.66	0.82	0.018	17.1	25.9	0.09	0.67	0.03	38.4	n.d.	0.15	0.083	0.055	3.42
9	37.3	0.46	10.1	3.08	0.025	9.35	12.1	0.20	4.02	0.08	19.0	n.d.	0.05	0.310	0.010	2.17
10	14.4	0.19	4.10	1.25	0.018	17.9	23.1	0.14	1.66	0.07	36.8	n.d.	0.03	0.130	0.045	0.310
11	33.9	0.42	9.67	2.89	0.023	7.60	13.0	0.24	3.73	0.07	18.1	n.d.	0.04	0.300	0.005	5.52
12	15.4	0.20	4.44	1.30	0.018	17.6	22.7	0.14	1.79	0.06	36.4	n.d.	0.06	0.140	0.035	0.340
13	23.8	0.37	6.75	2.18	0.017	14.3	18.1	0.21	2.36	0.06	30.0	n.d.	0.08	0.170	0.080	0.700
14	11.5	0.13	3.45	1.43	0.021	18.6	25.0	0.14	1.18	0.04	38.7	n.d.	0.18	0.120	0.050	0.630
15	23.0	0.21	4.74	1.60	0.026	13.8	20.0	0.11	2.24	0.08	29.6	n.d.	0.16	0.130	0.040	2.62
16	14.6	0.15	3.36	1.04	0.010	6.81	27.3	0.14	1.49	0.05	13.5	n.d.	0.45	0.240	0.100	18.1

SAMPLE	Li	B	Sc	V	Cr	Co	Ni	Cu	Zn	Br	Rb	Sr	Y	Zr	Nb	Sb	Cs	Ba	Pb	Th	U
1	83	80	4.8	32	22	6.0	19	10	22	8.5	40	280	10	<10	10	0.2	1.8	40	20	3.3	2.4
2	130	140	5.8	37	28	9.0	24	12	26	4.8	50	280	20	20	20	0.5	2.6	50	20	3.4	1.6
3	240	220	12	75	59	16	33	16	51	6.3	110	110	20	120	30	0.6	4.9	290	16	8.8	2.5
4	20	30	0.8	12	4.0	3.0	12	7.0	7.5	8.3	30	11240	<10	<10	<10	0.4	<0.4	70	24	0.8	1.0
5	240	200	11	68	52	13	31	14	47	5.8	120	80	20	160	<10	0.5	4.9	250	14	8.8	2.5
6	29	40	1.7	12	10	3.0	10	3.0	9.0	7.7	<10	210	10	<10	10	<0.2	0.8	10	14	1.1	1.3
7	190	160	11	64	53	15	34	16	49	6.6	110	190	20	130	10	0.6	4.7	290	14	8.8	2.5
8	44	50	1.9	14	9.0	5.0	16	12	12	7.1	20	2150	<10	<10	10	0.7	0.6	10	22	1.4	1.6
9	270	230	11	72	57	15	33	19	48	5.4	100	110	30	110	<10	0.6	3.9	260	14	8.5	2.3
10	100	90	4.3	28	22	6.0	18	7.5	20	8.3	50	130	<10	10	10	0.3	2.5	40	14	2.8	2.6
11	220	190	11	69	53	15	34	14	50	5.5	100	210	<10	100	<10	0.5	4.6	240	20	8.0	2.5
12	120	90	0.3	32	2.0	7.0	19	8.0	23	0.5	60	130	10	20	<10	<0.2	<0.4	60	16	<0.4	2.4
13	88	200	7.6	53	39	12	28	32	29	12	90	8080	10	50	10	0.6	4.3	140	36	6.6	2.4
14	73	60	3.7	26	20	6.0	17	8.5	19	10	30	300	30	20	<10	0.3	2.6	20	18	2.7	2.1
15	110	70	5.0	30	25	8.0	23	11	25	8.6	40	2190	10	40	<10	0.6	1.8	130	20	3.9	2.1
16	130	70	3.4	19	25	8.0	24	12	21	11	30	900	<10	20	<10	0.6	1.5	<10	52	3.1	2.0

TABLE 148.5 ANALYSES OF SALINA SEDIMENTS (continued)

SAMPLE	LOCATION	HOLE	DEPTH (m)	UNIT	S102	T102	A1203	FeO	MnO	MgO	CaO	Na20	K20	P205	LOI	C02	TOC	F	Cl	S
17	Fletcher F.	33411	272.0	G	0.69	0.00	0.09	0.85	0.012	14.1	32.9	0.04	0.08	0.01	28.2	n.d.	0.16	0.045	0.090	13.5
18	Fletcher F.	33411	275.5	F	32.6	0.35	7.37	3.00	0.022	13.1	14.7	0.42	3.05	0.08	24.0	n.d.	0.05	0.220	0.275	0.750
19	Fletcher F.	33411	278.0	F	9.51	0.09	2.04	1.03	0.025	19.3	26.2	0.10	0.84	0.03	41.1	n.d.	0.17	0.077	0.165	0.360
20	Fletcher F.	33411	281.0	F	33.5	0.44	9.54	3.24	0.026	9.75	14.2	0.31	3.74	0.10	18.2	n.d.	0.04	0.220	0.180	3.73
21	Fletcher F.	33411	284.0	F	28.7	0.31	6.06	2.06	0.026	13.6	17.4	0.18	3.04	0.09	28.0	n.d.	0.05	0.100	0.180	0.520
22	Fletcher F.	33411	287.0	F	33.4	0.30	6.50	1.93	0.023	12.5	15.9	0.17	3.63	0.09	25.2	n.d.	0.06	0.100	0.065	0.530
23	Fletcher F.	33411	290.0	F	33.6	0.37	7.33	2.30	0.030	12.0	15.1	0.12	3.85	0.10	24.3	n.d.	0.06	0.130	0.085	0.690
24	Fletcher F.	33411	292.5	F	33.3	0.42	8.61	3.07	0.025	11.0	15.1	0.25	3.68	0.10	20.5	n.d.	0.07	0.210	0.135	2.86
25	Fletcher F.	33411	295.0	F	32.7	0.34	7.20	2.30	0.019	12.5	15.3	0.10	3.80	0.10	24.5	n.d.	0.06	0.180	0.155	0.890
26	Fletcher F.	33411	298.5	F	0.88	0.00	0.21	0.44	0.008	12.1	30.6	0.02	0.02	0.01	24.9	n.d.	0.12	0.030	0.065	16.4
27	Fletcher F.	33411	302.5	F	33.0	0.40	7.96	2.46	0.017	12.6	14.3	0.17	4.04	0.09	24.1	n.d.	0.16	0.270	0.095	0.600
28	Fletcher F.	33411	304.5	E	3.31	0.02	0.66	0.25	0.006	14.7	29.8	0.06	0.22	0.02	30.3	n.d.	0.11	0.078	0.030	12.7
29	Fletcher F.	33411	340.5	E	20.7	0.22	4.47	1.54	0.016	16.3	21.2	0.18	2.00	0.07	33.2	n.d.	0.09	0.260	0.160	0.450
30	Fletcher F.	33411	344.0	C	35.0	0.38	7.61	2.29	0.017	9.25	15.5	0.30	3.70	0.09	18.5	n.d.	0.04	0.110	0.210	4.10
31	Fletcher F.	33411	346.5	C	52.5	0.35	7.50	2.24	0.021	7.52	9.44	0.55	2.90	0.08	16.0	n.d.	0.12	0.120	0.375	0.580
32	Fletcher F.	33411	350.0	C	35.7	0.48	10.6	4.05	0.026	11.1	11.9	0.33	4.04	0.08	21.9	n.d.	0.04	0.200	0.230	0.380

SAMPLE	Li	B	Sc	V	Cr	Co	Ni	Cu	Zn	Br	Rb	Sr	Y	Zr	Nb	Sb	Cs	Ba	Pb	Th	U
17	8.0	40	0.2	5.0	<2.0	3.0	12	4.5	10	9.2	10	1360	<10	<10	<10	0.3	0.4	<10	24	0.3	2.1
18	240	140	7.4	43	51	13	37	19	41	24	70	170	20	110	10	0.7	2.9	230	22	6.5	2.5
19	47	50	2.1	15	12	4.0	15	7.0	12	14	10	1970	20	<10	0.2	1.4	20	22	1.7	0.9	
20	240	190	10	69	72	15	43	17	49	18	90	960	20	80	<10	0.6	4.7	200	20	7.3	2.7
21	90	90	6.5	38	40	9.0	29	18	32	18	60	2010	20	80	10	0.5	2.3	140	32	5.6	1.8
22	85	100	6.2	36	42	10	31	16	32	9.6	60	1090	20	80	<10	0.4	2.9	170	18	6.3	2.2
23	110	100	7.6	42	56	12	33	13	43	11	90	470	20	100	<10	0.4	3.1	200	24	7.0	2.1
24	220	170	9.0	57	64	13	36	15	49	13	90	260	20	80	10	0.5	5.0	200	20	7.3	2.5
25	180	110	6.6	45	51	11	29	17	35	13	70	150	<10	70	10	0.5	2.9	200	20	6.3	3.0
26	10	30	0.2	4.0	<2.0	3.0	11	1.5	6.5	8.7	10	1310	<10	<10	<10	<0.2	<0.4	<10	26	<0.5	1.2
27	290	140	7.3	57	59	13	40	15	44	11	80	90	<10	90	10	0.4	3.5	210	28	7.4	4.5
28	63	30	0.7	9.0	4.0	3.0	12	4.5	9.5	5.9	<10	2570	10	<10	<10	<0.2	<0.4	<10	22	0.4	2.7
29	140	80	4.6	31	26	8.0	22	13	25	15	30	140	10	30	20	<0.2	2.4	90	22	3.6	1.8
30	75	110	7.4	40	46	8.0	20	10	25	22	70	880	20	150	<10	0.3	2.7	240	12	6.6	2.7
31	100	130	7.0	40	38	13	35	19	33	38	60	200	20	250	10	0.9	2.8	300	20	6.5	2.9
32	130	220	12	74	70	33	71	82	59	23	110	100	10	80	30	1.2	5.2	260	16	6.8	3.9

TABLE 148.5 ANALYSES OF SALINA SEDIMENTS (continued)

SAMPLE	LOCATION	HOLE	DEPTH (m)	UNIT
33	Fletcher F.	33411	353.0	C
34	Fletcher F.	33411	356.0	C
35	Fletcher F.	33411	359.0	C
36	Fletcher F.	33411	362.0	C
37	Fletcher F.	33411	365.0	C
38	Fletcher F.	33411	368.0	C
39	Fletcher F.	33411	373.0	C
40	Fletcher F.	33411	375.5	B
41	Lambton	OGS-82-1	438.4	G
42	Lambton	OGS-82-1	448.2	F
43	Lambton	OGS-82-1	457.4	F
44	Lambton	OGS-82-1	459.6	F
45	Lambton	OGS-82-1	463.5	F
46	Lambton	OGS-82-1	467.7	F
47	Lambton	OGS-82-1	470.0	F
48	Lambton	OGS-82-1	475.7	F

SAMPLE	S102	T102	A1203	FeO	MnO	MgO	CaO	Na20	K20	P205	LOI	CO2	TOC	F	Cl	S
33	27.5	0.35	7.73	2.96	0.036	13.5	16.9	0.23	3.35	0.09	27.6	n.d.	0.10	0.110	0.160	0.410
34	37.3	0.44	9.63	2.90	0.028	10.4	12.3	0.36	4.04	0.09	22.2	n.d.	0.09	0.150	0.370	0.240
35	44.1	0.59	8.15	2.16	0.021	7.03	12.0	0.46	3.82	0.13	14.6	n.d.	0.02	0.960	0.330	3.29
36	14.2	0.14	3.57	1.26	0.021	6.88	25.5	0.15	1.63	0.06	14.5	n.d.	0.10	0.660	0.035	16.8
37	38.1	0.47	10.8	3.31	0.019	10.3	11.0	0.44	4.27	0.08	20.6	n.d.	0.07	0.300	0.395	0.490
38	17.5	0.24	4.87	1.36	0.014	16.9	21.5	0.14	2.19	0.05	35.1	n.d.	0.40	0.190	0.080	0.490
39	17.5	0.16	4.54	1.31	0.017	8.37	23.3	0.13	2.24	0.06	17.0	n.d.	0.34	0.230	0.050	13.4
40	9.03	0.08	2.18	0.76	0.010	7.68	29.6	0.10	1.08	0.04	15.2	n.d.	0.10	0.079	0.025	19.9
41	25.1	0.27	5.70	1.70	0.016	14.5	19.3	0.18	2.55	0.08	30.5	29.1	n.d.	0.110	0.260	0.840
42	27.3	0.39	7.30	2.52	0.022	13.8	17.1	0.26	2.78	0.09	28.1	25.7	n.d.	0.130	0.370	0.930
43	43.6	0.56	10.9	3.82	0.028	9.16	9.00	0.33	4.20	0.13	18.1	12.9	n.d.	0.190	0.630	0.490
44	39.2	0.52	10.7	3.89	0.035	10.5	10.3	0.33	3.67	0.09	20.3	16.1	n.d.	0.210	0.590	0.470
45	33.7	0.40	8.02	2.81	0.030	11.9	14.6	0.28	2.99	0.10	24.5	21.2	n.d.	0.110	0.560	0.780
46	36.6	0.47	8.77	2.67	0.031	11.0	13.0	0.48	2.93	0.12	23.5	19.0	n.d.	0.100	0.510	0.410
47	33.0	0.37	7.38	2.43	0.028	12.5	15.0	0.35	2.57	0.10	26.1	21.8	n.d.	0.110	0.380	0.370
48	30.3	0.40	7.92	2.96	0.030	13.0	15.3	0.35	2.56	0.11	26.4	22.7	n.d.	0.120	0.450	0.670

SAMPLE	Li	B	Sc	V	Cr	Co	Ni	Cu	Zn	Br	Rb	Sr	Y	Zr	Nb	Sb	Cs	Ba	Pb	Th	U
33	57	120	8.5	48	55	16	46	40	47	18	70	120	30	50	<10	0.5	2.6	200	22	6.0	2.7
34	90	180	10	67	56	12	32	10	48	39	80	100	30	110	10	0.3	4.0	240	18	7.6	3.3
35	61	110	8.3	42	64	13	32	12	33	34	70	1000	40	440	20	0.2	3.0	300	20	14	3.8
36	46	70	4.8	21	25	10	26	16	26	6.5	20	1000	10	30	10	0.8	1.6	10	56	3.5	1.7
37	220	240	11	72	63	12	28	15	45	40	120	130	30	80	10	0.9	4.6	280	12	7.9	3.1
38	120	100	4.8	38	30	9.0	29	18	34	9.1	40	740	<10	30	10	0.5	2.0	60	20	4.2	5.2
39	220	120	4.7	28	23	10	27	12	24	6.3	40	1370	10	30	<10	0.6	2.0	40	26	3.3	1.7
40	49	80	2.2	14	11	7.0	20	16	13	8.2	20	2490	<10	<10	10	0.4	0.7	10	20	1.6	1.1
41	53	180	6.9	44	50	11	28	14	18	20	30	220	10	40	30	0.3	2.0	110	50	5.0	1.9
42	130	180	7.2	52	62	14	37	17	41	27	60	80	<10	60	20	0.4	3.0	170	58	5.0	4.5
43	220	230	10	74	120	16	45	13	60	48	120	190	40	130	30	0.2	4.0	350	24	8.0	3.0
44	240	260	11	72	82	23	60	53	63	45	90	250	20	90	20	0.9	4.0	320	40	7.0	3.9
45	130	160	8.0	56	66	14	38	16	44	41	60	350	10	100	20	0.2	3.0	220	36	6.0	3.1
46	110	150	8.4	60	68	16	41	18	51	39	50	280	20	100	20	0.2	4.0	280	32	7.0	2.7
47	120	140	7.4	50	56	13	36	14	41	29	50	180	10	130	10	0.2	3.0	220	36	7.0	2.2
48	110	140	8.3	62	64	16	48	23	46	39	60	1280	20	70	10	0.4	3.0	230	68	6.0	2.8

TABLE 148.5 ANALYSES OF SALINA SEDIMENTS (continued)

SAMPLE	LOCATION	HOLE	DEPTH (m)	UNIT	S102	T102	A1203	FeO	MnO	MgO	CaO	Na20	K20	P205	LOI	CO2	TOC	F	Cl	S
49	Lambton	OGS-82-1	482.3	F	27.0	0.31	5.72	1.60	0.019	14.4	18.0	0.19	1.98	0.08	30.4	25.7	n.d.	0.130	0.410	0.250
50	Lambton	OGS-82-1	486.2	F	39.1	0.50	10.2	3.04	0.023	10.7	10.8	0.40	4.12	0.10	20.4	15.9	n.d.	0.250	0.520	0.610
51	Lambton	OGS-82-1	487.7	F	18.5	0.23	4.68	1.57	0.013	7.30	27.3	0.13	1.97	0.07	14.0	12.0	n.d.	0.130	0.210	13.4
52	Lambton	OGS-82-1	537.0	C	23.3	0.31	6.05	2.26	0.036	14.7	19.1	0.32	0.99	0.08	32.8	27.9	n.d.	0.090	1.23	0.46
53	Lambton	OGS-82-1	543.5	C	38.2	0.65	5.20	1.37	0.019	6.26	8.65	7.66	2.11	0.21	24.7	11.6	n.d.	0.049	17.2	0.34
54	Lambton	OGS-82-1	552.2	C	42.8	0.54	10.8	3.65	0.040	7.67	8.24	2.07	2.12	0.14	21.8	10.4	n.d.	0.094	4.55	0.20
55	Lambton	OGS-82-1	557.7	C	29.6	0.38	7.87	2.83	0.028	12.7	15.2	0.51	1.52	0.08	28.7	21.9	n.d.	0.140	1.33	0.49
56	Lambton	OGS-82-1	568.2	B	0.22	<0.01	0.02	0.05	0.002	0.34	29.3	12.0	0.01	0.01	9.85	0.9	n.d.	0.014	19.9	18.8
57	Lambton	OGS-82-1	570.5	B	0.48	<0.01	0.09	0.13	0.004	11.3	38.0	<0.01	<0.01	0.01	23.9	22.9	n.d.	0.042	0.190	14.4
58	Lambton	OGS-82-1	663.0	A-2	0.89	0.01	0.21	0.05	0.003	16.9	23.2	5.37	0.64	0.01	44.8	33.9	n.d.	0.037	18.1	0.09
59	Lambton	OGS-82-1	672.8	A-2	4.44	0.06	1.67	1.22	0.009	18.3	27.0	0.01	0.03	0.02	47.2	39.6	n.d.	0.048	4.15	0.410
60	Lambton	OGS-82-1	677.6	A-2	7.85	0.11	3.41	0.86	0.007	10.9	35.3	0.01	0.08	0.03	41.1	36.5	n.d.	0.065	0.750	0.630
61	Lambton	OGS-82-1	687.0	A-2	17.4	0.31	6.27	2.16	0.013	9.63	24.1	0.24	1.85	0.06	23.0	20.0	n.d.	0.160	0.730	8.37
62	Lambton	OGS-82-1	695.7	A-2	5.50	0.05	1.57	0.45	0.005	7.35	36.7	0.11	0.17	0.02	16.5	15.3	n.d.	0.061	0.200	18.0
63	Lambton	OGS-82-1	729.0	A-1	1.91	0.01	0.68	0.67	0.005	21.4	29.0	<0.01	0.01	0.02	46.0	43.1	n.d.	0.060	2.15	0.550
64	Lambton	OGS-82-1	743.3	A-1	9.18	0.17	4.05	1.03	0.006	19.1	25.6	0.07	0.64	0.04	40.1	38.5	n.d.	0.097	0.340	0.900

SAMPLE	Li	B	Sc	V	Cr	Co	Ni	Cu	Zn	Br	Rb	Sr	Y	Zr	Nb	Sb	Cs	Ba	Pb	Th	U
49	140	90	5.8	40	46	11	26	14	32	30	40	1050	30	110	20	0.4	2.0	160	36	5.0	2.3
50	310	190	9.8	72	76	16	45	23	53	39	90	270	<10	90	40	0.5	3.0	340	50	7.0	6.1
51	190	100	4.7	36	42	12	31	11	34	19	30	1340	20	40	10	0.3	<2.0	50	58	3.0	1.7
52	59	110	6.0	42	42	15	30	28	35	110	20	160	20	80	20	0.4	3.0	140	34	5.0	1.7
53	22	70	5.2	26	38	9.0	14	13	30	83	40	100	20	250	10	<0.2	<2.0	210	54	9.0	2.2
54	87	150	10	72	70	25	46	24	64	170	40	220	30	120	20	0.7	4.0	450	32	7.0	3.0
55	130	120	8.4	52	56	15	38	17	49	160	30	170	10	70	20	0.3	4.0	230	38	6.0	2.1
56	3.0	80	<0.5	8.0	18	5.0	10	1.0	6.5	23	10	2280	<10	<10	<10	<0.2	2.0	<10	34	<1.0	<0.1
57	5.0	20	<0.5	10	18	5.0	11	1.0	6.0	13	20	1480	<10	<10	<10	<0.2	<2.0	<10	32	<1.0	0.9
58	6.0	20	<0.5	6.0	12	5.0	12	2.0	8.0	42	20	90	<10	<10	10	0.2	<2.0	<10	34	<1.0	1.7
59	19	120	1.8	20	26	7.0	18	6.0	14	100	<10	210	<10	<10	10	<0.2	<2.0	10	32	1.0	0.8
60	31	210	3.5	30	28	10	23	8.0	18	52	<10	250	<10	<10	10	<0.2	<2.0	<10	42	1.0	1.6
61	81	480	7.2	50	44	14	26	15	34	60	50	880	<10	30	20	0.6	5.0	50	34	5.0	1.3
62	29	120	1.6	16	20	8.0	19	3.5	11	16	20	1640	<10	<10	10	<0.2	<2.0	<10	46	1.0	0.5
63	8.0	40	0.7	12	14	7.0	16	3.0	12	24	10	1860	<10	<10	10	<0.2	<2.0	<10	40	<1.0	2.0
64	34	150	3.9	34	30	9.0	25	13	25	19	20	1030	<10	<10	10	0.3	<2.0	60	44	2.0	6.1

TABLE 148.5 ANALYSES OF SALINA SEDIMENTS (continued)

SAMPLE	LOCATION	HOLE	DEPTH (m)	UNIT																
SiO_2	TiO_2	Al_2O_3		FeO	MnO		MgO	CaO	Na_2O		K_2O	P_2O_5	LOI	CO_2	TOC	F		Cl	S	
Li	B	Sc	V	Cr	Co	Ni	Cu	Zn	Br	Rb	Sr	Y	Zr	Nb	Sb	Cs	Ba	Pb	Th	U
65	Michigan	Bradley-4	1470.7	A-1?																
0.54	<0.01	0.11		0.04	0.002		21.7	29.0	0.03		0.03	0.01	48.9	45.5	n.d.	0.095		3.63	0.450	
3.0	20	<0.5	12	14	7.0	18	2.0	9.5	12	10	110	10	<10	10	0.2	<2.0	<10	52	<1.0	2.0
66	Michigan	Bradley-4	1472.2	A-1?																
1.55	0.02	0.37		0.12	0.003		21.8	29.3	0.03		0.01	0.02	47.2	45.4	n.d.	0.085		0.950	0.340	
5.0	30	<0.5	14	14	6.0	15	5.0	12	7.0	10	120	<10	<10	10	<0.2	<2.0	<10	36	<1.0	2.1
67	Michigan	Bradley-4	1478.3	A-1?																
1.14	0.01	0.35		0.13	0.003		20.9	31.2	0.02		0.02	0.02	43.2	43.5	n.d.	0.960		0.110	21.4	
5.0	40	<0.5	12	12	6.0	15	3.5	9.5	8.0	10	370	<10	<10	10	<0.2	<2.0	<10	42	<1.0	1.8
68	Michigan	Bradley-4	1484.4	A-1?																
1.39	<0.01	0.31		0.12	0.004		4.78	48.3	<0.01		<0.01	0.02	43.5	40.9	n.d.	0.300		0.160	0.460	
3.0	30	<0.5	20	18	8.0	18	4.0	10	8.0	10	2780	<10	<10	10	0.2	<2.0	<10	52	<1.0	2.0

smectites are generally absent in pre-Mesozoic sediments. The favoured explanation (Mossman *et al.* 1982) involves complex crystalloblastic changes which may involve clay/water reactions of a net metasomatic character such as the alteration of smectite to illite. If so, the present composition of the rocks on the illite-dolomite join (Figure 148.8) may not accurately reflect initial sediment compositions and the present clay mineral paragenesis may not be the same as at the time of deposition.

It is not clear at this stage whether the clay mineral assemblages of the Salina sediments are of detrital or diagenetic origin. The relative abundance of albite and microcline however suggests that diagenetic or syngenetic changes were responsible for part of the present insoluble constituents. Vermiculite was similarly likely produced syn- or post-depositionally. The absence of sepiolite and other hypersaline indicator clays is tentatively ascribed to post-depositional alteration. This problem is worthy of further investigation.

ACKNOWLEDGMENTS

The authors wish to acknowledge the assistance of Kathy LaHay in the preparation and analysis of the clay samples. The Ontario Geological Survey provided access to the Lambton County core which provided a valuable and complete section through the formation in the interpinnacle shelf zone. Dr. D. Russell was instrumental in guiding and expediting this sampling. Core material from Michigan was provided by the Department of Geological Sciences at the University of Michigan. Fluid inclusion microthermometry was provided by Dr. J. Guha and his assistant Suzanne Morasse à L'Université du Québec à Chicoutimi.

REFERENCES

Allen, P., and Keith, M.L.
1965: Carbon Isotope Ratios and Paleosalinities of Purbeck Wealden Carbonates; Nature, Volume 208, Number 5017, p.1278-1280.

Bartholome, P.
1966: Sûr L'abondance de la Dolomite et de la Sepiolite Dans les Series Sedimentaires; Chemical Geology, Volume 1, p.33-48.

Brand, U., and Veizer, J.
1981: Chemical Diagenesis of a Multicomponent Carbonate System—2: Stable Isotopes; Journal of Sedimentary Petrology, Volume 51, Number 3, p.987-997.

Brehler, B., and Fuge, R.
1974: Bromine; p.457-502 *in* Handbook of Geochemistry, edited by K.H. Wedepohl, Springer-Verlag, Berlin and Heidelberg, Volume 2, Part 4.

Cosgrove, M.A.
1970: Iodine in the Bituminous Kimmeridge Shales of the Dorset Coast, England; Geochimica et Cosmochimica Acta, Volume 34, p.340.

Degens, E.T., Williams, E.G., and Keith, M.L.
1957: Environmental Studies of Carboniferous Sediments—Part 1: Geochemical Criteria for Differentiating Marine from Fresh Water Shales; American Association of Petroleum Geologists, Bulletin, Volume 41, p.2427-2455.

Dellwig, L.F.
1972: Primary Sedimentary Structures of Evaporites; p.53-59 *in* Geology of Saline Deposits, Proceedings of the Hanover Symposium, UNESCO.

Deuser, W.G., Degens, E.T., and Stoffers, P.
1978: ^{18}O and ^{13}C Contents of Carbonates from Deep Sea Drilling Sites in the Black Sea; *in* Initial Reports of the Deep Sea Drilling Project, edited by D.A. Ross *et al.*, Volume 42, Part 2, United States Government Printing Office, Washington.

Droste, J.
1963: Clay Mineral Composition of Evaporite Sequences; p.47-54 *in* First Symposium on Salt, Northern Ohio Geological Society.

Grim, R.E.
1968: Clay Mineralogy; Second Edition, McGraw Hill, New York, 596p.

Holser, W.T.
1966: Bromide Geochemistry of Salt Rocks; Second Symposium on Salt, Northern Ohio Geological Society, Volume 1, p.248-276.

Jeans, C.V.
1978: The Origin of the Triassic Clay Assemblages of Europe with Special Reference to the Keuper Marl and Rhaetic of Parts of England; Philosophical Transactions of the Royal Society of London, Volume 289, Series A, p.549-637.

Keith, M.L., Anderson, G.M., and Eichler, R.
1964: Carbon and Oxygen Isotopic Composition of Mollusk Shells from Marine and Freshwater Environments; Geochimica et Cosmochimica Acta, Volume 28, p.1757-1786.

Lapcevic, P.
1985: Stable Isotope Variations of Sulfate Minerals from the Salina Formation; Unpublished B.Sc. Thesis, University of Waterloo, Waterloo, Ontario.

Matthews, R.D., and Elgeson, G.C.
1974: Origin and Implications of Mid-Basin Potash Facies in the Salina Salt of Michigan; Fourth Symposium on Salt, Northern Ohio Geological Society, Volume 1, p.15-35.

Miles, M.C.
1982: A Study of the Isotopic Composition of the Salina Formation Gypsum Deposit at Caledonia, Ontario; Unpublished B.Sc. Thesis, University of Waterloo, Waterloo, Ontario.

Miles, M.C., Fritz, P., Frape, S.K., Lawson, D.E., and Appleyard, E.C.
1984: Geochemical Study of the Salina Formation of Southern Ontario—Isotopes, Major and Minor Elements; Grant 148, p.147-163 *in* Geoscience Research Grant Program, Summary of Research 1983-1984, edited by V.G. Milne, Ontario Geological Survey, Miscellaneous Paper 121, 252p.

Moine, B., Sauvan, P., and Jarousse, J.
1981: Geochemistry of Evaporite Bearing Series: A Tentative Guide for the Identification of Metaevaporites; Contributions to Mineral Petrography, Volume 76, p.401-412.

Mossman, D.J., Delabio, R.N., and MacIntosh, A.D.
1982: Mineralogy of Clay Marker Seams in Some Saskatchewan Potash Mines; Canadian Journal of Earth Sciences, Volume 19, p.2126-2140.

Nurmi, R.D.
1974: The Lower Salina (Upper Silurian); Stratigraphy of a Desiccated, Deep Michigan Basin; Proceedings of the Ontario Petroleum Institute, Thirteenth Annual Conference, p.1-25.

Nurmi, R.D., and Friedman, G.M.
1977: Sedimentology and Depositional Environments of Basin-centre Evaporites, Lower Salina Group (Upper Silurian), Michigan Basin; *in* Reefs and Evaporites—Concepts and Depositional Models, American Association of Petroleum Geologists, Studies in Geology, Number 5.

Olsen, E.R.
1975: Oxygen and Sulfur Isotope Geochemistry of Marine Evaporites; Unpublished Ph.D. Thesis, McMaster University, Hamilton, Ontario.

O'Shea, K.
1985: Fluctuations in the Isotopic Composition of the Carbonates of the Late Silurian Salina Formation of the Michigan Basin; Unpublished B.Sc. Thesis, University of Waterloo, Waterloo, Ontario.

Pierre, C.
1981: Formation Actuelle de Dolomite Supralittorale Dans Des Sables Quartzofeldspathiques: Un Exemple au Sud de La Lagune Ojo de Liebre (Basse Californie, Mexique); Comptes Rendus de l'Academie des Sciences, Paris, Serie II - 73.

Pierre, C., and Fontes, J.C.
1978: Isotope Composition of Messinian Sediments from the Mediterranean Sea as Indicators of Paleoenvironments and Diagenesis; p.635-650 *in* Initial Reports of the Deep Sea Drilling Project, edited by D.A. Ross *et al.*, Volume 42, Part 1, United States Government Printing Office, Washington.

Price, N.B., Calvert, S.E., and Jones, P.G.W.
1970: The Distribution of Iodine and Bromine in the Sediments of Southwestern Barents Sea; Journal of Marine Research, Volume 28, p.22.

Rickard, L.V.
1969: Stratigraphy of the Upper Silurian Salina Group, New York, Pennsylvania, Ohio, Ontario; New York State Museum and Science Service, Map and Chart Series Number 12.

Veizer, J., Holser, W.T., and Wilgus, C.K.
1980: Correlation of $^{13}C/^{12}C$ and $^{34}S/^{32}S$ Secular Variations; Geochimica et Cosmochimica Acta, Volume 44, p.579-587.

Walters, L.J., and Winchester, J.W.
1971: Neutron Activation Analysis of Sediments for Halogens Using the Szilard-Chalmers Reactions; Analytical Chemistry, Volume 43, p.1020.

Wedepohl, K.H., Editor
1979: Handbook of Geochemistry; Volume 2, Springer-Verlag, Berlin and Heidelberg.

Grant 149 Structural Signature and Tectonic History of Deformed Gold-bearing Rocks in Northwestern Ontario

Hervé Hugon and W.M. Schwerdtner

Department of Geology, University of Toronto

ABSTRACT

Detailed structural studies in the Red Lake and Hemlo areas lead the authors to conclude that whatever the initial gold source, the structural signature of the rocks which now host gold is predominantly that of either brittle, brittle-ductile, or ductile shear zones. The tectonic history as revealed by large-scale structural analysis and U-Pb age-dating of zircons indicates that the generation of gold-bearing shear zones occurred on a shield-wide scale and was intimately associated with batholith emplacement. These batholiths are benchmarks for an Archean major tectonic event that occurred around 2700 m.y. ago.

INTRODUCTION

Detailed structural studies conducted in the Red Lake and Hemlo areas by the authors (Hugon and Schwerdtner 1984; Hugon 1984a, 1984b), by H.K. Poulsen in the Mine Center Region (Poulsen 1983), and by Stott and Wallace (1984) in the Pickle Lake area, indicate that the only structural signature common to gold-bearing rocks throughout northwestern Ontario is that of intense shearing. Depending on a number of factors including the pressure-temperature conditions, the quantity and type of fluids present and the rheological properties of the rock materials involved, intense shearing induced various degrees of mylonitization. Therefore a comprehensive definition of mylonite and mylonitization is given below.

A consideration of the detailed structural analyses conducted during this project together with recent U-Pb age dating of zircons (Geochronological Laboratory, Royal Ontario Museum, Toronto) yields important constraints on the tectonic history of the Red Lake belt based on detailed observations in the Madsen area and the A.W. White (formerly Dickenson) Mine.

MYLONITE AND MYLONITIZATION

As defined by Lapworth (1885), the term "mylonite" describes the particular behaviour peculiar to a given protolith under restricted conditions of deformation. Sibson (1977) clearly demonstrated the inadequacy of a classification based on the so-called brittle-ductile transition as brittle or ductile behaviour merely depends on strain rates and the presence or absence of fluids as well as the temperature conditions. Sibson's classification of fault rocks based on the presence or absence of ductile strain features is more appropriate as it includes any kind of protolith. However, the examples of the cataclasite and the mylonite series given by Sibson (1977) are exclusively from deformed, crystalline quartzo-feldspathic rocks. To avoid the problem of genetic affiliation to a particular protolith one only needs to consider the derivation of the term mylonite. Mylonite comes from the Greek term "mylon", i.e. a mill. Therefore a mylonite is the end product of any kind of original rock material that has gone "through the mill" *sensu stricto*, whatever the strain features exhibited by the end product, i.e. brittle or ductile.

As illustrated by the mechanical action of old coffee and pepper mills, the deformation mechanism involved in a mill is one of simple shear. The natural analogies of this simple shear apparatus are faults, fault zones, or shear zones. As such, any rock material which has been deformed by a shearing mechanism within a narrow zone (relative to its length) is a mylonite. The terms protomylonite, mylonite, and ultramylonite define increasing degrees of shearing or mylonization. While the effects of mylonitization are somewhat obvious for granitoid protoliths they are unfortunately more difficult to recognize in pelitic or tuffaceous protoliths unless kinematic indicators of non-coaxial deformation are available. As is often the case this especially applies when these fine-grained protoliths are deformed in a homogeneous simple shear where curvature of foliation cannot be used as a kinematic indicator.

Figure 149.1 illustrates different behaviour of rock materials under an ideal, simple shear mechanism of deformation. These diagrams may be taken to represent a single protolith with variable behaviour due to changes in P, T, fluid or strain rate conditions; or variable protoliths under the same conditions of deformation. In the case of shearing coeval with a regional metamorphism, one can predict that a competent protolith will deform in a brittle manner during the early stages of the deformation that precede the peak of metamorphism. R and R′ Riedel shear fractures will develop as well as P and P′ conjugate shear fractures with increasing strain. As temperature rises, plastic or ductile behaviour progressively take over during the peak of metamorphism and ductile features such as the S, C, and C′ fabrics are generated with increasing shear intensities. During this stage of ductile behaviour of the rock material the early veins formed by shear fracturing will either be boudinaged and/or ductily stretched, or buckled and/or rotated in a passive manner depending on their relative position to the extensional or shortening field of the strain ellipsoid (Figure 149.2). If the shearing outlasts the regional metamorphism then new R, R′, P, and P′ shear fractures can develop as the deformed rock material cools down. At this stage the conjugate sets of Riedel shear fractures are expected to develop unless the degree of anisotropy (e.g. planar fabric) developed within the strained material during the ductile stage is too high. In that latter case, the strong anisotropy or fabric within the rock material will control the generation of conjugate shear fractures. These anisotropy-controlled shear fractures develop at low angles (<45°) to the fabric or foliation (Harris and Cobbold 1984). Therefore, the

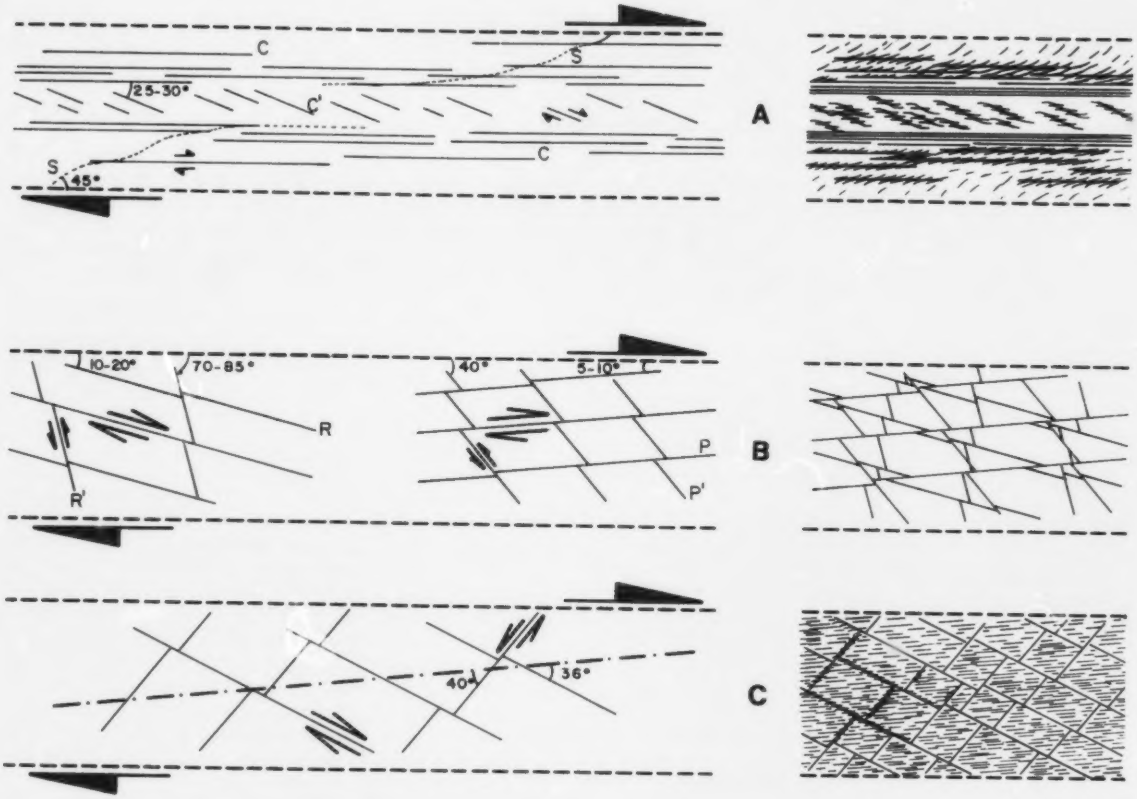

Figure 149.1. *Common geometric features occurring within shear zones. The diagrams on the left define the geometric features and the diagrams on the right give a representation of what these structures may look like in the field:*

A) Ductile features: Dashed lines = shear boundaries. Half arrows = sense of shearing. S.C and C' = fabrics that develop during a ductile simple shear. S = schistosity or foliation, C = secondary shear bands subparallel to the shear boundaries, C' = secondary shear bands affecting the C fabric.

B) Brittle to brittle-ductile features occurring in initially isotropic materials. R and R' = early conjugate set of Riedel shear fractures. P and P' = late conjugate sets of Riedel shear fractures. Note that the geometry of these shear fractures is referenced to the shear boundaries.

C) Brittle to brittle-ductile features occurring in initially anisotropic materials. The dotted-dashed line represents the trace of the anisotropy. Note that the conjugate set of shear fractures is referenced to the trace of the fabric (after Harris and Cobbold 1984).

structural interpretation of a strained or mylonitized protolith that has continuously recorded strain features through all the stages illustrated in Figures 149.1 and 149.2 is by definition complex. While such a deformed protolith would appear as rather a "mess", it is however possible to unravel the complex tectonic history with careful, systematic, structural analysis. Models like the ones illustrated in Figures 149.1 and 149.2 will tentatively be applied to the complex veining system of the A.W. White and Campbell Red Lake Mines during the course of this project.

GOLD–BEARING ROCKS OF THE RED LAKE BELT

Preliminary results from the Madsen area (Hugon and Schwerdtner 1984, p.168) show that foliation trajectories provide enough evidence to define a system of subparallel northeast-southwest-trending sinistral shear zones between Howey Bay and Flat Lake (Figure 149.3). These shear zones define the Howey Bay-Flat Lake deformation zone (Durocher and Hugon 1983, p.217). The narrowing of spacing between foliation trajectories is a clear indicator of increase in strain (Ramsay 1967, p.453) as one moves towards the sheared domain. These trajectories confirm therefore that deformation zones are narrow, linear zones, of higher deformation-intensity relative to that in the surrounding country rocks (Durocher and Hugon 1983; Andrews and Lavigne 1984; Hugon 1984b; Hugon and Schwerdtner 1984). The curvature of the foliation trajectories define sinistral shear zones in the Flat Lake-Howey Bay deformation zone. This implies that every rock material found within that deformation zone has been mylonitized to some extent.

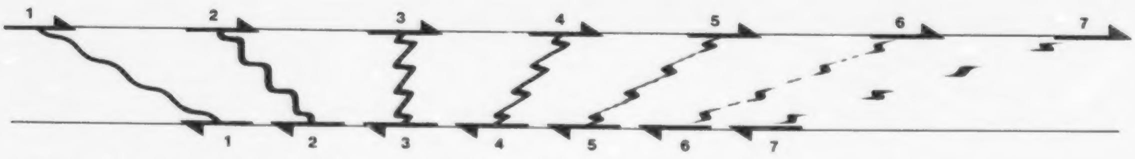

Figure 149.2. *Idealized sketch showing nearly passive amplification of early buckle folds in homogeneous simple shear. Progressive deformation is illustrated from right to left. The sinistral equivalent would be a mirror image of the illustration. The S asymmetry of the fold develops in the late stages of deformation in spite of dextral shear. The thickness variation in the folds may also be misinterpreted. Ramsay et al. (1983) suggested a similar, nearly passive amplification of earlier buckle folds at a larger scale.*

Field evidence including subhorizontal stretch lineation and subvertical intersection between schistosity planes, and small scale shear planes, indicate that the Flat Lake-Howey Bay deformation zone is composed of swarms of subparallel and anastomosing transcurrent, sinistral shear zones (Hugon and Schwerdtner 1984). Mylonitic to ultramylonitic fabrics are observed near and within outcrops of ore zones at the Madsen Mine site. Sinistral syn-metamorphic shearing is confirmed by the sense of rotation of metamorphic kinematic-indicators such as garnets, staurolites, and andalusites (Hugon and Schwerdtner 1984, p.171). Growth of metamorphic minerals during deformation is indicative of blastomylonitization, i.e. blastesis during deformation (Higgins 1971, p.72). Evidence of blastomylonitization is also revealed by the occurrence of 120° junctions of grain boundaries and the undulose extinction of the grains constitutive of fine-grained matrix.

Foliation trajectories (Figure 149.4) obtained form the foliation data available at the belt scale (Figure 149.5) demonstrate that large and small scale conjugate transcurrent shear zones developed within the supracrustal material of the belt. These sets of shear zones are particularly abundant in the area between the Dome Stock, Gullrock Lake, and Killala-Baird Batholith. Field observations in the Howey Bay and Chukuni River areas and the results obtained from the Madsen area demonstrate that the conjugate shear zones developed at the same period of time and were coeval with the emplacement of the Killalla-Baird Batholith (Hugon 1984b). These conjugate shear zones are indicative of a northwest-southeast to north-northwest-south-southeast direction of a maximum, horizontal finite-shortening component. Therefore this shortening event is of the same age as the Killalla-Baird Batholith. U-Pb analyses on zircons derived from a single sample of that batholith yielded an age of 2704±1 m.y. These conjugate shear zones seem to be a widespread feature in northwestern Ontario (Poulsen 1983; Stott and Wallace 1984) and are therefore indicative of a shield-wide shortening event. From the Red Lake study it can be deduced that this shield-wide tectonic event occurred about 2700 m.y.

While foliation trajectories are useful in outlining transcurrent, ductile-shear zones, they cannot be used in the same way for the map-determination of reverse or normal ductile shearing, as in these latter cases maximum curvature of foliation occurs in transverse cross sections. Preliminary observations conducted in the underground workings of the Campbell Red Lake and A.W. White Mines indicate that normal ductile faults trending northwest-southeast occur in that area. These normal structures fall into the inferred Cochenour-Gullrock Lake deformation zone (Hugon 1984b).

Examination of oriented thin sections of samples from the lower levels of the A.W. White Mine indicate that the normal shearing occurred during the peak of amphibolite grade of metamorphism. This is revealed by the inclusion-trail patterns within garnet, staurolite, cordierite, and amphibole porphyroblasts. A strong, downdip stretch lineation persists on shear planes throughout the mine. The schistosity plane-shear plane relationship indicates a downthrow of the southwest block relative to the northeast one. The stretch lineation is particularly well developed and exposed on the 26th level where the transition from well preserved pillowed basalt to a chlorite schist can be observed. Thin sections from this chlorite schist reveal the presence of garnet, amphibole, staurolite, cordierite, and chloritoid porphyroblasts as well as fibrolite aggregates.

Sillimanite has also been observed in thin sections from rock samples of the 30th level of this mine (A.J. Andrews, Geologist, Ontario Geological Survey, personal communication, 1985).

Although the detailed study of the A.W. White Mine is presently underway, it can be nonetheless stated that normal ductile shearing occurred during the peak of regional metamorphism. The regional metamorphism in that area is due to the emplacement of the Trout Lake Batholith as the isograds are conformable to the plutonic-supracrustal contact (Andrews 1984).

Ore horizons observed on the 24 to 30 levels of the A.W. White Mine crosscut lithologies (Lavigne and Crocket 1983) including an iron formation fold nose (M. Chowaniec, Geologist, A.W. White Mine, personal communication, 1985). At the mine scale the ore zones are axial-planar to this megastructure and yet also appear affected by the ductile shearing. Accordingly, it indicates that orebodies show both post-ductile and syn-ductile characteristics. It is therefore concluded that they occurred late in the ductile history of the deformation. The ductile shear deformation (including folding) is syn- to post-2757 m.y., the U-Pb zircon age of an isoclinally folded dike (Marmont 1983) located within the Cochenour-Gullrock Lake deformation zone. Accordingly, mineralization in the A.W. White Mine occurred late in the history of the Red Lake belt and significantly later than the deposition of the host volcanic

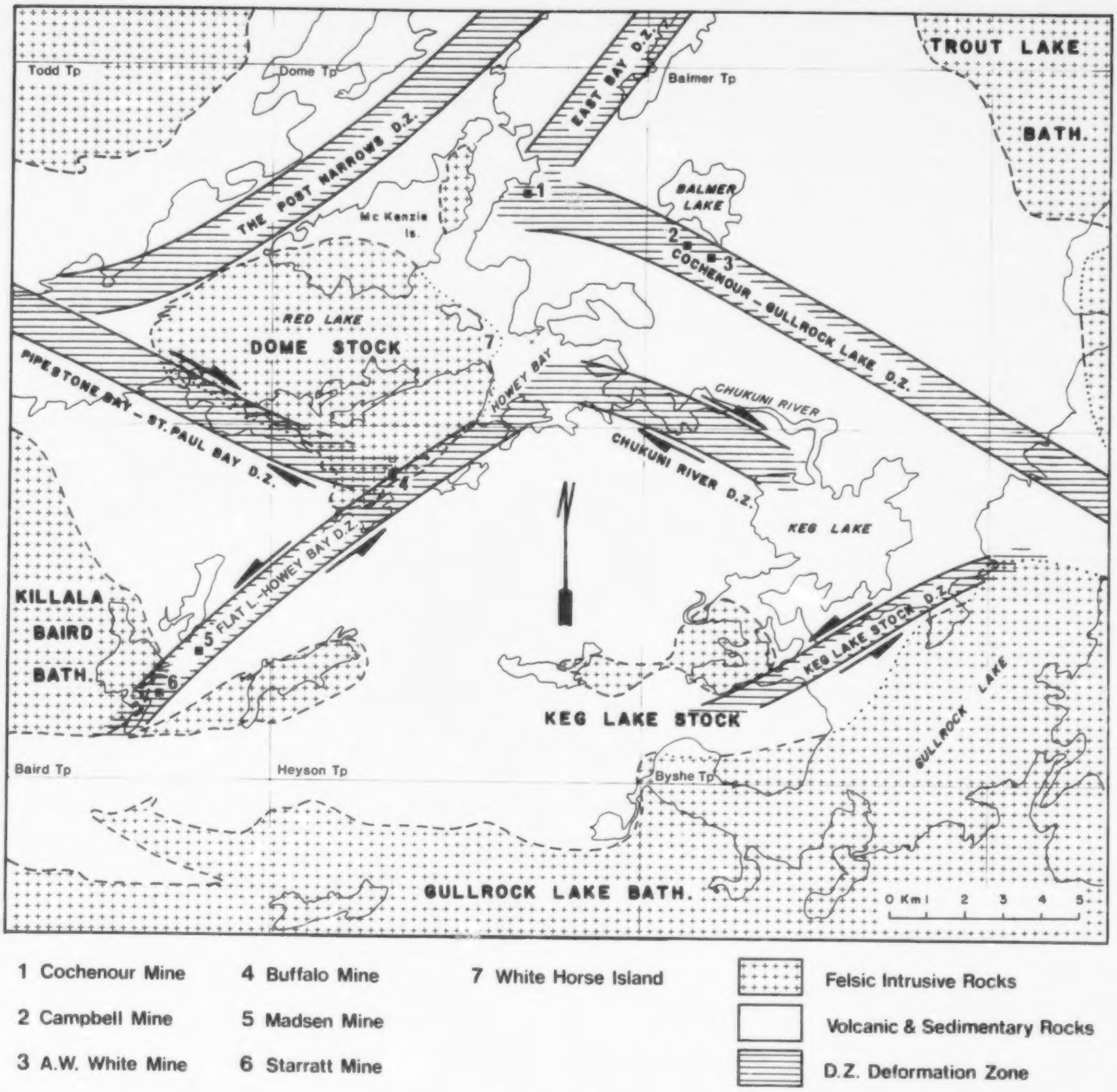
TROUT LAKE BATH.
Todd Tp
Dome Tp
Balmer Tp
EAST BAY D.Z.
THE POST NARROWS D.Z.
Mc Kenzie Is.
BALMER LAKE
1
2
3
COCHENOUR - GULLROCK LAKE D.Z.
RED LAKE
DOME STOCK
7
PIPESTONE BAY - ST. PAUL BAY D.Z.
HOWEY BAY
CHUKUNI RIVER
CHUKUNI RIVER D.Z.
4
KEG LAKE
N
FLAT L. HOWEY BAY D.Z.
5
6
KILLALA BAIRD BATH.
KEG LAKE STOCK D.Z.
KEG LAKE STOCK
GULLROCK LAKE
Baird Tp
Heyson Tp
Byshe Tp
GULLROCK LAKE BATH.
0 Km 1 2 3 4 5
1 Cochenour Mine
2 Campbell Mine
3 A.W. White Mine
4 Buffalo Mine
5 Madsen Mine
6 Starratt Mine
7 White Horse Island
Felsic Intrusive Rocks
Volcanic & Sedimentary Rocks
D.Z. Deformation Zone

Figure 149.3. *Structural framework of the Red Lake belt, eastern section. The patterned areas represent zones of most intense deformation. Deformation in the surrounding areas is pervasive but generally less intense.*

rocks dated at 2965-2982 m.y. (Marmont 1983). Ductile, normal shearing coeval with the peak of amphibolite grade of metamorphism within the Cochenour-Gullrock Lake deformation zone is most likely to be due to the diapiric rise of the adjacent Trout Lake batholith. Accordingly, gold mineralization intimately associated with the ductile, normal shearing in the A.W. White Mine is directly related to the emplacement of the Trout Lake batholith.

GOLD–BEARING ROCKS IN THE HEMLO AREA

Results from the preliminary structural study in the Hemlo area indicate that the main ore horizon (Figure 149.6) lies within the most deformed portion, or core (e.g. the central band of Figure 149.1A), of a heterogeneous dextral shear zone (Hugon 1984a).

Photo 149.1 illustrates the tremendous increase in strain that occurs towards the Lac Minerals "West Zone" over a horizontal distance of less than 10 m. The pictures follow a north-south sequence from isoclinal folding of primary layers to the complete overprinting of the primary features by a tectonometamorphic segregation, i.e. complete ultramylonitization. This mylonitization to ultramylonitization produced a planar, thin, subvertical, northwest-southeast-trending body of intensely strained rock material which will be mined for the next decades. The data presently available for this area indicate

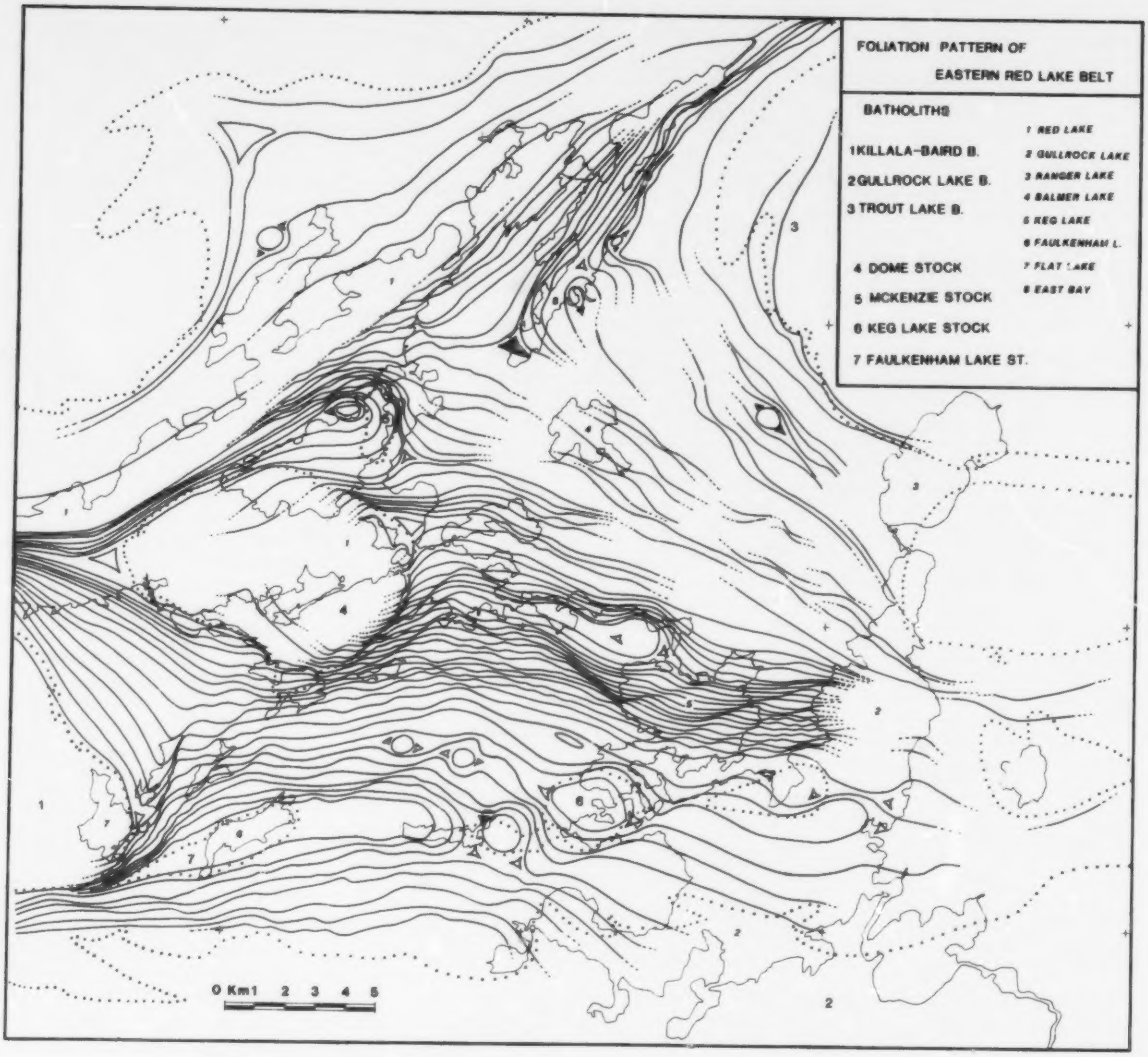
FOLIATION PATTERN OF
EASTERN RED LAKE BELT
BATHOLITHS
1 KILLALA–BAIRD B.
2 GULLROCK LAKE B.
3 TROUT LAKE B.
4 DOME STOCK
5 MCKENZIE STOCK
6 KEG LAKE STOCK
7 FAULKENHAM LAKE ST.
1 RED LAKE
2 GULLROCK LAKE
3 RANGER LAKE
4 BALMER LAKE
5 KEG LAKE
6 FAULKENHAM L.
7 FLAT LAKE
8 EAST BAY
0 Km 1 2 3 4 5
1
2
3
4
5
6
7

Figure 149.4. *Foliation trajectories of the eastern portion of the Red Lake belt. These foliation trajectories were obtained from the data available for the belt and presented in Figure 149.5. Note that trajectories are drawn by interpolation between strike data and are not a function of the density of measurements. Triangles denote areas of triple junction of foliation trajectories. The filled-triangle at the south end of East Bay outlines a zone of trajectory interference due to the diapiric rise of the large, adjacent plutonic bodies. These trajectories are presented as an approximation. The reader can check the general pattern of the trajectories by superposing Figures 149.4 and 149.5 under a stereoscope.*

that the ore zones do not follow the isoclinally folded primary layers. If this is further confirmed, then, the hypothesis of syngenetic origin of the gold mineralization in the Hemlo area may be ruled out.

Photo 149.2 exhibits evidence of mylonitization and blastomylonitization as well as obvious evidence of dextral displacement. Blastomylonitization involving recrystallization during deformation is responsible for the lack of preserved strain-features within the matrix (Photo 149.3). This recrystallization mechanism can mislead one to interpret the constitutive mineralogy of the ore horizon as fresh and pristine.

Ductile deformation occurred during the peak of the amphibolite grade of metamorphism in the Hemlo area. This is revealed by rotation of garnet and staurolite porphyroblasts during their growth (Photos 3a, 3b). Kyanite and sillimanite have been observed in thin sections from ore samples. In some instances, gold exhibits an intimate association with kyanite porphyroblasts (Photo 149.3c). The significance of such an association is not yet understood and will be further investigated.

Although a more detailed metamorphic study is needed, the data available presently indicate that the

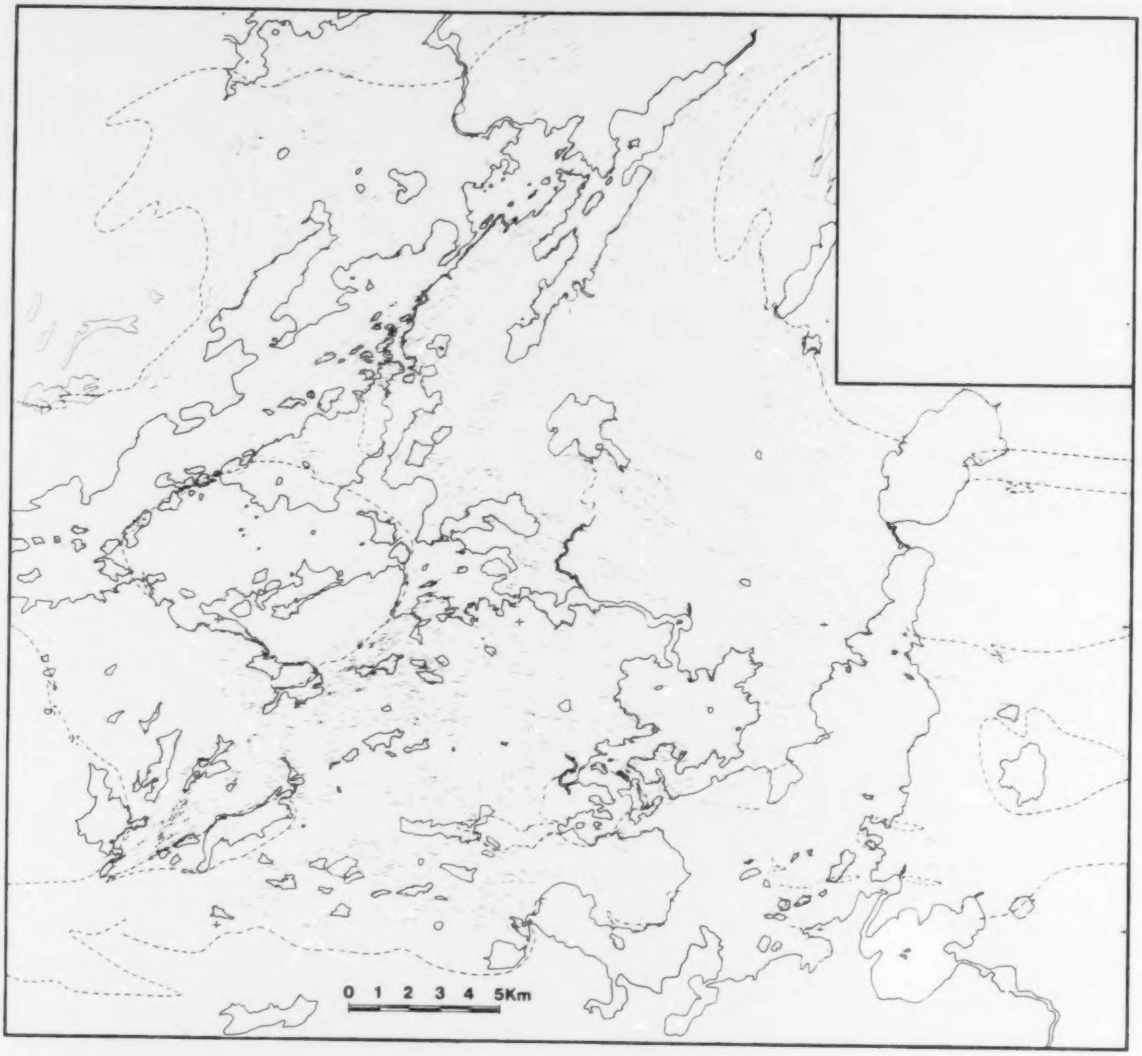

Figure 149.5. Strike data of the eastern portion of the Red Lake belt. Data of the southeastern portion of this foliation-strike map were obtained by the authors. Data for the other parts of the belt were compiled from Horwood (1945), Pirie and Sawitzky (1977a, 1977b), Pirie and Kita (1979a, 1979b, 1979c), Pirie and Grant (1978a, 1978b) and unpublished maps of Dome and Heyson Townships by Pirie and assistants. Half-arrowed foliation-strike symbols indicate sense of shearing of small-scale shear zones.

latest regional metamorphism in the Hemlo area is due to the Cedar Lake pluton.

CONCLUSIONS

The 3 examples of Archean gold deposits presented in this paper have the following points in common:

1. The mineralization occurs within the most deformed portions of heterogeneous ductile shear zones.
2. The ductile shearing occurred during a peak of amphibolite grade of metamorphism.
3. The only obvious sources of heat available in the vicinity of these shear zones capable of producing such metamorphism are large plutonic bodies.

From these 3 examples it appears that gold deposition occurred in close association with strong ductile shearing that developed during a regional metamorphism up to amphibolite grade due to the emplacement of large plutonic bodies.

The available data from zircon-U-Pb age-dating (Krogh *et al.* 1984) suggest that these large plutonic bodies were emplaced within a period of 2700±30 m.y. across northwestern Ontario, and therefore seem to be the benchmarks of a major Archean tectonic event. At the shield scale the structural expression of this major tectonic event are east-

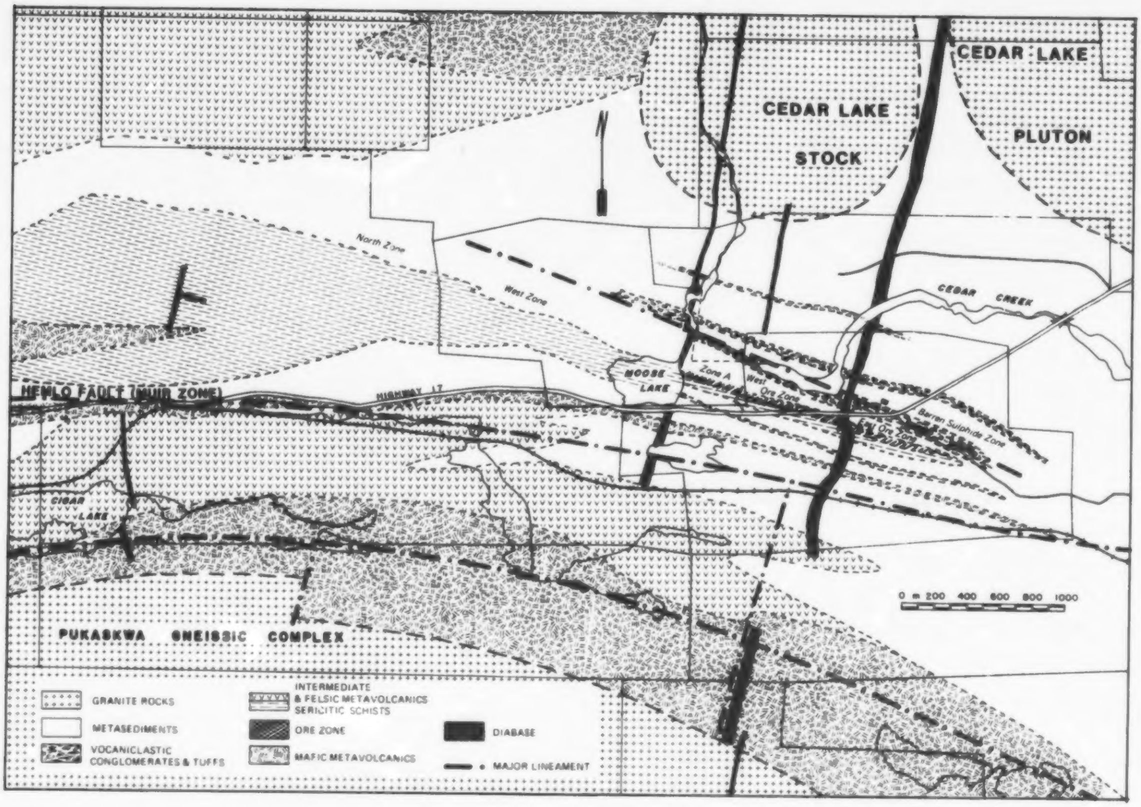
CEDAR LAKE
CEDAR LAKE STOCK
PLUTON
N
North Zone
West Zone
CEDAR CREEK
MOOSE LAKE
Zone A
West Ore Zone
Barren Sulphide Zone
HEMLO FAULT (MUIR ZONE)
HIGHWAY 17
CEDAR LAKE
0 m 200 400 600 800 1000
PUKASKWA GNEISSIC COMPLEX
GRANITE ROCKS
METASEDIMENTS
VOCANICLASTIC CONGLOMERATES & TUFFS
INTERMEDIATE & FELSIC METAVOLCANICS SERICITIC SCHISTS
ORE ZONE
MAFIC METAVOLCANICS
DIABASE
MAJOR LINEAMENT

Figure 149.6. *General Geology of the Hemlo area after Muir (1982), Patterson (1984) and Milne et al. (1972).*

west transcurrent dextral shear zones, limiting domains that exhibit conjugate sets of shear zones. These patterns suggest a northwest-southeast to north-northwest-south-southeast direction of finite maximum shortening (Schwerdtner *et al.* 1979, p.169).

ACKNOWLEDGMENTS

The authors wish to thank A.J. Andrews and A.C. Colvine of the Ontario Geological Survey (Mineral Deposits Section), Fernando Corfu of the Royal Ontario Museum (Geochronology Laboratory), M.J. Lavigne, Jr., of the Ministry of Natural Resources (Resident Geologist, Red Lake), James Pirie (Esso Minerals Exploration) and the staff of the Geology and Engineering Departments of the A.W. White Mine and Phil Walford (Chief Geologist, Lac Minerals Limited) for their help, co-operation, and helpful discussion.

REFERENCES

Andrews, A.J., and Lavigne, M.J., Jr.
1984: Gold Studies in the Red Lake Area; p.158-161 *in* Summary of Field Work, edited by John Wood, Owen L. White, R.B. Barlow, and A.C. Colvine. Ontario Geological Survey, Miscellaneous Paper 119, 309p.

Andrews, A.J.
1984: Alteration, Metamorphism, and Structure Associated with Archean Volcanic-Hosted Gold Deposits, Red Lake District; p.162-166 *in* Summary of Field Work, edited by John Wood, Owen L. White, R.B. Barlow, and A.C. Colvine, Ontario Geological Survey, Miscellaneous Paper 119, 309p.

Durocher, M.E., and Hugon, Hervé
1983: Structural Geology and Hydrothermal Alteration in the Flat Lake-Howey Bay Deformation Zone, Red Lake Area; p.216-219 *in* Summary of Field Work, 1983, by the Ontario Geological Survey, edited by John Wood, Owen L. White, R.B. Barlow, and A.C. Colvine, Miscellaneous Paper 116, 313p.

Harris, L.B., and Cobbold, P.R.
1984: Development of Conjugate Shear Bands During Bulk Simple Shearing; Journal of Structural Geology, Volume 7, Number 1, p.37-44.

Higgins, M.W.
1971: Cataclastic Rocks; United States Geological Survey, Professional Paper 687, 97p.

Horwood, H.C.
1945: Geology and Mineral Deposits of the Red Lake Area; Ontario Department of Mines, Annual Report for 1940, Volume 49, Part 2, 231p.

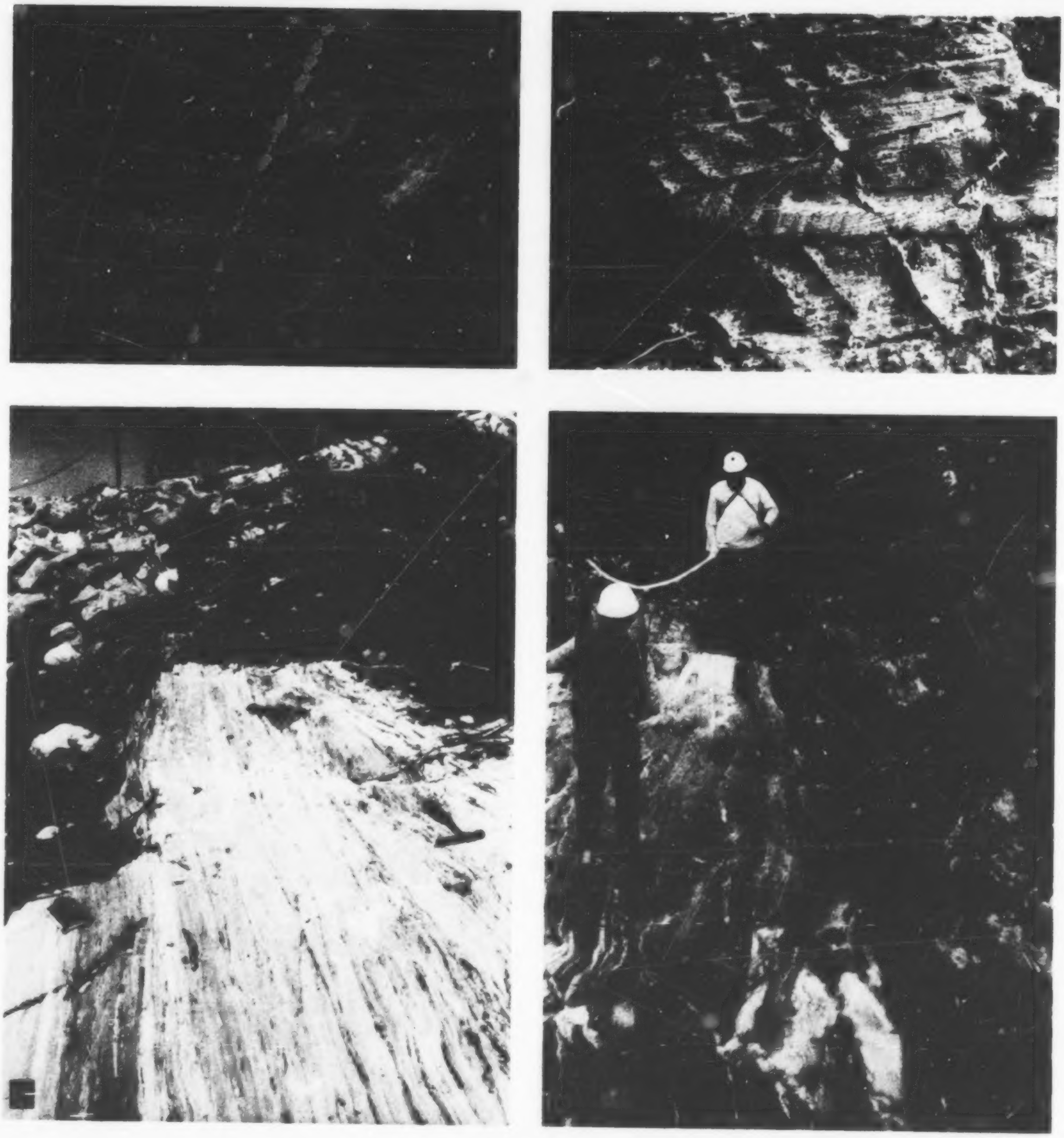

Photo 149.1. Lac Minerals Property

A) Isoclinal fold. Note that the upper limb is relatively thicker than the lower one. This feature is compatible with dextral, ductile shearing. The handle of the hammer points towards the south.

B) Detail of an isoclinal fold nose showing the overprinting of the folded primary layers by an axial planar tectono-metamorphic layering.

C) This picture is taken from an outcrop located 3 m south of the one shown in B. Here the isoclinal folding is not even recognizable because of a complete overprinting by the development of an extremely strong tectono-metamorphic segregation due to a very intense mylonitization to ultramylonitization.

D) Located 2 m south of the area shown in C this picture shows the finely schistosed "West Zone" on the Lac Minerals property. Thin sections from this zone reveal similar features as the one presented in Photo 149.3.

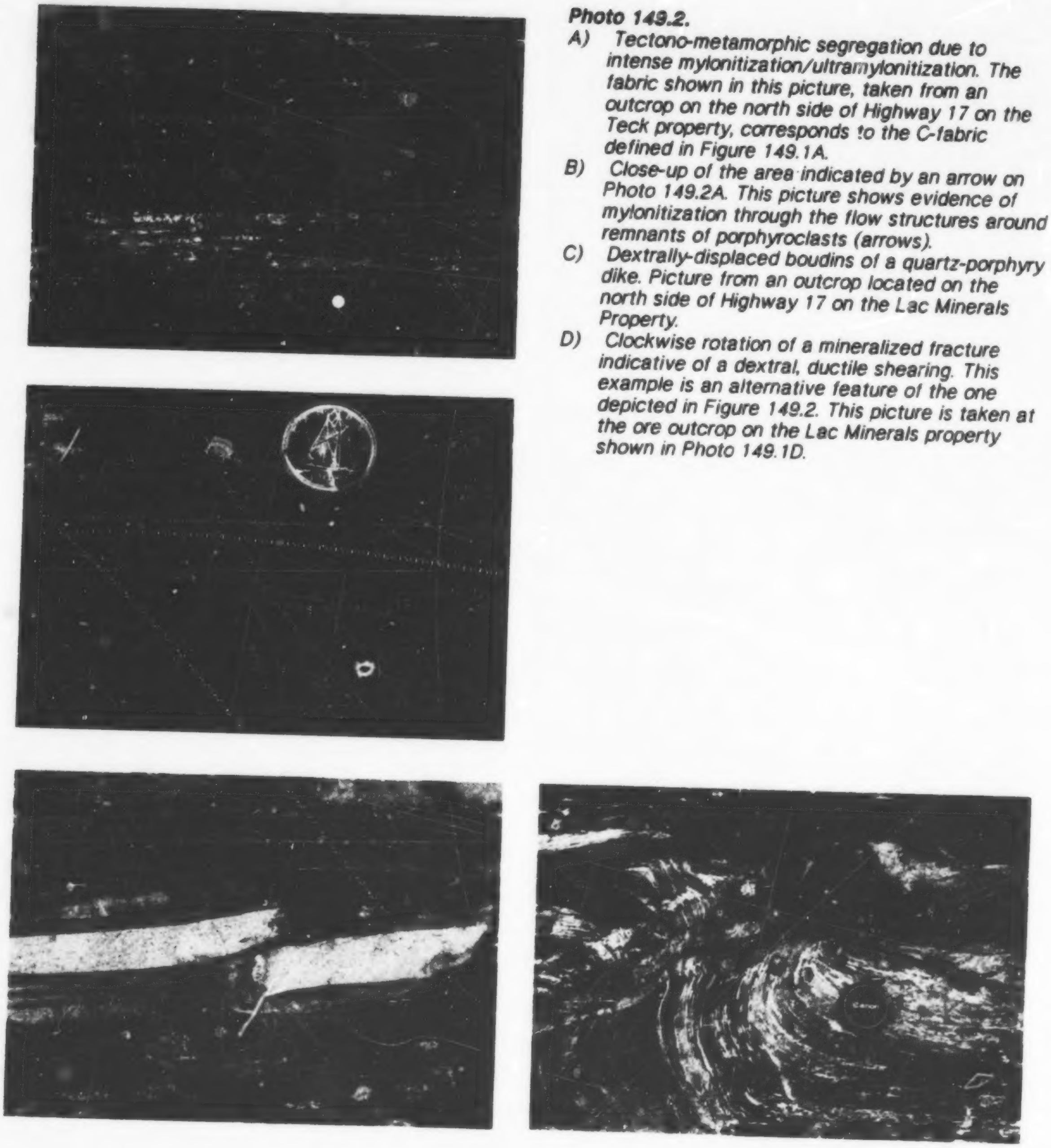

Photo 149.2.

A) Tectono-metamorphic segregation due to intense mylonitization/ultramylonitization. The fabric shown in this picture, taken from an outcrop on the north side of Highway 17 on the Teck property, corresponds to the C-fabric defined in Figure 149.1A.

B) Close-up of the area indicated by an arrow on Photo 149.2A. This picture shows evidence of mylonitization through the flow structures around remnants of porphyroclasts (arrows).

C) Dextrally-displaced boudins of a quartz-porphyry dike. Picture from an outcrop located on the north side of Highway 17 on the Lac Minerals Property.

D) Clockwise rotation of a mineralized fracture indicative of a dextral, ductile shearing. This example is an alternative feature of the one depicted in Figure 149.2. This picture is taken at the ore outcrop on the Lac Minerals property shown in Photo 149.1D.

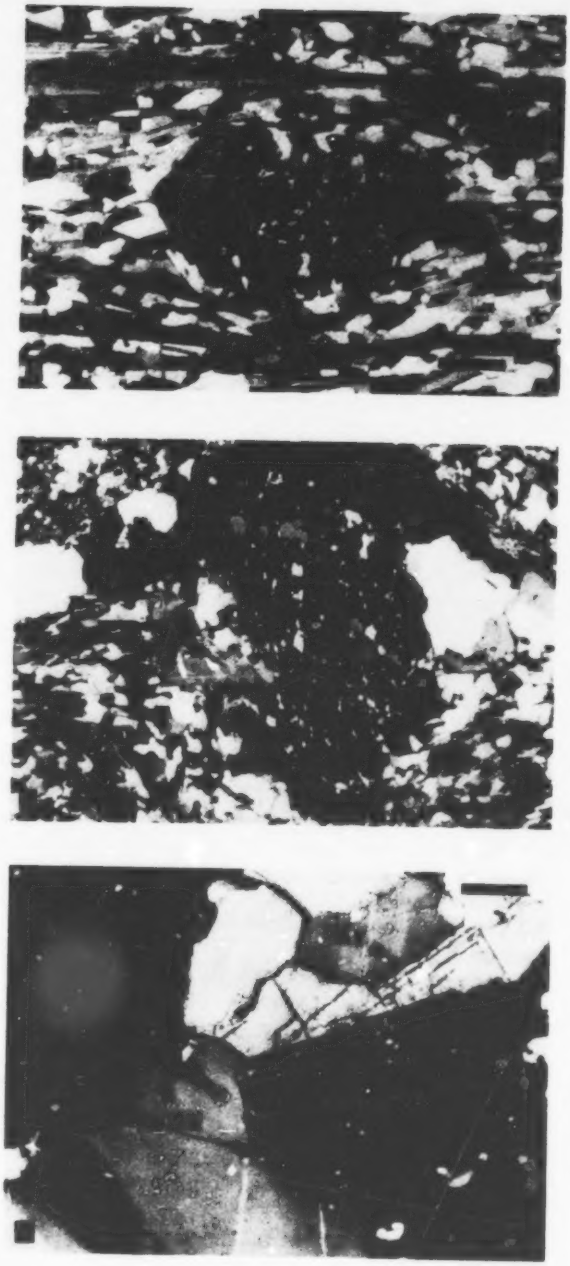

Photo 149.3.

A) Z-shaped inclusion trails within a garnet porphyroblast. The photomicrograph is oriented like the outcrop face; scale bar is 0.35 mm; section parallel to stretch lineation and perpendicular to foliation.

B) Z-shaped inclusion-trails within a staurolite porphyroblast. The photomicrograph is oriented like the outcrop face; scale bar is 0.35 mm; section parallel to stretch lineation and perpendicular to foliation.

C) Kyanite (Ky) porphyroblast and gold (Au) intimately associated; scale bar is 0.05 mm.

Note the 120° boundary-junctions between the grain of the matrix in Photos 149.3A, 149.3B, and 149.3C. Some grains show undulose exctinctions. These features are indicative of blastomylonitization especially when found in the central portion of a shear zone as is the case here.

Hugon, Hervé

1984a: The Hemlo Deposit: Gold Mineralization Within a Dextral Shear Zone; p.212-217 *in* Summary of Field Work, 1984, by the Ontario Geological Survey, edited by John Wood, Owen L. White, R.B. Barlow, and A.C. Colvine. Ontario Geological Survey, Miscellaneous Paper 119, 309p.

1984b: Ductile Deformation Zones and Their Significance in the Tectonic and Mineralization History of the Red Lake Belt; p.167-172 *in* Summary of Field Work, 1984, by the Ontario Geological Survey, edited by John Wood, Owen L. White, R.B. Barlow, and A.C. Colvine, Ontario Geological Survey, Miscellaneous Paper 119, 309p.

Hugon, Hervé, and Schwerdtner, W.M.

1984: Structural Signature and Tectonic History of Deformed Gold-Bearing Rocks in Northwestern Ontario. p.164-176 *in* Geoscience Research Grant Program, Summary of Research 1983-1984, edited by V.G. Milne, Ontario Geological Survey, Miscellaneous Paper 212, 252p.

Krogh, T.E., Davis, D.W., and Corfu, F.

1984: Implications of Precise U-Pb Dating for the Geological Evolution of the Superior Province; GAC-MAC Joint Annual Meeting, London, May 1984. Program with Abstracts, p.79.

Lapworth, C.

1885: The Highland Controversy in British Geology: Its Causes, Course and Consequences; Nature, London, Volume 32, p.558-559.

Lavigne, M.J., Jr., and Crocket, J.H.

1983: Geology of the East South C Ore Zone, Dickenson Mine, Red Lake; p.141-158 *in* The Geology of Gold in Ontario, edited by A.C. Colvine, Ontario Geological Survey, Miscellaneous Paper 110, 278p.

Marmont, Soussan

1983: Application of Age-Dating to Gold Mineralization; p.229-236 *in* Summary of Field Work, 1983, by the Ontario Geological Survey, edited by John Wood, Owen L. White, R.B. Barlow, and A.C. Colvine, Ontario Geological Survey, Miscellaneous Paper 116, 313p.

Milne, V.G., Giblin, P.E., Bennett, G., Thurston, P.C., Wolfe, W.J., Giguere, J.F., Leahy, E.J., and Rupert, R.J.

1972: Manitouwadge-Wawa Sheet, Algoma, Cochrane, Sudbury, and Thunder Bay Districts; Ontario Department of Mines, Map 2220, Geological Compilation Series, scale 1:253 440 or 1 inch to 4 miles. Compilation 1966-1971.

Muir T.L.

1982: Geology of the Hemlo Area, District of Thunder Bay; Ontario Geological Survey, Report 217, 65p. Accompanied by Map 2452, scale 1:31 680 or 1 inch to 1/2 mile.

Patterson, G.C.

1984: Field Trip Guidebook to the Hemlo Area; Ontario Geological Survey, Miscellaneous Paper 118, 33p.

Pirie, James, and Grant A.

1978a: Balmer Township Area, District of Kenora (Patricia Portion); Ontario Geological Survey, Preliminary Map P.1976A, Geological Series, scale 1:12 000 or 1 inch to 1000 feet.

1978b: Bateman Township, District of Kenora (Patricia Portion); Ontario Geological Survey, Preliminary Map P.1563, Geological Series, scale 1:12 000 or 1 inch to 1000 feet.

Pirie, James, and Kita, J.H.

1979a: Ranger Township, District of Kenora (Patricia Portion); Ontario Geological Survey, Preliminary Map P.2212, Geological Series, scale 1:12 000 or 1 inch to 1000 feet.

1979b: Willans Township, District of Kenora (Patricia Portion); Ontario Geological Survey, Preliminary Map P.2214, Geological Series, scale 1:12 000 or 1 inch to 1000 feet.

1979c: Byshe Township, District of Kenora (Patricia Portion); Ontario Geological Survey, Preliminary Map P.2213, Geological Series, scale 1:12 000 or 1 inch to 1000 feet.

Pirie, James, and Sawitzky, E.

1977a: McDonough Township, District of Kenora (Patricia Portion); Ontario Geological Survey, Preliminary Map P.1240, Geological Series, scale 1:12 000 or 1 inch to 1000 feet.

1977b: Graves Township, District of Kenora, (Patricia Portion); Ontario Geological Survey, Preliminary Map P.2214, Geological Series, scale 1:12 000 or 1 inch to 1000 feet.

Poulsen, H.K.

1983: Structural Setting of Vein-Type Gold Mineralization in the Mine Center-Fort Frances Area: Implications for the Wabigoon Subprovince; p.174-180 *in* the Geology of Gold in Ontario, edited by A.C. Colvine, Ontario Geological Survey, Miscellaneous Paper 110, 278p.

Ramsay, J.G.

1967: Folding and Fracturing of Rocks; New York, McGraw Hill Book Company, 568p.

Ramsay, J.G., Casey, Martin, and Kligfield, Roy

1983: Role of Shear in Development of the Helvetic Fold-Thrust Belt of Switzerland; Geology, Volume 11, Number 8, p.439-442.

Sibson, R.H.

1977: Fault Rocks and Fault Mechanisms; Journal of the Geological Society, London, Volume 133, p.191-213.

Schwerdtner, W.H., Stone, D., Osadetz, K., Morgan, J., and Stott, G.M.

1979: Granitoid Complexes and the Archean Tectonic Record in the Southern Part of Northwestern Ontario; Canadian Journal of Earth Sciences, Volume 16, Number 10, p.1965-1977.

Stott, G.M., and Wallace, Henry

1984: Regional Stratigraphy and Structure of the Central Uchi Subprovince: Meen Lake-Kasagiminnis Lake and Pashkokogan Lake Sections; p.7-13 *in* Summary of Field Work, 1984, Ontario Geological Survey, edited by John Wood, Owen L. White, R.B. Barlow, and A.C. Colvine, Ontario Geological Survey, Miscellaneous Paper 119, 309p.

Grant 168 Petrogenesis of Mineralized Horizons in Uchi Lake Metavolcanic Rocks

S.R. Noble[1], **N.M. Evensen**[2], **and T.E. Krogh**[2]

[1]Department of Geology, University of Toronto

[2]Jack Satterly Geochronology Laboratory, Royal Ontario Museum

ABSTRACT

The Uchi-Confederation Lakes greenstone belt and spatially related Trout Lake batholith are being examined using field, geochemical, and isotopic methods in order to elucidate mechanisms of Archean crustal growth and factors leading to the development of massive sulphide mineralization in the metavolcanic rocks.

Previous workers have shown that the volcanic rocks occur in 3 major cycles, with volcanism in the belt spanning 220 Ma. In addition, it has been suggested that sulphide mineralization, which is found only in the uppermost cycle is in part a consequence of the development of zoned magma chambers beneath a thickening volcanic crust.

Data obtained for this study show that the batholith is comprised of at least 2 major gneiss enclaves which are surrounded or intruded by trondhjemite-diorite-granodiorite and late felsic dikes. The oldest components of the batholith have a probable minimum age of 2800 Ma based on preliminary U-Pb zircon analyses.

Geochemical and Sm-Nd isotope data have been collected from part of the second volcanic cycle, and substantiate the hypothesis that zoned magma chambers were developing in the Uchi-Confederation belt. Preliminary Sm-Nd isotopic data obtained for samples in all 3 cycles suggests that the source regions for the volcanics were becoming progressively depleted as the belt developed. Although this is only a tentative hypothesis, it is supported by Hf-isotope data obtained by Patchett *et al.* (1981).

INTRODUCTION

This research project is primarily concerned with the problem of understanding the origin of the mineralized horizons in the Uchi-Confederation Lakes greenstone belt and their relationship, if any, with the adjacent Trout Lake batholith. To study this problem precise U-Pb zircon geochronology, major and minor element analyses, and Sm-Nd isotopic analyses are being employed in conjunction with field and petrographic observations.

The Uchi-Confederation Lakes belt (*see* Figure 168.1) and the ore deposits contained within it have been extensively studied. The belt is unique in demonstrating 3 major mafic to felsic volcanic cycles (Goodwin 1967; Pryslak 1971) which were erupted over a period of 220 Ma (Nunes and Thurston 1980). The oldest volcanic cycle has been dated at 2959 Ma

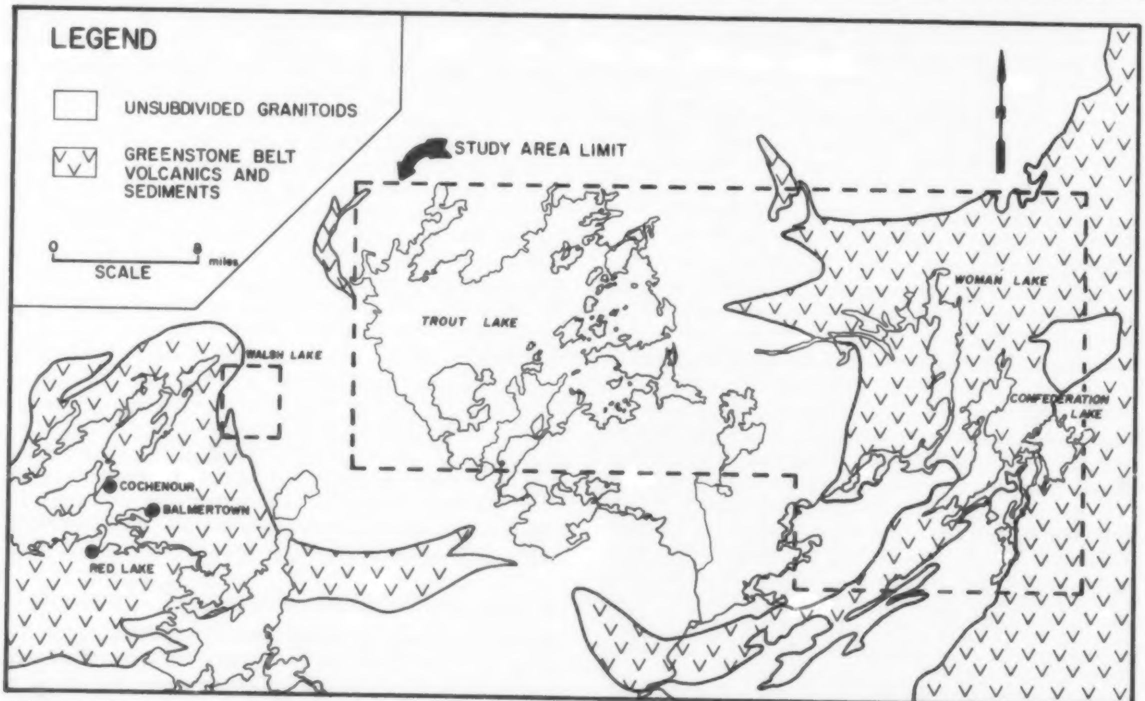

Figure 168.1. *Location map of study area, showing regional geology.*

TABLE 168.1. SUMMARY OF TROUT LAKE LITHOLOGIES.

1. Hornblende-biotite trondhjemite gneiss.
   (a) Migmatitic trondhjemite gneiss: medium-grained tonalitic leucosomes and hornblende-biotite melanosomes. Migmatitic gneiss is tightly folded.
   (b) Trondhjemite gneiss: Apparent precursor of 1(a), also forms mesosomes of 1(a).
   (c) Trondhjemite dikes: Discordant leucocratic dikes cutting 1(a) and 1(b).

2. Banded diorite-granodiorite gneiss.
   (a) Dioritic layers 1-20 cm thick locally boudinaged and disrupted by felsic layers.
   (b) Granodioritic layers 1-10 cm thick both concordant and discordant to dioritic layers.

3. Trondhjemite-diorite-granodiorite.
   (a) Foliated trondhjemite-granodiorite comprising most of the batholith. Equigranular, biotite/hornblende >1.
   (b) Foliated porphyritic hornblende granodiorite. Biotite/hornblende <<1.
   (c) Hornblende diorite. Biotite/hornblende >1, abundant sphene.

4. Late granodiorite-granite.
   (a) Biotite granodiorite. Irregular intrusions and dikes cutting units 1 and 3.
   (b)Late granitic pegmatitic pods and graphic granite.

5. Mafic dikes. Mafic dike intrusion spans the history of the batholith.

by U-Pb in zircons (Nunes and Thurston 1980), and represents some of the earliest volcanic activity in the Superior Province. The great age of these volcanic rocks, coupled with the 220 Ma time span for volcanism, make the Uchi-Confederation belt an excellent location in which to study Archean crustal growth.

Massive sulphide deposits present in the uppermost volcanic rocks possess unusual rare earth element (REE) patterns (Thurston 1982), which have been recognized elsewhere as being characteristic of ore-related felsic volcanic rocks (Campbell *et al.* 1982). Campbell *et al.* (1981) have suggested that large magma chambers are important in ore genesis, and examine trace element evolution in these felsic volcanic settings. Evidence supporting this hypothesis as applied to the Uchi-Confederation belt has been presented by Thurston and Fryer (1983) who suggested that the volcanic rocks were derived from large compositionally zoned magma chambers, and that the cycle 3 volcanic rocks associated with massive sulphide mineralization formed as a consequence of the evolution of the magma chamber beneath a progressively thickening crust.

In the previous report (Noble *et al.* 1984), field data were presented which showed that the Trout Lake granitoids were comprised of 4 major lithologic units. These lithologies included 2 gneiss enclaves within the main trondhjemite-diorite-granodiorite phase, and a series of late felsic dikes.

This report summarizes the field data obtained in 1984, and presents preliminary geochemistry and U-Pb data for the Trout Lake batholith, along with preliminary geochemistry and Sm-Nd isotope data for the volcanic rocks.

TROUT LAKE GRANITOIDS

Field work in 1984 concentrated on examining selected areas of the Trout Lake batholith in order to observe detailed geological relationships after studying lithologies in 1983.

LITHOLOGIES

A summary of lithologies encountered in 1983 and 1984 in the batholith is presented in Table 168.1.

Migmatitic Trondhjemite Gneiss

The grey gneiss enclave has been previously described (Noble *et al.* 1984) as trondhjemite orthogneiss comprised of leucocratic layers containing equigranular quartz-oligoclase-microcline and melanocratic layers of biotite-hornblende-sphene. It was suggested that this enclave was similar to "old grey gneiss" described elsewhere (Condie 1981; Jahn *et al.* 1984; Hillary and Ayres 1980). During field work in 1984 some portions of the enclave were found to be migmatitic (non-genetic definition describing a rock composed of 2 contrasting lithologies; Mehnert 1968).

The migmatitic portions of the enclave are mainly exposed on the easternmost portions of Trout Lake. The migmatites contain medium-grained plagioclase-quartz leucosomes up to 5 cm wide, biotite hornblende-sphene ± allanite melanosomes 0.5 to 1 cm thick, and mesosomes of fine- to medium-grained biotite-hornblende trondhjemite similar to the non-migmatitic trondhjemite gneisses found elsewhere in the enclave (migmatite terminology after Johannes and Gupta 1982). It appears that segregation of the ferromagnesian minerals and quartz and feldspar into thick discrete layers is gradational from the relatively homogeneous gneiss.

The migmatitic trondhjemites have suffered at least one major period of deformation during and/or after migmatization. This is shown by tight folds in the migmatites and veining of competent amphibolite xenoliths by material from the leucosomes. Syndeformational basaltic dikes have been disrupted to varying degrees, with the most disrupted dikes occurring now as mafic xenoliths and schlieren. It seems likely that the mafic xenoliths in the trondhjemite enclave are primarily related to the break-up of these basaltic dikes (Nielsen and Weiblen 1980).

Banded Diorite-Granodiorite Gneiss

Banded gneiss forms a large enclave west of the migmatitic trondhjemite. The gneiss was examined briefly in 1983, and was examined in greater detail in 1984.

The gneisses are composed of fine-grained amphibolite layers and medium-grained granodioritic

TABLE 168.2. BATHOLITH MAIN PHASE MODAL ANALYSIS.

Mineral	Sample SN-102	SN-103	SN-104	SN-105	SN-107	SN-112	SN-117	SN-118
Quartz	36.2	37.1	34.4	37.8	20.3	39.6	39.6	42
Plagioclase	46.2	39.6	47.8	32.2	62.5	38.9	43.1	51.5
Microcline	4.2	11.5	3.6	17.3	.6	14.1	10.6	2.5
Myrmekite				7			.5	
Biotite	6.7	5.4	8.1	7.1	4.8	2.1	4.1	8.9
Hornblende								
Muscovite	2.4	.9	.4	2.1	2.5	3.4	1.6	.1
Sphene	.3	.2	.4		.4	<.1		
Epidote								
Clinozoisite	1.9	4.6	3.3	3.2	7.6	1.6		1.2
Chlorite	1.[illegible]	.3	1.9	<.1	.6			.1
Apatite	.5	.1	<.1	.1	.2	<.1		.3
Zircon	.2	.2	<.1	.1	.2	.1		
Magnetite	.3						.4	
Allanite	.1	<.1						
Carbonate								

Mineral	SN-119	SN-121	SN-122	SN-135	SN-141	SN-146	SN-150
Quartz	28.9	39.4	36.8	29.3	33.3	38.1	32.8
Plagioclase	29.9	52.9	55.3	49.6	48.6	50	42.8
Microcline	28.8	1.2	1.73		12.6	5.7	21.8
Myrmekite							.2
Biotite	4.3	5.8	4.5	11.7	3.5	4.4	
Hornblende				2.9			
Muscovite	3.9	.1	1.0		1.4	1.2	3.8
Sphene	.1			.5			
Epidote		.5	.5				
Clinozoisite	2.3			5.3	<.1	.4	.4
Chlorite	.8				<.1	<.1	.6
Apatite	.1	.1	.1	.3	.2	.1	
Zircon	.1			<.1			
Magnetite	.6		.1	.1	.1	<.1	
Allanite				.2			.1
Carbonate				.1	.2		.2

layers. Amphibolite bands generally show internal layering due to varying grain size and relative proportions of hornblende, biotite, plagioclase, and quartz. The granodiorite layers are composed of quartz, plagioclase, potassium feldspar, and minor biotite and hornblende. Contacts between the 2 contrasting lithologies are usually very sharp. Some outcrops are dominated by amphibolite layers which are cut by discordant felsic dikes, or show irregular banding of amphibolite and felsic layers with occasional extreme disruption of amphibolite layers.

Based on outcrops examined in 1984, the banded gneisses seem to be comprised of a metavolcanic protolith which has been invaded by discordant and concordant layers or dikes of felsic material.

Trondhjemite-Diorite-Granodiorite

Previous work on the trondhjemite-diorite-granodiorite unit showed that trondhjemite was the principal rock type in the Trout Lake batholith, that is was generally foliated, and that identification of discrete plutons was not possible (Noble *et al.* 1984).

The mineralogy of the main portion of the batholith is summarized in Table 168.2. The composition of the trondhjemites based on modal composition falls primarily within the tonalite field (Streckeisen 1976), with some samples in the granodiorite field. Also shown in Table 168.2 are 2 late felsic dikes which have granodiorite to granite (*sensu stricto*) composition.

Important ubiquitous accessory minerals in the trondhjemites are magnetite, zircon, sphene, and epidote-clinozoisite. In some trondhjemites, especially those at the Uchi-Confederation Lake greenstone belt contact, epidote and clinozoisite occur primarily as inclusions in plagioclase, suggesting a predominantly metamorphic origin.

Care has been taken to identify minor mineral phases which are likely to be important to the trace element distribution of the trondhjemites. In some specimens, allanite and sphene are present as interstitial grains and appear to be primary. These 2 minerals have been shown to be important in controlling the REE budget of granodiorites (Gromet and Silver 1983) and their presence must be considered when constructing geochemical models from the trace element data obtained from the trondhjemites.

CONTACT RELATIONSHIPS

Field work in 1984 illustrated the striking effect of metavolcanic inclusions on biotite/hornblende ratios in the host trondhjemites. In 1984, contacts of the Trout Lake batholith with mafic metavolcanics of the Red Lake belt and felsic volcanics of the Uchi-Confederation belt were examined in detail.

Red Lake Greenstone Belt Contact

The batholith-greenstone belt contact is exposed along the shoreline of Walsh Lake, northeast of Red Lake. The contact is well exposed at the southern extremity of the lake, and is extremely sharp. The contact phase of the granodiorite is fine- to medium-grained, with equigranular to seriate texture, containing angular xenoliths of amphibolite in varying degrees of separation from the volcanic rocks. The mafic volcanic rocks at the contact have been metamorphosed to amphibolites containing calc-silicate bands (calcite + (calcite + garnet ± pyroxene) which outline open rootless folds. Recognizable primary volcanic textures are not preserved in these rocks.

The granitoids at Walsh Lake are predominantly foliated, medium-grained granodiorite-quartz monzonite. In general, the foliation is parallel to the contacts with the Red Lake belt. The granitoids contain < 10% potassium feldspar phenocrysts in a seriate quartz plagioclase-hornblende-sphene groundmass. Some quartz-monzonites are dominated by potassium feldspar megacrysts (up to 2 cm) with only minor quartz, plagioclase, and hornblende in the matrix.

Xenolith morphology and orientation changes markedly moving away from the contact. Within a few metres of the contact, angular, unoriented blocks are observed. However, at distances greater than a few hundred metres, lens-shaped xenoliths and schlieren become dominant. The degree of rounding of xenoliths and proportions of schlieren to xenoliths increases away from the contact, as does the degree to which xenoliths are aligned with host rock foliation. The principal minerals in the xenoliths are hornblende and sphene with minor quartz and plagioclase.

Uchi-Confederation Lakes Contact

The contact of the batholith with amphibolite-grade intermediate and felsic volcanic rocks of cycle 1 contrasts sharply with the Red Lake belt contact. The contact phase of the batholith is biotite trondhjemite with minor granodiorite. The trondhjemites are fine to medium grained and equigranular. Porphyritic phases are completely absent.

The trondhjemites become increasingly strained approaching the contact. The rocks become more strongly recrystallized, with lens-shaped quartz and plagioclase surrounded by a foliated groundmass of biotite, fine-grained quartz, plagioclase, and minor potassium feldspar.

The most obvious xenoliths are irregular biotite-rich clots and large amphibolite blocks probably related to gabbro sills present in cycle 1. Less obvious are relicts of felsic volcanic rocks which form large rafts near the contact, but are rapidly assimilated by the granitoids further away. Felsic xenoliths are still visible 3 to 4 km from the contact. The orientation of relict volcanic textures (lapilli, bedding) allowed the xenoliths to be distinguished from the foliated trondhjemite host.

The incorporation of felsic volcanic rocks into the trondhjemites is reflected in the high biotite/hornblende ratios of the latter. This suggests that the type and degree of assimilation of xenoliths is an important factor in controlling the ferromagnesian minerals in the granitoids.

GEOCHEMISTRY

Geochemical data for the batholith (Table 168.3) has been obtained recently, and therefore we present only our preliminary comments. Major element data from the migmatitic orthogneiss enclave are similar to the high alumina tonalite-trondhjemite gneisses common in other Archean terranes (Condie 1981). Data from samples of the trondhjemite-diorite-granodiorite are also similar to the high alumina tonalites.

Rare earth element data for lithologies in the batholith are presented in Figures 168.2 and 168.3. The migmatitic gneisses exhibit moderately sloping patterns with positive Eu anomalies for 2 samples. Similar patterns are shown by the trondhjemite-diorite granodiorite, supporting field and major element evidence that the gneisses are largely igneous in origin. One sample from the Uchi Confederation belt contact is unusual in that it is highly enriched in the LREE (300 times chondrites) and has a prominant negative Eu anomaly. This pattern is similar to those obtained from cycle 1 felsic volcanic rocks by Thurston (1981) and this study, and is suggestive of some degree of assimilation of cycle 1 material.

In contrast to the gneisses and trondhjemites, 2 samples from the late felsic dikes have relatively primitive REE patterns, characterized by moderate slopes and positive Eu anomalies. Both of these patterns were obtained from dikes cutting the migmatitic orthogneiss. A third sample shows a fairly fractionated pattern with a small negative Eu anomaly similar to the host trondhjemites.

ZIRCON GEOCHRONOLOGY

Our preliminary attempts to bracket the age of the batholith used samples from the migmatitic trondhjemite enclave and late undeformed felsic dikes. Although 70 kg samples were collected, zircons were unusually sparse. Those zircons which were obtained were not of high quality and were likely from several individual populations. Crystals with subrounded stubby morphology and smaller acicular grains predominated. U-Pb isotopic analyses of zircons from these 2 rocks are presented in Figure 168.4.

Zircons from the 2 samples do not define an age for the batholith. Analyses from the enclave suggest an approximate minimum age of 2800 Ma. Zircons from the dike have an uncertain origin and may be assimilated from the host trondhjemites. Further ef-

TABLE 168.3. GEOCHEMICAL ANALYSES OF THE TROUT LAKE BATHOLITH.

Sample Rock Name	SN-102 tr	SN-104 tr	SN-108 tr	SN-112 tr	SN-113 tr	SN-117 tr	SN-118 tr
SiO_2	70.40	69.60	69.20	71.50	75.50	72.00	70.50
Al_2O_3	14.80	14.80	15.50	14.80	13.90	15.50	16.00
CaO	2.91	3.41	3.40	2.91	0.62	2.32	3.34
MgO	0.70	1.03	0.79	0.68	0.06	0.48	0.83
Na_2O	4.42	4.19	4.36	4.39	4.72	5.47	5.32
K_2O	1.83	1.36	2.00	1.81	4.12	2.23	1.25
Fe_2O_3	2.66	3.86	3.25	2.74	0.50	1.25	1.75
MnO	0.05	0.06	0.05	0.04	0.02	0.02	0.02
TiO_2	0.28	0.40	0.31	0.30	0.03	0.16	0.22
P_2O_5	0.09	0.14	0.10	0.09	0.03	0.04	0.07
LOI	0.93	1.31	1.16	0.70	0.54	0.39	0.47
Total	99.07	100.30	100.20	100.10	100.10	100.00	99.90
Rb	58	63	85		148	29	30
Sr	201	235	195		28	400	473
Ba	517		367		146		577
Rb/Sr	0.29	0.27	0.43		5.33	0.07	0.06
U	1.83		2.70		2.27		0.35
Th	22.04		11.93		7.29		3.60
Ta	0.58		1.10		0.13		0.11
Cs	2.30		3.80		0.73		1.90
Cr	8.30		5.50		32.07		10.00
Hf	5.60		3.30		1.31		3.24
Co	4.30		6.20		17.79		3.80
Sc	1.80		5.80		11.57		2.40
Zn	52.00		62.00				41.30
Au ppb	0.07		0.20		0.10		0.05
Y	11.65	18.05	11.90		10.10	1.60	1.80
Zr	214	210	128		47	98	123
Ni	2.20	3.56	2.08		0.00	0.00	2.07
Cr	0.87	0.00	0.83		0.00	0.00	1.18
V	7.20	21.66	38.00		0.00	6.40	11.55
Ti	1232	1600	1278		48	597	897
La	67.39		25.41		7.28		12.71
Ce	92.42		52.44		3.79		17.79
Nd	33.81		12.87		4.36		6.96
Sm	6.39		2.54		1.33		1.25
Eu	0.79		0.73		0.75		0.42
Tb	0.38		0.32				0.14
Ho	0.04		0.03		0.18		
Tm	0.11		0.17				0.07
Yb	1.85		1.19		1.08		0.44
Lu	0.28		0.20		0.17		0.05
Zr/Hf	38.18		38.73		35.80		37.64
Sm/Nd	0.19		0.20		0.31		0.18

Abbreviations:
tr - trondhjemite
gd - granodiorite
tr gn - trondhjemite gneiss
di gn - diorite xenolith in trondhjemite gneiss

Table 168.3 cont'd.

Sample Rock Name	SN-119 gr dk	SN-121 tr	SN-122 tr	SN-123 tr	SN-133 tr	SN-135 tr	SN-136 m dk
SiO_2	71.60	71.20	72.30	70.20	72.90	67.40	53.10
Al_2O_3	15.00	16.00	15.50	16.00	14.30	16.00	15.50
CaO	1.07	3.08	3.02	3.35	1.56	3.76	8.18
MgO	0.44	0.64	0.56	0.81	0.89	1.25	6.55
Na_2O	4.14	5.76	5.51	5.46	5.22	4.72	3.53
K_2O	5.06	1.06	0.90	1.12	1.86	1.39	1.60
Fe_2O_3	1.53	1.60	1.59	2.06	1.94	4.05	9.12
MnO	0.02	0.02	0.02	0.03	0.04	0.06	0.14
TiO_2	0.24	0.22	0.17	0.23	0.19	0.38	0.80
P_2O_5	0.11	0.08	0.06	0.09	0.06	0.14	0.27
LOI	0 85	0.54	0.47	0.62	1.39	1.23	1.47
Total	100.30	100.30	100.20	100.10	100.50	100.50	100.40
Rb	172	21	16	44		49	44
Sr	458	510	508	209		242	537
Ba	1219		301			328	533
Rb/Sr	0.37	0.04	0.03	0.21		0.20	0.08
U	6.75		0.24			1.51	0.78
Th	16.57		1.30			9.47	2.53
Ta	1.79		0.07			0.43	0.22
Cs	3.40		1.02			2.20	2.00
Cr	5.10		3.90			13.90	215.90
Hf	5.60		3.14			4.98	2.63
Co	2.40		2.50			7.20	34.90
Sc	1.60		1.70			6.60	21.90
Zn	28.00		41.50			76.60	
Au ppb	0.04		0.07				0.02
Y	10.70	2.00	1.10	5.80		12.30	14.70
Zr	252	140	127	152		230	118
Ni	2.24	0.00	0.00	0.00		6.11	88.17
Cr	0.00	0.00	0.00	0.00		9.69	175.42
V	6.66	8.75	7.98	12.59		30.17	134.78
Ti	846	735	661	790		1523	2847
La	44.47		5.60			18.66	9.46
Ce	96.27		9.98			32.88	48.81
Nd	24.70		3.20			9.38	6.00
Sm	5.80		0.60			2.30	1.34
Eu	1.24		0.42			0.71	1.31
Tb	0.39		0.02			0.34	0.50
Ho			0.13			0.11	0.06
Tm	0.17		0.11			0.06	
Yb	0.94		0.18			1.04	0.54
Lu	0.17		0.05			0.12	0.08
Zr/Hf	44.91		40.51			46.12	44.94
Sm/Nd	0.23		0.19			0.24	0.22

Abbreviations
tr - trondhjemite
gd - granodiorite
tr gn - trondhjemite gneiss
di gn - diorite xenolith in trondhjemite gneiss
gr dk - granitic dike
m dk - mafic dike

Table 168.3 cont'd.

Sample Rock Name	SN-137	SN-140 m dk	SN-141 qm	SN-142 gr dk	SN-143 m dk	SN-144 tr	SN-147
SiO_2	62.90	50.70	71.50	73.10	54.40	67.60	61.60
Al_2O_3	16.60	12.20	15.70	15.40	17.20	17.10	18. 00
CaO	5.00	8.98	2.24	1.75	7.12	4.24	5.48
MgO	2.51	12.00	0.43	0.20	5.00	1.05	2.07
Na_2O	4.83	2.21	5.40	5.44	3.73	5.54	5.42
K_2O	1.26	1.93	2.38	2.93	2.19	1.20	1.21
Fe_2O_3	4.29	8.64	1.11	0.34	7.40	2.29	4.81
MnO	0.05	0.14	0.01	<0.1	0.10	0.02	0.06
TiO_2	0.62	0.60	0.17	0.07	0.80	0.33	0.56
P_2O_5	0.19	0.24	0.05	0.03	0.28	0.12	0.18
LOI	1.93	1.33	0.85	0.47	1.62	0.54	0.70
Total	100.40	99.90	100.00	99.90	100.00	100.20	100.30
Rb		75	54	58	64		
Sr		699	521	447	663		
Ba		685	917	742			
Rb/Sr		0.11	0.10	0.13	0.10		
U		1.11	0.78	0.53			
Th		7.71	3.00	1.30			
Ta		0.39	0.15	0.47			
Cs		9.20	4.50	1.70			
Cr		1026.62	2.60	3.30			
Hf		2.70	2.30	1.70			
Co		49.60	1.30	0.93			
Sc		25.40	1.60	1.10			
Zn		100.30	33.60	15.10			
Au ppb			0.06	0.07			
Y		15.10	4.00	2.40	17.00		
Zr		108	100	64	164		
Ni		296.62	0.00	2.43	52.03		
Cr		823.35	0.00	1.02	80.06		
V		119.32	7.79	3.10	104.49		
Ti		2230	655	234	2975		
La		38.53	9.46	3.71			
Ce		84.95	18.42	8.10			
Nd		40.85	6.00	2.40			
Sm		7.95	1.34	0.75			
Eu		1.81	0.57	0.45			
Tb		0.57	0.15	0.10			
Ho		1.29	0.09	0.13			
Tm		0.22	0.02	0.07			
Yb		1.08	0.54	0.37			
Lu		0.16	0.13	0.06			
Zr/Hf		40.04	43.43	37.76			
Sm/Nd		0.19	0.22	0.31			

Abbreviations
tr - trondhjemite
gd - granodiorite
tr gn - trondhjemite gneiss
di gn - diorite xenolith in trondhjemite gneiss
qm - quartz monzonite
gr dk - granitic dike
m dk - mafic dike

Table 168.3 cont'd.

Sample	**SN-149**	**SN-151**	**SN-159**	**SN-161**	**SN-159**	**SN-173**	**SN-205**
Rock Name	**m dk**	**tr gn**	**tr gn**	**tr gn**	**tr gn**	**gd**	**tr gn**
SiO_2	49.00	68.60	65.80	71.00	65.80	65.20	69.80
Al_2O_3	17.00	16.60	16.60	15.70	16.60	15.00	15. 30
CaO	8.40	1.55	3.89	3.38	3.89	3.56	3.16
MgO	5.24	1.15	1.23	0.66	1.23	2.26	1.01
Na_2O	3.95	6.22	5.32	5.41	5.32	3.89	4.87
K_2O	1.50	1.60	1.32	1.06	1.32	4.15	1.60
Fe_2O_3	10.70	2.62	4.65	1.98	4.65	4.22	3.26
MnO	0.16	0.02	0.06	0.02	0.06	0.06	0.04
TiO_2	1.09	0.29	0.46	0.26	0.46	0.68	0.39
P_2O_5	0.30	0.12	0.17	0.09	0.17	0.28	0.15
LOI	0.93	1.54	0.77	0.54	0.77	0.62	0.70
Total	98.27	100.50	100.40	100.20	100.40	100.20	100.40
Rb	37	45	70	34			
Sr	557	363	302	339			
Ba		243	681	299			
Rb/Sr	0.07	0.12	0.23	0.10			
U	0.63	0.61	0.65	0.44			
Th	2.66	10.16	2.55	1.88			
Ta	0.39	0.21	0.87	0.18			
Cs	1.99	1.09	8.00	1.20			
Cr	53.00	3.54	8.30	3.10			
Hf	2.85	4.09	3.52	3.77			
Co	37.96	5.54	8.20	3.70			
Sc	22.87	2.14	14.20	2.40			
Zn	105.60	45.60		47.80			
Au ppb	0.07	0.00	0.03	0.10			
Y	17.00	4.10	17.40	3.70			
Zr	117	182	136	167			
Ni	29.58	0.79	6.33	0.00			
Cr	40.56	0.00	3.47	0.00			
V	162.46	15.75	41.04	13.73			
Ti	3900	1200	1800	1100			
La	20.90	33.03	11.91	6.96			
Ce	54.74	55.53	27.04	12.17			
Nd	23.00	15.85	11.79	3.41			
Sm	5.56	2.16	3.40	0.86			
Eu	1.66	0.71	0.81	0.45			
Tb	0.59	0.22	0.56	0.14			
Ho	1.38		1.21	0.35			
Tm	0.26		0.39	0.11			
Yb	1.29	0.04	1.15	0.27			
Lu	0.25	0.03	0.21	0.07			
Zr/Hf	41.19	44.51	38.55	44.24			
Sm/Nd	0.24	0.14	0.29	0.25			

Abbreviations:
tr - trondhjemite
gd - granodiorite
tr gn - trondhjemite gneiss
di gn - diorite xenolith in trondhjemite gneiss

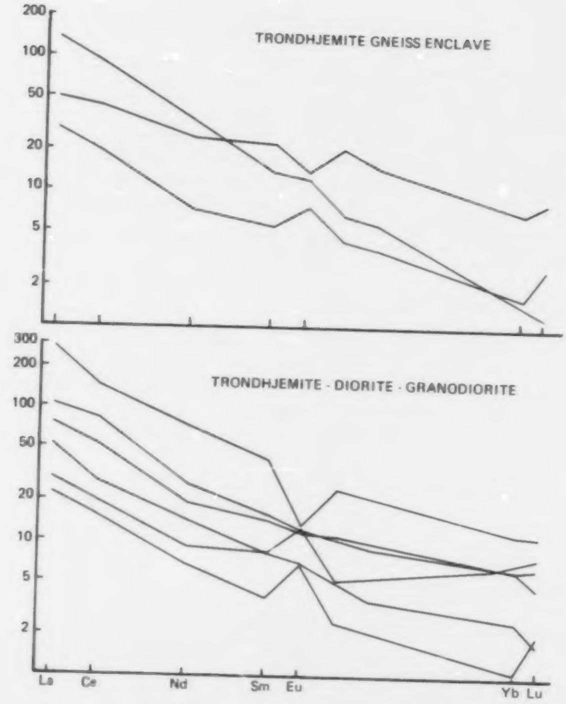

Figure 168.2. Chondrite normalised REE plots for the migmatitic trondhjemite enclave and trondhjemite-diorite-granodiorite main phase of the batholith.

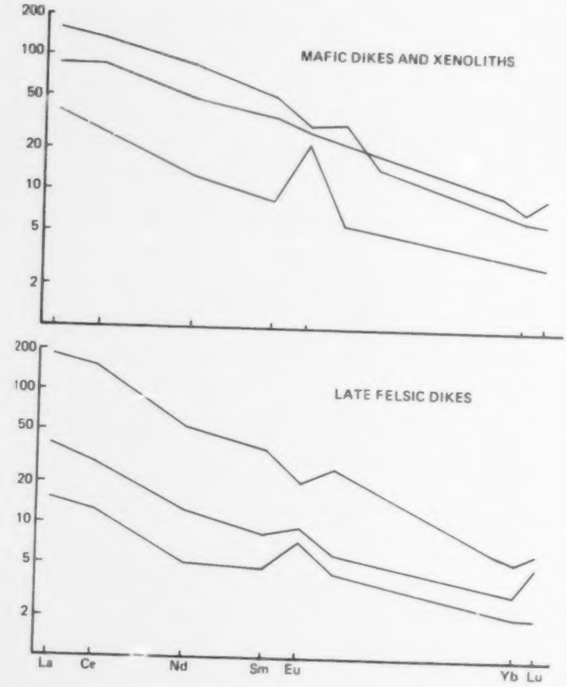

Figure 168.3. Chondrite normalised REE plots for the mafic dikes and xenoliths, and late felsic dikes.

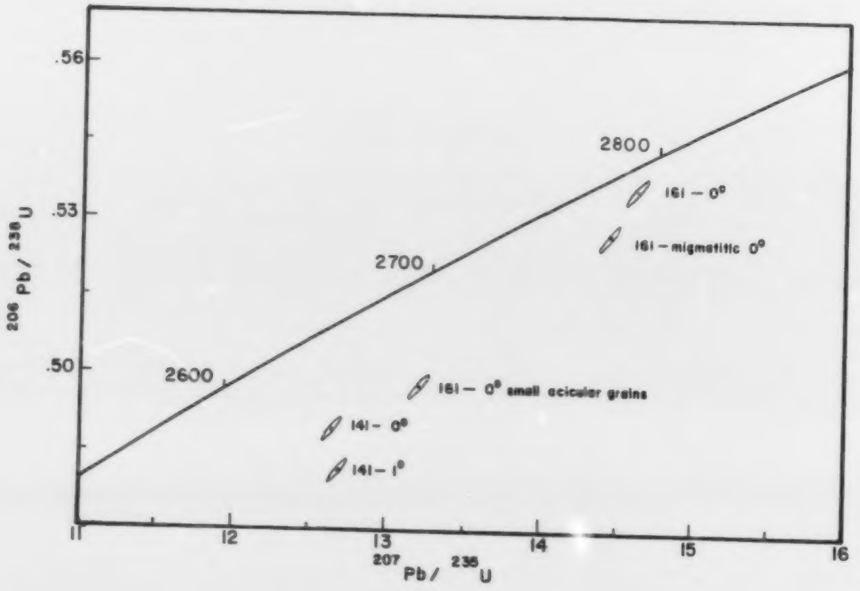

Figure 168.4. Concordia plot of U-Pb isotopic analysis of the Trout Lake batholith. Sample 141 is a late felsic dike, while sample 161 is a trondhjemite orthogneiss with some migmatitic portions. Angles preceding sample numbers refer to Frantz magnetic separator settings.

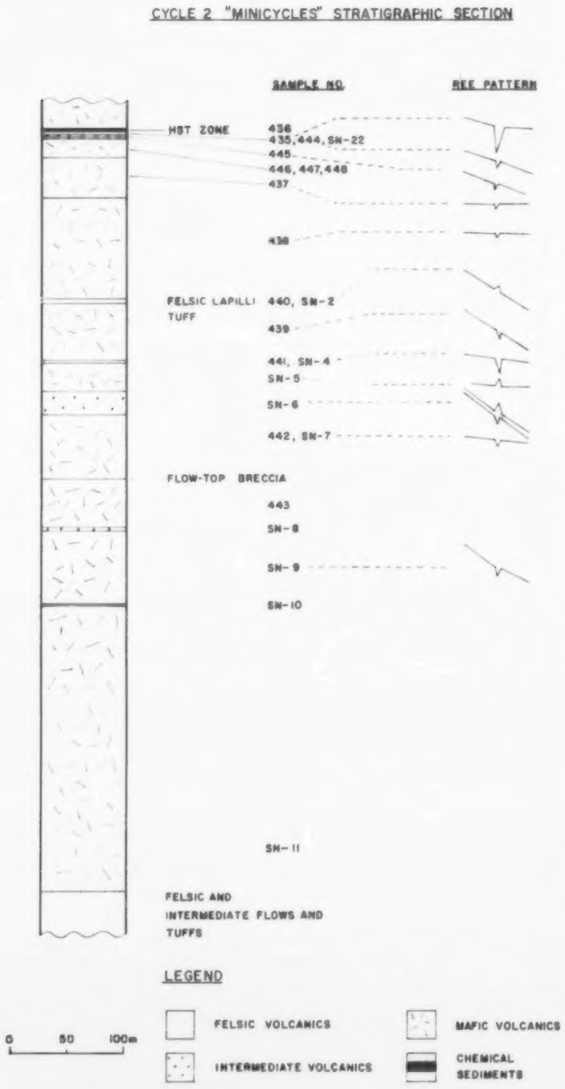
CYCLE 2 "MINICYCLES" STRATIGRAPHIC SECTION
SAMPLE NO.
REE PATTERN
HST ZONE
436
435, 444, SN-22
445
446, 447, 448
437
438
FELSIC LAPILLI TUFF
440, SN-2
439
441, SN-4
SN-5
SN-6
442, SN-7
FLOW-TOP BRECCIA
443
SN-8
SN-9
SN-10
SN-11
FELSIC AND INTERMEDIATE FLOWS AND TUFFS
LEGEND
FELSIC VOLCANICS
MAFIC VOLCANICS
INTERMEDIATE VOLCANICS
CHEMICAL SEDIMENTS
0
50
100m

Figure 168.5. *Stratigraphic section through part of the cycle 2 minicycles showing schematic REE patterns for the various lithologies. Data are obtained from this study and Thurston and Fryer (1983). 400 series samples are from Thurston (1981), SN series samples are from this study.*

forts to date the batholith are being concentrated on the foliated trondhjemite.

UCHI-CONFEDERATION LAKE VOLCANICS

We are examining several sections through the 3 volcanic cycles using major and minor elements, and Sm-Nd isotope analyses. We have completed a preliminary survey of Sm-Nd data for samples of all 3 cycles, and a geochemical traverse through part of cycle 2.

MINICYCLES

The "minicycles" are located near the eastern portions of Lost Bay, Confederation Lake near the Uchi Lake Mine (Au; Thurston 1981). The minicycles are a series of 4 mafic to felsic minor volcanic cycles within the eastern limb of cycle 2. Previous geochemical analyses of 2 minicycles (Thurston 1981; Thurston and Fryer 1983) indicated that these volcanic rocks may be the product of a previously recharged magma chamber. Therefore, these volcanic rocks are a reasonable location to test for variable degrees of assimilation of magma chamber host rock and for fractionation of those magmas concurrent with repeated influx of new magma, using a combination of trace element and Sm-Nd isotope analyses. Data from this section may in turn aid in determining whether crustal recycling has been important elsewhere in the volcanic rocks.

A stratigraphic section of part of the minicycles and the location of the samples collected by the authors and Thurston (1981) are shown in Figure 168.5. A summary of geochemical data for the minicycles from both this study and Thurston (1981) are given in Table 168.4.

Each minicycle has a basalt or basaltic andesite base. This base is usually a massive flow with a thin flow-top breccia, although some flows are pillowed. Intermediate to felsic tuffs overlie the mafic flows. The tuffs are primarily vitric and fine upwards.

The minicycles have the following geochemical characteristics:

1. Smooth fractionation trends are not observed on plots of relatively immobile trace elements (e.g. Zr vs TiO_2; Zr vs Y) for data from all the minicycles.
2. There is a progressive enrichment in LREE up the stratigraphy within a minicycle, with prominent positive Eu anomalies and enrichment in HREE in the most fractionated rhyolites. These rhyolites therefore bear some resemblance to "tholeiitic rhyolites" found in cycle 3 and elsewhere (Campbell *et al.* 1982; Hart 1984).

The REE pattern variation over small stratigraphic distances and repetition of the REE trends in other minicycles suggest that these rocks are indeed the result of periodic influxes of magma followed by fractionation.

Sm-Nd ISOTOPE GEOCHEMISTRY

Preliminary Sm-Nd data from the 3 cycles have been obtained. The philosophy at this stage of the study has been to use a combination of U-Pb ages and

TABLE 168.4. ANALYSES FOR MINICYCLES SAMPLES.

Sample	SN-4	SN-5	SN-6	SN-7	SN-8	SN-9
SiO_2	77.15	48.23	66.21	45.41	65.06	51.25
Al_2O_3	12.05	15.87	16.79	11.89	15.19	14.58
CaO	2.12	12.11	2.94	10.09	3.05	8.21
MgO	1.21	8.71	2.06	6.63	3.26	5.36
Na_2O	2.09	1.63	3.37	1.73	3.50	3.37
K_2O	2.70	.38	4.02	.40	2.23	.32
Fe_2O_3	2.32	11.48	3.92	20.71	4.92	13.15
MnO	.04	.17	.08	.19	.08	.17
TiO_2	.20	.81	.53	2.17	.64	1.49
P_2O_5	.02	.11	.11	.19	.43	.23
Total	99.89	99.50	100.02	99.41	98.76	98.12
LOI	2.93	4.16	5.31	2.39	4.39	2.54
Rb	57	9	66	10	41	7
Sr	98	425	181	396	157	381
Ba	591	22	1040	55	810	92
Rb/Sr	.58	.02	.36	.03	.26	.02
U	2.60	.08	.99	.35	.97	.41
Th	14.11	.40	3.06	2.54	3.65	2.15
Ta	2.01	.16	.34	.20	.31	.25
Cs	.68	.17	.49	.47	.41	.56
Cr	3.45	371.49	48.42	6.12	104.30	170.62
Hf	11.71	1.35	3.09	1.46	3.42	2.70
Co	2.75	54.15	9.86	71.94	16.43	43.61
Sc	1.72	32.29	6.45	48.49	9.40	29.47
Zn	74.65	83.20		133.81	126.50	128.56
Au ppb	.08			.27		
Y	67.34	13.94	6.95	17.80	7.43	20.48
Zr	383	55	144	70	155	101
La	55.64	4.83	16.30	17.22	18.73	20.20
Ce	128.13	12.42	27.36	42.06	34.43	50.53
Nd	44.63	6.46	8.89	22.01	12.15	22.50
Sm	10.61	1.86	2.11	4.51	2.56	4.96
Eu	1.30	.84	.81	1.39	.88	1.54
Tb	2.34	.41	.29	.88	.50	.96
Ho	2.44	.56	.43	.60	.46	1.44
Tm	1.52	.42	.19	.57	.30	.44
Yb	9.32	1.68	.90	1.65	.64	2.08
Lu	1.42	.27	.14	.27	.12	.32
Zr/Hf	32.72	40.75	46.62	47.80	45.32	37.41
Sm/Nd	.24	.29	.24	.20	.21	.22

Geochemical data for 400 series samples are found in Thurston (1981).

Sm-Nd isotopic data from the same samples to indicate the span of Nd initial ratios for the belt. Detailed analyses of cogenetic suites, if they can be reliably identified, will follow at a later date.

Table 168.5 lists initial ratios and epsilon Nd for 8 samples of reliably known age from each of the 3 main volcanic cycles. Samples SN-96 and SN-59 have been dated by Nunes and Thurston (1980) at 2959 Ma and 2738 Ma respectively. Samples SN-62 and SN-63 are granodiorite subvolcanic sills closely related to SN-50 (their REE patterns are virtually identical), while SN-4, SN-5, SN-6, and SN-7 are from the minicycles and have an approximate age of 2840 Ma (F. Corfu, J. Satterly Geochronology Laboratory, Royal Ontario Museum, Toronto, personal communication, 1984).

Figure 168.6 shows the relationship of the Uchi data to data from a variety of sources. Included are

TABLE 168.5. Sm-Nd ISOTOPIC DATA FOR UCHI VOLCANICS.

Assumed Age(Ga)	Sample	Sample Sm/Nd	Present 143/144	Initial 143/144	epsilon Nd (T)	T(CHUR) (Ga)
2.74	SN 59	.13958	.512055	.509531	8.80	1.56
2.74	SN 62	.13441	.511915	.509485	7.88	1.77
2.74	SN 63	.14861	.512142	.509455	7.30	1.58
2.84	SN 4	.11080	.511462	.509385	8.49	2.08
2.84	SN 5	.13284	.511871	.509381	8.41	1.83
2.84	SN 6	.09814	.511137	.509297	6.77	2.31
2.84	SN 7	.10892	.511328	.509286	6.56	2.27
2.96	SN 96	.06837	.510358	.509022	4.45	2.70

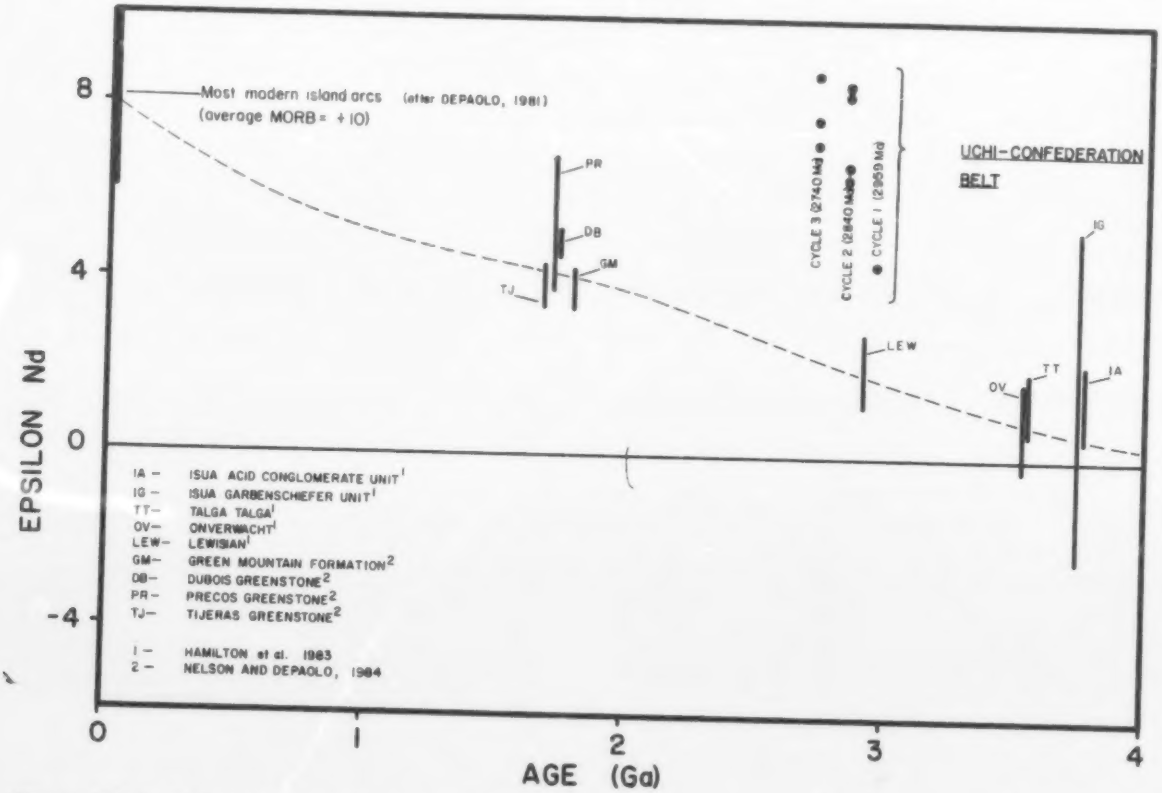

Figure 168.6. Epsilon Nd versus age diagram showing relationships of Uchi-Confederation belt analyses to other Archean and Proterozoic terranes. The modern island arc field is also shown.

data from other granodiorite belts, Archean Isua sediments and volcanics, Lewisian gneisses, and modern island arcs. The dashed line is an inferred bulk mantle epsilon Nd evolution line (Nelson and De Paolo 1984). Uchi data have epsilon Nd well above the bulk mantle evolution line suggesting an unusual source. This unusual source is not unexpected, because epsilon Hf data for a slightly post-cycle 3 pluton gave the oldest indication of depleted mantle in the global Hf survey by Patchett *et al.* (1982).

Figure 168.6 shows that in moving upwards through the volcanic stratigraphy from cycle 1 to the top of cycle 3, there is a positive increase of 4 epsilon Nd units. The positive increase is unusual because it suggests that magmas are being derived from a source region undergoing remarkable depletion, a surprising finding in view of the following points:

1. Crustal recycling via partial melting of the lower portions of the belt or assimilation of earlier volcanic rocks (with the less positive epsilon Nd due to a period of crustal residence and/or derivation from a presumably less depleted source than the younger volcanics) would be more likely to occur if a thick succession of volcanic rocks were already present. Therefore, there would be a greater tendency for younger volcanics to have epsilon Nd biased downward.
2. It is difficult to visualize a magma source region undergoing such marked depletion when it is generally considered that mantle convection and Archean tectonics were probably more vigorous than at the present time.
3. While the Nd isotope data indicate the volcanic rocks are derived from progressively depleted sources, REE data indicate that the volcanic rocks are becoming increasingly fractionated.

Data from the minicycles are particularly interesting. The 4 samples analyzed are mafic-felsic volcanic pairs from 2 minicycles. Epsilon Nd for samples in the same minicycles are consistent, considering that the error in epsilon Nd is approximately ± 0.5 epsilon units. However, the 2 minicycles differ by at least 1.6 epsilon units. This difference cannot be due to crystal fractionation and must result from varying degrees of contamination of the magma and/or varying magma source regions with different Nd isotopic characteristics.

CONCLUSIONS AND FUTURE OBJECTIVES

The following conclusions are based on a combination of essentially complete field work and preliminary geochemical and isotopic data:

1. U-Pb dating of zircons from the migmatitic trondhjemite and orthogneiss enclave show that portions of the Trout Lake batholith are at least 2800 Ma old and therefore predate cycle 3 volcanic rocks in the adjacent Uchi-Confederation Lake belt.
2. Additional geochemical analyses of the cycle 2 "minicycles" and re-examination of previously obtained data show that the repetitive stratigraphy is probably representative of a periodically recharged magma chamber. Nd-isotope data for 2 of the minicycles support this hypothesis and suggests that there are dramatic differences in the degree of assimilation of magma chamber host rocks and/or of Nd-isotopic characteristics of the magma sources for different minicycles.
3. If the preliminary Nd-isotopic data are reliable, then it appears that the magmatic source regions for the volcanic rocks in the Uchi-Confederation belt were becoming progressively depleted. It is remarkable that magma could have been tapped from such a mantle reservoir over a period spanning at least 220 Ma.

FUTURE OBJECTIVES

Field work and sample collection are essentially complete. The emphasis of the project has now shifted to laboratory based work.

Geochemical analyses of the samples from the Uchi belt are on-going and are expected to be completed by mid-1986.

Zircon U-Pb analyses will continue on 5 samples. Three samples are from the trondhjemite-diorite-granodiorite unit of the batholith, one sample is from a felsic crystal-vitric tuff from the lowermost cycle 2 minicycle, and one sample is from cycle 1 on the eastern portions of the belt. All samples have been reduced to heavy mineral separates and now await picking and analysis of the zircons. This group of samples is intended to give an age for the main phase of the batholith, to confirm the existence of, and aid in, obtaining Nd-initial ratios for cycle 1 volcanic rocks in the eastern part of the belt and to date the cycle 2 minicycles more precisely.

As with the geochemical analyses, Sm-Nd isotope analyses are on-going. We are now completing a new isotope preparation laboratory at the Department of Geology, University of Toronto, which will improve on the quality and quantity of analyses.

REFERENCES

Campbell, I.H., Coad, P., Franklin, J.M., Gorton, M.P., Scott, S.D., Sowa, J., and Thurston, P.C.
1982: Rare Earth Elements in Volcanic Rocks Associated with Cu-Zn Massive Sulphide Mineralization: A Preliminary Report; Canadian Journal of Earth Sciences, Volume 19, p.619-623.

Campbell, I.H., Franklin, J.M., Gorton, M.P., Hart, T.R., and Scott, S.D.
1981: The Role of Subvolcanic Sills in the Generation of Massive Sulfide Deposits; Economic Geology, Volume 76, p.2248-2253.

Condie, K.C.
1981: Archean Greenstone Belts; Elsevier, New York, 434p.

De Paolo, D.J.
1981: Nd Isotopic Studies: Some Perspectives on Earth Structure and Evolution; EOS, Volume 62, p.137-140.

Goodwin, A.M.
1967: Volcanic Studies in the Birch-Uchi Lakes Area of Ontario; Ontario Department of Mines, Miscellaneous Paper 6, 96p.

Gromet, L.P., and Silver, L.T.

1983: Rare Earth Element Distribution Among Minerals in a Granodiorite and their Petrogenetic Implications; Geochimica et Cosmochimica Acta, Volume 47, p.925-946.

Hart, T.R.

1984: The Geochemistry and Petrogenesis of a Metavolcanic and Intrusive Sequence in the Kamiskotia Area, Timmins, Ontario; Unpublished M.Sc. Thesis, University of Toronto, 179p.

Hamilton, P.J., O'Nions, R.K., Bridgewater, K., and Nutman, A.

1983: Sm-Nd Studies of Archean Metasediments and Metavolcanics from West Greenland and their Implications for the Earth's Early History; Earth and Planetary Science Letters, Volume 62, p.263-272.

Hillary, E.M., and Ayres, L.D.

1980: Trondhjemitic Basement Enclave Near the Archean Favourable Lake Complex, Northwestern Ontario, Canada; Canadian Journal of Earth Sciences, Volume 17, p.652-667.

Jahn, B., Vidal, P., and Kröner, A.

1984: Multi-Chronometric Ages and Origin of Archean Tonalitic Gneisses in Finnish Lapland: A Case for Long Crustal Residence Time; Contributions to Mineralogy and Petrology, Volume 86, p.398-408.

Johannes, W., and Gupta, L.N.

1982: Origin and Evolution of a Migmatite; Contributions to Mineralogy and Petrology, Volume 79, p.114-123.

Mehnert, K.R.

1968: Migmatites and the Origin of Granitic Rocks; Elsevier, New York, 393p.

Nelson, B.K., and DePaolo, D.J.

1984: 1700 Myr Greenstone Volcanic Successions in Southwestern North America and Isotopic Evolution of Proterozoic Mantle; Nature, Volume 312, p.143-146.

Nielsen, B.V., and Weiblen, P.W.

1980: Mineral and Rock Compositions of Mafic Enclaves in the Morton Gneiss; p.95-103 *in* Selected Studies of Archean Gneisses and Lower Proterozoic Rocks, Southern Canadian Shield, edited by G.B. Morey and G.H. Hanson, Geological Society of America, Special Paper 182.

Noble, S.R., Evensen, N.M., and Krogh, T.E.

1984: Petrogenesis of Mineralized Horizons in Uchi Lake Metavolcanics; Grant 168, *in* Geoscience Research Grant Program, Summary of Research 1983-1984, Ontario Geological Survey, Miscellaneous Paper 121, p.188-195.

Nunes, P.D., and Thurston, P.C.

1980: Two Hundred and Twenty Million Years of Archean Evolution: A Zircon U-Pb Age Stratigraphic Study of the Uchi-Confederation Lakes Greenstone Belt, Northwestern Ontario; Canadian Journal of Earth Sciences, Volume 17, p.710-721.

Patchett, P.J., Kouvo, O., Hedge, C.E., and Tatsumoto, M.

1981: Evolution of Continental Crust and Mantle Heterogeneity: Evidence from Hf Isotopes; Contributions to Mineralogy and Petrology, Volume 78, p.279-297.

Pryslak, A.P.

1971: Corless Township, District of Kenora (Patricia Division); Ontario Department of Mines and Northern Affairs, Preliminary Map P.634, scale 1:15 840.

Streckeisen, A.

1976: To Each Plutonic Rock its Proper Name; Earth Science Reviews, Volume 12, p.1-33.

Thurston, P.C.

1981: The Volcanology and Trace Element Geochemistry of Cyclical Volcanism in the Archean Confederation Lake Area, Northwestern Ontario; Unpublished Ph.D. Thesis, University of Western Ontario, 553p.

1982: Economic Evaluation of Archean Felsic Volcanic Rocks Using REE Geochemistry; Geological Society of Australia, Special Publication 7, p.439-450.

Thurston, P.C., and Fryer, B.J.

1983: The Geochemistry of Repetitive Cyclical Volcanism from Basalt Through Rhyolite in the Uchi-Confederation Greenstone Belts, Canada; Contributions to Mineralogy and Petrology, Volume 83, p.204-226.

Grant 173 Sedimentary Rocks and Strata-Bound Mineralization in the Cobalt Region

J.A. Donaldson[1], **F.A. Michel**[1], **P.S. Mustard**[1], **R. Rainbird**[1], **B.R. Rust**[2], **D.H. Watkinson**[1], **and B. Wilson**[1]

[1]Department of Geology, Carleton University

[2]Department of Geology, University of Ottawa

ABSTRACT

Detailed mapping in the Cobalt area (1:2000) has allowed subdivision of the Gowganda Formation into subunits diagnostic of particular depositional environments. The lower part of the Gowganda Formation (Coleman Member) comprises a basal breccia (periglacial regolith); basal diamictite (primary till); an upward-coarsening sequence of rhythmically laminated argillite, siltstone, and fine-grained sandstone, overlain by interbedded medium- to coarse-grained sandstone and pebble-granule ortho-conglomerate (prograding subaqueous outwash fan and interfan deposits); and bedded heterolithic diamicton resulting from subaqueous sediment gravity flows. The Gowganda Formation at Cobalt fits an inner-shelf grounded ice sheet model. Substantial subaqueous deposition is inferred to have occurred in a glaciomarine tidewater environment. The local depositional environment was an area of low to moderate relief, on the inner shelf of a slowly subsiding continental margin.

The upper part of the Gowganda Formation (Firstbrook Member) is inferred to have been deposited in a prograding, river-dominated, deltaic environment. Deposition probably occurred within a marine basin influenced by weak tidal and oceanic currents. Laminated mudstones in the lower part of the Firstbrook Member are inferred to represent quiet-water prodeltaic deposition subject to anoxic conditions. Laminated mudstone, siltstone, and fine-grained sandstone of the middle part of the Firstbrook are assigned to a delta-slope setting that was subject to oxidizing conditions promoted by wave agitation and tidal currents. Graded beds of arkose in this unit represent sporadic turbidity current deposits. Fine-grained sandstone and interbeds of siltstone and mudstone in the upper part of the Firstbrook Member represent deposition in a delta foreslope setting. The succession coarsens upward to the fluvial braidplain deposits of the overlying Lorrain Formation. Structures indicative of penecontemporaneous deformation are abundant in strata of the upper part of the Firstbrook Member.

The degree of chemical weathering of mudstones in the Cobalt Group, as assessed in terms of the chemical index of alteration (CIA), is in agreement with upward transition from chemically immature sediments of glacial provenance to chemically mature sediments developed in a temperate to tropical climate. An abrupt increase in the CIA index occurs across the Coleman-Firstbrook boundary.

Prograding subaqueous outwash fan deposits in the Coleman Member are potential sites for placer gold. Although samples from the Cobalt area yielded disappointing analytical results, outwash fans elsewhere in the Gowganda Formation should not be completely dismissed as targets for placer gold exploration.

Many of the sulphide minerals in the Coleman Member are not of detrital origin, as is indicated by their increase in abundance proximal to veins, their textures, and the presence of Ag, Ni, Co, and As minerals within many of the sulphide grains. However, some detrital sulphides may have been mobilized during vein formation or during emplacement of the Nipissing Diabase. Sulphur isotope work (in progress) should help to establish the origin of the sulphides in the Gowganda Formation.

INTRODUCTION

Although much of the mineral wealth of the Cobalt region (Ag, Pb, Zn, Cu, Pt, Co) has been derived from Proterozoic and Archean sedimentary rocks, few detailed sedimentological investigations, apart from the present study, have been carried out in this region. Whereas considerable research efforts have been directed at mineralogy, metamorphism, and relationship of the ore deposits to emplacement of the Nipissing diabase (e.g., Jambor 1971); most sedimentary studies of the Cobalt Group have been directed at regional syntheses (Young 1973). The present research project involves systematic studies of stratigraphic components of the Cobalt Group and subjacent Archean basement rocks (Figure 173.1), as well as the regolith at the Archean-Proterozoic unconformity (Patterson 1979; Rainbird 1980). The principal aims have been to establish criteria for recognizing specific lithofacies, to infer depositional environments, and to evaluate possible associations of mineral deposits with these facies.

With regard to the latter aim, we have focused in this report on the possible detrital origin of sulphide minerals in the Gowganda Formation (Halls and Stumpfl 1969; Patterson 1979; Kim 1979). We are now concentrating on evaluating the possible derivation of silver veins in the Cobalt area from Archean basement sources as well as the potential for stratabound Ag, Pb, Zn, and Cu deposits in the Gowganda Formation. (*See* Lovell 1978, for a review of earlier assessments).

SEDIMENTOLOGY OF THE COLEMAN MEMBER

Completion of 1:2000 scale mapping in the immediate Cobalt area (Figure 173.1) has resulted in the definition of individual subunits of the lower Gowganda Formation (Coleman Member). A review of assessment files, mine plans, and the notes of Robert Thomson, former resident geologist (all documents are stored in the Ontario Geological Survey Resident Geologist's Office, Cobalt), provided substantial data on subsurface stratigraphy of the Coleman Member. Combined with the well documented subsurface information of Knight (1924), the detailed surface geology from this study, and structure contour maps of the Archean-Proterozoic unconformity surface

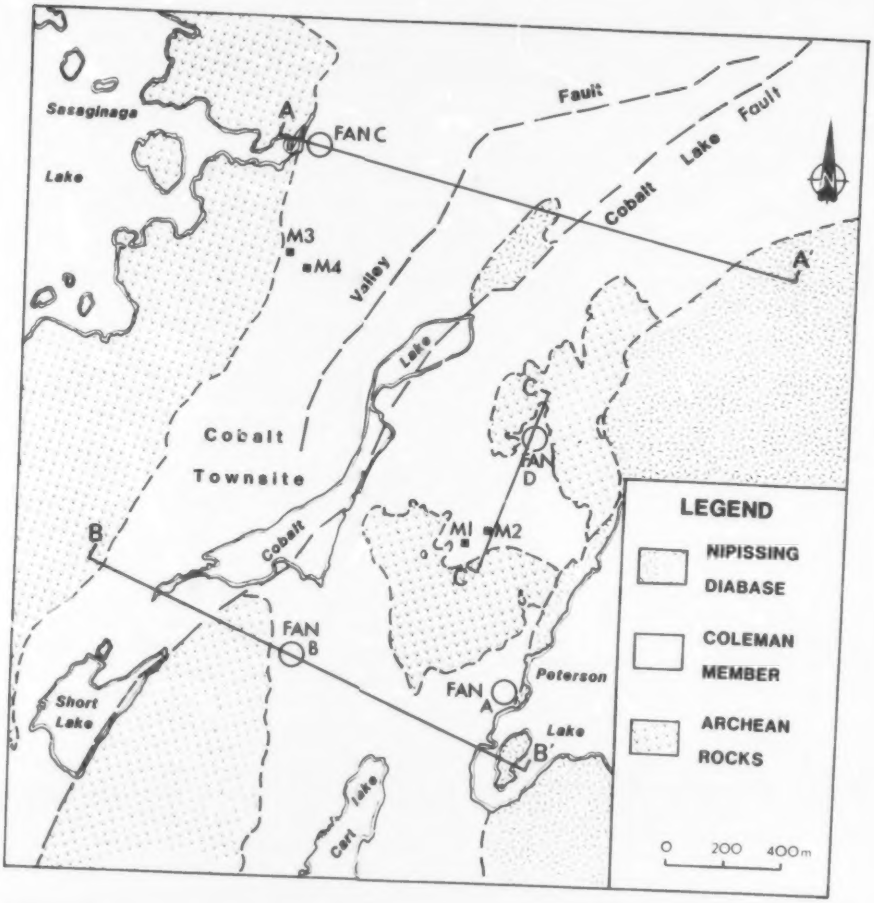

Figure 173.1. *Area mapped at 1:2000 scale for study of Coleman Member sedimentology (Mustard, in preparation). A-A', B-B', and C-C' correspond to the cross-sections illustrated in Figure 173.2; sites of samples analyzed for gold (Table 173.1) are indicated by letters and numbers. Little Silver Vein is within Fan B.*

(Thomson 1961, Legun 1984), cross-sections were generated which show the mutual relationships of Coleman Member lithofacies as well as their relationship to the Archean unconformity surface. Examples are illustrated in Figure 173.2.

The sections illustrate that thinning and pinch-out of Coleman Member lithofacies at the edges of apparent paleohighs occur only in the lowermost units (approximately the basal 30 m). However, even the extensive basal diamictite unit thins only slightly and mantles most paleohighs. The lithofacies contacts are subparallel to the unconformity surface, and many of the units do not noticeably thin or thicken with respect to paleotopography.

These observations confirm the original interpretation of Knight (1924) that Proterozoic and Archean rocks in the Cobalt area are gently folded. This is supported by Symons' (1970) paleomagnetic study of the Nipissing Diabase, in which he demonstrated that broad northeast-trending folds are superimposed on the gentle basin-and-dome configuration of the diabase. Our new evidence does not support Legun's (1984) conclusion that "considerable relief" was present on the unconformity surface. The minor pinch-out of lower stratigraphy requires a paleorelief of no more than a few tens of metres. Allowing for the effects of folding, the maximum paleorelief at Cobalt is estimated to be 100 m. The paleotopography is envisaged as a series of broad, north- to northeast-trending valleys separated by low ridges.

These conclusions indicate that the effects of differential compaction at Cobalt were less significant than previously proposed, and thus Legun's (1981, 1984) suggestion, that differential compaction related to basement paleotopography was an important component in the development of fracture patterns and related silver mineralization, should be re-evaluated. A detailed structural study of the Cobalt region is warranted, especially in view of preliminary results (Donaldson *et al.* 1984) which indicate a possible relationship between joint patterns, silver vein orientations, and regional compressional stress patterns inferred from major faults in the area.

The compilation of data required for the generation of these cross-sections also allowed a check on the accuracy of published structure-contour maps of the unconformity surface (Thomson 1961; Legun 1984). When subjected to this cross-checking, the hand-drafted map of Thomson (1961) proved to be more accurate than the computer-generated version of Legun (1984).

The sedimentological component of this study has resulted in an advanced understanding of the glaciogenic paleoenvironment at Cobalt during deposition of the Coleman Member. Our preliminary interpretations (Donaldson *et al.* 1984) have been con-

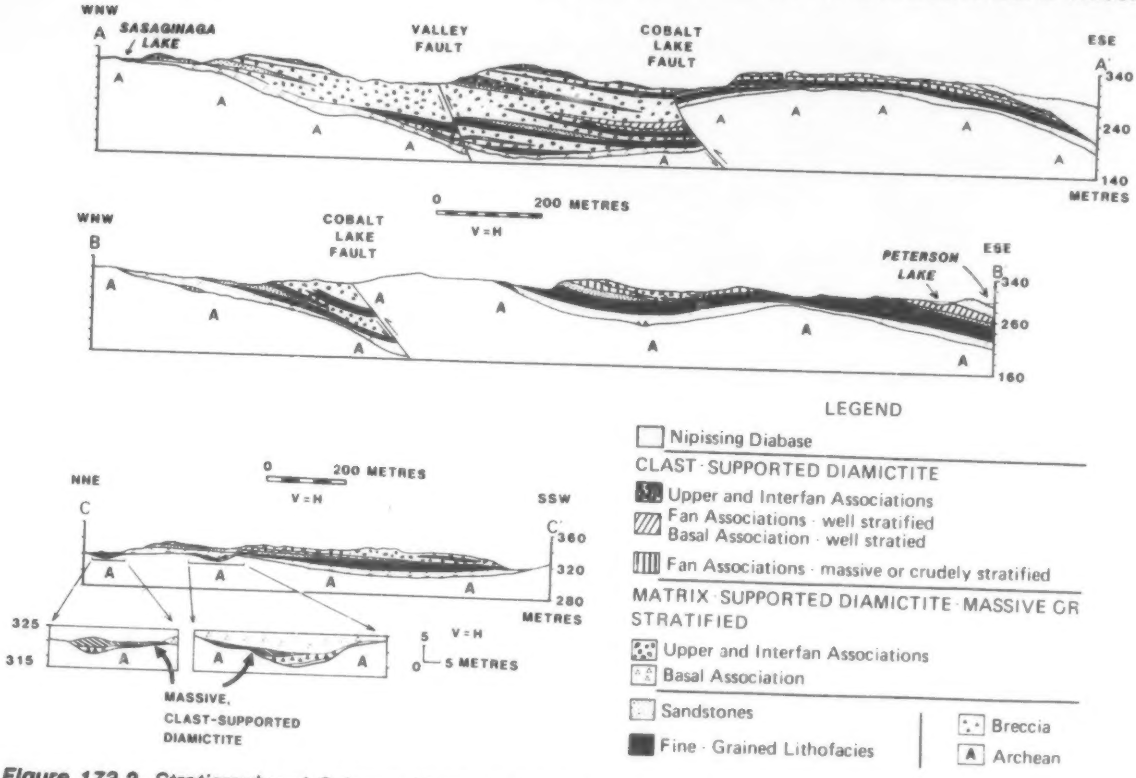
WNW
A
SASAGINAGA LAKE
VALLEY FAULT
COBALT LAKE FAULT
ESE
A'
340
240
140 METRES
0
200 METRES
V=H
WNW
B
COBALT LAKE FAULT
PETERSON LAKE
ESE
B'
340
260
160
NNE
C
0
200 METRES
V=H
SSW
C'
360
320
280 METRES
325
315
5
V=H
0
5 METRES
MASSIVE, CLAST-SUPPORTED DIAMICTITE
A
LEGEND
Nipissing Diabase
CLAST-SUPPORTED DIAMICTITE
Upper and Interfan Associations
Fan Associations - well stratified
Basal Association - well stratied
Fan Associations - massive or crudely stratified
MATRIX-SUPPORTED DIAMICTITE-MASSIVE OR STRATIFIED
Upper and Interfan Associations
Basal Association
Sandstones
Fine-Grained Lithofacies
Breccia
Archean

Figure 173.2. Stratigraphy of Coleman Member at Cobalt. Locations of sections are shown in Figure 173.1. Gravel-sized lithologies are referred to using the general term "diamictite". This embraces previously used terms such as orthoconglomerate (clast-supported diamictite) and paraconglomerate or pebbly mudstone (matrix-supported diamictite).

firmed in most respects. However, we have now concluded that the complex grading patterns, textures, and contact relationships in the fined-grained sandstone/siltstone/claystone rhythmites reflect a proximal to distal transition from areas where meltwater underflows dominated, to areas where meltwater interflow/overflows were more prevalent. Mackiewicz *et al.* (1984) and Domack (1984) have documented this pattern in Recent and Pleistocene ice-proximal glaciomarine environments. Such a pattern is unlikely in ice-contact glaciolacustrine environments because underflows dominate throughout the basin (Gustavson *et al.* 1975, Ashley *et al.* 1985). A glaciomarine interpretation is favoured here over previously proposed glaciolacustrine models. A second new conclusion is that the highest stratigraphy at Cobalt, confined approximately to the area between the Valley fault and Cobalt Lake fault (Figure 173.1), represents a change in depositional style from the lower stratigraphy exposed throughout most of the study area. This may reflect deposition during a separate readvance of the previously grounded ice sheet as a floating or partially floating ice shelf.

The summary of the depositional sequence at Cobalt presented below is based on a detailed analysis of interrelationships among the lithofacies we have defined. The documentation required to substantiate our conclusions will be presented elsewhere (Mustard, in preparation; Mustard and Donaldson, in review), and in the final report supported by the grant for this project.

SUMMARY OF COLEMAN MEMBER DEPOSITIONAL SEQUENCE AT COBALT

1. The local depositional environment was an area of low to moderate relief, on the inner shelf of a slowly subsiding continental margin. A regolith was developed on at least part of the subaerially exposed unconformity surface.
2. Continental-scale glaciation involved southerly advance of an ice-sheet which may have caused isostatic loading below sea level.
3. Subglacial processes caused plucking, brecciation, and shaping of the unconformity surface. The regolith was incorporated by the advancing ice sheet except where cavitation occurred over paleotopographic lows. Lee-side till was deposited in these subglacial cavities, protecting the regolith. A primary basal till was deposited over much of the unconformity surface.
4. Deposition during retreat was from a tidewater glacier grounded approximately 50 to 300 m below sea level. A wet-based thermal regime during this period contributed to a high meltwater influx into the basin.

5. Retreat rates were generally slow but fluctuating, perhaps with quasi-stationary periods and minor readvances. This resulted in deposition of prograding subaqueous outwash fans where subglacial/englacial meltwater channels entered the basin. Meltwater underflow deposition dominated in proximal areas, changing to interflow/overflow distally.
6. Morainal banks formed at the grounding line in interfan areas due to englacial/subglacial melt-out and fluctuations in ice-sheet retreat rates.
7. Oversteepening of fan and morainal bank slopes, collapse of banks during retreat, and perhaps shock effects from ice calving, initiated sediment gravity flows into interfan areas. Sediment-support mechanisms varied among the flows, resulting in a variety of flow types and a complex intercalation of deposits.
8. Fluctuating retreat rates resulted in complex overlapping of fan and interfan facies.
9. Ice calving deposited ice-rafted debris in areas adjacent to the ice front. Rapid transport of icebergs out of the immediate area resulted in much less dropstone deposition in relatively distal areas.
10. The upper stratigraphy probably was deposited by readvance of a floating or partially floating ice sheet. Undermelt diamictons were deposited near the grounding line (north of the study area), and redeposited as sediment gravity flows within the study area. Ice-rafted debris from melt-out beneath the shelf was partially deposited as dropstone diamicton.

PALEOPLACER GOLD POTENTIAL AT COBALT

Previous studies of the lower Gowganda Formation (Coleman Member) have concluded that there is little potential for paleoplacer gold concentration (Long 1981, Long and Leslie 1982; Mossman and Harron 1983, 1984). However, in none of these studies was the immediate Cobalt area specifically examined.

A major component of Coleman Member deposition at Cobalt is inferred to comprise prograding subaqueous outwash fans (of the type documented by Rust and Romanelli 1975) resulting from subglacial and/or englacial meltwater streams entering a proglacial body of water. Preserved parts of these small fans (areas of less than 2 to 3 km^2 in the Cobalt region) consist of a coarsening upward sequence of siltstone-mudstone rhythmites overlain by horizontal- and planar-crossbedded fine- to medium-grained sands, some trough-crossbedded sands, and pebbly sands with sparse pebble lags, all capped by moderately to poorly sorted orthoconglomerates.

On the basis of pebble-cobble long-axis orientations, Lindsey (1967) suggested south-southwesterly directed movement of the Gowganda ice sheet. This was confirmed by the discovery during this study of lee-side glacial quarrying features on the unconformity surface at Cobalt. The combination of an excellent gold source area to the north (the Abitibi greenstone belt) and the abundance of current-worked sands and gravels at Cobalt, indicated to us that sampling and analysis of Gowganda strata was justified.

The results of our sampling program are shown in Table 173.1. Some high values were obtained in the initial analyses. However, analysis of the retained portions of these samples resulted in only trace values, suggesting lab error or perhaps the presence of isolated gold-rich volcanic or sulphide clasts (D. Long, Laurentian University, personal communication, 1984). One replicate sample (A8) yielded a slightly anomalous value (0.012 ounce per ton), but a split of the latter sample preparation yielded only 0.003 ounce per ton, again suggesting that no real anomaly exists. Additional sampling resulted in more low values. Thus, in spite of the sedimentologically promising setting, we are forced to conclude that these results from the Cobalt area complement those obtained from other areas. The Coleman Member at Cobalt thus appears to hold little paleoplacer gold potential.

SEDIMENTOLOGY OF THE FIRSTBROOK MEMBER

Regional mapping (1:20 000 scale) and detailed studies of stratigraphic sections have led to the conclusion that the Firstbrook Member was deposited in a prograding river-dominated deltaic environment (Figure 173.3). Sedimentological comparisons, substantiated by geochemical data, provide support for proposing that deposition probably took place within a marine basin influenced by weak tidal and oceanic currents.

Laterally continuous, thinly laminated mudstone of the lower part of the Firstbrook Member are inferred to be representive of a quiet-water, relatively deep (>30 m), prodelta setting. Deposition was primarily by suspended load rainout; however, thin, graded siltstone interlaminations indicate a significant component of deposition from distal density underflows. The occurrence of black graphitic beds and lack of red hematitic strata is suggestive of anoxic conditions.

Laminated mudstone, siltstone, and minor fine-grained sandstone that compose the middle unit of the Firstbrook Member were deposited from both bedload and suspension load processes within the delta slope subenvironment (Figure 173.3). A shallow-water (10 to 30 m) oxidizing environment is indicated by an overall increase in grain size and by the appearance of variegated hematite-bearing strata. Isolated ripple bedforms near the top of the unit suggest reworking of the substrate by wave agitation and tidal currents. Thick (up to 2 m), graded arkose beds displaying Bouma divisions, sole marks, and other bedding irregularities are interpreted as turbidity current deposits (sediment gravity flows, Figure 173.3). Extreme river flood incursions, storms, and possibly seismic activity, triggered the failure of oversteepened delta foreslope sands, which were incorporated as density currents, and transported to the lower delta slope and prodelta. Coleman *et al.* (1983) noted that rapid sedimentation rates can cause pore pressures to approach geostatic values, thereby reducing sediment shear strength, causing failure on relatively low-angle slopes. Analogous deposits from

TABLE 173.1. ASSAY RESULTS FROM COLEMAN MEMBER OF THE LOWER GOWGANDA FORMATION IN THE COBALT STUDY AREA. ASSAYS ARE GROUPED WITHIN FAN COMPLEXES AND ALSO ARE ARRANGED ACCORDING TO RELATIVE STRATIGRAPHIC POSITION. NUMBERS IN PARENTHESES AFTER ASSAY VALUES INDICATE NUMBER OF SAMPLES FROM A SINGLE UNIT. SAMPLE SITES ARE SHOWN IN FIGURE 173.1.

Sample	Gold Value (oz/ton) Initial	Gold Value (oz/ton) Repeat	Sample Description	Interpretation
Fan A				
A1	nil(2)	nil(2)	top of granule-pebble orthocgl.	Upper
A2	trace(2)	nil(2)	upper zone, A1 unit	(Proximal)
A3	0.019	nil 0.001(2)	mid A1 unit	Fan
A4	trace	-	med-crs pebbly sandstone	
A5	nil(3)	-	med-crs sandstone	
A6	nil	nil	peb. SS, base of graded trough	Mid to
A7	nil	-	med sandstone	
A8	0.112	0.012 0.003 nil	peb. lag, trough X-bedded SS	Upper
A9	nil(2)	-	graded granule cgl-crs SS	
A10	nil(2)	nil	crs, pebbly, horiz. bedded SS	Fan
A11	0.006	nil	graded crs-med sandstone	
A12	nil	-	crs sandstone	
Fan B				
B1	0.004	0.002	pebble-cobble orthocgl.	Upper
B2	0.002	-	base: same as B1	Fan
B3	0.006	nil	top: med-crs peb. SS	Mid to
B4	0.004	nil	base: trough X-bedded SS	Upper Fan
Fan C				
C1	nil	-	med-large peb. orthocgl.	Upper Fan
C2	trace	-	small peb. orthocgl.	Mid to
C3	nil	-	peb. lag, graded trough SS	Upper Fan
Fan D				
D1	trace	-	med-crs, graded peb. SS	Mid
D2	trace	-	med-grained pebbly SS	Fan
Misc.				
M1	trace	-	small-peb. orthocgl. on	Subglacial
M2	0.002	nil	Archean unconf. surface	Channel
M3	nil	-	graded horiz. bed peb. crs SS	Mass Flow
M4	nil	-	small peb. orthocgl lens in diamictite (matrix supported)	Mass Flow in interfan zone

AA Fire Assay analyses by Temiskaming Laboratories, MNR, Cobalt, Ontario (Initial) and Bondar Clegg, Ottawa (Repeat).

the Mississippi delta require slopes of less than 1 degree (Coleman and Prior 1980). Related to this are coherent and non-coherent slump folds (Figure 173.3), representing slow gravity-induced sliding down the delta slope. Discordant breccia zones that contain plastically deformed angular clasts likely are related to synsedimentary growth faulting. Paleocurrent data from the middle unit indicate consistent transport to the south and southwest.

Fine-grained sandstone and interbedded siltstone and mudstone in the upper unit of the Firstbrook Member represent deposition in a delta foreslope setting. The coarsening-upward sequence forms a transition from upper delta foreslope to fluvial braidplain deposits represented by trough-crossbedded arkose of the Lorrain Formation. Abundant wavy, lenticular, and flaser bedding are reminiscent of the tidal bedding described by Reineck and Singh (1980, p.112-118), and of Proterozoic tidalites of the An-

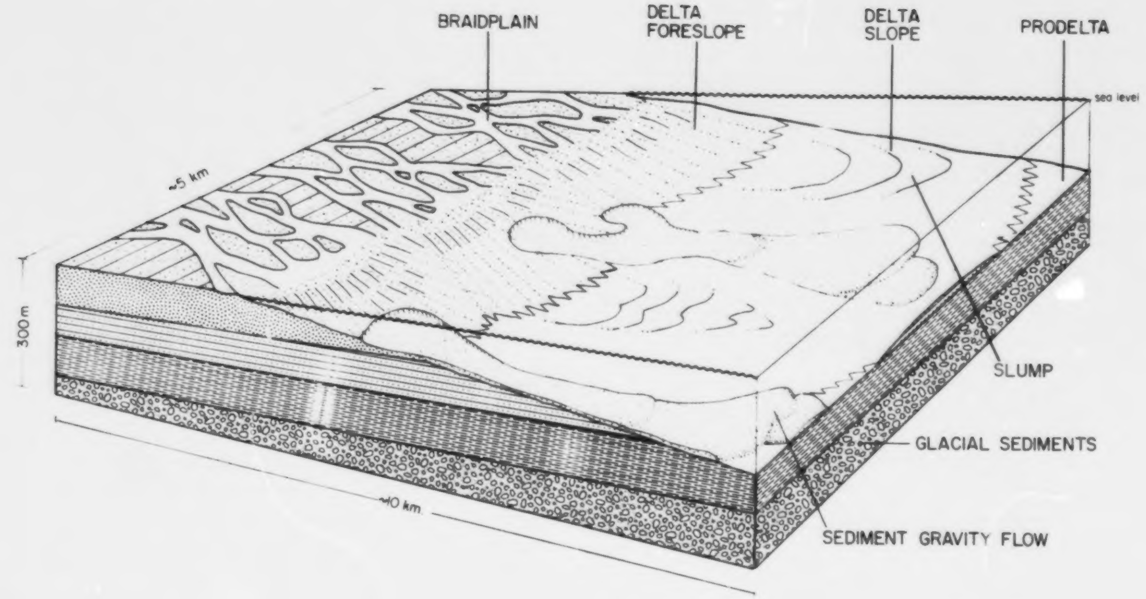

Figure 173.3. *Prograding river-dominated delta model proposed for the Firstbrook Member of the Gowganda Formation (from Rainbird 1985).*

imikie Basin (Ojakangas 1983). Starved ripples show opposing senses of transport, providing support for the postulation of tidal influence. However, the overall paleocurrent patterns show a multidirectional to southward-directed trend, suggesting a strong component of both river- and wave-generated currents in relatively shallow water (<10 m).

Penecontemporaneous deformation is recorded by load structures, ball-and-pillow structures, slump folds, and flame structures in strata of the upper unit. These structures appear to be intimately related to rapid slope-controlled deposition of relatively thick sand layers over mud-rich, water-saturated sediments.

A lack of tidal channels and interdistributary fines, and the abundance of soft-sediment structures, all suggest that the Firstbrook Member was deposited in a constructive river-dominated lobate delta modified by minor tidal and wave influence.

GEOCHEMISTRY OF MUDSTONES IN THE COBALT GROUP

Several previous studies of Cobalt Group rocks have suggested a rapid amelioration of the climate from the cold regime implied by lower Gowganda glaciogenic deposits, to humid and possibly subtropical conditions during deposition of the overlying Lorrain Formation (Chandler *et al.* 1969; Young 1973; Nesbitt and Young 1982). If these interpretations are correct, evidence should be manifest within upper Gowganda (Firstbrook Member) rocks which mark the transition between these 2 climatic extremities.

Pettijohn (1975, p.492-493) noted that the degree of chemical weathering of a rock is a direct function of the climatic regime which prevails at the time of weathering. Nesbitt and Young (1982) have applied this principle to geochemical analysis of Huronian mudstones. Assuming that the dominant process operative during chemical weathering of the Earth's crust is the breakdown of feldspars to form clay minerals, a chemical weathering index, referred to by Nesbitt and Young (1982) as the chemical index of alteration (CIA), can be calculated on the basis of molar proportions:

$$\mathrm{CIA} = [\mathrm{Al_2O_3} / \mathrm{Al_2O_3} + \mathrm{CaO}^{*} + \mathrm{Na_2O} + \mathrm{K_2O}] \times 100$$

where CaO^{*} is the amount of CaO in the silicate fraction of the rock. The index is derived on the assumption that during chemical weathering, the proportion of alumina to alkalis increases with increasing residual character. According to Nesbitt and Young (1982), Pleistocene clays yield values in the 60 to 65 range, whereas average shales plot between 70 and 75. Extensively weathered residual clays generally show CIA values greater than 85.

Twenty-three mudstone samples were collected from different levels in drill core from the Gowganda Formation and lower Lorrain Formation in the northern part of the study area. Samples were analyzed for major element oxide content, and their CIA values were computed. Results, presented stratigraphically in Figure 173.4, indicate an overall increase in weathering up-section. Coleman Member mudstones plot just below the values for Pleistocene clays. Nesbitt and Young (1982) have suggested that low CIA values in Gowganda mudstones reflect incorporation of unweathered material such as glacial flour, supporting a glacial origin for this unit. In contrast, Firstbrook Member mudstones plot closer to the values for average shale, suggesting the incorporation of extensively weathered material. An extremely abrupt increase in the CIA index across the Coleman Member-

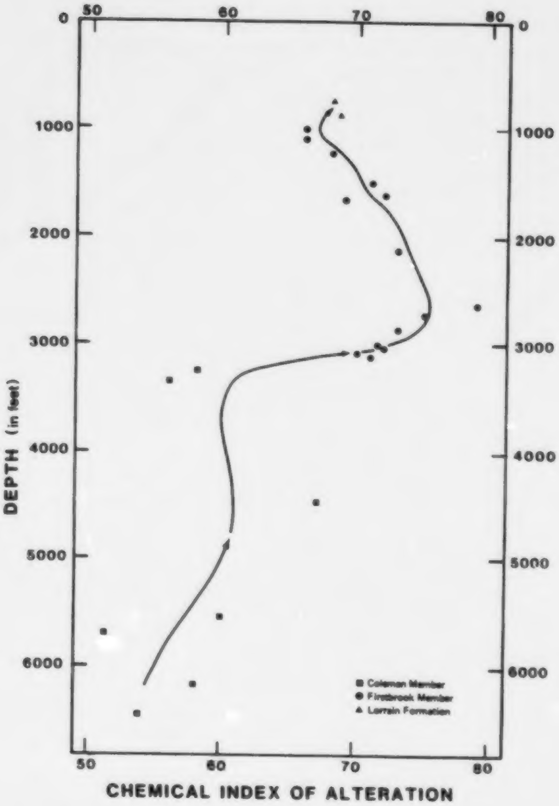

Figure 173.4. Chemical index of alteration (CIA) values for lower Cobalt Group mudstones from the Eplett drill hole, Henwood Township, Ontario. Black arrowed line is moving-average trend through these points. XRF analyses by Ron Hartree, University of Ottawa.

Firstbrook Member boundary is interpreted to be a function of increased weathering associated with rapid amelioration of the climate. The decreasing trend in CIA values for the upper Firstbrook Member is more difficult to interpret, but likely is due to an upsection increase in grain size.

A total of 60 samples collected from different localities were analyzed, including several samples from the overlying Lorrain and Gordon Lake Formations, and 2 samples from the matrix of the Coleman Member diamictite. A distinct bimodal pattern is evident in data plotted on the Feldspar-Clay diagram (Figure 173.5). Coleman Member samples are relatively enriched in CaO^*+ Na_2O, reflecting their unweathered character (low CIA values). Samples from the Firstbrook Member, Lorrain Formation, and Gordon Lake Formation are notably depleted in CaO^*+ Na_2O, and have slightly higher K_2O contents, reflecting stronger chemical weathering (higher CIA values). These data support rapid amelioration of the climate after deposition of the Coleman Member.

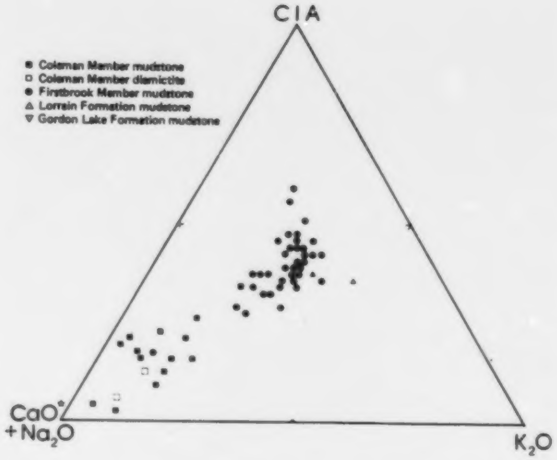

Figure 173.5. Feldspar-clay content of Cobalt Group rocks from the eastern Cobalt basin. Baseline of the triangle represents a chemical index of alteration (CIA) value of 50.

Initial comparisons of trace elements indicate that Firstbrook Member mudstones (compared to Coleman Member mudstones) contain significantly higher concentrations of boron and rubidium. This enrichment may be related to an increase in basin salinity brought on by the reduction or cessation of glacial meltwater influx toward the end of deposition of the Coleman Member. Additional sampling and mineralogical comparisons are required to verify this interpretation.

BASE–METAL MINERALIZATION IN THE FIRSTBROOK MEMBER

Firstbrook Member strata exhibit many characteristics which are considered favourable for sediment-hosted stratiform copper mineralization. These include:

1. *Redbeds.* The presence of redbeds within the middle and upper units of the Firstbrook Member suggest that oxidizing conditions prevailed during deposition and diagenesis. This is in accordance with previous observations that relatively high Eh and low pH conditions are required for the uptake and transport of metals (*see*Rose 1976).
2. *Aquifers.* Thick, laterally continuous and permeable turbidite beds in the middle unit could act as aquifers for the transport of mineralizing fluids.
3. *Source rocks.* Gustavson and Williams (1981) have noted that volcanic detritus, particularly that derived from tholeiitic basalts, is most desirable. Paleocurrent data suggest that a significant source area for Firstbrook Member sediments may have been the Abitibi greenstone belt to the north, which is known to contain mineralized tholeiites.
4. *Host beds.* Drab-coloured (anoxic) lower unit strata (perhaps containing some organic carbon) could act as reductants to high-Eh fluids containing dissolved metals.

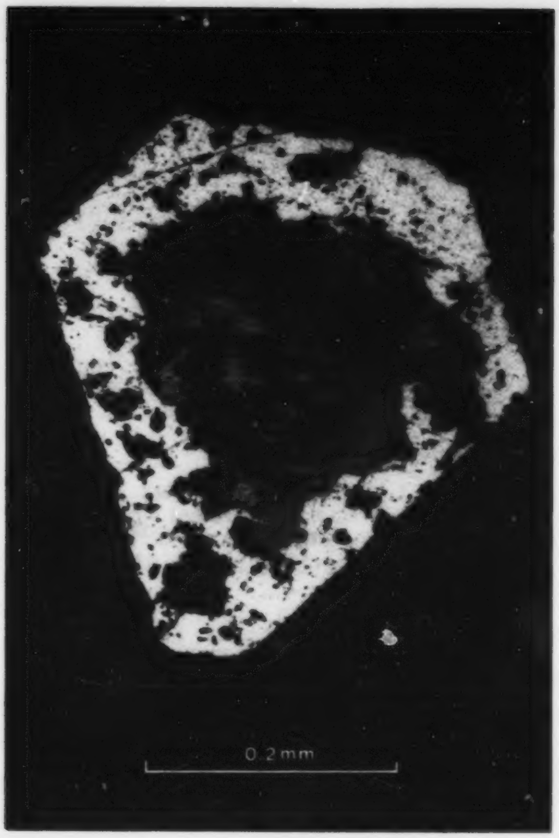

***Photo 173.1** Photomicrograph of sulphide minerals in sample from the Coleman Member of the Gowganda Formation: poikilitic sulphide grain consisting of chalcopyrite in the core of a euhedral pyrite grain. Magnetite forms a partial rim around the pyrite (reflected light).*

5. *Traps.* A common feature of sediment-hosted stratiform copper deposits is the association of ore with a pinch-out or pinch-down of host or footwall beds at paleotopographic highs (Gustavson and Williams 1981). A regional correlation of stratigraphic sections from the eastern part of the study area shows that a rapid thinning or pinch-out toward the margins of the basin is controlled by the presence of underlying Archean basement topography.

On the basis of observations, the most favourable strata for mineralization are the lower Firstbrook Member mudstones which are interbedded with red sandy turbidite horizons. Specific target areas could be selected where these strata pinch out against Archean paleotopographic highs.

SULPHIDE MINERALIZATION IN THE COBALT AREA

Metallic minerals occur not only in the silver veins at Cobalt, but also within the Archean interflow sediments and the Coleman Member of the Gowganda Formation. Information regarding the origin of the economic silver veins may be gained by understanding the origin of sulphides in the Coleman Member. Sulphides and other metallic minerals identified to date in this study of the Coleman Member are: pyrite, pyrrhotite, galena, sphalerite, chalcopyrite, arsenopyrite, gersdorffite, pyrargyrite, tetrahedrite, acanthite, native silver, and antimonial silver.

LITTLE SILVER VEIN

The principal study area has been at Little Silver Vein, where the rocks are exposed in a prominent 30 m cliff (Fan B, Figure 173.1). The base is composed of laminated siltstones which are overlain by a coarsening-upward succession of sandstones and orthoconglomerates. Samples have been collected throughout this stratigraphic succession, and from selected units at various distances from the vein.

The siltstones at Little Silver Vein contain minor concentrations of sulphide minerals (0.2% to 2.0%, estimated from polished thin sections), with ubiquitous pyrite composing 95% to 100% of the sulphide mineralogy. Characteristics such as composition and morphology of the sulphides and associated minerals change with respect to distance from the vein. Closest to the vein, the sulphides are pyrrhotite (65%), chalcopyrite (30%), gersdorffite (5%), and (rarely) pyrite. They occur in 0.5 to 2.0 mm clusters of irregular grains associated with TiO_2 and chlorite spots. Gersdorffite occurs as tiny euhedra within grains of chalcopyrite and pyrrhotite. More than 3 m from the vein, the sulphide mineralogy consists predominantly of pyrite with lesser amounts of chalcopyrite, and rarely pyrrhotite and galena. With the exception of 1 sample containing a late chalcopyrite veinlet, and another containing several percent chalcopyrite, rocks farther than 5 m from the vein contain little or no chalcopyrite. Within the sandstones and orthoconglomerates overlying the siltstones, the sulphide content also is greatest in samples closest to the vein. Samples collected near the vein contain pyrrhotite, galena, acanthite, sphalerite, tetrahedrite (friebergite), arsenopyrite, and gersdorffite, whereas those farther away contain pyrite and/or chalcopyrite (or no sulphides at all).

Zoning of the sulphide minerals occurs in other Proterozoic sediments in the Cobalt camp. For example, near Drummond Cairn, chalcopyrite is uncommon adjacent to a prominent vein, whereas pyrrhotite and sphalerite are abundant. A few metres away, pyrrhotite and chalcopyrite are common, and sphalerite is rare.

Within the siltstones at Little Silver Vein, sulphides are associated with chlorite, TiO_2, and a rare-earth silicate (tentatively identified on the basis of qualitative microprobe data as allanite).

The pyrite morphology ranges from euhedral, with sharp, well developed crystal faces (Photo 173.1) within 7 m of the vein wall, to subhedral and anhedral farther away. At distances greater than 20 m from the vein, pyrite occurs predominantly in the form of spherical shells with anhedral to subhedral outlines (Photo 173.2).

Euhedral pyrite crystals show prominent development of octahedral crystal faces (111), and smaller or equal-sized pyritohedron faces (102). The spherical shells of pyrite are ring-like in section. The cores of the pyrite rings commonly are composed of chlorite-free silt-sized detritus, chalcopyrite, or of intergrown quartz (presumably detrital) and allanite (Photo 173.2). In a few specimens, the cores consist of galena and pyrrhotite. Most pyrite in the sediments is to some degree poikiloblastic, and contains inclusions of detrital quartz.

Pyrite is most abundant in the fine-grained siltstone laminae. In some samples the pyrite distribution appears to be random throughout the laminae, but where it occurs in the coarse-grained layers, the pyrite grains generally are more anhedral or irregular in shape than pyrite in the fine-grained layers. Most pyrite grains range in size from less than 0.1 to 1.0 mm, although grains within chlorite spots may be as large as 2.5 mm. The grain size, almost invariably, is many times larger than the grain size of the siltstone host.

Where present as large grains (>2 mm), the pyrite tends to occur where a chlorite spot has grown outward into a finer grained mud-rich layer. Pyrite grains from many sample locations have partial rims of chlorite, where the chlorite tends to occur only on the stratigraphic tops and bottoms of the grains.

In some samples, the pyrite has been partially altered to magnetite, which occurs as rims around pyrite (Photo 173.1), as well as in irregular embayments and net-like patterns. In a few places, the magnetite displays the pseudomorphed euhedral outline of pyrite, and also contains tiny cores of relic pyrite. Rare magnetite-coated chalcopyrite occurs as irregular masses between silt grains.

Chalcopyrite commonly occurs as tiny blebs within the pyrite, and may account for 2% to 10% of the sulphide content in a single grain. In most samples it occurs in very low concentrations; however, it appears to be more abundant within a 5 m zone adjacent to the vein wall, and also is anomalously abundant in 2 samples more than 20 m from the vein. Chalcopyrite within pyrite rings occasionally occupies the entire core (approximately 30% to 60% of the area of the pyrite ring, Photo 173.1) but, less commonly, occupies small areas within the cores of silt-sized detritus. At one locality, chalcopyrite occurs as discontinuous blebs in a single planar orientation that cross-cuts several pyrite grains.

The distinct morphology, and the increase in both abundance and grain size exhibited by pyrite within the chlorite spots, implies that these features are genetically linked. The morphology, however, may be explained by the fact that the chlorite spots almost everywhere occur in the coarse-grained layers. Where pyrite occurs outside the spots in the coarse-grained beds, it is irregularly shaped. The chlorite spots at Silverfields Mine (Appleyard 1980) and elsewhere in the Cobalt camp (Boyle *et al.* 1969) typically contain abundant sulphides. The possible relationship of pyrite to the chlorite spots still presents a problem because the origin and timing of the spots is uncertain, and not necessarily related to fluids which precipitated the silver ores. Chlorite spotting differs locally in intensity, is neither more nor less abundant near productive silver veins, and, commonly, is particularly abundant in a 100 m halo adjacent to the Nipissing Diabase sill. This has led some workers (Jambor 1971; Dass 1971) to conclude that the spotting is caused by thermal metamorphism in the contact aureole adjacent to the Nipissing Diabase. If this were the case, pyrite formation should be earlier than vein emplacement. The pyrrhotite, chalcopyrite, and gersdorffite adjacent to the vein would then be the result of alteration of pyrite by a later mineralizing fluid. Appleyard (1980) presented evidence based on volumetric and geochemical data related by Gresens general metasomatic equation, that the chlorite spots are genetically related to silver mineralization (which occurs within a zone about 220 m from the diabase contacts, Petruk 1971b). Appleyard (1980) suggested that intraformational fluids developed into ore-forming fluids by the leaching of Ag, Sb, and As from the siltstones, and that the chlorite spots developed as leaching proceeded. Thus Appleyard (1980) considers the vein constituents to have originated in the

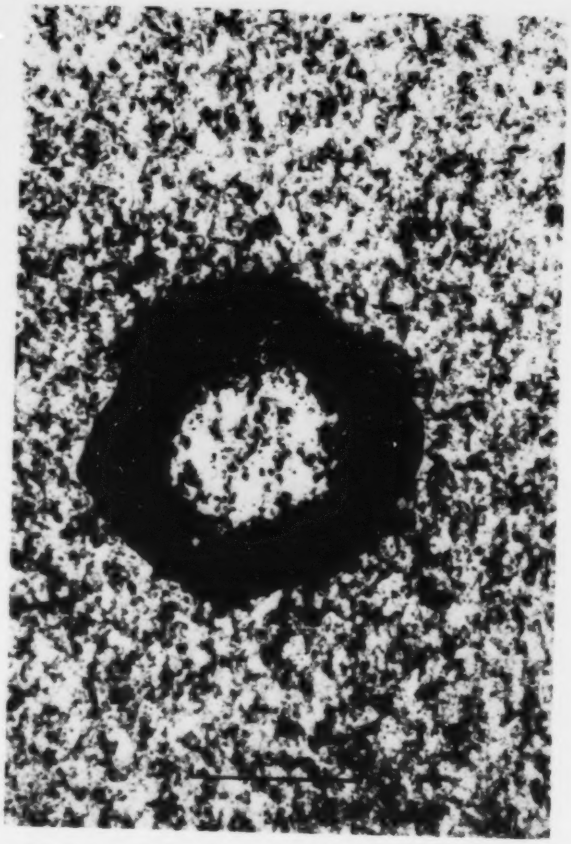

***Photo 173.2** Photomicrograph of sulphide minerals in sample from the Coleman Member of the Gowganda Formation: core of bleached siltstone enveloped by allanite, which in turn is rimmed by pyrite.*

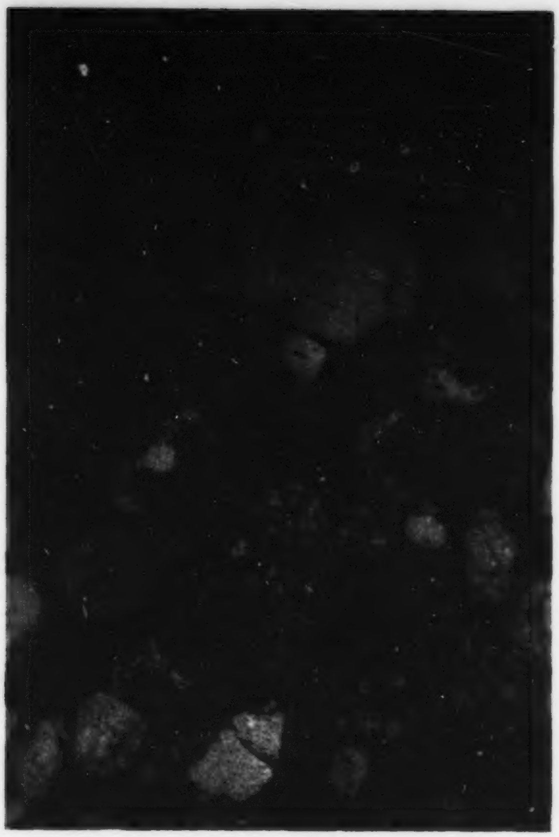

Photo 173.3 *Photomicrograph of sulphide minerals in sample from the Coleman Member of the Gowganda Formation: chalcopyrite that has infilled and partially replaced sand-sized detritus.*

chlorite-spotted rock, and to have migrated toward the veins.

At Coniagas-Tretheway Mine, metallic minerals occur in a manner similar to the chlorite spots. The metallic mineral spots occur both randomly in single beds and closely follow bedding planes elsewhere. The spots consist of native silver, tetrahedrite, gersdorffite, chalcopyrite, pyrite, acanthite, and pyrargyrite which have replaced the matrix, and to a lesser extent, the detrital clasts.

Allanite, invariably, is associated with pyrite and most commonly forms in the centre of the pyrite spheres which occur farthest from the vein. Allanite was not observed in samples close to the vein.

The presence of gersdorffite closest to the vein, and diminishing concentrations of chalcopyrite within the pyrite away from the vein, suggest that the sulphides are genetically related to the Ag-Ni-Co-As mineralization event. Pyrrhotite was observed in samples closest to the vein, whereas galena, which is absent adjacent to the vein, occurs in a narrow zone beyond the gersdorffite. Boyle *et al.* (1969) investigated the Little Silver Vein area and obtained similar results. Enrichment in As, Co, and Cu reported by Boyle *et al.* (1969) within these siltstones probably corresponds to the increased chalcopyrite content and the presence of gersdorffite. Their data show that the Pb concentration is low immediately adjacent to the vein, but increases in a narrow zone beyond that, consistent with the distribution of galena observed in this study. Boyle *et al.* (1969) also observed a distinct Cu peak and minor Pb, Zn, and Ag peaks about 20 m from the vein. It is in this area that an anomalous increase in chalcopyrite was observed in 2 samples collected for this study, one of which formed a small fracture-controlled veinlet. This slight increase in metals could have been caused by an influx of fluids along a minor vertical fault approximately 20 m from the vein. This fault has a displacement of 7 cm, with a sense of movement indicating north-side-up.

Adjacent to the silver-bearing veins throughout much of the Cobalt camp, a halo of low-grade silver ore is common. This halo generally is widest within the siltstones, as is evident from the greater width of stoping in the siltstones at Little Silver Vein and elsewhere in the Cobalt camp (e.g., Silverfields: Petruk 1968; University No. 3 Vein: Petruk 1971b: and the Langis Mine). At the Langis Mine, silver occurs in the low-grade halo as fine films of native silver and acanthite on bedding planes and tiny vertical fractures.

Sulphides in the siltstones at Little Silver Vein are characterized by a blastic growth, whereas sulphides in the overlying sandstones and conglomerates have, in most places, infilled spaces between clastic grains and have partially replaced some clasts (Photo 173.3). The associated carbonate and chlorite have behaved in a similar fashion. Some samples clearly show growth of plagioclase crystals around clasts. This stage was followed by deposition of suphides and associated chlorite, carbonate, and TiO_2 in the remaining pore spaces (Photo 173.4). Galena and chlorite occasionally are intimately intergrown; chalcopyrite completely surrounds some detrital grains (Photo 173.5). Sulphide minerals less commonly occur as discrete grains with slightly irregular outlines; the sulphide minerals include chalcopyrite, with or without tetrahedrite, and arsenopyrite (Photo 173.6). In 1 sample, arsenopyrite grains with sharp euhedral outlines occur within a detrital clast of crystal tuff or porphyritic volcanic rock.

SULPHIDE-RICH CLASTS

Sulphide-rich fragments up to 12 cm in diameter occur sporadically throughout the conglomerates within the Cobalt camp. Sphalerite, galena, tetrahedrite, and chalcopyrite occur as partial replacements within some clasts at Nipissing Hill (M1 and M2, Figure 173.1). The fine-grained matrix on the periphery of a clast of porphyritic volcanic rock has been predominantly altered to galena and tetrahedrite. The phenocrysts are unreplaced; the sulphides extend from the clast into the matrix.

Petruk (1971a) also observed suphides that have replaced rock-forming minerals in pebbles, and Kim (1979) reported that some granitic clasts contained finely disseminated chalcopyrite and/or sphalerite. Gebert (1985) investigated sphalerite-rich clots within

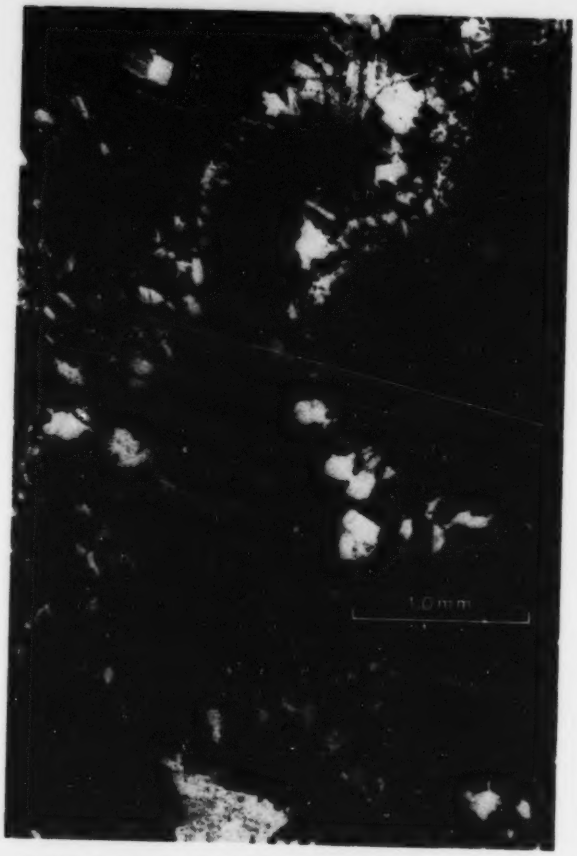

Photo 173.4 *Photomicrograph of sulphide minerals in sample from the Coleman Member of the Gowganda Formation: fringe of plagioclase crystals rimming volcanic clasts. The remaining space is occupied by chlorite (Cl), carbonate (cbt), and galena plus pyrite (central opaque area).*

Coleman Member strata near Drummond Cairn (3 km east-southeast of Little Silver Vein) and concluded that the clots were primary detrital clasts, but that the silver-bearing minerals (tetrahedrite and acanthite) on the margins of the clasts were introduced during subsequent silver mineralization.

Several sulphide-rich fragments observed during this study are mineralogically zoned. One such fragment from the Langis Mine, 12 by 15cm, has a core of chalcopyrite and a double rim. The inner rim, consisting of about 5 mm of galena, is enveloped by an outer 3 to 7 mm rim of sphalerite. Sphalerite is disseminated in a halo around this fragment. Another 2 by 3 cm fragment at Little Silver Vein consists of a pyrrhotite core with a discontinuous layer of chalcopyrite up to 3 mm thick, a layer of galena 1 to 2 mm wide, and an outer 1 to 2 mm rim of sphalerite.

Although a few sulphide-rich clasts may be detrital, all clasts examined so far in this study may be interpreted to have had their sulphide components emplaced *in situ*.

Photo 173.5 *Photomicrograph of sulphide minerals in sample from the Coleman Member of the Gowganda Formation: clastic quartz grain enveloped by chalcopyrite.*

SUMMARY

Many of the sulphide minerals in the Coleman Member are not of primary detrital origin, as is indicated by their increase in abundance proximal to veins, their textures, and the close association of Ag, Ni, Co, and As minerals with the suphides. Pyrite in the siltstone clearly formed after the sediment was deposited, and is not detrital, as indicated by its poikiloblastic nature, euhedral and spherical shape, and large size of the pyrite grains relative to the host-rock detrital grains. The common primary sulphides in the Archean basement rocks are base-metal sulphides: galena, sphalerite, chalcopyrite, pyrite, and pyrrhotite. Minerals such as tetrahedrite, gersdorffite, arsenopyrite, and acanthite suggest that some of these sulphides are related to silver vein emplacement.

Although most sulphides in the Coleman Member do not appear to be detrital, possibly some original detrital sulphides have been mobilized during vein formation or during emplacement of the Nipissing diabase. The detrital sulphide component probably is minor, so that most of the sulphides owe their origin to mineralizing fluids. Sulphur isotope data (work in progress) should help to establish the origin of sulphides in the Coleman Member of the Gowganda Formation.

ACKNOWLEDGMENTS

J.A. Donaldson and B.R. Rust express thanks to B.O. Dressler, A.C. Colvine, and John Wood, Ontario Geological Survey, for their helpful advice during preliminary planning of this project. Leo Owsiacki, Resident Geologist, Ontario Geological Survey (Cobalt), together with his staff, provided invaluable advice and access to their library and laboratory facilities. Zaira Arias and Elaine Dodd provided cheerful assistance during the 1984 field season.

The effort, time, and accessibility to the Beaver-Temiskaming and Langis Mines provided by Agnico-Eagle Mines Limited, Cobalt, was greatly appreciated. Special thanks are extended to Douglas Robinson and David Marek, the mine geologists for these 2 mines. Field work was supported in part by Natural Sciences and Engineering Research Council Grants A5536 (J.A. Donaldson), A2646 (F.A. Michel), and A7874 (D.H. Watkinson).

REFERENCES

Photo 173.6 Photomicrograph of sulphide minerals in sample from the Coleman Member of the Gowganda Formation: sulphides and clastic detritus in a sample from Nipissing Hill. The large sulphide grain is composed of chalcopyrite, arsenopyrite, and tetrahedrite.

Appleyard, E.C.
1980: A Preliminary Metasomatic Assessment of Laminated Siltstones at the Silverfields Mine, Cobalt, Ontario; Grant 70, p.1-10 *in* Geoscience Research Grant Program, Summary of Research, 1979-1980, edited by E.G. Pye, Ontario Geological Survey, Miscellaneous Paper 93, 262p.

Ashley, G.M., Shaw, J., and Smith, N.D.
1985: Glacial Sedimentary Environments; Society of Economic Peleontologists and Mineralogists, Short Course Number 16, Lecture Notes, 246p.

Boyle, R.W., Dass, A.S., Church, D., Milailov, G., Durham, C., Lynch, J., and Dyck, W.
1969: Research in Geochemical Prospecting Methods for Native Silver Deposits, Cobalt Area, Ontario, 1966; Geological Survey of Canada, Paper 67-35, 91p.

Chandler, F.W., Young, G.M., and Wood, J.
1969: Diaspore in Early Proterozoic Quartzites (Lorrain Formation) of Ontario; Canadian Journal of Earth Sciences, Volume 6, p.337-340.

Coleman, J.M., and Prior, D.B.
1980: Deltaic Sand Bodies; American Association of Petroleum Geologists, Short Course Notes, Series 15.

Coleman, J.M., Prior, D.B., and Lindsey, J.F.
1983: Deltaic Influence on Shelfedge Instability Processes; Society of Economic Paleontologists and Mineralogists, Special Publication Number 33, p.121-137.

Dass, A.S.
1971: A Study of Chlorites Associated with the Native Silver Deposits of the Cobalt Area, Ontario, Canada; The Indian Mineralogist, Volume 12, p.14-24.

Domack, E.W.
1984: Rhythmically Bedded Glaciomarine Sediments on Whidbey Island, Washington; Journal of Sedimentary Petrology, Volume 54, p.589-602.

Donaldson, J.A., Goodz, M.D., Michel, F.A., Mustard, P.S., Rainbird, R.H., Rust, B.R., Watkinson, D.H., and Wilson, B.
1984: Sedimentary Rocks and Strata-bound Mineralization in the Cobalt Region; Grant 173, p.198-210 *in* Geoscience Research Grant Program, Summary of Research 1983-1984, edited by V.G. Milne, Ontario Geological Survey, Miscellaneous Paper 121, 252p.

Gebert, J.S.
1985: Base Metal Mineralization along the Archean-Proterozoic Unconformity at Drummond Cairn, Cobalt, Ontario; Unpublished B.Sc. Thesis, Carleton University, Ottawa.

Gustavson, K.B., and Williams, N.
1981: Sediment-hosted Stratiform Deposits of Copper, Lead and Zinc; Economic Geology, 75th Anniversary Volume, p.139-178.

Gustavson, T.C., Ashley, G.M., and Boothroyd, J.C.
1975: Depositional Sequences in Glaciolacustrine Deltas; p.264-280 *in* Glaciofluvial and Glaciolacustrine Sedimentation, edited by A.V. Jopling and B.C. McDonald, Society of Economic Paleontologists and Mineralogists, Special Publication Number 23, 320p.

Halls, C.H., and Stumpfl, E.F.
1969: Geology and Ore Deposition, Western Kerr Lake Arch, Cobalt, Ontario; Ninth Commonwealth Mining and Metallurgical Congress, Mining and Petroleum Geology Section, Offices of the Congress and of the Institution of Mining and Metallurgy, London, Paper 18.

Jambor, J.L.
1971: Spotted Chloritic Alteration; The Canadian Mineralogist, Volume 11, p.305-319.

Kim, W.S.
1979: Sulfide Mineralogy in the Coleman Member in the Cobalt Area, Ontario; Unpublished M.Sc. Thesis, Carleton University, Ottawa.

Knight, C.W.
1924: Geology of the Mine Workings of Cobalt and South Lorraine Silver Areas; Ontario Department of Mines, Annual Report for 1922, Volume 31, Part 2, 374p.

Legun, A.S.
1981: Huronian Sedimentation in the Cobalt Area; p.88-92 *in* Summary of Field Work 1981, edited by J. Wood, Owen L. White, R.B. Barlow, and A.C. Colvine, Ontario Geological Survey, Miscellaneous Paper 100, 255p.
1984: Stratigraphy and Sedimentation in the Cobalt Area; Ontario Geological Survey, Open File Report 5508, 60p.

Lindsey, D.A.
1967: The Sedimentology of the Huronian Gowganda Formation, Ontario, Canada (with Special Reference to the Whitefish Falls Area); Unpublished Ph.D. Thesis, Johns Hopkins University, 296p.

Long, D.G.F.
1981: The Sedimentary Framework of Placer Gold Concentrations in Basal Huronian Strata of the Cobalt Embayment; p.218-223 *in* Summary of Fieldwork, 1981, edited by J. Wood, Owen L. White, R.B. Barlow, and A.C. Colvine, Ontario Geological Survey, Miscellaneous Paper 100, 225p.

Long, D.G.F., and Leslie, C.
1982: Placer Gold Potential of the Gowganda Formation along the Northern Margin of the Cobalt Embayment; p.198-200 *in* Summary of Fieldwork, 1982, edited by J. Wood, Owen L. White, R.B. Barlow, and A.C. Colvine, Ontario Geological Survey, Miscellaneous Paper 100, 235p.

Lovell, H.L.
1978: Possibilities for Large Tonnage Low Grade Silver Production; Unpublished Report, Resident Geologist, Ministry of Natural Resources, Kirkland Lake, Ontario, 65p.

Mackiewicz, N.E., Powell, R.D., Carlson, P.R., and Molina, B.F.
1984: Interlaminated Ice-proximal Glaciomarine Sediments in Muir Inlet, Alaska; Marine Geology, Volume 57, p.113-147.

Mossman, D.J., and Harron, G.A.
1983: Origin and Distribution of Gold in Huronian Supergroup, Canada—the Case for Witwatersrand-type Paleoplacers; Journal of Precambrian Geology, Volume 20, Number 2-4, p.543-583.
1984: Witwatersrand-type Paleoplacer Gold in the Huronian Supergroup of Ontario, Canada; Geoscience Canada, Volume 11, Number 1, p.33-40.

Mustard, P.S.
In Preparation: Sedimentology of The Lower Gowganda Formation Coleman Member (Early Proterozoic) at Cobalt, Ontario; Unpublished M.Sc. Thesis, Carleton University, Ottawa, Ontario.

Mustard, P.S., and Donaldson, J.A.
In Review: Early Proterozoic Ice-proximal Glaciomarine Deposition: the Lower Gowganda Formation at Cobalt, Ontario, Canada; *in* Glacigenic Deposystem Models, edited by D.E. Lawson and R.D. Powell, Plenum Press.

Nesbitt, H.W., and Young, G.M.
1982: Early Proterozoic Climates and Plate Motions Inferred from Major Element Chemistry of Lutites; Nature, Volume 299, Number 5885, p.715-717.

Ojakangas, R.W.
1983: Tidal Deposits in the Early Proterozoic Basin of the Lake Superior Region—The Palms and Pokegama Formations: Evidence for Subtidal-shelf Deposition of Superior Type Banded Iron Formation; Geological Association of America, Memoir 160, p.49-66.

Patterson, G.C.
1979: Metallogenic Relationships of Base-Metal Occurrences in the Cobalt Area; p.222-229 *in* Summary of Field Work, 1979; by the Ontario Geological Survey, edited by V.G. Milne, Owen L. White, R.B. Barlow, and C.R. Kustra, Ontario Geological Survey, Miscellaneous Paper 90, 245p.

Petruk, William
1968: Mineralogy and Origin of the Silverfields Silver Deposit in the Cobalt Area, Ontario; Economic Geology, Volume 63, p.512-531.
1971a: Sulphur Isotope Abundance Ratios for the Sulfides in the Cobalt-Gowganda Ores; The Canadian Mineralogist, Volume 11, p.391-395.
1971b: General Characteristics of the Deposits; The Canadian Mineralogist, Volume 11, p.76-107.

Pettijohn, F.J.
1975: Sedimentary Rocks; Third Edition, Harper and Row, New York, 718p.

Rainbird, R.H.
1980: The Geology of an Area Straddling the Archean-Proterozoic Unconformity near Cobalt, Ontario; Unpublished B.Sc. Thesis, Carleton University, Ottawa, 52p.

1985: Sedimentology of the Firstbrook Member of the Gowganda Formation in the Eastern Cobalt Basin, Ontario; Unpublished M.Sc. Thesis, Ottawa-Carleton Centre for Geoscience Studies, Carleton, University, Ottawa, Ontario.

Reineck, H.E., and Singh, I.B.
1980: Depositional Sedimentary Environments; Second Edition, Springer-Verlag, Berlin, Heidelberg, New York.

Rose, A.W.
1976: The Effect of Cuprous Chloride Complexes in the Origin of Redbed Copper and Related Deposits; Economic Geology, Volume 285, p.470-472.

Rust, B.R., and Romanelli, R.
1975: Late Quaternary Subaqueous Outwash Deposits Near Ottawa, Canada; p.177-192 *in* Glaciofluvial and Glaciolacustrine Sedimentation, edited by A.V. Jopling and B.C. McDonald, Society of Economic Paleontologists and Mineralogists, Special Publication Number 23, 320p.

Symons, D.T.A.
1970: Paleomagnetism of the Nipissing Diabase, Cobalt Area; Canadian Journal of Earth Sciences, Volume 7, p.86-90.

Thomson, Robert
1961: Part of Underground Workings and Approximate Structural Contours, Coleman Tp., concessions V and VI, lots 1 to 6, District of Timiskaming, Ontario; Ontario Department of Mines, Provisional Map P-97A, Scale 1 inch = 400 feet.

Young, G.M.
1973: Tillites and Aluminous Quartzites as Possible Time Markers for Middle Precambrian Rocks of North America; *in* Huronian Stratigraphy and Sedimentation, edited by G.M. Young, Geological Association of Canada, Special Paper Number 12.

Grant 179 The Petrogenesis and Metallogenesis of the Atikwa-Lawrence Volcanic-Plutonic Terrain

D.W. Davis[1] **and G.R. Edwards**[2]

[1]Department of Mineralogy and Geology, Royal Ontario Museum

[2]Earth and Atmospheric Science, York University

ABSTRACT

Combined field investigation, geochemistry, and geochronology of plutonic rocks in the Atikwa-Lawrence volcanic-plutonic terrain has served to divide these rocks into 5 main groups.

Group 1: Diorite to tonalite which accompanies layered mafic intrusions that are locally at the margins of the batholiths. These rocks are contemporaneous with the basic intrusions, at 2733 ± 1 Ma. The most likely origin for these rocks is the mixing of differentiation products of the layered intrusions with partial melts of their metabasaltic host rocks. Group 1 magma may represent sources for andesitic volcanism.

Group 2: Tonalite to granodiorite which accompanies and is contemporaneous with rocks of Group 1. Field, chemical, and age evidence suggests that the origin of these rocks is by differentiation within the Group 1 system. Group 2 magmas may represent sources for rhyolitic volcanicsm. Gold has been found in pyritized, sericitized, and locally hematitized zones, and in quartz veins adjacent to faults in this group and in overlying rhyolites. This group of rocks appears to be of greatest interest as a potential host for economic mineralization.

Group 3: Tonalite to granodiorite occupies the central parts of the batholiths. It intruded rocks of Group 1. U-Pb zircon analyses indicate that Group 3 rocks post-date Group 1 by 10 to 14 Ma. Steeply fractionated chondrite normalized REE patterns suggest that the origin of these rocks is by partial melting of metabasalt, leaving an amphibole-rich or garnetiferous residue.

Group 4: Dikes of ultramafic to felsic composition intrude many of the batholithic rocks. Mafic dikes appear to grade into intermediate dikes through a process of brecciation, remobilization, and magma mixing between dike and granitoid host rocks. Chemical and mineralogical evidence suggests that this process may be important in producing rocks of Group 5.

Group 5: Late tectonic plutons of quartz diorite, syenodiorite, granodiorite, or quartz monzonite composition occur throughout the volcanic and plutonic terrain of the Wabigoon Subprovince. The granodioritic Chuck Lake intrusion in the centre of the Lawrence lobe probably belongs to this group. These rocks have high Sr (≥ 1000 ppm) and high modal sphene. One U-Pb analysis gave an age of 2718 Ma for the cores of zircons in the Chuck Lake intrusion. These rocks may be derived by partial melting of Group 3 rocks following injection and underplating by Group 4 rocks.

INTRODUCTION

Over 80% of surface outcrop in the Superior Province consists of granitoid rocks which largely control the structural style of adjacent metavolcanic sequences. The problem of granitoid genesis is of fundamental importance to an understanding of crustal evolution in the Archean, but has received scant attention relative to the metavolcanic rocks partly on account of the lack of mineral potential. There is, however, evidence that the structural, age, and geochemical relationship between volcanic rocks and subjacent batholiths may be of considerable importance in determining their potential for mineralization (Campbell *et al.* 1981; Davis *et al.* in press).

This is a report of work done during the second year of an investigation into the field, petrochemical, and geochronological relationship between volcanism and plutonism in the Atikwa-Lawrence terrain of the western Wabigoon Subprovince. The results of additional geochemistry, a second season of field investigation, and preliminary geochronology, are presented. The data are synthesized into a preliminary model for evolution of the Archean crust in the Atikwa-Lawrence area.

GENERAL GEOLOGY

The Atikwa-Lawrence volcanic-plutonic terrain forms a circular complex about 70 km in diameter (Figure 179.1). The arrangement of lithologies is roughly concentric with an outer sequence of folded mafic to felsic volcanic rocks intruded by gabbroic and tonalitic plutons which form a discontinuous, arcuate rim around the central batholith. These in turn were intruded by massive and foliated trondhjemite and granodiorite phases which form the core of the batholith. Work has concentrated on the northwest Atikwa lobe of the batholith and on the southern Lawrence lobe.

ATIKWA LOBE

The northern and western parts of the Atikwa lobe are comprised mostly of gabbroic intrusions and intermediate plutonic rocks ranging from diorite to granodiorite. These plutons are largely intrusive into mafic metavolcanic rocks, although they were intruded into a dacitic volcanic centre to the north. The central part of the lobe mostly consists of a complex mixture of trondhjemite, granodiorite, and quartz monzonite phases which are intrusive into the border phase tonalites.

Previous geochronology in the area is reported in Davis *et al.* (1982). The sample locations are keyed into the map in Figure 179.1:

1. 2731.8 $^{+1.6}_{-1.3}$ Ma—trondhjemite, Atikwa lobe
2. 2742.8 $^{+1.4}_{-1.2}$ Ma—dacite volcanic rock, Atikwa lobe

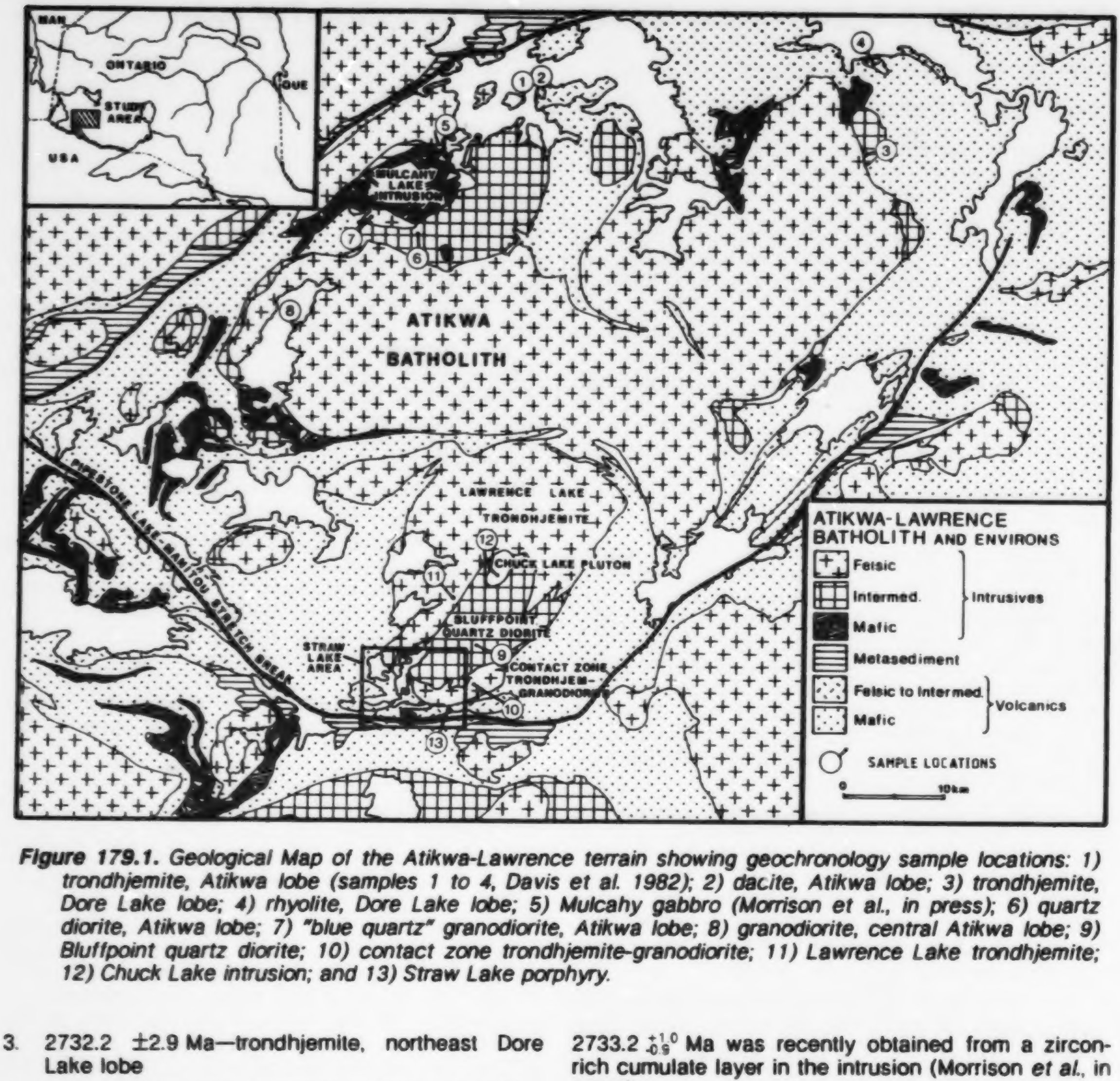
MAN
ONTARIO
QUE
STUDY AREA
USA
MULCAHY LAKE INTRUSION
ATIKWA BATHOLITH
LAWRENCE LAKE TRONDHJEMITE
CHUCK LAKE PLUTON
BLUFFPOINT QUARTZ DIORITE
STRAW LAKE AREA
CONTACT ZONE TRONDHJEM-GRANODIORITE
PIPESTONE LAKE-MANITOU STRETCH BREAK
1
2
3
4
5
6
7
8
9
10
11
12
13
ATIKWA-LAWRENCE BATHOLITH AND ENVIRONS
Felsic
Intermed.
Mafic
Intrusives
Metasediment
Felsic to Intermed.
Mafic
Volcanics
SAMPLE LOCATIONS
0
10km

Figure 179.1. *Geological Map of the Atikwa-Lawrence terrain showing geochronology sample locations: 1) trondhjemite, Atikwa lobe (samples 1 to 4, Davis et al. 1982); 2) dacite, Atikwa lobe; 3) trondhjemite, Dore Lake lobe; 4) rhyolite, Dore Lake lobe; 5) Mulcahy gabbro (Morrison et al., in press); 6) quartz diorite, Atikwa lobe; 7) "blue quartz" granodiorite, Atikwa lobe; 8) granodiorite, central Atikwa lobe; 9) Bluffpoint quartz diorite; 10) contact zone trondhjemite-granodiorite; 11) Lawrence Lake trondhjemite; 12) Chuck Lake intrusion; and 13) Straw Lake porphyry.*

3. 2732.2 ±2.9 Ma—trondhjemite, northeast Dore Lake lobe
4. 2734.8 $^{+4.0}_{-3.1}$ Ma—rhyolite, north of Dore Lake lobe.

These indicate contemporaneity of some tonalitic phases with the presence of contemporaneous and slightly older volcanic rocks.

The northwest contact between the Atikwa lobe and the volcanic rocks is partly occupied by the Mulcahy Lake layered basic intrusion. This is a remarkably well preserved body which forms one of an arcuate series of gabbroic plutons along the northern and western margins of the batholith. Early mapping by Moorhouse (1939) and Davies (1956) suggested that the Mulcahy gabbro was intruded as a large sill into metavolcanic rocks, and then was itself intruded by tonalitic phases of the Atikwa batholith. Recently, a detailed mapping of the Mulcahy intrusion has been carried out by Sutcliffe (1985). Extensive geochemical work has also been carried out by Morrison and Phinney (1985), who observed that the intrusion had a markedly more evolved, iron-rich character than its host metabasalts. A high precision age of 2733.2 $^{+1.0}_{-0.9}$ Ma was recently obtained from a zircon-rich cumulate layer in the intrusion (Morrison *et al.*, in press).

One of the main purposes of this investigation was to study the contact relations of the Mulcahy intrusion with its surrounding volcanic and granitoid rocks, and the relationship between the various granitoid phases of the Atikwa batholith. The occurrence of large basic intrusions is widespread in the Wabigoon Subprovince and they may have played an important role in the generation of Archean crust. In addition, intermediate plutonic rocks associated with the Mulcahy intrusion and overlying volcanic rocks are host to at least 10 gold and copper occurrences, so that crustal processes involving the intrusion may have played a role in favouring mineralization.

The similarity in age between the gabbro and the border tonalites of the Atikwa batholith, as well as the evolved chemistry of the basic intrusion as a whole, suggests a close link between gabbroic plutonism and the generation of tonalitic rocks. Detailed field investigations of the contact relations

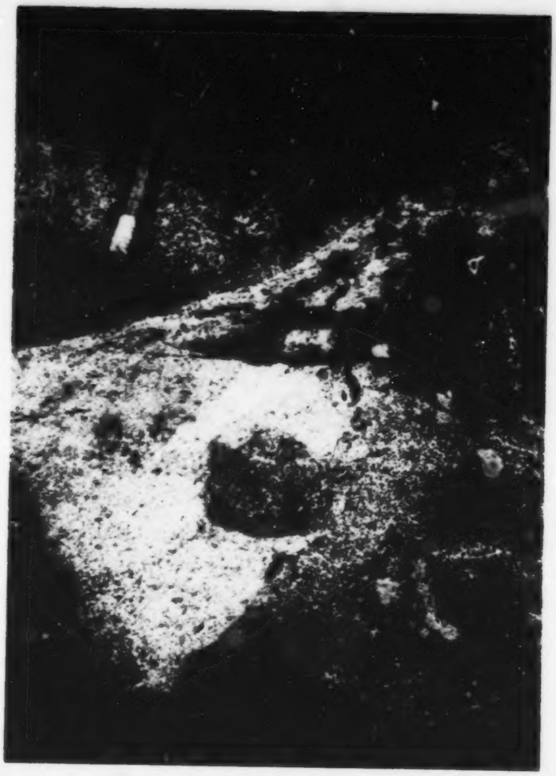

Photo 179.1a. *Fluidal contact between Mulcahy gabbro and quartz diorite. South margin of Mulcahy intrusion.*

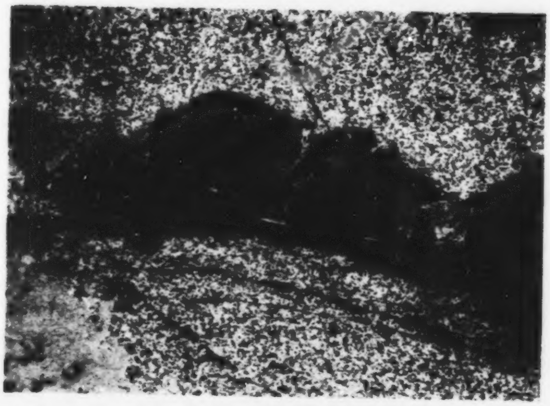

Photo 179.1b. *Back veining in a mafic dike intruded into tonalite. Eagle Lake, west of Mulcahy intrusion.*

show fluidal textures and gradational relationships which indicate that both gabbro and tonalite were liquid at the same time (Photo 179.1). This suggests that either both phases were generated simultaneously and therefore are most likely interrelated, or that the gabbro was intruded into tonalite, remobilizing its host rock due to the high temperature of the mafic liquid.

Photo 179.2 *Pegmatite patches in metabasalts adjacent to the Mulcahy intrusion.*

Selected rare earth element (REE) patterns for gabbroic and adjacent tonalitic rocks were given in a previous report (Edwards and Davis 1984). These demonstrated that within the range of variation, gabbro and tonalite cannot be distinguished. The border phase gabbro has a characteristic light rare earth enriched pattern which contrasts with flat or light rare earth depleted patterns in the host metabasaltic rocks (Figure 179.2). Tonalitic phases surrounding the layered basic intrusion have a generally similar rare earth pattern to the border phase gabbros. The composition of these phases ranges from quartz diorite immediately adjacent to the gabbro to "blue quartz" granodiorite (Davies 1956), which occupies a large area northwest of the basic intrusion and intrudes locally elsewhere near its boundary.

The composition of the intermediate rocks sometimes shows a gradational variation. For example, a series of tonalitic samples collected from the eastern boundary of the basic intrusion, along a 10 km line eastward to the border of the batholith, shows a small but continuous variation with increasing amounts of silica (Table 179.1). Figure 179.3 gives REE patterns for these samples. A quartz diorite nearest the basic intrusion has the most depleted pattern. The more distant samples have slightly negative Eu anomalies.

On the southwestern side of the basic intrusion, where it is in contact with pillowed metabasaltic rocks, pegmatite patches were developed in the host metavolcanic rocks adjacent to the intrusion (Photo 179.2). Locally, the metavolcanic rocks appear to be bleached and metasomatized. In places, these bleached rocks have a netted texture composed of a fine-scale veining of granodioritic material (Photo 179.3). At the extreme western end of the intrusion, these rocks grade through a quartz porphyry zone into massive "blue quartz" granodiorite.

These observations suggest that generation of the tonalites was by partial melting of metavolcanic rocks previously hydrated by seawater interaction. The heat source for this would have been the intru-

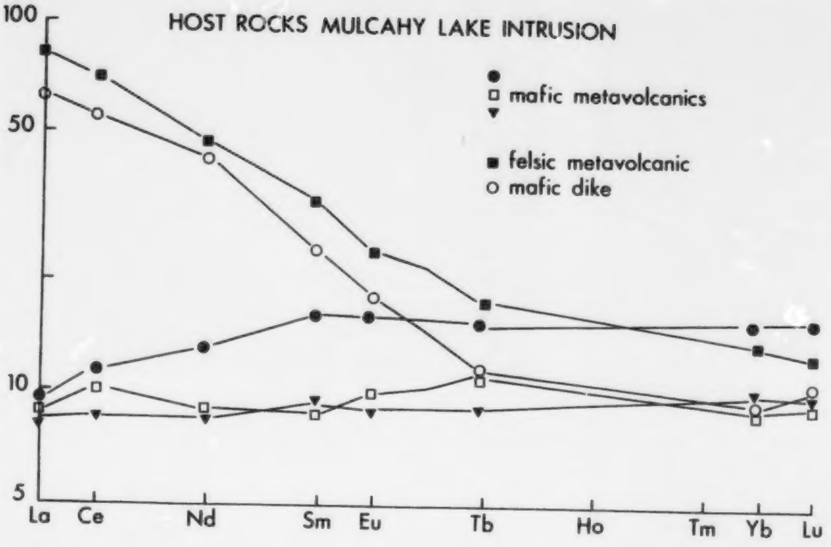

Figure 179.2. *Chondrite normalized rare earth element patterns for volcanic rocks adjacent to the Mulcahy intrusion and for a mafic dike intruding quartz diorite.*

sion of basic magmas, such as the Mulcahy gabbro. The highly evolved, Fe-rich character of the gabbro suggests that it was generated by fractionation in a deeper magma chamber, perhaps at the base of the crust (Sutcliffe 1985). The existence of more primitive magma chambers is also suggested by slightly later ultramafic dikes in the tonalite adjacent to the intrusion.

In contrast to the border phase plutons, rare earth element data for trondhjemite to quartz monzonite in the interior of the batholith, show distinctly different, more fractionated patterns (Figure 179.4).

Preliminary zircon work on a quartz diorite phase, which forms the bulk of the host rock to the Mulcahy intrusion, and a "blue quartz" granodiorite phase, which should be the latest phase associated with the gabbro (Davies 1956), is given in Figure 179.5. These results confirm the previous suggestion that all border phases are contemporaneous at about 2733 ± 1 Ma. In contrast, a concordant zircon fraction from one of the central granodiorite phases gives a distinctly younger age of 2719 Ma. The age-chemistry relationship parallels very closely the relationship previously found between volcanic and plutonic rocks at Sturgeon Lake (Davis *et al.*, in press), 150 km to the northeast.

All granitoid phases of the batholith are intruded by intermediate dikes of varying composition. In some cases, these dikes pre-date intrusion of the later central granitoid phases. The central part of the Atikwa lobe has rare clinopyroxenite dikes up to 5 m in width. In some cases, they appear to grade along strike into intermediate dikes, apparently by contamination with the host rock. Locally, the more mafic dikes show zones of brecciation and magma-mixing textures. Rapakivi-textured K-feldspar megacrysts were sometimes locally developed at the contact with their granitoid host rocks.

The field relations suggest that the dikes were intruded into a hot, perhaps partially molten host rock (Photo 179.4). They may represent a significant source of heat input into the batholith. The major and trace element chemistry of 2 intermediate dikes is given in Table 179.2 while the rare earth element distribution is given in Figure 179.4, where it can be compared with the granitoid host rocks of the Atikwa batholith. A striking feature of this data is that the enrichment in trace incompatible elements is greater in the sample with more primitive major element chemistry. It appears that trace elements are being selectively mobilized from the host rock and enriched in the dikes, perhaps by a process of volatile transfer. This is presumably a disequilibrium effect. Eventual dilution of the mafic magma during the mixing process would cause it to have more normal chemistry.

LAWRENCE LOBE

The Lawrence lobe comprises the southern part of the Atikwa-Lawrence batholith (Figure 179.1). The oldest phase is the Bluffpoint quartz diorite (BQD). This was intruded on its northern contact by the Lawrence Lake trondhjemite (LLT), a fairly uniform, massive trondhjemite pluton and by the Chuck Lake pluton, a small K-feldspar megacrystic granodiorite stock. The southern margin of this lobe is occupied by the contact zone trondhjemite to granodiorite (CZT). Although this was thought to be intrusive into the BQD, investigation of the contact relations shows a nebulous, gradational zone between the 2 phases with the development of hybrid textures that suggests the 2 phases were liquid at the same time. Preliminary age data are shown in Figure 179.6. The ages of BQD and CZT are the same, within error, and agree with the ages of the border tonalites and gabbro in the northern part of the batholith. In contrast, the age of LLT is distinctly younger, and is close to the age measurement of the central Atikwa trondhjemite (Figure 179.5).

The Lawrence lobe is overlain by an intermediate-felsic volcanic pile in the south. Field relations indicate that diorite of BQD grades into andesite flow at the base of the sequence. A comagmatic relationship between andesites and BQD was

TABLE 179.1. MAJOR AND SELECTED TRACE ELEMENT DATA FOR TONALITIC ROCKS EAST OF THE MULCAHY LAKE LAYERED BASIC INTRUSION (SEE FIGURE 179.3 FOR SAMPLE LOCATIONS).

	1	2	3	4	5	6
SiO_2	62.7	62.1	63.4	64.1	69.1	66.8
Al_2O_3	16.0	15.6	15.9	15.8	14.5	15.4
CaO	5.37	5.59	5.38	5.02	3.20	3.97
MgO	2.50	2.52	2.27	2.13	1.19	1.33
Na_2O	4.46	4.25	4.59	4.53	4.65	4.50
K_2O	1.03	0.93	0.91	1.08	1.65	1.82
Fe_2O_3	5.80	6.69	6.30	5.57	3.58	4.33
MnO	0.08	0.10	0.09	0.08	0.05	0.05
TiO_2	0.67	0.75	0.77	0.65	0.41	0.47
P_2O_5	0.13	0.15	0.17	0.14	0.10	0.09
L.O.I.	0.70	0.77	0.62	0.62	0.70	1.16
Total	99.5	99.5	100.5	99.8	99.2	100.0
ppm						
Sr	420	340	360	360	250	290
Zr	120	190	230	230	170	240
Rb	10	20	20	20	50	70

also supported by rare earth element distributions given in a previous report (Edwards and Davis 1984). The volcanic rocks are slightly more enriched in rare earths than the quartz diorites but they have a similar pattern of fractionation. Similarity in trace element composition and age between BQD and the Mulcahy tonalites suggests that BQD may be associated with, and possibly underlain by, a basic intrusion similar to the Mulcahy intrusion.

CZT grades southward into a fine-grained porphyry which metasomatizes and intrudes andesitic rocks. Rhyolites occur in abundance near the top of the volcanic sequence where they are quite sheared. Rare earth element distributions were determined for rocks of the CZT and the felsic volcanics in the previous report (Edwards and Davis 1984). Most of these rocks, especially those of CZT are characterized by a negative Eu anomaly. The similarity in chemistry suggests that the felsic volcanic rocks may be the eruptive equivalents of CZT.

One of the latest igneous events in the area was intrusion of the Chuck Lake pluton. This contains

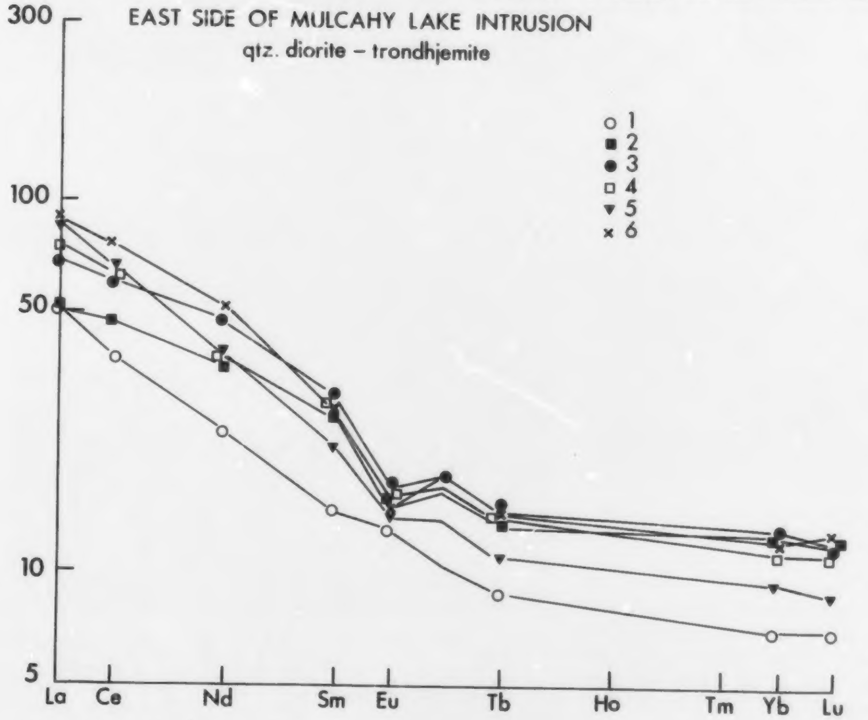

Figure 179.3. Chondrite normalized rare earth element patterns for tonalitic rocks east of the Mulcahy intrusion. For the following samples, the distances were measured going east along the road from the boundary of the intrusion: 1 - 2.0 km; 2 - 6.0 km; 3 - 6.5 km; 4 - 10.0 km; 5 - 10.5 km; and 6 - DD78-6 geochronology sample (Davis et al. 1982), South Twin Island, Eagle Lake.

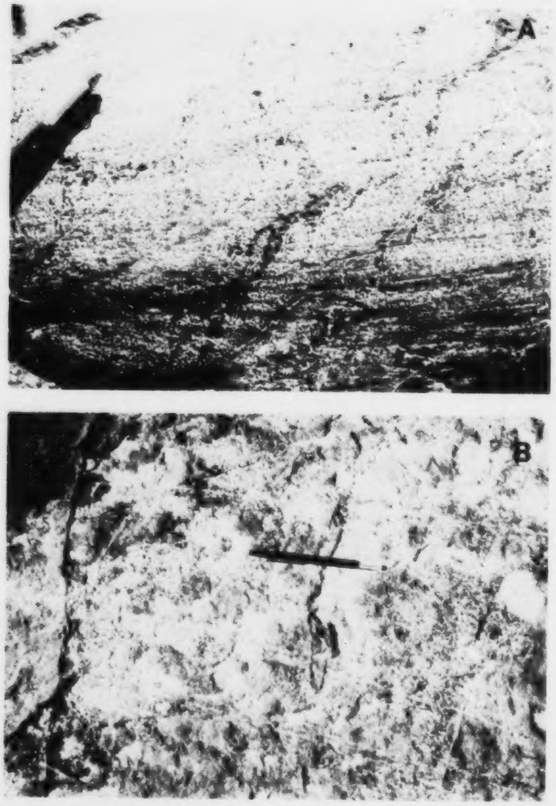

Photo 179.3a,b. *Net texture of granodiorite in metavolcanic rocks adjacent to the Mulcahy intrusion.*

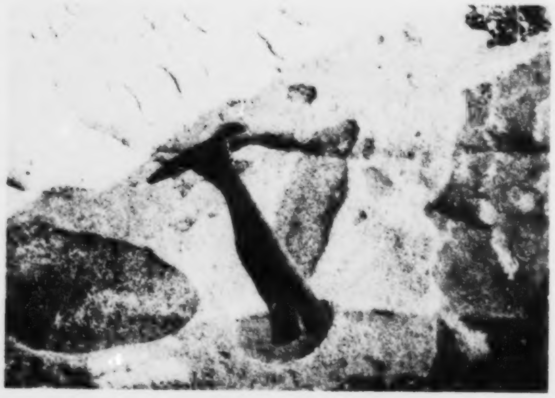

Photo 179.4a. *Intermediate dike containing more mafic fragments, central Atikwa lobe.*

zircons with low uranium cores and high uranium overgrowths. Analysis of some of the core material gives 2718 Ma (Figure 179.6), close to the age of the interior trondhjemite. This may be an inherited age and indicates that the granodiorite was derived by partial melting of LLT.

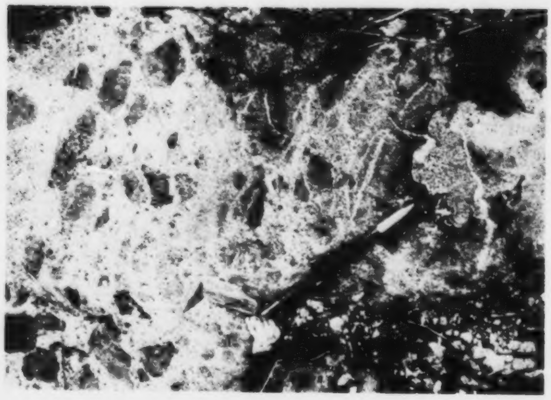

Photo 179.4b. *Breccia zone with evidence for magma mixing adjacent to clinopyroxenite dike, central Atikwa lobe.*

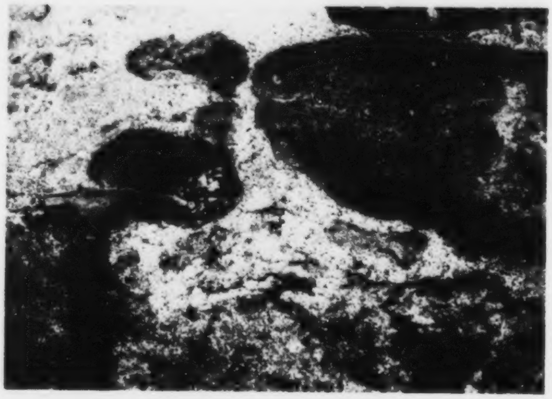

Photo 179.4c. *"Pillows" of mafic material in a felsic host. Mafic material shows magma-mixing texture, central Atikwa lobe.*

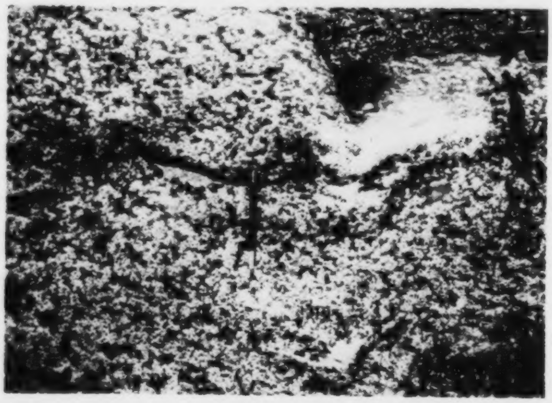

Photo 179.4d. *"Snowflake" texture resulting from incomplete mixing of mafic and felsic magmas, central Atikwa lobe.*

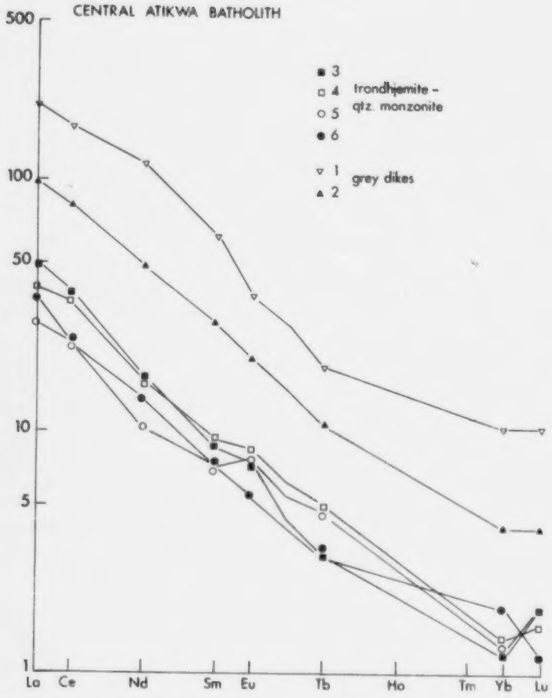

Figure 179.4. *Chondrite normalized rare earth element patterns for felsic plutonic rocks and for 2 samples of intermediate dikes in the central Atikwa lobe.*

The contact between the Chuck Lake intrusion and BQD is occupied by a breccia zone containing mostly intermediate inclusions, but also rare clinopyroxenite fragments, and local accumulations of K-feldspar megacrysts (Photo 179.5). The intrusion itself contains numerous metasomatized xenoliths. The chemistry of this intrusion (Table 179.2) is characterized by very high strontium, as is that of 2 of the intermediate dikes. Table 179.2 also gives chemistry for 2 late tectonic intrusions in the western Wabigoon Subprovince. Although these bodies have varying major element composition, they are all characterized by very high Sr, and also have very high modal sphene, as does the Chuck Lake intrusion and the intermediate dikes. In addition, association with local breccia zones is a characteristic of many of these late plutons. It therefore seems likely that the Chuck Lake pluton and other late tectonic Wabigoon plutons may have a common origin, perhaps by partial melting of slightly earlier trondhjemite.

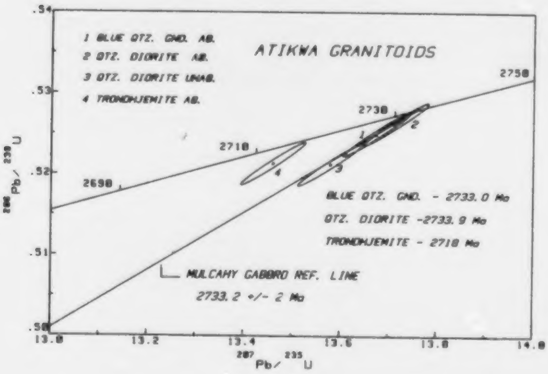

Figure 179.5. *U-Pb zircon data for granitoid rocks adjacent to the Mulcahy intrusion and for a sample of granodiorite from the central Atikwa lobe. The lead loss line for the Mulcahy gabbro is shown for reference (Morrison et al., in press).*

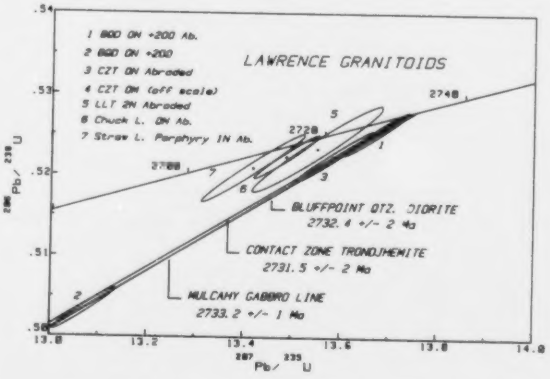

Figure 179.6. *U-Pb zircon data for granitoid rocks in the Lawrence lobe. The lead loss line for the Mulcahy gabbro (Morrison et al., in press) is shown for reference.*

MINERALIZATION

Gold occurs in CZT in silicified and hematitized rocks and quartz veins adjacent to faults transecting the area (Edwards and Davis 1984). A past-producing mine has also been found in a quartz vein in the rhyolite. Several attempts to date the rhyolite have been unsuccessful due to the absence of zircon. Although the rocks are high in zirconium, the absence of quartz phenocrysts indicates that crystallization of the magma had not proceeded far enough to form sizable zircon crystals before eruption. A quartz porphyry near a gold showing gives an age of about 2715 Ma (Figure 179.6). This is distinctly younger than CZT and may be younger than the age of LLT. Since the porphyry is sheared, it indicates that gold mineralization, which is syn- or post-shearing, was relatively late, and perhaps associated with fluid mobility at some time after intrusion of the LLT.

In the areas of study, gold appears to be associated with particular lithologies such as CZT, the "blue quartz" granodiorite in the area of the Mulcahy intrusion, and overlying felsic volcanic rocks. The association of late gold mineralization with these rocks may be due to their behaviour during brittle deformation in providing focussed pathways for ore-bearing solutions along fracture zones. On the other hand, the magmatically evolved nature of these rocks

TABLE 179.2. MAJOR AND SELECTED TRACE ELEMENT DATA FOR GRANITOID ROCKS IN THE ATIKWA-LAWRENCE TERRAIN AND TWO LATE TECTONIC PLUTONS ELSEWHERE IN THE WABIGOON SUBPROVINCE.

	1	2	3	4	5	6	7	8	9
SiO_2	59.2	64.7	69.0	69.5	70.9	70.9	70.1	68.0	58.9
Al_2O_3	15.5	14.7	16.0	15.7	15.5	14.8	15.6	15.4	17.4
CaO	4.24	3.81	2.95	3.00	2.21	1.80	2.08	2.82	5.76
MgO	3.03	2.50	0.86	1.04	0.55	0.56	0.77	1.42	2.96
Na_2O	4.16	4.61	5.85	5.59	5.46	5.11	5.91	4.72	5.37
K_2O	3.93	2.89	1.24	1.53	2.45	3.27	2.99	3.55	1.62
Fe_2O_3	6.83	3.63	1.96	2.18	1.34	1.28	1.47	3.00	5.79
MnO	0.10	0.05	0.02	0.02	0.01	0.01	0.03	0.04	0.09
TiO_2	0.80	0.44	0.28	0.28	0.18	0.18	0.19	0.39	0.56
P_2O_5	0.49	0.19	0.09	0.09	0.06	0.06	0.09	0.17	0.28
L.O.I.	1.08	0.54	0.62	0.47	0.54	0.54	0.93	0.77	0.54
Total	99.6	98.2	99.0	99.5	99.3	98.6	100.3	100.5	99.5
ppm									
Sr	1540	1080	920	750	920		1130	1250	1490
Zr	210	150	100	90	100		120	150	140
Rb	100	90	60	50	70		80	90	60

1. Intermediate dike, central Atikwa batholith
2. Intermediate dike, central Atikwa batholith
3. Trondhjemite, central Atikwa batholith
4. Trondhjemite, central Atikwa batholith
5. Granodiorite, central Atikwa batholith
6. Quartz monzonite, central Atikwa batholith
7. Chuck Lake intrusion
8. Ottertail stock, Rainy Lake area
9. Heronry diorite, Kakagi Lake area

(Numbers 8 and 9 are late tectonic plutons for comparison with 7.)

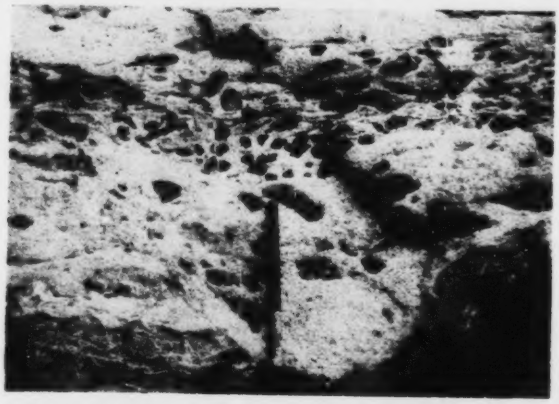

***Photo 179.5a.** Breccia zone between the Chuck Lake intrusion and the Bluffpoint quartz diorite.*

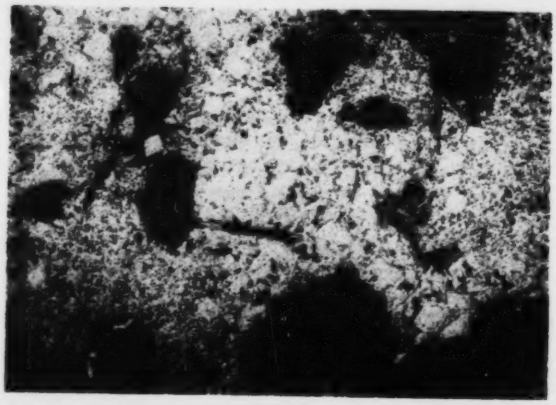

***Photo 179.5b.** Local, K-feldspar-rich zone in the Chuck Lake breccia.*

suggests that a pre-concentration stage during CZT-type magmatism may have been important.

PRELIMINARY MODEL FOR CRUSTAL EVOLUTION

Currently available field, geochemical, and geochronological evidence allows the development of a working model for the formation and evolution of the Archean crust in the Atikwa-Lawrence terrain. The primary head source driving the igneous system is ultramafic-basaltic magmatism, derived from the mantle. Igneous activity must have begun with eruption of thick piles of basaltic lava, presumably in some sort of rift environment, with local development of felsic centres, perhaps due to differentiation of mafic rocks in subvolcanic magma chambers. The volcanic rocks were hydrated due to interaction with seawater. The intrusion of large, hot, basic sills into the volcanic pile led to partial melting of the basaltic host rocks, fluxed by their water of hydration. This produced tonalitic magmas which re-invaded and mixed with the basic magmas. This occurred very rapidly in the Atikwa-Lawrence terrain at about 2733 ± 1 Ma. In some cases, as in the southern part of the Lawrence lobe, the tonalitic magma chambers became compositionally zoned, perhaps by a process of volatile transfer, to form a more felsic upper portion such as CZT. This process may also have resulted in concentration of rare elements such as gold. At any point during the process, the magma chambers may have erupted to form intermediate or felsic volcanic rocks.

At this time, plutonism was conformable to the volcanic pile and apparently did not produce major deformation. After a gap of about 10 to 14 Ma, there was another pulse of igneous activity. The head source must again have been intrusion and/or underplating of the crust by mafic magmas from the mantle. The crust, which was now thicker and of more intermediate composition, may have acted as a more effective barrier to the ascent of dense mafic or ultramafic magmas. This would have resulted in partial melting at deeper levels, either of amphibolite or garnet granulite, to produce intermediate magmas with heavy rare earth depleted patterns. A certain amount of mixing and remobilization of these magmas occurred through the continued injection of hot, primitive liquids. Volcanic equivalents of these magmas appear to be relatively rare in the Atikwa-Lawrence terrain although they occur in the Sturgeon Lake area (Davis *et al.*, in press).

Deformation of the overlying volcanic and tonalitic rocks in the Atikwa-Lawrence terrain may have occurred at this time due to the rise and emplacement of these magmas. However, this appears not to have been the case elsewhere in the Wabigoon Subprovince where the ages of 4 late tectonic intrusions occupy a narrow time span from about 2710 to 2695 Ma (Davis *et al.* 1982; Davis and Edwards, in preparation). In the Kakagi Lake area, large-scale regional folding has been shown to post-date intrusion of the major batholiths (Davis and Edwards 1982, in preparation). Regional deformation may have been the result of the diapiric emplacement of remobilized batholith material during a third pulse of thermal activity at about 2700 Ma.

Mantle-derived mafic magmas, unable to rise through the thick, low density crust, would intrude and underplate the trondhjemitic rocks. Partial melting of these intermediate rocks could produce granodiorites and quartz monzonites similar to the Chuck Lake intrusion. It is these light, buoyant magmas which may have caused diapiric remobilization of the overlying trondhjemites. Occasionally, the underlying melts breached through the gneiss domes to form central, late-tectonic plutons such as the White Otter Lake pluton, 90 km to the southeast in the Irene-Eltruit Lakes complex, or they intruded around the gneiss domes, in a zone of weakness at the contact between mafic volcanic and granitoid rocks, to form crescentic intrusions (Schwerdtner *et al.* 1979, 1983) such as the Jackfish-Weller Lake pluton south of the Atikwa-Lawrence terrain. This event would have resulted in deformation and cratonization of the crust. Over most of the Superior Province, this was the final large-scale Archean igneous event, perhaps as a result of having depleted the mantle and lower crust in heat-producing elements. It may have been during this event that much of the gold mineralization occurred.

SUMMARY

Based on field association, chemistry, and age, the plutonic rocks of the Atikwa-Lawrence terrain and, by extension, of the Wabigoon Subprovince, can be divided into 5 distinct groups as follows:

Group 1. (Pyroxene)-biotite-amphibole diorite and quartz diorite to amphibole-biotite tonalite. This group of rocks accompanies and partially surrounds layered mafic to ultramafic rocks that are locally at the contact between the batholith and the host metavolcanic rocks. The rocks show light REE enriched chondrite normalized patterns with La/Yb increasing with SiO_2 enrichment. More fractionated members may have small negative Eu anomalies. At least 4 rocks of this group have zircon U-Pb ages which agree at 2733 ± 1 Ma (Davis *et al.* 1982), *see* Figures 179.5, 179.6. This agrees within error with a 2733.2 $^{+1.0}_{-0.9}$ Ma age for gabbro in the Mulcahy Lake layered basic intrusion (Morrison *et al.*, in press). Field evidence suggests that both rock types were emplaced simultaneously. The most likely origin for this group is the mixing of the differentiation products of the layered intrusion with partial melts of its basalt host. Group 1 magmas may be related to andesitic volcanism.

Group 2. Amphibole-biotite tonalite and trondhjemite to granodiorite. This group of rocks accompanies rocks of Group 1. Field relations and zircon geochronology confirm that they were emplaced at approximately the same time as rocks of Group 1. Group 2 is chemically characterized by more enriched REE concentrations and by negative Eu anomalies, and a differentiated major element signature with SiO_2 ranging from 72% to 76% and Al_2O_3 from 12.3% to 14.5% (Edwards and Davis 1984). Gold has been found in pyritized, sericitized, and locally hematitized zones and in quartz veins adjacent to faults in this group. In addition, Campbell (1981) has pointed out that Group 2 rocks in the Sturgeon Lake area may play an important role in base-metal mineralization. Therefore, this group of rocks appears to be of the greatest interest as a potential host for economic mineralization. Group 2 rocks may have originated by partial melting of basalt, leaving a pyroxene-rich residue, or by differentiation of the Group 1 system. They may be important as sources of rhyolitic volcanism.

Group 3. (Amphibole)-biotite tonalite to trondhjemite and granodiorite. These rocks occupy the central part of the batholith, and from field relationships post-date Groups 1 and 2. Zircon age determinations indicate that they were intruded approximately 10 to 14 Ma after rocks of Group 1. SiO_2 ranges from 67% to 75% with concomitant ranges of Al_2O_3 from 14% to 16.6%, which is generally higher than Group 2 rocks of similar silica content (Edwards and Davis 1984). They also have more Sr, less Zr, and greater La/Yb than rocks of Groups 1 and 2. Group 3 rocks of the central Atikwa lobe are also distinctly higher in Sr than interior trondhjemites of the Lawrence lobe

(Edwards and Davis 1984). Chondrite normalized REE patterns show a depletion in heavy REE, sometimes with a slight positive Eu anomaly that increases with decreasing total REE (Edwards and Davis 1984). The fractionated REE pattern is consistent with the origin of these rocks by partial melting of metabasalt leaving an amphibole-rich or garnetiferous residue.

Group 4. Ultramafic to felsic dikes. Dikes of ultramafic to felsic composition intrude many of the batholithic rocks. They vary in width from a few centimetres to tens of metres. The ultramafic dikes are usually amphibolitic biotitic clinopyroxenite, or amphibolite with some relict olivine and abundant opaque oxides. The dikes grade into plagioclase- and biotite-bearing gabbro. The intermediate to felsic dikes may be amphibole, plagioclase, or biotite phyric, and are notably enriched in Sr and modal sphene. The dike suite probably has a common origin resulting from injection of mafic magma into the lower part of the batholith. The surrounding felsic rocks are fluxed and partly mixed with the more mafic magma and injected higher into the crust. In the field, there is considerable evidence for melting of the host granitoid, and concomitant magma mixing adjacent to ultramafic or mafic dikes. Group 4 rocks may be instrumental in producing the late plutons described below.

Group 5. Quartz diorite, syenodiorite, granodiorite, or quartz monzonite. Late tectonic plutons are scattered throughout the volcanic and plutonic terrain of the Wabigoon Subprovince. They may be quartz diorite, amphibole-biotite granodiorite or quartz monzonite in composition. They are characterized by Sr values in excess of 1000 ppm and by high modal sphene, up to 4%. Zircon geochronology defines a narrow time span of 2710 to 2695 Ma for their intrusion, late in the greenstone cycle (Davis *et al.* 1982; Davis and Edwards, in preparation). A slightly older age of 2718 Ma for the Chuck Lake intrusion may be due to inheritance. These magmas may be the result of partial melting of Group 3 rocks following injection and underplating by Group 4 rocks. Their production may lead to gravitational instabilities, resulting in the diapiric rise of earlier plutons.

In conclusion, the fundamental heat source for igneous evolution appears to be mafic-ultramafic magmas derived by partial melting of the mantle. The different types of igneous activity are a result of various kinds of interaction (e.g., crustal filtering, partial melting, and remobilization) between these magmas and pre-existing crust at a given time in the crustal development process. The entire process from initial mafic volcanism to regional deformation and cratonization appears to have occurred over a time span of about 30 Ma. The model in its present form does not require the presence of an Archean subduction process for which direct evidence appears to be lacking, but only the existence of a narrow rift. The absence to date of any inheritied zircon component in the rocks studied suggests that this rift occurred in an oceanic, simatic environment, or that partial melting of pre-existing sialic crust was very limited.

ACKNOWLEDGMENTS

We would like to thank R.H. Sutcliffe of the Ontario Geological Survey and D.A. Morrison of the National Aeronautics and Space Administration whose excellent work in the Mulcahy Lake area complements our own, and for a free and stimulating exchange of ideas and data.

Discussions with, and references by W.H. Schwerdtner have greatly improved our understanding of diapirism and regional deformation. To the best of our knowledge, he was the first to suggest the mechanism of diapiric remobilization through underplating by bouyant felsic magmas.

The technical assistance of Sandra Kamo, Nick Keehn, Barbara Every, and Jim Shaver is gratefully acknowledged.

Rare earth element analyses were done on the SLOWPOKE reactor at the University of Toronto with the cooperation and assistance of Ron Hancock.

Drawings were prepared by Rob Mason and Susan Kesmarky.

The manuscript was word processed by Lisa Phipps.

REFERENCES

Campbell, I.H., Franklin, J.M., Gorton, M.P., Hart, T.R., and Scott, S.D.

1981: The Role of Subvolcanic Sills in the Generation of Masive Sulfide Deposits; Economic Geology, Volume 76, p.2248-2253.

Davies, J.C., and Watowich, S.N.

1956: Geology of the Populus Lake Area; Ontario Department of Mines, Annual Report, Volume 65, Part 4, 24p.

Davis, D.W., Blackburn, C.E., and Krogh, T.E.

1982: Zircon U-Pb Ages from the Wabigoon-Manitou Lakes Region, Wabigoon Subprovince, Northwest Ontario; Canadian Journal of Earth Sciences, Volume 19, p.254-266.

Davis, D.W., Krogh, T.E., Hinzer, J., and Nakamura, E.

In Press: Zircon Dating of Polycyclic Volcanism at Sturgeon Lake and Implications for Base Metal Mineralization; Economic Geology.

Davis, D.W., and Edwards, G.R.

1982: Zircon U-Pb Ages from the Kakagi Lake Area, Wabigoon Subprovince, Northwest Ontario; Canadian Journal of Earth Sciences, Volume 19, p.1235-1245.

In Preparation: Crustal Evolution of Archean Rocks in the Kakagi Lake Area, Wabigoon Subprovince, Ontario, as Interpreted from High Precision U-Pb Geochronology; Submitted to Canadian Journal of Earth Sciences.

Edwards, G.R., and Davis, D.W.

1984: Petrogenesis and Metallogenesis of the Atikwa-Lawrence Volcanic-Plutonic Terrane; Grant 179, p.222-239 *in* Geoscience Research Grant Program, Summary of Research 1983-1984, edited by V.G. Milne, Ontario Geological Survey, Miscellaneous Paper 121, 252p.

Moorhouse, W.W.
1939: Geology of the Eagle Lake Area; Ontario Department of Mines, Annual Report, Volume 48, Part 4, 31p.

Morrison, D.A., Davis, D.W., Woode, J.L. Bogard, D.D., Maczuga, D.E., Phinney, W.C., and Ashwal, L.D.
In Press: Age of the Mulcahy Lake Intrusion, N.W. Ontario; Earth and Planetary Science Letters.

Morrison, D.A., and Phinney, W.C.
1985: The Mulcahy Lake Gabbro and Related Intrusions (Abstract); Institute on Lake Superior Geology, 31st Annual Meeting, Kenora, Ontario, Abstracts, p.60.

Schwerdtner, W.M., Stott, G.M., and Sutcliffe, R.H.
1983: Strain Patterns of Crescentic Granitoid Plutons in the Archean Greenstone Terrain of Ontario; Journal of Structural Geology, Volume 5, p.419-430.

Schwerdtner, W.M., Stone, D., Osadetz, K., Morgan, J., and Stott, G.M.
1979: Granitoid Complexes and the Archean Tectonic Record in the Southern Part of Northwestern Ontario; Canadian Journal of Earth Sciences, Volume 16, p.1965-1977.

Sutcliffe, R.H.
1985: Mulcahy Lake Gabbro: A Well Preserved Archean Layered Intrusion; Institute on Lake Superior Geology, 31st Annual Meeting, Kenora, Ontario, Abstracts, p.90.

Grant 187 Sedimentology of the Cambro-Ordovician Sandstones of Eastern Ontario

Rainer R. Wolf and Robert W. Dalrymple

Department of Geological Sciences, Queen's University

ABSTRACT

The Potsdam Group in the Kingston-Brockville-Big Rideau Lake area consists of the lower "Covey Hill" Formation and the overlying Nepean Formation. Six depositional facies are recognized in these units: (1) massive to cross-stratified, feldspathic conglomerates and crossbedded, conglomeratic arkoses, which formed in a proximal, braided fluvial environment; (2) quartz arenites containing giant crossbeds deposited by eolian dunes; (3) alternating crossbedded and bioturbated, quartz arenites in sequences 1 to 3 m thick which represent repeated progradation of tide-dominated, subtidal to intertidal-flat environments; (4) flat-bedded quartz arenites, containing isolated ripple and small megaripple crossbeds separated by parallel lamination and ripple cross-lamination, which represent a wave-dominated, nearshore deposit; (5) graded quartz arenites, which pass upwards from laminated to burrowed in each bed, produced by storms in an (offshore?) marine setting; and (6) trough crossbedded, quartz arenites containing variable amounts of gravel, plus isolated burrows in the most distal equivalents, which formed in a braided fluvial to estuarine (?) environment. The first of these facies is restricted to the "Covey Hill" Formation, whereas the others jointly comprise the Nepean Formation; we recommend, however, that facies 2 be given formal stratigraphic status. The restriction of the wave- and storm-dominated facies to the south side of the Frontenac Axis, together with paleocurrent trends in several of the facies, strongly suggest that a topographic high existed in the location of the Frontenac Axis during deposition of the Postdam Group.

The initial detritus derived from the Shield (facies 1) was mineralogically immature; the major purification which occurred to produce the quartz arenites of the Nepean Formation probably took place in the eolian environment of facies 2. Subsequent reworking by rivers and the transgressing sea redeposited much of the eolian sand in fluvial and marine facies (facies 3 to 6). Early silica cementation of the eolian sands helped to prevent the later introduction of carbonate cements which reduce the bulk silica content of many of the marine sandstones.

INTRODUCTION

In Eastern Ontario, all of the post-Grenville, siliciclastic sediments which underlie the Beekmantown Group belong to the Potsdam Group (Carson 1982a, 1982b; Williams and Wolf 1984a, 1984b). This Group is subdivided into a lower unit consisting of feldspathic conglomerates and conglomeratic arkoses which are tentatively correlated with the Covey Hill Formation of Quebec, and the overlying, quartz-rich sandstones (and minor, basal conglomerates) of the Nepean Formation (Williams and Wolf 1984a, 1984b). The age of these units is not known with certainty. The Nepean Formation contains a Lower Ordovician (Tremadocian) conodont fauna in the Ottawa area (Brand and Rust 1977), while its correlative in New York State (the Keeseville Formation) is Upper Cambrian in age (Fisher 1977). The "Covey Hill" Formation is believed to be older than this, and could even be Precambrian in age (Wolf and Dalrymple 1984).

Due to the continued interest in the silica sand potential of the Potsdam Group, we initiated a study in 1983 to determine the depositional environments of these sediments, and the extent of their control on silica grade. An additional goal was to map the facies distribution within the Postdam Group in detail so as to provide a better means of internal correlation than had existed previously. The study area consisted of the 2500 km^2 triangular area between Kingston, Brockville, and Big Rideau Lake (Figure 187.1), straddling the Frontenac Axis and including the southwestern margin of the Ottawa Valley. In our previous annual report (Wolf and Dalrymple 1984) we gave preliminary descriptions and environmental interpretations of the depositional facies based on incomplete field work. Since then, we have completed our mapping. In total, 350 outcrops have been examined in detail, allowing us to refine our previous descriptions and interpretations, and subdivide the undifferentiated "nearshore" facies (facies 4) of Wolf and Dalrymple (1984). In addition, the framework petrography and diagenetic history of the major facies have been examined. In this report we outline these new findings. Details of our methodology are provided by Wolf and Dalrymple (1984).

DEPOSITIONAL FACIES

INTRODUCTION

We now recognize 6 facies within the Potsdam Group of the study area: (1) pebbly arkose and feldspathic conglomerate (braided fluvial); (2) sandstone with very large-scale crossbeds (eolian); (3) alternating crossbedded and bioturbated sandstone (tide-dominated marine); (4) flat-bedded sandstone (wave-dominated nearshore); (5) graded, laminated to burrowed sandstone (storm-dominated marine); and (6) trough crossbedded sandstone (braided fluvial to estuarine?). Facies 1 is restricted to, and constitutes the entirety of, the "Covey Hill" Formation, whereas the remaining facies are quartz arenites (with minor quartz-rich conglomerates) of the Nepean Formation. The first 3 facies were described and interpreted by Wolf and Dalrymple (1984), and only brief summaries, together with any newly discovered features, will be presented. Facies 4, 5, and 6 represent the subdivided facies 4 of Wolf and Dalrymple (1984). Despite the greater subdivision, all of the Nepean facies of aqueous origin (facies 3 to 6) exhibit a considerable range in their characteristics, and intergradations can occur between them. The scattered nature and small size of most outcrops, and the absence of shale makes further refinement, inter-outcrop correla-

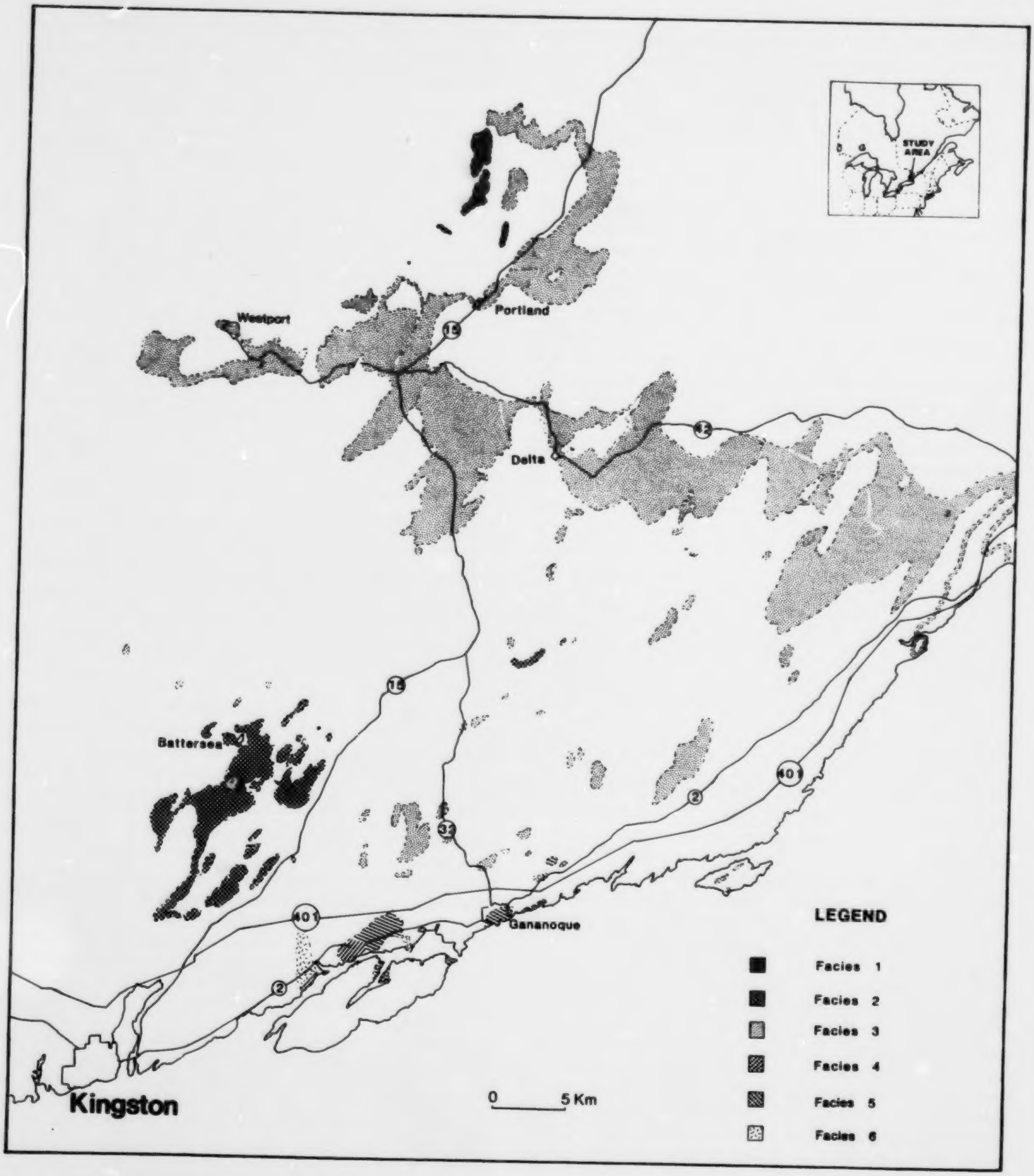
STUDY AREA
Westport
Portland
15
Delta
42
15
Battersea
32
401
Gananoque
401
2
2
Kingston
0 5 Km
LEGEND
Facies 1
Facies 2
Facies 3
Facies 4
Facies 5
Facies 6

Figure 187.1. *Location map and distribution of facies within the Potsdam Group of the Kingston-Brockville-Big Rideau Lake area (modified after Wolf and Dalrymple 1984).*

tion, and environmental interpretation very difficult; therefore, highly detailed environmental reconstruction is not possible at this time.

FACIES 1: PEBBLY ARKOSE AND FELDSPATHIC CONGLOMERATE

Description

The feldspathic conglomerates and pebbly arkoses of this facies are poorly sorted and contain subrounded to well rounded pebbles set in angular to subrounded, coarse to medium sand. The conglomerates are massive, crudely horizontally stratified, and cross-stratified, whereas the sandstones exhibit low- to high-angle, planar, and trough crossbedding in sets up to 2 m thick. Paleocurrents are to the east and north. Both fining- and coarsening-upward sequences exist. Wolf and Dalrymple (1984) interpreted this facies as a proximal, braided, fluvial deposit which is believed to predate the quartz arenites of the Nepean Formation because Paleozoic clasts and the rounded quartz sand grains which characterize the Nepean sandstones are absent.

Petrology

The gravel clasts consist primarily of quartzite and granite with lesser amounts of gneiss, schists, and marble. The marble clasts are commonly partially leached, and schist fragments are usually sericitized and slightly deformed (bent) around adjacent clasts. The sands have a diverse and variable framework mineralogy (Dorr 1984) that averages 63% quartz (polycrystalline grains are 10% to 60% of the total), 30% feldspar (microcline is slightly more abundant than orthoclase, and plagiocalse is relatively uncommon), 5% lithic fragments (schist is most abundant, but granite, gneiss, and marble also occur), and 2% other minerals (including, in approximate order of decreasing abundance, amphibole, goethite and/or hematite, biotite, sphene, garnet, zircon, and pyroxene). The quartz content generally increases upward through the unit, and marble fragments are present only near the base. The sandstones contain 10% to 20% matrix on average, which consists of sericite, hematite, chlorite, and quartz. It is almost entirely diagenetic in origin, having formed from the alteration of feldspars and lithic fragments, and the crushing of schist grains. Both quartz and feldspar overgrowths are present as well, but the unit is poorly indurated, possibly due to the dissolution of a previous cement (calcite?). The degree of compaction and diagenetic alteration suggests that the area was buried to a depth of approximately 2000 m, a finding that is in agreement with microfossil alteration indices in the overlying carbonates (Legall *et al.* 1981).

Occurrence

No new outcrops of this facies were discovered this year; consequently, occurrences of this facies are essentially restricted to down-faulted blocks in the Big Rideau Lake area (Figure 187.1), with additional, minor outcrops scattered on the eastern part of the Frontenac Axis.

FACIES 2: SANDSTONE WITH VERY LARGE-SCALE CROSSBEDS

Description

This facies is characterized by very large, simple crossbeds composed of well sorted, medium-grained quartz sand. The sets have thicknesses between 2 m and 10 m, and most are very broad troughs, with widths up to 100 m. These crossbeds consist primarily of long, sweeping toesets and extensive bottomsets; maximum dips rarely exceed 20° and foresets are very uncommon. Third-order bounding surfaces (Brookfield 1977), planes where dip angle and/or direction changes slightly within an otherwise continuous crossbed, break the continuity of the sets at widely spaced intervals. Paleoflow directions were generally to the southeast and southwest. The laminae within the sets are thin, laterally extensive, and very uniform in thickness. They are believed to represent predominantly climbing translatant strata and grainfall lamination (Hunter 1977), with rare, coarser, grainflow laminae associated with higher-angle foresets. Small reverse faults and deformed laminae also occur sporadically. On bedding planes, adhesion warts and ripples (Kocurek and Fielder 1982) are moderately common, occurring in close association with less common eolian ripples. In addition, wave ripples have been observed on bottom and toesets in 2 locations near the contact with the overlying marine sandstones, at approximately the same stratigraphic level where arthropod crawling traces (*Protichnites*) occur on toeset laminae.

The set boundaries are commonly inclined, and many show no textural change, while others are lined either by a thin granule layer, or by a thicker bed or lens of unsorted conglomerate with a quartz sand matrix. Locally, these pebble-cobble layers may extend some distance up the toesets. In 2 adjacent outcrops approximately 5 km southeast of Battersea (Figure 187.1; about midway between Sunbury and Brewers Mills), cobbles and boulders up to 0.5 m long also occur scattered in the toe- and bottomsets of the large crossbeds. Many of these clasts are triangular in shape (ventifacts?), and none appear to deform the surrounding lamination.

Petrology

The sand comprising the crossbeds consists of 99.5% quartz, with only trace amounts of stable heavy minerals such as rutile and zircon. Syntaxial quartz overgrowths are extensively developed, leaving little porosity. Some of these overgrowths may have formed very early, as evidenced by syndepositional breccias (Selleck 1978), and clasts of sandstone in other facies. Hematite occurs both as a dust rim separating the well rounded quartz core from the overgrowth and as a later, pore-filling cement. The latter is the more abundant form however. Bitumen is also present locally.

The clasts in the conglomerates are composed predominantly of quartzite and quartz-rich granite, but gneiss and gabbro also occur locally. The sand matrix is similar in composition to the sand in the crossbeds. In the outcrop with the scattered cobbles and boulders, the feldspar grains within the clasts show strong kaolinitic (?) alteration, and the exteriors of the clasts are deeply pitted. It is suggested that the pits represent the locations where altered feldspars have been removed by abrasion, which implies that the alteration is Cambro-Ordovician in age.

Interpretation

The previous interpretation of this facies as an eolian deposit (Wolf and Dalrymple 1984) remains unchanged by the new observations. The bimodal (southeast-southwest) paleocurrent suggests that the dunes may have been north-south oriented, longitudinal dunes, which may have reached 100 m in height as indicated by the thickness of the grainflow laminae (Kocurek and Nielson 1984). Based on the presence of *Protichnites* traces and wave ripples, it was also suggested that the dune complex formed in a coastal setting where it experienced intermittent marine inundation (for another example of such eolian-marine interaction, *see* Pulvertaft 1985). This is supported by the discovery that these features occur near the top of the unit, where it is overlain by marine sandstones. The conglomerate layers and lenses are interpreted as the deposits of ephemeral streams in interdune areas. Eolian deflation may have aided in the concentration of these layers, but the scarcity of ventifacts suggests that this process was not particularly important. The origin of the dispersed cobbles and boulders within the crossbeds remains unresolved.

Occurrence

The most extensive outcrops of this facies occur in the vicinity of Battersea, high on the Frontenac Axis (Figure 187.1). Additional small outcrops, many of them too small to appear on Figure 187.1, are scattered throughout the study area, most notably east of the junction of Highways 15 and 32, and near Charleston Lake and Delta. Stratigraphically, this facies rests unconformably on the Precambrian wherever it occurs; previous indications that the eolian deposits overlie marine sandstones has not been supported by further mapping. Usually, the upper contact is not exposed, but in 3 places it is sharply overlain by marine sandstone (facies 5), and in one place by trough crossbedded sandstones of facies 6. These contacts are generally abrupt, and marked by a thin layer of granules or pebbles. The occurrence of marine indicators in the underlying eolian crossbeds suggests, however, that this contact does not represent a major disconformity. Because of the distinctive nature of this facies and its regional extent, including outcrops in the Ottawa and northern New York State areas, we plan to propose formally that this unit be given member, or even formation, status, with a type section located across the River Styx (Cataraqui) from Joyceville. We would welcome comments on this.

FACIES 3: ALTERNATING CROSSBEDDED AND BIOTURBATED SANDSTONE

Description

This facies is charcterized by 1 to 3 m thick, cyclic alternations of crossbedded and bioturbated, medium- to fine-grained, quartz sandstone. The ideal sequence begins with an erosional surface which is mantled by conglomerate in some areas adjacent to Precambrian hills. This is overlain locally by a thin unit (<0.15 m) of horizontal stratification, which is in turn overlain by trough and planar crossbedding in sets 0.2 to 0.5 m thick. Formsets of bedforms with heights of 0.25 m and lengths of 10+ m occur in some outcrops. These crossbeds typically display a bimodal, bipolar ("herringbone") paleocurrent pattern with a dominant east-west orientation; regularly spaced reactivation surfaces are also common. Toward the top of the physically structured portion of the cycles, discrete, vertical burrows (*Skolithos, Diplocraterion, Arenicolites*, and *Monocraterion*) are found. The very top of this interval may display wave ripples.

The overlying, bioturbated portion of the cycle contains no physical structures, and generally shows pervasive, biogenic mottling. Where discrete burrows can be identified, they are primarily horizontal types (*Palaeophycus, Phycodes*, and *Teichichnus*), except in a small number of pipe-rock beds situated near the top of the formation which contain abundant *Arenicolites*. Fragments of lingulid brachiopods, gastropods, and bivalves are also found rarely, as are thin mud-cracked layers. In a few places just below the contact with the March Formation, the tops of the cycles are disrupted by soft-sediment deformation, due either to the leaching of evaporites or to (earthquake induced?) liquifaction. In general, the bioturbated intervals are thinner than the crossbedded sandstones in the lower part of the section, but the proportions are reversed toward the top of the Nepean Formation. Individual cycles cannot be traced great distances due to lateral changes in the amount of bioturbation which obliterates the crossbedded portion of the cycles.

Petrology

The framework grains in this facies are predominately well to very well rounded quartz (98% to 99%), with minor amounts (<1%) of fine-grained, sericitized feldspar (orthoclase and plagioclase), and heavy minerals (e.g. zircon, rutile, magnetite). Again, syntaxial quartz overgrowths are common, but they have been corroded in many places by a later calcite cement, particularly in the burrowed intervals. The calcite cement is itself dolomitized locally, and burrow linings commonly contain dolomite rhombs, even in otherwise carbonate-free quartz arenites. In fault zones, the diagenetic history is even more complex, with multiple generations of silica, calcite, and, most importantly, hematite cement.

Interpretation

The previous interpretation of this facies as a tide-dominated deposit composed of stacked, progradational, subtidal to intertidal flat sequences (Wolf and Dalrymple 1984) is supported by the additional observations. The upward increase in burrowing, and the change from vertical to horizontal burrows within each cycle results from the decrease in energy upward into the intertidal zone; periodic exposure is indicated by the scattered desiccation cracks. Evaporite moulds in one outcrop of this facies near

Gananoque and in the overlying carbonates give evidence of elevated salinities, a finding that is compatible with an evaporite-solution origin of the soft-sediment deformation features. Mud is absent from this facies, not because energy levels prevented deposition, but because the fine-grained material was blown away by the winds which formed facies 2 (Dalrymple *et al.*, in press).

Occurrence

This facies is the most areally and stratigraphically widespread of the facies in the Nepean Formation. It outcrops most extensively along the Ottawa Valley margin of the Frontenac Axis, and to a lesser extent on the crest of the Axis. Wherever it is found, it rests directly on the Precambrian, except for one possible occurrence near Gananoque where it rests on facies 6. It is overlain conformably (?) by the March Formation, and is, therefore, the youngest facies in the study area, although it may be contemporaneous with the other marine facies (4 and 5).

FACIES 4: FLAT-BEDDED SANDSTONE

Description

The fine- to medium-grained quartz sandstones of this facies generally occur in thin, tabular beds, with flat, or very gently undulatory, bedding planes which give the unit its flat-bedded appearance. Scattered throughout, however, are trough and planar crossbeds, and formsets of ripples and small megaripples. Crossbed sets are smaller than in facies 3 and rarely exceed 0.1 m in thickness, although in one case, an isolated set which reaches 0.5 m in thickness sits in an erosional scour amongst the smaller-scale structures. The crossbeds are separated from each other by one or more, thin tabular beds in which the detailed structures consist of either parallel lamination or ripple cross-lamination. Some of the undulatory bedding may be hummocky cross-stratification. Laterally extensive quartz granule and pebble layers, 1 grain thick, occur throughout the facies. Trace fossils were not observed.

Interpretation

Facies 4 is believed to represent a high-energy, wave-dominated, nearshore deposit, formed under alternating storm (granule and pebble beds, megaripples, and possible hummocks) and fairweather conditions (ripples). The bottom must have experienced relatively continuous wave action, however, as biogenic structures did not form. A very shallow setting above fairweather wave base, facing onto an open body of water, is envisaged.

Occurrence

This facies occurs in only a few isolated outcrops in the Kingston-Gananoque area, on the southwest flank of the Frontenac Axis, a location which suggests that the open body of water lay to the southwest. These nearshore sandstones lie on the Precambrian in some places, and on facies 6 elsewhere. Facies 4 is overlain by both facies 5 and 6 in separate instances. This facies is also represented by the lower portion of the Nepean type section, west of Ottawa.

FACIES 5: GRADED, LAMINATED TO BURROWED SANDSTONE

Description

This facies is characterized by repeated, parallel-sided beds with thicknesses from a few centimetres to approximately 0.2 m. Each bed begins with a sharp base that may be erosional, overlain by a thin (1 cm or less) quartz granule layer in many cases. This passes abruptly upwards into fine- to medium-grained quartz arenite containing parallel lamination and/or ripple cross-lamination. Both *Diplocraterion*, and *Bergaueria* burrows are present within this interval, and horizontal *Treptichnus* traces have been seen on the bases of some beds. This physically structured zone is gradationally overlain by a thoroughly bioturbated interval in fine-grained sandstone, from which *Palaeophycus* and *Bergaueria* traces have been recovered. Decimetre-scale crossbeds are virtually absent from this facies, and hummocky cross-stratification has not been observed.

Interpretation

These graded beds, which contain an upward transition from physical to biogenic structures, closely resemble the graded storm layers described by many workers from shallow marine environments (*see* Walker (1984) for a summary). The abundance of bioturbation at the top of each bed suggests that the fairweather conditions were quiet, which might place this facies below fairweather wave base. Normally, shale would be present between the beds in such a setting, but its absence due to prior wind removal (Dalrymple *et al.*, in press) makes relative depth determination difficult. The occurrence of beds with monospecific trace-fossil assemblages indicates, however, that the environment was probably not normal marine.

Occurrence

Occurrences of facies 5 are limited in number, and are restricted to the region between Kingston and Gananoque (associated with facies 4), and to 2 localities southwest of Battersea. In the former area, facies 5 overlies facies 4, an arrangement which suggests an upward, nearshore to offshore, transgressive succession. Sediments which also have features in common with facies 5 (but which contain larger crossbeds) are also laterally equivalent to facies 6 in one outcrop. In the Battersea area, facies 5 overlies eolian facies 2 with an abrupt contact that is marked by a granule or pebble layer. The upper portion of the Nepean type section has strong similarities with this facies.

FACIES 6: TROUGH CROSSBEDDED SANDSTONE

Description

The quartz arenites of facies 6 are characterized by abundant trough crossbedding in sets 0.2 to 0.5 m thick. The very few, widely scattered outcrops of this facies differ markedly in detail from each other, and 3 (intergradational?) variants of this facies exist. The most northerly outcrop is also the coarsest, and consists of 0.2 to 0.8 m thick co-sets of crossbedding, separated by quartzite pebble and cobble beds. The crossbeds themselves are composed of medium- to coarse-grained quartz with scattered pebbles along set boundaries. Just east of Gananoque, facies 6 sandstones are medium grained, and contain only a minor amount of gravel which occurs both as isolated clasts along set boundaries, and as thin (1 grain thick), continuous, quartz-pebble horizons which subdivide the outcrop into co-sets 1 to 3 m thick. There is no evidence of trace fossils in either of these occurrences of facies 6. Between Kingston and Gananoque, the fine- to medium-grained sandstones of facies 6 lack gravel completely and occur in co-sets 1 to 2 m thick separated by horizontal erosion surfaces. Sporadic *Skolithos* burrows are also present at the top of crossbeds. In addition, the crossbedding grades laterally into a section that contains graded and partially bioturbated beds between the crossbeds. The paleocurrent direction in all outcrops of this facies is generally to the south. Reactivation surfaces have not been seen.

Interpretation

The unimodal paleocurrent pattern, the lack of reactivation surfaces, and the absence of trace fossils in most occurrences of this facies, together with the gravel layers in the more northerly (up-current) outcrops and the lack of well defined fining-upward sequences, suggests that facies 6 represents a braided fluvial deposit. The marine trace fossils in the most southerly (distal) outcrop may indicate that an estuarine environment existed in that location; this outcrop does, in fact, sit in a north-south, elongate depression in the Precambrian surface.

Occurrence

As already stated, this facies is primarily restricted to the southwestern flank of the Frontenac Axis. To the north, it rests directly on the Precambrian, whereas farther south, it lies on the nearshore sandstones of facies 4. It is seen to be overlain by sandstones at 3 localities; in 2 of these, they are flat-bedded sandstones of facies 4, and in the other (just east of Gananoque) they are intermediate in character between facies 3 and 4.

SUMMARY AND DISCUSSION

The sandstones and conglomerates of the Potsdam Group in Eastern Ontario contain a complex assemblage of terrestrial and marine deposits. The earliest deposits are represented by the arkosic sandstones and feldspathic conglomerates of the "Covey Hill" Formation, which formed in a proximal, braided, fluvial environment, in which flow was to the north and east. Subsequent to this, but before the marine transgression in the Late Cambrian or Early Ordovician, eolian conditions prevailed. Terrestrial weathering and eolian abrasion during this interval, as evidenced by the highly altered feldspars and pitted pebbles described from facies 2, is believed to be responsible for most or all of the quartz enrichment that is evident in the Nepean Formation. (The efficiency of eolian action in the generation of quartz-rich sands has long been recognized (Kuenen 1960).) Eolian conditions continued in the coastal zone of the advancing sea, until the marine waters drowned the dune complex. During the transgression, eolian sand was reworked to form the marine deposits of facies 3, 4, and 5. Rivers may also have transported sand to the advancing sea as evidenced by the interbedding of facies 6 with facies 3 and 4. In the sea, physical energy levels decreased, and/or biological activity increased, through time as the transgression continued, leading to the upward increase in bioturbation. This may not have been caused by deepening, however, as evidenced by the presence of exposure features in the overlying March Formation and its New York equivalent, the Theresa Formation (Selleck 1984). Instead, the increasing width of the cratonic sea may have damped energy levels, while the upward change to carbonate sedimentation probably also reflects the increasing distance to the shoreline and the reduction in the size of the source area. Small amounts of detrital carbonate matrix, and/or diagenetic introduction of calcite from the overlying carbonates, accounts for the greater impurity of the marine facies in many areas. In addition, these sediments may not have had the early phase of silica cementation that is evident in the eolian sandstones.

Both tide-dominated (facies 3) and wave/storm-dominated (facies 4 and 5) conditions existed in the Cambro-Ordovician seas. Geographic separation of the 2 assemblages precludes establishing the exact age relationship between them without biostratigraphic control, but both pass upward into similar, more thoroughly biturbated sandstones which are transitional with March Formation lithologies. This suggests that they are broadly contemporaneous. If this is so, then the presence of wave/storm sedimentation on the southwest side of the Axis while tide-dominated sedimentation existed in the Ottawa Valley argues strongly for the existence of a paleo-Frontenac Axis in the Late Cambrian and Early Ordovician. It is possible, in fact, that the tidal conditions recorded in the Ottawa Valley are a direct result of the existence of a paleo-embayment which promoted tidal amplification. The upward decrease in tidal energy recorded in facies 3 might be due, therefore, to the flooding of the embayment as transgression progressed. Other indirect evidence for a paleo-Frontenac Axis includes the northeasterly paleocurrents in facies 1, the southerly paleocurrents in facies 6, and the east-west paleocurrents in the tidal sediments (approximately parallel to the embayment axis?).

ACKNOWLEDGMENTS

Our appreciation is extended to the landowners in the study area who granted permission to examine exposures on their property. The various quarry owners are especially thanked. We also thank Drs. G.M. Narbonne and L. Smith, Queen's University, and Dr. A.G. Plint, McMaster University, for helpful discussions on the paleontology, stratigraphy, and environmental interpretations. The financial support of the Ontario Geological Survey is gratefully acknowledged.

REFERENCES

Brand, U., and Rust, B.R.
1977: The Age and Upper Boundary of the Nepean Formation in its Type Section Near Ottawa, Ontario; Canadian Journal of Earth Sciences, Volume 14, p.2002-2006.

Brookfield, M.E.
1977: The Origin of Bounding Surfaces in Ancient Eolian Sandstones; Sedimentology, Volume 24, p.303-332.

Carson, D.M.
1982a: Paleozoic Geology of the Brockville-Mallorytown Area, Southern Ontario; Ontario Geological Survey, Preliminary Map P.2495, Geological Series, scale 1:50 000.
1982b: Paleozoic Geology of the Gananoque-Wolfe Island Area, Southern Ontario; Ontario Geological Survey Preliminary Map P.2496, Geological Series, scale 1:50 000.

Dalrymple, R.W., Narbonne, G.M., and Smith, L.
In Press: Eolian Action and the Distribution of Cambrian Shales in North America; Geology.

Dorr, J.J.
1984: The Sedimentological Study of the Feldspathic Conglomerates and Sandstones of the Big Rideau Lake Area, Ontario; Unpublished B.Sc. Thesis, Queen's University, Kingston, Ontario, 98p.

Fisher, D.W.
1977: Correlation of the Hadrynian, Cambrian, and Ordovician Rocks of New York State; New York State Museum, Map and Chart Series, Number 25, 75p.

Hunter, R.E.
1977: Basic Types of Stratification in Small Eolian Dunes; Sedimentology, Volume 24, p.361-387.

Kocurek, G., and Fielder, G.
1984: Adhesion Structures; Journal of Sedimentary Petrology, Volume 52, p.1229-1241.

Kocurek, G., and Nielson, J.
1984: Determination of Original Eolian Dune Height from Ancient Cross-strata; Society of Economic Paleontologists and Mineralogists, First Midyear Meeting, Abstracts, p.44.

Kuenen, Ph.H.
1960: Sand; Scientific American, Volume 202, p.94-110.

Legall, F.D., Barnes, C.R., and MacQueen, R.W.
1981: Thermal Maturation History, and Hotspot Development, Paleozoic Strata of Southern Ontario-Quebec, from Conodont-Acritarch Colour Alteration Studies; Bulletin of Canadian Petroleum Geology, Volume 29, p.492-540.

Pulvertaft, T.C.R.
1985: Aeolian Dune and Interdune Sedimentation in the Middle Proterozoic Dala Sandstone, Sweden; Sedimentary Geology, Volume 44, p.93-111.

Selleck, B.W.
1978: Syndepositional Brecciation in the Potsdam of Northern New York State; Journal of Sedimentary Petrology, Volume 48, p.1177-1184.
1984: Stratigraphy and Sedimentology of the Theresa Formation (Cambro-Ordovician) in Northeastern New York State; Northeastern Geology, Volume 6, p.118-129.

Walker, R.G.
1984: Shelf and Shallow Marine Sands; p.141-170 *in* Facies Models (Second Edition), edited by R.G. Walker, Geoscience Canada, Reprint Series 1, 317p.

Williams, D.A., and Wolf, R.R.
1984a: Paleozoic Geology of the Westport Area, Southern Ontario; Ontario Geological Survey, Preliminary Map P.2723, Geological Series, scale 1:50 000.
1984b: Paleozoic Geology of the Perth Area, Southern Ontario; Ontario Geological Survey, Preliminary Map P.2724, Geological Series, scale 1:50 000.

Wolf, R.R., and Dalrymple, R.W.
1984: Sedimentology of the Cambro-Ordovician Sandstones of Eastern Ontario; Grant 187, p.240-252 *in* Geoscience Research Grant Program, Summary of Research 1983-1984, edited by V.G. Milne, Ontario Geological Survey, Miscellaneous Paper 121, 252p.

Grant 189 Preliminary Report on the Stratigraphy and Sedimentology of the Bar River Formation

D.J. Wright and B.R. Rust

University of Ottawa

ABSTRACT

The Bar River Formation is the uppermost unit of the Cobalt Group and thus represents the last phase of Huronian sedimentation.

From the 2 locations examined (near Flack Lake and Bay Finn) the formation can be subdivided into 4 subunits:

1. Laminated quartzite
2. Cross-bedded quartzite
3. Quartzite and hematitic quartzite
4. Interbedded quartzite, sandstone, and siltstone

Features indicating bimodal or multimodal paleocurrents are present throughout the formation in the form of herringbone crossbed sets, reactivation surfaces, and multidirectional ripple crests. In the Flack Lake section desiccation cracks provide evidence for exposure.

Paleocurrent measurements indicate predominantly northeastward transport in the Bay Finn area, and a southerly transport direction in the Flack Lake area.

A preliminary interpretation is that the sediments of the Bar River Formation were deposited in a shallow marine, meso- to macro-tidal environment and that the sequence is transgressive. The gradational upward change from the underlying Gordon Lake Formation indicates increasing influence of more open marine conditions.

INTRODUCTION

The Bar River Formation is the uppermost unit in the Cobalt Group, which in turn is the uppermost group of the Huronian Supergroup. The formation, comprising mainly quartzites, has been treated by several authors in the context of regional reports (Frarey 1977; Frarey and Cannon 1968; Wood 1975; Siemiatkowska 1978; Card 1976, 1978; Card *et al.* 1973). It has been examined in more detail by Wood (1970) in the Flack Lake area, and by Card (1978) in the Bay Finn area, but no comprehensive study of the formation has been made.

Recent interest in apparently stratabound copper mineralization in the Cobalt Group has drawn attention to the need to understand the sedimentology of these rocks. The Bar River Formation, like other Huronian rock units, has been subject to several environmental interpretations. Frarey (1977) and Frarey and Roscoe (1970) suggested a fluvial origin for the unit, whereas Wood (1970, 1975) favoured shoreline deposition with eolian influence. Card (1976, 1978) proposed a general marine shelf environment and a tidal marine regime with emergent sand shoals was suggested by Chandler (1984). Some of this conflicting interpretation may be due to the fact that these authors worked on widely separated exposures of the formation. By examining as much of the unit as possible, we hope to arrive at a reasonable interpretation of the Bar River Formation applicable to all exposures.

The Bar River Formation has been recognized in 5 locations, the Flack Lake, Bay Finn, Welcome Lake, McGiffin Lake, and Gordon Lake areas (Figure 189.1). Work done to date consists of stratigraphic and sedimentological examination of the 2 most extensive exposures, herein referred to as the Flake Lake and Bay Finn areas (Figures 189.2a, 189.2b respectively.)

PRESENT STUDY

FLACK LAKE AREA

This area contains some 300 to 450 m of almost flat lying Bar River quartzites. The lower contact with the Gordon Lake Formation is sharp but conformable, and the upper boundary is a profound unconformity partially overlain by unconsolidated Cenozoic material (Robertson 1973; Wood 1975; Siemiatkowska 1978).

The formation is divisible into 2 intergradational units, based on lithology, bedding thickness, and the abundance of sedimentary structures. The lower unit is approximately 175 m thick, and consists of over 90% white quartzite with occasional thin beds, lenses, and drapes of green siltstone. Stratification, where visible, is commonly of medium thickness, although some thick beds were observed. Sedimentary structures include planar and trough crossbeds, commonly with mud chip or rarely, granule lags, herringbone crossbed sets, overturned crossbed sets, symmetrical and asymmetrical straight-crested ripples, and desiccation and rare syneresis cracks. Planar crossbeds range in size from small to large scale, with those of medium scale being the most common.

Pockets of poorly cemented coarse quartz sandstone are associated with large scale crossbeds. The unit containing these structures corresponds to Siemiatkowska's (1978) lower massive orthoquartzite.

Quartzite is the only lithology in the upper unit apart from thin desiccated skins of green and brown siltstone. This unit is approximately 125 m thick, and corresponds to Siemiatkowska's thinly bedded, well rippled quartzite. Bedding is well developed in the quartzite on a scale varying from medium to thin. Ripples occur on most bed surfaces, with both symmetrical and asymmetrical forms represented. The ripple crests vary from straight to wavy, and the crest tops from sharp to rounded. Wavelengths and amplitudes are low, averaging 3 cm and 0.8 cm respectively. Crest orientation is quite variable and interference patterns are common. An interesting feature observed in this unit and also reported from the Lorrain Formation (Frarey 1977; Young 1969; Wood 1975) are vermicular structures found in some ripple troughs. Despite their fossil-like appearance, these structures are probably the result of inorganic pro-

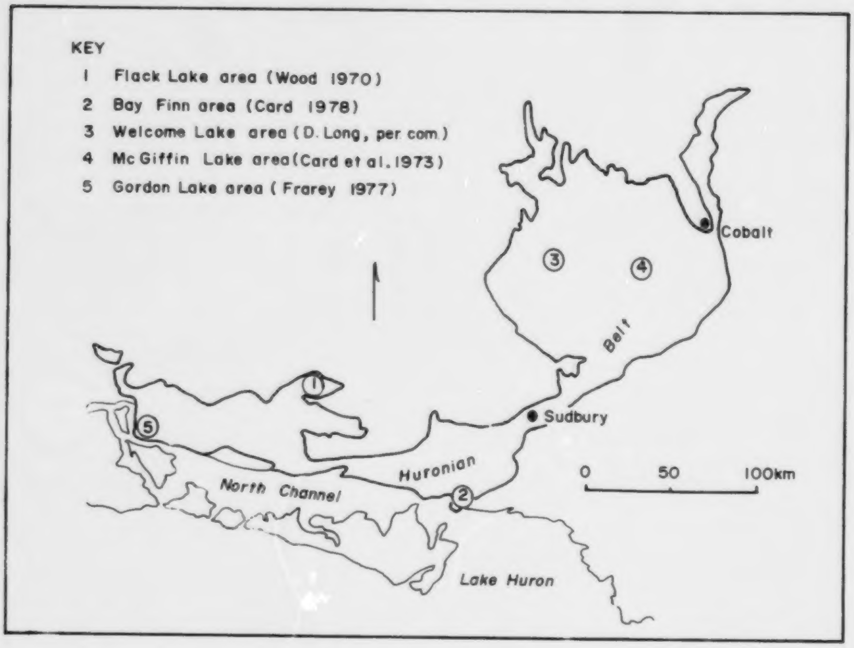
KEY
1 Flack Lake area (Wood 1970)
2 Bay Finn area (Card 1978)
3 Welcome Lake area (D. Long, per. com.)
4 McGiffin Lake area(Card et al. 1973)
5 Gordon Lake area (Frarey 1977)
Cobalt
③
④
Belt
①
Sudbury
⑤
Huronian
North Channel
②
0
50
100km
Lake Huron

Figure 189.1. *Locations of Bar River Formation within the Huronian Belt.*

cesses (Young 1969; Wood 1975), possibly infilling, and disturbance of syneresis cracks.

Paleocurrent data, derived from planar cross-strata, trough cross-strata, and ripple crests, indicate a predominantly southward transport direction (Figure 189.4).

BAY FINN AREA

The most complete section, over 900 m, of Bar River quartzites and siltstones is exposed in this area. The lower contact with the Gordon Lake Formation is gradational over about 30 m. In this area the Gordon Lake Formation is made up of interbedded siltstone and sandstone. Through the transition zone, the sandstone beds gradually become thicker and more frequent. The lower boundary of the Bar River Formation has been placed at the base of the first thick quartzite bed above which there is only minor siltstone (Card 1978). The topographic expression of this boundary is commonly a marked increase in slope. The upper boundary of the Bar River Formation is an angular unconformity, in places overlain by flat-lying Paleozoic strata (Card 1978; Card *et al.* 1973).

In the course of regional mapping, Card (1976) subdivided the Bar River Formation into 5 intergradational units. This subdivision has been modified for the present project into the following 4 units:

Laminated quartzite: This unit, approximately 90 m thick, consists of fine- to medium-grained quartzite with silty laminae and lenses common near the base. It is white and locally red in colour. Bedding is generally of medium thickness and sedimentary structures include coarse laminae and planar cross-strata. Bedding tops, where visible, are commonly rippled.

Cross-stratified quartzite: White and locally blue or red quartzites make up this 180 m thick unit. Structures, where visible, are medium-scale, planar cross-strata with rippled bed tops. The colouration in this unit is patchy and commonly discordant with sedimentary structures. Further evidence of migration of iron-bearing fluids is found in red staining on joint surfaces. Cubic vugs, believed to be impressions of pyrite cubes, are present on joint surfaces at several locations.

Quartzite and hematitic quartzite: In this unit black, red, blue, and white colouration is more extensive and commonly concordant with bedding and structures. These quartzites are medium- to thinly bedded and sedimentary structures are commonly outlined with hematite. The structures include trough cross-strata, planar cross-strata with common herringbone sets and reactivation surfaces, symmetrical and asymmetrical low amplitude, and wavelength ripples. This unit is approximately 230 m thick.

Interbedded siltstone, sandstone and quartzite: This unit has a different expression in different parts of the area. In the western portion it is confined to the top 400 m of the section. Typically, it is made up of 2 or more cycles beginning with red to bluish, medium- to thinly bedded quartzite followed by thinly interbedded fine sandstone and siltstone which is, in turn, followed by red to white, medium-bedded quartzite. The base of this cycle is erosional at 1 location.

To the east, the silty portions thicken, and the unit interfingers with units lower in the section (Card 1978). Sedimentary structures in the quartzites include planar cross-strata with herringbone sets and reactivation surfaces, and symmetrical and asymmetrical ripples. The interbedded siltstone and sandstone portions show symmetrical and asymmetrical ripples,

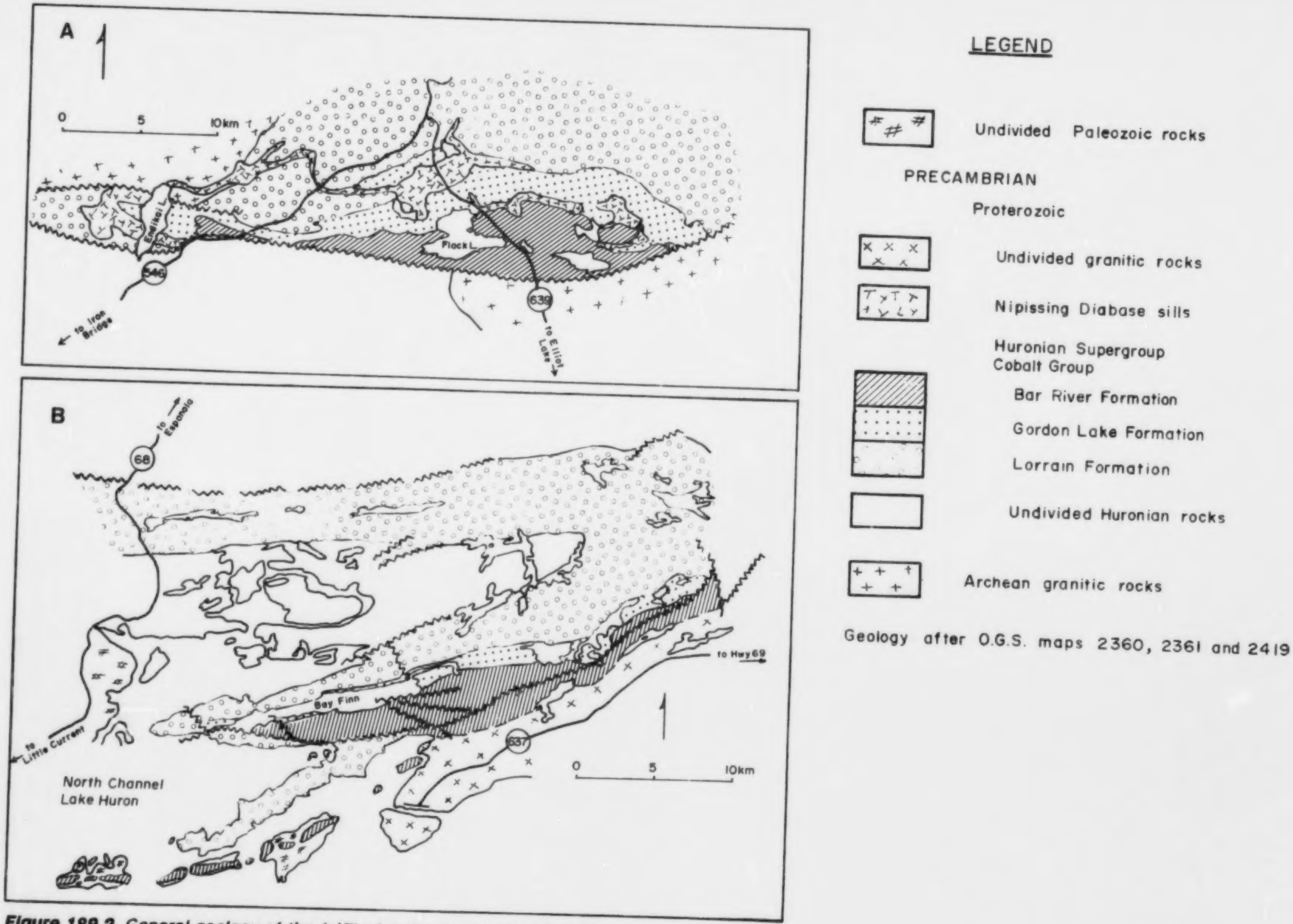
A
0
5
10km
Endikai L.
Flack L.
546
639
to Iron Bridge
to Elliot Lake
B
68
to Espanola
to Little Current
North Channel
Lake Huron
Bay Finn
637
to Hwy69
0
5
10km
LEGEND
Undivided Paleozoic rocks
PRECAMBRIAN
Proterozoic
Undivided granitic rocks
Nipissing Diabase sills
Huronian Supergroup
Cobalt Group
Bar River Formation
Gordon Lake Formation
Lorrain Formation
Undivided Huronian rocks
Archean granitic rocks

Geology after O.G.S. maps 2360, 2361 and 2419

Figure 189.2. General geology of the (a)Flack Lake area, and (b)Bay Finn area.

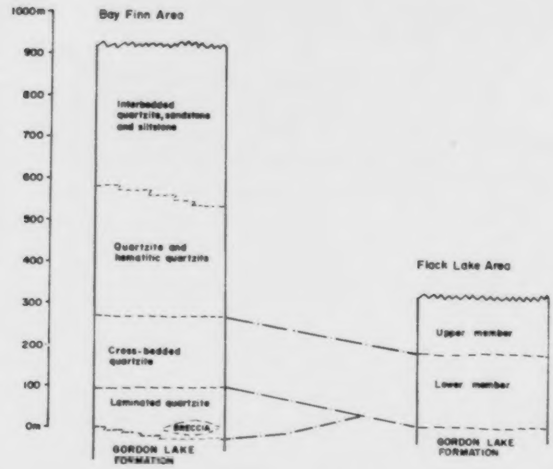

Figure 189.3. *Correlation of the members of the Bar River Formation between the Bay Finn and Flack Lake areas.*

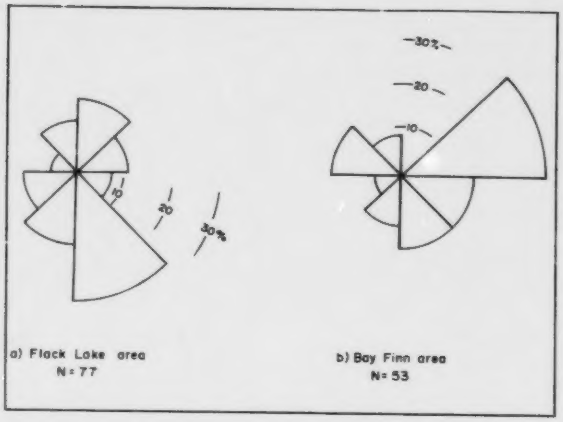

Figure 189.4. *Paleocurrent roses, Bar River Formation, based on measurements of ripples, and trough and planar crossbeds.*

starved ripples, and rare load structures, but are most commonly laminated. Some of the siltstones are very dark in colour and appear to be iron rich. Hematite blebs and nodules occur in one such unit and Card (1978) reported up to 15% total Fe_2O_3 in some samples.

A fifth rock type, previously unreported, was found near the base of the formation (Figure 189.3). This is a lens of breccia located about 500 m north of the Pool. This lens, approximately 10 m thick and extending 40 m along strike is composed of angular clasts of transition zone sandstone and laminated quartzite in a gritty green matrix. Clasts range in size from 1 cm to at least 10 cm. In view of the numerous faults in the area, the breccia is most likely of tectonic origin.

Measurements taken from planar cross-strata and ripple crests indicate a polymodal current pattern with a stonger northeast component (Figure 189.4).

DISCUSSION

The similarity in lithology, bedding style, thickness, and types of sedimentary structure indicate a possible correlation between the Flack Lake area and the middle 2 units in the Bay Finn area (Figure 189.3). The basal and top units at the Bay Finn area are absent from the Flack Lake area, but the lack of the upper unit is presumably due to erosion.

A notable difference between the 2 areas is that no desiccation features were observed the Bay Finn area. Paleocurrent data indicate almost opposing major currents between the 2 areas.

PRELIMINARY INTERPRETATION

Data collected to date indicate that the sediments of the Bar River Formation in the Flack Lake and Bay Finn areas were deposited in a marine environment. Although much of this data is not diagnostic, features indicating opposing and asymmetrical currents abound (i.e., reactivation surfaces, herringbone crossbed sets, silty drapes on planar and trough cross-strata). This variability in current direction and strength is unlikely in a fluvial environment, and quite typical of a tidally influenced marine regime (Stride 1982, p.172; Johnson 1978). Small-scale ripples with low amplitudes and wavelengths suggest deposition in shallow water and the desiccation features in the Flack Lake area indicate periodic emergence. Some sort of sandy barrier or shoal, cut by tidal channels, would explain many of the features found in this northern area.

In the Bay Finn area, a more complete section probably represents several coexisting and related environments. The sandy shoals were still present, but lower relief or a lower tidal range prevented emergence. Landward of the shoals, washover or spillover may have deposited laminated sands; and seaward, sand deposition would give way to deposition of finer grained sediment. The difference in paleocurrent directions between the 2 areas may be a result of basin configuration. Tidal currents are known to be variable between different parts of a basin (Johnson 1978, p.237).

In short, the preliminary interpretation is that the sediments of the Bar River Formation were deposited in a shallow marine, meso- to macro-tidal environment, and that the sequence is transgressive.

REFERENCES

Card, K.D.
1976: Geology of the McGregor Bay-Bay of Islands Area, Districts of Sudbury and Manitoulin; Ontario Division of Mines, Geoscience Report 138, 63p.
1978: Geology of the Sudbury-Manitoulin Area, Districts of Sudbury and Manitoulin; Ontario Geological Survey Report 166, 238p.

Card, K.D., McIlwaine, W.H., and Meyn, H.D.
1973: Geology of the Maple Mountain Area, Districts of Temiskaming, Nipissing and Sudbury; Ontario Division of Mines, Geological Report 160, 131p.

Chandler, F.W.
1984: Sedimentary Setting of an Early Proterozoic Copper Occurrence in the Cobalt Group, Ontario; A Preliminary Assessment; *in* Current Research, Part A, Geological Survey of Canada, Paper 84-1A, p.185-192.

Frarey, M.J.
1977: Geology of the Huronian Belt between Sault Ste. Marie and Blind River, Ontario; Geological Survey of Canada, Memoir 383, 87p.

Frarey, M.J., and Cannon, R.T.
1968: Notes to Accompany a Map of the Geology of the Proterozoic Rocks of Lake Panache-Collins Inlet Map-Areas, Ontario (41 I/3, H/4); Geological Survey of Canada, Paper 68-63, 5p.

Frarey, M.J., and Roscoe, S.M.
1970: The Huronian Supergroup north of Lake Huron, p.143-157 *in* Symposium on Basins and Geosynclines of the Canadian Shield; edited by A.J. Baer, Geological Survey of Canada. Paper 70-40.

Johnson, H.D.
1978: Shallow Siliciclastic Seas; p.207-258 *in* Sedimentary Environments and Facies, edited by H.G. Reading, Elsevier.

Robertson, J.A.
1973: A Review of Recently Acquired Geological Data, Blind River-Elliot Lake Area, p.171-198 *in* Huronian Stratigraphy and Sedimentation, edited by G.M. Young, Geological Association of Canada, Special Paper 12.

Siemiatkowska, K.M.
1978: Geology of the Endikai Lake Area, District of Algoma; Ontario Geological Survey, Report 178, 79p.

Stride, A.H.
1982: Offshore Tidal Sands—Processes and Desposits; Chapman and Hall, London, New York.

Wood, J.
1970: The Stratigraphy and Sedimentation of the Upper Huronian Rocks in the Rawhide Lake-Flack Lake Area, Ontario; Unpublished B.Sc. Thesis, University of Western Ontario, London, 235p.
1975: Geology of the Rawhide Lake Area, District of Algoma; Ontario Division of Mines, Geoscience Report 129, 67p.

Young, G.M.
1969: Inorganic Origin of Corrugated Vermiform Structures in the Huronian Gordon Lake Formation near Flack Lake, Ontario; Canadian Journal of Earth Sciences, Volume 6, p.795-799.

Grant 192 Geochemical Exploration For Gold

Ian Nichol and Gene S. Shelp

Department of Geological Sciences, Queen's University

ABSTRACT

The investigation is concerned with an examination of the nature of gold distribution in glacial till associated with a number of gold deposits. The objective of the study is to assess the reliability of currently adopted procedures and hopefully identify ways by which exploration reliability may be increased. A number of problems have been identified relating to sample representivity, sample processing, and interpretation. Work is continuing on identifying ways of overcoming these problems.

INTRODUCTION

The background to the investigation lies in the recognition that gold deposits of the Canadian Shield have a wide variety of characteristics relevant to the search for further deposits. These include occurrence in a range of host rocks, structural settings, varying mineralogy with gold occurring alternatively in pyrite, free gold, or as tellurides and wide variations in the grain size of the gold. Superimposed on this diversity of characteristics of the gold deposits themselves, exploration is further complicated by wide diversities in the nature of associated glacial overburden. It is to be expected that the geochemical response due to gold mineralization in glacial overburden will vary according to features both of the primary deposits and surface overburden. Effective exploration should as far as possible be capable of detecting as wide a range of deposit types in different environments.

One of the commonest geochemical exploration procedures adopted for areas of glacial overburden involves the sampling of glacial till, although the sampling of specific soil horizons and humus is also employed in certain cases. Depending upon the depth of the glacial overburden, till samples may be obtained by surface sampling, trenching, or deep overburden sampling employing various drilling techniques. Treatment of the sample may involve the direct analysis of a certain size fraction of the till. Frequently a heavy mineral concentrate is obtained from the sample by tabling and heavy liquid separation. Documented case histories indicate the contribution of these methods to the discovery of several important gold deposits (Gray 1983; Averill and Zimmerman 1984; Sauerbrei *et al.* 1985; and Thomson *et al.* 1985) or alternatively their ability to identify known deposits (Closs and Sado 1979; Bird and Coker 1985).

The objective of the current investigation is to examine the nature of gold dispersion associated with a variety of gold deposits and thereby assess the effectiveness of commonly adopted methodology. On the basis of the results, it is hoped to identify ways by which exploration effectiveness may be increased.

This report presents a review of results obtained during the first year of the investigation (Shelp and Nichol 1985).

AREAS OF INVESTIGATION

The areas selected for examination were the Owl Creek, Hemlo, and McBean Deposits, and the Green Lake occurrence. The Hemlo and Green Lake mineralization is overlain by relatively thin overburden and the basal till, where present, is fairly accessible.

The Owl Creek and McBean Deposits have both open pits and offer good access to lodgment till overlying and immediately down-ice from mineralization.

SAMPLING

Bulk samples, in excess of 50 kg, have been collected by hand from all areas to avoid as far as possible any bias introduced by sampling method.

SAMPLE PROCESSING PROCEDURE

The investigation undertaken to date has involved an examination of gold distribution in heavy mineral concentrates and the silt- and clay-sized or minus 63 μm fraction of tills.

Two heavy mineral processing procedures were used in the investigation, one involving the use of a gravity table and heavy liquids, and the second involving wet panning and heavy liquids.

To clarify some of the terms used in the text of the report, the heavy mineral concentrating procedure using gravity separation is outlined in Figure 192.1. The procedure basically involves the removal of the plus 2 mm (10 mesh) fraction of the sample and passing the minus 2 mm fraction over a separatory table. In some cases wetting agents are used to reduce surface tension effects and to aid in the recovery of fine-grained particles. Similarly, the sample may be passed more than once over the separatory table. The heavy mineral concentrate from the table is then treated by heavy liquids, frequently methylene iodide (S.G. = 3.3), to further concentrate the heavy minerals. In some cases, tetrabromoethane may be used (S.G. = 2.9) which allows for the recovery of slightly lighter heavy minerals and is thus suitable for the recovery of particles of fine-grained gold in quartz grains. The heavy mineral concentrate produced from the heavy liquid separation is then divided into non-magnetic and magnetic fractions. Of the 4 fractions produced by the process only the non-magnetic heavy mineral concentrate is analyzed in most geochemical exploration programs but all fractions were analyzed in the current project. It should be noted that in using this general technique fine-grained material, particularly that of low specific gravity, is lost from the table as effluent and no reliable data are available as to the gold lost in this manner.

The panning system involves using a series of pans submerged in water, each pan producing a heavy mineral concentrate. The greater the number of pans used, the more restricted the particle size range that is concentrated by an individual pan. Three pans were used for the preparation of heavy

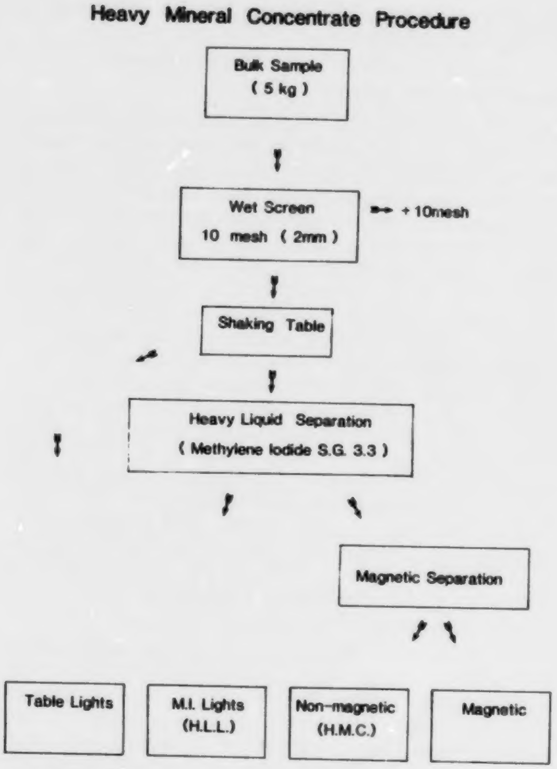

Figure 192.1. *Flow sheet for heavy mineral concentrate procedure.*

mineral concentrates for this project with the corresponding particle size fractions being: minus 2000 plus 500 µm, minus 500 plus 125 µm, and minus 125 µm. The concentrate from each pan was further processed by heavy liquids. To determine the amount of gold lost by using methylene iodide (S.G. = 3.3) the concentrates were also treated with a somewhat lower specific gravity liquid-tetrabromoethane (S.G. = 2.9). This procedure separated the samples into 4 fractions:

1. heavy mineral concentrate (S.G. >3.3)
2. intermediate heavy mineral concentrate (S.G. >2.9 and <3.3)
3. light fraction (S.G. <2.9)
4. material in suspension

The minus 63 µm or silt- and clay-sized fraction was sieved from selected samples to investigate the usefulness of the gold content of this fraction as an indicator of mineralization.

A cyclosizer was employed to classify the minus 63 µm fraction into hydraulically equivalent fractions. The cyclosizer consists of a series of 5 inverted cyclones through which water will pass and a series of interconnecting pipes through which water progressively increases in velocity due to a decrease in the diameter of the interconnecting piping from the first to the last cyclone. The increase in velocity causes material with progressively lower hydraulic equivalence to be captured in the top of each succeeding cyclone. The size of the particles captured in each cyclone is based on hydraulic equivalence related to specific gravity and shape.

ANALYSIS

All samples were analyzed by instrumental neutron activation analysis (INAA) carried out by Nuclear Activation Services, Hamilton, Ontario. The technique offers the advantage that it is non-destructive and therefore a sample may be stored for future reference.

ASPECTS CONSIDERED

To gain an understanding of the relevance of several aspects to the overall problem, a series of tests have been carried out by examining:

1. grain size analyses of bulk till samples, to establish the grain size distribution
2. grain size analyses of heavy mineral concentrates, to establish the grain size distribution of the heavy mineral concentrates and were compared with the grain size distribution of the bulk till samples
3. the gold content of the non-magnetic heavy mineral fractions and other fractions of the heavy mineral concentrate procedure, to establish the extent of gold concentration in the heavy mineral concentrates
4. the mode of occurrence of gold in different components of the heavy mineral procedure
5. the size distribution of gold in different size fractions in various components of the heavy mineral concentrate procedure
6. the absolute content of gold in different fractions
7. the variations in the concentration and contained gold in heavy mineral concentrates prepared by different laboratories
8. the distribution of gold within the silt- and clay-sized fraction of the till associated with mineralization
9. a comparison of dispersion associated with heavy mineral concentrates and the silt- and clay-sized fraction

RESULTS

Results relating to investigations on bulk till samples are described first, followed by data on heavy mineral concentrates prepared by gravity tabling, followed by information on heavy mineral concentrates prepared by wet panning, and finally information on gold distribution in the silt- and clay-sized fractions is given.

TILLS

Grain Size Analysis of Tills

The grain size distribution of till samples from the Owl Creek and Hemlo Deposits, and the Green Lake Occurrence; show that the silt- and clay-sized fraction (minus 63 µm) constitutes between 20% and 50% of the sample (Figure 192.2).

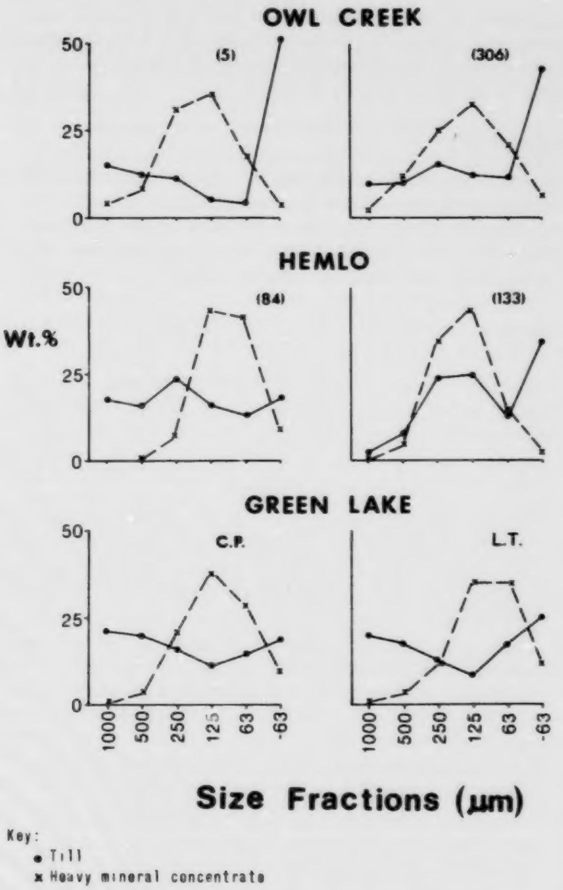

Figure 192.2. Comparison of grain size distribution of till and heavy mineral concentrates.

HEAVY MINERAL CONCENTRATES (GRAVITY TABLES)

Grain Size Distribution

Grain size analysis of heavy mineral concentrates indicates a consistent majority of material in the minus 500 plus 63 µm fraction (Figure 192.2) with <10% in the minus 63 µm fraction. This systematic difference between the grain size composition of the till samples and equivalent heavy mineral concentrate indicates that the heavy mineral concentrate is not quantitatively representative of all size fractions of the original till, and is in fact biased towards the intermediate size fractions.

Gold Concentration

Considering the contrast between the non-magnetic heavy mineral fraction and the heavy liquid light fraction, a pronounced preferential concentration of gold occurs in the heavy mineral concentrate (Table 192.1). Contrasts between the concentrations of the non-magnetic heavy mineral (HMC) and heavy liquid light (HLL) fraction vary in the range 33- to 105-fold, indicating a marked enrichment of gold in the heavy mineral concentrate.

Separation Efficiency

The efficiency of the heavy mineral concentrating procedure for concentrating the gold in the heavy mineral concentrate according to grain size can be assessed by comparing the gold content of equivalent size fractions of the non-magnetic heavy mineral fraction and the heavy liquid light fraction. The heavy liquid separation of the table concentrate is very effective in the intermediate to coarse fraction but appears inefficient in the finest fraction (minus 63 µm) as comparable gold contents are apparent in the non-magnetic heavy and heavy liquid light fractions (Figure 192.3). In contrast, sample #306 (a loosely compacted, silty, oxidized till) shows poor separation with >1000 ppb of Au remaining in most size fractions of the heavy liquid lights. The study was extended to tills from the Hemlo Deposit and the Green Lake occurrence. Anomalous gold is still present in the heavy liquid lights of the oxidized till samples from Hemlo and Green Lake but not in the unoxidized till sample from Green Lake. The efficiency of the heavy liquid separation of tills even within a deposit type appears variable.

The existence of significant gold concentrations in the heavy liquid light fraction as indicated in the case of sample #306 (Figure 192.3) was a point of some concern. Mineralogical examination of the heavy liquid light fraction and equivalent non-magnetic heavy mineral fraction has indicated that the gold occurs as free gold of the same size and morphology in both fractions. However, at this stage it is not known whether free gold accounts for all the gold in the heavy liquid light fraction. The fact that similar gold concentrations are found in both the heavy liquid lights and the table lights indicates the possibility that comparable gold may occur in the table lights. This feature is currently being examined but if the mineralogy of the gold is the same as the gold in the concentrate, then questions must be raised concerning the reliability of the separatory table as a concentrating method.

TABLE 192.1. VARIATIONS IN THE PARTITIONING OF GOLD BETWEEN NON-MAGNETIC HEAVY MINERAL CONCENTRATES AND HEAVY LIQUID LIGHT MINERAL FRACTIONS.

Sample Number	HMC (Au-ppb)	HLL (Au-ppb)	Contrast
5	5570	53	105
306	137060	1977	69
84	2828	86	33
133	9026	258	35

Key:
HMC - non-magnetic heavies
HLL - heavy liquid lights
Contrast - ratio of gold content of HMC to HLL

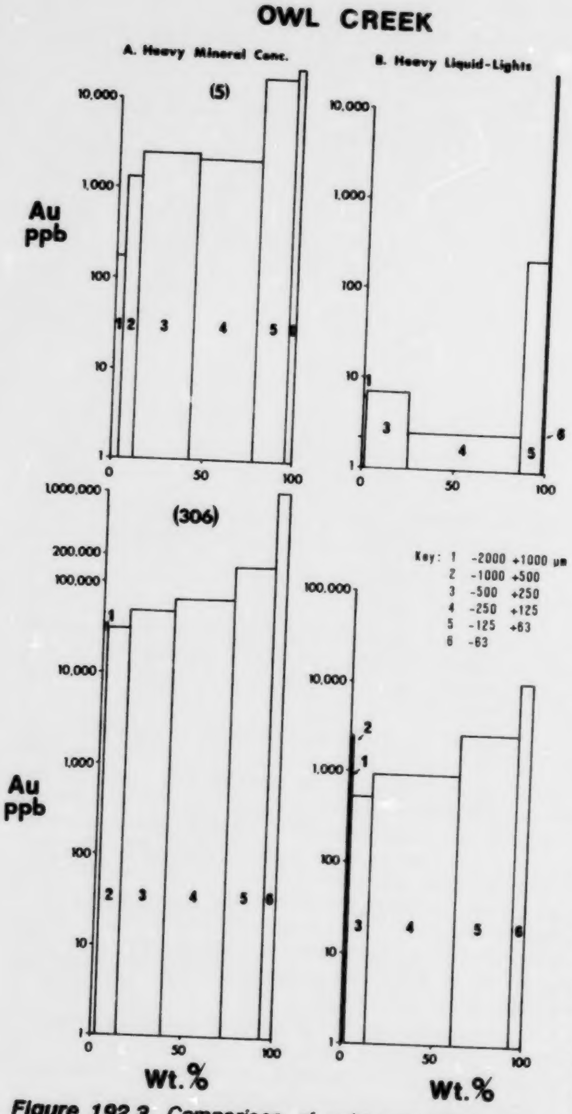

Figure 192.3. Comparison of gold contents in the non-magnetic heavy mineral concentrate and the heavy liquid light fractions of 2 tills.

Proportional Concentration of Gold in Heavy Mineral Concentrate

To determine the relationship of the amount of gold in the heavy mineral concentrate to the total gold in the original sample, neglecting that lost in the effluent, the gold contained in the non-magnetic heavy mineral concentrate was compared to the total of the original sample based on the combined gold contained in the non-magnetic and magnetic content of the heavy mineral concentrates, the heavy liquid lights, and the table lights fractions. The proportion of gold in the non-magnetic heavy mineral concentrate as a percentage of the total gold in the original sample is <15%, indicating that the vast majority of the gold is being left in fractions other than the non-magnetic heavy mineral fraction (Figure 192.4).

An additional feature is that the proportion of the gold being recovered in the non-magnetic heavy mineral fraction varies between 4% and 15% of the total indicating that it bears a variable relationship to the total gold of the original sample.

Size Analyses

In considering the proportion of gold in different size fractions, it is necessary to determine the weight of gold for each fraction on the basis of the weight and gold concentration of the fraction. Greater than 90% of the gold present in the non-magnetic heavy mineral fraction occurs in the minus 500 µm fraction with the majority of the gold in the minus 125 µm fraction (Figure 192.5). Although the majority of the gold in the heavy mineral concentrates is found in the finer fractions based on the analysis of bulk minus 63 µm fractions of the samples, the amount of gold present in the minus 63 µm fraction of the heavy mineral concentrates represents only 6 ±5% of the total gold in the minus 63 µm fraction of the original sample. This feature emphasises the fundamental limitation of the separatory table for separating fine-grained material, Wang and Poling (1983) Figure 192.6. This is a serious limitation of the separatory table when, as in this case, the majority of the fine-grained gold occurs in size fractions only partially recoverable by the table.

INTER-LABORATORY COMPARISON

Separation Efficiency

In order to assess the possible extent of variations in the gold contents of heavy mineral concentrates prepared by laboratories using essentially the same concentrating procedure (e.g. the use of wetting agents, repeated tabling and table operating conditions), 2 samples were sent to 3 laboratories. The concentration of gold in sample #5 recovered by Laboratory 3 is 54- and 26-fold higher than Laboratories 1 and 2 respectively (Table 192.2). Common practice involves evaluating gold data on the basis of concentration of gold in the heavy mineral concentrate, thus the order of decreasing economic significance would be in the order of Laboratories 3, 2, and 1. However, considering the weight of heavy mineral fractions recovered by the different laboratories and the concentrations of gold in the heavy mineral concentrates, the absolute amount of gold expressed in nanograms ($\eta g = 10^{-9}g$) recovered by the Laboratory 3 is 33- and 52-fold higher than Laboratories 1 and 2 respectively. It should be noted that although the concentration of gold recovered by Laboratory 1 is approximately half that of Laboratory 2, the actual weight of gold recovered by the 2 Laboratories is comparable. Smaller scale variations are noted in the case of sample #306. Intuitively one might expect consideration of the absolute amount of gold present in a sample would be a more reliable indicator of mineralization than the concentration of gold in the concentrate in view of varying degrees of concentration.

In order to examine these features further, approximately 10 kg of 2 samples were homogenized

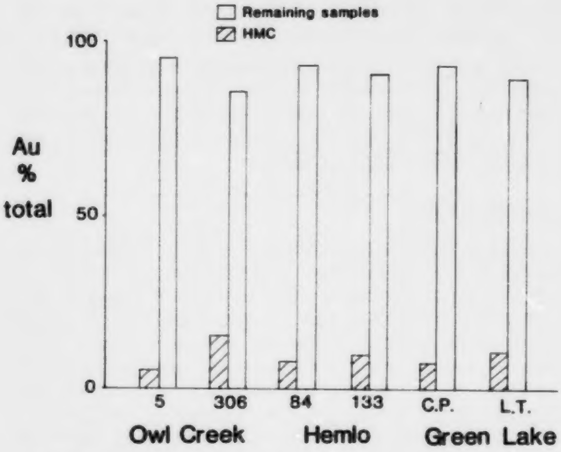

***Figure 192.4.** Partitioning of gold between heavy mineral concentrate and bulk sample.*

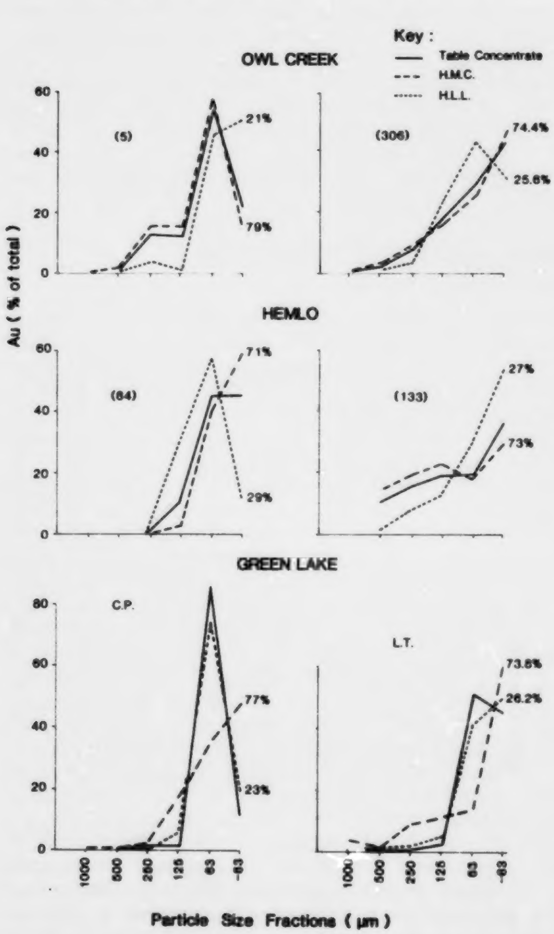

***Figure 192.5.** Variation of gold content with grain size of heavy mineral concentrate.*

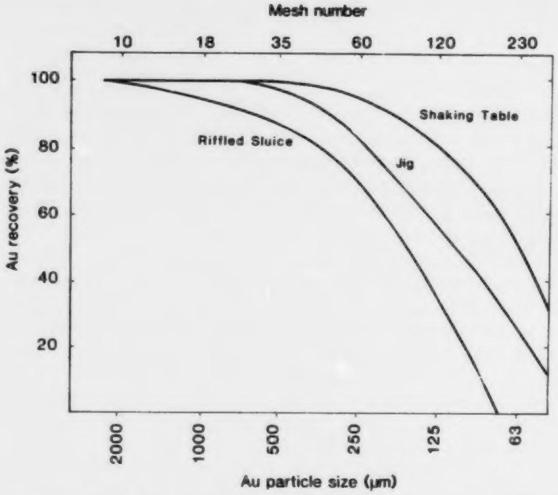

***Figure 192.6.** Recovery of different size gold particles by gravity devices (after Wang and Poling 1983).*

by coning and quartering to reduce the risk that any of the above differences could be due to sample heterogeneity, and then 5 kg sub-samples were sent to Laboratories 2 and 3.

Analyses of the heavy mineral concentrates produced by the 2 laboratories show over a 30-fold variation in both the concentration of gold in the heavy mineral concentrates and the absolute weight of gold recovered, in sample #5, but generally equivalent values in sample #223 (Table 192.3). In the case of both samples; Laboratory 3 collects more gold in the concentrate (expressed as ηg of Au per 5 kg); for example from sample #5, Laboratory 3 recovers 209 479 ηg compared to 6655 ηg by Laboratory 2; while in the case of sample #223, 149 679 ηg compared to 103 714 ηg.

Considering the total amount of gold present in the original sample, less that lost in the effluent, on the basis of gold recovered in the individual fractions (non-magnetic heavies, magnetic heavies, heavy liquid lights and table lights) and the weight of these fractions, a 7-fold variation in the total gold exists between Laboratories 2 and 3 in the case of sample #5. This suggests a loss of gold in the table effluent by Laboratory 2. To a lesser degree, for sample #223, more gold is also contained in the original sample processed by Laboratory 3.

Size Analyses

Considering the distribution of gold in different size fractions of the heavy mineral concentrate, the majority of the gold in the heavy mineral concentrates of samples #5 and #223 from Laboratory 2 is found in the minus 125 µm size fraction whereas the majority of the gold present in the concentrates from Laboratory 3 is found in the minus 500 plus 250 µm fraction, Figure 192.7. In both cases, sample #5 and #223, there are considerable differences in the size of gold being recovered by the 2 laboratories.

TABLE 192.2. COMPARISON OF GOLD CONTENTS OF HEAVY MINERAL CONCENTRATES OF TWO SAMPLES PREPARED BY THREE LABORATORIES.

		Lab 1	Lab 2	Lab 3
Au in HMC of sample #5	Conc'n (ppb)	2,657	5,570	143,337
	Wt. (g)	7.1	2.9	4.4
	Wt. (ηg)	18,853	16,153	626,044
Au in HMC of sample #306	Conc'n (ppb)	77,598	137,060	258,018
	Wt. (g)	9.9	11.2	1.9
	Wt.(ηg)	765,706	1,535,072	493,793

TABLE 192.3. COMPARISON OF GOLD CONTENTS OF VARIOUS FRACTIONS OF THE HEAVY MINERAL CONCENTRATING PROCEDURE ON TWO SAMPLES PREPARED BY TWO LABORATORIES.

			Sample #5 Laboratory		Sample #223 Laboratory	
			2	3	2	3
Au	HMC	(ppb)	2,175	69,135	19,945	29,177
		(ηg)	6,655	209,479	103,714	149,679
	HLL	(ppb)	19	42	667	1,068
		(ηg)	540	1,625	15,465	24,751
Total Au*			82,200	583,315	1,232,817	1,404,440
$\frac{\text{Au HLL}}{\text{Au HLL + HMC}}$ %			8	0.8	15	16.5
Wt. of HMC (grams)			3.06	3.03	5.20	5.13
Wt.(ηg) Au in -63μm fraction of HMC			3,200	4,433	31,957	32,189
% of total Au in HMC			48	2	31	22
Wt.(ηg) Au -500 + 250μm fraction of HMC			1,477	167,164	11,870	63,863
% of total Au in HMC			22	80	12	43

*The total gold in the original sample is calculated based on analyses of all fractions returned by the laboratory.

Consideration of the absolute amounts of gold in the minus 63 μm fraction of the heavy mineral concentrates produced by different laboratories is broadly similar, Table 192.3. However, the amount of gold in the minus 500 plus 250 μm fraction of the concentrates between laboratories is quite different with Laboratory 3 recovering a considerably higher amount of gold in this size fraction than Laboratory 2. This discrepancy cannot be explained by the nugget effect in the minus 500 plus 250 μm fraction because the same pattern is noted in the heavy liquid light fraction of both samples. The reason for this variation in recovery size range is not understood. Possible explanations may be the variations in the mineralogy or morphology of the gold-bearing material being recovered. However, an ongoing investigation at Queen's University is examining the reasons for the discrepancy.

The weight of heavy minerals recovered by Laboratory 2 and 3 is the same (Table 192.3) which may suggest that the original samples were homogeneous in so far as the majority of the heavy mineral concentrate is composed of non-gold-bearing material. The difference in the amount and size distribution of gold recovered indicates that the gold in the sample

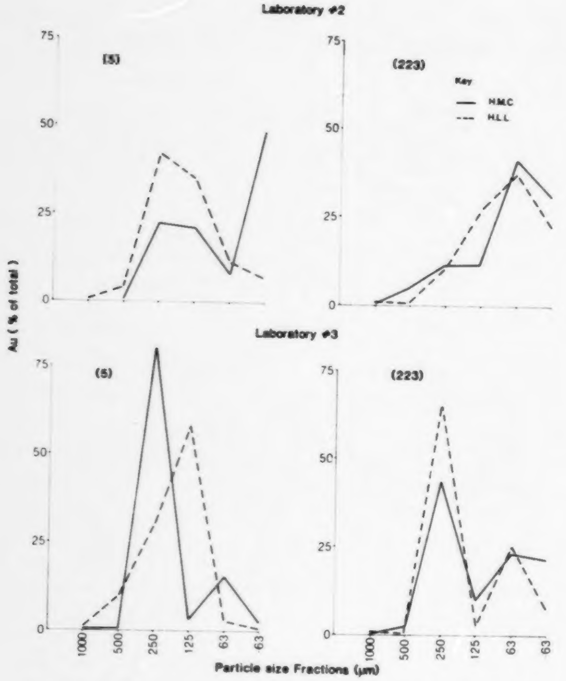

Figure 192.7. Variation of gold content with size fraction of heavy mineral concentrates between laboratories.

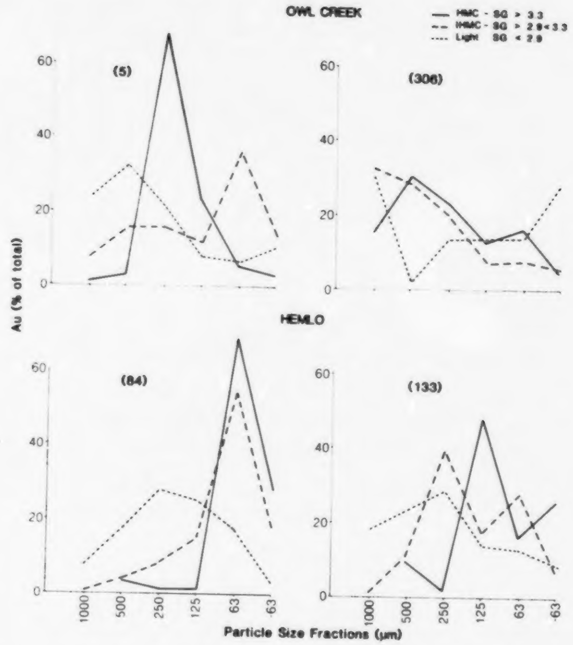

Figure 192.8. Variation of gold content with grain size in various fractions from panning concentration.

TABLE 192.4. GOLD CONTENT IN VARIOUS FRACTIONS OF HEAVY MINERAL CONCENTRATING PROCEDURE INVOLVING PANNING. (VALUES BASED ON 5 KG OF MINUS 2 MM.)

		Owl Creek		Hemlo	
		#5	#306	#84	#133
Au in HMC	Conc'n (ppb)	8,651	52,451	1,574	7,346
	Wt.(ηg)	72,666	2,376,042	6,847	147,645
	% of total Au	3.6	30.4	1.4	11.0
Au in Intermediate HMC	Conc'n (ppb)	44	3,810	85	547
	Wt.(ηg)	1,043	459,065	4,628	96,514
	% of total Au	0.1	5.9	1.0	7.2
Au in Light Mineral Fraction	Wt.(ηg)	4,225	1,991,659	236,650	756,775
	% of total Au	0.2	26.0	47.0	56.3
Au in Suspension	Wt.(ηg)	1,948,804	2,995,036	256,756	342,589
	% of total Au	96.2	37.7	50.6	25.5
Total Au in the sample (ηg)		2,026,740	7,821,802	504,881	1,343,523
Wt.of HMC (grams)		8.4	45.3	4.3	20.1

is acting differently from the rest of the heavy minerals during the concentrating process.

In conclusion, the different amounts and size of gold-bearing particles recovered by the 2 laboratories suggest different behaviour of gold-bearing particles in the concentrating procedure adopted by the 2 laboratories. In the tabling procedure up to 45% of the sample is lost as effluent, thus the "total" gold contents calculated for the tabling procedures may be grossly underestimated in view of the observation that the majority of the gold in tills occurs in the fines.

HEAVY MINERAL CONCENTRATES (PANNING)

The testing of 2 different laboratories using gravity table separations produced widely different results in terms of gold concentrations in the sample (ppb), total contained gold (ηg), and size range of the gold recovered. For further comparison, 4 samples were sent to Laboratory 4 which adopts the wet panning separatory system in which little material is lost. In contrast to the loss of up to 45% of the sample as effluent by the traditional tabling procedures, the wet panning procedure collected 90% to 99% of the original sample. The total gold content of the original sample can be determined by a summation based on the weight and gold content of each fraction.

Partitioning of Gold

As discussed previously, the concentration of gold in the different fractions of a sample is quite variable, and evaluating data based only on the concentration of gold can be misleading. For example, the concentrations of the heavy mineral concentrate fractions of samples #5 and #133 are 8651 and 7346 ppb of Au, respectively, which might be considered to be of equivalent exploration significance (Table 192.4). However, considering the more than 2-fold greater heavy mineral concentrate of sample #133 compared to sample #5, the total gold in sample #133 is some 2-fold higher than sample #5, and therefore, presumably of greater economic significance. Therefore, to eliminate the effect of the dilution of the gold by the heavy minerals all further discussion of results will be restricted to the absolute amount of gold present in the various fractions unless specifically stated to be otherwise.

The amount of gold collected in the heavy mineral concentrates (S.G. >3.3) obtained from the 4 samples ranges from 1.4% to 30.4% of the total gold while in the intermediate heavy mineral concentrates the amount of gold ranges from 0.1% to 7.2% of the total gold in the original sample. The amount of gold in the intermediate fraction of sample #5 is insignificant but for samples #306, #84, and #133, the amount of gold is considerable with similar amounts of gold in the intermediate and heavy mineral fractions of samples #84 and #133. Therefore, these results suggest that tetrabromoethane is useful for recovering gold held in minerals of lower specific gravity.

It must also be noted that the material remaining in suspension contains a large amount of gold; in the case of sample #5, the gold in suspension represents 96% of the total gold in the original sample. This further substantiates the need to retain all material at the sampling stage as well as at the processing stage in order to determine the true gold content of the original sample, and possibly lead to a more reliable assessment of an area. It should be noted that the total gold recovered in sample #5, 2026.740 ηg, by Laboratory 4 using the wet panning process (Table 192.4) is 24- and 3.5-fold higher than the total gold recovered by Laboratories 2 and 3 using the gravity table (Table 192.3).

Size Analyses

The distribution of the gold in the different size fractions of the various separatory fractions is variable, Figure 192.8. In the case of sample #5, the majority of the gold is in the minus 500 plus 125 μm fraction of the heavy mineral concentrate (S.G. >2.9 <3.3) and present in the minus 1000 plus 250 μm fraction of the light material. The variable distribution of the gold between different fractions is also apparent in the other 3 samples. The fact that gold may occur in a variety of mineralogical forms and that native gold may occur in a variety of shapes may account for the different distribution patterns observed.

COMPARISON OF GOLD RECOVERY USING DIFFERENT TECHNIQUES

In order to place the characteristics of different concentrating procedures on a firmer basis, data on 4 samples processed by Laboratories 2 and 4 are now considered.

The concentration of gold in the non-magnetic heavy mineral concentrate shows up to a 2.6-fold variation (e.g. sample #306), and up to a 4-fold difference when expressed as the total contained gold of the heavy mineral fraction (sample #5, Table 192.5). A comparison of the total contained gold shows reasonable agreement for samples #306, #84, and #133. However, a 6.5-fold difference exist for sample #5. It is conceivable that these differences could be explained by the heterogeneity of the samples. In the case of sample #306, Laboratory 4 collects greater than 2.5 times more gold in terms of a percentage of the total gold while for sample #84 the reverse is true with Laboratory 2 collecting a percentage that is 3 times greater.

A more detailed examination of the gold distribution within the size fractions of the heavy mineral concentrate shows that Laboratory 4 generally collects a higher proportion of gold in the plus 250 μm fraction than Laboratory 2 (Figure 192.9). On the other hand, Laboratory 2 collects at least an equal amount of gold in the minus 63 μm size fraction of the concentrates with up to 7 times more gold in sample #306. In all cases, Laboratory 4 produced a greater weight of heavy mineral concentrate from the same initial sample weight. The discrepancies may be due to the fact that each technique is most efficient at concentrating gold which occurs in a specific size range and mineralogy or due to the heterogeneity of the samples.

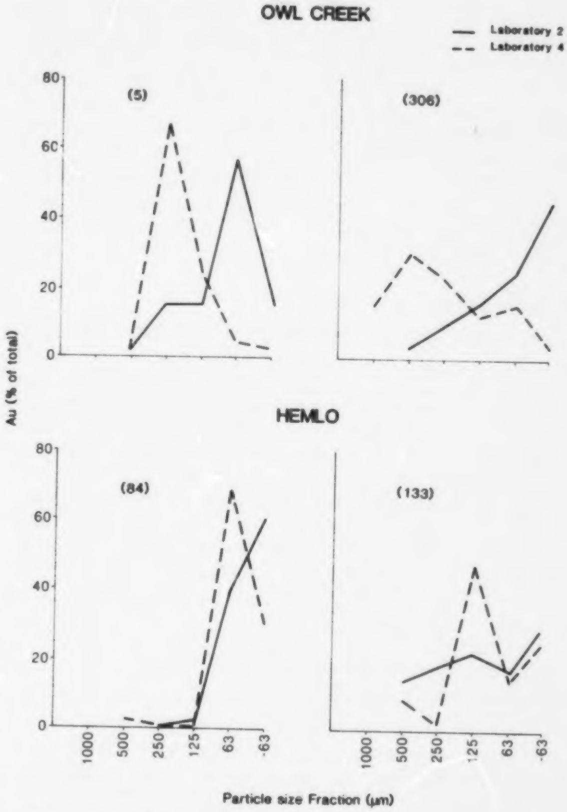

Figure 192.9. Comparison of variation in grain size of gold in heavy mineral concentrates prepared by 2 laboratories.

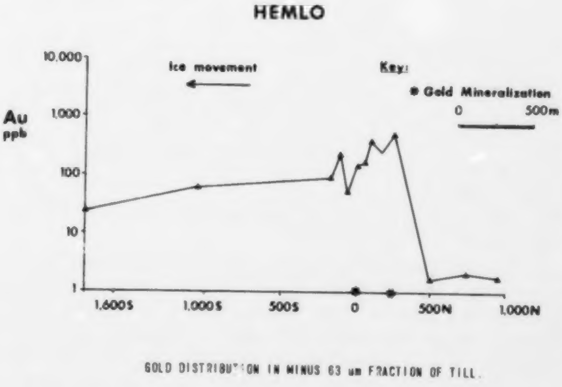

Figure 192.10. Gold distribution in the minus 63 μm fraction of till associated with mineralization at Hemlo.

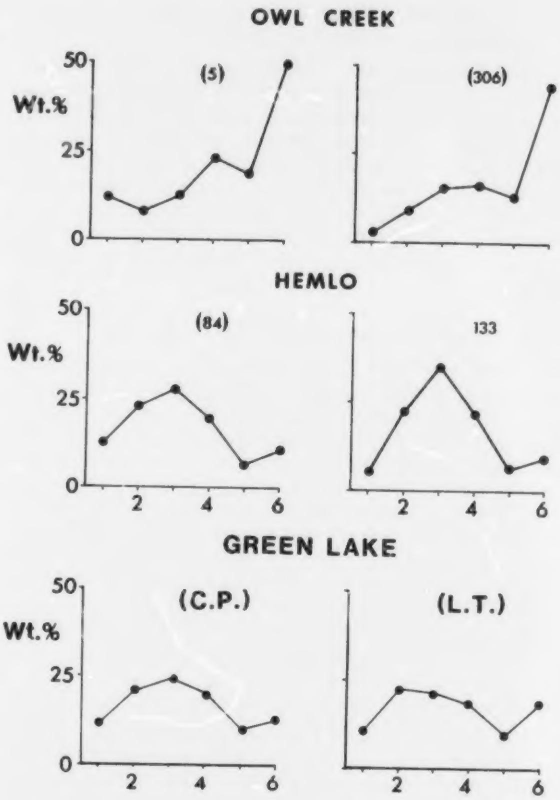

Key:	1	2	3	4	5	6
Quartz	44	33	22	14	11 um	Effluent
Gold	21	16	10	7	5 um	Effluent

Figure 192.11. Distribution of hydraulically equivalent fractions within the minus 63 μm fraction of tills.

SILT AND CLAY FRACTION

In view of the recognized occurrences of the majority of the gold in the minus 125 plus 63 μm fraction or the minus 63 μm fraction of tills, it was considered possible that anomalous gold concentrations might be detectable by the direct analyses of the minus 63 μm fraction of tills. Analyses of the minus 63 μm fraction of till associated with mineralization at the Hemlo Deposit shows clearly defined anomalous gold contents overlying mineralization at 1600 feet and down-ice from mineralization (Figure 192.10).

A comparison of the relative proportion of the different hydraulically equivalent fractions within the minus 63 μm fraction of tills indicates that at the Owl Creek Deposit there is a majority of finer particles with lowest hydraulic equivalence while at the Hemlo Deposit, and to a lesser extent the Green Lake Occurrence, the majority of particles are of intermediate hydraulic equivalence (Figure 192.11).

Considering the distribution of gold within the different hydraulically equivalent fraction it is appar-

TABLE 192.5. COMPARISON OF GOLD RECOVERED IN NON-MAGNETIC HEAVY MINERAL FRACTION PREPARED BY LABORATORY 2 AND 4. (VALUES BASED ON 5 KG OF MINUS 2 MM.)

	Lab	#5	#306	#84	#133
Au in HMC (ppb)	2	5,570	137,060	2,900	6,524
	4	8,651	52,451	1,574	7,346
Wt. of the HMC (g)	2	2.9	11.20	6.74	16.30
	4	8.40	45.30	4.35	20.10
Wt. of Au in HMC (ηg)	2	16,153	1,535,072	19,574	106,341
	4	72,666	2,376,042	6,847	147,645
Total Au (ηg)	2	310,795	11,335,581	449,935	1,332,330
	4	2,026,740	7,821,802	504,881	1,343,523
Au in HMC as % of total Au	2	4.0	13.2	4.4	8.0
	4	3.6	30.4	1.4	11.0
Conc'n of Au in original sample (ppb)*	2	2.4	300	3.9	21.3
	4	14.5	475	1.4	29.5

*The concentration of gold in the original sample is based on the premise that all the gold has been extracted into the HMC.

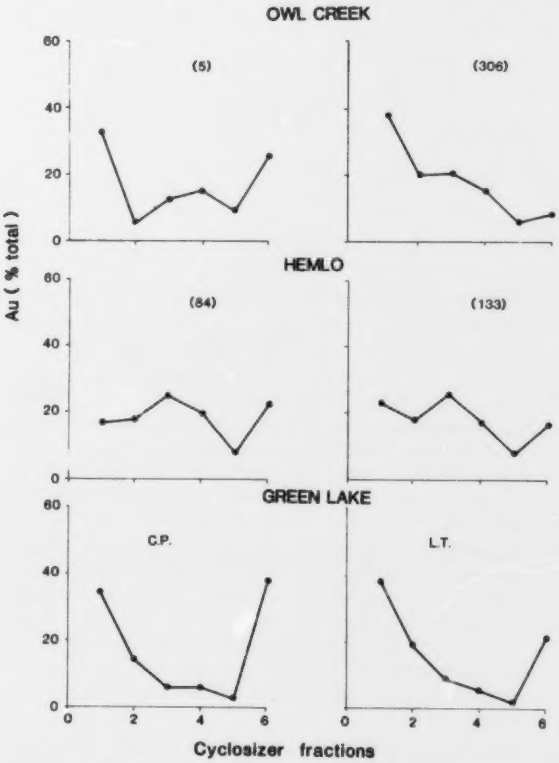

Figure 192.12. *Distribution of gold in hydraulically equivalent fractions of minus 63 μm fraction of tills.*

ent that the distribution is similar for tills from the same deposit but variable when comparing tills from different deposits (Figure 192.12). A bimodal distribution of the gold is present in the Owl Creek Deposit and Green Lake Occurrence samples with the greatest proportions of gold in the fractions with highest and lowest hydraulic equivalence. In the Hemlo samples the gold is evenly distributed throughout the minus 63 μm fraction of the tills except in the 5 to 7 μm range where little gold is present. This variation in the size of the gold within the minus 63 μm fraction indicates that the size of a representative sample will vary from deposit to deposit.

Comparison of the Silt and Clay Fraction to the Heavy Mineral Concentrates

Sonic core samples taken down-ice from the Owl Creek Deposit were made available to the project by Kidd Creek Mines Limited. The minus 63 μm fraction of each sample was analyzed and the results are compared to the heavy mineral data (courtesy of Kidd Creek Mines Limited) on Figure 192.13. The minus 63 μm gold data and the heavy mineral concentrate data show similar patterns. The existence of comparable responses in the heavy mineral concentrate and the minus 63 μm fraction of till is a further indication of the usefulness of analyses of the fine fraction in identifying mineralization. In this instance, the information provided by the gold distribution in the minus 63 μm fraction is no different from that of the non-magnetic heavy mineral fraction. However, if fine-grained gold deposits occurred in an area and the gold was liberated in the till, these deposits would have a small chance of detection on the basis of heavy mineral concentrate analysis but would be more amenable to detection by analysis of the minus 63 μm fraction.

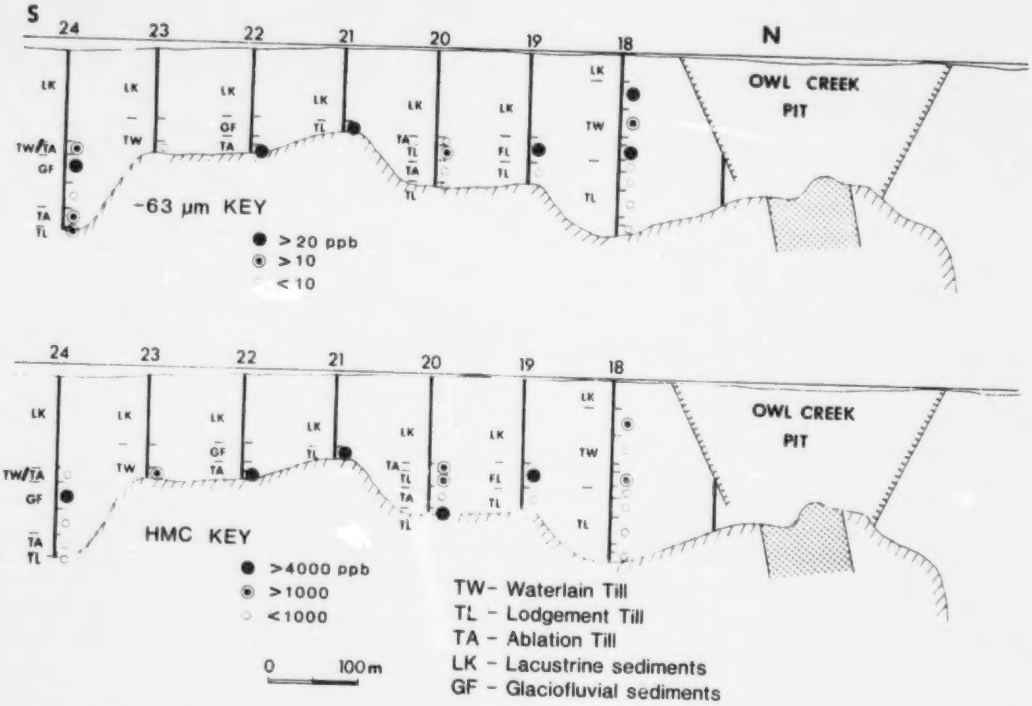

Figure 192.13. *Comparison of gold distribution in heavy mineral concentrates and minus 63 µm fraction of till from Owl Creek.*

CONCLUSIONS

To date, work undertaken has been based on a relatively small number of samples but the consistency of the results allows some preliminary conclusions to be drawn:

1. Till samples contain from 20% to 50% of silt- and clay-sized material.
2. Heavy mineral concentrates are biased towards recovering the minus 500 plus 63 µm fractions and include only an insignificant proportion of silt- and clay-sized material.
3. The non-magnetic heavy mineral concentrates show a marked enhancement of gold content relative to the light mineral fraction.
4. The extent to which gold particles are preferentially enriched in the heavy mineral concentrate tends to decrease with decreasing particle size.
5. In certain instances significant concentrations of gold remain in the light mineral fractions.
6. The proportion of total gold content concentrated in the heavy mineral fraction varies in the range 4% to 15%.
7. The majority of gold in heavy mineral concentrates occurs in the minus 125 µm fraction where there is a marked reduction in the recovery efficiency of the gravity table.
8. Inter-laboratory comparisons display marked variations in the concentration of gold in the heavy mineral concentrates, the weight of the heavy mineral concentrates, and thus the absolute weight of gold recovered in the heavy mineral concentrates.
9. Comparisons of the grain size distribution of gold in heavy mineral concentrates indicates in some cases marked variation between laboratories.
10. A heavy mineral concentrating procedure involving a closed system of wet panning and heavy liquid separation indicates that significant proportions of the total gold in a sample occur in the intermediate heavy mineral fraction (S.G. >2.9 <3.3) and a major proportion in the light mineral fraction.
11. Notwithstanding the limitations of gold exploration based on heavy mineral concentrate analyses, heavy mineral concentrates can provide unique information on the type of source mineralization, and distance of transport based on a consideration of the mineralogy of the heavy mineral concentrate and shape of the gold grains.
12. Anomalous gold contents occur in the silt- and clay-sized fraction of tills associated with both the Owl Creek and Hemlo Deposits.
13. The distribution of gold in hydraulically equivalent fractions of the minus 63 µm portion of the sample varies with deposit type.
14. Comparison of gold dispersion in the non-magnetic heavy mineral fraction and the minus 63 µm fraction of tills associated with the Owl Creek Deposit shows very comparable dispersion trains.

15. The analyses of the silt- and clay-sized fraction, however, is also suited to the detection of fine-grained gold deposits that are not amenable to detection on the basis of heavy mineral concentrate analyses.
16. Analyses of silt- and clay-sized fractions reduce the sample representivity problems associated with analyzing coarser fractions.
17. It may be concluded that the minus 63 μm fraction and the heavy mineral concentrate analyses provide different information for a diversity of exploration targets and surface environments. Exploration reliability can be increased by analyzing both the silt- and clay-sized fraction and the heavy mineral concentrate.

FUTURE WORK

Future work will be directed towards:

1. substantiating the validity of the preliminary results by analyzing more samples from more deposit types and with varying spatial relationship to mineralization
2. investigating the mineralogical mode of occurrence of gold in silt-sized fractions
3. examining the representivity of samples collected by a variety of drilling systems and ways of improving the representivity of samples collected from different systems
4. examining ways of improving the reliability that can be attached to gold analyses of heavy mineral concentrates
5. identifying an exploration methodology that will improve the overall effectiveness of geochemical exploration applied to gold exploration.

ACKNOWLEDGMENTS

In addition to the Ontario Geoscience Research Fund, assistance for this investigation was provided by Cominco Limited, Exxon Minerals Corporation, Inco Limited, Kidd Creek Mines Limited, Lac Minerals Limited, Noranda Explorations Limited, Placer Development Limited, and Teck Explorations Limited and is greatly appreciated. In particular we would like to thank Dr. Eric Hoffman of Nuclear Activation Services for contributing the analytical data.

REFERENCES

Averill, S.A., and Zimmerman, J.R.
1984: The Riddle Resolved: The Discovery of the Partridge Gold Zone Using Sonic Drilling in Glacial Overburden at Waddy Lake, Saskatchewan; *in* 86th Annual General Meeting, Ottawa, April 15-19, 1984, Canadian Institution of Mining and Metallurgy.

Bird, D.J., and Coker, W.B.
1985: Quaternary Stratigraphy and Geochemistry at the Owl Creek Gold Mine, Timmins, Ontario (Abstract); *in* 11th International Geochemical Exploration Symposium, Toronto, April 28 to May 1, 1985, Abstracts, Association of Exploration Geochemists.

Closs, L.G., and Sado, E.V.
1979: Geochemical Drift Prospecting Studies Near Gold Mineralization, Beardmore-Geraldton Area, Northwest Ontario, Canada; p.459-477 *in* Geochemical Exploration, 1978, edited by J.R. Watterson and P.K. Theobald, Association of Engineering Geologists.

Gray, R.S.
1983: Overburden Drilling as a Tool for Gold Exploration; *in* 85th Annual General Meeting, Winnipeg, April 17-20, 1983, Canadian Institution of Mining and Metallurgy.

Sauerbrei, J.A., Pattison, E.F., and Averill, S.A.
1985: Till Sampling in the Case Berardi Area, Quebec: A Case History in Orientation and Discovery (Abstract); *in* 11th International Geochemical Exploration Symposium, Toronto, April 28 to May 1, 1985, Abstracts, Association of Exploration Geochemists.

Shelp, G.S., and Nichol, I.
1985: Dispersion of Gold in Glacial Till Associated with Gold Mineralization in the Canadian Shield (Abstract); *in* 11th International Geochemical Exploration Symposium, Toronto, April 28 to May 1, 1985, Abstracts, Association of Exploration Geochemists.

Thomson, I., Burns, J.G., and Faulkner, F.H.
1985: Gold Exploration in Deep Glaciated Overburden: Experiences from the Belore Case History (Abstract); *in* 11th International Geochemical Exploration Symposium, Toronto, April 28 to May 1, 1985, Abstracts, Association of Exploration Geochemists.

Wang, W., and Poling, G.W.
1983: Methods for Recovering Fine Placer Gold; Bulletin, Canadian Institute of Mining and Metallurgy, Volume 76, Number 860, p.47-56.

Grant 193 The Geological Setting and Genesis of the Cameron Lake Gold Deposit

D.R. Melling[1], **D.H. Watkinson**[1], **K.H. Poulsen**[2], **and L.B. Chorlton**[3]

[1]Ottawa-Carleton Centre for Geoscience Studies, Carleton University
[2]Economic Geology and Mineralogy Division, Geological Survey of Canada
[3]Mineral Deposits Section, Ontario Geological Survey

ABSTRACT

The Cameron Lake gold deposit, located in the Wabigoon Subprovince of the Superior Province in northwestern Ontario, is situated near the stratigraphic transition between a lower, mafic volcanic succession, and an upper mixed mafic to felsic, partly pyroclastic succession, but within the latter. The deposit is epigenetic, structurally controlled, and occurs in sheared mafic metavolcanic rocks adjacent to a sheared intrusive contact with a metagabbroic sill. The shear zone containing the deposit, here called the Cameron Lake Shear Zone, is a brittle-ductile, dextral strike-slip system with an attitude of 315/70°NE and an inferred displacement vector pitching 5°NW. It is tentatively interpreted as a splay related to the major Pipestone-Cameron Fault.

Three distinct vein types have been recognized in the carbonatized rocks of the Cameron Lake Shear Zone: a) early barren, extensional, quartz-carbonate veins which have been buckled, b) a major system of gold-bearing, pyritic, quartz-rich, breccia veins, and c) a late group of straight, *en echelon* quartz-carbonate-chlorite-hematite-gold extension veins.

The deposit is essentially of the vein type enveloped by a large, gold-bearing hydrothermal alteration zone. The characteristic alteration assemblage consists of ferroan dolomite-sericite-pyrite. The alteration is chemically expressed by the addition of major amounts of CO_2, K, Ca, and S, and minor amounts of Ag, Au, B, Hg, Rb, Sr, and W. Precipitation of pyrite at the expense of primary magnetite was related to gold mineralization.

The localization of economic quantities of gold along the Cameron Lake Shear Zone is related to the development of oblique, secondary, bedding-controlled, sympathetic shear zones. At the intersection of the 2 shear systems a steeply pitching, dilatant zone was created in which ascending hydrothermal solutions precipitated gold. The shear zone intersection model serves to explain the complex subsurface geometry of the deposit, as well as the existence of hanging wall and footwall zones on either side of the main zone of gold enrichment.

INTRODUCTION

The history of gold exploration in the Kenora-Fort Frances area of northwestern Ontario dates back to the mid-1800s. Activity peaked between 1890 and 1910 when the area accounted for over 55% of Ontario's total gold production (Beard and Garrett 1976). Although the area hosts no major presently producing gold mines, optimism is again high in view of the recent "Cameron Lake Gold Rush" (Northern Miner 1983).

The Cameron Lake gold deposit is located in northwestern Ontario about 80 km south-southeast of Kenora. It was originally discovered in 1960 by 2 prospectors working for Noranda Mines (Hunter *et al.* 1984). Low gold prices at that time, coupled with a complex subsurface geometry and poor outcrop exposure, discouraged investment and development. Four separate diamond-drilling programs were conducted on the property prior to the discovery of a major gold zone in 1983 by 2 junior mining companies, Nuinsco Resources and Lockwood Petroleum. Proven reserves presently total 1 328 000 tons grading 0.16 ounce Au per ton, including 900 000 tons grading 0.20 ounce Au per ton (Nuinsco Resources Limited 1984).

Although several workers have characterized the gold occurrences in the region (Blackburn 1982; Blackburn and Janes 1983; Mackasey *et al.* 1974; Thompson 1935; Trowel *et al.* 1980), few detailed studies have focused directly on the development of descriptive and genetic models of gold emplacement in this promising region of the Superior Province. The purpose of this project is to document the possible roles of lithological, structural, and geochemical controls % gold concentration in the Cameron Lake deposit, and to evaluate their significance and implications for gold deposits in the Cameron-Rowan Lakes belt. This research should lead to an improved understanding of the factors influencing gold mineralization in the area, and a better description of their geological setting.

REGIONAL GEOLOGIC SETTING AND ITS BEARING ON GOLD MINERALIZATION

Cameron Lake lies at the western extremity of the Archean, Savant Lake-Crow Lake metavolcanic-metasedimentary belt (Trowell *et al.* 1980) in the Wabigoon Subprovince of northwestern Ontario (Figure 193.1). The region is divided geologically by the southeast-trending, northeast-dipping Pipestone-Cameron Fault (Figure 193.2). Southwest of the fault lies the north- to east-facing, Kakagi Lake greenstone terrain (KLGT) (Schwerdtner *et al.* 1979), and to the northeast the south-facing Rowan Lake greenstone terrain (RLGT). The fault is a major zone of deformation and displacement which has been defined over 100 km of strike length. Exposure of the fault in the Cameron Lake area is poor, often being obscured by lakes and low swampy depressions. Correlation of lithologies across the fault, although suspected, has not been possible to date (Trowell *et al.* 1980).

The geology of the RLGT is dominated by the Shingwak Lake Anticline. The axial surface of the fold has an east-northeast strike and the plunge is steep toward the southwest (Kaye 1973). Based on field mapping and lithogeochemical analyses, Blackburn and Hailstone (1983) have shown that the RLGT may be subdivided into the Rowan Lake and Cameron Lake Volcanics. All rocks have been

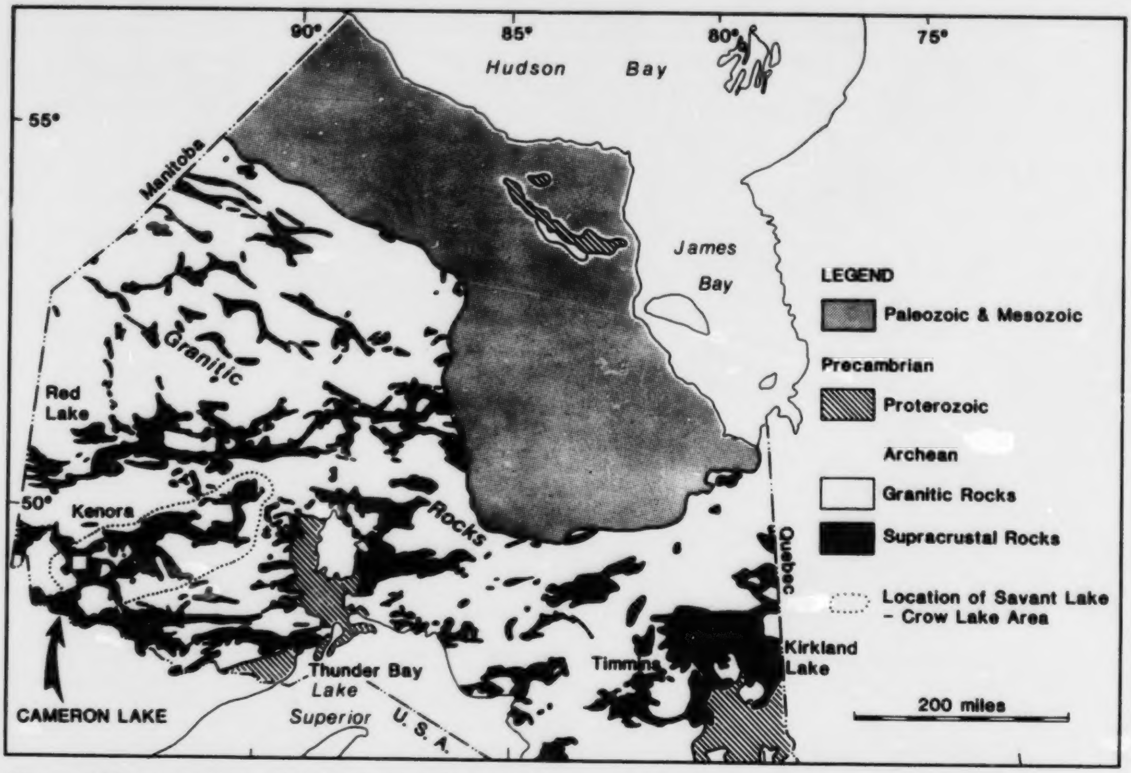

***Figure 193.1.** Location of the Cameron Lake gold deposit within the Savant Lake-Crow Lake metavolcanic-sedimentary belt and its position within Ontario (modified after Trowell et al. 1980).*

metamorphosed to greenschist facies assemblages. The Rowan Lake Volcanics form a thick, predominantly pillowed, subaqueous mafic flow succession in the core of the Shingwak Lake Anticline. These rocks are overlain by the Cameron Lake Volcanics, a mixed succession of subaqueous pillowed and massive mafic flow rocks, and intermediate to felsic pyroclastic rocks. Top determinations define a steeply dipping homocline facing southward.

Subvolcanic gabbroic sills were emplaced at all levels in the stratigraphy prior to folding. Felsic porphyry sills and dikes, and quartz monzonite stocks intrude many of the earlier strata.

Blackburn and Hailstone (1983) have shown that the lower succession (Rowan Lake Volcanics) is tholeiitic, and mainly magnesium-rich, while the upper succession (Cameron Lake Volcanics) is variable, from tholeiitic to calc-alkaline. The most significant gold occurrences within the RLGT (including the Cameron Lake Deposit) are located within the Cameron Lake Volcanics (Blackburn and Janes 1983) and tend to be associated with zones of high strain. Several of these occurrences are situated at or near gabbroic-volcanic contacts. Two such gold-bearing high strain zones, previously unnamed, are referred to here as the Cameron Lake and Monte Cristo Shear Zones. They are at present the principal targets for exploration.

LOCAL GEOLOGY OF THE CAMERON LAKE DEPOSIT

The Cameron Lake Deposit is situated on the north shore of Cameron Lake (Figure 193.2) about 700 m northwest of the present Nuinsco bush camp. The area is underlain by mafic volcanic rocks and interbedded intermediate to felsic pyroclastic rocks of the Cameron Lake Volcanics. Two subcordant gabbro sills intruded the pyroclastic units and are interpreted as subvolcanic intrusions related to large masses of mafic to ultramafic intrusive rocks to the northwest of the map area (Kaye 1973). A large concordant quartz-feldspar porphyry sill is present, as are numerous thin dikes of similar composition which are markedly discordant. Associated with the felsic pyroclastic rocks are subordinate graphitic units and epiclastic rocks.

The Cameron Lake gold deposit occurs in sheared mafic volcanic rocks adjacent to their highly deformed contact with a gabbroic sill. To date, mapping, trenching, and drilling have indicated that tuffaceous rocks and siliceous sinters (essential to syngenetic, volcanogenic exhalative, or epithermal hotspring type deposits) are not present within the host rocks of the Cameron Lake Deposit. The mafic volcanic rocks are predominantly massive and pillowed flows. The massive flows may be subdivided into fine-grained and distinctly medium- to coarse-grained

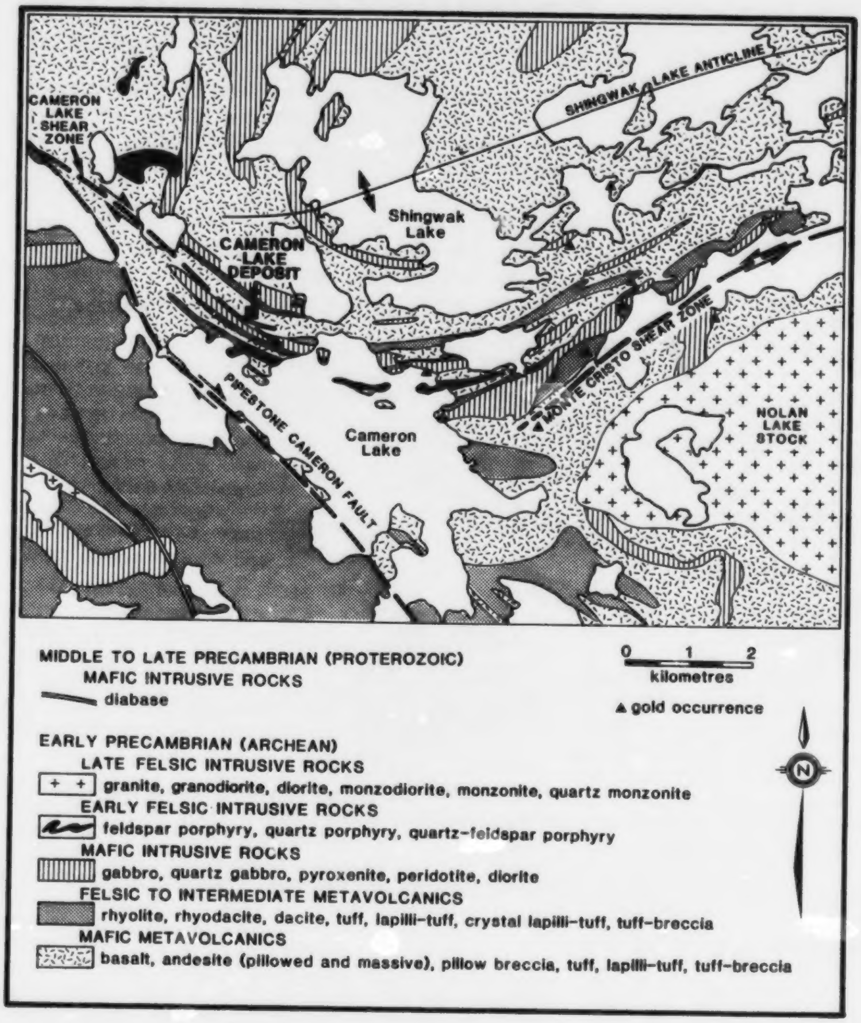
CAMERON LAKE SHEAR ZONE
SHINGWAK LAKE ANTICLINE
Shingwak Lake
CAMERON LAKE DEPOSIT
MONTE CRISTO SHEAR ZONE
NOLAN LAKE STOCK
PIPESTONE CAMERON FAULT
Cameron Lake
0 1 2
kilometres
▲ gold occurrence
N
MIDDLE TO LATE PRECAMBRIAN (PROTEROZOIC)
MAFIC INTRUSIVE ROCKS
diabase
EARLY PRECAMBRIAN (ARCHEAN)
LATE FELSIC INTRUSIVE ROCKS
granite, granodiorite, diorite, monzodiorite, monzonite, quartz monzonite
EARLY FELSIC INTRUSIVE ROCKS
feldspar porphyry, quartz porphyry, quartz-feldspar porphyry
MAFIC INTRUSIVE ROCKS
gabbro, quartz gabbro, pyroxenite, peridotite, diorite
FELSIC TO INTERMEDIATE METAVOLCANICS
rhyolite, rhyodacite, dacite, tuff, lapilli-tuff, crystal lapilli-tuff, tuff-breccia
MAFIC METAVOLCANICS
basalt, andesite (pillowed and massive), pillow breccia, tuff, lapilli-tuff, tuff-breccia

Figure 193.2. *Geology of the Cameron Lake area (modified after Kaye 1973) and the location of the Cameron Lake deposit.*

types. Minor interdigitated pillow-breccia is also present.

The gabbroic sill in the footwall of the deposit is approximately 100 m thick. It is fine- to medium-grained and locally contains small quartz megacrysts. Its contact with the mafic volcanic rocks is always sheared, carbonatized, and variably sericitized. At depth this structure is parallel to the mineralized shear zone, and located about 50 m in the footwall. Drilling data indicate that the 2 structures merge along strike and at surface.

Thin quartz-feldspar porphyry dikes, 1 cm to 3 m in thickness, intrude the mafic volcanic succession. They commonly occur within the zones of shearing and have been traced by drilling for several hundred metres along strike. They are tentatively interpreted to post-date the formation of the deposit as inferred from the apparent structural control on their orientation, and their inclusions of pervasively altered and sheared rock fragments similar in texture and mineralogy to those containing anomalous gold concentrations.

The following features were observed in an attempt to document the kinematics of the Cameron Lake Shear Zone:

1. passive bedding markers curved into the plane of the shear zone
2. minor active Z-folds developed on the foliation
3. syntectonic, extensional, *en echelon* vein arrays oriented obliquely to the shear zone
4. buckled non-passive markers

All of these features suggest a dextral component of displacement but quantitative estimates of throw on the Cameron Lake Shear Zone are unavailable. Aspect ratios of pillows within zones of high strain are always less than 10:1 and the early veins are rarely dismembered so that displacements probably did not exceed more than a few hundred metres.

The shear zone hosting the Cameron Lake gold deposit has an attitude of 315/70°N, a minimum strike length of over 1000 m and width from 11 to 60 m. Two planar fabrics are locally present within the zones of high strain; a cleavage parallel to the

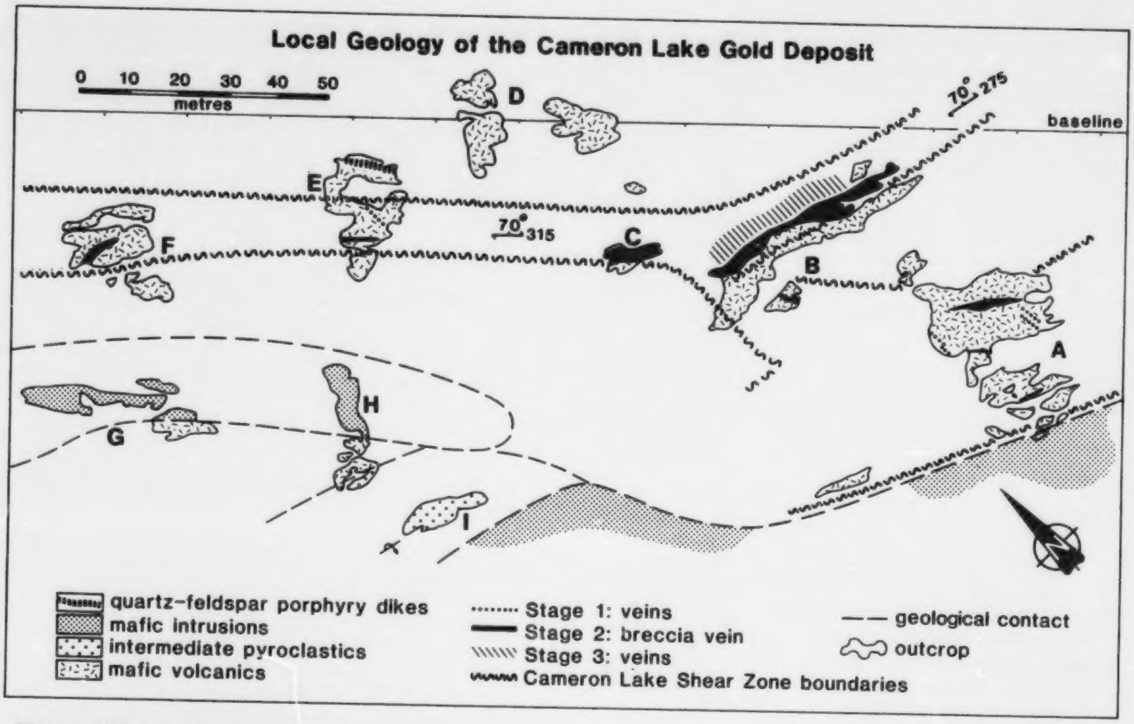

Figure 193.3. Local geology of the Cameron Lake gold deposit. Letters refer to: Discovery outcrop (A), North trench (B), Vic's trench (C), NC-19 trench (D), Island trench (E), Blood trench (F), Gabbro trench (G), Hunter's trench (H), and Controversy trench (I).

shear zone, and a planar mineral alignment (flattening plane foliation) inclined at angles less than 45° to the shear zone. The intersection of these foliations defines a lineation which pitches 85°E within the shear zone. This lineation is perpendicular to the inferred displacement vector, which pitches 5°W within the shear plane.

The relationship between the Cameron Lake Shear Zone and regional geological features has not yet been established. Deformation zones at Cameron Lake may represent tectonic slides (Hutton 1979) either associated with an episode of flexural slip folding, or related to the Pipestone-Cameron Fault system. Regional mapping by the Ontario Geological Survey defined a distinct geometric relationship between the orientation of lithological contacts and the fault. The consistent merging of rock units into the plane of the fault (Figure 193.2) implies dextral, dominantly strike-slip movement. The sense of shear on the Cameron Lake Shear Zone is also dextral and subhorizontal. Observations of this type are compatible with the Cameron Lake Shear Zone representing a minor splay from the major Pipestone-Cameron Fault (Figure 193.2). Further work on the Pipestone-Cameron Fault will be required in order to fully document and assess its role with respect to gold deposits.

GEOMETRY OF THE CAMERON LAKE DEPOSIT

Figure 193.3 is a generalized geological map of the deposit compiled from surface mapping and core logging. Note the orientation of the splay which bifurcates from the main zone of deformation. Its attitude is similar to that of bedding measured outside the shear zone. This geometrical relationship is seen on scales which range from one metre to tens of metres. Systematic channel sampling across these surface exposures indicates that the locus of gold concentration occurs at the intersection of 2 of these structures.

It is concluded, therefore, that the localization of highly anomalous quantities of gold along the Cameron Lake Shear Zone corresponds to the development of oblique, secondary, bedding-controlled sympathetic shear zones (275/70°N). This is illustrated on a dipping longitudinal section compiled from drill data (Figure 193.4). Note the approximate 70°W pitch of the gold zones, and the periodicity of the high-grade shoots. Figure 193.5 is a simplified stereographic projection of the Cameron Lake Shear Zone and the oblique, bedding-controlled, sympathetic splays. The pitch of the deposit, as defined by drilling, is coincident with the intersection of these 2 shear systems. The relationship between the 2 shear systems and the deposit is illustrated diagramatically in Figure 193.6. This model serves to explain the

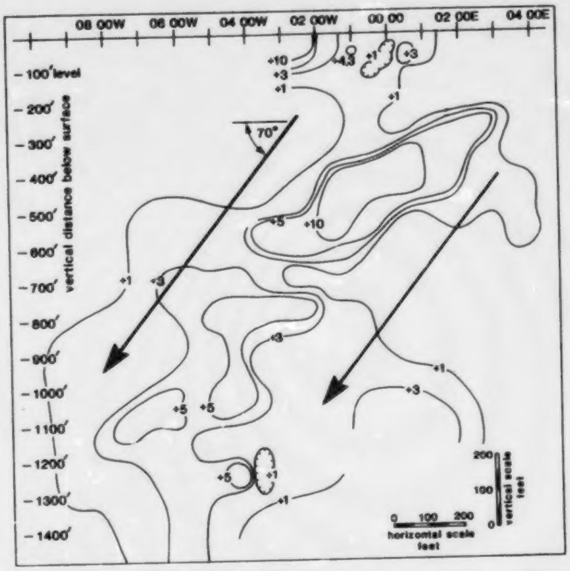

Figure 193.4. Longitudinal section dipping 65°N from the baseline. Contours represent the value of grade times thickness (e.g., 0.2 oz/ton Au over 50 feet = 10). The contours are based on approximately 75 drill hole piercing points.

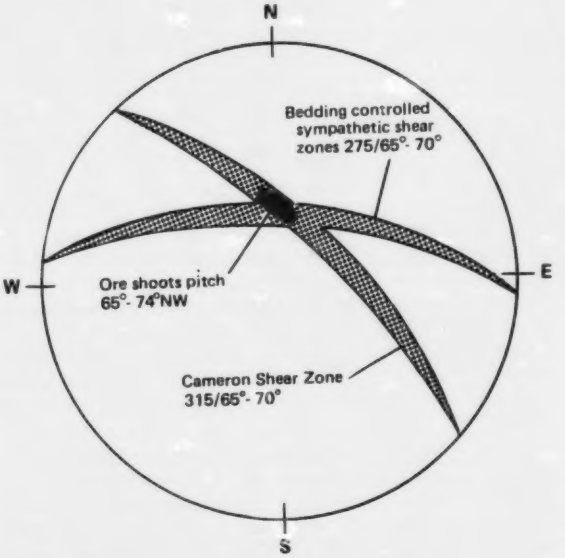
N
W
E
S
Bedding controlled sympathetic shear zones 275/65°- 70°
Ore shoots pitch 65°- 74°NW
Cameron Shear Zone 315/65°- 70°

Figure 193.5. Simplified stereographic projection illustrating the coincidence of the pitch of the ore shoots with the line of intersection of the Cameron Lake Shear Zone and bedding-controlled shear zone splays.

complex subsurface geometry of the gold shoots, as well as the existence of hanging wall and footwall zones on either side of the main zone of gold enrichment. At this stage of investigation, the periodicity of the high grade gold shoots cannot yet be adequately explained.

VEIN PARAGENESIS

During 1983 and 1984 an extensive trenching program was conducted at Cameron Lake. Prior to that time very little outcrop exposure of the deposit existed. In 1984 all the excavated exposures of the deposit were mapped at 1:60 scale, the objectives being to resolve the vein paragenesis and interpret the kinematics of the Cameron Lake Shear Zone.

Three distinct vein types were recognized in the carbonatized rocks of the Cameron Lake Shear Zone:

1. early, barren, extensional, quartz-carbonate veins which have subsequently been buckled (Photo 193.1)
2. a major system of gold-bearing pyritic, quartz-rich breccia veins (Photo 193.2)
3. a late group of straight, cross-cutting, *en echelon*, extension veins which contain quartz-carbonate-chlorite-hematite-gold (Photo 193.3)

The stage 1 veins are typically 1 to 2 m in length and 3 to 4 cm in width. They consist of coxcomb-textured quartz with a median seam of rusty-weathering carbonate. They are interpreted as having been formed during the early stages of development of the shear zone. These buckled veins have no associated pyrite and chip samples indicate that they are barren of gold.

The breccia veins range from centimetre size to large structures with strike lengths exceeding 175 m and widths in excess of 4 m. They commonly pinch and swell, and may terminate abruptly. Their margins are often the sites of pronounced shearing. They are approximately planar and parallel to the shear zone in which they occur, and have orientations of either 315/70°N or 275/70°N.

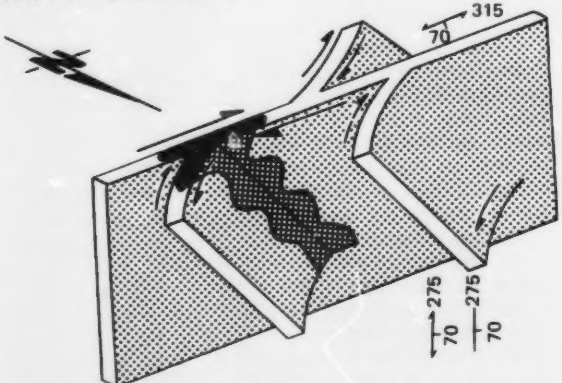

Figure 193.6. Diagrammatic represenlation of the spatial relationship between ore shoots and the northwest-trending Cameron Lake Shear Zone and the northeast- to east-trending bedding-plane splays.

Photo 193.1. Early barren, extensional, quartz-carbonate veins which have subsequently been buckled. Note the median seam of carbonate and axial planar cleavage. This type of vein commonly displays Z-fold asymmetry.

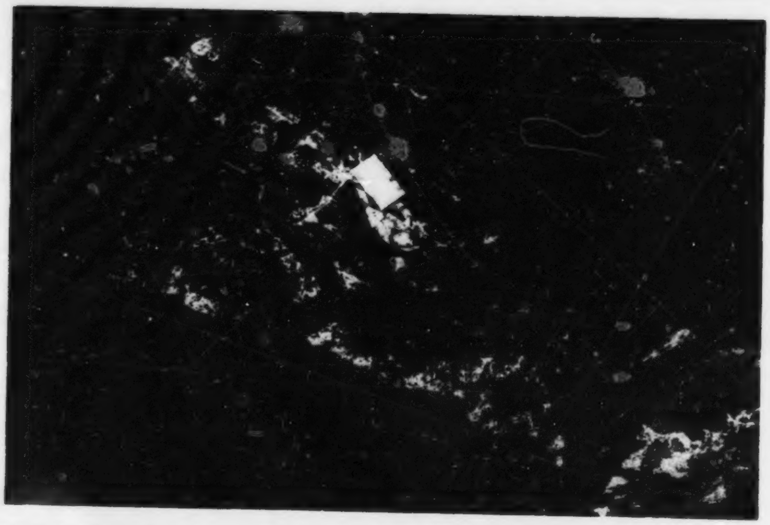

Photo 193.2. Gold-bearing, pyritic, quartz-rich breccia-vein. Note the angular nature of the fragments indicating little comminution.

Photo 193.3. Late array of straight, en echelon extension veins cross-cutting a breccia-vein.

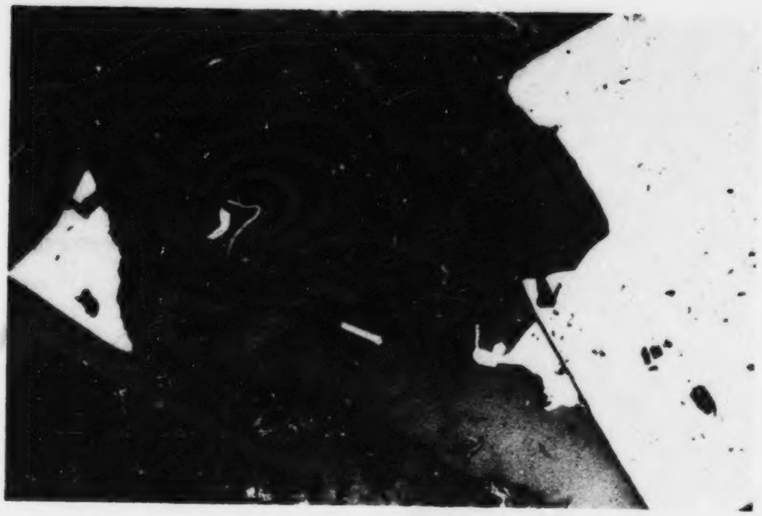

Photo 193.4.
Photomicrograph of a pyrite grain which has been fractured. Note the extensive pressure shadow linking the detached part to parent crystal. Chalcopyrite has been mobilized by pressure solution with quartz and carbonate into the pressure shadow. Field of view is 2.4 mm.

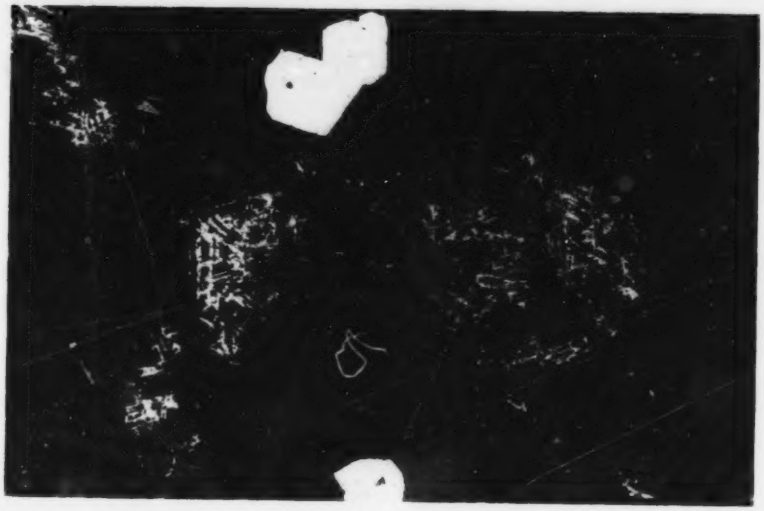

Photo 193.5.
Photomicrograph of rutile laths pseudomorphing ilmenite oxyexsolution lamellae displaying an inherited, ordered orientation. Field of view is 0.6 mm.

The breccia veins contain angular, often elongate, fragments of altered basalt which range from 1 mm to greater than 30 cm in size. Breccia fragments often have a strong internal fabric and may be in contact or separated by a matrix (10% to 50%) of quartz, carbonate, and plagioclase. The matrix may be massive or consist of mineral fibres elongate perpendicular to the fragment boundaries. Groups of fragments commonly have shapes suggesting that, by removing the vein material, they could be fitted together like pieces in a jigsaw puzzle. Pyrite rarely exceeds 10%, is concentrated within the fragments, and forms narrow envelopes surrounding the breccia veins. Gold is locally present in hand sample as inclusions within pyrite grains, as free gold interstital to pyrite, and rarely, in the siliceous vein matrix. Less than 1% chalcopyrite is also present.

The stage 3 veins form arrays of the type described by Roering (1968), Beach (1975), and Kerrich and Allison (1978). The veins are planar, strike north-south, and dip vertically. They are in general only 1 to 2 m in length, 1 to 2 cm in width, and in the North trench (Figure 193.3) they are spaced at fairly regular intervals of 6 to 10 cm. They cut the breccia veins and the pervasively altered, foliated phyllonitic rocks of the shear zone. Internal fibrous quartz textures suggest that these veins formed by crack-seal mechanisms (Ramsay 1980), and propagated normal to the least principal stress directions. The quartz carbonate-chlorite-hematite-gold assemblage infilling the veins is thought to be locally derived by solution transfer.

The significance of the stage 2 breccia veins has been previously underestimated. They represent a specific gold-bearing rock type at Cameron Lake which commonly contains greater than 0.3 ounce Au per ton. The other, lower-grade rock type consists of pervasively altered carbonate-sericite-pyrite-rich phyllonitic rocks; they occupy a large volume of the Cameron Lake Shear Zone, enveloping the breccia veins. This subdivision of gold-bearing rock types is readily visible in surface exposures of the deposit and diamond-drill core. Figure 193.7 is a frequency plot of assay results from drill holes intersecting the

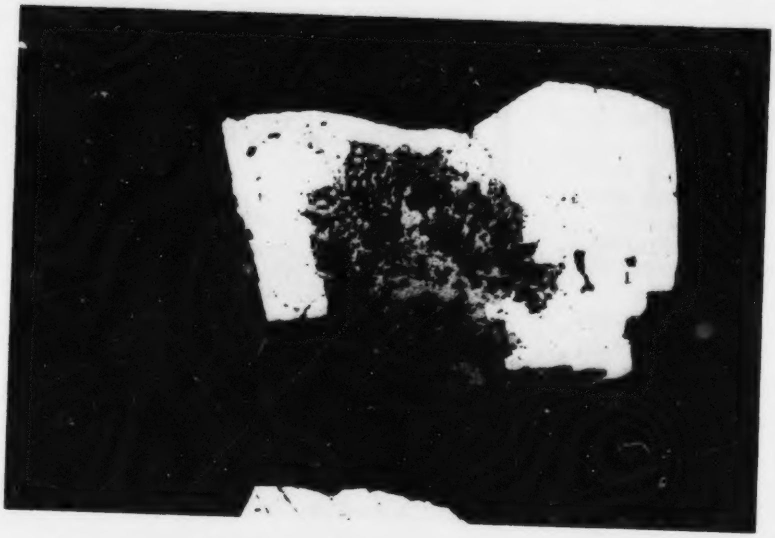

Photo 193.6. *Photomicrograph illustrating the nucleation of pyrite on skeletal rutile intergrowths, with carbonate. Field of view is 0.6 mm.*

main zone of gold concentration. Note the bimodal character of the assay data. The lower values correspond to the pervasively altered basaltic rocks while the higher grades are from the breccia veins.

ALTERATION

Three types of alteration are recognized in the rocks hosting the Cameron Lake deposit. The first is considered to be the result of a primary metamorphic event that produced greenschist facies assemblages in the mafic volcanic rocks which envelop the gold-bearing alteration zones. The other 2 types are clearly related to gold enrichment and are characterized by carbonate plus sericite alteration and sulphidation.

Carbonate and sericite are alteration products commonly found associated with many Archean lode gold deposits (Colvine *et al.* 1984) and the Cameron Lake deposit is no exception. Carbonate is by far the most abundant mineral associated with the deposit. On weathered surfaces the carbonate imparts a distinct, rusty brown rind of discolouration, whereas the sericite occurs in light buff to tan coloured aggregates and foliated lamellae.

Outside the pervasively altered shear zone, rhombohedral carbonate is present in the weakly altered, massive basalts. Its distribution is erratic and tends to occur in the upper sections of the deposit and may locally increase in abundance with proximity to the ore zones. Caution should be used in applying it as an exploration guide, as there appears to be a primary control on its distribution related to flow contacts, and coarser grain sizes in the volcanic rocks.

The pervasively altered phyllonitic rocks consist predominantly of carbonate and sericite. No primary mineralogy or textures are preserved. In hand sample, the carbonate may appear rather massive, although in thin section a planar fabric is observed. With increasing amounts of sericite a distinct foliation is developed. Core samples taken from the pervasively altered zone in several drill holes, and samples obtained from surface exposures were stained for carbonate (Dickson 1965). The carbonate minerals in both veins and phyllonitic rocks are Fe-bearing dolomite. These results were verified by X-ray diffraction.

The second type of alteration is related to the formation of breccia veins. Sulphidation is common in rocks surrounding the breccia veins and the basaltic fragments within them. Pyrite, the most common sulphide, envelops breccia veins, is concentrated within breccia fragments, and forms diffuse patches within the pervasively altered phyllonitic rocks. Rarely does pyrite occur within the quartz-vein matrix.

A distinct correlation exists between pyrite and gold as shown by core assays and channel samples. In polished section, gold is seen as inclusions and fracture fillings within pyrite and as coatings on pyrite grains. Occasionally gold occurs as free grains interstitial to pyrite, and more rarely within the quartz-rich matrix between breccia fragments. Continued deformation postdating the formation of pyrite is reflected in the development of pressure shadows and the mobilization of quartz, carbonate, and chalcopyrite into them (Photo 193.4).

Albitic plagioclase commonly occurs in the siliceous matrix of the breccia veins. It should be stressed that silicification, in terms of a pervasive alteration facies, is not observed, although silica is a critical component within the breccia-vein matrix.

Rutile is present in almost all the samples from Cameron Lake. Textural evidence suggests that it formed during the oxidation of ilmenite oxyexsolution lamellae within magnetite (Rumble 1976); magnetite is common in the unaltered basalts near the deposit. The alteration of the magnetite-ilmenite assemblage to hematite and rutile is not only restricted to the zones of gold enrichment; in both the hanging wall and footwall to the deposit a curious "brown fleck" alteration is locally developed. The brown flecks have been identified as aggregates of small skeletal rutile grains. Hematite is quite often localized in veins

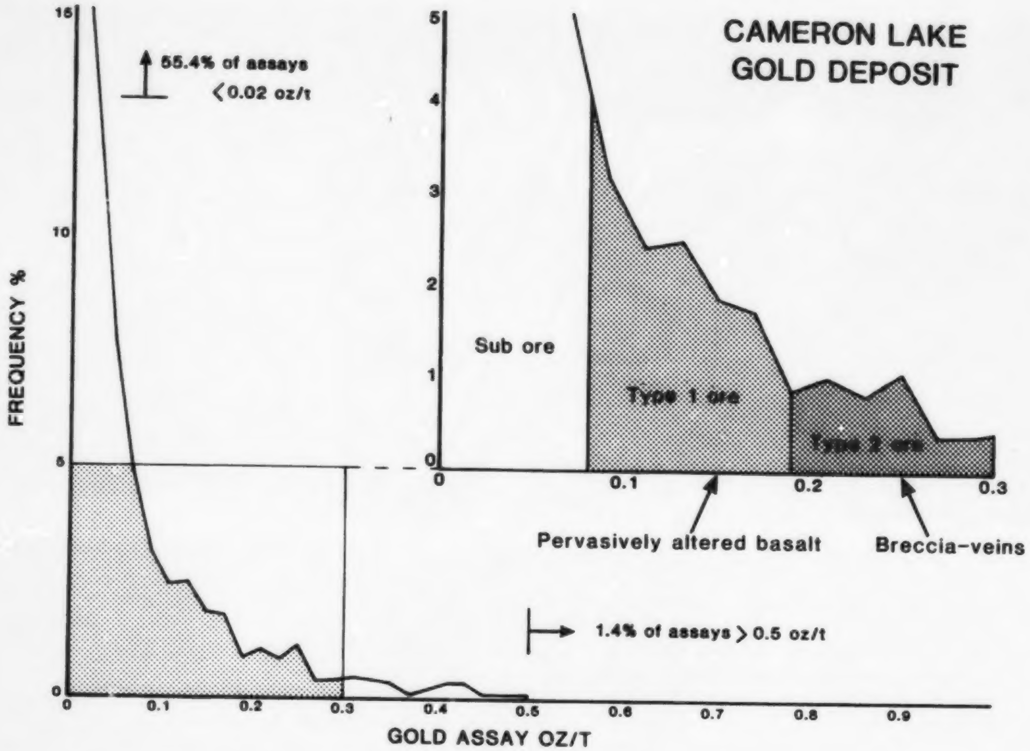

Total assays 1958

Composite of 52 DDHs through "The Main Zone"

Figure 193.7. *Frequency versus gold assay histogram plot of drill hole data from the Cameron Lake deposit. Two distinct gold-bearing rock types are present: carbonate-sericite-pyrite phyllonitic rocks (0.08 to 0.19 oz/ton Au) and breccia-veins (greater than 0.19 oz/ton Au).*

and fractures. The magnetite is also a site for pyrite nucleation (Photos 193.5 and 193.6).

LITHOGEOCHEMISTRY

Samples were collected from the deposit for lithogeochemical analysis:

1. to identify the elemental associates of the gold
2. to supplement and assist in the interpretation of petrographic and mapping data
3. to provide some insight into the chemical processes operative during alteration

The concentrations of Ag, As, Au, B, Ba, Be, Bi, Cd, Co, Cr, Cu, Hg, Li, Mo, Ni, Pb, Rb, Sb, Se, Sn, Sr, Ta, Te, U, V, W, and Zn were determined on samples from the Cameron Lake deposit. Major element analyses of SiO_2, Al_2O_3, Fe_2O_3 total, FeO, MgO, CaO, Na_2O, K_2O, TiO_2, P_2O_5, MnO, CO_2, and S, and loss on ignition were also obtained. Analytical work was performed by Bondar-Clegg and Company Limited, Ottawa.

METHODOLOGY AND SAMPLING PROCEDURES

A profile through the deposit was obtained by sampling DDH NC-29. This hole, considered representative of the deposit, was chosen for several reasons. First the rocks in both the hanging wall and footwall adjacent to the gold-bearing phyllonitic rocks apparently had the same primary basaltic compositon. Hanging wall and footwall gold zones are absent. Horses of unaltered, weakly deformed rocks, which commonly occur within broad zones of shearing (Simpson 1983), are not present in this part of the deposit. Thin quartz-feldspar porphyry dikes intrude the altered phyllonitic rocks, as well as the sheared contact between the basalt and gabbro.

Material sampled outside the shear zone provided composite samples obtained by selecting several homogeneous, vein-free, 4 to 5 cm pieces of core over a total core length of 1 to 2 m. Samples representing the altered and mineralized zone were obtained from the assay rejects which represent complete composite samples of split core over lengths averaging about 1.2 m.

Nine samples of gold-bearing, breccia veins were collected from the excavated outcrops exposed during the 1984 trenching program. The samples represent 6 different vein structures. Polished slabs, and polished thin sections corresponding to these samples were retained for mineralogical and textural studies.

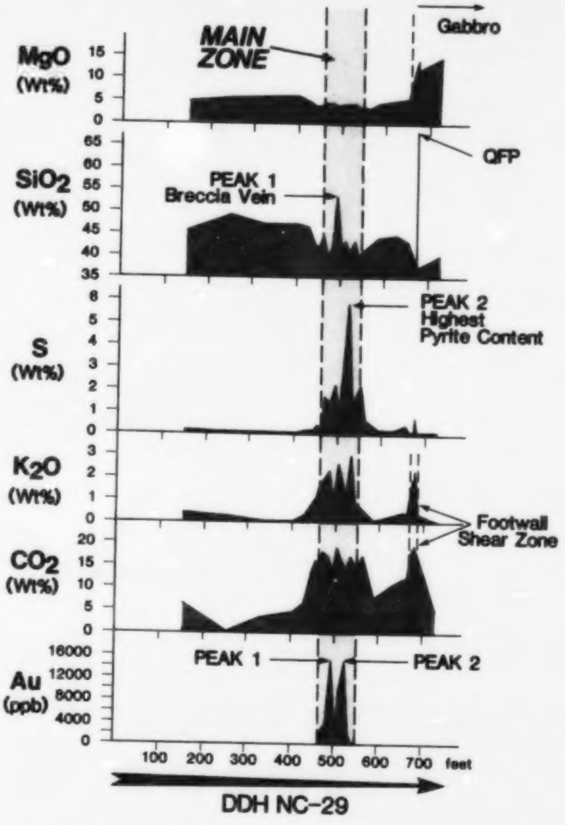

Figure 193.8. *Downhole lithogeochemical profile which illustrates the broad alteration envelopes which surround the gold deposit.*

The data were grouped according to rock type (basalt, gabbro, and quartz-feldspar porphyry dikes) and the basalts were subdivided into weakly altered and pervasively altered phyllonitic rock sub-types. None of the samples could be considered unaltered. Breccia veins were grouped as a distinct class of gold-bearing rock type.

RESULTS

WHOLE ROCK GEOCHEMICAL DATA

Figure 193.8 consists of lithogeochemical profiles based on the data obtained from DDH NC-29 (intersection: 57.2 feet grading 0.26 ounce Au per ton). There is a tight zone of gold enrichment and corresponding high CO_2, K_2O, and S, reflecting carbonate, sericite, and pyrite respectively. CO_2-rich rocks form an extremely broad halo around the deposit; this is also characteristic of the barren footwall shear which separates the mafic volcanic rocks from the gabbroic sill. High K_2O values are also diagnostic of both shear zones, but the distribution is somewhat more restricted and is not as extensive as CO_2. S alone serves to distinguish the shear zone containing gold enrichment. It displays a strong correlation with gold and is absent in the footwall shear zone which lacks gold concentrations. Two high gold peaks occur within the data, one associated with a breccia vein (note high corresponding silica) and another correlated with an extremely high pyrite content.

MgO is useful in monitoring the primary composition of the host rocks since it is less susceptible to chemical migration than Si or K (Jensen 1976). Figure 193.8 illustrates that even in pervasively altered rocks the MgO content is approximately equal to that of the unaltered basalts.

Figures 193.9, 193.10, and 193.11 are scatter plots of lithogeochemical data obtained from the Cameron Lake deposit. CO_2 and SiO_2 were chosen as parameters upon which to base this discussion since field evidence suggests 2 styles of alteration and/or veining are present, characterized by early carbonatization and later breccia veining accompanied by sulphidation.

A positive correlation of CO_2 with Au, S, K_2O, and CaO exists as a function of degree of alteration (Figure 193.9). The breccia veins show similar trends; however, the data must be interpreted with caution.

If it is assumed that 2 somewhat distinct types of alteration have occurred, then the pervasively altered phyllonitic rocks may have been carbonatized prior to their inclusion as fragments within the breccia veins. CO_2 versus SiO_2 (Figure 193.10a) illustrates this point. Among the basalts, silica displays no systematic variation with carbonatization. The breccia veins, however, never have CO_2 values which exceed those of the pervasively altered phyllonites, and CO_2 decreases with increasing silica. Since quartz is present in the form of a vein matrix, this relationship may be thought of as simply a dilution of pervasively carbonatized basalt. In other words, the more vein matrix (SiO_2), the fewer rock fragments (altered phyllonites) and therefore lower levels of CO_2, K_2O, and CaO.

These trends are more clearly reflected in data plotted against SiO_2 (Figures 193.10b, 193.10d, 193.11a, and 193.11c). Note the negative correlations which exist among CO_2, CaO, Na_2O, and K_2O data. Silica shows no systematic variation during the carbonatization and sericitization of the basalt.

Several statements concerning gold precipitation within this hydrothermal system may also be made. Within the breccia veins the highest S and Au values are associated with the lowest silica values (Figures 193.10c and 193.11b). Consequently, the presence of phyllonitic rock fragments within the breccia veins seems critical in terms of having provided sites for sulphidation and Au precipitation. The highest gold grades are found in those breccia veins containing the greatest percentage of fragments and in the wall rocks adjacent to the veins. However, a quartz vein of the same generation lacking breccia fragments, may still contain gold (Figures 193.9a and 193.9b). As CO_2 values approach zero, S and Au do not, but rather reach minima of 1% S and 1000 ppb Au. This is compatible with observations that Au and pyrite do locally occur within the siliceous vein matrix.

Because iron shows no positive correlation with CO_2 content (Figure 193.11d), ferroan dolomite must have been derived from the alteration of iron-rich minerals.

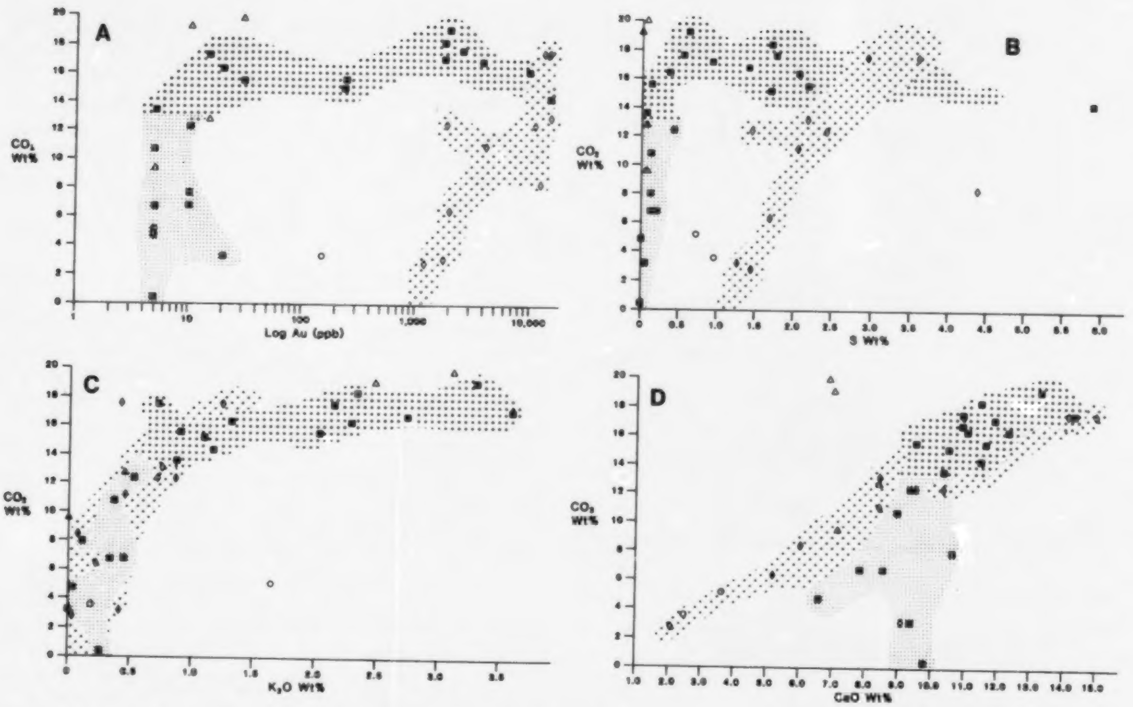

***Figure 193.9.** Scatter plots of geochemical data from the Cameron Deposit. (A) CO_2 against Log Au. Log or (B) CO_2 against S. (C) CO_2 against K_2O. (D) CO_2 against CaO. Half-filled squares are weakly altered basalt, solid squares are pervasively altered basalts. Diamonds are breccia-veins, circles are quartz-feldspar porphyry dikes, and triangles are gabbros. Fields are specified for weakly altered basalts (light dots), pervasively altered basalts (dark dots), and breccia veins (crosses).*

Na_2O within the breccia veins (Figure 193.11a) displays a higher concentration than in any of the basalts, but has an overall negative correlation with silica. This may relate to local albitization of basalt spatially associated with the breccia veins or albite as a vein mineral.

K_2O values within the least siliceous breccia veins (Figure 193.11c) are approximately equal to those transitional from weakly altered to pervasively altered basalts. If sericitization occurred prior to breccia-vein formation, the silica-poor veins might be expected to reflect much higher K_2O values, similar to those occurring in the most altered phyllonites. One possible explanation for this apparent inconsistency may be that during breccia-vein development, K_2O was locally mobilized immediately adjacent to veins. Alternatively, sericite may occupy a crude alteration zone located distally from the breccia veins.

TRACE ELEMENT GEOCHEMISTRY

Of the trace elements studied, only 6 (Ag, Ba, Hg, Rb, Sr, and W) correlate positively with gold (Figure 193.12).

Hg exhibits a maximum value of 45 ppm in the breccia veins which is at best only twice the background in both the unaltered and altered basalts.

Ag, Ba, Rb, Sr, and W are enriched in both the altered basalts and the breccia veins. Ag has a strong correlation with gold and has a maximum value of 4.2 ppm; it probably occurs alloyed with the gold. Ba is also associated with gold and has a maximum value of 161 ppm, which is only about twice background levels. W shows a weak but positive correlation with gold and has a maximum value of 28 ppm. Both Rb and Sr are related to the mineralization and have maxima of 107 ppm and 410 ppm respectively.

DISCUSSION

Carbonatization in the rocks which host the Cameron Lake deposit is wide-spread; however, it alone should not be considered indicative of deformation or of gold enrichment. Studies at Cameron Lake and elsewhere in the Superior Province have shown that carbonate alteration occurs relatively early with respect to gold mineralization (Colvine *et al.* 1984), and that it is often localized in areas other than shear zones (Fyon and Crocket 1982). Fluids move along all zones of high permeability including shear zones, flow contacts, dike margins, or unconformities.

Field relationships suggest that early carbonatization and sericitization occurred during ductile deformation and were followed by brittle deformation, the formation of breccia veins, and sulphidation. This is compatible with changes in the composition of the hydrothermal fluids, which may have been initially

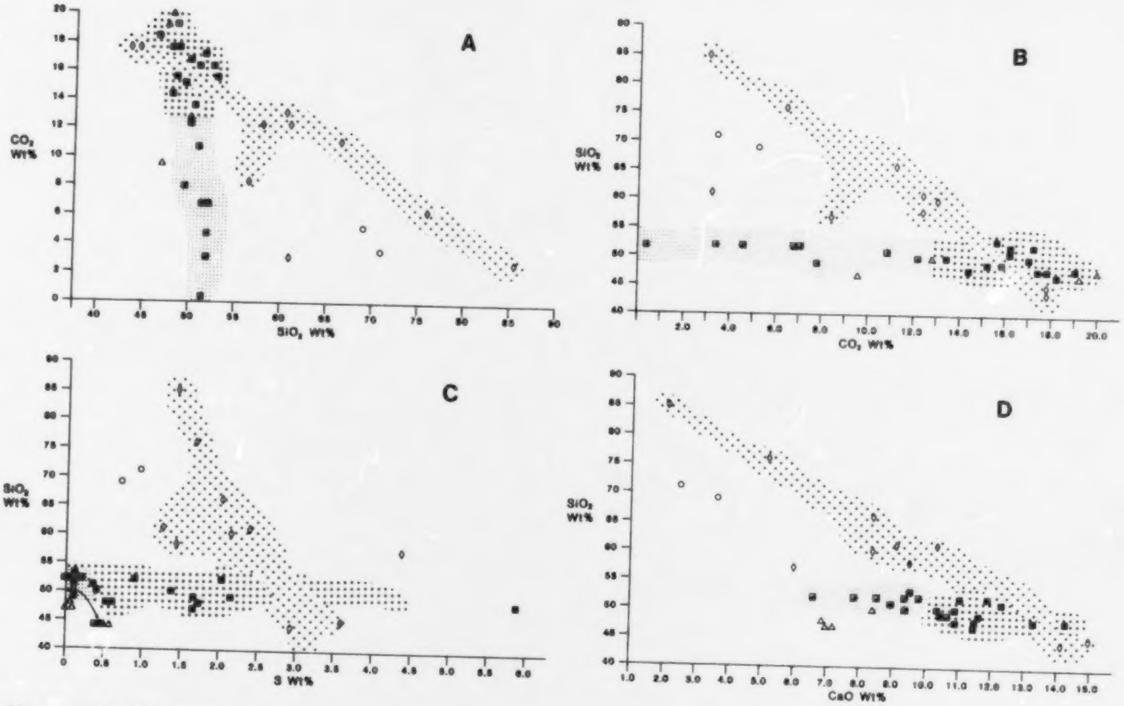

Figure 193.10. Scatter plots of geochemical data from the Cameron Lake deposit. (A) SiO_2 against CO_2. (B) CO_2 against SiO_2. (C) SiO_2 against S. (D) SiO_2 against CaO.

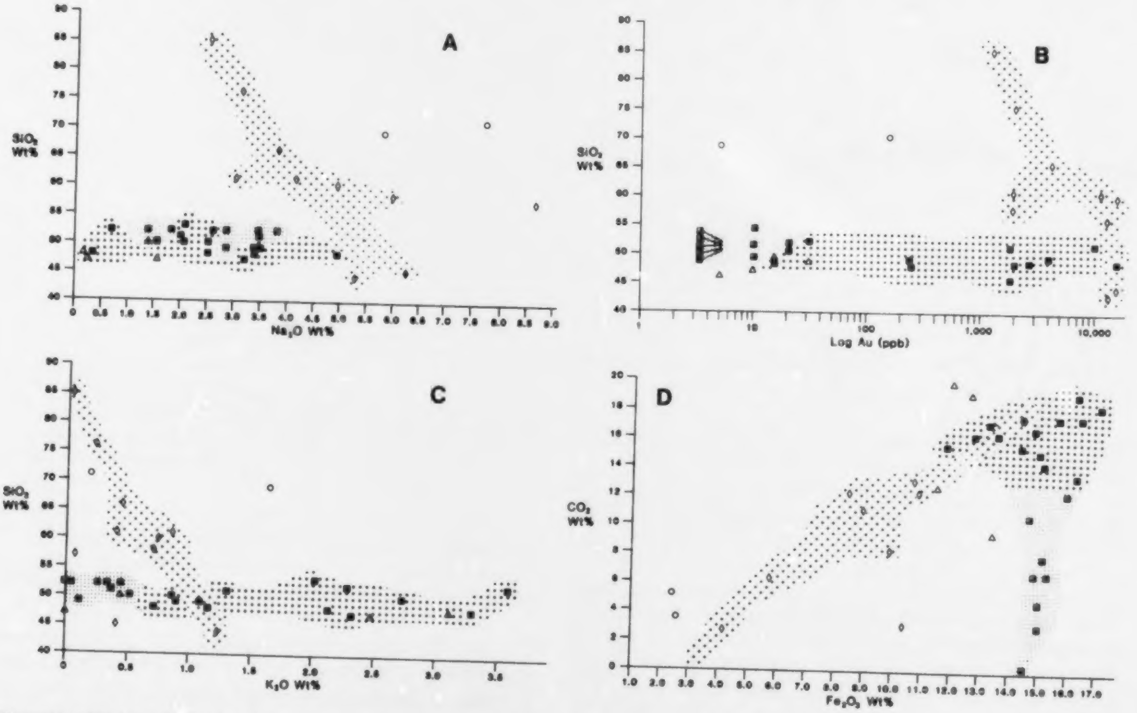

Figure 193.11. Scatter plots of geochemical data from the Cameron Lake deposit. (A) SiO_2 against Na_2O. (B) SiO_2 against log Au. (C) SiO_2 against K_2O. (D) CO_2 against Fe_2O_3.

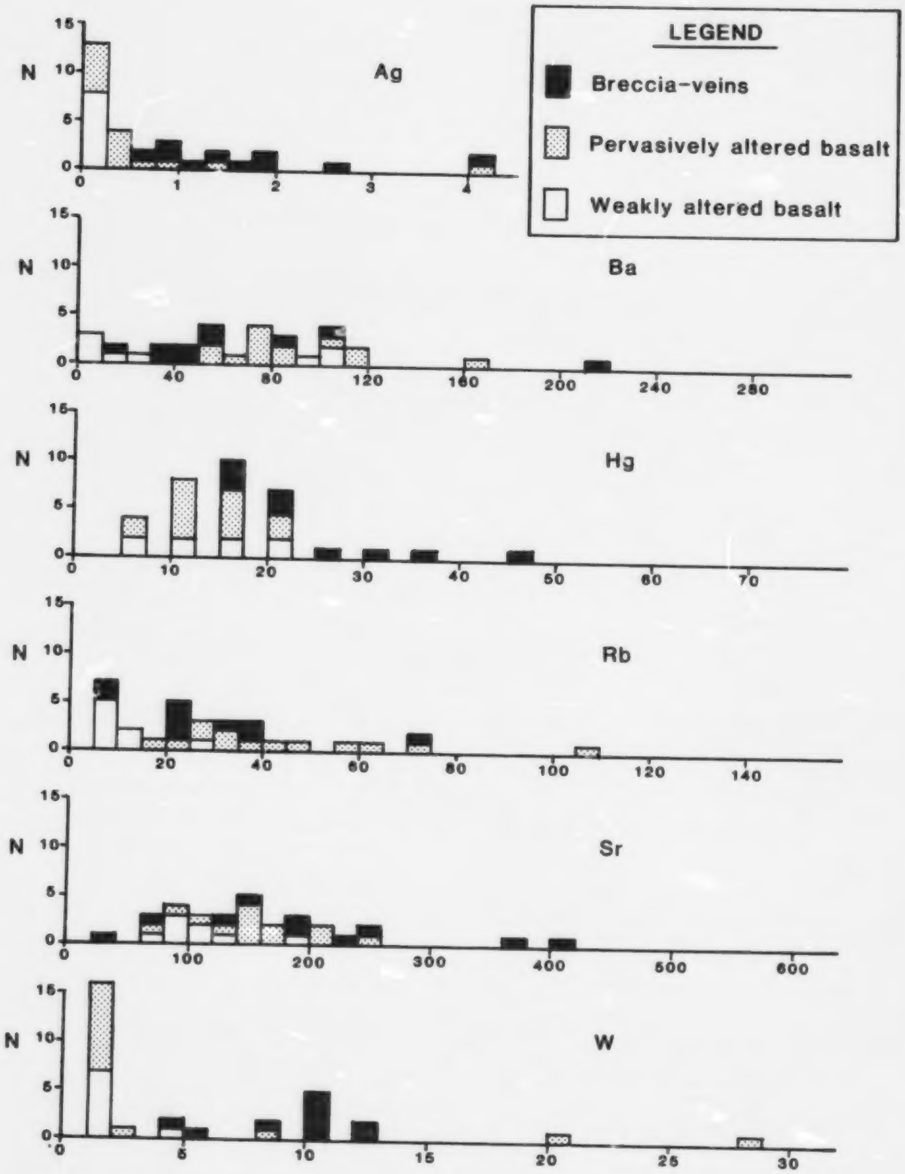

Figure 193.12. *Frequency histograms for trace elements which exhibit a positive correlation with gold. N is the frequency occurrence. Total number of analyses equals 31. All analyses are in ppm.*

CO_2 + K rich and later CO_2 + H_2O + S rich; gold precipitation was most significant from the latter.

The transition from ductile cleavage development to brittle processes within the Cameron Lake Shear Zone is manifested in the formation of veins and vein-breccias. The change from ductile to brittle behavior may have been the result of local increases in fluid pressure which facilitated brittle deformation and vein formation by reducing the effective normal stresses. The breccia veins probably formed major conduits for fluid circulation; gold complexes with sulphur-bearing species may have become unstable, precipitating gold when these fluids reacted with the iron-rich phyllonitic rocks to form pyrite.

CONCLUSIONS

Several of the more significant conclusions which may be made on the basis of progress to date are:

1. The Cameron Lake deposit occurs in mafic volcanic rocks of the Cameron Lake Volcanics and is associated with a discordant zone of high strain, which may be related to the Pipestone-Cameron Fault.
2. The deposit is essentially of the vein-type associated with a large hydrothermal alteration zone.
3. The localization of highly anomalous gold concentrations occurred in response to the development of oblique, bedding-controlled, sympathetic

splays, which also appear to control the geometry of the deposit.

4. The characteristic alteration assemblage consists of Fe-dolomite + sericite + pyrite associated with quartz-rich breccia veins.
5. The alteration is chemically expressed by the addition of major amounts of CO_2, K_2O, CaO, S, and minor amounts of Ag, Au, B, Hg, Rb, Sr, and W.
6. Precipitation of pyrite at the expense of primary magnetite was related to gold mineralization.

ACKNOWLEDGMENTS

The study of gold mineralization in the Cameron-Rowan Lakes belt is part of an M.Sc. thesis by David R. Melling, in progress at Carleton University, under the supervision of David H. Watkinson and Lesley B. Chorlton. The authors express their gratitude to the staff of Nuinsco Resources Limited for their assistance in the field and for providing the excavated exposures. Without the field support and unrestricted access to data provided by Nuinsco, this study would have been rendered impractical.

Appreciation is also extended to Gold Fields Canadian Mining Limited, Inco Limited, Canolan Resources Limited, Bigstone Minerals Limited, Tantalus Resources Limited, Calaveras Explorations Limited, and Silver Lake Resources Incorported for providing access to the data they have accumulated while conducting exploration programs within the Cameron-Rowan Lake belt.

The authors would also like to thank C.E. Blackburn, (Resident Geologist, Kenora) for his lively discussions, insight into the regional geology, and providing the data upon which his regional stratigraphic subdivisions are based.

Finally warm appreciation is expressed to Doug Hunter of Earthunt Explorations for suggesting this project to Melling and for his contributions which have brought the deposit closer to development.

REFERENCES

Beach, A.
1975: The Geometry of *En Echelon* Vein Arrays; Tectonophysics, Volume 28, p.245-263.

Beard, R.C., and Garrett, G.L.
1976: Gold Deposits Fort-Frances Area, Districts of Kenora and Rainy River; Ontario Division of Mines, Mineral Deposits Circular 16, 46p. Accompanied by Chart A, scale 1:253 440 or 1 inch to 4 miles.

Blackburn, C.E.
1982: Geology of the Manitou Lakes Area, District of Kenora, (Stratigraphy and Petrochemistry); Ontario Geological Survey Report 223, 61p. Accompanied by Map 2476, scale 1:50 000.

Blackburn, C.E., and Janes, D.A.
1983: Gold Deposits in Northwestern Ontario; p.194-210 *in* The Geology of Gold in Ontario, edited by A.C. Colvine, Ontario Geological Survey, Miscellaneous Paper 110, 278p.

Blackburn, C.E., and Hailstone, M.R.
1983: The Geological Environment of Gold Mineralization, Cameron-Rowan Lakes, N.W. Ontario; Geoscience Research Seminar, Program with Abstracts, December 6-7, 1983, Toronto, Ontario, 13p.

Colvine, A.C., Andrews, A.J., Cherry, M.E., Durocher M.E., Fyon, A.J., Lavigne, Jr., M.J., Macdonald, A.J., Marmont, Soussan, Poulsen, K.H., Springer, J.S., and Troop, D.G.
1984: An Integrated Model for the Origin of Archean Lode Gold Deposits; Ontario Geological Survey , Open File Report 5524, 98p.

Dickson, J.A.D.
1965: A Modified Staining Technique for Carbonates in Thin Section; Nature, Volume 205, Number 497, 587p.

Fyon, J.A., and Crocket, J.H.
1982: Gold Exploration in the Timmins District Using Field and Lithogeochemical Characteristics of Carbonate Alteration Zones; p.113-129 *in* The Geology of Canadian Gold Deposits, edited by R.W. Hodder and W. Petruk, Canadian Institute of Mining and Metallurgy, Special Volume 24, 286p.

Hunter, A.D., Curtis, L.W., and Melling, D.R.
1984: The Cameron Lake Gold Deposit, N.W. Ontario: Pioneering in a Dormant Gold Camp; (Abstract) Canadian Institute of Mining and Metallurgy Bulletin, Volume 77, Number 863, p.60.

Hutton, D.H.W.
1979: Tectonic Slides: A Review and Reappraisal; Earth Science Reviews, Volume 15, p.151-172.

Jensen, L.S.
1976: A New Cation Plot for Classifying Subalkalic Volcanic Rocks; Ontario Division of Mines, Miscellaneous Paper 66, 22p.

Kaye, L.
1973: Rowan Lake Area, District of Kenora; Ontario Division of Mines, Preliminary Map P.831, Geological Series, scale 1 inch to 1/4 mile. Geology 1972.

Kerrich, R., and Allison, I.
1978: Vein Geometry and Hydrostatics During Yellowknife Mineralization; Canadian Journal of Earth Sciences, Volume 15, p.1653-1660.

Mackasey, W.O., Blackburn, C.E., and Trowell, N.F.
1974: A Regional Approach to the Wabigoon-Quetico Belts and its Bearing on Exploration in Northwestern Ontario; Ontario Division of Mines, Miscellaneous Paper 58, 30p.

Northern Miner
1983: Cameron Lake Gold Rush Builds Momentum; The Northern Miner, June 23, Volume 69, Number 16, p.1, 16.

Nuinsco Resources Limited
1984: Annual Report to Shareholders; 16p.

Ramsay, J.G.
1980: The Crack-Seal Mechanism of Rock Deformation; Nature, Volume 284, Number 5752, p.133-139.

Roering, C.
1968: The Geometrical Significance of Natural *en echelon* Crack Arrays; Tectonophysics. Volume 5, p.107-123.

Rumble, D. (Editor)
1976: Oxide Minerals; Mineralogical Society of America, Short Course Notes, Volume 3.

Schwerdtner, W.M., Stone, D., Osadetz, K., Morgan, J., and Scott, G.M.
1979: Granitoid Complexes and The Archean Tectonic Record in the Southern Part of Northwestern Ontario; Canadian Journal of Earth Sciences, Volume 16, p.1965-1977.

Simpson, C.
1983: Strain and Shape-fabric Variations Associated with Ductile Shear Zones; Journal of Structural Geology, Volume 5, Number 1, p.61-72.

Thompson, J.E.
1936: Geology of the Rowan-Straw Lakes Area; Ontario Department of Mines, Annual Report for 1935, Volume 44, Part 4, p.1-28.

Trowell, N.F., Blackburn, C.E., and Edwards, G.R.
1980: Preliminary Synthesis of the Savant Lake-Crow Lake Metavolcanic-Metasedimentary Belt, Northwestern Ontario, and its Bearing upon Mineral Exploration; Ontario Geological Survey, Miscellaneous Paper 89, 30p. Accompanied by Chart A.

Grant 202 Sulphur Isotope Studies of Archean Gold Deposits

H.P. Schwarcz and C.E. Rees[a]

Department of Geology, McMaster University

ABSTRACT

Pyrite from lode gold deposits in the Superior Province of Ontario has been analyzed for sulphur isotope ratios. There is a general clustering of values between 0 and +2‰, suggesting that the principal source of sulphur is of mantle derivation. However, significant fractionation is observed in some deposits. ^{34}S is enriched in some ores of the McIntyre and Dome Mines, and is very strongly depleted in the ores of the Canadian Arrow Deposit, Matheson. The latter shift is due to displacement of sulphur chemical equilibrium, due to oxidation. A positive correlation between $\delta^{34}S$ and Au content is observed in some deposits.

INTRODUCTION

Pyrite is a nearly ubiquitous component of gold ore in lode deposits of the Archean greenstone belts. Frequently, nearby pyritiferous rocks are barren of significant gold values. It would be useful to obtain geochemical criteria which would allow us to discriminate between potentially auriferous and barren, pyritic rocks. The purpose of this study was to test one such well established geochemical technique, namely, sulphur isotope ratio measurement, to see whether it could be used to characterize auriferous rocks, and also to see, in general, what relationship exists between S isotope ratios and other, better known, geological and geochemical characteristics of Au deposits.

The method employed in this preliminary study was to use samples of rock and ore which had previously been collected and studied by members of the Mineral Deposits section of the Ontario Geological Survey (OGS). In this way, we were able to make sure that any sample which we analyzed had already been placed in a meaningful geological context, and that we could relate the isotopic results to that geological setting. This report will set out the isotope data as it stands at present, and some aspects of the geology of each site as it appears to relate to these isotope results.

ANALYTICAL PROCEDURES

The samples were provided either as already purified pyrite separates, or as whole rock. Rock samples were crushed and sieved, and the 100 to 200 mesh fraction was suspended in a vertical flowing water column, which allowed the separation of an essentially pure pyrite sample, based on its higher settling velocity.

For some samples, pyrite was hand-picked from crushed rock, since only about 100 mg was generally required for analytical work. In all cases, the pyrite samples were given a final hand-picking under a binocular microscope to remove traces of other sulphides and silicates.

Sulphur isotope analyses were carried out on SO_2 gas which was prepared by reacting the pyrite directly with CuO, under vacuum. In some cases the pyrite was previously converted, chemically, to Ag_2S, and this was oxidized to SO_2. The SO_2 was analyzed on a mass spectrometer to determine $\delta 34_S$, with a precision of ± 0.2‰. The results are given with respect to the Canyon Diablo standard troilite (CDT).

Analyses for gold were carried out by instrumental neutron activation analysis (INAA), by Nuclear Activation Services at McMaster University. The detection limit of the method is 5 ppb (parts per billion), and the precision is about 5 ppb. Some gold analyses were also carried out by the analytical services laboratory of the OGS, using atomic absorption spectrophotometry (AAS).

THEORETICAL EXPECTATIONS AND PREVIOUS WORK

It is useful, before presenting the data, to consider the possible significance of such a study. Variations in S-isotope ratios can arise from various causes such as:

1. mixing between S sources of differing isotopic composition, e.g., magmatic and sedimentary
2. fractionation of S-isotopes during chemical speciation of sulphur (Ohmoto and Rye 1979)
3. biogenic reduction of sulphate to sulphide

Each of these processes has a characteristic effect on the sulphur isotope distribution and on correlation between S-isotope ratios and other geochemical parameters (redox state, C/S ratio, trace element concentrations, etc.). At this early stage in the investigation of S-isotopes in gold ore deposits, we can make only preliminary inferences about the causes of the observed isotope distributions. In particular we might expect the following trends, based on prior geological data.

First, we know that most of the lode ores are closely associated with igneous rocks, both volcanic and intrusive. We would therefore expect isotopic ratios typical of igneous sources, with $\delta^{34}S$ values near zero. Secondly, we have some evidence of variations in oxidation state of the ore-depositing solutions as shown by reddening of wall rock, by interaction between hydrothermal solutions and oxide facies iron formation (in at least one deposit studied here), and the presence of anhydrite as an alteration phase. We would expect that, as the mole fraction of sulphate in the hydrothermal solution increases, $\delta^{34}S$ will decrease due to the partitioning of $\delta^{34}S$ into sulphate. Finally, we might expect that where sulphides have been deposited in relatively large amounts as a result of pervasive alteration of a volcanic or intrusive host rock, that some fractionation of the sulphur reservoir ("Rayleigh distillation") would occur leading to progressive isotopic enrichment, the sign and magnitude of which would depend on the fractionation factor between the sulphide (principally pyrite) and the solution species (HS^- or $S^=$).

---

[a]deceased

Previous studies of S-isotopes in Archean gold ores have been carried out in Australia by Lambert *et al.* (1984) who found that there were significant differences between $\delta^{34}S$ values of pyrite depending on the host-rock environment, even within a single gold camp. Pyrite from barren igneous rock tended to be more positive (up to +8‰), as was pyrite in auriferous stockwork of a carbonatized intrusion; sulphides in metabasalt were generally somewhat negative (to -7‰). Lavigne (1983) found at the Red Lake camp that pyrite and pyrrhotite were generally positive, with values ranging from 0 to +8‰, clearly distinguishable from associated sulphide facies BIF; the high $\delta^{34}S$ values he attributed to desulphurization reactions liberating ^{34}S-enriched sulphur from pyrite.

ANALYTICAL DATA AND INTERPRETATION

In the present study, we have mainly analyzed samples from deposits in north-central Ontario (Geraldton, Terrace Bay), and the Abitibi belt (Dome, McIntyre, and Hollinger Mines at Timmins; Canadian Arrow Deposit at Matheson). The data are shown in Table 202.1 and in Figure 202.1. We shall discuss these data in sequence from west to east.

HARD ROCK MINE, GERALDTON

Auriferous pyrite occurs in veins cutting oxide facies banded iron formation (BIF) at this deposit. Macdonald (1984) considers various explanations for the close spatial relationship between ore and BIF including primary enrichment of Au in the BIF sediment, structural localization of the conduit of hydrothermal solutions, and chemical trapping of Au through oxidation of a sulphide complex. We have analyzed pyrite from 3 settings within this deposit: a) massive pyrite replacing BIF; b) in a vein cutting BIF; and c) disseminated in albite porphyry which also hosts Au at this mine. The $\delta^{34}S$ values for pyrite from each setting are indistinguishable (Table 202.1); the average for the entire population is 2.1 ± 0.8‰, slightly enriched with respect to an "igneous" source. Macdonald suggests that pyrite may have precipitated due to the reaction between bisulphide ions and magnetite (resulting in Au deposition through breakdown of the bisulphide complex). This reaction involves no change in oxidation state of the sulphur, and therefore is not likely to be accompanied by a large isotope fractionation factor. This is consistent with the small range of $\delta^{34}S$ values observed.

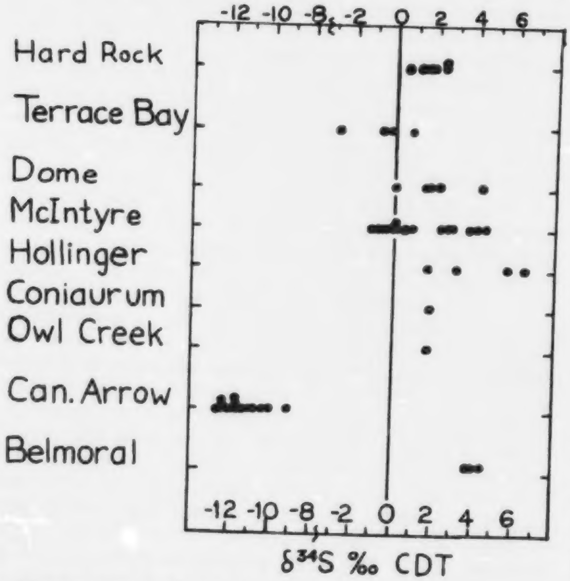

***Figure 202.1** Distribution of $\delta^{34}S$ values in pyrite from Archean gold deposits, Ontario.*

TERRACE BAY DEPOSIT

The Terrace Bay batholith is located on the north shore of Lake Superior, due south from Geraldton. While no major deposits have yet been developed in the area, it possesses many of the characteristics of a potential Au camp, and mineralization in the area has been extensively studied by Marmont (1984). The suite of samples analyzed here comes from a series of veins cutting a basalt flow, near a contact with the granodiorite phase of the batholith. The main interest in these pyrite samples arises from the striking differences in crystal habit which they exhibit. The samples are:

SM 519r	euhedral cubes of pyrite from metabasalt
SM 519v	vein cutting this rock, containing pitted (corroded) pyrite
SM 401	Au-bearing vein
SM 402	Au-bearing vein
JS 20	Coarse pyrite with visible gold

Where present, gold is exclusively found associated with the pitted variety of pyrite. The average of the auriferous samples is -0.7 ± 1.6‰; the single euhedral sample analyzed here is indistinguishable from the other samples, -0.2‰. Again, the average of all the pyrites, 0.8 ± 1.6‰, is close to igneous values, as might be expected from the close spatial association of these veins with the west end of the batholith, a zone of intense hydrothermal alteration.

MINES OF THE TIMMINS CAMP: DOME, HOLLINGER, AND MCINTYRE

These 3 deposits will be treated together as they are closely associated in space and style of deposition. In each mine there is a sequence of carbonatized and chloritized mafic to ultramafic volcanic rocks, intruded by silicic porphyries which are themselves highly altered. The samples analyzed in this study were largely collected by J.S. Springer of the OGS in a study of trace element and textural characteristics of gold-bearing pyrite. They do not represent an exhaustive sampling of any of these deposits, but were intended only to get the "flavour" of the $\delta^{34}S$ distributions at each deposit.

In the Dome, we analyzed a total of 5 samples (Table 202.1), representing various ore types encoun-

TABLE 202.1. SULPHUR ISOTOPE ANALYSES OF PYRITE SAMPLES FROM ARCHEAN GOLD DEPOSITS.

Sample Number	Description (locality)	$\delta^{34}S$ ‰,CDT	Log (Au) ppm
1. GERALDTON: Hard Rock Mine			
AJM 4B		2.1 ± 0.2	
AJM 6C		0.9 ± 0.2	
AJM 9B	A= replaces BIF	2.4 ± 0.4	
AJM 19A	B= vein cuts BIF	2.3 ± 0.1	
AJM 21C	C= in albite porphyry	2.0 ± 0.3	
AJM 36A		2.0 ± 0.2	
AJM 46B		1.4 ± 0.6	
AJM 59		3.6 ± 0.0	
2. TERRACE BAY			
SM 519 R	Qtz-py vein in metabasalt near granite contact:	-0.2	
SM 519 V	R = rock (euhedral py) V= vein (pitted py)	0.8	
SM 402 V		-2.9	
SM 401 V		-0.4	
JS 20(V)	Euhedral py with gold	-0.4	3.05
3. TIMMINS			
a) Dome Mine, 1200′ Level			
JS 5C	vein sulphides between V8/V10 flow; interflow	2.1	0.52
JS 6C	tourmaline zone, vein	1.4	-0.80
JS 7C	Preston porphyry, schistose	4.2	-1.30
JS 8C	sulphides in greenstone, cut by vein	2.1	-0.12
JS 9C	Preston porphyry	1.6	-1.04
b) McIntyre Mine			
JS 10C	stope 122907 platy porphyry	2.5	-0.32
JS 11C	stope 122907: vein margin	0.8	0.00
JS 12C	1250′ level: "barren py" in greenstone	2.7	-1.15
JS 13C	stope 125701: "Gold rich"	4.4	1.49
JS 14B	stope 122907: brassy py; chloritic vein	0.4	
JS 14C		2.2	-0.72
JS 15C	stope 122907: greyish	5.3 ± 1.1	0.78
MCI 1	stope 122907	-0.9	-0.62
MCI 2	do	-0.2	-0.68
MCI 3	do	-0.4	-0.72
MCI 4	do	-0.5	-0.52
MCI 5	do	-0.1	-1.05
MCI 6	do	-0.3	-1.24
MCI 7	do	-0.6	-1.00
MCI 8	do	-1.3	-0.92
MCI 9	do	-0.1	-0.43
MCI 10	do	3.6	1.04

Table 202.1 cont'd.

Sample Number	Description (locality)	$\delta^{34}S$ ‰CDT	Log (Au) ppm
c) Hollinger Mine			
JS 16C	1250′ level, stope 120702: fine vein py	5.5	0.57
JS 17C	Same stope: coarse py	1.6	0.60
JS 18C	1200 level: coarse py 10 m from porphyry in fissile greenstone	3.0	-1.52
JS 19C	same loc., fine py; 5 m from porphyry	6.3	-0.92
d) Coniaurum property			
JS 4	Euhedral py	1.7	-0.37
e) Owl Creek Pit			
JS 3C	several generations of py; free Au on qtz/graphite boundary	0.7	-0.38
4. MATHESON: Canadian Arrow Mine			
	(tj = trondhjemite; Q = vein; R = reddened rock; F = fresh rock)		
MC 1	white tj; q/carb vein; red halo		
Q		-11.7	
R		-11.9	
F		-10.1	
MC 14	reddened tj with qtz vein		
R		-12.4	
F		-12.6	
MC 19	pink tj, no halo; no py in vein		
Q		-11.5	
R		-12.2	
MC 21 F	red tj; q vein; no py in vein	-10.4	
MC 24 F	pale pink tj; no halo (early)	-10.1	
MC 25 F	grey tj, q vein; no halo	-12.3	
MC 26 F	fresh tj	-11.7	
MC 28 F	fresh tj	-9.2	
MC 34 F	red tj with q veins; no py in veins	-10.8	
Q		-12.4	
MC 47 F	reddened tj	-12.5	
R		-12.0	
MC 60-1	"felsite" (flow laminated diorite)	-6.0	
NORANDA: Belmoral Mine			
SM 7/VO	coarse py	4.0 ± 0.5	
SM 7/VO	rock	3.9	
JS 2C	auriferous py	4.5	1.71

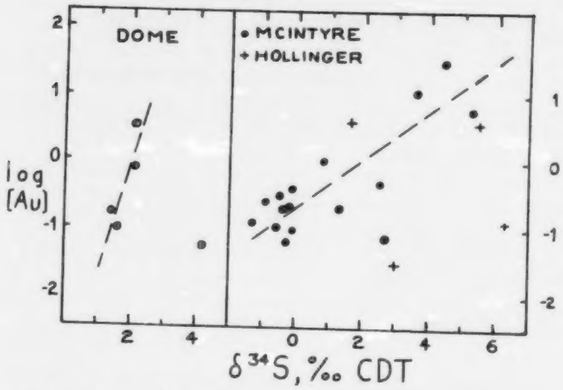

Figure 202.2 Correlation between $\delta^{34}S$ and gold content (log(Au, ppm)) in mines of the Timmins Camp: a) Dome; b) Hollinger and McIntyre.

tered on the 1200-foot level, including veins, sulphides disseminated in metabasalt, and schistose Preston porphyry. Pyrite from the metavolcanic rocks gave a mean value of 1.8 ±0.3 ‰, while one of the samples from the Preston porphyry (7C) gave a significantly higher value of 4.2‰.

One of the goals of this study was to test whether $\delta^{34}S$ is a possible indicator of (proxy for) Au content. In this case, we observed a poorly defined positive correlation between $\delta^{34}S$ and log(Au) (Figure 202.2a), suggesting that there was a tendency for more auriferous sulphides to be richer in ^{34}S. One of the analyses from the Preston porphyry diverges from this trend, having the lowest gold content of any of the samples analyzed here.

A similar relationship is seen, even more clearly, in the data from the McIntyre Mine (Figure 202.2b). There is a larger range in isotopic composition in this deposit, from -0.5 to +5.3‰, and a positive correlation between $\delta^{34}S$ and log(AU), although with a distinctively lower slope than that observed in the Dome Mine. The samples from the 1250-foot level tend to be generally richer in ^{34}S than those from the 2907-foot level, but both sets of samples define a single trend of $\delta^{34}S$ versus log(Au).

We do not at present understand the significance of these isotope/Au-grade trends, but they present an interesting potential guide to ore within a single vein system. It does not appear to be possible to extend these trends outside a single vein system. Indeed, and quite surprisingly, the samples from the Hollinger Mine do *not* show this correlation (Figure 202.2b) although they are presumably deposited from the same mega-plumbing system of hydrothermal veins as the McIntyre ores. Note, also, the strong tendency for the fine pyrite to be enriched in ^{34}S with respect to coarse pyrite in these Hollinger specimens.

One possible cause for the origin of the relatively high $\delta^{34}S$ values of some of these samples may be found in the presence in the McIntyre Mine of a zone enriched in anhydrite. While we have not yet analyzed the isotopic composition of this mineral, we might expect that it will be enriched in ^{34}S with respect to coexisting sulphide. We also note that the ores are closely associated with graphite-bearing interflow sediments. We might imagine a scenario in which the ore-forming fluid was first oxidized to form some ^{34}S-enriched sulphate, and that this sulphate, on encountering the graphitic sediments, was quantitatively reduced to sulphide, which either preserved the original ^{34}S-rich composition of the sulphate, or was mixed with light (^{34}S-depleted) sulphide.

Single samples were also analyzed from 2 other minor deposits of the Timmins camp, Owl Creek pit, and a surface exposure on the Coniaurum Property. Their $\delta^{34}S$ and Au values are similar to those of the samples from the McIntyre Mine.

CANADIAN ARROW DEPOSIT, MATHESON

This deposit consists of a series of pyritic quartz veins traversing a contact between trondhjemite and metabasalt. The trondhjemite exhibits a reddened halo adjacent to some of the veins while the rock adjacent to other veins (with a different structural trend) is comparatively fresh (Cherry 1983). The latter veins are cut by the former. Gold values are highest in the vicinity of the reddened, pyritic haloes and associated veins. The reddening is presumed to be due to oxidation of iron from the silicates of the trondhjemite, and might be inferred to be associated with elevated $f(O_2)$ in the hydrothermal fluid at the time of vein emplacement. The $\delta^{34}S$ data clearly support this inference (Table 202.1, Figure 202.3). All sulphides from this deposit are strikingly depleted in ^{34}S, as would be expected if a large proportion of the total sulphur in the hydrothermal fluid had been oxidized to sulphate. No anydrite or barite has been recognized in these veins, however. It is also striking that the depletion in ^{34}S is observed equally in the reddened and non-reddened vein systems, showing that the oxidation of the fluid occurred prior to its introduction into this vein system, and was equally intense whether or not there was a reddening of the wall rock (Figure 202.3). This is the only deposit in the present study in which ^{34}S-depleted sulphides are observed.

BELMORAL DEPOSIT, NORANDA

Only 1 sample form this deposit was analyzed. It is isotopically quite enriched (+4.4‰); 2 other analyses of the same sample yield similar values (Table 202.1). This sample plots on a log(Au) vs $\delta^{34}S$ diagram on the same trend as the McIntyre samples, which may be coincidental.

CONCLUSIONS

We have seen that the variation in $\delta^{34}S$ of pyrite from Archean gold deposits is much wider than could be accounted for by simple derivation of the sulphur from a single, homogeneous, "igneous" (mantle) source. To a first approximation there is a clear tendency for analyses to cluster between 0 and 2‰ (Figure 202.1), but many deposits exhibit intradeposit dispersion of $\delta^{34}S$ suggestive of either mixing with an extraneous sulphur source, or major isotopic fractionation. Further study of this phenomenon, focusing on a single, readily accessible deposit, is clearly called for. Unfortunately, the deposit which shows

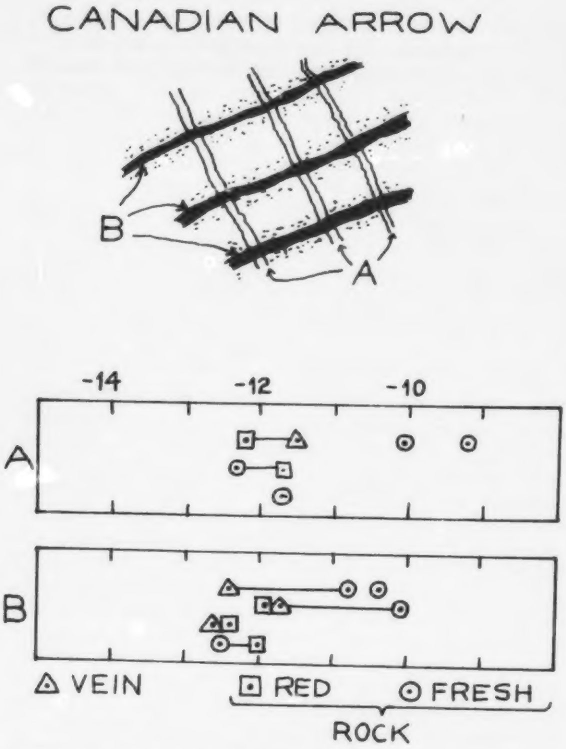

Figure 202.3 *Distribution of $\delta^{34}S$ values in the Canadian Arrow Deposit: A = earlier generation of quartz veins; B = later generation, associated with reddened haloes, and higher Au content.*

the correlation between $\delta^{34}S$ and Au most clearly (McIntyre) is no longer accessible. The role of redox equilibria in determining sulphur speciation is clearly defined in the Canadian Arrow case. We expect similar shifts to negative $\delta^{34}S$ values in other deposits exhibiting reddish alteration haloes. Whether this may also provide information about Au paragenesis (in relation to alteration) remains to be seen. In the Canadian Arrow example, all the samples studied (auriferous and barren) are uniformly ^{34}S-depleted.

ACKNOWLEDGMENTS

We acknowledge the assistance of the staff of the Mineral Deposits Section of the Ontario Geological Survey in providing us with samples and information on the geological relationships of the sample sites. We also are grateful to the sulphur isotope analysis laboratory at McMaster University for carrying out some of the analyses here. A. Fyon contributed valuable suggestions for the improvement of the manuscript, and has been continuously helpful in the execution of this study.

REFERENCES

Cherry, M.E.
1983: Felsic Intrusion Associated Lode Gold Deposits in the Matheson Area, Cochrane District; p.176-179 *in* The Geology of Gold in Ontario, edited by A.C. Colvine, Ontario Geological Survey, Miscellaneous Paper 110, 278p.

Lambert, I.B., Phillips, G.N., and Groves, D.I.
1984: Sulphur Isotope Compositions and Genesis of Archean Gold Mineralization, Australia and Zimbabwe; *in* Proceedings of the Symposium on Gold '82, Geological Society of Zimbabwe, Special Publication Number 1, A.A. Bulkema, Rotterdam, The Netherlands.

Lavigne, M.J., Jr.
1983: Geological, Geochemical and Sulphur Isotopic Investigations of Gold Mineralization and Sulfide Facies Banded Iron Formation at the Dickenson and Campbell Red Lake Mines, Red Lake, Ontario; Unpublished M.Sc. Thesis, McMaster University, Hamilton, Ontario.

Macdonald, A.J.
1984: Gold Mineralization in Ontario, I: The Role of Banded Iron Formation; p.412-430 *in* Chibougamou-Stratigraphy and Mineralization, edited by J. Guha and E.H. Chown, Canadian Institute of Mining and Metallurgy, Special Volume 34.

Marmont, Soussan
1984: The Terrace Bay Batholith and Associated Mineralization; Unpublished Report to Mineral Deposits Section, Ontario Geological Survey, 55p.

Ohmoto, H., and Rye, R.
1979: Isotopes of Sulfur and Carbon; p.509-567 *in* Geochemistry of Hydrothermal Ore Deposits, Volume 2, edited by H.L. Barnes, J. Wiley, New York.

Grant 205 Clay Mineralogy of Two Selected Carbonate Reservoirs in Southwestern Ontario

P.L. Churcher and M.B. Dusseault

Department of Earth Sciences, University of Waterloo

ABSTRACT

The importance of adequately defining the clay mineral distribution in hydrocarbon reservoirs has only recently been acknowledged. The presence of clay minerals in a reservoir can severely limit the effectiveness of an Enhanced Oil Recovery project. When foreign fluids are introduced into the reservoir, the clay minerals react by swelling *in situ*, dislodging and migrating to the pore throats, or by adsorbing chemical additives, thus limiting oil recovery or adding to the cost of production.

A study is underway to define the distribution and behaviour of clay minerals in 2 Silurian age carbonate reservoirs in southwestern Ontario. The 2 reservoirs being studied are the Fletcher patch reef and the Wilkesport pinnacle reef, both stratigraphically located in the Guelph Formation.

Four complete cores were logged and thin sections were made to define the facies distributions within the 2 reservoirs. Samples were then chosen for a preliminary X-ray diffraction and scanning electron microscope study aimed at delineating the clay minerals present in each facies. Since the study is at an early stage, this report will cover only the results of the facies mapping and preliminary scanning electron microscope phases of the project.

INTRODUCTION

Enhanced Oil Recovery (EOR) techniques may be employed in Ontario to recover a significant percentage of the estimated 100 x 10^6 m^3 of oil remaining in depleted and partially depleted carbonate reservoirs. It is estimated that only 10% to 30% of the original oil in place is produced during the primary recovery phase of any reservoir's history. This leaves a valuable untapped resource underground. In order to maintain Canada in energy self sufficiency, researchers must learn to develop new EOR techniques to meet the special problems that carbonate reservoirs pose. To implement proper planning for EOR requires some fundamental reservoir geological parameters, among the most important of which are clay content and behaviour. All reservoirs contain some amount of clay minerals which can have a dramatic effect on reservoir performance. Clay minerals are sensitive to foreign fluids introduced to the reservoir and react by either breaking free and migrating, usually getting lodged in the narrow pore throats, by swelling *in situ*, or by adsorbing the chemical additives. The result is usually a drop in permeability, and thus a drop in production. Clay minerals are particularly abundant in sandstone reservoirs (Berea, Cardium, etc.), but are also found in carbonate reservoirs as detrital grains or authigenic precipitates. This is especially true if the primary sediment is highly argillaceous. Diagenetic events have been observed by the authors in carbonates of Ordovician age which appear to result in the reprecipitation of the clays as authigenic constituents in the pore space between dolomite rhombs.

Very little is known about clay mineral speciation and distribution in carbonates, and to the best of the authors' knowledge there has been virtually no work done on the clay mineralogy of carbonate reservoirs in Ontario.

The objectives of this study are to define the distribution, type, and relative abundance of clay minerals in 2 selected reservoirs in southwestern Ontario. This project is being undertaken on a facies specific basis in order to define any relationships which may exist between clay mineral speciation and depositional environment. It is postulated that the original depositional environment may have not only controlled the clay mineral species deposited as detrital grains, but may also have controlled the pathways for migration of diagenetic fluids capable of precipitating authigenic clay minerals in the pore space. If relative amounts of different clay species can be correlated to specific facies, this may represent a useful tool for visually evaluating oil and gas reservoirs of this age for EOR potential.

As this study is in progress, the contents of this first report will cover only what has been accomplished to date.

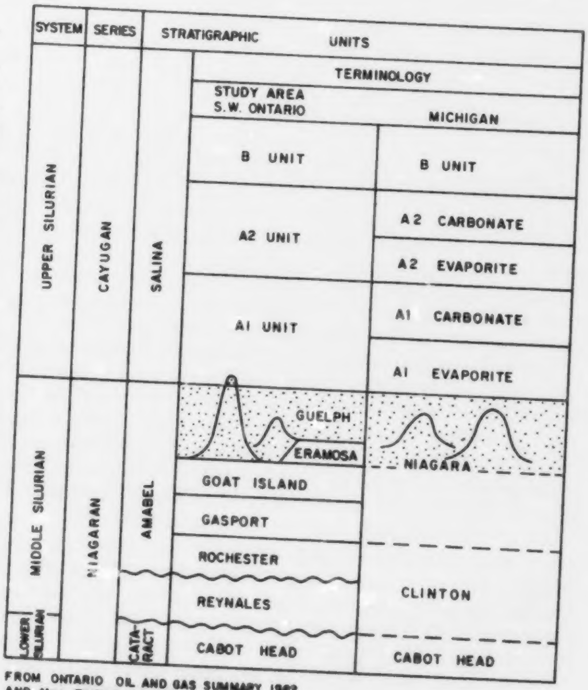

FROM ONTARIO OIL AND GAS SUMMARY 1982 AND MSc THESIS (PEARSON, 1980)

Figure 205.1 Generalized stratigraphic column for the Michigan basin.

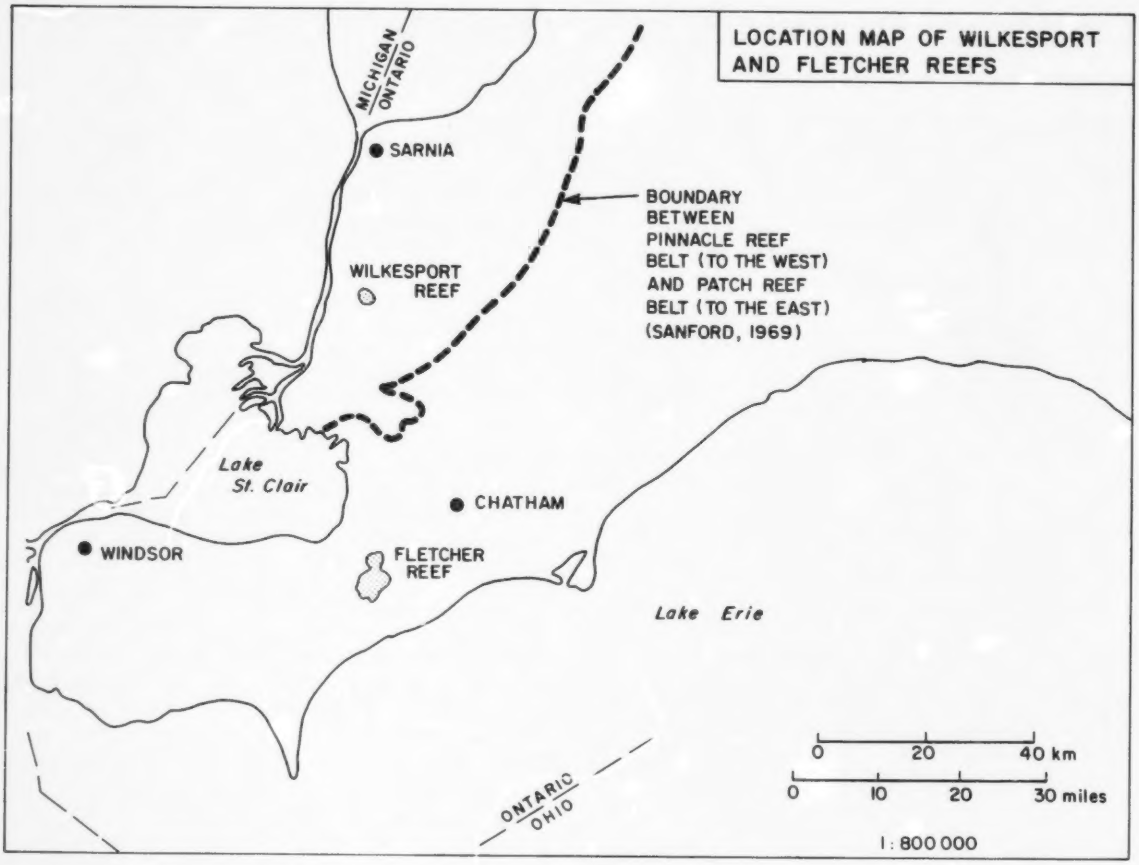
LOCATION MAP OF WILKESPORT AND FLETCHER REEFS
MICHIGAN
ONTARIO
SARNIA
BOUNDARY BETWEEN PINNACLE REEF BELT (TO THE WEST) AND PATCH REEF BELT (TO THE EAST) (SANFORD, 1969)
WILKESPORT REEF
Lake St. Clair
CHATHAM
WINDSOR
FLETCHER REEF
Lake Erie
0
20
40 km
0
10
20
30 miles
1 : 800 000
ONTARIO
OHIO

Figure 205.2 Location map.

BACKGROUND INFORMATION AND GEOLOGY

There are numerous carbonate reservoirs, ranging in age from Cambrian to Devonian, on the Ontario side of the Michigan basin which produce oil and gas. It was decided that only 2 Silurian reservoirs would be studied in detail. The 2 reservoirs chosen were the Fletcher patch reef and the Wilkesport pinnacle reef, both of which are stratigraphically located in the Guelph Formation (Figure 205.1). The 2 different types of reef were chosen because the vast majority of carbonate reservoirs in southwestern Ontario are of one type or the other. The 2 fields were selected based on the availability of diamond-drill core, company reports, well logs, and core analysis data which will be incorporated into the final synthesis.

The Fletcher Field, located in Kent County (Raleigh and Tilbury East Townships, Figures 205.2 and 205.3), produced 190 794.6 m^3 of oil, mostly between the years 1905 and 1915. The field was then abandoned until 1982 when Consumers' Gas began work once again on the play. Eleven development holes were drilled and cored to define any further primary production and the EOR potential of the reservoir. It was discovered that the primary production had not only been from the A-1 carbonate, but that there was also production coming from the dolomitized reef core itself. Results of the study conducted on this reservoir are still pending.

The Wilkesport pinnacle reef, located in Lambton County (Sombra Township, Figures 205.2 and 205.4), produced 567.3 m^3 of oil and 237 105.4 x 10^3 m^3 of natural gas since its discovery in 1965 (Habib and Trevail 1984). In 1978 the reservoir was redesignated for gas storage. The value of a gas reservoir, such as the Wilkesport, is increased by a factor of 12 when it is redesigned as a gas storage facility (R.A. Trevail, Senior Petroleum Geologist, Petroleum Resources Laboratory, London, Ontario, personal communication). Keeping this in mind, it is unlikely that any EOR scheme will ever be implemented. However, the reservoir still serves as a medium for study because it is considered to be a typical pinnacle reef. The reservoir consists of a dolomitized reef top and base, and a limestone core, with an impermeable anhydrite cap.

APPROACH AND RESULTS TO DATE

Three cores, totalling 62 m in length, were obtained for study from the Fletcher Field, and one complete core, totalling 116 m was obtained from the Wilkesport reef. The cores were slabbed (axially) to facilitate core logging and sample acquisition. They were then geologically logged and over 40 thin sec-

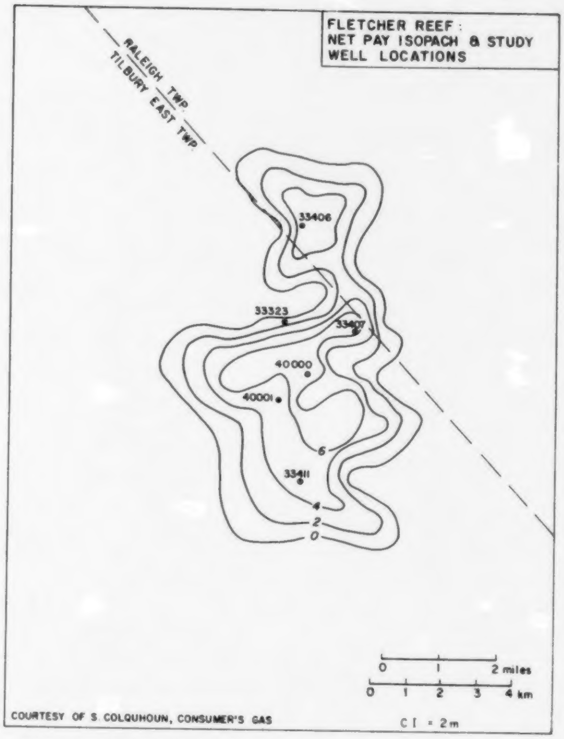

COURTESY OF S. COLQUHOUN, CONSUMER'S GAS

Figure 205.3 *Isopach map of the reef net pay, Fletcher Field.*

tions were cut and stained with alizarin red solution in order to determine the facies distribution and the degree of dolomitization in each reservoir. In addition to the normal parameters obtained during core logging (fossil type and relative abundance, sedimentary structure, lithology, etc.), notes were made regarding stylolite type (Wanless 1984). The nature of the dolomitization in the Fletcher Field also allowed the authors to log stylolite concentration per metre. In the absence of argillaceous material (indicated by the gamma response), stylolite type and concentration are believed to be directly related to the "graininess" of the original sediment before diagenesis. The importance of this will be made clear when details of the facies distribution are discussed. The results of this phase of the study are illustrated in Figures 205.5 and 205.6. For simplicity, only 1 section from each field is presented.

The facies distribution in the Fletcher Field is simple, and although the reservoir has been extensively dolomitized, fossil remains and structures were still readily discernible in the core. The following is a general description of each of the 4 main facies. The A-1 carbonate represents a supratidal/tidal flat facies consisting of pelletal grainstones and algal mats. The unit is virtually devoid of fossils, probably due to highly saline conditions believed to be prevalent at the time of its deposition. Stylolites present in the A-1 are generally flat and anastomosing. They are relatively abundant due to the large amount of argillaceous material in the original sediment, as evidenced by the gamma log response. The Guelph-A-1 contact is indicated by the presence of a series of green "shale" beds which produce a pronounced spike on the gamma log. This green "shale" has been interpreted by some authors to represent an erosional unconformity. The authors believe that new evidence brought forth by Wanless (1984), regarding the Muav Limestone in Arizona may indicate that this layer is simply the end result of concentrated pressure solution at the contact between a relatively argillaceous unit (the A-1 carbonate) and a non-argillaceous unit (the Guelph Formation). The evidence for this is the fact that these so-called "shale" beds grade laterally into stylolites, and contain remnant pods of dolomitized parent material. These pods are thought to represent the only material remaining of a once more extensive unit destroyed by progressive and intense pressure solution (Wanless 1984). Further work will refine the nature of this contact.

Directly below the contact, the first facies encountered in the Guelph Formation is a lagoonal facies. The fossil assemblage consists of pelecypods, gastropods, brachiopods, and algae, all of which appear to be floating in a "sea" of dolomitized micrite. The stylolite concentration is much lower than the overlying A-1 carbonate, and the type is transitional between the flat and jagged forms. Below this layer lies a zone which has been interpreted as a deeper water lagoon (S. Colquhoun, Consumers' Gas, personal communication). It is believed that this facies represents a micritized reef top/lagoonal facies which was the result of an imbalance of destructive over constructive forces after the reef ceased to grow. The evidence for this interpretation is the lack of extensive burrowing in the facies as compared to the upper lagoon, the presence of the first stromatoporoid fragments, which appear to be randomly oriented and extensively bioeroded by boring sponges and possibly algae, and by the rapid change in stylolite concentration and type in this zone. The gamma log indicates the amount of shaley/argillaceous material is less, therefore, this change in stylolite concentration is believed to be due to an increase in the grain to grain contacts. In other words, there is evidence that the facies has changed from a predominantly mudstone/wackestone to a grainstone, although this is difficult to verify visually because of the degree of dolomitization. Below this zone lies the true reef core facies with its high faunal content and diversity. Fossils in this zone consist of tabulate corals, globular, tabular, and hemispherical stromatoporoids, cladopora, rugosa, and brachiopod/shell debris. There appears to be no distinct zoning in this unit that would warrant futher division into subfacies.

The facies distribution in the Wilkesport pinnacle reef is considerably more complex than that of the Fletcher reef. There have been numerous papers written describing the facies found in pinnacle reefs of the Michigan basin. So as to not belabour this subject, the authors suggest reference to Gill (1977), or Balogh (1981) to obtain details regarding the facies delineated in Figure 205.6. The only difference between the Wilkesport and many of the other reefs is the fact that it lacks a massive stromatoporoid facies and that it has a distinct calcarenite basal unit,

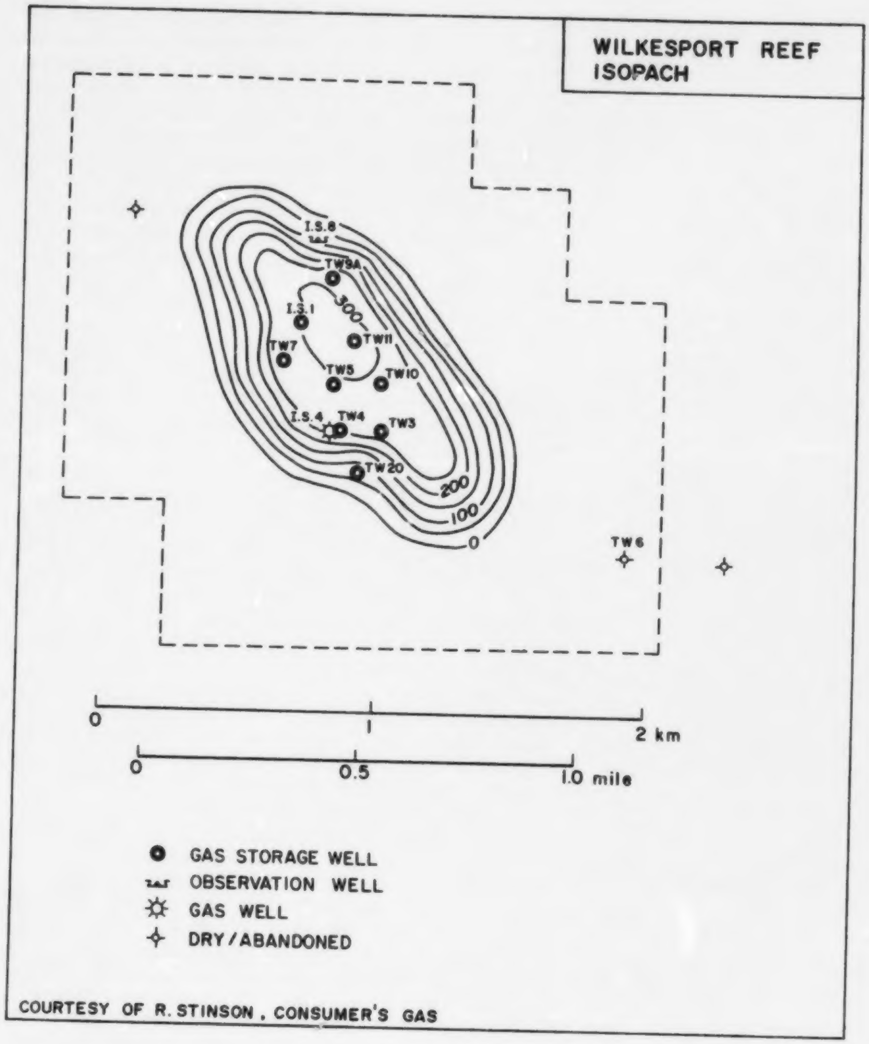
WILKESPORT REEF
ISOPACH
I.S.8
TW9A
I.S.1
300
TW11
TW7
TW5
TW10
I.S.4
TW4
TW3
TW20
200
100
0
TW6
0
1
2 km
0
0.5
1.0 mile
GAS STORAGE WELL
OBSERVATION WELL
GAS WELL
DRY/ABANDONED
COURTESY OF R. STINSON, CONSUMER'S GAS

Figure 205.4 Isopach map, Wilkesport pinnacle reef.

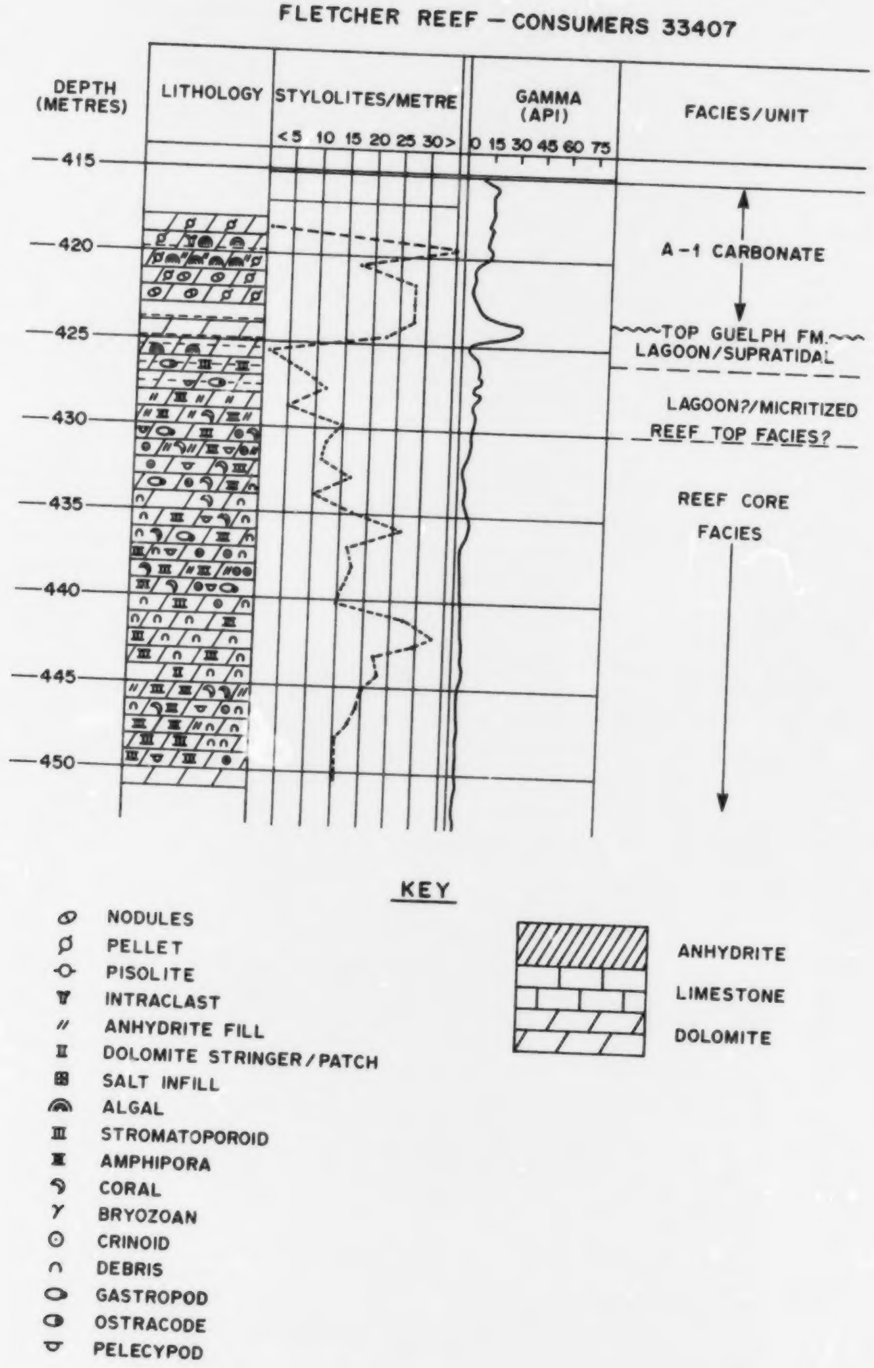

Figure 205.5 Results of the core logging and geophysical well log correlation, Fletcher Field.

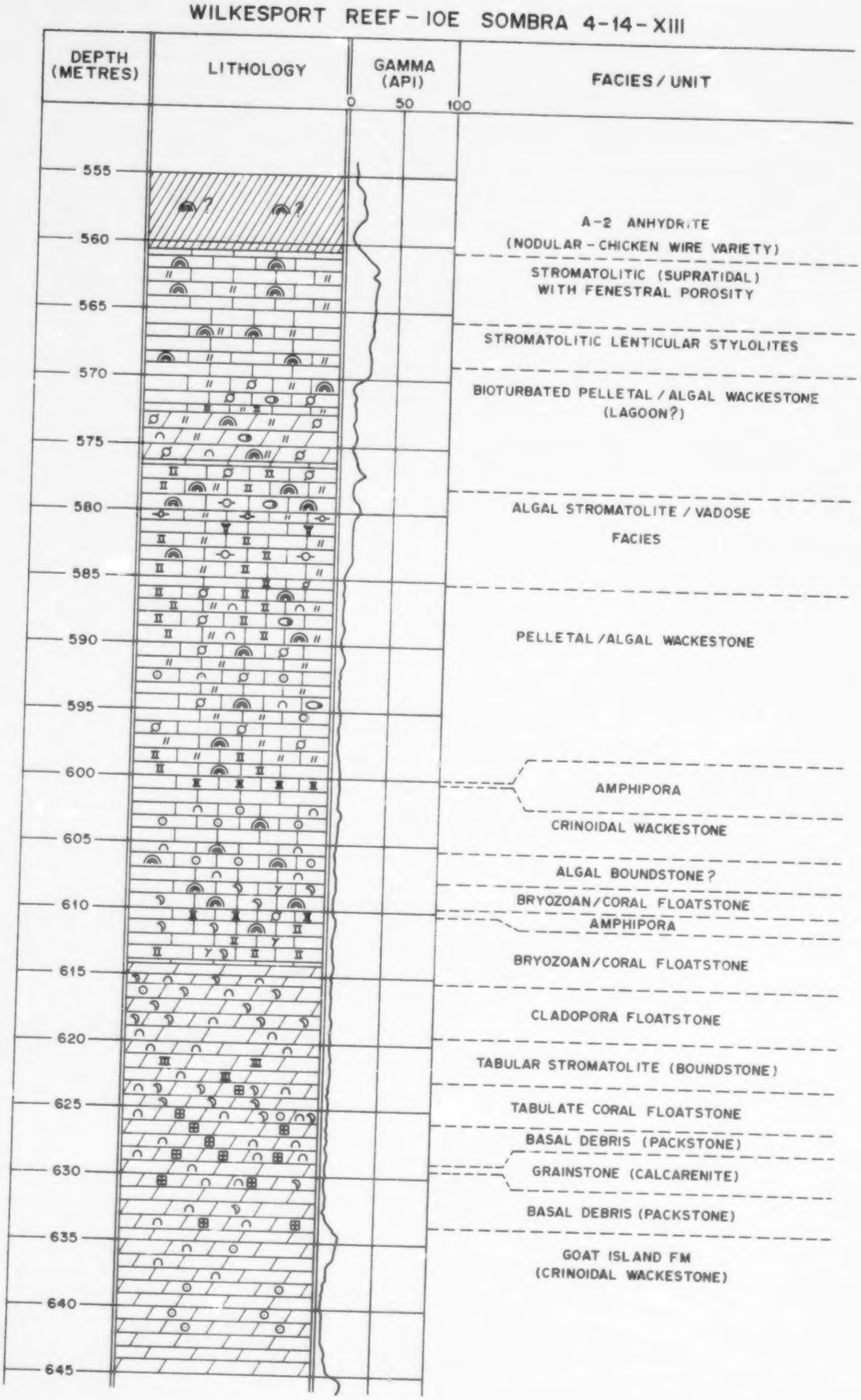
WILKESPORT REEF - IOE SOMBRA 4-14-XIII
DEPTH (METRES)
LITHOLOGY
GAMMA (API)
0
50
100
FACIES / UNIT
555
560
565
570
575
580
585
590
595
600
605
610
615
620
625
630
635
640
645
A-2 ANHYDRITE (NODULAR - CHICKEN WIRE VARIETY)
STROMATOLITIC (SUPRATIDAL) WITH FENESTRAL POROSITY
STROMATOLITIC LENTICULAR STYLOLITES
BIOTURBATED PELLETAL / ALGAL WACKESTONE (LAGOON?)
ALGAL STROMATOLITE / VADOSE FACIES
PELLETAL / ALGAL WACKESTONE
AMPHIPORA
CRINOIDAL WACKESTONE
ALGAL BOUNDSTONE?
BRYOZOAN/CORAL FLOATSTONE
AMPHIPORA
BRYOZOAN/CORAL FLOATSTONE
CLADOPORA FLOATSTONE
TABULAR STROMATOLITE (BOUNDSTONE)
TABULATE CORAL FLOATSTONE
BASAL DEBRIS (PACKSTONE)
GRAINSTONE (CALCARENITE)
BASAL DEBRIS (PACKSTONE)
GOAT ISLAND FM (CRINOIDAL WACKESTONE)

Figure 205.6 *Results of the core logging and geophysical well log correlation, Wilkesport pinnacle reef.*

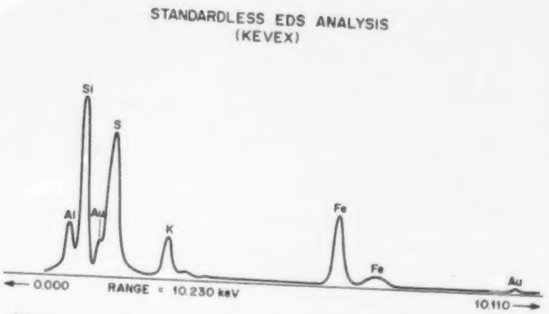

Figure 205.7 *Typical KEVEX response trace indicating the presence of illite in the sample by the relative magnitudes of the Al, Si, and K peaks.*

which is interpreted as a carbonate shoal. In all other respects the reef is similar to the Belle River Mills or Ray reef in Michigan (Balogh 1981).

The detailed core logging was a vital phase of the project for it was with this geological description that a sampling scheme could rationally be developed. A preliminary set of samples representing each facies was obtained from the core for the X-ray diffraction phase of the study. Representative cuttings were retained from these samples for work to be done at a later date on the scanning electron microscope. The samples were cleaned with distilled water and acetone to remove surface contamination, crushed to -60 mesh, and then solvent extracted to remove hydrocarbons which would reduce the efficiency of the acid attack and the sharpness of the X-ray diffraction response. The samples were then acidified in a buffered solution to free the clay minerals from the host carbonate. The method followed was designed to reduce the risk of damage to the clay minerals themselves, details of which may be found in Ostrom (1961). The results of this preliminary X-ray diffraction study are not available for publishing at this time.

In addition to the X-ray diffraction work, a limited scanning electron microscope and KEVEX Elemental analysis study was conducted on 14 selected cuttings. Preliminary findings indicate the presence of illite and possibly chlorite in the stylolites. Figure 205.7 shows a typical KEVEX response plot. The presence of the clay mineral illite is indicated by the Al, Si, and K peaks, and by its classical whispy form shown in Photo 205.1. The iron and sulphur peaks on the KEVEX trace are due to disseminated sulphides. The illite in the photograph was found outside the stylolite in pore space and is believed to be authigenic, possibly remobilized by pressure solution. It is, however, still too early in this project to say anything conclusive regarding the clay mineral content and distribution.

FUTURE WORK

The project activity was initiated in September 1984, and a considerable amount of work is to be done before its scheduled completion date of May 1986. An additional 55 X-ray diffraction analyses will be performed to provide an adequate data base on which conclusions can be based. In addition to this, scanning electron microscope and KEVEX studies will be conducted to refine the results obtained from the X-ray diffraction traces. It is the authors' hope that this project will provide a valuable starting point for future work that needs to be done on the clay minerals of other carbonate reservoirs being considered for EOR projects. Only by adequately defining the materials encountered can a successful EOR project be designed and implemented.

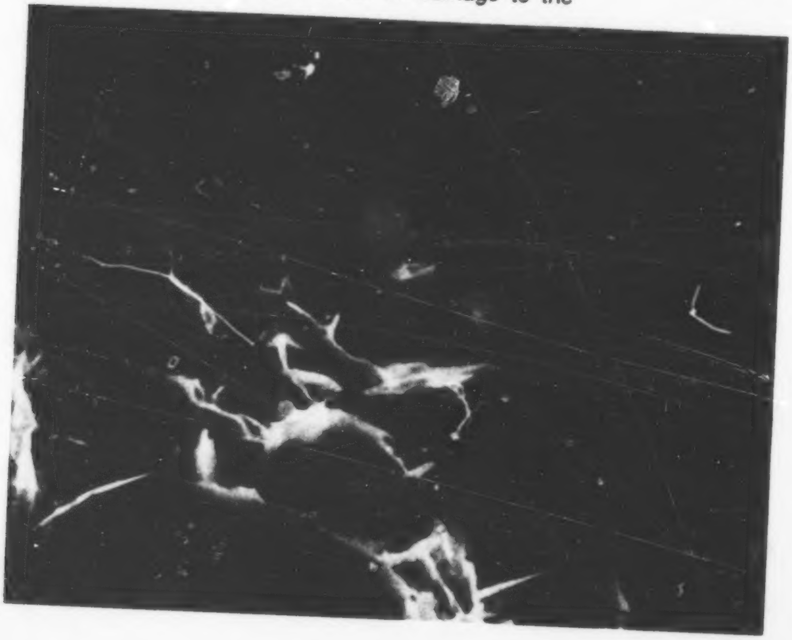

Photo 205.1 *Scanning electron photomicrograph showing whispy illite in the pore space outside of a stylolite. Magnification: x 1800. Scale bar represents 10 micrometres.*

ACKNOWLEDGMENTS

The authors would like to thank Mr. R.A. Trevail, Senior Petroleum Geologist, Petroleum Resources Laboratory, London, Ontario, and S. Colquhoun, R. Stinson, and R. Craig, of Consumers' Gas, Scarborough, Ontario, for assistance in the project.

REFERENCES

Balogh, R.J.
1981: A Study of the Middle Silurian Belle River Mills, Peters, and Ray Pinnacle Reefs from the Michigan Basin; Unpublished M.Sc. Thesis, Bowling Green State University, 202p.

Gill, D.
1977: The Belle River Mills Gas Field: Productive Niagaran Reefs Enclosed by Sabkha Deposits, Michigan Basin; Michigan Basin Geological Society, Special Papers Number 2, 187p.

Habib, H.E., and Trevail, R.A.
1984: Oil and Gas Exploration, Drilling and Production Summary, 1982; Ontario Ministry of Natural Resources, Oil and Gas Paper Number 5, 216p.

Ostrom, M.E.
1961: Separation of Clay Minerals from Carbonate Rocks by Using Acid; Journal of Sedimentary Petrology. Volume 31, Number 1, p.123-129.

Pearson, E.M.
1980: Sedimentology and Diagenesis of the Warwick Reef (Silurian), Lambton County, Southwestern Ontario; Unpublished M.Sc. Thesis, University of Waterloo, 302p.

Sanford, B.V.
1969: Silurian of Southwestern Ontario; *in* Ontario Petroleum Institute, 9th Annual Conference, Technical Paper Number 5.

Wanless, H.R.
1984: Burial Diagenesis in Limestone; *in* Sediment Diagenesis, edited by A. Parker and B.W. Sellwood, Proceedings of the NATO Advanced Study Institute on Sediment Diagnesis, Reading, United Kingdom, July 12-15, 1981.

Grant 216 Sedimentology of the Long Rapids Formation, Preliminary Results

R.K.A. Bezys and M.J. Risk

Geology Department, McMaster University

ABSTRACT

In order to determine the paleoecology of the Moose River Basin during the Upper Devonian, carbon isotope and organic carbon analyses were obtained for shale samples from the Long Rapids Formation. Distribution of ichnofauna (trace fossils) were also used to help correlate any trends through the different lithologies. The evidence suggests a marine origin for the shales, but isotopic signatures give evidence of a terrestrial source for the organic carbon. The organic material may originally have been enriched in ^{13}C, but with time and diagenetic alterations (biological and non-biological), depletion in ^{13}C possibly occurred. A marine setting is still proposed for the environment of deposition, but isotopic fractionation has altered the final signatures.

The cyclic stratification found in these shales may be caused by a variety of mechanisms. One possible mechanism is the seiching model that explains oxygen fluctuations due to turbidity currents elsewhere in the basin. The organic richness in these sediments may have been caused by high surface productivity of the water column, floating mats of vegetation, or large storms.

INTRODUCTION

The Long Rapids shale of the Moose River Basin (Figure 216.1) has been correlated with similar Upper Devonian deposits in the Illinois, Michigan, and Appalachian Basins. The Long Rapids shale is considered as a possible source of shale oil. The formation consists of alternating beds of brownish black shale and greenish grey shales/mudstones with scattered concretionary horizons. Bioturbation is abundant in the greenish grey lithologies, but rare in the dark shales. Body fossils are also rare, though the greatest abundances occur in the lighter coloured beds.

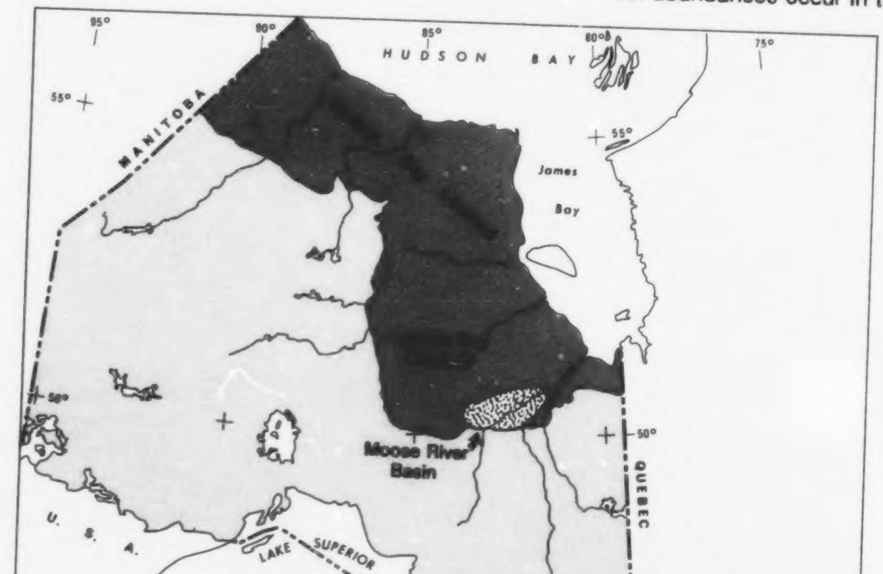

Figure 216.1. *Location map, showing the position of the Moose River Basin. From Telford and Verma (1982).*

Total organic carbon content values were determined for some of these units, and carbon isotope analysis was done, as an aid in determining the source of organic matter. Identifying the organic matter type will help in reconstruction of the paleoenvironment. Early workers have interpreted the basin to be overlain by an epicontinental sea in Devonian times. The sediments deposited in this area are, therefore, marine, as suggested by the presence of marine body fossils. Numerous trace fossils occur at specific horizons, and their inter-relationships have helped in the paleobathymetric reconstruction.

The cyclicity of the black and greenish grey units suggests an epicontinental sea environment with shallow-to- moderate depths. The facies changes are probably caused by oxygen fluctuations, and several models have been proposed to explain the variations in oxygen. One such model, the seiching model, suggests that turbidity currents in the basin caused a surge of oxygenated water elsewhere. Other hypotheses include floating mats of vegetation that increased organic matter content of the water column, or storms that brought in large amounts of organic detritus. Increased productivity of the overlying water column may also have contributed to the organic matter amount and type.

An understanding of the paleoecology of the Long Rapids Formation is critical to our understanding of the history of this Upper Devonian sedimentary basin.

GEOLOGY

SETTING

Devonian rocks occur in 2 separate areas of the Hudson Bay Platform in northern Ontario. One area, the Moose River Basin, is located in the James Bay Lowlands, the southern part of the Hudson Bay Lowlands (Figure 216.1). The second area, the Hudson Bay Basin, is completely covered by water and was discovered by drilling (Sanford and Norris 1975).

Early investigations in the area, over a century ago, were concerned with deposits of lignite, fireclay, kaolin, silica sand, gypsum, and iron. Although interest in the region has been keen, a complete study of the entire area has never been undertaken, due largely to inaccessibility, lack of good outcrop exposures, and high costs.

Drilling has been the easiest method of obtaining data, but has its difficulties. Due to the swampiness of the terrain in the summer months, and the extreme cold of the winter, there are no easy solutions. Winter drilling is usually easier technically, but accessibility and housing for work crews are problems.

STRATIGRAPHY

Depending on the locality, Upper Devonian strata in the Moose River Basin overlie Middle Devonian rocks, both conformably and unconformably, and in turn are overlain by Cretaceous sediments. The formation name, Long Rapids, was first introduced by Savage and Van Tuyl (1916, 1919). These early workers were sponsored by the University of Illinois, and based their interpretations on outcrop exposures along the Abitibi and Moose Rivers. Dyer (1931, 1932) summarized the results of the first drillhole to penetrate the entire sedimentary section in the Moose River Basin (Onakawana Drillhole "A"). In March, 1985, Onakawana Drillhole "B" was drilled by the Ontario Geological Survey in the same location as Onakawana Drillhole "A".

Dyer and Crozier (1933) subdivided the Long Rapids Formation into 3 members:

Upper Member: Interbedded pale greenish grey clay and grey shale.

Middle Member: Dark-grey bituminous shale with thin bands of greenish grey clay.

Lower Member: Pale greenish grey to grey shaley clays with bands of dark black shale and abundant hard concretionary layers and nodules (compared to upper members).

The Long Rapids Section in the Onakawana Drillhole "B" was approximately 80 m thick and could be subdivided into these 3 members. Outcrops of Long Rapids rocks are rare in the basin and only one, located on the east bank of the Abitibi River at Williams Island, is mappable. Its base sits on identifiable Middle Devonian carbonates, and therefore a proper stratigraphic section can be erected. The approximately 35 m of section exposed at the location can be correlated with Dyer and Crozier's (1933) Lower Member.

SEDIMENTOLOGY

The dominant lithology of the Long Rapids Formation is shale. The colours vary from black to brownish black to greenish grey. Shale (Blatt 1982) is a fissile mudrock with various silt percentages. Mudstones and claystones can also possess similar amounts of silt, but do not have a fissile nature.

In outcrop, the black shales are very fissile, and in some places are cut by long, near-vertical joints (up to 1 m long). In core, the shales are massive and fracture subconchoidally. The dark colour of the rock is due to the presence of organic matter, but not necessarily due to the percentage of organic matter. The colour difference may be due to the nature of the organic material itself (refractory or labile; Goldhaber 1978). Other constituents include clay-sized quartz, pyrite, mica, illite, and chlorite. X-ray fluorescence spectroscopy (XRF) and X-ray diffraction (XRD) analyses will be conducted to identify and determine percentages of these constituents. Lamination in the shales (which leads to fissility), is due to quartz-rich, clay-rich, and organic-rich layers $\leq$ 1 mm in thickness. The lighter coloured lithologies (greenish grey) are similar in grain size and sedimentology to the darker shales, but lack the organic matter content and fissility.

The lower member of the formation has abundant calcareous beds and nodules (Photo 216.1). Calcite is the dominant carbonate mineral in concretionary layers, although dolomite crystals have been found inside calcite nodules. Many of these calcareous horizons and nodules cap green shales or mudstones and may be sharply overlain by black shales. The sequence may then repeat itself (Figure 216.2). The hard concretionary horizons vary in colour from mottled grey to white. Abundant pellets and shell frag-

Photo 216.1. *Pinch-and-swell nature of concretionary horizons. Hammer for scale.*

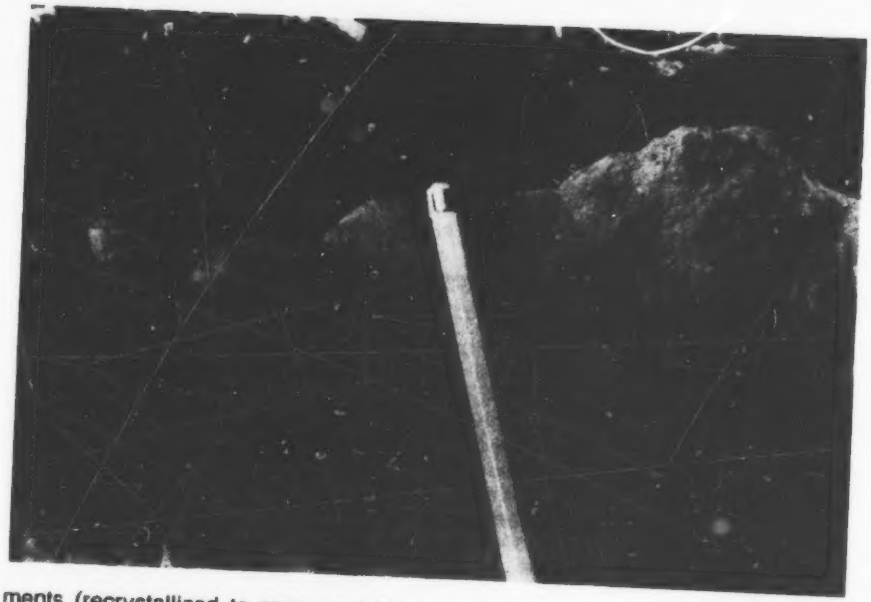

Photo 216.2. *Goniatite (Manticoceras sp.) in concretionary layer. Pen for scale.*

ments (recrystallized to sparry calcite) were seen in this section (Figure 216.3).

Some greenish grey beds contain abundant goniatite remains (*Manticoceras*) that range in size from 3 to 5 cm (Photo 216.2). One bivalve shell (*Pectin*) and plant remains were discovered in a hard concretionary unit. Rare coal seams (up to 0.5 cm thick) were found also.

METHODOLOGY

SAMPLING PROCEDURES

Samples of Long Rapids rocks were taken from the Abitibi River outcrop during a detailed mapping of the outcrop section (36 m) in September 1984. In total, approximately 160 samples were obtained from the site.

ANALYTICAL PROCEDURES

All samples were crushed manually and then in a shatter box in a tungsten carbide container. Samples that were analyzed for total organic carbon values were treated initially with heated 20% hydrochloric acid to dissolve any carbonates. The samples were then filtered through 0.45μ filters. The filtrate and filter paper were placed in a LECO crucible and allowed to dry completely. A LECO carbon determinator was used for total organic carbon (TOC) values.

Samples were prepared in a similar manner for carbon isotope analyses. The samples were acid and

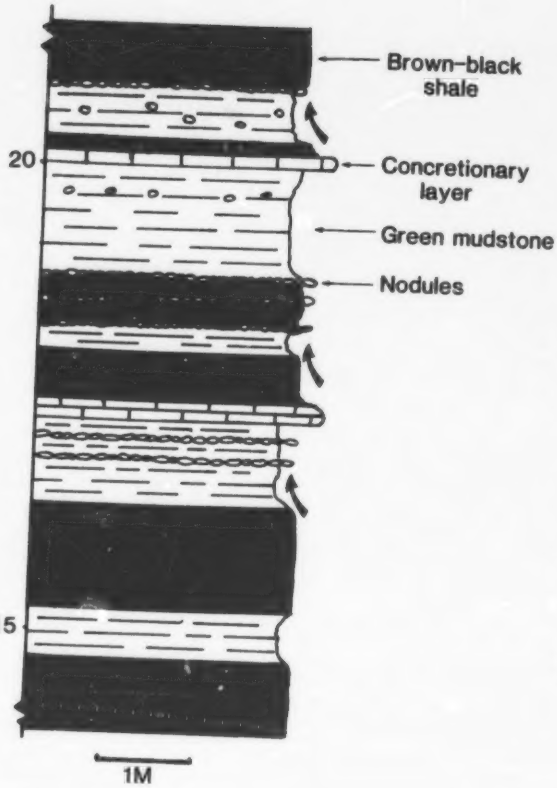

Figure 216.2. *Typical facies sequence for the Long Rapids Formation, showing succession of black shale, greenish-grey mudstone, and concretionary layer.*

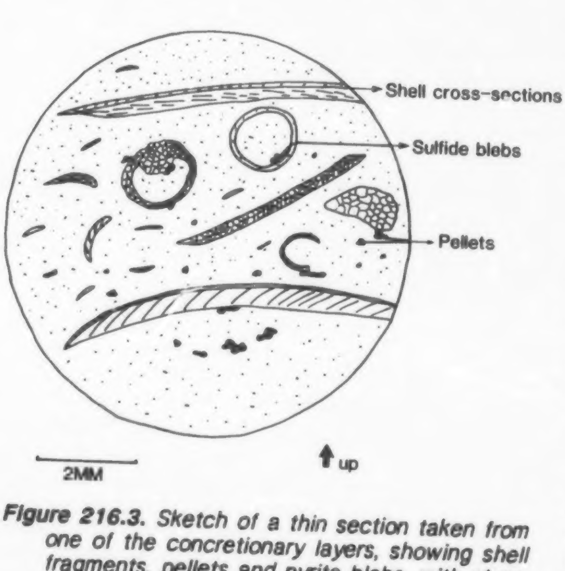

Figure 216.3. *Sketch of a thin section taken from one of the concretionary layers, showing shell fragments, pellets and pyrite blebs, with abundant sparry calcite infill and micritic matrix.*

TABLE 216.1. CARBON ISOTOPE AND ORGANIC CARBON COMPOSITION.

SAMPLE NUMBER	$\delta^{13}C$ (%)	C_{TOC}(%)
10-2-Db	-30.00	-
10-2-Dbx	-29.85	2.10
11-5-Ea	-29.60	-
11-5-Eax	-29.62	0.79
11-8-Ec	-30.32	2.02
12-2-Fa	-29.73	0.90
12-5-Fa	-30.36	4.12
12-9-Fa	-29.33	0.56
19-1-Ma	-25.29	0.76
Coal fragment	-22.90	-
Plant fragment	-22.67	-

water washed, but not filtered. The residue was allowed to dry and then weighed out into a 10 mm quartz tube with some cupric oxide wire. The tubes were placed under a vacuum, evacuated, and then sealed off. The tubes were heated for 2 hours at 900°C. Carbon isotope values were then determined on a Micromass 602D mass spectrometer. All $\delta^{13}C$ isotope data are expressed relative to the Pee Dee Belemnite (PDB) standard and have the δ-notation:

$$\delta^{13}C_{PDB}\ 0/100 = 1000\left[\frac{(^{13}C/^{12}C)\ \mathrm{SAMP}}{(^{13}C/^{12}C)\ \mathrm{std}}\right]^{-1}$$

Standard is Pee Dee formation Belemnite (PDB).

CARBON ISOTOPE COMPOSITION

Marine (sapropelic) organic matter contains hydrogen-rich aliphatic compounds that are a likely source of petroleum, or will yield greater volumes of shale oil upon pyrolysis. Carbon isotope analysis of the organic matter in the shale can help identify the organic type.

The bulk of the plant kingdom (C_3 - pathway) has $\delta^{13}C$ values between -24 to -37‰ (mean -27‰), whereas aquatic plants (CAM - pathway) have values of -9 to -19‰ (mean -17‰). C_4 - pathway plants have values ranging from -9 to -16‰ (mean -12‰) and algae have values from -12 to -22‰ (Hoefs 1980). Natural marine phytoplankton populations vary in $\delta^{13}C$ values, due to different water surface temperatures; $\delta^{13}C$ values for plankton at 2°C is about -30‰, and at 15°C the $\delta^{13}C$ values increase to about -20‰ (Sackett *et al.*, *in* Hoefs 1980).

The $\delta^{13}C$ values of the total organic carbon of 9 samples of Long Rapids shale range from -25.29‰ to -30.36‰ with a mean of -29.42‰ (Table 216.1). Coal and plant samples were also analyzed, and had values of -22.90‰ and -22.67‰ respectively. These shale samples are depleted in ^{13}C as compared to organic matter in modern marine sediments. An average value of -21‰ was recorded for modern marine sediments in Atlantic Ocean sediments by Sackett (1964). The Long Rapids values suggest a terrestrial input for the organic matter, yet paleoecologically that is unlikely since the shales are interpreted to be marine. Other possibilities for this isotopic shift may be diagenetic processes or contamination of the sediment.

Hailer *et al.* (1983) obtained similar carbon isotope results on the Upper Devonian New Albany Shale. The formation consists mainly of black shale horizons with intermittent green mudstone beds. Carbon isotope values for 137 samples ranged from -24.5 to -31.0‰, with a median value of -29.35‰. These shales are also paleoecologically interpreted to be marine, and yet have depleted isotope values. Quiescent, warm, and productive conditions are thought to have existed in the Illinois Basin where the shale was deposited, and these conditions would not have caused extreme photosynthetic fractionations that would result in large ^{13}C depletions. The authors suggest that diagenetic alteration of carbon isotope abundances is the most likely cause of the observed depletion of ^{13}C.

Ancient marine sedimentary organic matter is generally lighter than recent sedimentary organic matter. Hoefs (1980) explains that this may be due to the observed enrichment in ^{12}C as a result of diagenetic elimination of more perishable ^{13}C-rich carbohydrate-protein fractions from the marine sediments. Therefore, the existence of light δ^{13}C values in ancient sediments cannot be used as a criterion for land-derived organic matter (especially for rocks greater than Tertiary in age). Stahl (1977) claims that this trend may be caused by variations in the intensity of photosynthesis through time, which would change the isotopic composition of atmospheric carbon dioxide.

Two degradation processes may alter the isotope values. Nonbiological alteration could arise from the thermal degradation of heavier ^{13}C compounds, such as proteins and carbohydrates. The remaining residue would then be enriched with more refractory ^{12}C-rich lipids. Biologically, anaerobic bacteria may alter the isotope values by consuming the proteins and carbohydrates in the sediments and leaving behind the lipids that are relatively resistant to biological degradation. Also, the recycling of any sediment already depleted in ^{13}C could produce these similar results. For the New Albany Shale, Hailer *et al.* (1983) predict the most likely cause of the observed depletion in ^{13}C is diagenetic alteration.

TOTAL ORGANIC CARBON CONTENT

A total of 134 samples were analyzed for total organic carbon (TOC) percentages. The values range from 0.02% to 8.04% with a mean value of 2.24%. These data represent samples from all lithology types, except hard concretionary layers. Table 216.1 shows no correlation of TOC with carbon isotope values.

The amount of organic matter preserved in a sediment depends on its rate of accumulation and the rate of sedimentation (of sediments other than organic matter). Under oxic water conditions, there is a positive correlation between sedimentation rates and organic carbon content in recent sediments. Demaison and Moore (1980) place the range for organic carbon between 0.3% to 4.0%. In modern anoxic sediments, this correlation does not apply, and the range (1% to +20%) is wider and higher, regardless of sedimentation rates (Demaison and Moore 1980).

What is a significant amount of organic matter so that sufficient shale oil can be extracted? The temperature of pyrolysis is never greater than 500° to 600°C and the energy required to raise the temperature of the sample to 500°C is about 250 calories per gram of rock (Macauley 1984). The heat value of the indigenous organic matter is approximately 10 000 calories per gram. Thus, the minimum organic content at which the amount of energy recovered as shale oil could theoretically balance the input heat is 2.5%. Mining, transportation, and other costs are not included in this calculation. The frequently used lower limit for economic recovery is 5% (Macauley 1984).

ICHNOFAUNA (= TRACE FOSSILS)

Trace fossils in the Long Rapids rocks occur where there is a colour change between shales or mudstones. Of the 3 previous members described, burrowing is present in the 2 lower members, but is not found in the Upper Member (only seen in Onakawana Drillhole "B"). The outcrop section (encompassing the Lower Member) also records abundant burrowing. The recognizable burrows occur within black shales units, directly below green-grey shale or mudstone beds.

Cross sections of calcareous concretionary horizons do not reveal any bioturbation, but some of these horizons are quite mottled, and therefore may be so bioturbated that no distinct burrows can be seen. Weathered, planar views of some of these horizons reveal burrows, so bioturbation is suspected throughout. The smaller concretionary nodules (3 by 6 cm) contain spaghetti-like burrows oriented at various angles.

In core and outcrop, all trace fossils discovered were found in association with greenish grey shales or mudstones and concretionary horizons or nodules. Trace fossils were found in black shales only when they were overlain by green beds (Photo 216.3). Distinct, green sediment-infilled burrows sometimes extend 20 cm into black shale units.

SYSTEMATIC ICHNOLOGY

Zoophycos Massalongo 1855. Figure 216.4.

Description: Broad, near-horizontal whorls containing spreiten. The spreiten consist of mined and unmined sediments. The burrows can contain a marginal cylindrical tube. Preserved as endichnia. Interpreted as a feeding structure of soft-bodied, wormlike organisms. A whorl represents the action of the organism as it mined through the sediments. Each successive whorl is constructed as the organism retracted in its cylindrical tube and proceeded on a new whorl. Whorl diameters generally increase downward and diameters up to 60 cm have been recorded (Häntzschel 1975).

Remarks: Two specimens of *Zoophycos* have been recorded from the Long Rapids Formation, both in core. The best specimen is preserved as a horizontal tunnel in vertical section. It is located directly

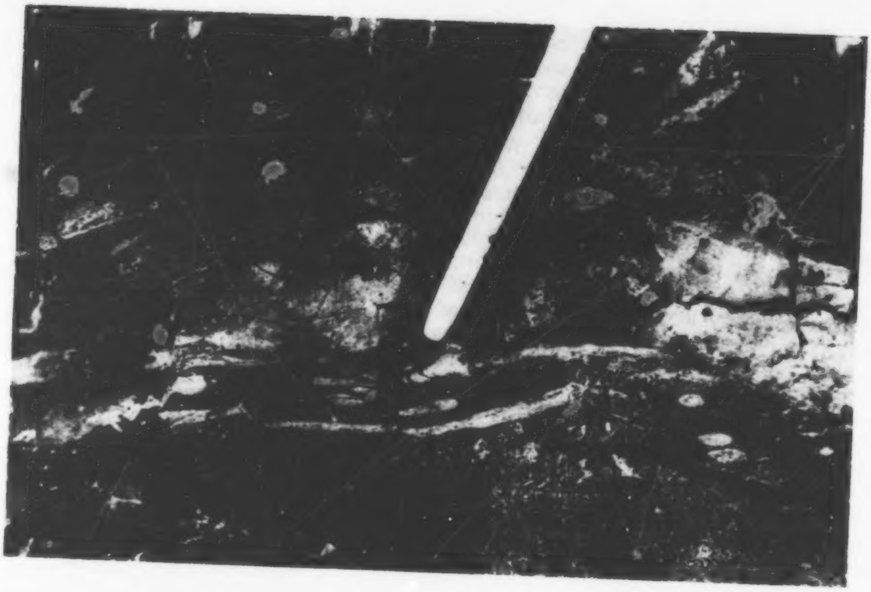

***Photo 216.3.** Planolites (large) and Chondrites (small) burrows, preserved as green infillings in a black shale layer. Pen for scale.*

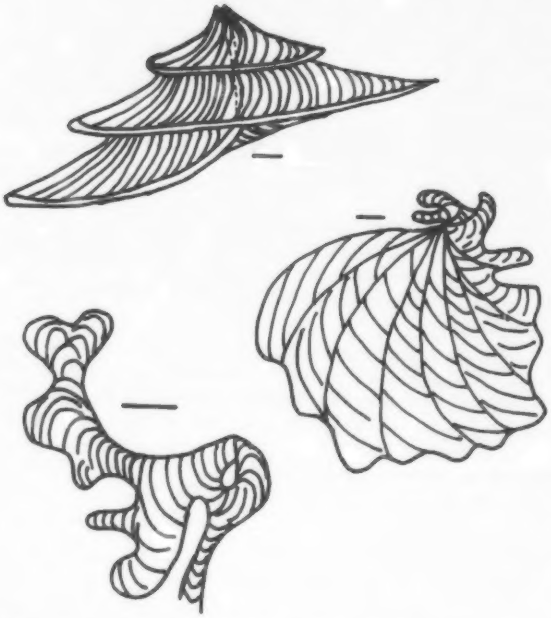

***Figure 216.4.** Various morphologies exhibited by Zoophycos. Scale bars 1 cm. From Hantzschel (1975) Figure 75 1a,b, and c.*

underneath a green mudstone in a black shale unit (about 3 to 5 mm down), and possesses excellent backfill menisci with alternating light and dark green laminae. This tunnel is up to 0.5 cm thick and extends the entire width of the bore (7 cm across). Small *Chondrites* cross-cut the burrow. The other specimen is smaller (2.0 by 0.7 cm in diameter) and more lobate; it too contains distinct, concentric green mud backfill. This specimen lies parallel to bedding in a black shale bed with wispy green mud laminae. *Chondrites* burrows are present, but do not cross-cut the *Zoophycos*.

Teichichnus Seilacher 1955. Figure 216.5.

Description: This trace fossil consists of long, horizontal burrows with spreiten structures stacked vertically to bedding. It represents the progressive vertical movement of a horizontal burrower that mined the sediments for organic matter (a deposit feeder). They are commonly retrusive (a response to sudden sediment influxes), but can also be protrusive. They can be up to 50 cm long and about 10 cm or more in height (Häntzschel 1975). One species, *T. rectus*, is noted by Häntzschel.

Remarks: Only 1 possible *Teichichnus* burrow was found, located at the top of a black shale bed, 3.5 cm below a green shale unit. It possesses indistinct protrusive menisci and is .4 cm long and 3 mm wide. It is associated with *Chondrites*, pelleted *Chondrites*, and *Planolites*. A small *Chondrites* burrow cross-cuts the *Teichichnus* structure. The green shale unit (10 cm thick) lies in a thick sequence of black shale (over 2 m).

Planolites Nicholson 1873. Figure 216.6.

Description: *Planolites* consist of straight to contorted, non-branching, horizontal to subhorizontal burrows. The tubes are circular in cross section where they are not compacted. Burrow walls may be smooth or irregular, and sediment fills contrast with the host stratum. Lengths vary from about 1 cm to over 25 cm, and diameters range from 1 cm to about 1.5 cm. It can be preserved as endichnia, hypichnia, and epichnia. It is distinguished from *Palaeophycus* by having unlined walls and burrow fills differing in texture from that of the surrounding rock. It is interpreted to be the burrow of deposit-feeding worms. Infills of *Planolites* represent sediment that has been ingested by the tracemaker and passed through the alimentary canal.

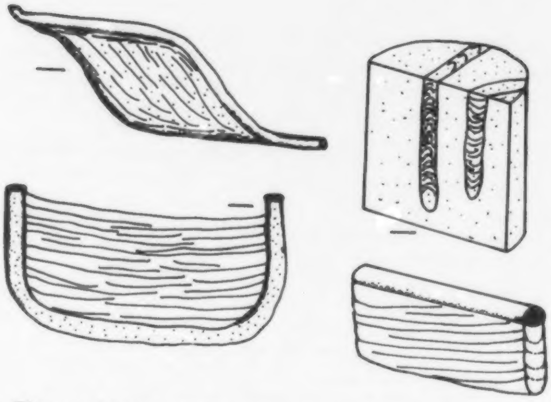

Figure 216.5. Various morphologies exhibited by Teichichnus. Scale bars 1 cm. From Chamberlain (1978) Figures 57, 58, and 60.

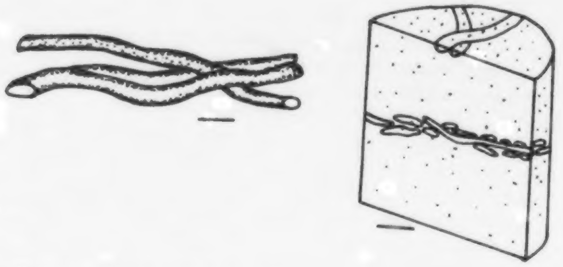

Figure 216.6. Various morphologies exhibited by Planolites. Scale bars 1 cm. From Chamberlain (1978) Figures 40 and 41.

Three species of *Planolites* are currently recognized (Pemberton and Frey 1982):

1. Small, curved to tortuous burrows—*P. montanus* (average diameter, 3 mm)
2. Large, straight to gently curved burrows—*P. beverleyensis* (average diameter, 10 mm)
3. Transversely annulated burrows—*P. annularis*

Remarks: *Planolites* is one of the most common traces in the Long Rapids section. Both longitudinal and cross-sectional views are exposed. Lengths are up to 10 cm, and diameters range from 3 to 7 mm. The best traces are found in black shales that are overlain by greenish grey units. The burrow infills are green, in contrast to the black shale host. In this section, *Planolites* and *Chondrites* burrows show no distinct changes in grain size across the burrow boundary. The major difference is that the burrow infills lack the brownish black organic matter that imparts the dark colour.

Burrow margins show no grain alignment. Many invertebrate organisms reinforce their burrow walls to prevent cave-ins or collapse. This reinforcement of burrow walls can be indicated by a concentration of larger grain sizes around the margin or an alignment of the grains. These types of burrows are built by organisms that intend to use the burrow as a permanent dwelling. When abandoned, the open burrows usually become passively infilled by subsequent sedimentation. Slight grain alignment can also occur when an organism moves through the sediments, ingests organic-rich particles, and then passes them through its alimentary canal. This type of movement represents actively infilled burrows and usually results in unstructured burrow walls.

All *Planolites* burrows present in the Long Rapids formation possess smooth, unornamented walls. The dominant species is *P. beverleyensis*. *P. montanus* may be present, but would be difficult to distinguish from *Chondrites*. *P. montanus'* curved and tortuous nature has not been observed.

Chondrites Sternberg 1833.

Description: *Chondrites* consists of three-dimensional burrow systems branching in a plant-like, dendritic pattern, at 25° to 45° from a main tube. The burrow systems tend to level off horizontally after the main inclination and are generally straight. Tube diameters remain equal throughout. Tunnels never interpenetrate or cross each other. It is thought that one or more main axes are open to the surface. Häntzschel (1975) notes that some tunnels may have transversally built-in ellipsoidal pills, but he doubts they are fecal in origin. The trace is interpreted to have been made by deposit-feeding sipunculan or echiuroid worms having retractable proboscises. The proboscis allowed the animal to work from a fixed point to mine the substrate (Simpson 1957). Possibly the pellets found in some traces are actually fecal in origin and the burrower may have back-filled its tube with pellets. Most authors (Bromley and Ekdale 1984; Jordan 1985) believe *Chondrites* burrows are passively infilled, where the burrow is excavated and then left open. Overlying sediments then passively infill the open cavities.

Remarks: *Chondrites*, like *Planolites*, is one of the most common trace fossils in the Long Rapids. Lengths can reach 4 cm, although most are approximately 2.5 cm. Diameters range from 1 to 2 cm. As with the previous trace, *Chondrites* is found just below green mudstone/shale units within black shales. None showed distinct dendritic branching patterns, which may be due to oblique viewing angles. Some had pellets within the burrows instead of green infill. The pellets are green in colour but lie in a matrix of black mud. The branches of some of these tubes are larger than typical *Chondrites* size. This type of pelletted burrow structure has not as yet been described in the literature, except for the above-cited mention by Häntzschel. *Chondrites* burrows penetrate deeper into black shales than do the other traces. They also tend to cross-cut previous burrows.

TRACE FOSSIL DISTRIBUTIONS

Overall, it appears that *Chondrites* burrows are more abundant than *Planolites* burrows, though the difference is not great. Pelleted *Chondrites* is the next most abundant trace. The others, *Zoophycos* and *Teichichnus*, are rare. Distinct assemblages cannot be modelled definitely. *Chondrites* and *Planolites* nearly always occur together, and *Zoophycos* and *Teichichnus* never occur without the previous two. As was mentioned before, *Chondrites* is seen cross-cutting both *Zoophycos* and *Teichichnus* burrows. The densest burrow concentrations occur in black shales directly below green shale/mudstone units. Rare burrows are found deep within black shale units (never greater than 20 cm from the top of the unit). They are usually *Chondrites* or pelleted *Chondrites*.

Since trace fossils are rarely transported, they are excellent tools to help interpret energy conditions at the depositional interface, substrate type, sedimentation rates, and oxygen and food availability. The fine laminations in a black shale imply quiet-water deposition. Each lamina could be a product of seasonal or other periodic events. The presence of lamination also proves the lack of benthos. If there is any oxygen present, it would be utilized in the decay process of the organic matter where oxygen is taken up to produce carbon dioxide (Tissot and Welte 1978). The high amount of organic matter present in these shales implies that oxygen was limited and organic matter was not reworked by benthic fauna, and hence was preserved from microbial degradation.

In the Long Rapids Formation, there are cyclic repetitions of black shale and greenish grey shale/mudstone units. In the Middle and Lower Members, bioturbation is observed in black shale units underlying greenish grey units. There is no bioturbation in the Upper Member even though it consists of greenish grey mudstones with minor amounts of black-grey shale interbeds. In contrast, the Middle Member consists of black shale units with minor interbeds of greenish grey units, and it contains abundant burrows. The cyclicity that is present in the Long Rapids Shale is due to varying oxygen conditions in the basin. The black shales are deposited under anoxic conditions, whereas the greenish grey units probably represent periods of oxygenation. But since these cyclic units can be separated by mere centimetres, it is hard to define the mechanisms that cause the oxygen fluctuations. In a basin environment, oxygen content is thought to change with water depth (Byers 1977). If bottom waters are anoxic in the deeper portions of the basin, then, at the edge of the basin, where the water is shallower, more oxygenation would occur. In low oxygen waters, benthic life is best adapted to the conditions by being small infaunal and epifaunal deposit feeders. As oxygen levels increase (> 1 ml/l), body size, abundance, and diversity of the organisms also increase (Rhoads and Morse 1971).

Rhoads and Morse (1971) subdivide an oxygen-stratified water column into aerobic, dysaerobic, and anaerobic levels based on oxygen contents, wherein benthic fauna and ichnofauna abundance decrease with increasing water depths. If the dysaerobic zone were to constantly move over the shelf margin of a basin, due to sea level changes or continental uplifts, repetitive variations in the stratigraphy could occur. This can explain why a non-bioturbated, laminated black shale can be overlain by a greenish grey unit that has a base bioturbated into the black shale. The conditions may have markedly changed from anaerobic to aerobic (or dysaerobic) to allow for the existence of benthic life. As conditions change once again, another black shale unit is deposited.

The introduction of oxygen to the bottom sediments also leads to the decay of any organic matter present. Organisms must quickly exploit the sediment for food before it is eaten by competitors. This may lead to a hierarchy amongst the burrowers. Semi-complex to complex burrows (such as *Zoophycos* and *Teichichnus*) would be near the sediment-water interface to keep a close connection to the overlying water column. Other burrowers, such as *Chondrites* and *Planolites*, could also coexist with the previous burrowers. As the organic matter is eaten up or decayed, less food is available and the opportunists seek other food sources. They could dig deeply to get at organic matter that has not been affected by the decay processes, with *Chondrites* being the most exploitable. Another explanation could be that as the oxygen supply is again turned off, the other burrowers flee or die off to leave *Planolites* and *Chondrites* to further exploit the sediments. Yet another explanation is that as more oxygenated sediments are being deposited, *Chondrites* digs deeper to exploit organic matter left behind. This could explain cross-cutting relationships of *Chondrites* with other traces. Jordan (1985) notes the *Chondrites* traces are cross-cut by those of larger infaunal deposit feeders such as *Planolites*, *Zoophycos*, and *Phycodes* in the New Albany Shale in east-central Kentucky. This relationship is due to *Chondrites* representing the pioneer burrower in the black sediments, with later infestation by larger infaunal deposit feeders.

Another problem is the question of active or passive infill of *Chondrites*. Active infill occurs as the burrower ingests the sediment, passes it through its alimentary canal, and refills its burrow. Passive infill implies the burrow was first mined out and later infilled by sediments from the overlying units. Many authors (Bromley and Ekdale 1984; Jordan 1985) believe *Chondrites* to be passively infilled in black shale environments. This argument may never be resolved, but we feel some of the Long Rapids *Chondrites* are actively infilled. In close inspection of the burrows in thin sections, there are no sharp burrow margins or grain alignments. The grain size of the sediments inside the burrow is similar to the sediment outside the burrow, except that the colour is lighter and rare organic matter is present. The burrow infill shows no meniscate or geopetal structures. The burrows have no dewatering halos, which would indicate thixotropic muds. Therefore, the sediments remained firm as the organism passed through. The presence of pelleted burrows can possibly be used as evidence that the burrows were actively infilled. The discrete, individual pellets (1 mm in diameter) could not have been passively infilled by sediments from a distance of about 20 cm (the sediment-water interface).

CONCLUSIONS

The repetitive and cyclic nature of the black and greenish grey shales in the Long Rapids Formation indicate an environment that experienced periodic changes in water column oxygen. Benthic fossils and ichnofauna are mainly associated with greenish grey units, which represent periods of oxygenation. The black shale units contain large amounts of organic matter and very rare body fossils. Trace fossils found in black shales always occur at the top of the unit and lie directly underneath greenish grey units. The greenish grey units have rare organic matter within them. The burrows in the Long Rapids Shale consist of *Zoophycos, Teichichnus, Planolites, Chondrites*, and pelleted *Chondrites*. The most common traces are *Planolites, Chondrites*, and pelleted *Chondrites*. The organisms were probably small, vermiform, infaunal deposit feeders that lived in a semi-restrictive environment. Influxes of fresh, oxygenated water introduced benthic life that scavenged the bottom sediments that were rich in organic matter. As organic matter content decreased due to scavenging and decay, certain burrows were excluded whereas others, such as *Planolites, Chondrites*, and pelleted *Chondrites*, tested the deeper sediments (the black shales) for food. The mechanism for the emplacement of these cyclic beds may have been varied. Numerous factors such as active tectonism, increased organic matter contents (due to upwellings or large influxes off the continent), changes in the position of the dysaerobic zone, and oxygenation due to turbidity currents may have caused these lithology fluctuations.

Total organic carbon content of the shales is about 2.2%. Stable carbon isotope values are consistent with a terrestrial origin for the organic matter, though a marine setting is still proposed for the basin.

ACKNOWLEDGMENTS

We are grateful to Dr. Peter Telford, Jim Sanderson, and Dave Russell, Ontario Geological Survey, for geological introductions to the area and their general assistance. We also thank Wendy Smith, Martin Knyf, and Jerome Richardson at McMaster University.

REFERENCES

Blatt, H.
1982: Sedimentary Petrology; W.H. Freeman and Company, San Francisco, 564p.

Bromley, R.G., and Ekdale, A.A.
1984: *Chondrites*: A Trace Fossil Indicator of Anoxia in Sediments; Science, Volume 224, p.872-875.

Byers, C.W.
1977: Biofacies Patterns in Euxinic Basins: A General Model; p.5-17 *in* Deep-water Carbonate Environments, edited by H.E. Cook and P. Enos, Society of Economic Paleontologists and Mineralogists, Special Publication Number 25.

Chamberlain, C.K.
1978: Recognition of Trace Fossils in Cores; p.119-166 *in* Trace Fossil Concepts, edited by B. Basan, The Society of Economic Paleonotologists and Mineralogists, Short Course Number 5.

Demaison, G.J., and Moore, G.T.
1980: Anoxic Environments and Oil Source Bed Genesis; American Association of Petroleum Geologists, Bulletin, Volume 64, p.1179-1209.

Dyer, W.S.
1931: Stratigraphy and Structural Geology of the Moose River Basin, Northern Ontario; Transactions of the Royal Society of Canada, Series 3, Volume 25, Section 4, p.85-99.
1932: Stratigraphy and Oil and Gas Possibilities of Moose River Basin; p.98-103 *in* Oil and Gas of Eastern Canada, edited by G.S. Hume, Geological Survey of Canada, Economic Geology Series, Number 9.

Dyer, W.S., and Crozier, A.R.
1933: Lignite and Refractory Clay Deposits of the Onakawana Lignite Field; Ontario Department of Mines, Annual Report for 1933, Volume 42, Part 3, p.46-78.

Goldhaber, M.
1978: Euxinic Facies; *in* Encyclopedia of Sedimentology, edited by R.W. Fairbridge and J. Bourgeois, Dowden, Hutchinson, and Ross, Publishers, 901p.

Hailer, J.G., Leininger, R.K., and Hayes, J.M.
1983: Marine vs. Terrestrial Sources and Other Influences on the Carbon Isotopic Composition of the Organic Matter in the New Albany Shale; p.207-213 *in* Proceedings of 1983 Eastern Oil Shale Symposium, Lexington, Kentucky, November 1983.

Häntzschel, W.
1975: Trace Fossils and Problematica; *in* Treatise on Invertebrate Paleonology, Part W, Miscellanea, Supplement 1, edited by C. Teichert, University of Kansas Press, and Geological Society of America, Lawrence, Kansas, 269p.

Hoefs, J.M.
1980: Stable Isotope Geochemistry; Springer-Verlag, 200p.

Jordan, D.W.
1985: Trace Fossils and Depositional Environments Upper Devonian Black Shales, East-Central Kentucky, USA; p.279-298 *in* Biogenic Structures: Their Use in Interpreting Deposition Environment, edited by H. Curran, Society of Economic Paleontologists and Mineralogists, Special Publication Number 35.

Macauley, G.
1984: Geology of the Oil Shale of Canada; Geological Survey of Canada, Paper 81-25, 65p.

Pemberton, S.G., and Frey, R.W.
1982: Trace Fossil Nomenclature and the *Planolites-Palaeophycus* Dilemma; Journal of Paleontology, Volume 56, p.843-881.

Peterson, M.Sl., Rigby, K.J., and Hintze, L.F.
1980: Historical Geology of North America; Wm. C. Brown Company, 232p.

Rhoads, D.C., and Morse, J.W.
1971: Evolutionary and Ecologic Significance of Oxygen-Deficient Marine Basins; Lethaia, Volume 4, p.413-428.

Sackett, W.M.
1964: The Depositional History and Isotopic Organic Carbon Composition of Marine Sediments; Marine Geology, Volume 2, p.173-185.

Sanford, B.V., and Norris, A.W.
1975: Devonian Stratigraphy of the Hudson Platform, Part I—Stratigraphy and Economic Geology, Part II—Outcrop and Subsurface Sections; Geological Survey of Canada, Memoir 379, 372p.

Savage, T.E., and Van Tuyl, F.M.
1916: The University of Illinois "Hudson Bay Expedition"; Science, Volume 44, Number 1140, p.632.
1919: Geology and Stratigraphy of the Area of Paleozoic Rocks in the Vicinity of Hudson and James Bay; Bulletin of the Geological Society of America, Volume 30, p.339-377.

Simpson, S.
1957: On the Trace-fossil *Chondrites*; Geological Society of London, Quarterly Journal, Volume 112, p.475-499.

Stahl, W.J.
1977: Carbon and Nitrogen Isotopes in Hydrocarbon Research and Exploration; Chemical Geology, Volume 20, p.121-149.

Telford, P.G., and Verma, H.M.
1982: Mesozoic Geology and Mineral Potential of the Moose River Basin; Ontario Geological Survey, Study 21, 193p.

Tissot, B.P., and Welte, D.H.
1978: Petroleum Formation and Occurrence; Springer-Verlag, 538p.

Grant 221 The Significance and Genesis of Chloritoid Alteration in Volcanic Rocks of the Michipicoten Belt, Ontario

M.B. Lockwood[1], **J.M. Franklin**[2], **J.M. Moore**[1]

[1]Ottawa-Carleton Centre for Geoscience Studies, Ottawa

[2]Geological Survey of Canada, Ottawa

ABSTRACT

Four properties, three with iron formation (Rand No. 2, "C", Josephine), and one with Pb-Zn-Ag showing (Kozak) have been mapped. Volcanic textures on all 4 properties indicate that deposition occurred under shallow subaqueous to possibly subaerial conditions. Alteration facies and their distributions have been defined. For the felsic rocks, in increasing order of alteration, facies are: least altered, feldspar-sericite, sericite, chloritoid, chlorite, and cordierite. For the mafic rocks, in increasing order of alteration, facies are: epidote-actinolite, quartz-chlorite, and chloritoid-chlorite. The chloritoid and chloritoid-chlorite alteration facies have the widest distribution of the most intense alteration assemblages. Beneath the iron formations they form zones that are parallel to stratigraphy, possibly indicative of diffuse fluid venting or the widespread blockage and storage of trapped fluids. Around the Kozak Pb-Zn-Ag occurrence, the zones are in small patches near the areas of mineralization. Distribution of alteration facies near all of the deposits does not define large-scale pipe structures.

Chloritoid is a post-tectonic mineral, formed due to the metamorphism of some precursor alteration assemblage. Its ubiquitous association with carbonate minerals suggests that a high PCO_2 was necessary for its formation.

INTRODUCTION

Chloritoid has long been recognized as a common constituent of iron-rich aluminous pelitic schists, and more recently, as a product of alteration in a variety of volcanic and intrusive rocks. More importantly, its association with various types of ore deposits, including base-metal massive sulphide deposits (Franklin *et al.* 1975; Groves 1984; S. Osterburg, M.Sc. student, University of Minnesota, 1985, personal communication), Algoma-type iron deposits (Goodwin 1962; LaTour *et al.* 1980; Morton and Nebel 1984), and shear-zone-hosted copper-gold deposits (Eckstrand 1963), suggests that its occurrence may serve as a possible exploration guide. Chloritoid is common throughout the volcanic rocks of the Wawa area, associated both with rocks of economic mineral potential and those apparently without. Very little is known about this alteration type relative to processes leading to the formation of the magnesian alteration patterns in Precambrian rocks (Riverin and Hodgson 1980; Walford and Franklin 1982; Costa *et al.* 1983).

The objectives of this research are to obtain an understanding of the following:

1. Whether chloritoid is an indicator of focused hydrothermal discharge or widespread subsurface water rock reaction.
2. To establish the physical parameters (P, T, PCO_2) required for chloritoid formation.
3. To define the volcanic setting and to establish the controls imposed on alteration by the physical nature of the volcanic rocks.
4. To determine the chemical changes between altered rocks and their unaltered precursors.

Four areas associated with potentially economic mineralization have been chosen to represent a wide range of chloritoid occurrences. They are:

1. The Rand No. 2: a sulphide-facies iron formation.
2. The "C" Property: a deformed sulphide-facies iron formation.
3. The Kozak Lake Showing: Pb-Zn-Ag showing with no iron formation.
4. The Josephine Iron Range: oxide-carbonate iron formation.

GEOLOGICAL BACKGROUND

The 4 study areas are located northeast of Wawa on Algoma Central Railway (ACR) land (Figure 221.1). The Josephine Iron Range is located 13 km northeast of Wawa in the southwestern corner of Corbiere Township, accessible by private gravel road. The Rand No. 2 is situated 2 km south of Goudreau, and west of the ACR tracks in Abotossaway Township. The Kozak Property is located 3 km south of S. s, also in Abotossaway Township. The "C" Property is situated about 2 km east of Goudreau, on the north side of the Goudreau-Localsh road.

RAND NO. 2 PROPERTY

The Rand No. 2 Property (Figure 221.2) contains 2 east-west striking stratigraphic units of predominantly sulphidic iron formation, each between 16 and 50 m in thickness. Pillow lavas indicate that the facing direction is north. The facies succession within the iron formation is carbonate, sulphide, and silicate facies, in ascending order, with minor variations. Both the southern and northern iron formations are underlain by very altered felsic pyroclastic rocks and overlain by a massive mafic flow. They are separated by up to 200 m of mafic flow rocks. The repetition of stratigraphy has been interpreted by Sage (1983) to be fault-related.

Conformable mafic units, either flows or sills, separate the iron formations. They are massive and coarse grained, and have some flow banding. Unlike the massive and pillowed mafic flows above the northern iron formation at the Rand, they contain epidote clots and rare "felsic" patches, which are possibly assimilated host material or local areas of

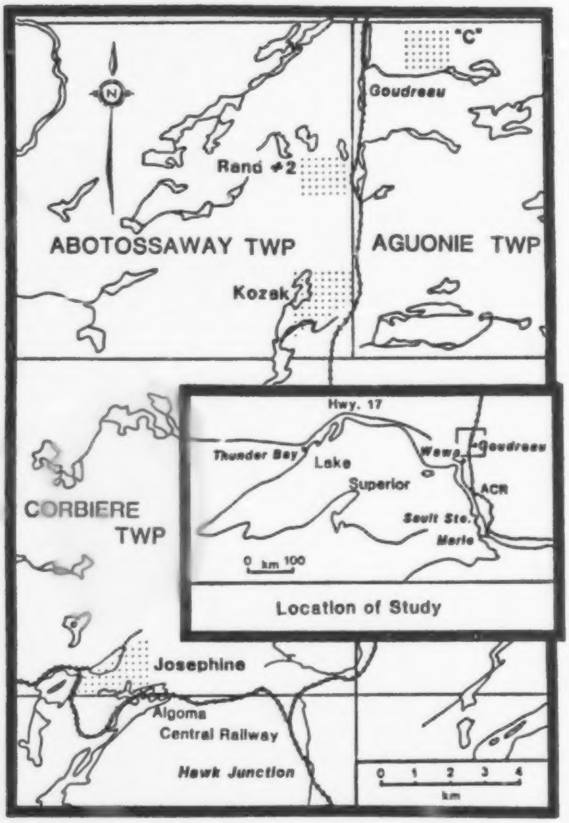
"C"
Goudreau
Rand #2
ABOTOSSAWAY TWP
AGUONIE TWP
Kozak
CORBIERE TWP
Hwy. 17
Thunder Bay
Lake
Superior
Wawa
Goudreau
ACR
Sault Ste.
Marie
0 km 100
Location of Study
Josephine
Algoma
Central Railway
Hawk Junction
0 1 2 3 4
km

Figure 221.1 Location of the four areas relative to Goudreau.

silicification. The mafic units do not have chilled margins.

Little primary texture remains in the footwall felsic rocks. A homogeneous sericite schist with ghost outlines of highly altered lapilli fragments forms the footwall section. The coarsest fragment size occurs at the base of the felsic volcanic accumulation, fining upward from a matrix-supported monolithic felsic breccia, to lapilli tuff, to fine tuff, over a stratigraphic interval of about 50 m.

THE "C" PROPERTY

The "C" Property is a structurally complex area, consisting of the northern half of an "s"-shaped fold (Bruce 1942), defined by iron formation (Figure 221.3). In the central part of the map area (Figure 221.3) there is fault-related repetition of the middle fold limb and truncation of the fold nose by a gabbroic intrusion. The stratigraphic succession of felsic volcanic rocks, iron formation, and mafic volcanic rocks, is similar to that at the Rand Property. The north-facing northern iron formation, also known as the "McPhail" (Moore and Armstrong 1946), includes an underlying layer of sulphide-bearing marble, reported to laterally grade into siderite facies iron formation (Collins and Quirke 1926). Within the felsic footwall rock a thin layer of monolithic brecia, similar to that at the Rand Ocurrence, underlies the iron formation. Beneath this, the rocks consist of fine tuff and crystal tuff with intensely altered pumiceous lapilli. Iron formation in the central part of the southern limb is very thick, possibly the result of tectonic thickening accompanying the major deformation.

In the hanging wall, the mafic volcanic rocks consist of fine-grained mafic flows, commonly strongly foliated. They have been truncated by the intrusion of large, fine fine- to coarse-grained metagabbro bodies covering much of the western map area. Thin

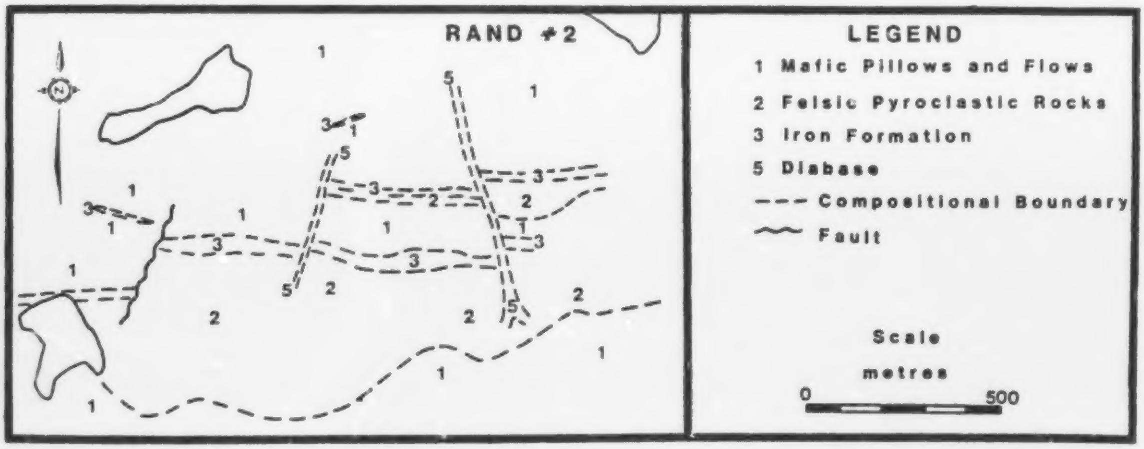
RAND #2
N
1
2
3
5
LEGEND
1 Mafic Pillows and Flows
2 Felsic Pyroclastic Rocks
3 Iron Formation
5 Diabase
--- Compositional Boundary
~~ Fault
Scale
metres
0 500

Figure 221.2 Simplified geologic map of the Rand No. 2 property.

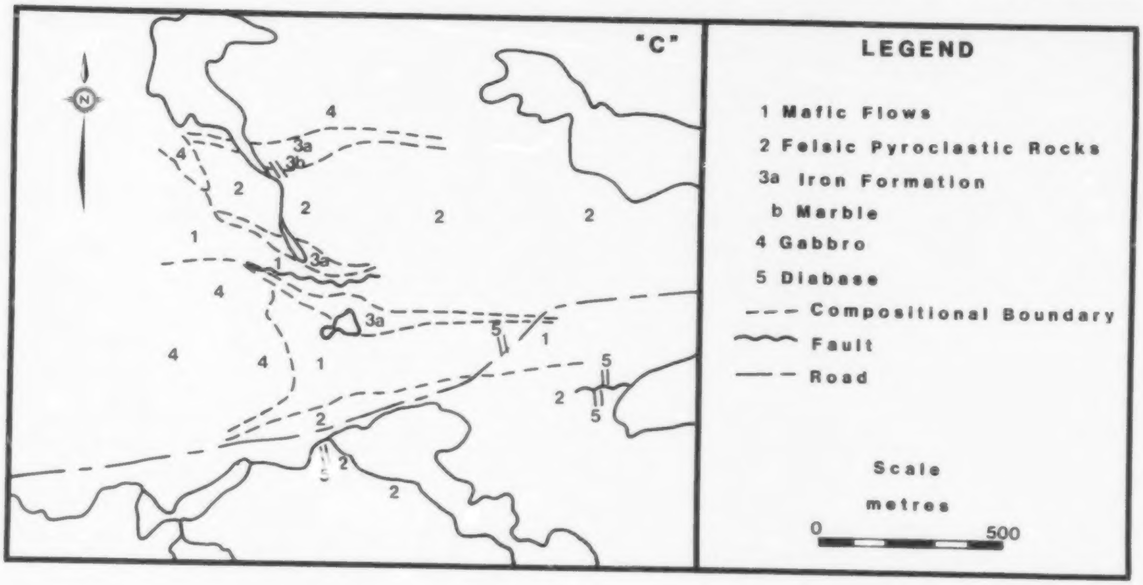

Figure 221.3. Simplified geologic map of the "C" property.

layers of felsic tuff have been observed in 2 places at the tops of mafic flow layers.

THE KOZAK LAKE SHOWING

Pb-Zn-Ag mineralization in the Kozak Lake Showing (Figure 221.4) is in felsic flows and pyroclastic rocks. The sulphides occur in quartz-carbonate veins associated with areas of silicification, similar to the sulphide veins in the Favourable Lake area (Adams 1976). Deformation has been intense, 2 foliation directions are common. One direction is regionally subparallel to bedding, striking approximately east-west and dipping steeply north. The other is approximately north-south with steep to shallow westward dips. The latter is thought by Sage (1982a) to be related to the north-trending MacVeigh Creek Fault, which lies to the east. Alternatively, it could be related to a north-trending fault noted by R.P. Sage (Geologist, Ontario Geological Survey, Toronto, 1983, personal communication) to the west of the Kozak Property.

Footwall rocks contain corroded crystals and pumiceous lapilli. Toward the mineralization, volcanic textures include well preserved crystal tuff, 3 to 5 m thick felsic flows with well defined, parallel and contorted flow banding extending over distances of 20 to 30 m, lapilli tuff, and monolithic and heterolithic breccias. A lack of differential weathering within the coarser felsic monolithic pyroclastic rocks suggests a compositional similarity between the clasts and the matrix. A pipe-like felsic body, up to 10 m wide, is internally structureless with well defined edges. It cuts all the other structures. Small *en echelon* faults have cut the pipe resulting in a saw-tooth pattern along the pipe's western edge. Breccia zones are common along the edge of this intrusion, in the adjacent felsic rocks. The hanging wall volcanic rocks are composed of a 450 m thick layer of undeformed to strongly sheared crystal tuff. This, in turn, is intruded by a quartz diorite body, which is present across a large extent of the northern part of the map area (Figure 221.4).

THE JOSEPHINE IRON RANGE

The Josephine area (Figure 221.5) consists of, in ascending stratigraphic order, (a) massive and pillowed mafic flows with intercalated mafic tuff, (b) a thin discontinuous tuffaceous iron formation, (c) mafic pyroclastic rocks, (d) a discontinuous ferruginous dolomite layer, and (e) a thick sequence of felsic pyroclastic rocks. The succession is capped by the Josephine Iron Formation.

Deformed mafic flows with elongate pillows form the base of the section. Pillows face north and range up to 2 m in diameter, with numerous centimetre-sized vesicles and amygdules. Mafic fragmental rocks form a unit up to 200 m thick in the central part of the map area, along the southeastern shore of Parks Lake (Calvert 1983). This latter unit is composed predominantly of lapilli tuff, with less common clasts of breccia-block size; fragment size increases upwards, from 10 to 20 m of fine mafic tuff at its base, through 10 m of mafic crystal tuff, and upwards into lapilli-sized mafic fragmental rocks. Clasts are supported by a mafic matrix and are heterolithic, composed mostly of aphanitic felsic clasts with about 15% mafic and 15% chert clasts. Sulphide clasts can be observed in this layer immediately south of Parks Lake. Some felsic clasts have reaction rims, and all tend to be subangular, weakly imbricated, unsorted, and unstratified. Calvert (1983) suggested that this mafic pyroclastic unit is the product of a heated debris flow. However, if it was formed during one event, clast size distribution may have resulted from more turbulent flow, such as in a pyroclastic surge. The variable clast composition indicates that this unit is either epiclastic, or that the flow had an erosive

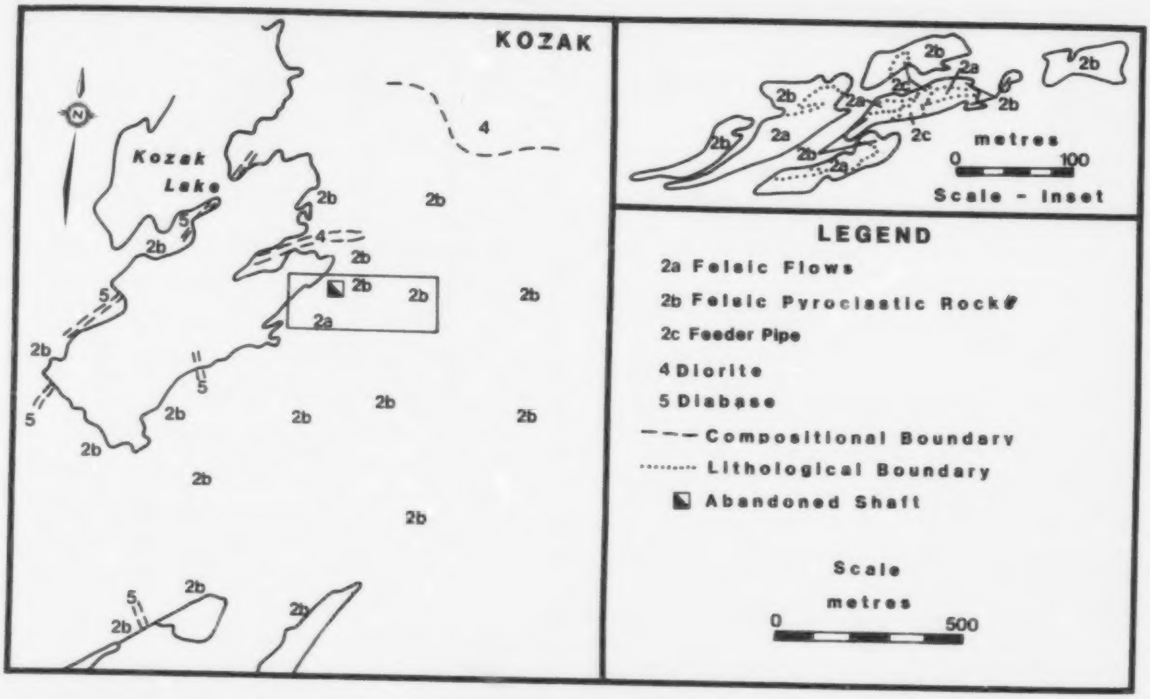
KOZAK
N
Kozak Lake
4
2b
5
2a
2c
metres
0
100
Scale - Inset
LEGEND
2a Felsic Flows
2b Felsic Pyroclastic Rocks
2c Feeder Pipe
4 Diorite
5 Diabase
Compositional Boundary
Lithological Boundary
Abandoned Shaft
Scale
metres
0
500

Figure 221.4. *Simplified geologic map of the Kozak property. The inset shows, in more detail, the distribution of felsic flow and pyroclastic rocks in the outcrops near the mine shaft.*

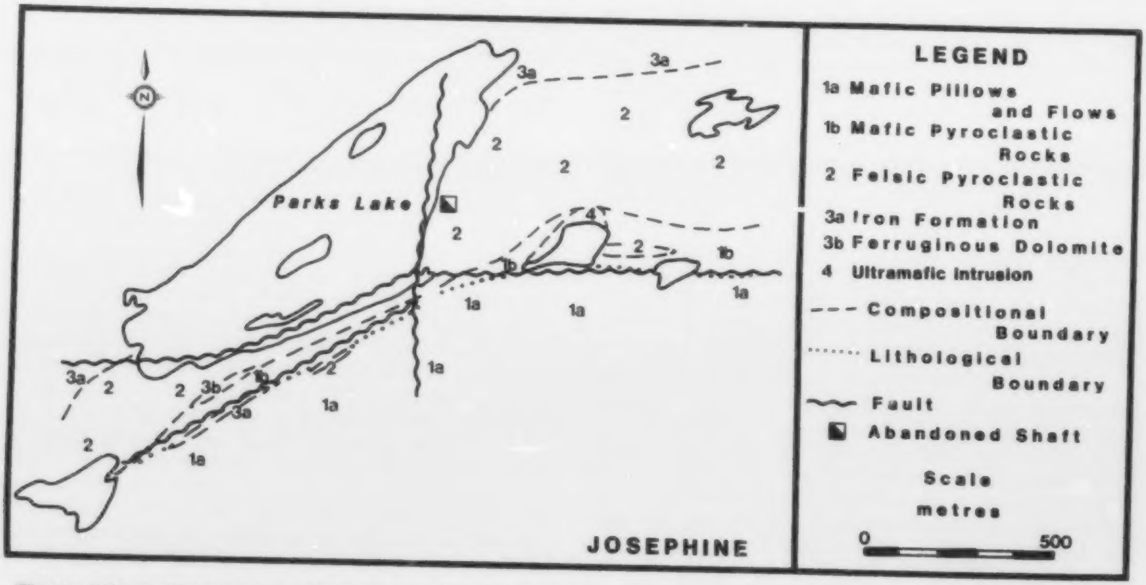
N
Parks Lake
3a
2
4
1b
1a
3b
LEGEND
1a Mafic Pillows and Flows
1b Mafic Pyroclastic Rocks
2 Felsic Pyroclastic Rocks
3a Iron Formation
3b Ferruginous Dolomite
4 Ultramafic Intrusion
Compositional Boundary
Lithological Boundary
Fault
Abandoned Shaft
Scale
metres
0
500
JOSEPHINE

Figure 221.5. *Simplified geologic map of the Josephine Iron Range (partly adapted from Calvet 1983).*

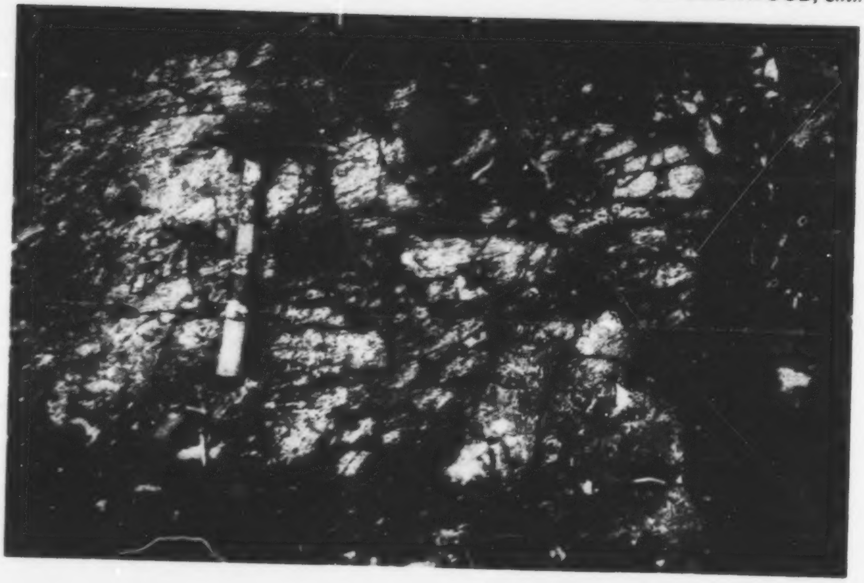

Photo 221.1. *Breccia pipes cross-cutting the middle of the felsic pyroclastic rocks at the Josephine Iron Range. Clasts are composed of locally derived rock and the matrix is iron-rich carbonate.*

base, also in keeping with a pyroclastic surge deposit (Fisher 1982).

The overlying felsic pyroclastic rocks to the east of Parks Lake are texturally diverse, and form the thickest part of the felsic succession, up to 400 m thick. The lower contact is not exposed. No individual flow or surge deposits could be distinguished. Clast sizes increase upwards from the base, reaching a maximum size about 100 m from the mafic floor, in a small band of heterolithic breccia with angular felsic clasts and some mafic clasts. Above this is a felsic tuff unit with 10% to 20% sericitized fiamme and 10% lapilli fragments, gradually changing upward into a 100 to 200 m thick, fine-grained tuff. This is in turn overlain by the Josephine Iron Formation.

To the west of Parks Lake, the felsic pile is considerably thinner. Here felsic pyroclastic rocks grade upward from crystal tuff at the base to heterolithic lapilli tuff. The latter member is overlain by fine-grained bedded tuff and crystal tuff members, which in turn are overlain by highly deformed and altered felsic rock, probably of pyroclastic origin. Two important trends are notable from east to west: the pyroclastic pile becomes thinner, and there is an overall decrease in grain size.

Throughout the lower felsic sequence, rocks are cut by breccia pipes which have an average width of 1 m (Photo 221.1). They contain angular clasts of host rock, up to 30 cm in diameter, set in a matrix of ferruginous carbonate. The mouth of one pipe is located in the felsic volcanic rocks to the southwest of Parks Lake, this pipe has a matrix of ankerite. Delicately laminated carbonate beds, up to 1 m wide, occur within tuff beds at the same stratigraphic level but farther along strike.

ALTERATION

Alteration facies have been defined by thin section and X-ray studies, following geological mapping done during the 1984 field season. The minerals used in defining each facies generally comprise 10% or more of the rock. The rocks containing the assemblages typical of the more intense alteration may also contain minerals typical of the less altered facies. Alteration facies are listed in increasing intensity of alteration. For the felsic rocks they are:

1a. Least Altered: Quartz (30%-45%), Feldspar (20%-40%), Sericite (5%-15%), Carbonate (10%-15%), Chlorite (<1%-2%)

1b. Feldspar-Sericite: Quartz (30%-50%), Feldspar (10%-30%), Sericite (10%-25%), Carbonate (2%-25%), Chlorite (2%-10%)

2. Sericite: Quartz (25%-75%), Sericite (10%-50%), Feldspar (10%-30%), Carbonate (1%-30%), Chlorite (2%-15%), Chloritoid (0%-7%), Stilpnomelane (<1%-3%)
3. Chloritoid: Quartz (20%-60%), Sericite (5%-40%), Feldspar (0%-5%), Carbonate (3%-30%), Chlorite (3%-15%), Chloritoid (7%-50%)
4. Chlorite: Quartz (35%-50%), Sericite (5%-7%), Chlorite (20%-35%), Carbonate (5%-20%), Chloritoid (<1%-3%), Garnet (3-5%)
5. Cordierite: Quartz, Sericite, Chloritoid, Cordierite (Calvert 1983)

For the mafic rocks, mineral assemblages are very different:

1. Epidote-Actinolite: Quartz (5%-10%), Chlorite (30%-40%), Feldspar (10%-50%), Carbonate (15%-20%), Epidote (3%-5%), Actinolite (0%-15%)
2. Quartz-Chlorite: Quartz (10%-50%), Chlorite (10%-50%), Feldspar (0%-15%), Sericite

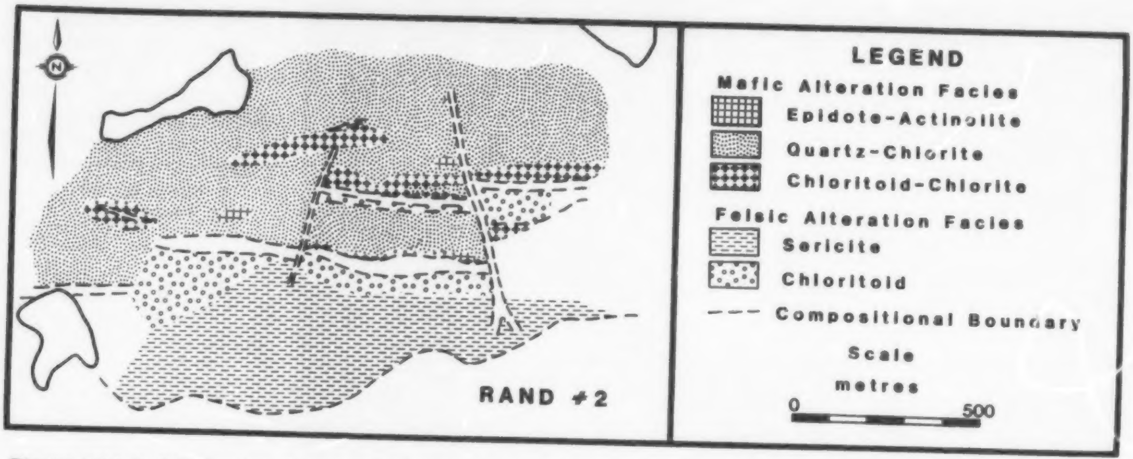

Figure 221.6. *Distribution of alteration facies of the Rand No. 2 property.*

(1%-15%), Carbonate (15%-30%), Chloritoid (0%-3%), Stilpnomelane (0%-3%)

3a. Chloritoid-Chlorite: Quartz (25%-60%), Chlorite (0%-35%), Sericite (1%-20%), Carbonate (5%-35%), Chloritoid (10%-65%)

3b. Staurolite-Chlorite: Quartz (20%-40%), Chlorite (20%-30%), Sericite (0%-10%), Biotite (0%-15%), Staurolite (5%-10%), Carbonate (10%-30%)

Feldspar observed within the mafic rocks varies from albite to andesine, whereas within the felsic rocks it varies from albite to oligoclase. Siderite and ankerite are the 2 principal carbonate minerals. Chloritoid occurs as laths and radial bowtie aggregates up to 3 mm in length. In all 4 study areas, chloritoid is randomly oriented, and cuts both foliation and vein boundaries.

Changes in alteration facies are a reflection of differing intensities of fluid/rock reaction as well as initial rock composition. The latter is demonstrated by the fact that the alteration mineral assemblages of adjacent mafic and felsic rocks are invariably different, although they may have been affected by the same fluid and similar physical conditions. Primary textural controls were also important. Unfractured massive flows generally are less intensely altered than their tuffaceous counterparts, because their primary permeability was less.

RAND NO. 2 PROPERTY

The felsic footwall rocks of both the north and south units of the Rand No. 2 Property have undergone relatively advanced alteration (Figure 221.6). For an interval of 60 m below the southern band, chloritoid becomes an important mineral. Chloritoid alteration occurs in a zone parallel to stratigraphy, and is traceable beneath the entire strike-length of both iron formations. Directly beneath both layers of iron formation is breccia, typically 5 m thick, with deformed clasts up to 1 m in length. The clasts are replaced by chloritoid (Photo 221.2). The matrix is microcrystalline quartz with carbonate intergrowths. Chloritoid is also in veinlets through both the siderite and sulphide layers of the iron formation, as well as in the lower 2 m of the overlying mafic flows. Increased carbonate content is apparent generally at least 10 m below the iron formations and commonly persists for 5 m above. Chloritoid is usually associated with the carbonate. Mafic flows, between the iron formation layers and the hanging wall mafic volcanic rocks, have undergone less alteration, usually of the quartz-chlorite facies. Around small isolated iron formation layers within the hanging wall, the chloritoid-chlorite facies is evident.

THE "C" PROPERTY

The "C" Property displays a wider range of alteration types than the Rand (Figure 221.7). Chloritoid occurs as a minor phase (<10%) throughout much of the sericite facies in the felsic footwall. Chloritoid facies alteration exists beneath the iron formation, but is not traceable in the footwall along its entire length due to lack of exposure. In 2 areas within the footwall immediately beneath the iron formation, the chloritoid facies gives way to the chlorite facies. In the central area of the property (Figure 221.7) chlorite facies alteration occurs in veins which cut rocks containing the chloritoid facies. Poorly developed garnets, up to 1 mm in diameter, occur in these veins. In the western part of the area (Figure 221.7), chlorite facies is more predominant. The mafic rocks overlying the iron formation have been somewhat altered, and contain scattered relict chloritoid laths, now pseudomorphically replaced by staurolite. Biotite is an essential mineral in this assemblage. Farther south, above another segment of iron formation, the epidote-actinolite assemblage is predominant.

THE KOZAK LAKE PROPERTY

The Kozak property contains the smallest range of alteration types of any of the properties studied (Figure 221.8). Varying amounts of sericite replacement of feldspar occur in irregularly distributed zones throughout the footwall. Sericite is pervasive; its distribution is controlled by fractures and vein swarms, and it has corroded the edges and fractures of the abundant feldspar grains. Silicification is also fracture controlled, but occurs only locally, unlike the more widespread sericite alteration. Irregulr veins of very fine grained cherty quartz are exposed on the lakeshore just southwest of the mine shaft.

Chloritoid zones occur near but not directly within the zone of base-metal mineralization. These zones are surrounded by areas of complete primary feldspar breakdown. Chloritoid occurs within the sericite veinlets as small laths up to 1 mm in length. Chloritoid is nowhere as concentrated (usually <10%) as at the Rand or the "C" Properties but, as with the latter 2 occurrences, it is associated with great amounts of carbonate. Hanging wall alteration is minor.

THE JOSEPHINE IRON RANGE

In the mafic rocks at Josephine (Figure 221.9), a chloritoid zone up to 100 m thick occurs throughout the map area and continues to the east for at least 3 km (R.P. Sage, 1982, personal communication). This zone forms the top of a unit consisting of mafic pillows and massive flows. Chloritoid occurs as disseminations and in chloritoid-chlorite fracture fillings in pillows and flows. In the layered tuffs, it is very abundant in coarser layers, and locally it is disseminated in massive tuff units (Lockwood 1983). Chloritoid has also been noted in the overlying mafic fragmental rocks.

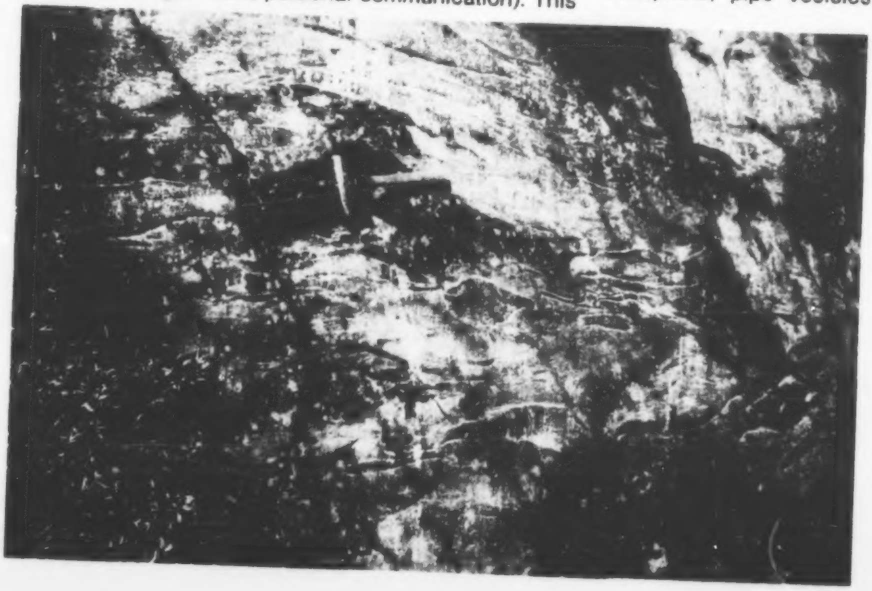

Photo 221.2. *Chloritoid-replaced breccia underlying both layers of iron formation at the Rand No. 2 property. The clasts are composed of up to 60% chloritoid and almost 40% sericite. The matrix is microcrystalline quartz and carbonate.*

Within the felsic pyroclastic rocks, sericite-facies alteration ranges from moderate to intense with almost all primary pyroclastic rock being replaced by sericite. Chloritoid occurs in two areas to the extreme west of the map area, one at the base of the felsic rocks, the other in the upper felsic rocks close to the base of the iron formation. Cordierite is a minor phase in the felsic rocks in the central map area at the base of the felsic rocks (Calvert 1983). It probably formed by contact metamorphism adjacent to a small ultramafic intrusive body immediately beneath this felsic unit, within mafic fragmental rocks.

DISCUSSION

VOLCANOLOGICAL CHARACTERISTICS

Detailed examination of the volcanologic attributes reveals that, in most areas, deposition took place in a shallow subaqueous environment, although in a few locations, a possible subaerial depositional environment is evident. The breccia pipes at Josephine, and the felsic breccia zones in the footwall of both the Rand No. 2 and the "C" Deposits, indicate that hydroexplosion may have accompanied hydrothermal activity. Boiling of these fluids may also have caused the deposition of carbonate in the matrix to these breccia zones. Thus, confining pressures at the depositional sites were low. Extensively vesiculated pillows, commonly with pipe vesicles along pillow bottoms (Jones 1969), at both the Rand No. 2 and Josephine, pipe vesicles along the base of these flows at the Rand No. 2, and fiamme in the felsic rocks at the Josephine, also support this conclusion. Well preserved felsic flows at Kozak indicate that the depositional environment was either shallow subaqueous or subaerial.

From the similarity of stratigraphy, it would appear that the "C" and the Rand No. 2 were formed in virtually indentical environments. The felsic footwall rocks at both localities are composed of similar fine tuffs to crystal tuffs. Both iron formations are underlain by units of hydroexplosion breccia which are extensively replaced by chloritoid alteration. Both iron formations are overlain by mafic flow rocks.

The principal difference between the Rand and the "C" Deposits is the repetition in stratigraphy at the Rand. Mafic units separating the iron formations at the Rand may be, at least in part, sills. Their lack of chilled margins is characteristic of sills of the

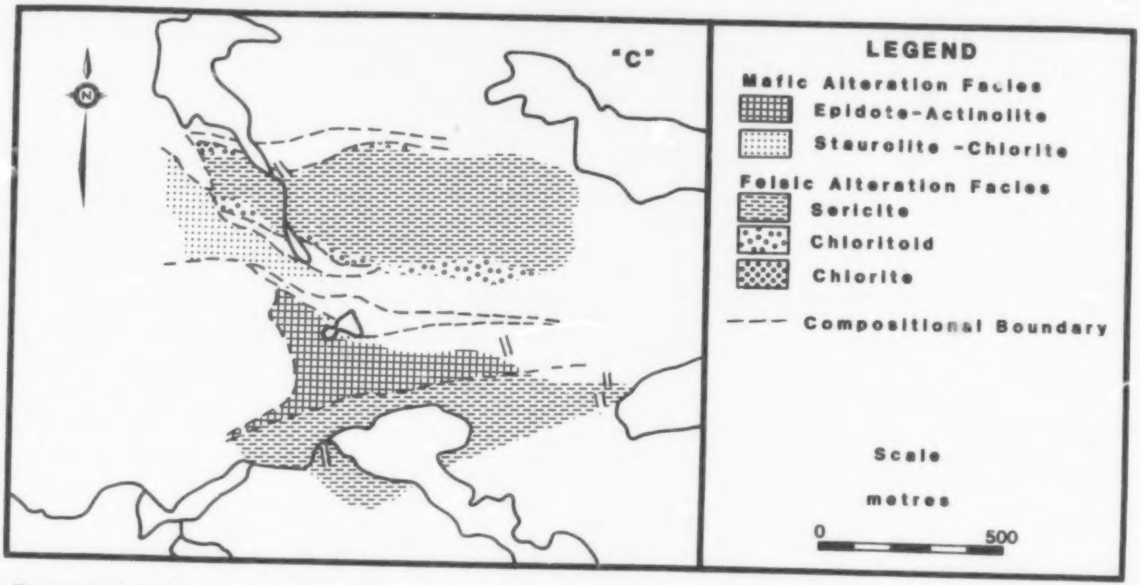

Figure 221.7. Distribution of alteration facies of the "C" property.

region and was thought by Goodwin (1962) to indicate that their emplacement occurred in rocks of similar temperature. If sills, they were probably introduced penecontemporaneously with volcanism, as their lower 2 m are affected by chloritoid alteration.

At Kozak Lake, the presence of flow banding adjacent to the breccias may indicate that these felsic rocks formed as an exogenous dome. The lack of coarse pyroclastic material indicates that the environment was relatively quiescent, and that the eruptive centre was probably small. The massive pipe-like body of felsic rock at Kozak has been tentatively interpreted as a feeder pipe to the volcanic rocks farther up in the section. This would support the contention that this area is proximal to a small volcanic centre.

At the Josephine, the volcanic environment is complex. The decrease in thickness of the felsic pile to the west and overall eastward increase in clast size may indicate a local easterly source, contrary to the overall trend for the belt (R.P. Sage, personal communication). It would be difficult to discern, judging from the felsic accumulation east of Parks Lake, whether the felsic volcanic rocks within the central area are the accumulated product of a series of flows and falls, or are the remnants of a single flow event. Thinly bedded pyroclastic flows and flow variations in the western map area indicate that the former is most probable. The thinly laminated carbonate beds within these flows to the west of Parks Lake may indicate that appreciable time gaps occurred between successive flows. They also may signify that formation of hydrothermal pipes and continued hot spring activity occurred penecontemporaneously with the deposition of the felsic pyroclastic rocks.

Heat sources needed to drive hydrothermal systems for the Rand No. 2, the "C", Kozak, and Josephine are not apparent. No sizeable subvolcanic bodies have been noted in their footwall successions. They may lie unexposed, or else the ore-producing hydrothermal systems may have relied solely upon the heat inherent within their respective volcanic accumulations. It has been demonstrated by Cathles (1978), Campbell *et al.* (1981), and others that such bodies were necessary to provide heat for the formation of volcanic-associated base-metal deposits, such as the Japanese Kuroko deposits, and Mattabi and Kam-Kotia deposits in the Canadian Shield. However, oxygen isotope work by LaTour *et al.* (1980) has demonstrated that fluids involved in the formation of the Helen Iron Formation were considerably cooler (<2250°C). This may relieve some of the apparent need for a specific heat source such as a subvolcanic intrusion.

ALTERATION

Almost without exception, the chloritoid and chlorite zones are the only readily mappable alteration zones. Other alteration facies (e.g. sericite) are usually impossible to recognize in the field. It is likely that lower grades of alteration observed throughout the felsic accumulations represent the regional metamorphism evident in virtually all the felsic volcanic rocks throughout the belt (R.P. Sage, personal communication). Hence, the first 2 facies of felsic alteration recognized here may not be the direct consequence of the processes responsible for the overlying mineralization.

The association of chloritoid-facies alteration with the iron formation throughout the Wawa belt suggests that it is a product of relatively low temperature alteration (<250°C) (LaTour 1980; Goodwin *et al.* 1985). The ubiquitous association of this alteration with carbonates (Sage 1982b) may be indicative that a high PCO_2 environment is necessary for its forma-

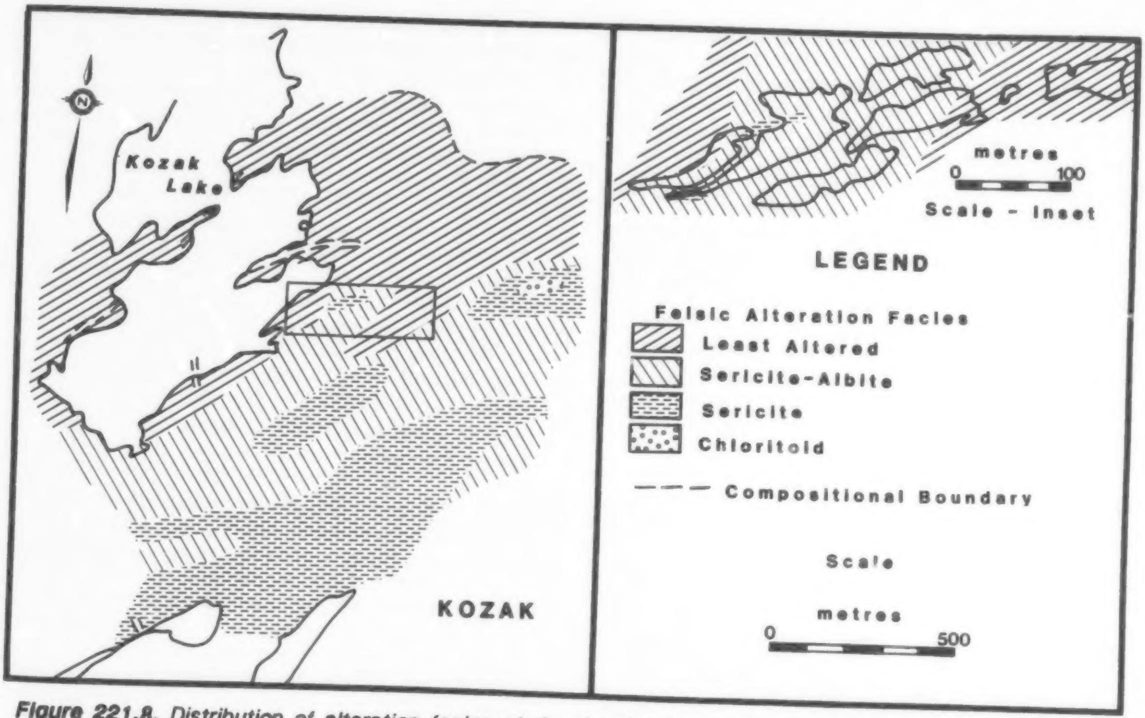
N
Kozak Lake
KOZAK
metres
0
100
Scale - Inset
LEGEND
Felsic Alteration Facies
Least Altered
Sericite-Albite
Sericite
Chloritoid
Compositional Boundary
Scale
metres
0
500

Figure 221.8. Distribution of alteration facies of the Kozak property. The inset shows, in more detail, the distribution of alteration facies in outcrops near the mine shaft.

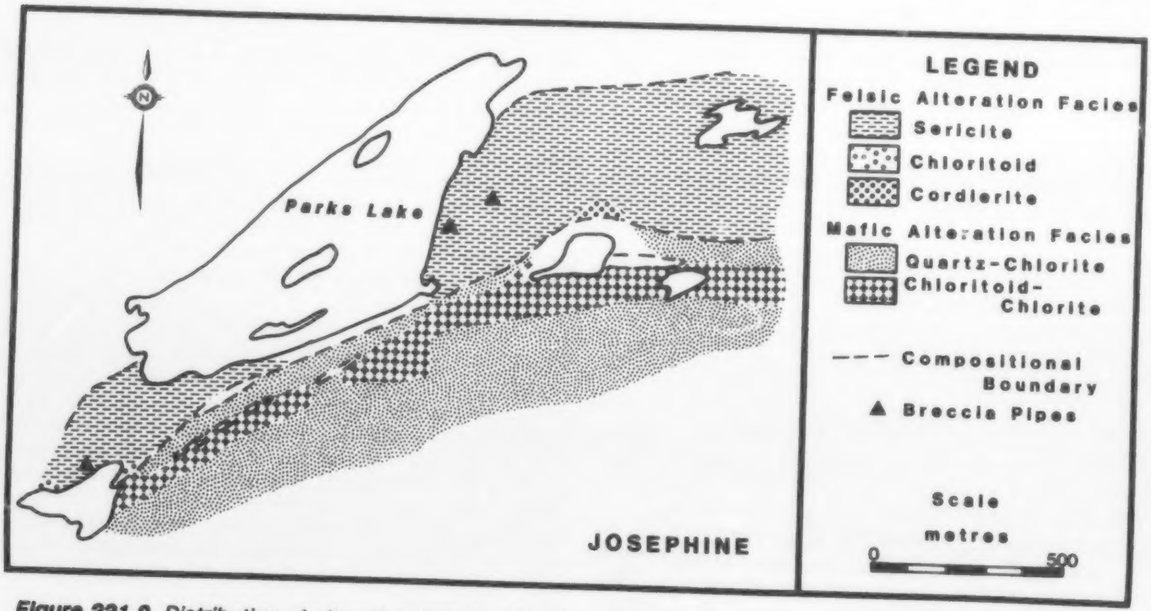
N
Parks Lake
JOSEPHINE
LEGEND
Felsic Alteration Facies
Sericite
Chloritoid
Cordierite
Mafic Alteration Facies
Quartz-Chlorite
Chloritoid-Chlorite
Compositional Boundary
Breccia Pipes
Scale
metres
0
500

Figure 221.9. Distribution of alteration facies of the Josephine Iron Range.

tion. In the Sturgeon Lake area, it occurs in areas also enriched in ferruginous carbonate and in base metals. This is probably a high temperature alteration sequence (Franklin *et al.* 1975). At Onaman River, it is not associated with carbonate, and may also be within a high temperature alteration sequence (S. Osterburg, 1985, personal communication).

The chloritoid alteration at the Rand, the "C", and at Josephine are, conformable to semi-conformable "blanket type" zones. This is consistent with chloritoid zones throughout most of the Wawa belt, which generally occur in stratigraphically conformable zones up to several kilometres long and 300 or more metres thick (Sage 1981). This could reflect an alteration path of a diffuse nature (MacMillan 1981) rather than a focused system. Chloritoid zones could also represent areas that acted as reservoirs for fluids trapped by overlying impermeable layers.

The sequence of alteration recognized here is different from that within a cross-cutting pipe in the footwall to the Helen Iron Formation, as recognized by Morton and Nebel (1984). The areas mapped for this study lack the discontinuous chlorite-rich pods and lenses observed beneath the Helen Iron Formation. Morton and Nebel (1984) considered these zones to represent a less intense amount of alteration than the chloritoid zones. Instead, chlorite-rich zones, where observed at the "C", are considered to represent a greater intensity of alteration than that represented by the chloritoid zone, due to their proximity to the iron formation. The chlorite zones are gradational with the chloritoid zones, but were not observed in proximity to the sericite zones. Ankerite zones, as defined by Morton and Nebel (1984), were also observed beneath the iron formatin at the "C" but are too small to be considered of consequence.

Within the mafic rocks, the least intense facies of alteration may be representative of no more than simple spilitization. Fewer alteration minerals are present in the mafic rocks, possibly due to the generally lower permeability of these rocks compared to that of felsic pyroclastic rocks. The presence of chloritoid within these rocks, as well as the felsic rocks, demonstrates that chloritoid production may be explained by more than one set of reactions, and that its production is not particular to one initial rock compositon.

CONCLUSIONS AND FUTURE PLANS

The following tentative conclusions and generalizations have been made as a result of the work conducted to the present time:

1. All of the rocks near the deposits examined in this study were deposited in a shallow subaqueous environment, with a possible subaerial depositional environment for the felsic pyroclastic rocks at the Kozak Occurrence.
2. No well defined pipe structures are evident from the distribution of the alteration patterns in the areas studied. Chloritoid zones exist as stratigraphically parallel zones beneath, and locally above, the iron formations. This may indicate that venting of hydrothermal fluids was very diffuse. It may also indicate that these rocks acted as reservoirs for trapped hydrothermal fluids.
3. Alteration assemblages are dependent upon the initial compositions of the host rocks. Mafic and felsic rocks invariably have different alteration mineral assemblages, in spite of having undergone alteration at similar temperature, pressure, and water/rock ratio conditions.
4. Alteration facies defined for the felsic rocks in an increasing order of alteration are: Least Altered (Feldspar-Sericite), Sericite, Chloritoid, Chlorite, and Cordierite.
5. Alteration facies defined for the mafic rocks in an increasing order of alteration are: Epidote-Actinolite, Quartz-Chlorite, and Chloritoid-Chlorite (Staurolite-Chlorite).
6. Chloritoid nucleation is post-tectonic. It overgrows the regional foliation in all the areas studied.
7. Chloritoid is ubiquitously associated with elevated carbonate concentrations. This may indicate that a high PCO_2 is necessary for chloritoid precursor development in rocks that have undergone relatively low temperature alteration.
8. The presence of stratiform chloritoid alteration away from either iron formation or base-metal occurrences in the Wawa area, indicates that this type of alteration is not useful as a means of identifying areas that are potentially base-metal bearing.

Through the upcoming year, further petrographic studies of the rock suites collected during the 1984 field season will be undertaken. This will be accompanied by additional X-ray diffraction and microprobe studies.

Chemical data for rocks representing the complete range of alteration facies will also be used for mass balance analysis to determine the chemical changes which affected these rocks to produce the observed metamorphic mineral assemblages, and to help trace the chemical evolution of the fluids involved in the alteration process.

ACKNOWLEDGMENTS

The author would like to thank R.P. Sage, of the Ontario Geological Survey, and Gord Yule, of Canamax Limited, for the valuable suggestions and information they have given throughout this project. Thanks are also due to Toivo Taal, for his excellent field assistance, Ron Conlon for assistance with the X-ray work, and Dan Marshall and Ross Taylor for thin sections. Chris Findlay, Stuart Roscoe, and Ron Sage reviewed earlier versions of the manuscript.

REFERENCES

Adams, G.W.
1976: Precious Metal Veins of the Berens River Mine, Northwestern Ontario; Unpublished M.Sc. Thesis, University of Western Ontario, 114p.

Bruce, E.L.

1942: Geology of the Goudreau-Localsh Area; Ontario Department of Mines, Annual Report for 1940, Volume 49, Part 3, 50p.

Calvert, H.T.

1983: Petrography and Geochemistry of an Archean Volcanic Sequence of the Josephine Area, Wawa, Ontario; Unpublished B.Sc. Thesis, Brock University, 69p.

Campbell, I.H., Franklin, J.M., Gorton, M.P., and Scott, S.D.

1981: The Role of Subvolcanic Sills in the Generation of Massive Sulphide Deposit; Economic Geology, Volume 76, p.2248-2253.

Cathles, L.H.

1978: Hydrodynamic Constraints on the Formation of Kuroko Deposits; Mining Geology, Volume 28, p.257-265.

Collins, W.H., and Quirke, T.T.

1926: Michipicoten Iron Ranges; Geological Survey of Canada, Memoir 147, 170p.

Costa, U.R., Barnett, R.L., and Kerrich, R.

1983: The Mattagami Lake Mine Archean Zn-Cu Sulfide Deposit, Quebec; Hydrothermal Coprecipitation of Talc and Sulfides in a Sea-Floor Brine Pool—Evidence from Geochemistry, Oxygen/Isotope, and Mineral Chemistry; Economic Geology, Volume 78, p.1144-1203.

Eckstrand, O.R.

1963: Crystal Chemistry of Chlorite; Unpublished Ph.D. Thesis, Harvard University, 128p.

Fisher, R.V.

1982: Pyroclastic Surges; p.71-110 *in* Pyroclastic Volcanism of Cenozoic Intermediate to Felsic Volcanic Islands with Implications for Precambrian Greenstone-Belt Volcanoes, edited by L.D. Ayres, Geological Association of Canada, Short Course Notes, 365p.

Franklin, J.M., Kasarda, J., and Poulsen, K.H.

1975: Petrology and Chemistry of the Alteration Zone of the Mattabi Massive Sulphide Deposit; Economic Geology, Volume 20, p.63-79.

Goodwin, A.M.

1962: Structure, Stratigraphy, and Origin of Iron Formations, Michipicoten Area, Algoma District, Ontario, Canada; Geological Society of America, Bulletin, Volume 73, p.561-586.

Goodwin, A.M., Thode, H.G., Chou, C.L., and Karkhansis, S.N.

1985: Chemostratigraphy and Origin of the Late Archean Siderite-Pyrite-rich Helen Iron Formation, Michipicoten Belt, Canada; Canadian Journal of Earth Sciences, Volume 22, p.72-84.

Groves, D.A.

1984: Stratigraphy and Alteration of the Footwall Volcanic Rocks Beneath the Archean Mattabi Massive Sulphide Deposit, Sturgeon Lake; Unpublished M.Sc. Thesis, University of Minnesota, 115p.

Jones, G.G.

1969: Pillow Lavas as Depth Indicators; American Journal of Science, Volume 267, p.181-195.

LaTour, T.E., Kerrich, R.W., Hodder, R.W., and Barnett, R.L.

1980: Chloritoid Stability in Very Iron-rich Altered Pillow Lavas; Contributions to Mineralogy and Petrology, Volume 74, p.165-173.

Lockwood, M.B.

1983: The Nature and Significance of Chloritoid in Footwall Basalt of the Josephine Iron Formation of the Michipicoten Area, Algoma District, Ontario; Unpublished B.Sc. Thesis, University of Western Ontario, 75p. MacMillan, D.

1981: The Significance of Chloritoid within the Footwall Volcanic Rock of the Helen Iron Range, Wawa, Ontario; Unpulished B.Sc. Thesis, University of Western Ontario.

Moore, E.S., and Armstrong, H.S.

1948: Iron Deposits in the District of Algoma; Ontario Department of Mines, Annual Report for 1946, Volume 55, Part 4, p.1-118.

Morton, R.L., and Nebel, M.

1984: Hydrothermal Alteration of Felsic Volcanic Rocks at the Helen Siderite Deposit, Wawa, Ontario; Economic Geology, Volume 79, p.1319-1333.

Riverin, G., and Hodgson, C.J.

1980: Wall-Rock Alteration at the Millenbach Cu-Zn Mine, Noranda, Quebec; Economic Geology, Volume 75, p.424-444.

Sage, R.P.

1981: Josephine Area, District of Algoma; p.41-44 *in* Summary of Field Work, 1981, by the Ontario Geological Survey, edited by John Wood, Owen L. White, R.B. Barlow, and A.C. Colvine, Ontario Geological Survey, Miscellaneous Paper 100, 253p.

1982a: Josephine Area, District of Algoma; p.28-33 *in* Summary of Field Work, 1982, by the Ontario Geological Survey, edited by John Wood, Owen L. White, R.B. Barlow, and A.C. Colvine, Ontario Geological Survey, Miscellaneous Paper 106, 235p.

1982b: Preliminary Appraisal of Alteration of Metavolcanics in the Wawa Area, District of Algoma; p.34-35 *in* Summary of Field Work, 1982, by the Ontario Geological Survey, edited by John Wood, Owen L. White, R.B. Barlow, and A.C. Colvine, Ontario Geological Survey, Miscellaneous Paper 106, 235p.

1983: Josephine Area, District of Algoma; p.45-49 *in* Summary of Field Work, 1983, Ontario Geological Survey, edited by John Wood, Owen L. White, R.B. Barlow, and A.C. Colvine, Ontario Geological Survey, Miscellaneous Paper 116, 312p.

Walford, D.C., and Franklin, J.M.

1982: The Anderson Lake Mine, Snow Lake, Manitoba; p.481-524 *in* Precambrian Sulphide Deposits, H.S. Robinson Memorial Volume, edited by R.W. Hutchinson, C.D. Spence, J.M. Franklin, Geological Association of Canada, Special Paper 25, 791p.

Grant 225 Genesis of Pegmatites in the Quetico Gneiss Belt of Northwestern Ontario—Rare-Element Pegmatites and Associated Granitoids of the Georgia Lake Pegmatite Field

S.A. Kissin and B. Zayachkivsky

Department of Geology, Lakehead University

ABSTRACT

The Georgia Lake pegmatite field lies immediately east of the Nipigon Plate in the northern portion of the Quetico Gneiss Belt. Granitoid rocks in the area are divisible into 3 groups on the basis of petrography and geochemistry: two-mica leucogranites, including the Glacier Lake pluton, forming the southern portion of the study area; I-type granitoid stocks of the Kilgour Lake Group; and tonalitic dikes and sills. The two-mica leucogranites appear to be the likely parental magmas to rare-element pegmatites on the grounds of their peraluminous, S-type character and extensive fractionations in terms of high K/Ba, Ba/Sr, and Rb/Sr, and low K/Rb, Ba/Rb, Mg/(Li x 10), and Zr/Sn ratios. The muscovite, perthitic microcline, and Ta-Nb-Sn oxide minerals of the Li-bearing, rare-element pegmatites were analyzed for trace elements, and the subdivision of the pegmatites into 3 groups on textural grounds was supported by trace element fractionation patterns. The Central Group shows a strong fractionation pattern from east to west, culminating in pegmatites bearing Ta-Nb mineralization. The Northern Group pegmatites show little fractionation within the group, and have trace element abundances and ratios at about the midpoint of the trend established in the Central Group. Unlike the unzoned or weakly zoned Northern and Central Group pegmatites, the MNW pegmatite of the Southern Group is distinctly zoned. High fractionation of trace elements from wall to core zones is present. Differences among the pegmatite groups are thought to have arisen from differing processes of internal evolution.

INTRODUCTION

The Quetico Gneiss Belt extends across northwestern Ontario, from the International Border in the western reaches of Quetico Provincial Park, in a direction slightly north of east, until it is disrupted by the Kapuskasing Zone in the east, a distance of approximately 700 km (Stockwell *et al.* 1970). Within, and immediately adjacent to, the northern and southern boundaries of the Quetico Belt are found numerous pegmatite bodies, generally in the form of dikes or small pods. These pegmatite bodies contain low but significant amounts of uranium in the area west of the Nipigon Plate, and Franklin (1978) has attributed unconformity-type occurrences to a source in these uraniferous pegmatites. To the east of the Nipigon Plate, Proterozoic cover rocks, consisting of diabase sheets, the Sibley Group clastic sediments (Stockwell *et al.* 1970), and the Archean Quetico gneisses and associated pegmatites, re-emerge. In this easterly region, known as the Georgia Lake pegmatite field, the pegmatites are rich in lithium and contain traces of beryllium, tantalum, and niobium mineralization. Thus, one continuous terrain provides a spectrum of mineralized pegmatites and a basis for field study of the generation of differing types of pegmatites. The relationship to various "fertile", parental granitoids in the area to the pegmatites is also a subject for investigation. The current year's research efforts have been directed towards studies of the geochemistry and mineralogy of rare-element pegmatites and related granitoid intrusions within the Georgia Lake pegmatite field.

The Georgia Lake pegmatite field is contained within Map Area 2056 (Pye 1965), and is located southeast of Lake Nipigon in Thunder Bay District, Ontario (Figure 225.1). The area was studied from the standpoint of the staking rush for lithium deposits in the late 1950s (Pye 1965), and a Ph.D. thesis (Milne 1962) dealt with the mineralogy and petrography of some of the more prominent occurrences. General descriptions of the pegmatite occurrences were also provided by Mulligan (1965).

The entire northern part of the study area is underlain by metasedimentary rocks of the Quetico Gneiss Belt, which have been intruded by various sills, dikes, and stocks of granitoid rocks. The granitoids are in turn cut by dikes and pods of pegmatite. The southern portion of the study area is a batholithic-sized body, the Glacier Lake pluton (McCrank *et al.* 1981), at present an unstudied granitoid. The western portion of the study area is covered by diabase sheets of Proterozoic age, the Logan diabase sills. Adjacent areas to the east and south are unmapped, while the Geraldton greenstone belt lies immediately to the north.

METHODOLOGY

Granitoid rocks were analyzed in whole rock, while, due to the inhomogeneity of pegmatites, their alkali feldspars, muscovites, and Ta-Nb-Sn oxide minerals were analyzed as mineral separates. Granitoids were analyzed for SiO_2, TiO_2, Al_2O_3, total iron, MnO, CaO, Na_2O, K_2O, P_2O_5, Rb, Sr, Ba, Zn, Zr, and Nb by X-ray fluorescence spectrometry. FeO was determined by wet chemical titration and CO_2 and H_2O on a carbon-hydrogen-nitrogen analyzer. Analyses for Li, Be, and Sn were carried out by the Geoscience Laboratories of the Ontario Geological Survey by means of atomic absorption spectrophotometry.

The minerals of the pegmatites were also analyzed by a combination of methods. SiO_2, Al_2O_3, and K_2O in feldspar and muscovite, and TiO_2, total iron, and MgO in muscovite were determined on the electron microprobe. Rb and Cs in feldspar and muscovite, and Sc, Ta, and Co in muscovite, were determined by instrumental neutron activation analysis. X-ray fluorescence spectrometry was used for analysis of Sr, Ba, and Zr in feldspar and muscovite, and

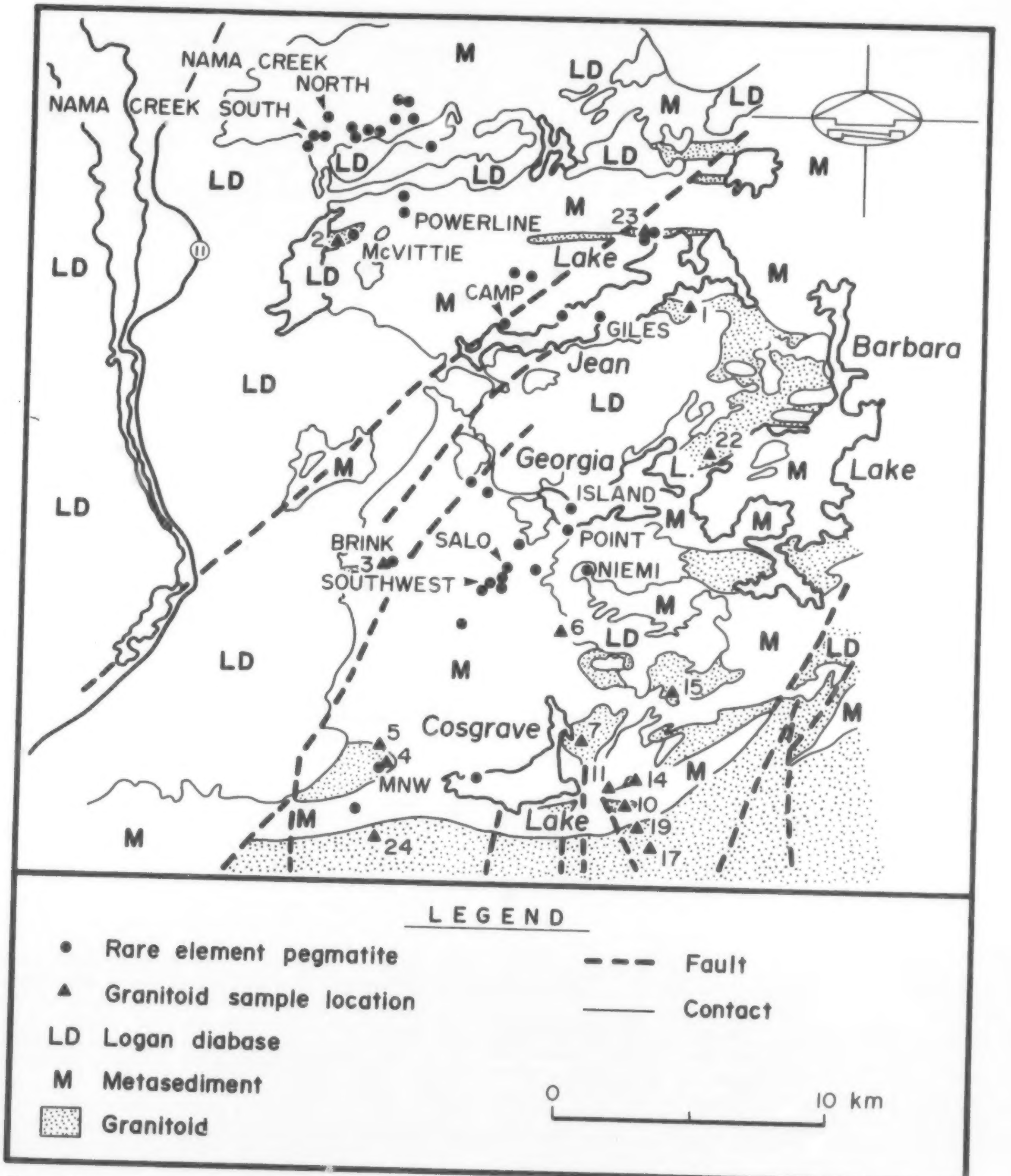
NAMA CREEK NORTH
NAMA CREEK SOUTH
M
LD
POWERLINE
23
2
McVITTIE
11
Lake
CAMP
GILES
1
Jean
Barbara
Lake
22
Georgia
L.
ISLAND
BRINK
3
SALO
POINT
SOUTHWEST
NIEMI
6
15
Cosgrave
Lake
5
4
MNW
7
11
14
10
19
17
24
LEGEND
● Rare element pegmatite
▲ Granitoid sample location
LD Logan diabase
M Metasediment
Granitoid
Fault
Contact
0
10 km

Figure 225.1. The Georgia Lake pegmatite field showing the distribution of sampling locations for pegmatites and granitoids (after Pye 1965).

Nb in muscovite. Li and Na_2O in muscovite were determined by atomic absorption spectrophotometry and H_2O by carbon-hydrogen-nitrogen analyzer. Sn in selected muscovite samples was determined by atomic absorption by the Geoscience Laboratories, Ontario Geological Survey. Analyses of Sn-Ta-Nb oxide minerals were performed on the electron microprobe using synthetic oxide standards by R. Chapman of the University of Manitoba. Complete details of the analytical procedures are given by Zayachkivsky (1985).

GRANITOIDS

GEOLOGICAL SETTING

The study area contains 2 differing portions of the Quetico Subprovince characteristically found east of the Nipigon Plate: a northern metasedimentary sequence with minor granitic dikes and sills; and a southern plutonic zone characterized by a granitic pluton of batholithic proportions and numerous stock-like bodies in adjacent high-grade metasediments. The southern batholithic body, the Glacier Lake pluton (McCrank *et al.* 1981), together with adjacent satellite stocks, are two-mica leucogranites. Interspersed with the stocks of leucogranite are stocks and plugs of more mafic granitoids, ranging from tonalites to granodiorites to monzodiorite, here called the Kilgour Lake Group. Throughout the area, but particularly in the north, is a group of tabular intrusions mostly oriented in an east-west direction. These are tonalites and are virtually identical from body to body (*see* Figure 225.1).

PETROGRAPHY

The two-mica leucogranites contain abundant quartz, albite to oligoclase, and perthitic microcline with minor muscovite and biotite. No mafic minerals other than biotite are present, and only traces of opaque oxides and apatite occur. Traces of magmatic garnet occur near the foliated border of the Glacier Lake pluton, but the garnet and foliation diminish away from the contact, and are absent 0.5 km from the margin of the intrusion.

The Kilgour Lake Group intrusions are notably more mafic than the leucogranites, all containing hornblende as well as biotite. One intrusion, designated the Kilgour Lake-Stein Lake metagabbro by Pye (1965), contains clinopyroxene as well. All of these intrusions are of granitoid affinity, with more than 50% feldspar in the mode, and abundant to minor quartz and microcline. Plagioclase is more calcic than in the leucogranites, and microcline is rarely perthitic. Sphene, apatite, and opaque oxides are minor but ubiquitous constituents, while zircon and allanite occur in many but not all bodies.

The tonalitic sills and dikes contain abundant plagioclase and quartz, but minor to absent microcline. All contain biotite with lesser muscovite, but are free of mafic minerals, and contain no consistent suite of trace minerals.

GEOCHEMISTRY

Representative samples from all the two-mica leucogranite and Kilgour Lake intrusions and selected tonalites were analyzed in whole rock. The results, given in Table 225.1, refer to localities indicated in Figure 225.1. Differentiation into 3 groups on petrographic grounds is supported by distinctive whole-rock geochemistry in each case.

The two-mica leucogranites all contain normative corundum > 1% and $Al_2O_3/(CaO+Na_2O+K_2O)$ ($\equiv$ A/CNK) ratios $\geq$ 1.1, both indicators of peraluminous, S-type granitoids (Hine *et al.* 1978; Chappell 1978). While the Kilgour Lake Group granitoids contain normative corundum > 1%, except in the case of analysis no. 11, the Kilgour Lake-Stein Lake monzodiorite, A/CNK is nearly always $\leq$ 1.1, indicating I-type character. As well, field characteristics of low quartz content and the presence of hornblende are consistent with those of I-type granitoids (Chappel and White 1974; Pitcher 1979). The tonalites are more difficult to characterize, as they possess characteristics of both I- and S-type granitoids.

Patterns of minor and trace element abundances and ratios also distinguish the 3 groups of granitoids. The two-mica leucogranites are enriched in Li and Rb and depleted in Sr, Ba, Zr, and Zn with respect to the Kilgour Lake Group, while the values for the tonalites are intermediate. The high values for Li and Rb in no. 23 (Parole Lake sill) may reflect contamination by pegmatitic material. These abundance patterns yield high K/Ba, Ba/Sr, and Rb/Sr ratios and low K/Rb, Ba/Rb, Mg/(Li x 10), and Zr/Sn ratios in the leucogranites, as compared to those in the tonalites and the Kilgour Lake Group. Abundances of Be, Nb, and Sn show little variation. The two-mica leucogranites are thus likely parental magmas to rare-element pegmatites, based on these abundance and fractionation data, which are considered indicative by Goad and Černý (1981) and Trueman and Černý (1982).

Considerable fractionation is evident in a comparison of the various two-mica leucogranite bodies. Figure 225.2 illustrates fractionation trends as a function of K/Rb in the Glacier Lake pluton (GL), together with its core (c) and border (b) zones, and satellite bodies, the Barbara Lake-Jean Lake stock (BL-JL), and the MNW stock (MNW). While the satellite bodies and the main mass of the Glacier pluton show similar fractionations, the core to border trend reveals that the border is the most highly fractionated of the granitoids, or portions of those that have been considered. The K/Rb ratio of the main mass and border phase of the Glacier Lake pluton is, in fact, lower than that of the satellite bodies or the core zone. Zr is also markedly lower in the main mass, while Rb/Sr and K/Ba are similar to the values in the satellite bodies. As can be seen in Table 225.2, most other trace element ratios and abundances reach maxima or minima in the border zone (no. 19).

RARE-ELEMENT PEGMATITES

GEOLOGIC SETTING

Rare-element pegmatites in the Georgia Lake area are generally hosted in metasedimentary rocks, but occasionally they intrude tonalite dikes and sills.

TABLE 225.1. ANALYSES OF GRANITOIDS FROM THE GEORGINA LAKE PEGMATITE FIELD.

	Two-mica Leucogranites							Kilgour Lake Group granitoids						Tonalites		
	1	22	4	5	17	19	24	6	7	10	11	14	15	2	3	23
SiO$_2$(%)	74.19	74.24	73.44	73.76	74.68	77.17	74.05	64.18	65.17	62.66	56.12	66.76	67.40	73.99	68.87	63.46
TiO$_2$	0.22	0.17	0.27	0.22	0.09	0.04	0.15	1.47	0.40	0.42	0.70	0.53	0.36	0.24	0.14	0.93
Al$_2$O$_3$	13.58	13.89	13.64	14.20	14.05	13.07	14.61	16.37	16.97	17.77	14.39	16.96	16.31	13.66	17.45	18.47
Fe$_2$O$_3$	0.78	1.49	1.62	1.01	0.74	0.76	0.75	1.49	2.06	2.84	1.27	1.66	1.46	0.91	0.94	1.27
FeO	0.71	0.33	0.53	0.50	0.29	0.19	0.37	1.62	1.41	1.89	6.29	0.98	1.36	0.59	0.38	1.58
MnO	0.02	0.02	0.03	0.03	0.01	0.02	0.02	0.05	0.04	0.12	0.14	0.03	0.04	0.03	0.02	0.04
MgO	0.37	≤0.30	0.32	≤0.30	≤0.30	≤0.30	≤0.30	2.12	2.01	2.67	4.58	1.75	1.46	1.07	1.20	2.82
CaO	0.10	0.42	0.18	0.24	0.40	0.04	0.35	2.42	3.10	2.53	6.86	2.14	2.75	1.60	2.97	2.88
Na$_2$O	3.55	3.59	3.51	3.53	3.95	4.24	4.60	4.64	4.65	3.99	3.89	4.77	4.74	4.99	5.67	4.91
K$_2$O	5.68	5.34	5.47	5.29	4.66	4.07	4.50	3.16	3.03	4.61	4.05	3.15	3.31	1.49	1.27	1.62
P$_2$O$_5$	0.10	0.13	0.21	0.20	0.12	0.11	0.12	0.30	0.30	0.47	0.93	0.20	0.25	0.11	0.13	0.21
CO$_2$	≤0.15	≤0.15	≤0.15	≤0.15	0.40	≤0.15	≤0.15	0.22	≤0.15	0.22	≤0.15	≤0.15	≤0.15	0.22	0.18	≤0.15
H$_2$O	0.63	≤0.36	0.54	0.63	0.63	≤0.36	≤0.36	1.70	0.71	0.36	0.89	0.63	0.54	0.98	0.71	0.80
Total	99.93	99.62	99.76	99.61	100.02	99.71	99.52	99.74	99.85	100.19	100.11	99.56	99.98	99.88	99.93	98.99
CIPW cor	1.59	1.74	1.95	2.67	2.51	1.69	1.82	2.07	1.07	3.14	-	2.34	0.47	1.68	2.05	3.86
Li(ppm)	26	107	176	104	28	66	112	30	36	27	14	51	150	42	280	900
Rb	357	303	377	377	168	351	332	109	103	160	97	101	122	30	85	414
Be	5	4	5	6	3	4	6	2	2	4	4	2	3	1	2	3
Sr	104	114	97	97	118	44	99	674	792	807	1158	562	686	360	458	635
Ba	756	686	598	600	553	408	559	1088	1141	1145	1590	976	991	663	685	944
Zn	≤18	20	24	29	≤18	27	27	66	59	76	72	56	50	41	≤18	73
Zr	145	138	139	138	81	40	99	152	128	218	219	110	133	45	58	116
Nb	18	9	17	19	8	12	11	10	9	14	14	7	10	8	6	7
Sn	4	5	5	6	4	10	6	1	2	2	1	2	2	1	3	4
K/Rb	132	146	120	167	230	96.3	113	240	244	239	346	258	255	413	124	32.4
K/Ba	62.4	64.6	75.9	73.2	70.0	82.8	66.9	24.1	22.1	33.5	21.1	26.7	27.8	18.7	15.3	14.2
Ba/Rb	2.12	2.26	1.59	1.59	3.29	1.16	1.68	9.98	11.08	7.16	16.39	9.66	8.12	22.1	8.06	2.28
Ba/Sr	7.27	6.02	6.16	6.19	4.69	7.27	5.65	1.61	1.44	1.42	1.37	1.74	1.44	1.84	1.50	1.49
Rb/Sr	3.43	2.66	3.89	3.89	1.42	7.98	3.35	0.162	0.130	0.198	0.084	0.180	0.178	0.083	0.186	0.652
Mg/(Li x 10)	8.4	-	1.1	-	-	-	-	43	34	60	197	21	5.9	16	2.6	1.9
Zr/Sn	36	28	28	23	20	4.0	17	152	64	109	219	55	67	96	19	29
A/CNK	1.12	1.12	1.14	1.19	1.15	1.14	1.12	1.06	1.03	1.10	0.62	1.12	1.00	1.06	1.09	1.23
FeO/Fe$_2$O$_3$	0.91	0.22	0.33	0.50	0.39	0.25	0.49	1.09	0.68	0.67	4.95	0.59	0.93	0.65	0.40	1.24

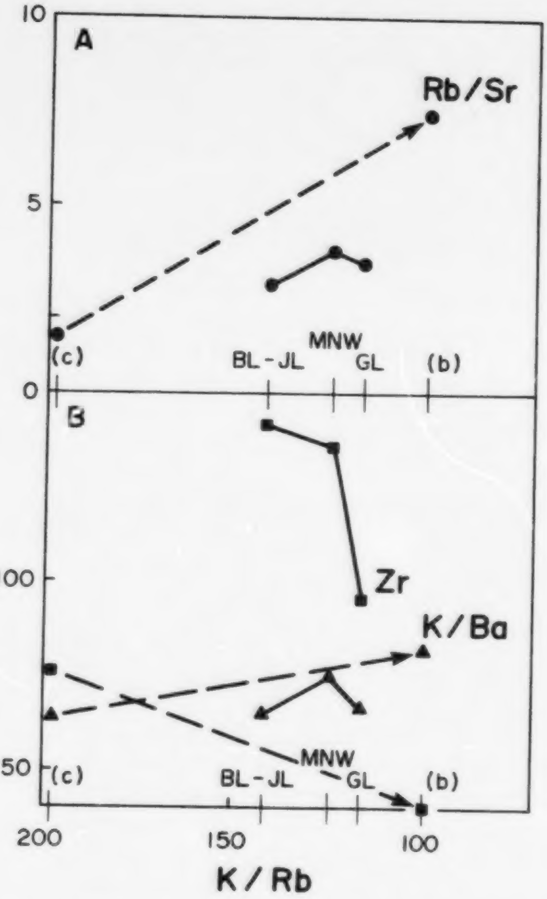

Figure 225.2. *Fractionation as a function of K/Rb ratio for the two-mica leucogranites: a) Rb/Sr vs K/Rb; b) Zr and K/Ba vs K/Rb. Intrusions and sample numbers as follows: BL-JL, 1 and 22—Barbara Lake-Jean Lake stock; MNW, 4 and 5—MNW stock; GL, 24—Glacier Lake pluton. Arrows show the trend from the (c) core zone, 17 to (b) border zone, 19, in the Glacier Lake pluton (see Figure 225.1 and Table 225.1).*

Only the MNW pegmatite is hosted in two-mica leucogranite, the MNW stock. All of the rare-element pegmatites occur as dikes of maximum width about 10 m. The dikes strike easterly to northeasterly to northerly and have dips ranging from near vertical to near horizontal (Pye 1965). The apparent irregular distribution of the pegmatites within the study area is probably largely a function of outcrop and ground-cover conditions.

The pegmatites sampled have been here subdivided into a Northern Group, including the Nama Creek North and South, Giles, Camp, McVittie, and Powerline pegmatites; a Central Group, including the Brink, Southwest, Salo, Niemi, Point, and Island pegmatites; and a Southern Group with 1 member, the MNW pegmatite. The Southern, Central, and Northern Groups correspond, respectively, to Groups 1, 2, and 4 of Milne (1962). Milne's Group 3 pegmatites were not sampled, but on the basis of their locations and published descriptions were believed to be essentially the same as Group 4.

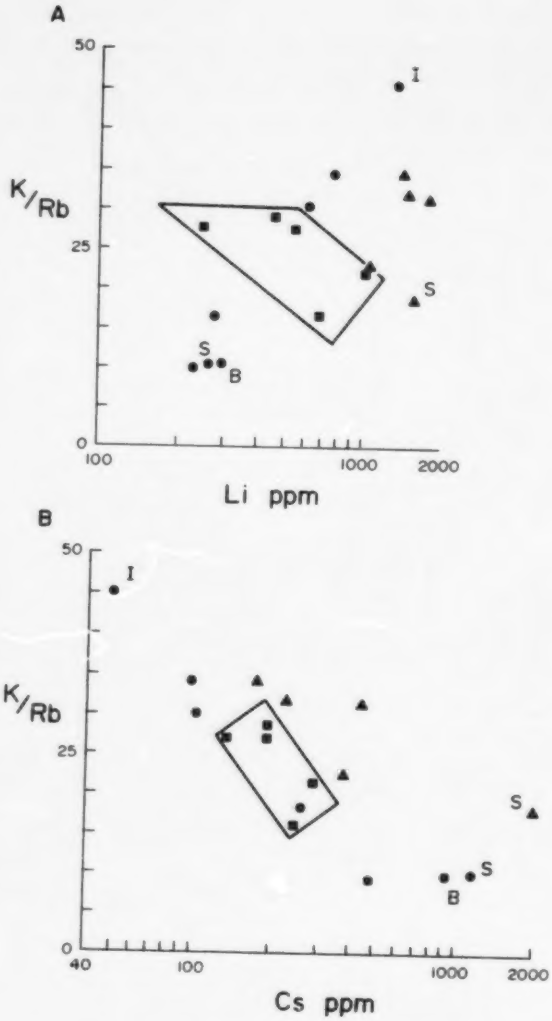

Figure 225.3. *Fractionation in terms of K/Rb in muscovite from rare-element pegmatites: a) K/Rb vs Li, b) K/Rb vs Cs. Northern Group pegmatites are outlined by a quadrilateral. Symbols are from Table 225.2.*

All of the pegmatites of the Northern and Central Groups are unzoned, with the exception of the Brink, which has a variably developed border zone. The MNW pegmatite of the Southern Group shows, on the other hand, distinct zones, which were described by Milne (1962) originally, and subsequently by others (Pye 1965; Mulligan 1965; Breaks 1980).

TABLE 225.2. SAMPLE LOCATIONS OF ANALYZED MUSCOVITE SPECIMENS.

Group	Pegmatite	Sample No.	Description
Southern ▲	MNW-wall zone-west	M74	book muscovite
	MNW-intermediate zone-west	M63	book muscovite
	MNW-intermediate zone-east	M79	book muscovite
	MNW-wall zone-east	M80	book muscovite
	MNW-core zone (S)	M73	microcrystalline
Central ●	Brink (S)	M10	microcrystalline
	Brink (B)	M12	book muscovite (green)
	Southwest	M95	book muscovite (green)
	Salo	M87	book muscovite
	Niemi	M103	book muscovite
	Point	M116	book muscovite
	Island (I)	M117	book muscovite
Northern ■	Nama Creek North	M49	fine-grained
	Nama Creek South	M50	fine-grained
	McVittie	M29	fine-grained
	Powerline	M6	fine-grained
	Camp	M32	fine-grained
	Giles	M131	fine-grained

TABLE 225.3. ANALYSES OF MUSCOVITE FROM THE MNW PEGMATITE.

wt.%	M74	M63	M79	M80	M73
SiO_2	45.68	46.50	43.42	45.45	44.97
TiO_2	0.26	0.25	≤0.24	0.25	≤0.24
Al_2O_3	33.56	33.78	34.91	33.26	36.14
FeO^*	2.54	2.21	1.80	2.32	0.70
MgO	0.96	1.06	0.42	0.79	0.36
Na_2O	0.79	0.79	0.64	0.82	0.46
K_2O	10.22	9.83	9.91	9.76	10.59
H_2O	5.31	5.76	6.93	5.13	4.41
Total	99.32	100.18	98.03	97.78	97.63
ppm					
Li	1399	1561	1060	1764	1570
Rb	2440	2557	3602	2578	4753
Cs	176	227	378	432	2053
Sr	48	52	61	49	70
Ba	508	457	387	453	398
Sc	12	11	1	10	2
Zr	23	20	14	17	11
Nb	213	213	177	229	46
Ta	56	65	61	77	141
Co	3	2	nd	nd	0.5
Sn	390	570	618	427	300
K/Rb	34.75	31.91	22.85	31.42	18.49

total iron as FeO
nd = not determined

TABLE 225.4. ANALYSES OF MUSCOVITE FROM THE CENTRAL GROUP PEGMATITES.

wt.%	M10	M12	M95	M87	M103	M16	M117
SiO_2	45.37	45.26	47.31	46.52	44.11	45.41	46.30
TiO_2	0.24	0.24	0.24	0.24	0.24	0.24	0.24
Al_2O_3	36.46	35.72	37.87	37.04	35.31	34.84	34. 66
FeO*	0.63	0.63	0.17	0.54	1.96	1.84	2.12
MgO	0.44	0.37	0.36	-	0.57	0.46	1.10
Na_2O	0.74	0.73	0.65	0.77	0.74	0.79	0.71
K_2O	10.31	9.82	9.45	9.59	10.21	9.86	10.45
H_2O	4.41	5.22	4.77	4.68	4.86	6.03	5.13
Total	98.36	97.75	100.58	99.14	97.76	99.23	100.46
ppm							
Li	261	291	238	273	618	758	1326
Rb	7864	8034	7871	4794	2808	2376	1888
Cs	1181	925	479	263	104	99	49
Sr	99	99	94	75	51	56	53
Ba	422	391	401	384	447	442	600
Sc	0.1	0.1	0.1	0.1	3	2	11
Zr	7	7	7	10	17	19	21
Nb	59	114	92	155	145	151	184
Ta	103	61	77	44	54	63	46
Co	0.5	0.5	0.5	nd	nd	3	2
Sn	405	480	280	nd	nd	nd	324
K/Rb	10.89	10.14	9.96	16.60	30.20	34.47	45.97

*total iron as FeO
nd = not determined

PETROGRAPHY

The petrography of the pegmatites has been discussed in detail by Milne (1962) and will be only briefly reviewed here. The pegmatites of the Georgia Lake pegmatite field are characterized by the presence of spodumene, with abundant quartz and perthitic microcline, and variable amounts of muscovite, albite, and other minerals. As noted previously, the Southern Group is differentiated from the Central and Northern Groups by the presence of zoning. The Northern Group pegmatites are differentiated texturally from those of the Central Group by the presence of coarse- to medium-grained spodumene and microcline in a finer grained matrix of quartz, muscovite, and albite. Aplite stringers and pods, frequently rimmed with muscovite and containing small garnets, occur only in the Northern Group.

The Central Group pegmatites are unzoned to weakly zoned, especially Brink. They are characterized by coarse to very coarse grained microcline and spodumene with finer albite, microcline, and quartz. Aggregates of apatite crystals occur together with subordinate and variable garnet, tantalite-columbite, purpurite-heterosite, and tourmaline. Saccharoidal albite is characteristic in the Central Group.

The MNW pegmatite of the Southern Group is symmetrically zoned into at least 5 zones, according to the classification of Cameron *et al.* (1949). The zoning is described in detail elsewhere (Milne 1962). However, in the inner zones, spodumene occurs in an intimate intergrowth with quartz (SQUI), which is interpreted as a breakdown product of petalite. Small relics of petalite are also visible in thin section. The inner zones of the pegmatite contain fairly abundant phosphate minerals and noticeable quantities of ferrocolumbite, ferrotantalite, and staringite, the Ta-rich polytype of cassiterite.

GEOCHEMISTRY

Fractionation trends in the rare-element pegmatites were investigated by analysis of microcline and muscovite, as well as Ta-Nb-Sn oxide minerals. Muscovite, as well, was studied as a potential carrier of Nb, Ta, and Sn, which might serve as an indicator of economic concentrations of these elements.

Muscovites of various habits from the various pegmatite groups (Table 225.2) are designated by symbols in subsequent diagrams. Muscovite books from the various zones of the MNW pegmatite of the Southern Group (Table 225.3) displayed minor but significant differences in trace element content. The Central Group pegmatites (Table 225.4) exhibited a strong fractionation trend from east to west among members of the group. The Northern Group pegmatites (Table 225.5) were of relatively constant trace element abundance with significant differences only in Rb and Li contents.

Representative fractionation trends in the muscovites are illustrated in Figure 225.3 as K/Rb vs Cs, and K/Rb vs Li plots. While the most fractionated pegmatites have the lowest K/Rb ratios, Cs and Li contents have opposite trends. Among the Central Group pegmatites nearly linear trends on semi-log plots exist between the least fractionated Island pegmatite (I) and the most fractionated Salo pegmatite (S). The Northern Group pegmatites form a tight cluster, outlined by quadrilaterals in Figure 225.3a and b, lying midway in the trend established by the Central Group. The MNW pegmatite zones show considerable fractionation in the K/Rb vs Cs plot (Figure 225.3b), with the core (S) showing the highest Cs of any of the pegmatites, but K/Rb somewhat less fractionated than in several of the Central Group pegmatites. Li in the MNW muscovite is highest of any of the pegmatites, but shows little variation in a semi-log plot.

Nb in muscovite is fairly constant in the Northern Group pegmatites (Table 225.5), but varies inversely according to degree of fractionation in the Central Group. The values in the Northern Group, clustering around 100 ppm, are rather high, and are not well distinguished from values obtained in pegmatites of the Central Group that carry tantalite-columbite (Brink and Southwest). Ta is more concentrated in the muscovite of the most fractionated Central Group pegmatites; however, these values, around 100 ppm, are not clearly separable from the Ta contents of the Northern Group. Data on Sn contents is not available for the Northern group, but the behaviour seems likely to be similar to that of Nb and Ta. Within the MNW pegmatite of the Southern Group, trends within the Central Group are duplicated in the sequence, wall to intermediate to core zone, indicating strong internal fractionation.

Microcline from the various pegmatites (Table 225.6) was analyzed for selected elements (Table 225.7). The trace elements Rb, Cs, Sr, Ba, and Zr are all strongly to moderately fractionated. Typical is a semi-log plot of K/Rb vs Cs (Figure 225.4). A nearly linear trend is again seen between the least fractionated Island (I) and the most fractionated Brink (B) pegmatites. The Northern Group microclines lie near the middle of this linear trend in a cluster. The MNW pegmatite of the Southern Group shows a linear trend from wall to core (c) zones, but with higher K/Rb ratios and Cs contents than in the Central Group.

Tantalite-columbite were found in the MNW and Brink pegmatites, as reported earlier (Pye 1965), and newly discovered in the Southwest pegmatite. Analyses of these (Table 225.8) show a variation from tantalite to columbite, with ferroan and manganoan varieties as well. Both ordered and disordered structures are present, as indicated by X-ray studies.

Cassiterite had been previously reported in the MNW pegmatite (Breaks 1980), but our analyses (Table 225.9) show significant Ta_2O_5 content. Powder and single crystal X-ray studies reveal the presence of superstructure, indicating that the mineral is staringite (Burke *et al.* 1969). The Ta_2O_5 content is lower than in type staringite, but higher than in most cassiterite (Foord 1982).

DISCUSSION

PETROGENESIS

The subdivision of the pegmatites on textural grounds into Northern, Central, and Southern Groups is well justified by the geochemical data presented. The

TABLE 225.5. ANALYSES OF MUSCOVITE FROM THE NORTHERN GROUP PEGMATITES.

wt.%	M48	M50	M29	M6	M32	M131
SiO_2	44.55	46.25	47.87	46.03	46.98	45.78
TiO_2	≤0.24	≤0.24	≤0.24	≤0.24	≤0.24	≤0.24
Al_2O_3	34.81	34.59	36.01	33.91	35.81	34.84
FeO*	1.26	2.79	1.31	3.09	1.20	2.77
MgO	0.35	-	-	0.33	0.36	0.45
Na_2O	0.83	0.78	0.65	nd	1.15	0.86
K_2O	10.29	10.43	9.53	10.15	9.65	10.40
H_2O	5.04	4.86	4.86	nd	4.68	4.77
Total	97.13	99.70	100.23	93.51	99.83	99.65
ppm						
Li	459	683	1034	nd	244	553
Rb	2929	5273	3479	nd	2920	3110
Cs	189	247	288	nd	189	135
Sr	61	60	62	97	72	60
Ba	395	398	494	415	434	516
Sc	0.8	0.1	1	nd	0.8	0.6
Zr	20	17	22	18	23	35
Nb	98	144	95	88	94	180
Ta	89	83	108	nd	2	0.7
Co	1	nd	nd	nd	nd	nd
K/Rb	29.16	16.42	22.74	-	27.43	27.75

*total iron as FeO
nd = not determined

TABLE 225.6. SAMPLE LOCATIONS OF ANALYZED PERTHITIC MICROCLINE SPECIMENS.

Group	Pegmatite	Sample No.
Southern ▲	MNW-wall zone-north	F71
	MNW-wall zone-south	F76
	MNW-core zone (c)	F72
Central ●	Brink (B)	F17
	Southwest	F100
	Salo	F88
	Niemi	F102
	Point	F114
	Island (I)	F120
Northern ■	Nama Creek North	F48
	Nama Creek South	F54
	McVittie	F24
	Powerline	F5
	Camp	F33
	Giles	F132

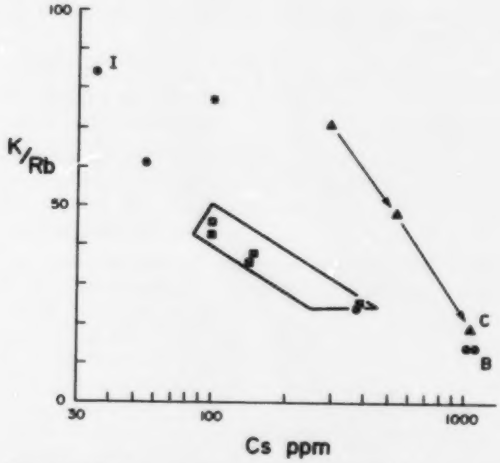

Figure 225.4. K/Rb vs Cs in microcline from rare-element pegmatites. Northern Group pegmatites are outlined by a quadrilateral. Arrows indicate the fractionation trend from wall to core (c) zones. Symbols are from Table 225.2.

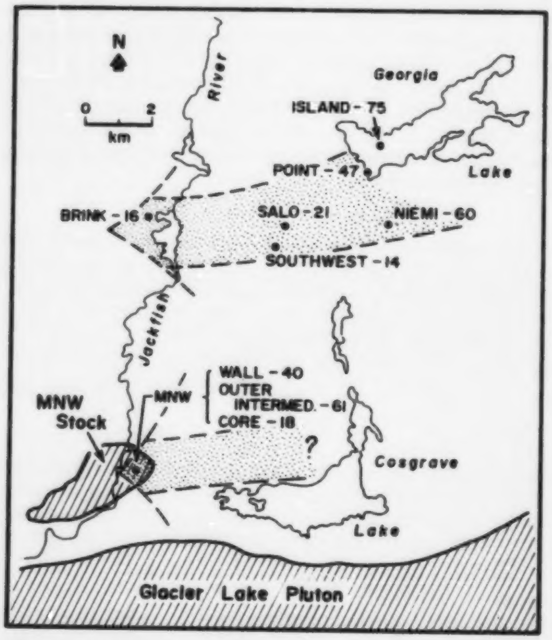
N
0
2
km
River
Georgia
ISLAND - 75
POINT - 47
Lake
BRINK - 16
SALO - 21
NIEMI - 60
SOUTHWEST - 14
Jackfish
WALL - 40
OUTER
INTERMED. - 61
CORE - 18
MNW
MNW
Stock
?
Cosgrave
Lake
Glacier Lake Pluton

Figure 225.5. Trend of K/Rb ratio in microcline of the Central Group pegmatites. Ratios are also given for zones within the MNW pegmatite of the Southern Group.

strong fractionation trends within the Central Group clearly distinguish it from the Northern Group, in which pegmatites show negligible differences in fractionation. A model of rare-element pegmatite zonation derived by Nedumov (1964) suggests that fractionation increases with distance from the parental magma due to continued evolution of late magmatic fluids. Within the Central Group increasing fractionation from east to west suggests a source area in the vicinity of Barbara Lake. However, intervening zones of beryl-bearing and barren pegmatite should also occur, and their presence is not yet established.

The problem of the Southern Group's origin is compounded by a lack of comparative data. The

TABLE 225.7. COMPOSITIONAL CHARACTERISTICS OF PERTHITIC MICROCLINE FROM THE GEORGIA LAKE RARE-ELEMENT PEGMATITES.

wt.%	F71	F76	F72	F17	F100	F88	F102	F114	F120	F48	F54	F24	F6	F33	F132
K_2O	16.04	16.21	15.32	15.09	15. 58	16.04	16.03	15.80	16.12	15.95	nd	15.88	15.79	16.14	16.05
ppm															
Rb	1886	2792	6707	8969	9149	5527	1717	2138	1596	3677	3397	3670	5152	3485	2864
Cs	287	537	1015	1120	1090	3374	106	54	34	103	117	149	382	144	104
Sr	114	94	92	140	118	93	218	224	260	78	71	77	75	75	60
Ba	891	455	416	428	425	429	486	729	1097	421	410	469	437	475	419
Zr	23	≤7	17	≤7	≤7	8	19	17	16	20	16	18	21	20	22
K/Rb	70.6	48.2	19.0	14.0	14.1	24.1	77.5	61.4	84.2	43.0	-	35.9	25.5	38.5	46.5

TABLE 225.8. SELECTED MICROPROBE ANALYSES OF Ta-Nb MINERALS FROM THE GEORGIA LAKE RARE-ELEMENT PEGMATITES.

wt.%	T2	T3A	T4-4	T6A	T1-1(L)	T1-1(D)
Ta_2O_5	59.59	46.84	19.63	25.40	53.85	44.62
Nb_2O_5	22.87	30.43	59.60	55.82	29.55	38.72
TiO_2	0.50	3.54	1.23	0.38	-	-
SnO_2	1.69	3.48	0.39	-	0.39	-
FeO*	4.60	13.90	14.13	9.74	3.81	3.62
MnO	10.60	2.06	4.95	8.81	12.86	13.48
Sc_2O_3	-	-	-	-	0.05	-
Total	99.86	100.24	99.93	100.14	100.53	100.64

Notes:
T2: core zone, MNW pegmatite
T3A: Intermediate zone, MNW pegmatite (inclusions in staringite)
T4-4: Intermediate zone, MNW pegmatite
T6A: Southwest pegmatite
T1-1(L): Brink pegmatite, light BSE image
T1-1(D): Brink pegmatite, dark BSE image
A dash denotes not detected
*All iron as FeO

TABLE 225.9. MICROPROBE ANALYSES OF Sn OXIDE MINERALS FROM THE MNW PEGMATITE.

wt.%	S7A	S7B	S8A	S8B	S9
Ta_2O_5	2.49	8.34	1.91	2.15	4.45
Nb_2O_5	-	1.52	-	0.29	1.87
TiO_2	-	-	-	-	0.42
SnO_2	98.39	89.42	97.78	97.16	91.90
FeO*	0.41	1.50	0.55	0.69	1.53
MnO	-	-	-	-	0.12
Total	101.28	100.78	100.25	100.29	100.30

Notes:
S7A and S7B: core zone (staringite)
S8A and S8B: intermediate zone (cassiterite?)
S9: intermediate zone (staringite)
A dash denotes not detected
*all iron as FeO

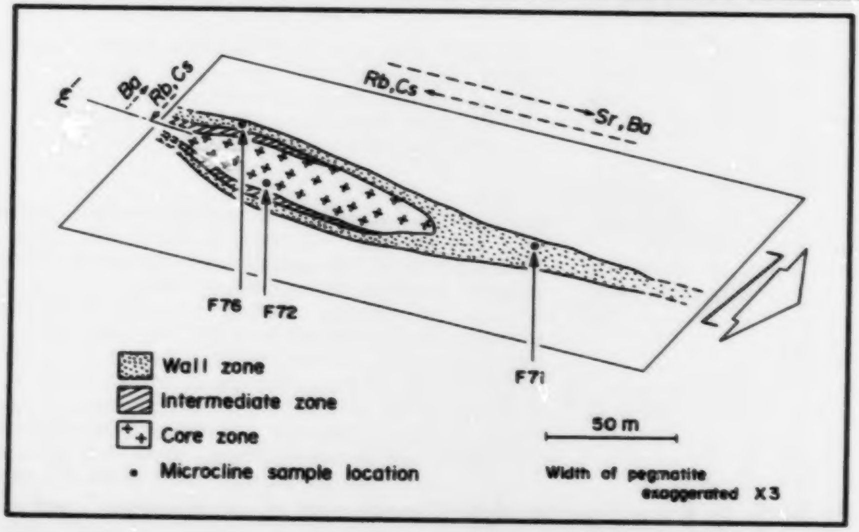

Figure 225.6. Trace element abundance trends in microcline within the MNW pegmatite, indicating the direction to pods of Ta-Nb-Sn mineralization within the dike. Sample numbers refer to Table 225.7.

group may be a southern extension of the pattern observed in the Central Group, or it may have been derived from a source centred on the MNW stock. Zonation patterns remain unclear.

The lack of significant fractionation within the Northern Group pegmatites, even though they occur over a greater area than the highly fractionated Central Group (*see* Figure 225.1), is strong evidence of differing origins for the 2 groups. The widely accepted Jahns and Burnham (1969) model of formation by differentiation from a parental magma may not apply in the Northern Group. Direct anatexsis of Li-rich sediments has been suggested as a mechanism by Norton (1973), although Černý (1982) has discussed some problematical aspects of such a hypothesis.

The internal evolution of the pegmatites may also have had a strong bearing on factors such as mineralogy, texture, and geochemistry. A number of characteristics, including the nature of the spodumene in the pegmatites, are suggestive of the influence of differing courses of internal evolution. Heinrich (1975, 1976) subdivided pegmatitic spodumene into 3 types: 1) phenocrystic, greenish spodumene of high (0.6 to 0.9 wt.%) Fe_2O_3, characteristic of unzoned or weakly zoned pegmatites; 2) zonal, white spodumene of low (0.01 to 0.03 wt.%) Fe_2O_3, characteristic of cores and intermediate zones of zoned pegmatites, and 3) secondary, white spodumene of very low (0.007 to 0.03 wt.%) Fe_2O_3, produced by breakdown of petalite to yield spodumene-quartz intergrowths (SQUI). In the Georgia Lake area, the Northern Group pegmatites contain phenocrystic spodumene exclusively and, together with the presence of late aplites, indications are that magmatic crystallization predominated. The lack of fractionation may also be attributed to minimal interaction with a late magmatic fluid.

The Central Group pegmatites also contain phenocrystic spodumene but lack the aplitic phase of the Northern Group. Development of weak zonation in the most fractionated Brink pegmatite, together with strong fractionation of trace elements, suggest a much greater role for a late magmatic fluid.

Finally, the MNW pegmatite of the Southern Group contains both secondary and zonal spodumene and is well zoned itself. The strong internal fractionation from wall to core zones is suggestive of a progression from magma + fluid-dominated to fluid-dominated crystallization.

The problem of parental magmas for the pegmatites can be only partially resolved in work completed so far. The highly fractionated, S-type two-mica leucogranites seem to be obvious parents to the pegmatites of the Central and Southern Groups. The magma parental to the Northern Group pegmatites, if it exists, is not readily apparent. The tonalitic dikes and sills, although of S-type, are not highly fractionated, and consideration of their small size, as well, does not make them likely parents. Differences in internal evolution, as discussed previously, may better account for the differences seen in the Northern Group than a search for a different parental magma.

ECONOMIC IMPLICATIONS

The present work suggests that the emphasis, in the past, on the Georgia Lake pegmatites, as a lithium resource has obscured a potential for tantalum and niobium and, perhaps, tin. The abundant mineralization visible in the MNW pegmatite suggests that this body is worthy of further investigation. Moreover, the degree of fractionation of pegmatites of the Central Group is also indicative of potential for Ta and Nb. The extent of fractionation in the MNW pegmatite of the Southern Group, and the Brink, Southwest, and Salo of the Central Group, is comparable to that found in muscovite and microcline of the former producer, the Tanco pegmatite of Manitoba (Goad and Černý 1981).

On a practical level, the fractionation trends determined within the Central Group pegmatites point precisely to areas of potential exploration interest. Figure 225.5 illustrates the K/Rb ratio decreasing to the west within the group, indicating quantitatively the most fractionated (lowest ratio) pegmatites. The situation with respect to the zoned MNW pegmatite in the lower portion of the figure is less clear, but presumably could be illuminated with additional data.

Fractionation as indicated by microcline in the MNW pegmatite (Table 225.7) is also a guide to the occurrence of more highly mineralized pods and zones. Figure 225.6 schematically illustrates that increasing Rb and Cs, and decreasing Sr and Ba in microcline may point in the direction of richer Ta and Nb mineralization along a pegmatite dike.

CONCLUSIONS AND FUTURE WORK

The work completed at present leads us to the following conclusions:

1. Subdivision of pegmatites into 3 groups, based on textural and mineralogical criteria, is supported by geochemical data. Northern Group pegmatites form a cluster with respect to trace element fractionation in microcline and muscovite, lying near the midpoint of a strong east to west fractionation trend exhibited by the Central Group. The zoned MNW pegmatite of the Southern Group has unclear affinities to the Central Group.
2. Trace element fractionation trends in pegmatite minerals serve as a guide to Ta, Nb, and Sn mineralization, pointing rather specifically to targets of interest.
3. The two-mica leucogranites of the Glacier Lake pluton and related satellite bodies appear to be the parental magmas for the Central and Southern Group pegmatites. The parental material for the Northern Group pegmatites is not obvious, but the group may have been formed by a different mechanism of internal evolution.

Further work on the following problems is suggested by our results and would serve to clarify some remaining questions:

1. Study of the internal features of the Glacier Lake pluton would clarify the relationships among it, the satellite plutons, and the pegmatites. At present, insufficient geochemical data are on hand

to determine precisely the parental body or bodies.

2. The presence of beryl-bearing and barren pegmatitic zones inward of the rare-element pegmatites requires further investigation, both to establish firmly the direction of fractionation trends, and indicate likely parental, magmatic bodies.

ACKNOWLEDGMENTS

Assistance in laboratory work at Lakehead University was provided by M. Artist-Downey, T.J. Griffith, A. MacKenzie, K. Pringnitz, and E. Jensen. C.M. Cermignani and M.P. Gorton assisted with electron microprobe analyses at the University of Toronto. Analyses of oxides were conducted at the University of Manitoba by R. Chapman through the generous support of P. Černý. F.W. Breaks provided much helpful advice, and analyses for selected elements were conducted by the Geoscience Laboratories of the Ontario Geological Survey through the support of G.C. Patterson, Thunder Bay District Geologist. Tables were typed by W.C. Bons, and drafting was done by S.T. Spivak.

REFERENCES

Breaks, F.W.
1980: Lithophile Mineralization in Northwestern Ontario, Rare Element Granitoid Pegmatites; p.5-9 *in* Summary of Field Work, 1980, by the Ontario Geological Survey, edited by V.G. Milne, Owen L. White, R.B. Barlow, J.A. Robertson, and A.C. Colvine, Ontario Geological Survey, Miscellaneous Paper 96, 201p.

Burke, E.A.J., Kieft, C., Felius, R.O., and Adusumilli, M.S.
1969: Staringite, a New Sn-Ta Mineral from Northeastern Brazil; Mineralogical Magazine, Volume 37, p.447-452.

Cameron, E.N., Jahns, R.H., McNair, A.H., and Page, L.R.
1949: Internal Structure of Granitic Pegmatites; Economic Geology, Monograph 2, 115p.

Černý, P.
1982: Petrogenesis of Granitic Pegmatites; p.405-461 *in* Granitic Pegmatites in Science and Industry, edited by P. Černý, Mineralogical Association of Canada, Short Course Handbook, Volume 8, 555p.

Chappell, B.W.
1978: Granitoids from the Moonbi District, New England Batholith, Eastern Australia; Journal of the Geological Society of Australia, Volume 25, p.267-283.

Chappell, B.W., and White, A.J.R.
1974: Two Contrasting Granite Types; Pacific Geology, Volume 8, p.173-174.

Foord, E.E.
1982: Minerals of Tin, Titanium, Niobium, and Tantalum in Granitic Pegmatites; p.187-238 *in* Granitic Pegmatites in Science and Industry, edited by P. Černý, Mineralogical Association of Canada, Short Course Handbook, Volume 8, 555p.

Franklin, J.M.
1978: Uranium Mineralization in the Nipigon Area, Thunder Bay District, Ontario; Current Research, Part A, Geological Survey of Canada, Paper 78-1A, p.275-282.

Goad, B.E., and Černý, P.
1981: Peraluminous Pegmatitic Granites and their Pegmatite Aureoles in the Winnipeg River District, Southeastern Manitoba; Canadian Mineralogist, Volume 19, p.177-194.

Heinrich, E.W.
1975: Economic Geology and Mineralogy of Petalite and Spodumene Pegmatites; Indian Journal of Earth Sciences, Volume 2, p.18-29.
1976: A Comparison of Three Major Lithium Pegmatites: Varutrask, Bikita, and Bernic Lake; p.50-54 *in* Lithium Resources and Requirements by the Year 2000, edited by J.D. Vine, United States Geological Survey, Professional Paper 1005.

Hine, R., Williams, I.S., Chappell, B.W., and White, A.J.R.
1978: Contrasts Between I- and S-type Granitoids of the Kosciusko Batholith; Journal of the Geological Society of Australia, Volume 25, p.219-234.

Jahns, R.H., and Burnham, C.W.
1969: Experimental Studies of Pegmatite Genesis. I. A Model for the Derivation and Crystallization of Granitic Pegmatites; Economic Geology, Volume 64, p.843-864.

McCrank, G.F.D., Misiura, J.D., and Brown, P.A.
1981: Plutonic Rocks in Canada; Geological Survey of Canada, Paper 80-23, 171p.

Milne, V.G.
1962: The Petrography and Alteration of Some Spodumene Pegmatites Near Beardmore, Ontario; Unpublished Ph.D. Thesis, University of Toronto, 242p.

Mulligan, R.
1965: Geology of Canadian Lithium Deposits; Geological Survey of Canada, Economic Geology Report 21, 131p.

Nedumov, I.B.
1964: The Process of Differentiation of Pegmatitic Melt and the Role of Tectonics in the Formation of Rare-Element Pegmatites; 22nd International Geological Congress, New Delhi, Reports, Part 6, p.116-139.

Norton, J.J.
1973: Lithium, Cesium, and Rubidium—The Rare Alkali Metals; p.365-378 *in* United States Mineral Resources, edited by D.A. Brobst and W.P. Pratt, United States Geological Survey, Professional Paper 820, 722p.

Pitcher, W.S.
1979: Comments on the Geological Environments of Granites; p.1-8 *in* Origin of Granitic Batholiths—Geochemical Evidence, edited by M.P. Atherton and J. Tarney, Shiva, Kent.

Pye, E.G.
1965: Georgia Lake Area; Ontario Department of Mines, Geological Report 31, 113p.

Stockwell, C.M., McGlynn, J.C., Emslie, R.F., Sanford, B.V., Norris, A.W., Donaldson, J.A., Fahrig, W.F., and Currie, K.L.
1970: Geology of the Canadian Shield, Introduction; p.44-54 *in* Geology and Economic Minerals of Canada, edited by R.J.W. Douglas, Geological Survey of Canada, Economic Geology Report 1, 838p.

Trueman, D.L., and Černý, P.
1982: Exploration for Rare-Element Granitic Pegmatites; p.463-493 *in* Granitic Pegmatites in Science and Industry, edited by P. Černý, Mineralogical Association of Canada, Short Course Handbook, Volume 8, 555p.

Zayachkivsky, B.
1985: Granitoids and Rare-Element Pegmatites of the Georgia Lake Area, Northwestern Ontario; Unpublished M.Sc. Thesis, Lakehead University, 234p.

Grant 227 A Structural Investigation between the Kirkland Lake and Larder Lake Gold Camps

D.J. Toogood and C.J. Hodgson

Department of Geological Sciences, Queen's University

INTRODUCTION

In 1984 a program was initiated to investigate the structural and lithological controls of gold mineralization along the Kirkland-Larder Lakes Break. Since related studies had already commenced in the Virginiatown area (Hamilton 1983), the focus of this season's field work extended from Virginiatown in the east to Dobie in the west.

GENERAL GEOLOGY

The study area is in the southwestern part of the Archean (2.7 Ga) Abitibi greenstone belt, in an area dominated by ultramafic to mafic volcanic assemblages and intruded by felsic stocks and plutons (MERQ-OGS 1983). Trending east-west across this section of the greenstone belt is a conspicuous, narrow (2 to 3 km wide) zone of mostly clastic sedimentary rocks and associated alkaline volcanic rocks, exposed over a strike length, in Ontario, of approximately 60 km. These units are collectively referred to as the Timiskaming Group. Pronounced changes between fluviatile and turbidite facies occur within the Timiskaming.

In general the Timiskaming is steeply dipping, fractured, and foliated, with numerous cross-cutting minor intrusive rocks. The Timiskaming Group may be a supracrustal expression of a fundamental tectonic lineament known as the Cadillac-Larder Lake Fault (the Kirkland-Larder Lakes Break, in Ontario), which can be traced as a distinct entity for at least 150 km between Kenogami Lake in Ontario and Val d'Or in Quebec.

The extent of the Timiskaming has recently been the subject of some discussion. Most workers have considered the sedimentary rocks, both north and south of the Kirkland-Larder Lakes Break, as being Timiskaming in age (Thomson 1943, 1949; Hewitt 1963; Ridler 1970; Hyde 1978, 1980), although it had been acknowledged that the absence of alkaline volcanic rocks and the presence of significant iron formations in the south indicated a different environment. It was further established by Hyde (1978) that a variation in clast composition across the Break implied major changes in provenance. These observations have led Jensen and Langford (1983) to reinterpret the sequence south of the Break, and to place it in the considerably older Larder Lake Formation, which they believe contains intercalated ultramafic lavas and subordinate felsic volcanic rocks previously thought to form the basement to the Timiskaming Group. This interpretation would tend to emphasize the Kirkland-Larder Lakes Break as a profound discontinuity. Current investigations (Hamilton and Hodgson 1984; Jensen, in preparation) should resolve the status of the sedimentary and volcanic rocks in this area.

STRUCTURE

REGIONAL

The Kirkland-Larder Lakes Break occurs in a zone of pervasive deformation. Since the full width of this zone has yet to be identified, and since there is no definitive account of the strain features it contains, it may be premature to refer to the Kirkland-Larder Lakes Deformation Zone. In order to assess the significance of structural pattern, it is essential to determine the state of strain in the surrounding rocks. An area in Hearst Township, about 10 km south of the Break, was examined for this purpose.

The disposition of contacts on the geological map (Thomson 1949) and the frequent opposed facing directions were found to be the result of tight and isoclinal folding of the sedimentary/volcanic sequence. Two sets of coaxial folds (D_1 and D_2) were identified, one with axial surfaces trending northwest, and the other, northeast. The first set (D_1) has a weakly developed axial plane cleavage in sedimentary rocks, but in mafic volcanic rocks this cleavage is paralleled by a strong foliation defined by flattened pillows. These early folds are cross-cut by undeformed syenite dikes. Interference patterns are produced by the overprinting of D_1 folds by the northeasterly trending D_2 structures which deform syenite dikes, indicating that the 2 episodes of folding were separated by a period of igneous activity. Cases were also encountered of foliated lamprophyre dikes cross-cutting syenite boudins in D_2 fold cores, which suggest that these were emplaced contemporaneously with the later deformation. High D_2 strain tends to be localized in linear zones resembling simple shear zones. However, bedding displacement effects, changing symmetry of minor folds, and foliation orientation indicate these high strain zones are related to the cores of strongly amplified D_2 folds.

The recognition of fold interference patterns involving northwest- and northeast-trending coaxial folds in the Larder Lake area is strikingly similar to the situation reported in Quebec (Hubert *et al.* 1984). It establishes a history of multiple deformation that is uniformly distributed throughout the Abitibi Belt, and is not confined to, and may not be associated with, narrow zones of deformation around faults.

Since the structures described here lie south of the Kirkland-Larder Lakes Break, in an area where chronostratigraphic correlations are disputed, the significance of the deformation will obviously depend on whether the sedimentary rocks eventually prove to be Timiskaming in age, or part of a basement succession predating the Timiskaming.

LARDER LAKE BREAK

The term "Larder Lake Break" classically refers to a linear feature of very limited lateral extent which displays strong foliation and carbonatization in mafic rocks (Thomson 1943). During the present study, it was found that the foliation and other strain features are characteristic of a zone at least 2 to 3 km in width, extending as far north as the contact of the Timiskaming with the Kinojevis Group, and as far south as the north shore of Larder Lake in McGarry and McVittie Townships. The nature of the deformation in this zone is controlled by the mechanical properties of the different rock types. The development of planar and linear fabrics is prominent in sedimentary and mafic volcanic rocks and to a lesser degree in the trachytes, while fracturing and vein formation is very noticeable in the rigid, isotropic syenite bodies. Contacts between these units were invariably found to be sheared and faulted, making stratigraphic correlation in the deformation zone difficult. In addition, large shear-bounded blocks in the zone may have been erroneously interpreted as folds (Spectacle Lake Antiform?, Thomson 1943).

FABRIC DESCRIPTION

Foliations of several orientations are present. In general they tend to fall naturally into 2 groups, based on a combination of orientation and type.

S_1/L_1

The earliest planar fabrics have an orientation which mirrors the overall strike of the Kirkland-Larder Lakes Break. In the majority of these cases this is approximately 070° to 090°, but in some localities, such as in parts of Gauthier Township where there is a pronounced change in the regional trend of the Break, this may be north-south. In many outcrops, 2 foliations with almost identical orientations and characteristics exist, and both are referred to as S_1. The foliations have an anastomosing character and wrap around trachyte horizons and intrusive rocks alike, while intensity of development is pronounced along the contacts. The contemporaneity of the S_1 fabric is demonstrated by lack of overprinting relationships where they occur together.

The fabric is well developed in the mafic volcanic horizons where it is represented by a chlorite schist. In the sedimentary rocks pressure solution cleavage passes into a fissile, transposition foliation accompanied by rootless folds in the most highly strained localities. Since bedding and S_1 are subparallel, the foliation may be difficult to identify in cases where movement has been accommodated in the more incompetent argillaceous material, or localized along contacts between beds. S_1 is seen to be axial planar on steeply plunging isoclinal folds defined either by bedding or dikes. Deformed conglomerate pebbles are flattened in the foliation plane and stretched parallel to the fold axes and to the S_1 foliation intersections, mineral streaks, quartz rods, and mullions. They plunge northeast to east on the north side of the Break, and south or southeast on the south side.

S_2/L_2

In contrast to the variable orientation of S_1, a later fabric, designated S_2, has a fairly constant 040° to 070° strike throughout the area examined, despite obvious changes in the trend of the deformation zone. Where S_1 and S_2 are present in the same outcrop, the 040° to 070° fabric is always seen to be the younger. S_2 may be a fracture cleavage, crenulation cleavage, a solution cleavage and, more rarely, a transposition foliation. Whatever its form, it nearly always displays a subvertical dip. Linear fabrics (L_2) are defined by S_2 bedding and S_2/S_1 intersections, stretched pebbles, mineral streaking, and ribbing. All L_2 fabrics plunge at steep to moderate angles to the northeast on the north side of the Break, and to the south or southeast on the south side.

In central McGarry Township near the Kerr Addison Mine, S_2 has been reoriented by small-scale, vertical, 070° trending, dextral shear zones. In the same locality a 10 cm wide ductile mylonite band was found with an identical orientation and sense of displacement. This was the only ductile mylonite observed in the area studied.

S_3/L_3

This is a poorly developed fabric that is only important in McVittie and McGarry Townships. It is characterized by a very weak subhorizontal (up to 20° dips) foliation associated with chevron folds and kink bands having gentle east or west plunges. A fine ribbing on S_1 is the most commonly encountered variety of L_3. The reason why this fabric is restricted to the eastern part of the area is not yet understood. Prominent quartz-carbonate veins near the Kerr Addison Mine share a similar orientation to S_3 and may be genetically associated.

EARLIER FABRICS

Fabrics S_1 to S_3 exhibit a strong spatial association with the Kirkland-Larder Lakes Break and must be considered genetically related to it. In a few isolated instances cleavages have been observed which appear to predate S_1. Where they can be distinguished from later overprints, they are seen to vary widely in orientation from north-south to east-west. As yet it is not possible to determine whether they mark an earlier stage in the development of the deformation zone, or whether, perhaps, they are preserved effects of other deformational events now visible outside the zone.

LATER FABRICS

Younger fabrics occur throughout the area and are clearly related to discrete, linear, ductile shear zones of limited lateral extent. Most common orientations of these zones are 170° to 180° and 020° to 030°. Brittle fractures with no accompanying foliations are common with several orientations.

KINEMATICS AND FABRIC DEVELOPMENT

Linear zones displaying anomalously high strain are normally interpreted as shear zones (*sensu lato*), and the ductile fabrics they contain are thought to be the product of dominantly progressive simple shear (Ramsay 1980). The deformation now revealed in the zone associated with the Kirkland-Larder Lakes Break clearly involves rocks with markedly divergent mechanical behaviour and, as would be expected in this situation, fabric orientation in particular shows no obvious relationship to increasing shear gradients across a clearly demarcated shear zone.

The determination of the amount and direction of displacement in any shear zone is a major objective, and both the linear and planar fabrics are potentially useful for this purpose. Most workers agree that the extension lineation in shear zones parallels the X axis of the simple shear strain ellipsoid, and is consequently parallel to the shear direction (Simpson and Schmid 1983). On these grounds, the consistently steeply plunging linear fabrics associated with both S_1 and S_2 in the deformation zone, including ribbing, mineral streaking, rods, mullions, and stretched pebbles, would indicate continued dip slip movement. However, problems of interpretation arise in the present case since the extension lineation is usually found to be parallel to the intersection lineation defined by bedding and foliation of S_1 and S_2. This relationship is not anticipated in a simple shear model where a high angle would be predicted between intersecting shear-related foliations, and the bulk extension lineation (Berthé *et al.* 1979).

The regional northeast orientation of S_2 in relationship to an east-west trending deformation zone suggests an origin parallel to the XY plane of a simple shear strain ellipsoid, which would unequivocally indicate dextral strike-slip movement. This sense of displacement is also confirmed by reoriented S_2 and mylonite bands in the dextral shear zones which parallel the strike of the deformation zone. The steeply plunging intersection lineation between S_1 and S_2 would be compatible with this movement.

Any model which is proposed for the sense of displacement in the deformation zone must therefore take into account that strike-slip movement prevailed, at least during and following the development of S_2. It is tentatively suggested that the ductile LS fabric in the deformation zone may reflect components of both pure shear and simple shear, with the extension lineation now parallel to the X axis of the pure shear finite strain ellipsoid (Lister and Price 1978). There are no quantitative data giving the relative magnitudes of these 2 components.

A kinematic model for S_1 has yet to be formulated. Although they now occur as shear-parallel foliations, they are not "C shear" surfaces of translation as described by Berthé *et al.* (1979). The subvertical foliations are axial planar on ductile isoclinal folds with thickened hinge zones and attenuated limbs. Fold axes, S_1 intersection lineations, and extension lineations are again mostly sub-parallel. There is no evidence of a consistent movement sense shown by the asymmetry of the folds, but this could be caused by variations in the shear gradient within the shear zone (Ramsay 1983). We regard the use of folds as indicators of the relative displacement to be suspect, and especially so when the folds in question occur outside the discernible limits of shear zone influence. The development of S_1 may mark the most important phase of movement in the deformation zone and may be associated with sinistral strike-slip movement, as suggested by the distribution of gold deposits and intrusive rocks in the deformation zone (Hodgson 1982).

East of McGarry Township, the next exposures of the deformation zone are associated with the Cadillac-Larder Lake Fault in Quebec. In this area, Hubert *et al.* (1984) describe the fabrics with similar orientations, except they report the presence of a strong horizontal lineation (L_1) in the northern block immediately adjacent to the fault, which is not seen in the Larder Lake area. From the description, L_1 is an intersection lineation defined by steeply dipping bedding and a foliation (S_1). It does not appear to have been recorded by Goulet (1978) in his structural study across the fault near Rouyn, and its significance is not readily apparent.

The spatial association of a unique volcano/sedimentary succession, such as the Timiskaming, with a linear deformation zone, is closely analagous to the tectonic evolution of major strike-slip fault systems (Reading 1980; Aydin and Nur 1982; Aydin and Page 1984).

The variation in sedimentary units, the disposition of volcanic rocks, and changes in the structural pattern can be accounted for in a zone of "transpression", featuring dextral strike-slip movement combined with compression normal to the strike. A key area in this interpretation is near Dobie in central Gauthier Township, where a noticeable change in sedimentary facies has been well documented by Hyde (1978). To the west, the Timiskaming contains fluviatile and eolian deposits, but where the belt changes strike, around the Lebel Stock, only turbidite sequences are encountered, while farther east, in McVittie and McGarry Townships, turbidites occur with fluviatile beds. The abrupt change from a fluviatile to a turbidite environment is accompanied by a break in the semi-continuous nature of the trachyte members. We believe that these features are best explained by the development of a pull-apart basin (herein referred to as the Dobie Basin) east of the Lebel Stock, following an early stage of fracture initiation (Figures 227.1A to 227.1C). According to Hyde (1978) the conglomerate bands within the turbidites near Dobie are exceptional in that they are the only recorded examples of conglomerates, north or south of the break, where Timiskaming sandstone clasts are found (well over 50% in some bands). These clasts could have resulted from rapid erosion of the previously deposited fluviatile material during the opening up of the Dobie Basin.

Timiskaming strata north of the Larder Lake Break have a fairly uniform subvertical dip over their entire exposed length. The very consistency of this orientation limits the kinematic models that can be invoked in explanation and virtually eliminates the possibility of localized compressional environments created in a zone of overall transcurrent movement. An exception to this rule is again found in the Dobie Basin where overturned beds with northward dips of 15° occur. Along the power line just east of Dobie, there is also evidence of disrupted beds and displacement along bedding surfaces associated with possible soft-sediment deformation. These features may collectively indicate a compressional phase in the deformation zone which generally resulted in near-vertical dips along the east-west trending segments, but in the Dobie Basin caused slumping and possible nappe-like structures (Figure 227.1D). Intru-

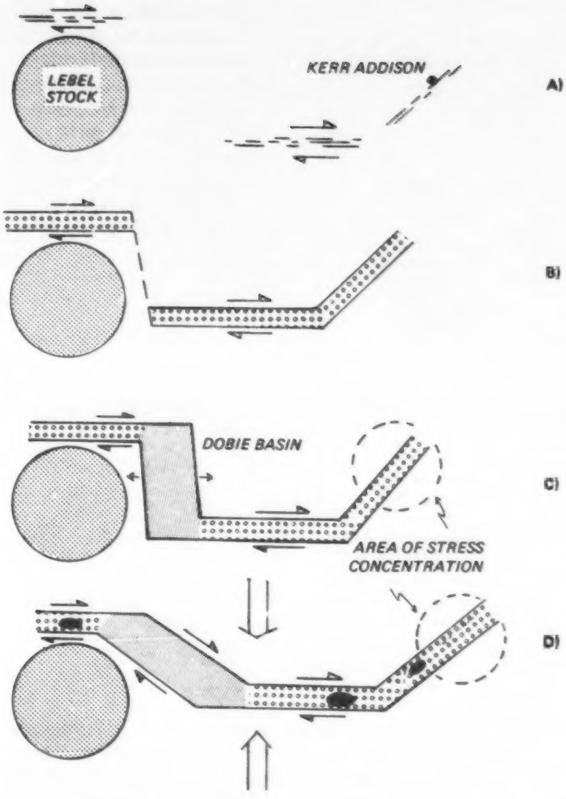

Figure 227.1. *Drawing showing the possible evolution of the deformation zone by "transpression" in an area east of the Lebel stock. A) Dextral strike-slip fracture initiations. B) Fracture extension, Timiskaming fluviatile sedimentation and trachytic volcanism (circles). C) Volcanism ceases, continued dextral strike-slip movement and turbidite sedimentation (hachured) in the pull apart Dobie Basin; stress buildup in northeastern segment of the deformation zone. D) Compressive phase, beds become vertical, intrusion of syenite bodies (solid) and continued strike-slip movement.*

sion of syenite bodies and the development of ductile fabrics commenced during this stage and continued during later stages of dextral strike-slip movement as evidenced by the S_2 foliation. This model of dextral movement would imply the existence of stress concentrations around the northeast-trending section of the deformation zone in McGarry Township. It is in this locality that the S_2 fabric has been deformed and a ductile mylonite recorded near the Kerr Addison Mine.

STRUCTURE RELATED TO GOLD MINERALIZATION

The interesting fact to emerge from a comparison of fabric data across the Larder Lake Break (Figure 227.2), is that there is a marked change in lineation plunge, a structural disparity first noted by Downes (1981). Also terminated abruptly by the break is a north-northwesterly foliation thought to be part of the D_3 event described in Hearst Township. Progressive simple shear models cannot easily account for this contrast within the deformation zone. Since the lineation is quite clearly produced by shear-related fabrics, the only adequate interpretation is that there has been late-stage movement along the Larder Lake Break. This movement may record a change from continuous to discontinuous deformation during the final stages of shear zone evolution and serves to reinforce the identification of the Larder Lake Break as a discrete surface within the wider high strain zone. Since the major gold deposits show a close spatial relationship to the Break, this tends to substantiate observations that gold mineralization marks a closing event in the strain history of the deformation zone (Colvine *et al.* 1984).

REFERENCES

Aydin, A., and Nur, A.
1982: Evolution of Pull-apart Basins and their Scale Independence; Tectonics, Volume 1, p.91-105.

Aydin, A., and Page, B.A.
1984: Diverse Pliocene-Quarternary Tectonics in Transform Environments, San Francisco Bay Region, California; Geological Society of America, Bulletin, Volume 95, p.1303-1317.

Berthé, D., Choukroune, P., and Jegouzo, P.
1979: Orthogneiss, Mylonite, and Non Coaxial Deformation of Granites: The Example of the South American Shear Zone; Journal of Structural Geology, Volume 1, p.31-42.

Colvine, A.C., Andrews, A.J., Cherry, M.E., Durocher, M.E., Fyon, A.J., Lavigne, M.J., Jr., Macdonald, A.J., Marmont, Soussan, Poulsen, K.H., Springer, J.S., and Troop, D.G.
1984: An Integrated Model for the Origin of Archean Lode Gold Deposits; Ontario Geological Survey, Open File Report 5524, 98p.

Downes, M.J.
1981: Structural and Stratigraphic Aspects of Gold Mineralization in the Larder Lake Area, Ontario; p.66-70 *in* Genesis of Archean Volcanic-Hosted Gold Deposits, Symposium Held at the University of Waterloo, March 7, 1980, edited by E.G. Pye and R.G. Roberts, Ontario Geological Survey, Miscellaneous Paper 97, 175p.

Goulet, N.
1978: Stratigraphy and Structural Relationships Across the Cadillac-Larder Lake Fault, Rouyn-Beauchastel Area, Quebec; Unpublished Ph.D. Thesis, Queen's University, 141p.

Hamilton, J.V.
1983: Geological Study of the Area of the Kirkland-Larder Lakes Break in Central McGarry Township; p.179-184 *in* Summary of Field Work, 1983, by the Ontario Geological Survey, edited by John Wood, Owen L. White, R.B. Barlow, and A.C. Colvine, Ontario Geological Survey, Miscellaneous Publication 116, 313p.

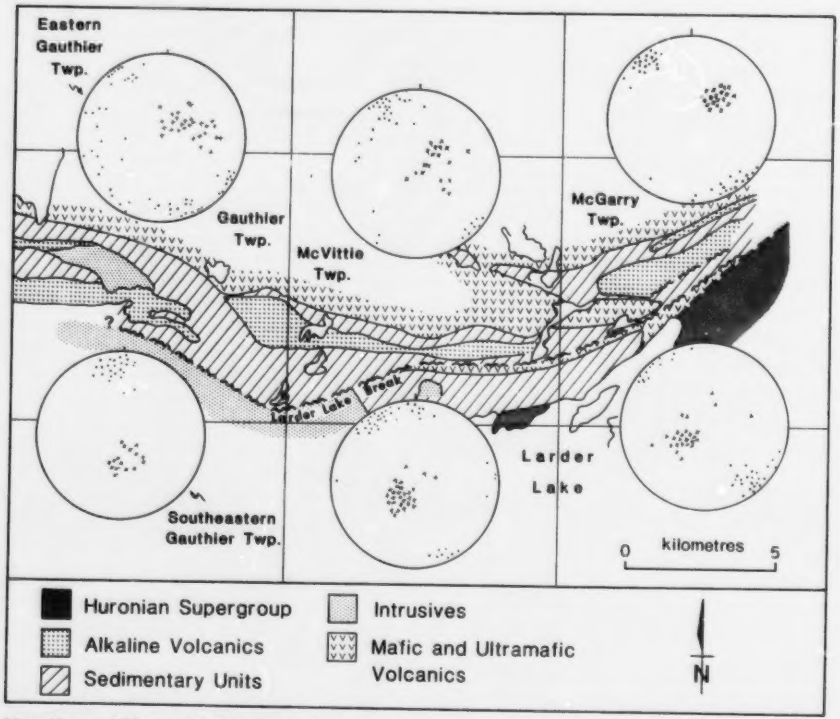

Figure 227.2. *A comparison of structural data across the Larder Lake Break in Gauthier, McVittie, and McGarry Townships. All data plotted on equal area pi diagrams. Lineations (L_1 and L_2) crosses, foliations (S_1 and S_2) dots.*

Hamilton, J.V., and Hodgson, C.J.

1984: Structural Geology and Gold Mineralization in the Kirkland-Larder Lake Deformation Zone; p.220-225 *in* Summary of Field Work, 1984, by the Ontario Geological Survey, edited by John Wood, Owen L. White, R.B. Barlow, and A.C. Colvine. Ontario Geological Survey, Miscellaneous Paper 119, 309p.

Hewitt, D.F.

1963: The Timiskaming Series of the Kirkland Lake Area; Canadian Mineralogist, Volume 7, p.497-522.

Hodgson, C.J.

1982: Gold Deposits of the Abitibi Belt, Ontario; p.192-197 *in* Summary of Field Work, 1982, by the Ontario Geological Survey, edited by John Wood, Owen L. White, R.B. Barlow, and A.C. Colvine, Ontario Geological Survey, Miscellaneous Paper 106, 235p.

1983: Preliminary Report of the Timmins-Kirkland Lake Gold File; Ontario Geological Survey, Open File Report 5467, 434p.

Hubert C., Trudel, P., and Gerlinas, L.

1984: Archean Wrench Fault Tectonics and Structural Evolution of the Blake River Group, Abitibi Belt, Quebec; Canadian Journal of Earth Sciences, Volume 21, p.1024-1032.

Hyde, R.S.

1978: Archean Timiskaming Group, Abitibi Greenstone Belt, Northeastern Ontario, Canada; Unpublished Ph.D Thesis, McMaster University, Hamilton, 422p.

1980: Sedimentary Facies in the Archean Timiskaming Group and their Tectonic Implications, Abitibi Greenstone Belt, Northeastern Ontario, Canada; Precambrian Research, Volume 12, p.161-195.

Jensen, L.S., and Langford, F.F.

1983: Geology and Petrogenesis of the Archean Abitibi Belt in the Kirkland Lake Area, Ontario; Ontario Geological Survey, Open File Report 5455, 512p.

Lister, G.S., and Price, G.P.

1978: Fabric Development in Quartz-Feldspar Mylonite; Tectonophysics, Volume 49, p.37-58.

MERQ-OGS

1983: Lithostratigraphic Map of the Abitibi Subprovince; Ontario Geological Survey, Ministere de l'Energie et des Ressources. Quebec, Map 2484 in Ontario and DJ 83-16 in Quebec.

Ramsay, J.G.

1980: Shear Zone Geometry: A Review; Journal of Structural Geology, Volume 2, p.83-99.

Ramsay, J.G., Casey, M., and Kligfried, R.

1983: Role of Shear in the Development of Helvetic Fold-Thrust Belt of Switzerland, Geology, Volume 11, p.439-442.

Reading, H.G.

1980: Sedimentation in Oblique-Slip Mobile Zones; edited by Ballance, P.F., and Reading, H.G., International Association of Sedimentologists, Special Publication 4.

Ridler, R.H.

1970: Relationship of Mineralization to Volcanic Stratigraphy in the Kirkland-Larder Lakes Area, Ontario; Geological Association of Canada, Proceedings 21, p.33-42.

Simpson, C., and Schmid, S.M.
1983: An Evaluation of Criteria to Deduce the Sense of Movement in Sheared Rocks; Geological Society of America, Bulletin, Volume 94, p.1281-1288.

Thomson, J.E.
1943: Geology of McGarry and McVittie Townships, Larder Lake Area; Ontario Department of Mines, Annual Report for 1941, Volume 50, Part 7, 99p.
1949: Geology of Hearst and McFadden Townships; Ontario Department of Mines, Annual Report for 1947, Volume 56, Part 8, p.1-54.

Grant 230 Petrology, Geochemistry, Isotopic Studies, and Platinum Group Element Potential of the Nipissing Diabase

D.M. Conrod and A.J. Naldrett

Department of Geology, University of Toronto

ABSTRACT

Field, petrological, and mineralogical studies have been initiated on 3 bodies of the Nipissing Diabase: at Cross Lake and at Portage Bay on the Montreal River, in the Cobalt area; and at Bonanza Lake, south of Lake Wanapitei, near Sudbury.

The bodies at Cross Lake and Portage Bay generally conform to the intrusive facies defined by Hriskevich (1968), however, the Portage Bay intrusion lacks the hypersthene zone typical of sills in this area. They generally consist of a quartz-rich basal and capping gabbro; a thick hypersthene-rich gabbro; and above this, a varied texture zone consisting of interdispersed coarse- and fine-grained gabbro, locally containing granodioritic pods and aplitic dikes.

The Bonanza Lake intrusion consists predominantly of gabbro-norite, with differentiated phases consisting of quartz diorite and granodiorite (containing syenogranitic pegmatite).

Microprobe analysis of orthopyroxene throughout the 363 m thick sill at Cross Lake has indicated no trend of cryptic variation with height. Analysis of the orthopyroxene from the Bonanza Lake intrusion has shown an increase in iron at the expense of magnesium toward the granodiorite differentiate. Analyses of the nickel content in olivine suggest that before or during crystallization of the hypersthene zone at Cross Lake, significant amounts of magmatic sulphide did not segregate from the magma. Olivine was not observed in the Bonanza Lake intrusion.

INTRODUCTION

The Nipissing Diabase, first referred to as such by Miller (1911), is composed of a suite of gabbroic intrusive rocks of tholeiitic composition and associated differentiated phases, that extends from Cobalt to Sault Ste. Marie, Ontario. Emplacement occurred 2150 ± 50 to 2160 ± 60 million years ago (Fairbairn 1960; Van Schmus 1969), based on Rb/Sr whole-rock analysis of samples from the Blind River and Gowganda areas, respectively. These bodies take the form of dikes, sills, and cone sheets (Figure 230.1) (Card and Pattison 1973).

Associated mineralization varies on a regional scale (Figure 230.2) (Card and Pattison 1973). For this reason, 3 areas (Portage Bay, Cobalt; South Wanapitei Lake, Sudbury; and Bruce Mines, Sault Ste. Marie) have been selected for a study of the petrology, geochemistry, and platinum group element potential of the intrusions. This mineralization includes silver-cobalt-nickel-arsenide vein deposits within the Cobalt area, copper-nickel sulphides within the Sudbury area, and copper sulphides within the Sault Ste. Marie area. One aim of this project is to determine why regional variation in the type and style of mineralization exists.

A full understanding of the emplacement, magmatic differentiation and mineralization associated with the Nipissing intrusions is somewhat lacking, and, therefore, this project commenced with detailed mapping during which over 400 samples were collected. Amongst a number of objectives for this study, the establishment of type sections of the Diabase for the 3 areas has received the most attention this past year.

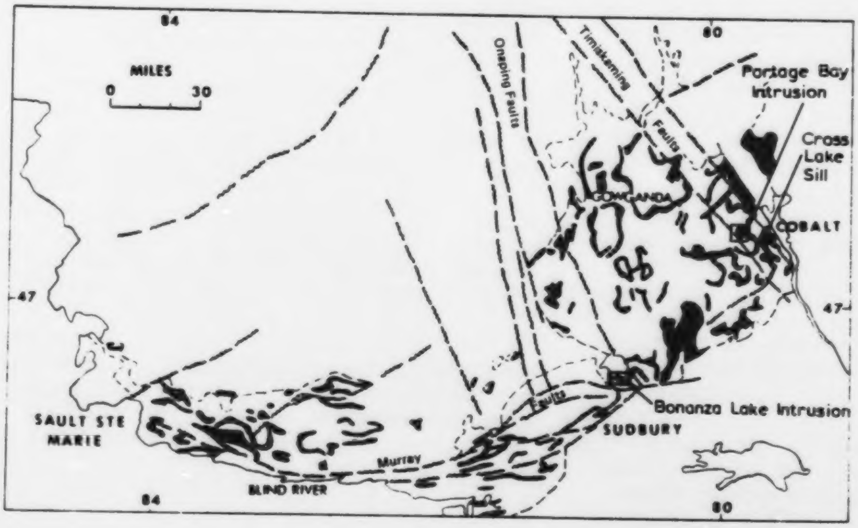

Figure 230.1. Distribution of Nipissing Diabase intrusions throughout Ontario (Card and Pattison 1973).

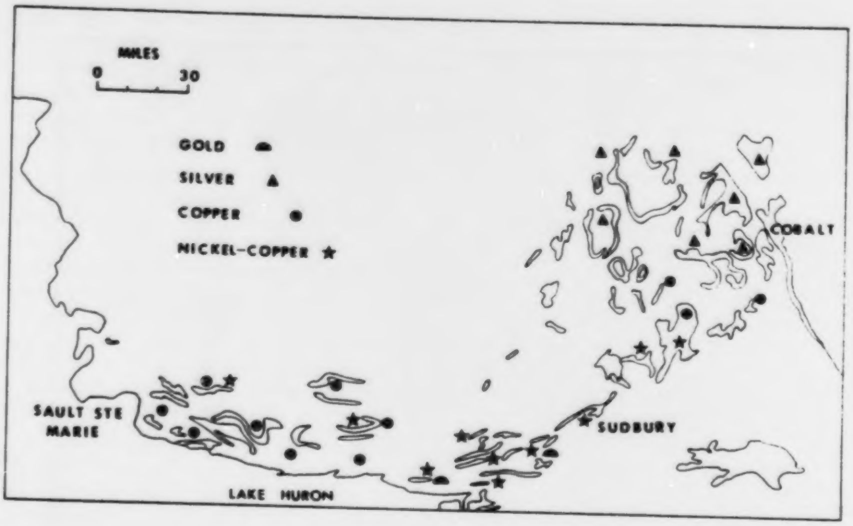

Figure 230.2. Various metallic types associated with the Nipissing Diabase (Card and Pattison 1973).

GEOLOGICAL FEATURES AND SETTING OF THE NIPISSING DIABASE

PORTAGE BAY AND COBALT INTRUSIONS

The Nipissing Diabase intrudes along the unconformity separating the underlying Keewatin volcanics and the generally flat-lying Huronian metasedimentary rocks in the Cobalt area (Hriskevich 1968). Many of the intrusions now display discontinuous, open ring to irregular shaped, outcropping patterns, similar to those found in the Karoo of South Africa. This pattern has led to their interpretation as large undulating sheets from which the arches have been removed by erosion. The sills within the Cobalt camp have been documented to consist of 4 distinct textural and mineralogical zones (Hriskevich 1968; Jambor 1971). These intrusions typically consist of a 24 to 26 m thick basal quartz- rich gabbro, followed by a 196 to 232 m thick hypersthene-rich gabbro, a 76 to 87 m thick varied texture zone, characterized by distinct pods of coarser grained gabbro set in a finer grained gabbro, presumably of the same composition, and a 9 m thick quartz-rich gabbro cap. Granophyre, aplite, and pegmatitic gabbro, occurring as small pods and dikes, are often found within the varied texture zone.

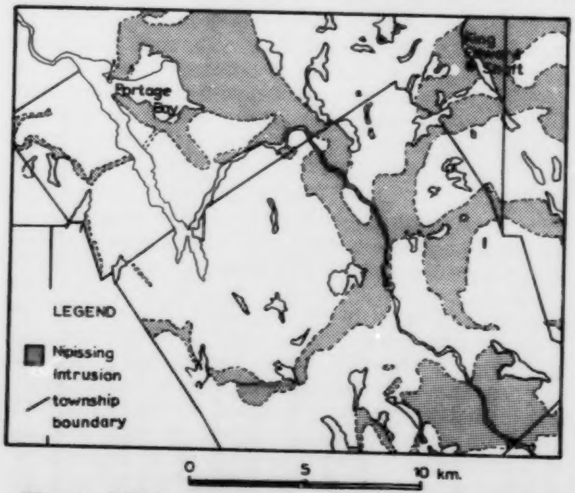

Figure 230.3. Distribution of Nipissing intrusions around the Cobalt area (Hriskevich 1968).

The Portage Bay area, approximately 9 km west of Cobalt (Figure 230.3), is a typical example of an intrusion with a concentric outcropping pattern. Although detailed mapping (1:7000), has been somewhat limited in this area, thus far, the completed mapping has indicated that the intrusion consists of a fine-grained, flinty, chilled zone occurring within 6 cm of the contact, quartz-rich gabbro, varied texture gabbro, pegmatitic gabbro, granophyre, and aplitic dikes. Numerous fine- to medium-grained mafic dikes cut the intrusion. The hypersthene zone has, thus far, not been observed in this area. Very rarely are the contacts between the intrusion and the host rocks exposed.

The Firstbrook and Coleman metasedimentary rocks around Portage Bay dip inward, toward the centre of the Bay (Figure 230.4). The northern contact between the intrusion and Lorrain arkose dips southward at approximately 41°. Contacts along the western and eastern sides of the bay are characterized by approximately 10 cm zones of flinty chilled gabbro, and baked and partially melted metasedimentary rock. Chilled gabbro taken from a pit dug through the Firstbrook siltstone at the southern edge of the Bay indicates the position of the contact there. The more differentiated phases of the intrusion are found around the Bay. Diamond-drill hole data has indicated that the vertical thickness of the intrusion at Fiddlers Island is at least 190 m, and at Eisen Lake is at least 276 m (Figure 230.4). The lower contact of the intrusion with the underlying Huronian metasedimentary rocks is almost horizontal in the Eisen Lake area.

These observations are consistent with the undulating sheet model proposed by Hriskevich (1968) for those intrusions within the Cobalt camp, although this is not the only model consistent with the avail-

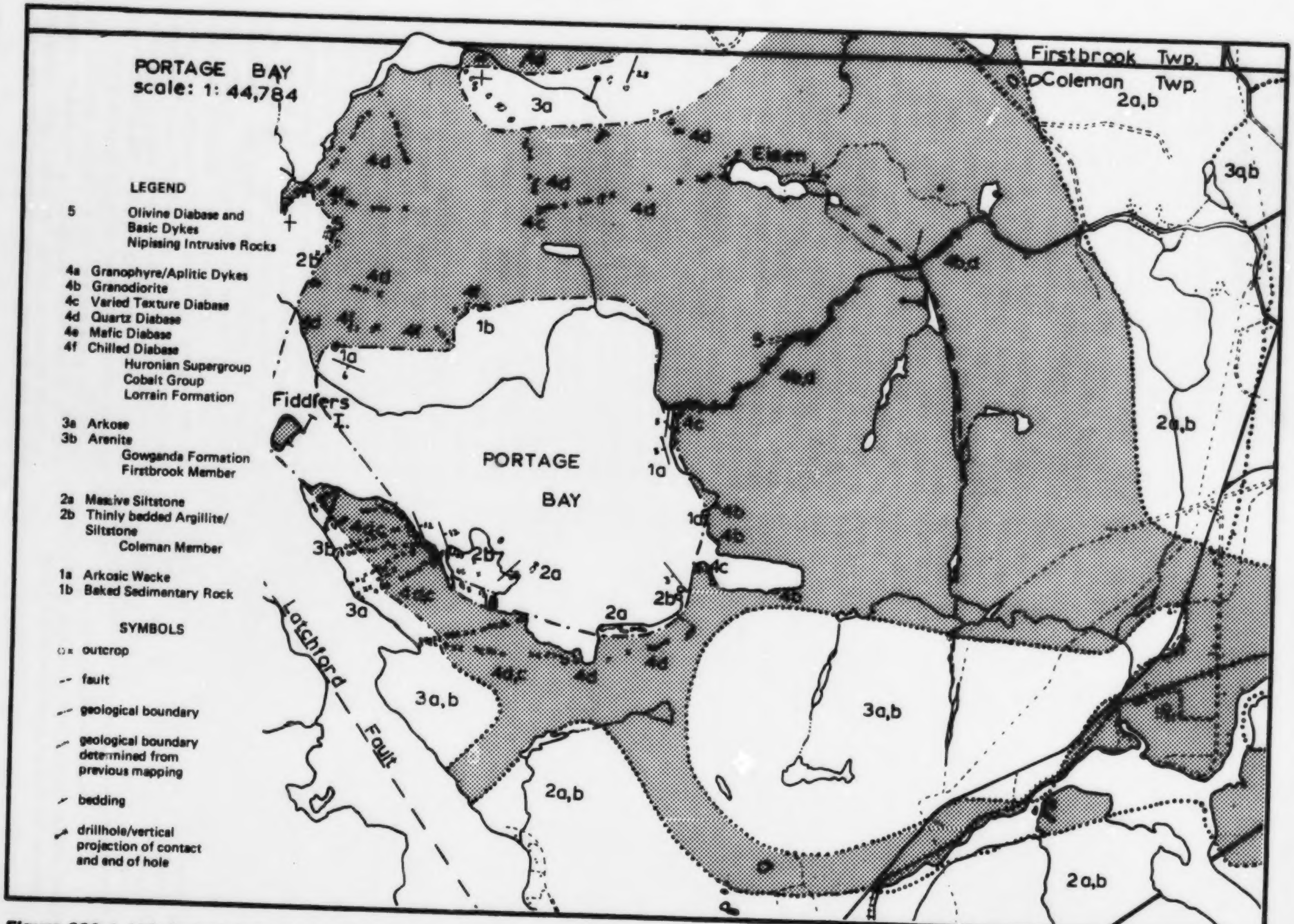
PORTAGE BAY
scale: 1: 44,784
LEGEND
5 Olivine Diabase and Basic Dykes
Nipissing Intrusive Rocks
4a Granophyre/Aplitic Dykes
4b Granodiorite
4c Varied Texture Diabase
4d Quartz Diabase
4e Mafic Diabase
4f Chilled Diabase
Huronian Supergroup
Cobalt Group
Lorrain Formation
3a Arkose
3b Arenite
Gowganda Formation
Firstbrook Member
2a Massive Siltstone
2b Thinly bedded Argillite/Siltstone
Coleman Member
1a Arkosic Wacke
1b Baked Sedimentary Rock
SYMBOLS
outcrop
fault
geological boundary
geological boundary determined from previous mapping
bedding
drillhole/vertical projection of contact and end of hole
Firstbrook Twp.
Coleman Twp.
PORTAGE BAY
Fiddlers I.
Eileen
Latchford Fault
3a
3a,b
2a,b
1a
1b
2a
2b
3b
4d
4c
4b
4d,c
4b,d
5

Figure 230.4. Lithological distribution within the Portage Bay intrusion.

able data. For example, an eastward tilting cone sheet feeding a sill to the east is also a possibility. Continued mapping of the distribution of the lithologies within the intrusion and a study of element fractionation trends should help determine which of the above interpretations is correct.

Because many of the samples collected around Portage Bay are altered, samples were collected at 10.5 m intervals along the King Edward Shaft through the 363 m thick sill at Cross Lake (Figure 230.3), as a type section for the Nipissing intrusion in the Cobalt area. Sample collection indicated that in this location the intrusion consisted of a 40 m thick basal quartz gabbro, a 166 m thick hypersthene zone, a 48 m thick varied textured zone, a 45 m thick medium-grained quartz gabbro zone, and a 63 m thick zone of fine-grained quartz gabbro.

Diamond drilling and surface mapping around the Portage Bay area has indicated that there is generally a gradational change from one facies to another. Fine-grained portions of the intrusion, as well as aplite dikes, however, appear to be scattered throughout the body in this area. Such often abrupt, but sometimes gradational, changes in texture and grain size may in fact suggest that emplacement involved more than 1 pulse. Chemical studies to follow may help in understanding these observations.

BONANZA LAKE INTRUSION, SOUTH WANAPITEI LAKE

The Bonanza Lake intrusion is located along the immediate south shore of Lake Wanapitei near Sudbury (Figure 230.5). Detailed mapping has indicated that this body consists predominantly of gabbro-norite, with lesser proportions of pegmatitic gabbro scattered throughout. Granodiorite and granitic differentiates are concentrated in the northeastern portion, with aplitic dikes and pods occurring generally along the northern contact. Numerous northwesterly trending olivine diabase dikes, 0.5 to 2 m in width, cut the intrusion.

The intrusion is emplaced between the Huronian Mississagi Formation and the Serpent Lake Formation. Previous mapping by Dressler (1982) indicated that most of the Huronian metasedimentary rocks dip moderately to the north, yet some of the Serpent Lake Formation near to the intrusive contact dips to the south. This observation was confirmed in this study.

Contacts between the intrusion and the country rock are very scarce and many are characterized by a 0.5 to 1.2 m wide zone of breccia, typically consisting of a very fine grained black matrix containing rounded clasts, 2 cm to 1 m in size, of both the intrusion and the country rock. The presence of such a zone often creates great difficulty in obtaining measurable contacts between the host rock and the intrusion. Contacts along the northern extent of the intrusion with the Serpent Lake Formation are characterized by small shear zones that dip moderately to the south (Figure 230.5). Directly observable contacts between the intrusion and the Mississagi Formation were not found, although the metasedimentary rocks within 2 m of the contact dip moderately toward the north.

The occurrence of granodiorite, with coarse-grained syenogranitic phases, and quartz diorite along the lake shore are believed to be magmatic differentiates of the main mass of gabbro-norite. Gradation from one phase into the other is fairly rapid over a short distance, however, petrological studies during this investigation led to the conclusion that the 2 are genetically related. Further chemical and isotopic studies will distinguish whether these differentiates have undergone significant contamination by the country rocks during their emplacement. It should be noted that during this study, no flow structures were observed in either the Cobalt or Bonanza Lake intrusions.

PETROGRAPHY AND PETROLOGY

Modal analyses of 54 selected samples taken from the King Edward Shaft and Portage Bay, Cobalt, and from the Bonanza Lake intrusion, Sudbury, are given in Table 230.1. These analyses (1000 counts per sample), plotted on the Q.A.P. diagram of Streckeisen (1976), show the transition from the gabbro through quartz diorite to granodiorite in the Bonanza Lake intrusion (Figure 230.6).

Figure 230.7 shows vertical modal variation across the Cross Lake sill, and modal variation along 2 south to north traverses (indicated in Figure 230.5) across the Bonanza Lake intrusion.

An increase in quartz and clinopyroxene (augite + pigeonite), accompanied by a decrease in plagioclase and orthopyroxene, occurs toward the base and top of the Cross Lake sill. Olivine occurs predominantly in the central and lower portions of the sill.

Modal variation across the south to north traverse a-b, within the Bonanza Lake intrusion, indicates an increase in quartz toward the southern contact with the Mississagi Formation. An increase in hornblende occurs toward both the northern and southern contacts. Increases in orthopyroxene are reflected in decreases of clinopyroxene throughout the central portion of the exposed body. Modal variation across the south to north traverse c-d, through the gabbro toward the granodiorite phase, indicates a pronounced increase in quartz, hornblende, and to some extent biotite, toward and into the granodiorite. A minor increase in quartz occurs toward the southern contact. Plagioclase decreases toward and into the granodiorite, apparently due to an increase in quartz and potassic feldspar. Extensive alteration of both orthopyroxene and clinopyroxene in the samples collected along this traverse has prevented the distinction of any meaningful variation of these minerals.

COBALT AREA

Much of the petrological study has been carried out on samples taken from the King Edward Shaft for the Cobalt area because of extensive alteration around Portage Bay; although samples from Portage Bay were also taken into consideration in this study.

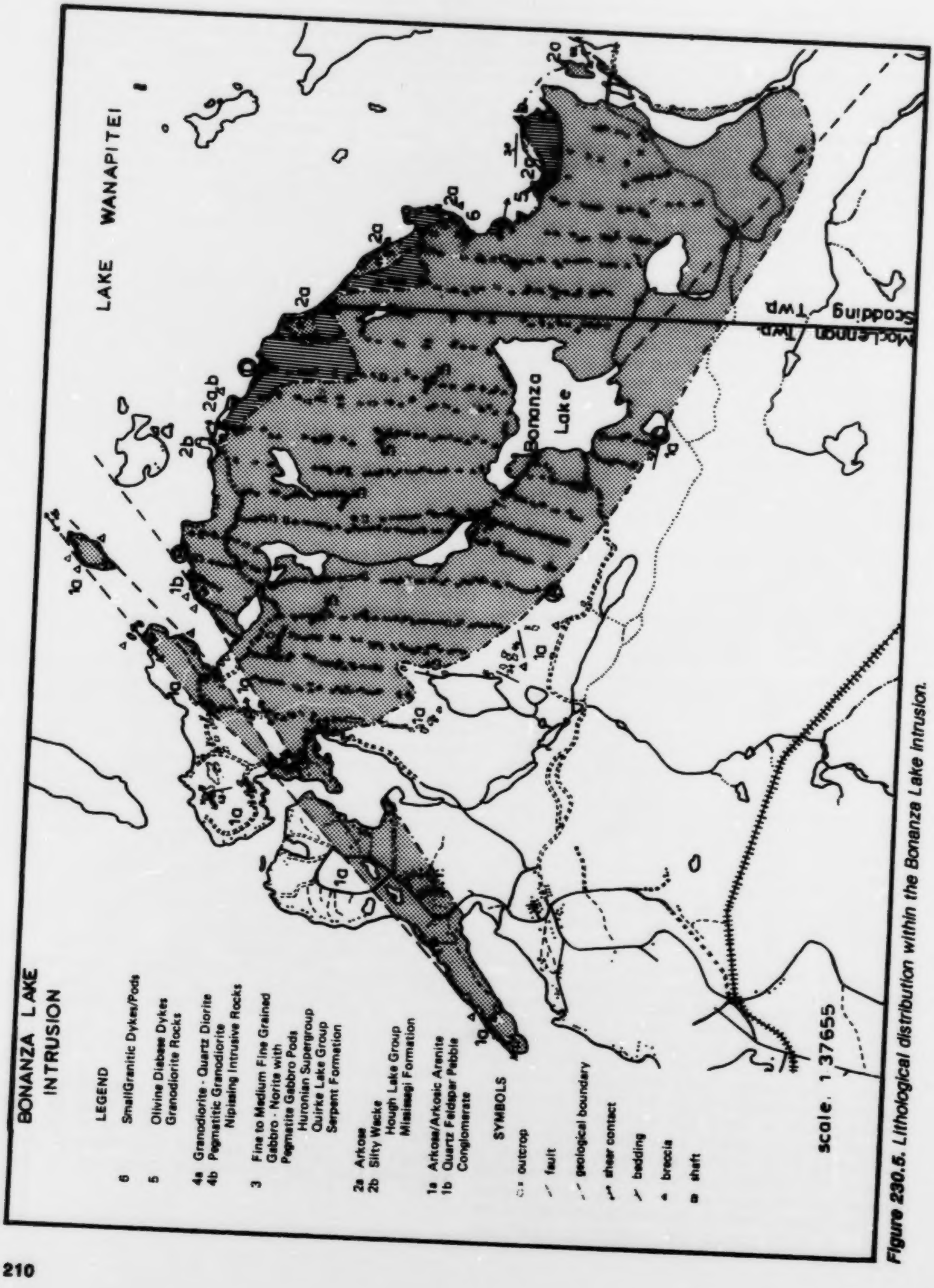
BONANZA LAKE INTRUSION
LEGEND
6 SmallGranitic Dykes/Pods
5 Olivine Diabase Dykes Granodiorite Rocks
4a Granodiorite - Quartz Diorite
4b Pegmatitic Granodiorite Nipissing Intrusive Rocks
3 Fine to Medium Fine Grained Gabbro - Norite with Pegmatite Gabbro Pods Huronian Supergroup Quirke Lake Group Serpent Formation
2a Arkose
2b Silty Wacke Hough Lake Group Mississagi Formation
1a Arkose/Arkosic Arenite
1b Quartz Feldspar Pebble Conglomerate
SYMBOLS
outcrop
fault
geological boundary
shear contact
bedding
breccia
shaft
LAKE WANAPITEI
Bonanza Lake
MacLennan Twp.
Scadding Twp.
scale. 1 37655
1a
1b
2a
2b
2a,b
3
4a
5
6

Figure 230.5. Lithological distribution within the Bonanza Lake intrusion.

TABLE 230.1. MODAL ANALYSES OF SELECTED SAMPLES FROM THE CROSS LAKE SILL (SC), THE PORTAGE BAY INTRUSION (PB), AND THE BONANZA LAKE INTRUSION (WL).

Sample Number	SC 35	SC 33	SC 31	SC 1	SC 2	SC 4	SC 6	SC 9	SC 10	SC 12	SC 13	SC 17	SC 19	SC 21	SC 22	SC 23	SC 25	SC 27	SC 29
Quartz	5.5	6.6	4.8	8.8	4.3	2.2	2.5	1.0	1.0			0.5		0.1	0.4	0.3	0.1	3.2	0.1
Plagioclase	10.9	0.5	18.2	9.3	13.0	34.5	42.3	46.5	40.3	40.7	39.2	18.4	54.2	41.2	48.1	28.0	28.0	26.5	8.4
Potassic Feldspar																			
Perthite																			
Clinopyroxene	5.7	27.6	38.7	40.6	29.9	26.2	24.5	23.5	28.1	24.3	20.3	27.0	20.7	26.7	25.2	21.9	24.1	32.0	38.5
Orthopyroxene				0.2	11.5	18.6	23.0	21.1	10.7	26.1	30.0		14.5	24.6	18.1	31.6	23.8		
Olivine									6.9	5.0	9.6		5.1		4.0	0.9			
Hornblende	0.1												3.1						
Biotite		0.2		0.2	0.1	0.3	0.2		0.4	0.2	0.5	0.7	0.7	1.0	0.4	1.8	0.2	0.1	tr.
Sphene																			
Zircon				tr															tr.
Muscovite												0.1				0.2	0.1	0.8	0.9
Apatite																			
Opaques	2.8	1.9	3.3	1.0	1.0	1.2	1.3	1.0	0.1	0.3	0.4		0.1	0.6	1.2	0.8	0.7	2.3	2.4
Leucoxene							0.1												
Actinolite/Tremolite/Talc*	39.4	9.5	9.0									18.8						16.8	16.3
Chlorite*	0.3	0.5		0.5	0.1		0.2		0.1	0.1		0.1	1.4	0.3		0. 2		0.2	0.4
Epidote/Saussurite/Sericite*	28.2	49.7	26.0	39.2	40.1	16.9	6.0	7.0	11.4	0.3		33.9		5.0	2.2	12.3	21.3	18.1	31.0
Carbonate*																			
Turbid Alteration*	9.1	3.5								2.5		0.5							
Hematite*																			
Serpentine Antigorite Talc*									1.0	0.5	tr.		0.2	0.5	0.3	2.0	1.7		2.0

*secondary alteration minerals
**altered pyroxene

Legend
SC 35-29—Nipissing Gabbro from King Edward Shaft, Cobalt (listed in order of increasing depth)

Table 230.1 cont'd.

Sample Number	PB 100	PB 102	PB 204	WL 251	WL 32	WL 63b	WL 63c	WL 63e	WL 63d	WL 139	WL 181	WL 182	WL 229	WL 184	WL 183	WL 219	WL 122	WL 215
Quartz	10.4	14.1	21.5	8.5				1.1	0.1	15.7	33.2	40.0	36.1	34.1	35.8	46.6	20.3	
Plagioclase		47.7	35.2	3.1	50.5	11.5	42.3	39.8	42.2	13.4	14.2	19.5	6.5		26.3	23.4	16.5	57.3
Potassic Feldspar		10.5	0.7							1.4	4.4	12.3	13.6	41.0	1.0	16.1		
Perthite																		
Clinopyroxene	33.0			2.9	29.1	1.2	19.8	16.0	18.1	7.7**								12.6
Orthopyroxene				1.0	15.5	0.4	25.9	12.9	29.9									
Olivine																		17.6
Hornblende				0.2		2.5	1.5	1.4	1.0	28.4	14.9	7.1	5.1	0.2	1.3		8.9	
Biotite	0.2		1.0		0.4	1.5	1.4	1.4	1.8	7.3	10.3	7.6	13.3	1.3	15.0		1.2	2.1
Sphene		1.3	4.9														1.4	
Zircon																		
Muscovite																		
Apatite						1.0												
Opaques	0.9	4.0	1.6	1.1	0.6	0.7	1.3	0.9	1.6	1.2	2.5	0.7	0.9		0.3		0.7	9.8
Leucoxene	2.6																2.2	
Actinolite/Tremolite/Talc*		19.5		39.6		57.7	5.3	20.9	3.6								39.3	
Chlorite*	0.8	2.1	25.4	0.2	1.9	0.1	0.6	0.4	0.7	1.2	0.3	0 .3	4.6		0.2	2.1	5.0	
Epidote/Saussurite/Sericite*	52.1	0.9	3.3	42.4	1.5	23.2	0.3	3.1		23.6	20.2	12.4	19.5	11.3	19.4	10.5	4.5	0.2
Carbonate*			6.4									0.1	0.4			0.9		
Turbid Alteration*				1.0	0.4	0.2	0.6	2.1	1.0	0.1				12.0	0.5	0.4		
Hematite*																		0.4
Serpentine Antigorite Talc*																		

*secondary alteration minerals

**altered pyroxene

Legend

PB 100-204—Nipissing Gabbro from Portage Bay, Cobalt

WL 251—Quartz-rich Gabbro-Norite from near contact locations in the Bonanza Lake Intrusion

WL 32-63e—Gabbro-Norite from Bonanza Lake Intrusion

WL 139—Transition Rock between Gabbro-Norite and Granodiorite

WL 181-229—Granodioritic Differentiates

WL 184—Pegmatic Granodioritic Phase

WL 183, 219—Quartz-rich Differentiate

WL 122—Pegmatitic Phase found within the Gabbro-Norite

WL 215—Olivine Diabase Dike

Table 230.1 cont'd.

Sample Number	WL 115	WL 116	WL 117	WL 37	WL 35	WL 34	WL 33	WL 198	WL 258	WL 259	WL 98	WL 94	WL 93	WL 92	WL 91	WL 90
Quartz	6.4	0.2	2.1	0.5		0.7	0.4	1.0	6.9	2.6	0.4	3.1	10.0	34.7	42.7	17.5
Plagioclase	37.2	41.8	39.6	40.9	45.3	39.2	37.4	3.7	33.0	41.5	40.7	39.2	35.1	13.4	14.8	1.8
Potassic Feldspar													tr.	10.3	8.2	0.4
Perthite																
Clinopyroxene	20.8	34.7	31.0	25.7	26.1	36.7	34.6	0.7	29.1	38.0	31.8	4.1	18.3			
Orthopyroxene	10.2	19.6	21.2	28.5	25.0	21.4	22.4		3.3	13 .6	19.6	2.0	3.7	0.9		
Olivine																
Hornblende	4.8	tr.	0.5	tr.	tr.	tr.	tr.	8.7	3.7	1.0	1.1	4.5	11.3	17.9		25.8
Biotite	2.0	1.2	1.7	0.8	0.6	0.7	0.4		3.9	0.9	0.4	3.4	0.7	6.3	14.7	9.3
Sphene																
Zircon	tr.		tr.			tr.	tr.	tr.	tr.	tr.		tr.	tr.	tr.	0.1	tr.
Muscovite															8.0	
Apatite																
Opaques	1.8	0.9	0.8	0.6	0.9	0.3	1.3		1.6	0.2	0.2	0.7	14.1		0.2	1.8
Leucoxene																
Actinolite/Tremolite/Talc*	10.0	0.2	1.1	1.5	1.7	0	0.8	46.0	10.9	0.1	0.2	37.7	4.4	0.4		5.8
Chlorite*		0.1	1.4	0.7	0.1	0.2	0.1	1.8	0.1	0.2				0.3	0.9	3.4
Epidote/Saussurite/Sericite*	6.8	1.3	0.7	0.8	0.3	0.8	2.6	38.1	7.5	1.9	5.6	5.3	2.4	15.8	10.4	34.6
Carbonate*																
Turbid Alteration*																
Hematite*																
Serpentine/Antigorite/Talc*																

*secondary alteration minerals
**altered pyroxene

Legend
WL 115, 258—Quartz-rich Gabbro-Norite from the Bonanza Lake Intrusion
WL 33-98-116-258—Gabbro-Norite
WL 93-94—Transition rock between the Gabbro-Norite and Granodiorite
WL 90-92—Granodiorite
WL 91—Quartz-rich Differentiate

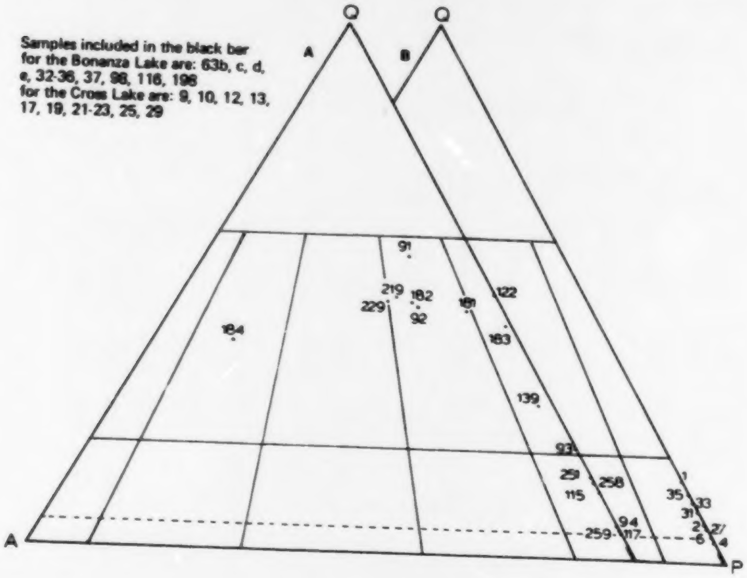

Figure 230.6. Plotted positions of samples from a) the Bonanza Lake, and b) Cross Lake intrusions on the Q.A.P. diagram of Streckeisen (1976).

Chilled Diabase of the Cobalt Area

The chilled diabasic gabbro at Portage Bay consists of very fine grained pyroxene, intergranular to plagioclase crystallites approximately 0.04 mm in size. Typical quench textures include sheaf-like growths of acicular plagioclase with hollow centres and forked edges. The occurrence of glomeroporphyritic plagioclase approximately 0.45 mm in size, suggests that some crystallization had occurred previous to emplacement. Alteration of the chilled zone includes epidote, zoisite, sericite, and chlorite afer plagioclase. Calcite has been introduced along veinlets also containing specular hematite. Although the chilled zone was not observed within the King Edward Shaft, Hriskevich (1968), described a similar rock for that sill.

Basal Quartz Diabase of the Cobalt Area

The basal quartz diabase from the King Edward Shaft consists of phenocrystic augite, pigeonite, and minor hypersthene, approximately 0.3 to 0.8 mm in size, phenocrystic plagioclase, approximately 0.4 mm in size, and clusters of antigorite, approximately 0.7 mm in size, are set in a finer grained matrix of the same mineralogy. The molding of pigeonite on augite is very common in this zone; and the intergrowths also developed between the 2 minerals suggest that, although augite is likely to have formed slightly earlier or to have nucleated more rapidly, some crystallization of these 2 pyroxenes was simultaneous. Orthopyroxene is sometimes observed molded on pigeonite, which in turn is molded on augite. Exsolution of clinopyroxene occurs as plates along 001 and 100, often displaying a herring bone texture within the pigeonite. The sequence of pyroxene crystallization determined includes: augite, followed by pigeonite, followed by inverted pigeonite, and hypersthene consistent with that observed by Hriskevich (1968).

Hypersthene Zone of the Cobalt Area Diabase

Samples taken from the hypersthene zone of the Cross Lake sill indicate that this zone is characterized by phenocrystic hypersthene, olivine, and plagioclase. Mineralogically, this zone is similar to the basal quartz diabase, however, distinct differences include a marked decrease in quartz occurring in micropegmatitic intergrowth with plagioclase, and a marked decrease in pigeonite accompanying the increase in hypersthene.

Hypersthene occurs as large subhedral equidimensional crystals up to 1 cm in size, often partially to totally enclosing plagioclase and augite. Frequently, hypersthene can be seen rimming olivine, which sometimes appears to have nucleated on a hexagonally shaped crystal now totally replaced by chlorite and possible serpentine. Augite occurs in a similar fashion as that found in the quartz diabase zone. Olivine occurs predominantly in the upper and middle portion of the hypersthene zone, as subhedral to anhedral grains approximately 1 mm in diameter. Alteration includes epidote, zoisite, chlorite, and sericite after plagioclase, actinolite-tremolite, talc, and antigorite after pyroxene, and antigorite and a green serpentine after olivine.

Varied-Texture Diabase of the Cobalt Area

The varied texture zone is so named because of its distinct differences in texture and grain size. Typically, coarse-grained gabbro, occurring in pods, is gradational to a finer grained gabbro of the same mineralogy (Hriskevich 1968). Augite, pigeonite, and minor inverted pigeonite occur in both the coarse- and fine-grained phases. No granodioritic or aplitic phases were observed within the King Edward Shaft. Aplitic dikes and granodioritic phases appear to be more common around Portage Bay, close to the contact with metasedimentary rocks along the shore.

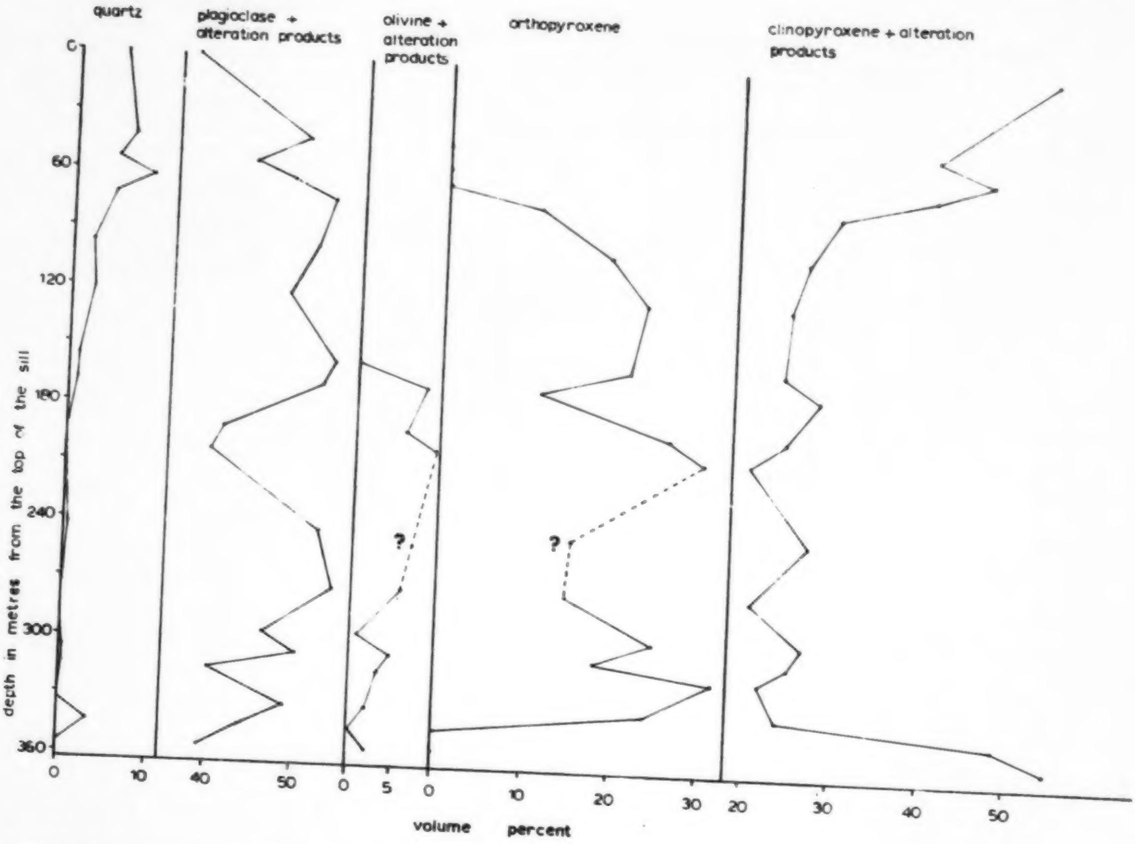

Figure 230.7a. Modal variations of selected minerals across the Cross Lake sill; (?) indicates an unobtainable value due to extensive alteration, although in some cases an estimation based on pseudomorphed grain shape was possible.

BONANZA LAKE INTRUSION

Much of the Bonanza Lake intrusion is characterized by a fine- to medium-grained, fairly uniform gabbro-norite, consisting of plagioclase, hypersthene (locally with blebby clinopyroxene exsolution-filled rims), augite, and minor quartz, biotite, hornblende, and opaque minerals. Alteration includes epidote-zoisite and sericite after plagioclase, and actinolite-tremolite and talc after pyroxene.

The minor pegmatitic phases found scattered across the intrusion consist of a monzodiorite described by Dressler (1982), and a quartz diorite determined in this study. This phase consists of large, strained quartz crystals, plagioclase, hornblende, up to 5 cm in length, and minor biotite, sphene, and opaque minerals. Alteration is usually fairly extensive with actinolite-tremolite after hornblende and epidote, sericite, and saussurite after plagioclase. Chlorite may be present.

Contacts between the pegmatitic phase and gabbro-norite may be sharp or diffuse, suggesting that at least some of the pegmatite simultaneously crystallized with the gabbro-norite, and some was most likely introduced after solidification of the main mass of gabbro-norite.

The granodiorite and quartz-rich differentiates of the intrusion are in gradational contact with the main mass of gabbro-norite. The granodiorite consists of quartz, plagioclase, potassic feldspar, hornblende, biotite, and opaque minerals. Zircon occurs in trace amounts throughout the body but appears to be concentrated in the more differentiated phases, where it occurs as grains up to 0.1 mm in size. Alteration is similar to that of the gabbro-norite.

A transition phase occurs between the typical gabbro-norite and granodiorite. This phase plots as a quartz-poor quartz diorite on the Q.A.P. diagram of Streckeisen (1976) (Figure 230.6), containing quartz, plagioclase, minor potassic feldspar, altered pyroxene, hornblende, biotite, and opaque minerals. Numerous examples of hornblende rimming and reacting with the pyroxene strongly suggests a genetic relationship between the gabbro-norite, containing augite, and the granodiorite containing hornblende and biotite. The granodiorite is, therefore, most likely a felsic differentiate of the tholeiitic magma, and the transition phase has nicely captured the pyroxene-hornblende reaction described by Bowen (1928). Fur-

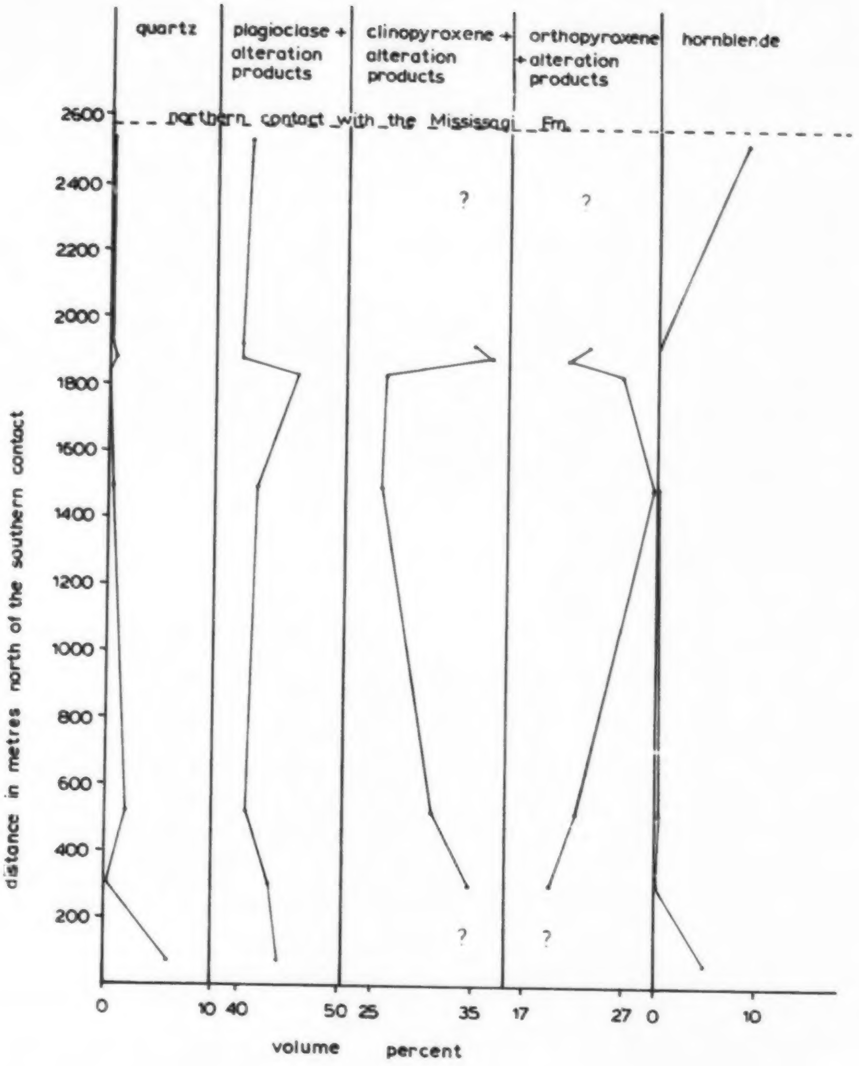

***Figure 230.7b.** Modal variations of selected minerals across traverse a-b of the Bonanza Lake intrusion; (?) indicates an unobtainable value due to extensive alteration, although in some cases an estimation based on pseudomorphed grain shape was possible.*

ther isotopic studies will determine the degree of crustal contamination within the granodiorite phase.

MINERAL CHEMISTRY

Electron microprobe analyses of major oxides were undertaken on orthopyroxene grains in samples from the Cross Lake sill and across the Bonanza Lake intrusion. The analyses indicate that there is no variation in the atomic ratio Mg/(Mg+Fe) with height throughout the Cross Lake sill (Figure 230.8).

Variation in this ratio across the Bonanza Lake intrusion, along traverses a-b and c-d, are shown in Figures 230.9a and 230.9b respectively. Little variation is shown along traverse a-b. However, it appears that the spread in values between the core and rim of a given grain increases toward the southern contact of the intrusion with the Mississagi Formation, perhaps reflecting a faster cooling rate near the southern contact.

Analyses show a decrease in this ratio across traverse c-d, indicating a normal differentiation trend toward the granodiorite phase, supporting the proposal of a genetic relationship between the gabbronorite and granodiorite.

All orthopyroxene grains from the Bonanza Lake intrusion which were analyzed showed normal zonation. Most grains from the Cross Lake sill showed normal zonation, however, a few showed reverse zonation.

Microprobe analysis of plagioclase within the Cross Lake sill indicate that both normal and reverse zonation occurs within the upper quartz gabbro and hypersthene zone. Only 25 analyses of the plagioclase have been completed and any further deductions at this point would be unwise.

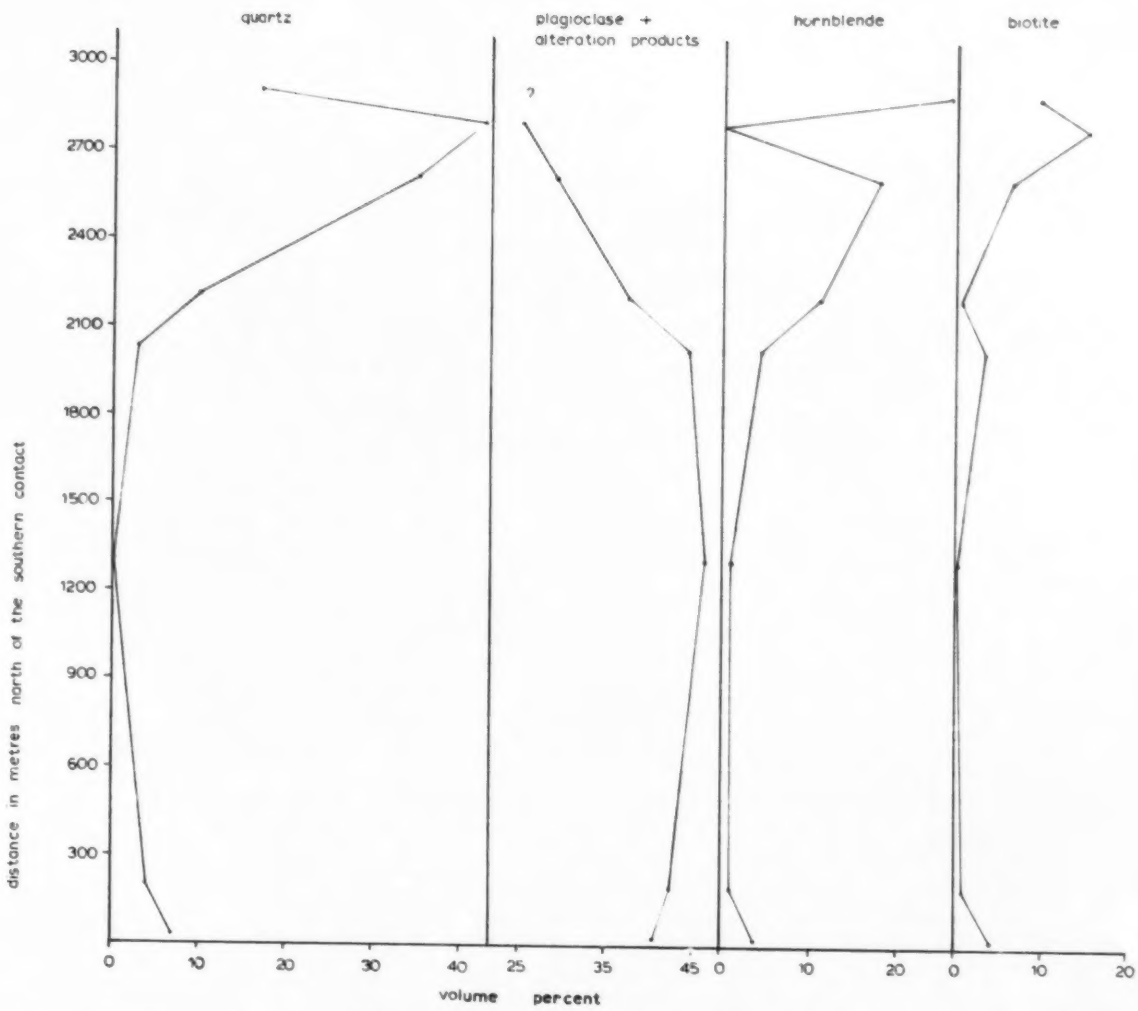

Figure 230.7c. *Modal variations of selected minerals across traverse c-d of the Bonanza Lake intrusion; (?) indicates an unobtainable value due to extensive alteration, although in some cases an estimation based on pseudomorphed grain shape was possible.*

POTENTIAL OF THE NIPISSING DIABASE AS A HOST FOR MAGMATIC SULPHIDES

Microprobe analysis of the nickel content within the olivine from the hypersthene zone of the Cross Lake sill indicates that the nickel content varies from 1430 to 1780 ppm (Table 230.2). The average mole percent of forsterite for each sample is also listed in Table 230.2.

The distribution coefficient for nickel into sulphides is considerably higher than for silicate melts. If significant amounts of sulphide had segregated before or during crystallization of the magma, the magma and thus the olivine would be expected to be depleted in nickel. The forsterite and corresponding nickel contents of the olivine from the hypersthene zone of the Cross Lake sill, have been plotted in Figure 230.10. Comparison of their plotted position to general nickel-Fo trends set by unmineralized samples of Simkin and Smith (1970) show that the olivine is slightly enriched in nickel, suggesting that significant amounts of sulphide had not segregated from the magma. Unfortunately, olivine was not observed in the Bonanza Lake intrusion and therefore this test could not be carried out.

DISCUSSION AND FUTURE PLANS

The major difference between the Nipissing Diabase of the Cobalt area and that of South Wanapitei Lake is the distinct lack of olivine, and the less well developed diabasic texture within the Bonanza Lake intrusion. During this study no evidence for flow structures have been observed. Finn (1981) has documented characteristics similar to those of the Bonanza Lake intrusion in the Wanapitei Lake intrusion, which is located in the northeastern corner of Lake Wanapitei. His studies indicated that a reverse

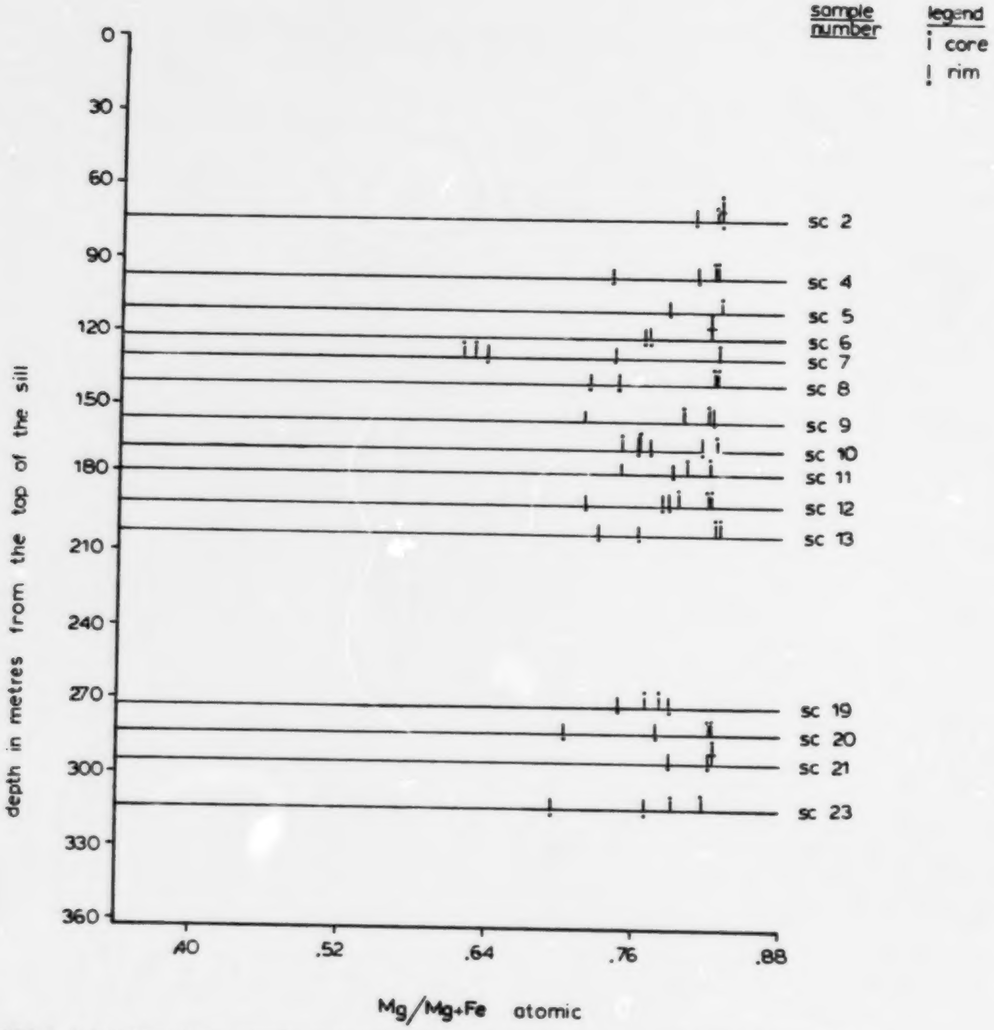

Figure 230.8. Variation of the atomic ratio Mg/(Mg+Fe) across the Cross Lake sill, Cobalt.

differentiation trend was found with increasing height from the base of the intrusion. Although insufficient analytical work has been completed in this study at this time, differentiation trends for the Portage Bay, Cross Lake, and Bonanza Lake intrusions will be determined.

The microprobe analysis of orthopyroxene from the Bonanza Lake intrusion has shown a normal differentiation trend from the southern contact toward the granodiorite. No cryptic variation was observed within the Cross Lake sill.

The immediate future plans involve the completion of mapping of the Portage Bay intrusion, and concentrated mapping of the southern contact of the Bonanza Lake intrusion with the Mississagi Formation. Whole-rock analysis of major oxides and trace elements will be carried out for Portage Bay, Bonanza Lake, and Cross Lake sill samples during the coming summer. Microprobe analysis of plagioclase and pyroxene will also be carried out to help define differentiation trends that may be related to the regional variations in mineralization. Nd-Sm and Rb-Sr isotopic studies, to be carried out in the Fall, will help define the degree of crustal contamination in each intrusion. Neutron-activation analyses are expected to be carried out on specific samples during the winter months, to evaluate the platinum element potential of the Nipissing intrusions.

ACKNOWLEDGMENTS

The authors wish to thank Dr. Burkhard O. Dressler and Mr. Leo Owsiacki for their suggestions of appropriate field areas and for their introductory field tours of the Bonanza Lake intrusion and Cobalt intrusions respectively. We would also like to thank Dr. C. Cermignani for his instruction and guidance at the microprobe. Thanks are also due to Stephany Thomas for her assistance in the field.

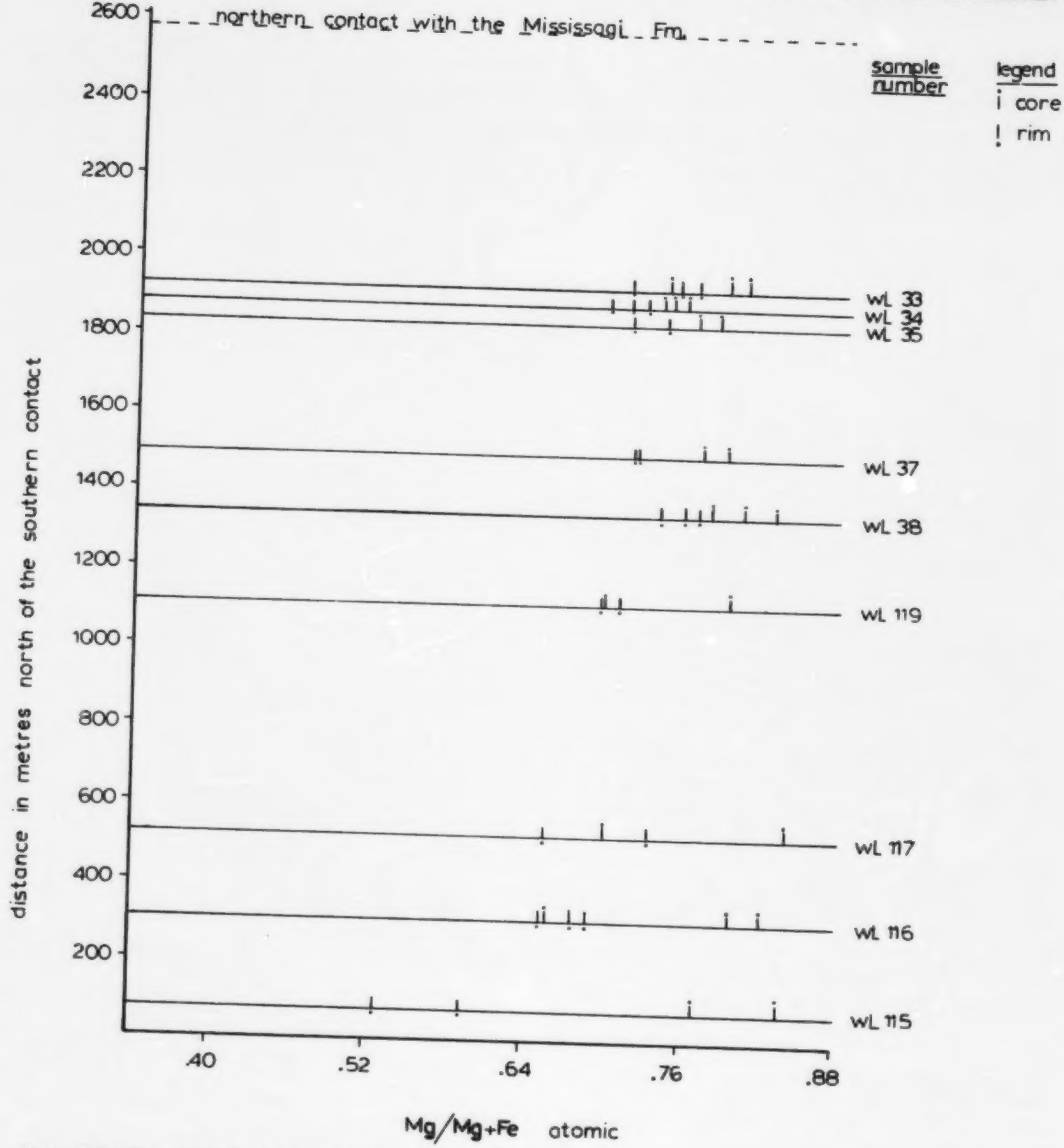

Figure 230.9a. *Variation of atomic ratio Mg/(Mg+Fe) across traverses a-b of the Bonanza Lake intrusion.*

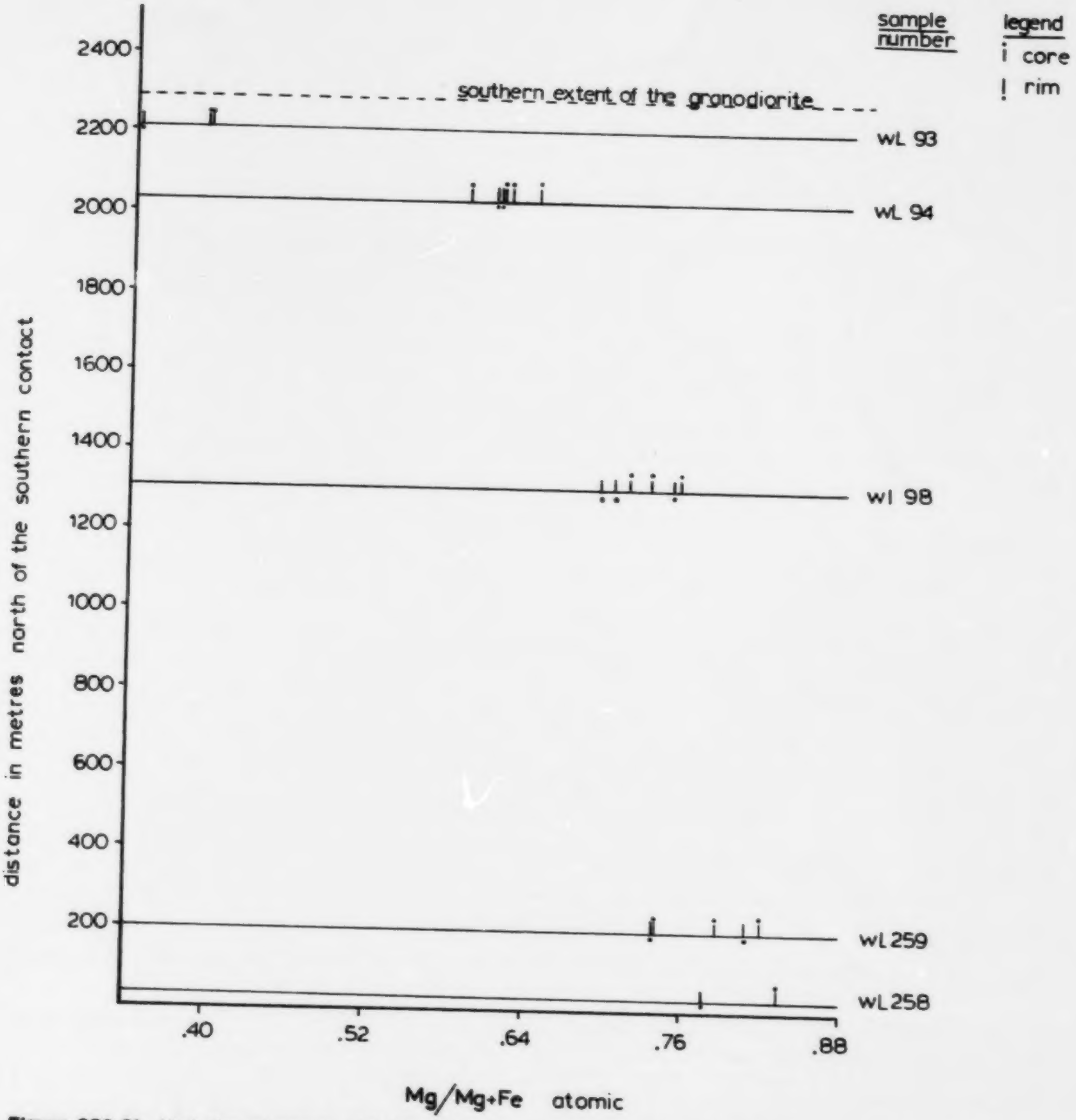

Figure 230.9b. Variation of atomic ratio Mg/(Mg+Fe) across traverses c-d of the Bonanza Lake intrusion.

TABLE 230.2. NICKEL CONTENT AND Fo VALUES IN OLIVINE FROM THE CROSS LAKE SILL.

Sample Number	Depth from the top of the sill (metres)	Ni content in the core of olivine grains (accuracy ± 85 ppm)	Average Fo content of olivine grains (mole % Fo)
SC 10	168	1650	66.79
SC 11	178	1760	68.37
SC 12	190	1760	68.79
SC 13	202	1735	68.13
SC 19	272	1780	67.70
SC 20	283	1595	64.20
SC 23	315	1430	60.63

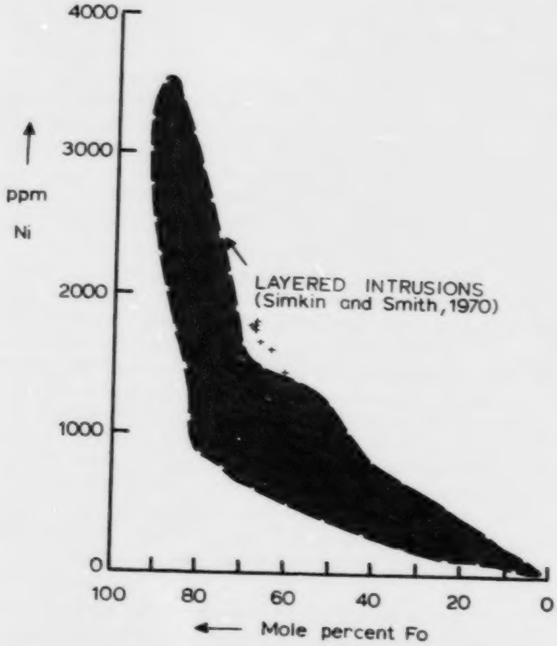

Figure 230.10. Nickel content plotted against mole percent Fo of olivine from the hypersthene zone of the Cross Lake sill, Cobalt.

REFERENCES

Bowen, N.L.
1928: The Evolution of the Igneous Rocks; Princeton University Press.

Card, K.D., and Lumbers, S.B.
1977: Sudbury-Cobalt, Algoma, Manitoulin, Nipissing, Parry Sound, Sudbury and Timiskaming District; Ontario Geological Survey, Map 2361, Geological Compilation Series, scale 1:253 440 or 1 inch to 4 miles. Revised compilation of Map 2188, 1974-75.

Card, K.D., and Pattison, E.F.
1973: Nipissing Diabase of the Southern Province, Ontario; Geological Association of Canada, Special Paper 12, p.7-30.

Dressler, Burkhard O.
1982: Geology of the Wanapitei Lake Area, District of Sudbury; Ontario Geological Survey, Open File Report 5287, and Map 2451, scale 1:31 680.

Fairbairn, H.W., Hurley, P.M., Card, K.D., and Knight, C.J.
1969: Correlation of Radiometric Ages of the Nipissing Diabase and Huronian Metasediments with Proterozoic Orogenic Events in Ontario; Canadian Journal of Earth Sciences, Volume 6, p.489-497.

Finn, G.C.
1981: Petrogenesis of the Wanapitei Gabbro-norite Intrusion, a Nipissing-type Diabase, from Northeastern Ontario; Unpublished M.Sc. Thesis, University of Western Ontario, 213p.

Hriskevich, M.E.
1968: Petrology of the Nipissing Diabase Sill of the Cobalt Area, Ontario, Canada; Geological Society of America, Bulletin, Volume 79, Number 10, p.1387-1404.

Jambor, J.L.
1971: The Silver-Arsenide Deposits of the Cobalt-Gowganda Region, Ontario; Mineralogical Association of Canada, Volume 11, p.34-72.

Johns, G.W.
1980: Geology of the Firstbrook Lake Area, District of Timiskaming; Ontario Geological Survey, Open File Report 5303, 79p. Accompanied by Map P.2279.

Miller, W.G.
1911: Notes on the Cobalt Area; Engineering and Mining Journal, Volume 92, p.645-649.

Naldrett, A.J.
1984: Magmatic Deposits and Platinum Group Elements; Ore Deposits Workshop Notes, University of Toronto, p.1-341.

Poldervaart, A., and Hess, H.H.
1951: Pyroxenes in the Crystallization of Basaltic Magma; Journal of Geology, Volume 59, p.472-489.

Simkin, T., and Smith, J.V.
1970: Minor Element Distribution in Olivine; Journal of Geology, Volume 78, Number 3, p.304-325.

Streckeisen, A.
1976: To Each Plutonic Rock its Proper Name; Earth Science Reviews, Volume 12, p.1-33.

Thomson, J.E.
1961: Maclennan and Scadding Townships; Ontario Department of Mines, Geological Report 2, 34p.

Thomson, R.
1964: Cobalt Silver Area, Southwestern Sheet, Timiskaming District; Ontario Department of Mines, Map 2051, scale 1:12 000.

Van Schmus, W.R.
1965: The Geochronology of the Blind River-Bruce Mines Areas, Ontario, Canada; Journal of Geology, Volume 73, p.755-780.

Grant 233 The Dating of Ontario's Gold Deposits

A. Masliwec, Derek York, P. Kuybida, and C.M. Hall

Department of Physics, University of Toronto

ABSTRACT

A study to test the applicability of dating gold deposits via the ^{40}Ar/^{39}Ar method, was confined to 2 areas: the Dome and Hollinger mines. A green mica alteration was found in association with gold in these mines. The green mica (fuchsite) is considered to be syngenetic with or to post-date the gold formation. Since the age of the host lithology is known from U-Pb zircon dating, it was hoped that ^{40}Ar/^{39}Ar analyses could help to bracket narrowly, for the first time, the age of gold formation.

INTRODUCTION

The purpose of the proposed project is to apply the ^{40}Ar/^{39}Ar method of dating to minerals associated with some of Ontario's gold deposits so that reliable estimates can be made of the time(s) of gold formation. Currently these times are only imprecisely known. While U-Pb dating of zircons is beginning to produce an accurate volcano-stratigraphic framework for the evolution of the gold-bearing greenstone belts, it remains extremely difficult to position the gold-forming events within this time-matrix.

What is required is a means of assigning ages to minerals and events associated with the gold-producing episodes. The advantages of the ^{40}Ar/^{39}Ar method in this context are the following: (a) a wide variety of minerals can be analyzed. This means that minerals in the ore-bearing veins themselves can be dated. Many of the deposits are associated with alteration haloes. Again, these contain minerals which can be analyzed with the ^{40}Ar/^{39}Ar approach. (b) Extremely high spatial resolution is attainable with a laser probe (accurate ages have been measured on 2500 Ma old biotite using sample sizes of several hundred nanograms), so that spatial pattern of ages associated with the veins can be sought on a variety of scales.

Initially, an approach is being developed in the Timmins camp which has already shown clear signs of being a major breakthrough in the dating of gold deposits. A number of the producing deposits are located in porphyries. The crystallization ages of these are being measured by Soussan Marmont (Geologist, Ontario Geological Survey, personal communication) by U-Pb dating of zircons. The gold is therefore younger than the associated zircon age. The gold is, however, apparently associated with a green mica alteration product which is considered to be syn- or post-gold. We are therefore ^{40}Ar/^{39}Ar dating the green mica to get a minimum age of gold formation. Already the mica has been shown to be a very suitable mineral for ^{40}Ar/^{39}Ar work and has enabled us to bracket the age of formation of the Hollinger Mine deposit at between 2617±5 Ma (from the micas) and 2685±3 Ma from the zircons. As a result, Hollinger may now be the most precisely dated Precambrian gold deposit in existence.

To the south, unaltered greenschist metamorphosed komatiite outside the ore zone is replaced by auriferous flow ore inside the Kerr-Addison Mine. Within the latter, original spinifex texture remains but is totally replaced by green mica, chlorite, and other minerals. Both these minerals will be dated in detail and the unaltered komatiite will also be dated (Lopez-Martinez 1984).

The approach adopted in the Abitibi region will be used in Red Lake, with samples from the Dome Stock, Dickenson Mine, and the Austin Tuff.

Finally, thermal histories of gold-related felsic intrusives will be analyzed in detail using the thermochronometric approach developed in Berger and York (1981).

The precise dating of gold and its positioning in the metamorphic and thermal histories of the greenstone belts will greatly aid theories of gold genesis and will be useful in the exploration for gold.

EXPERIMENTATION

The evolution of our experimental methods of handling mineral separates has been described earlier (York *et al.* 1981, 1982). All samples were irradiated in the McMaster University reactor along with Zartman hornblende standard (Zartman 1964). Milligram-size samples were used and cadmium shielding was used to reduce the hazard level of induced radioactivities. The irradiated samples were then fused in an ultra-high vacuum system and the purified argon was subsequently analyzed on a mass spectrometer. Mineral separations were performed with extreme care so that any contamination was removed as completely as possible.

PREVIOUS GEOCHRONOLOGY

Up to the present, geochronological work in the Timmins area has been very limited. Previous geochronological studies required interpolation of data from distant Abitibi areas to the Timmins area.

One such study (Gates and Hurley 1973) provided a detailed comparison of Rb-Sr and K-Ar dates on the Matachewan dike swarm (Matachewan is located approximately 75 km southeast of Timmins). K-Ar ages were found to be widely scattered and ranged from 1879 Ma to 2730 Ma A combined whole-rock and mineral Rb-Sr isochron produced an age of 2633±93 Ma The discrepancy in K-Ar ages was attributed to post-crystallization argon loss due to the geological complexity of the area. Since these dikes transect Kenoran fold structures and batholiths, they provide a minimum age for mineralization and regional deformation of the Timmins area.

In addition, a Sm-Nd whole-rock isochron from various komatiitic and tholeiitic rock formations within the Abitibi Belt yielded a best-fit isochron of 2662±120 Ma (Zindler 1977). The relatively large errors associated with this age were due, in part, to the restricted range of Sm and Nd ratios. However, a portion of the scatter was also attributed to the metamorphic history of the rocks. Lopez-Martinez (1984) has suggested that this scatter may be due to an event at approximately 1700 Ma ago which she found had reset the K-Ar clocks in the komatiites.

Reliable age estimates from the Abitibi Belt have come primarily from U-Pb investigations of zircon populations. To date, only 2 papers have been published on zircons from this area (Nunes and Pyke 1980; Nunes and Jensen 1980). Their data suggest that the upper units in both Timmins and Kirkland Lake to the east, are contemporaneous at 2703±2 Ma However, accumulation of the upper volcanic cycle in Kirkland Lake (7 Ma) took place over a much shorter time span than in the Timmins area (22 Ma). A preliminary age on the Timmins Millerton Porphyry gives a value of 2685±3 Ma (Soussan Marmont, personal communication). This suggests a time span of only 18 Ma between the last volcanic event and the emplacement of this porphyritic unit.

Kerrich *et al.* (1984) reported Rb-Sr ages on unspecified mineralization in the Hollinger, Kerr-Addison, and Dumagami Mines. Rb-Sr isochrons from mineral samples within these mines yielded ages of 2440±26 Ma, 2510±30 Ma, and 2420±19 Ma respectively. They interpreted these values as being disturbed Rb-Sr ages, since Pb-Pb and U-Pb ages in the area indicated a (much older) average value of 2697 Ma

RESULTS

Samples were obtained from 2 locations in the Timmins gold camp—the Dome and Hollinger Mines (Masliwec 1984). In each locality fuchsite was obtained from vein material and from the surrounding porphyritic host rock.

It is considered that K-metasomatic alteration present in association with the gold in the porphyries is either syngenetic or post the formation of the gold. Consequently, the age of the hosting porphyritic unit would provide an upper age limit for the gold mineralization, while the age of the altering event (creating the fuchsite) would provide a lower limit to the timing of gold emplacement. One such porphyry, the Millerton porphyry (which hosts the Hollinger gold), has been dated by U-Pb at 2685±3 Ma In addition, several other porphyries in the area give identical ages (Soussan Marmont, personal communication). Consequently an upper limit to the age of gold mineralization in Timmins was known. By dating the fuchsite (and therefore the alteration event) it would be possible to accurately bracket the time of emplacement of the gold mineralization.

DOME MINE RESULTS

The first sample shown in Figure 233.1 is vein associated, fuchsite material from the Dome Mine. The sample produced a stepwise monotonically increasing age spectrum. In the first fraction of gas released (0.2%), an age of 1535±192 Ma results. The next 0.5% of gas released produces a much more accurately defined age of 1765±39 Ma The ages then progressively increase to a maximum value of 2596±2 Ma Combining all the individual fractions gives a total integrated age of 2508±3 Ma

If the ^{39}Ar rate parameters are used a blocking temperature of 253.8°±26.6°C results, with a corresponding activation energy of 45.0±2.0 kcal/mole.

Sample OGS 585-600 is a repeat analysis of the Dome Mine vein sample shown in Figure 233.1. As before, the age spectrum (shown in Figure 233.2) produces a stepwise increasing age spectrum. The first least retentive step-heating fraction produces an age of 1343±91 Ma and then rises abruptly to a more precisely measured value of 1767±18 Ma The ages then progressively increase to a maximum age of 2579±4 Ma At the highest temperature the age drops slightly to 2567±15 Ma (2.6% of the total gas release). This is due possibly to slight fractionation of the argon isotopes at the highest temperature. The integrated age is 2480±6 Ma and is slightly lower than the previously mentioned integrated age. However, as the samples were irradiated in different cans, errors in the irradiation constants calculated from different irradiation cans may just account for the discrepancies.

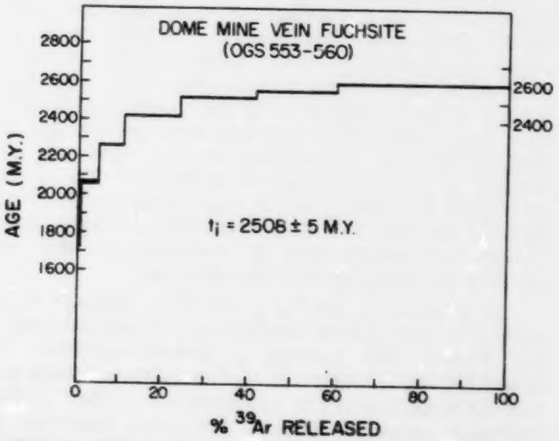

Figure 233.1. Age Spectrum for Dome Vein Fuchsite.

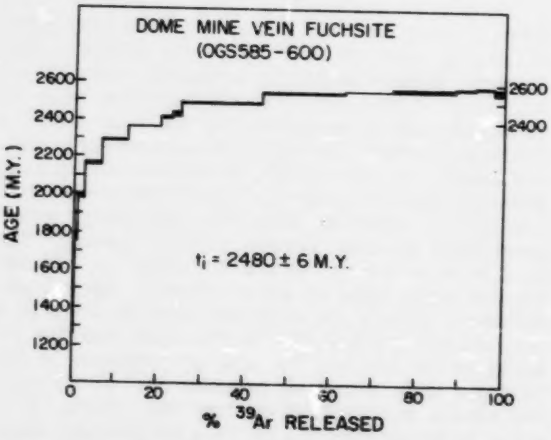

Figure 233.2. Age Spectrum for Dome Vein Fuchsite.

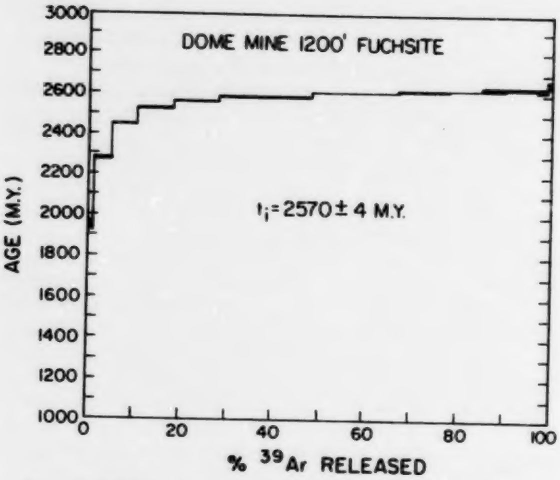

Figure 233.3. *Age Spectrum for Dome Vein Fuchsite.*

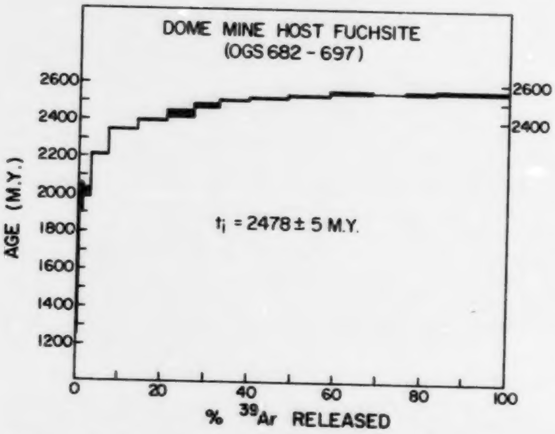

Figure 233.4. *Age Spectrum for Dome Host Fuchsite.*

Blocking temperatures and activation energy estimates from the ^{39}Ar rate parameters resulted in values of 240.3°±25.7°C and 47.3±1.8 kcal/mole respectively.

The age spectrum shown in Figure 233.3 is from vein-associated fuchsite from the Dome Mine, but from a different vein location than the 2 previously discussed age spectra. The minimum age at the lowest temperature step was 1693±58 Ma The ages then increased monotonically to a maximum age of 2633±6 Ma The integrated age of the sample was 2570±4 Ma

The argon data provide a blocking temperature estimate of 243.6°±14.9°C and an activation energy of 47.1±1.2 kcal/mole (using ^{39}Ar rate parameters).

A sample of fuchsite (OGS 682-697) from the host Preston porphyry was also analyzed. The resultant age spectrum is shown in Figure 233.4. In the first 1% of gas release (2 fractions), the age spectrum rises from 1403±148 Ma to an age of 1982±78 Ma The age values then increase with each rise in the extraction temperature to a maximum value of 2560±8 Ma This last temperature fraction approaches but does not reach the values attained in fusing the corresponding vein fuchsite. Nevertheless, the integrated age from sample OGS 585-600 is 2478±5 Ma, which is nearly identical to the value obtained from the vein.

Blocking temperature and activation energy calculations using the ^{39}Ar data produced values of 228.2°±36.6°C and 45.3±2.7 kcal/mole respectively.

Since the samples exhibit spectra which have monotonically increasing ages, the best estimate of formation age may be the oldest age obtained in the last few percent of gas release.

HOLLINGER MINE RESULTS

Figure 233.5 shows the age spectrum of a fuchsite sample (OGS 601-616) obtained from vein material from the Hollinger Mine. The age spectrum shows a rise with increasing temperature, similar to the Dome Mine fuchsites. In the first fraction of gas release (0.4%) an age of 1755±170 Ma is obtained. The age then rises to 2014±14 Ma in the next pulse of gas released. A maximum age of 2567±4 Ma is reached in the second last fraction of gas release. Since the integrated age includes the low ages produced by the least retentive argon sites the geological meaning of the 2502±5 Ma integrated age is debatable. A better approximation of the maximum age of the vein fuchsite may be 2567±4 Ma, which is only 2.6% older than the integrated age.

The ^{39}Ar rate parameters produce a blocking temperature and activation energy of 276.9°±23.6°C and 52.4±1.9 kcal/mole, respectively.

Sample OGS 617-632, shown in Figure 233.6 is fuchsite taken from the host rock of sample OGS 601-616. The age spectrum also shows a stepwise climb. The first 2 lowest temperature steps produce ages of 1233±60 Ma and 1682±50 Ma The third fraction then jumps to a value of 2013±47 Ma The ages then increase monotonically to a maximum age of 2607±5 Ma in the second last fraction of gas release. In the last 1% of argon release, the age drops slightly to 2558±35 Ma The high temperature drop was also observed in OGS 601-616, however, there is no readily apparent reason for this behaviour, other than possible fractionation effects.

A blocking temperature estimated from the ^{39}Ar rate parameters was 243.3°±31.2°C. The corresponding activation energy was 44.7±2.3 kcal/mole.

In order to demonstrate the capabilities of the new ultra-sensitive laser probe mass spectrometer just developed at the University of Toronto geochronology laboratory, a single grain of the Hollinger vein fuchsite was step heated. The resulting age spectrum is shown in Figure 233.7. A comparison with Figure 233.5 shows that, within expected experimental errors, the much more rapidly obtained laser dates agree completely with the more conventionally determined age. An age of 2617±5 Ma is indicated for the last cooling of the Hollinger deposit.

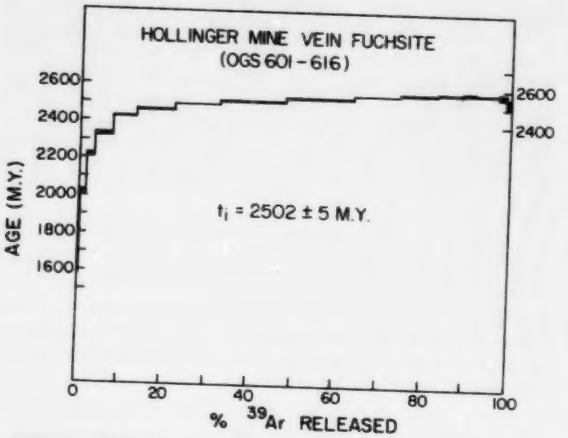

Figure 233.5. *Age Spectrum for Hollinger Vein Fuchsite.*

DISCUSSIONS

A preliminary study of fuchsite mineralization was initiated in the Timmins gold camp with the purpose of bracketing the time of emplacement of gold mineralization. Heretofore, the only knowledge of the time of gold emplacement was that the age of mineralization was essentially synchronous with, or younger than, the host lithology. Since several gold-hosting porphyries in the Timmins area had consistently produced U-Pb zircon ages of about 2685 Ma (Soussan Marmont, personal communication), this was the known maximum age of gold formation. Since it had been determined that potassic metasomatism of the host porphyries was syngenetic with or post gold formation, dating of the alteration event would provide a time span within which the gold formation would fall.

The results of dating the fuchsites that were formed during the potassic alteration event are summarized in Table 233.1. The formation ages in Table 233.1 were derived by assuming that the oldest ages found in the age spectra were derived from gas released from the most retentive phases. This assumption seems reasonable in light of the disturbed type of age spectra that were obtained.

TABLE 233.1. ANALYTICAL RESULTS FOR THE TIMMINS FUCHSITES

Sample	Mine	Formation Age (Ma)
TM 87-101 (vein)	Dome	2633±6
OGS 553-560 (vein)	Dome	2596±2
OGS 585-600 (host)	Dome	2579±4
OGS 682-697 (host)	Dome	2560±8
OGS 601-616 (vein)	Hollinger	2573±6
OGS 617-632 (host)	Hollinger	2607±5
Laser fusion (vein)	Hollinger	2617±5

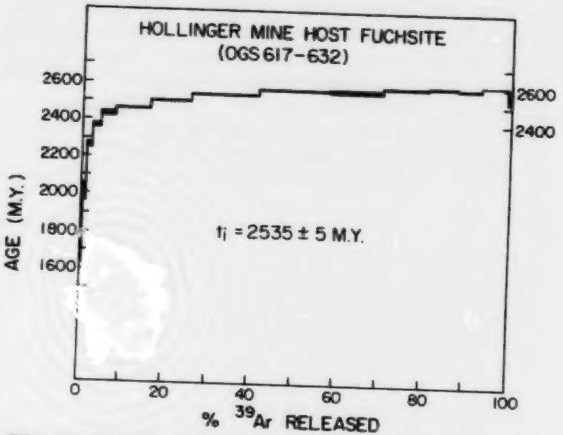

Figure 233.6. *Age Spectrum for Hollinger Host Fuchsite.*

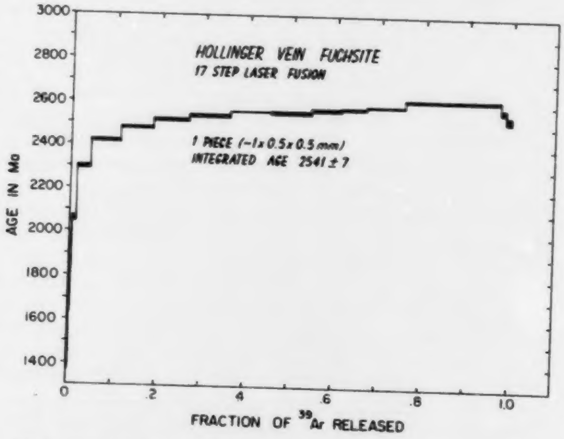

Figure 233.7. *Laser Generated Age Spectrum for Hollinger Vein Fuchsite.*

Since the 2 mines studied were separated by only 1.3 km, it seems reasonable to suppose that both mines have undergone similar thermal histories. The variance in maximum ages is, therefore, most likely due to different grain size or chemical composition of the fuchsites producing differences in blocking temperatures in the micas. If the maximum age of 2617 Ma from the Hollinger Mine is used as an upper limit of the alteration event, it is possible to bracket closely the Hollinger gold formation. It appears highly probable that gold in the Hollinger deposit was emplaced between 2617±5 and 2685±2 Ma ago. This is a very important result for studies in the Timmins area. In addition, if the porphyry hosting the Dome Mine is also approximately 2685 Ma old (*see* "Previous Geochronology"), then it is possible to even more closely bracket the formation of the gold to between 2633±6 and 2685 Ma It is the first time that the emplacement of gold in the Timmins area has been bracketed to this degree of accuracy. The authors are, in fact, unaware of any

Precambrian gold deposit which has been this accurately dated.

The preliminary analyses of fuchsites have given extremely exciting results for bracketing the age of gold emplacement in the Timmins area. It will obviously be worthwhile to perform a more detailed ^{40}Ar/^{39}Ar study of the locality. Since many other porphyry-related gold mines in the Timmins camp exist (several, whose host porphyries have been dated using U-Pb on zircons), it will be productive to date the associated alteration micas. By sampling alteration micas with larger grain sizes, different chemical compositions, or from different portions of the mining area, it should be possible to obtain samples with higher blocking temperatures and activation energies. These consequently could provide older formation ages and thus even more precisely constrain the time of Archean gold formation. Once the Timmins area has been adequately resolved, subsequent studies will be extended to other Abitibi and Archean gold areas in order to bracket the time of gold formation in those regions.

SUMMARY

In the course of the research presented here it has been established that:

1. By performing a preliminary ^{40}Ar/^{39}Ar study of fuchsite alteration assumed to be syngenetic with or post-dating gold mineralization, it has been possible to bracket (with the aid of U-Pb zircon ages), for the first time, the time of formation (to within 75 Ma) of an Archean gold deposit (Hollinger). If an age of 2685 Ma is reasonable for the porphyry hosting the Dome gold, then it is possible to bracket the gold formation even more closely (50 Ma). Previously, it was only known that the age of the gold mineralization in the Timmins area was younger than the host lithology (i.e. 2685 Ma).

2. The fuchsites from the Dome and Hollinger Mines exhibited nearly identical age spectra and diffusive properties. However, slight differences are detectable between samples. This extreme sensitivity of the ^{40}Ar/^{39}Ar dating method in delineating minor differences as demonstrated by the fuchsites, is testimony to the power of this technique as a geological tool. It would obviously be worthwhile to apply this dating method more widely to the Timmins area, with the intent of obtaining an even more accurate definition of the age of gold mineralization. It is conceivable that the age(s) of the gold could be delineated with an uncertainty limited mostly by uncertainties in the half-lives of the uranium and potassium isotopes.

3. Additional fuchsite samples have also been obtained from 6 different Archean gold deposits in Ontario. These will soon be subject to indepth argon isotope analyses.

4. As well, in an attempt to reduce the uncertainty surrounding the thermal history of the Red Lake gold camp, several hornblendes, micas, and K-feldspars have been obtained from this locality. With this suite of minerals it will be possible to perform a detailed ^{40}Ar/^{39}Ar thermochronometric study of the Red Lake area. Such a study will hopefully offer many new insights into gold formation.

ACKNOWLEDGMENTS

The project is principally funded by the Ontario Geoscience Research Grant Program, but is also significantly supported by Natural Sciences and Engineering Research Council (NSERC) grants. We are indebted to Soussan Marmont and A. Andrews for the provision of samples. The McMaster University reactor personnel were extremely helpful with all irradiations.

REFERENCES

Berger, G.W., and York, D.
1981: Geothermometry from ^{40}Ar/^{39}Ar Dating Experiments; Geochimica et Cosmochimica Acta, Volume 45, p.795-811.

Gates, T.M., and Hurley, P.M.
1973: Evaluation of the Rb-Sr and K-Ar Dating Methods Applied to the Matachewan, Abitibi, Mackenzie, and Sudbury Dike Swarms in Canada; Canadian Journal of Earth Sciences, Volume 10, p.900-919.

Kerrich R., Kishida, A., and Willmore, L.M.
1984: Timing of Abitibi Lode Gold Deposits: Evidence from ^{40}Ar/^{39}Ar and Rb-Sr; *in* GAC-MAC Program with Abstracts, p.78.

Lopez-Martinez, M.
1984: ^{40}Ar/^{39}Ar Study of Komatiites; Unpublished Ph.D. Thesis, University of Toronto, Toronto.

Masliwec, A.
1984: Applicability of the ^{40}Ar/^{39}Ar Dating Method to the Dating of Ore Deposits; Unpublished Ph.D. Thesis, University of Toronto, Toronto.

Nunes, P.D., and Jensen, L.S.
1980: Geochronology of the Abitibi Metavolcanic Belt, Kirkland Lake Area—Progress Report; p.40-45 *in* Summary of Geochronology Studies 1977-1979, edited by E.G. Pye, Ontario Geological Survey, Miscellaneous Paper 92, 45p.

Nunes, P.D., and Pyke, D.R.
1980: Geochronology of the Abitibi Metavolcanic Belt, Timmins-Matachewan Area—Progress Report; p.34-39 *in* Summary of Geochronology Studies 1977-1979, edited by E.G. Pye, Ontario Geological Survey, Miscellaneous Paper 92, 45p.

York, Derek, Masliwec, A., Hall, C.M., Kuybida, P., Kenyon, W.J., Spooner, E.T.C., and Scott, S.D.
1981: The Direct Dating of Ore Minerals; Grant 62, p.334-340 *in* Geoscience Research Grant Program, Summary of Research 1980-1981, Ontario Geological Survey, Miscellaneous Paper 98, 340p.
1982: Direct Dating of Ore Minerals; Grant 62, p.213-219 *in* Geoscience Research Grant Program, Summary of Research 1981-1982, edited by E.G. Pye, Ontario Geological Survey, Miscellaneous Paper 103, 219p.

Zartman, R.E.
1964: A Geochronologic Study of the Lone Grove Pluton from the Llano Uplift, Texas; Journal of Petrology, Volume 5, p.359-409.

Zindler,A.
1977: Nd-Sm Isotopic Studies of Komatiites and Related Rocks; *in* Komatiites, edited by N.T. Arndt and E.G. Nisbet, by G. Allen and Unwin, Publishers.

Grant 236 Geological, Fluid Inclusion, and Isotopic (Carbon and Sulphur) Studies of Au-Quartz-Carbonate-Pyrite-Scheelite Vein Mineralization and Intrusion-Hosted Cu-(Au-Mo) Mineralization in the Hollinger-McIntyre System, Timmins, Ontario

E.T.C. Spooner, P.C. Wood, D.R. Burrows, A.V. Thomas, and S.R. Noble

Department of Geology, University of Toronto

ABSTRACT

The Hollinger (Timmins)-McIntyre (Schumacher)-Coniaurum-Vipond-Moneta-Crown system is the largest Au-quartz-Fe-carbonate-pyrite ± tourmaline ± tellurides ± W (scheelite) ± MoS_2 vein deposit in the Superior Province, with end-1984 past-production plus reserves of 994.7 tonnes of recovered/recoverable gold. The McIntyre Mine also contains a Cu-(Au-Mo) orebody hosted in the strained Pearl Lake Porphyry (~10 million tonnes at 0.8% Cu, 0.05% Mo, and 1.2 g/tonne Au) which constitutes a poorly defined Archean exploration target. Gold mineralization is related to quartz dominated veins with prominent pyrite-Fe-carbonate-muscovite alteration envelopes. Geometrically, the veins are unusual, consisting of steeply dipping tabular sections from which extend flats and spurs which feather, bifurcate, and branch. Some aspects of these various vein geometries can be explained by hydraulic fracturing. It is concluded that the "porphyries" which mineralization cross-cuts, but with which mineralization has a spatial association, are intrusive. Their contacts cross-cut the regional strike of foliation and they coalesce at depth. Cu-(Mo-Au) mineralization and the associated alteration haloes *post-date*, to varying degrees, the distinctive L-fabric ubiquitous in both volcanics and porphyry intrusions in the central portions of the area. The main Au-(W) mineralization, although partly controlled by pre-existing structure, is later than almost all folding and fabric development.

Primary fluid inclusions in early scheelite, main stage scheelite, and quartz indicate a relatively pure CO_2-bearing fluid (CO_2 m.pt. = -56.7 ± 0.7°C, n = 100) of low to moderate salinity (4.3 ± 1.8 equiv. wt.% NaCl, n = 58). Evidence shows that H_2O-CO_2 phase separation did occur, and thus that formation temperatures are equivalent to total homogenization temperatures of 271° ± 47°C (n = 33). Furthermore, the thermal and chemical properties of the ore fluids derived from fluid inclusions in vein materials are applicable to adjacent mineralized wall rocks where the bulk (> 95%) of the Au is located. This is shown by the fact that, in 9 cases out of 10, the variance between vein and adjacent wall rock pyrite $\delta^{34}S$ values is less than the total $\delta^{34}S$ variance at >the 95% confidence level.

Carbonate $\delta^{13}C$ values for Timmins area Au vein mineralization (-3.1 ± 1.3‰; 1s; n = 289), which include 14 new, representative determinations for Hollinger and Golden Mile Au vein mineralization (-3.4 ± 0.4‰; n = 19), are remarkably similar to carbonate $\delta^{13}C$ values for Mink Lake intrusion MoS_2 mineralization (-3.3 ± 0.4‰; n = 13), with arithmetic means differing by only 0.3‰. This similarity suggests that Archean gold-quartz-Fe-carbonate-pyrite ± tourmaline ± tellurides ± W (scheelite) ± Mo vein mineralization could be magmatically derived.

In Hollinger, 97.1 volume % of gold in mineralized wall-rock material, where ~95% of the Au is located, is directly associated with pyrite (n = 342 Au particles). The $\delta^{34}S$ value of this pyrite is +3.5 ± 1.4‰ (n = 33), which is very similar to that in most Western Australian deposits (+3.0 ± 1.3‰; n = 37). Mann-Whitney U nonparametric significance tests show that vein and wall-rock pyrite $\delta^{34}S$ values are drawn from the same population with a high probability of 62%. $\delta^{34}S$ values of +3.0‰ to +3.5‰ do not appear to be very useful for distinguishing sources or processes involved in the formation of Archean vein Au deposits. Unfortunately, the possibility that potential for unusually large Archean vein gold deposits might be recognizable from negative $\delta^{34}S$ values (Lambert *et al.* 1984) appears to be unlikely.

PART 1. GEOLOGICAL RELATIONSHIPS

by D.R. Burrows, P.C. Wood, and E.T.C. Spooner

INTRODUCTION

The Hollinger (Timmins)-McIntyre (Schumacher)-Coniaurum-Vipond-Moneta-Crown vein system is ~5 km long, a maximum of ~2 km wide, and has been mined to a depth of 2.4 km (7875-foot level, McIntyre Mine). Located on the north limb of the east-northeast trending Porcupine Syncline (Figure 236.1) within the Tisdale Group (Central and Vipond subgroups of Ferguson 1968), it is the largest known Au vein system in the Superior Province, and one of the largest known in the world, probably the second largest, with end-1984 past-production plus reserves of 100.9 million tonnes at 9.9 g/tonne recovered/recoverable Au and ~2 g/tonne Ag (Bertoni 1983; Pamour Porcupine Mines Limited Annual Reports 1983-1985). The total amount of contained Au (994.7 tonnes with a current value of US$ ~11 x 10^9, at US$ 300 per troy ounce) is less than that in the Golden Mile system of lodes in the Yilgarn Block of Western Australia (~1200 tonnes; Lambert *et al.* 1984), but more than that in the Kolar Gold Field in southern India (825 tonnes; Mining Journal, April 26, 1985). Of the total contained Au, 60.2% occurred in the Hollinger deposit which, after staking by Benny Hollinger and Alec Gillies on October 1, 1909, has been in production with some interruptions since 1910. Underground mining ceased in October 1984, but surface mining continues. During the 1920s and 1930s, the Hollinger mine was the second largest hard-rock Au producer in the world, and between 1940 and 1953 it was the principal source of scheelite of the gold mines in the Archean of Canada (47 878.1 tonnes of ore at 0.78% WO_3; Allen and Folinsbee 1944; Ferguson 1968; Wood 1983). Of the total contained gold, 34.1% occurred in the McIntyre part of the system, where underground mining still continues. Hence the Hollinger-McIntyre system is an excellent example of an Archean gold-quartz-Fe-carbonate-pyrite ± tourmaline ± tellurides ± W (scheelite) ± MoS_2 type of vein deposit.

The McIntyre Mine also contains a Cu-(Au-Mo) orebody, hosted in the Pearl Lake Porphyry, with ~10 million tonnes at 0.8% Cu, 0.05% Mo, and 1.2 g/tonne Au (Davies and Lutha 1978). The latter constitutes a poorly defined Archean exploration target.

PORPHYRIES

Nine distinct plagioclase-quartz-phyric sodic intrusions occur in the system, as well as numerous smaller porphyry lenses (Ferguson 1968). The stocks strike 40° to 70°NE, dip 50° to 80°S, and generally plunge 45° to 60°E. These include the Pearl Lake (PLP), Acme, Millerton, Miller Lake, Northern, Gillies Lake, and Crown Porphyries in the Hollinger-McIntyre Property (Figure 236.1). At surface they range in size from 460 x 1680 m (Pearl Lake Porphyry) to 60 x 230 m (Millerton). However, with depth, the sizes of the stocks increase dramatically (Figure 236.2). For example, the Millerton is 90 x 1100 m at the 2000-foot level. The Northern and Miller Lake Porphyries merge with depth (≥ 1800-foot level), and the Millerton Porphyry merges with this body at greater than the 2000-foot level, or is connected by apophyses. Likewise, the Millerton joins with the more northern lobe of the coarse-textured granitoid Crown Porphyry below the 4250-foot level, while in the McIntyre, ~300 m northwest of the PLP, the Northern Porphyry joins the Gillies Lake Porphyry to form the largest intrusion in the property.

None of the porphyries has a fixed relationship to a particular horizon in the volcano-sedimentary sequence, and there are numerous apophyses and irregular lenses, all of which indicate intrusion of the porphyries into the limb of a folded structure.

The porphyry contacts observed were intrusive in nature in many cases, with small dikes, chilled contacts, and an unstrained, "subcrowded", porphyritic, igneous texture with zoned plagioclase phenocrysts up to 7 mm in size. The contacts are oblique to both the regional strike of foliation and the fabric developed within the porphyry itself. A heterolithic breccia commonly obscured the contact of the PLP and the Northern Porphyry with porphyry and volcanic fragments in a porphyry-like matrix.

The Northern and Miller Lake Porphyries on the 1250-foot level appear to cross-cut both stratigraphy

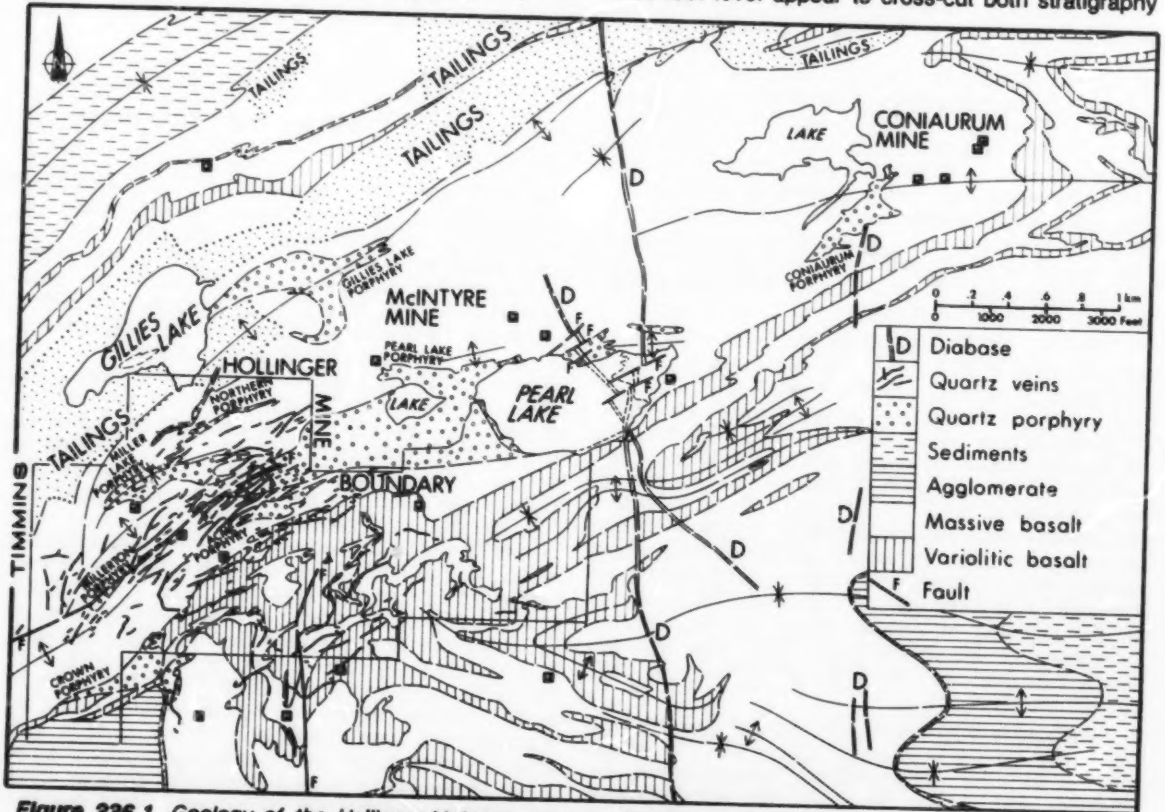
TAILINGS
TAILINGS
TAILINGS
TAILINGS
TAILINGS
TAILINGS
LAKE
CONIAURUM MINE
D
CONIAURUM PORPHYRY
GILLIES LAKE PORPHYRY
McINTYRE MINE
PEARL LAKE PORPHYRY
GILLIES LAKE
HOLLINGER
NORTHERN PORPHYRY
MINE
LAKE
PEARL LAKE
MILLER LAKE PORPHYRY
BOUNDARY
TIMMINS
MILLERTON PORPHYRY
CROWN PORPHYRY
F
0 .2 .4 .6 .8 1 km
0 1000 2000 3000 Feet
D Diabase
Quartz veins
Quartz porphyry
Sediments
Agglomerate
Massive basalt
Variolitic basalt
F Fault

Figure 236.1. Geology of the Hollinger-McIntyre system showing porphyry and vein distributions (modified after Ferguson 1968).

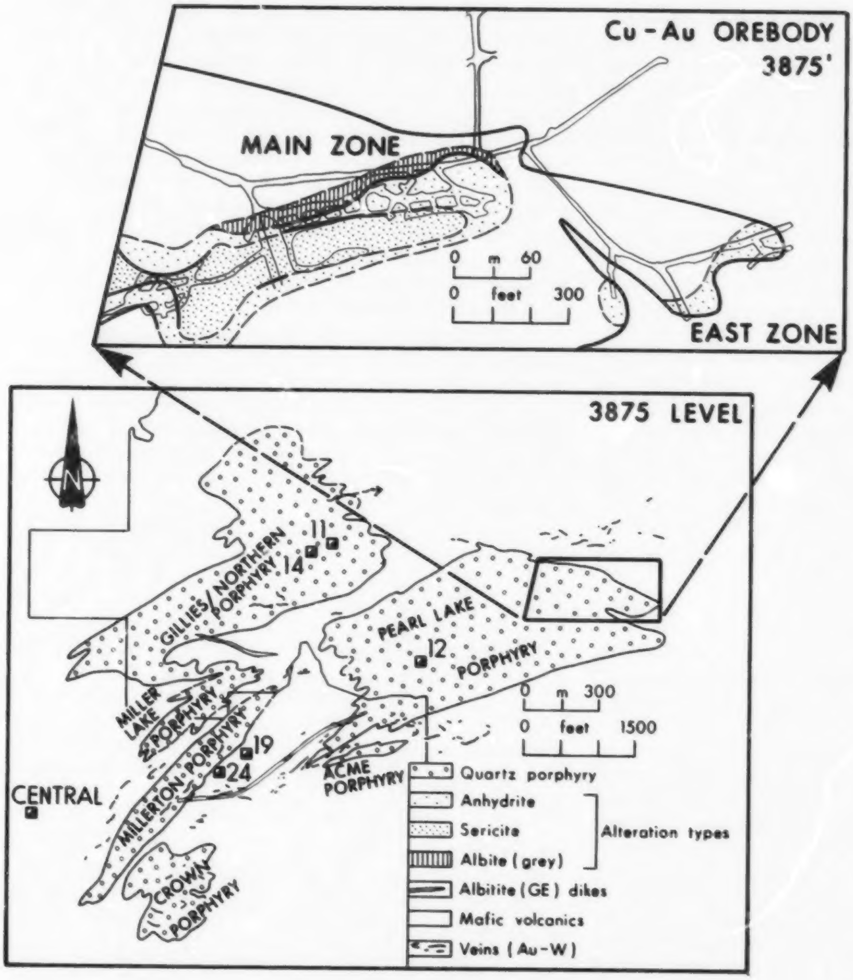
Cu - Au OREBODY
3875'
MAIN ZONE
0 m 60
0 feet 300
EAST ZONE
3875 LEVEL
N
GILLIES/NORTHERN PORPHYRY
11
14
PEARL LAKE PORPHYRY
12
0 m 300
0 feet 1500
MILLER LAKE PORPHYRY
MILLERTON PORPHYRY
19
24
ACME PORPHYRY
CENTRAL
CROWN PORPHYRY
Quartz porphyry
Anhydrite
Sericite
Albite (grey)
Alteration types
Albitite (GE) dikes
Mafic volcanics
Veins (Au-W)

Figure 236.2. *3875-foot Level plan showing relationships of porphyry intrusions to the main Au-(W) vein system and Cu-(Au-Mo) ore body.*

and the regional fabric developed in the volcanic rocks. The basal contacts of the porphyries, especially, are unstrained and strike 226° to 240°, dipping 50° to 60°SE. The unaltered porphyritic material at this contact changes over less than a metre into silicified, sericitized porphyry with a strong L-fabric, with only quartz eyes remaining of the original porphyritic texture evident in the fresh intrusion. This altered material is always distinguishable from silicified volcanics. Tongues and apophyses of this material, especially on the north flank of the PLP on the 3650-foot level, are true intrusive bodies, not silicified volcanic rocks or sheared-off portions of the main PLP. The contacts dipping 66°SE bear no relation to the steeper foliation. The same is true for the Crown Porphyry contact (194°/vertical) with the enclosing fragmental (? Krist) unit, which although interdigitated, is unaffected by subsequent shearing and is clearly intrusive.

Level plans indicate, therefore, that the individual stocks increase in size and merge, to give the appearance at depths greater than the 5300-foot level, of one large but irregular intrusion, with a more northwesterly portion comprising the Gillies Lake, Northern, Miller Lake, Crown, and Millerton Porphyries. Even the Pearl Lake and the Acme Porphyries, which are distinct at higher levels, tend to lose their identity.

The appearance and composition of the porphyries, although similar, show a range of colour, phenocryst content, and size, from the "crowded" PLP to the "subcrowded" Northern Porphyry (with large phenocrysts), to the granitoid textured Crown Porphyry. This information suggests that they represent fractionation of a single parent magma. Variable degrees of strain and alteration are probably largely responsible for the variation in texture.

ALBITITE / GE DIKES

Porphyries are cut by pre-ore "albitite" dikes from 0.5 to 5 m wide. Five dikes were sampled on levels 2375-foot, 2750-foot, and 3875-foot (one of them at different locations along strike) in the McIntyre Mine, and also one 274°/70°S dike (parallel to the fabric within volcanic rocks) on the 2750-foot level in the Hollinger Mine.

The dikes are distinctive in that they cross-cut stratigraphy and porphyry contacts, and are less strained than their surrounding lithologies. Another diagnostic feature is the presence of rounded to ellipsoidal, 1 to 30 cm in size, felsic inclusions of unstrained adamellite and microgranitic material termed "Goose Eggs" (hence GE dikes).

The albitite intrusions have an extremely consistent strike between 262° and 280° (East), but a more variable dip between 40° and 85°S, with the exception of one more felsic example with a 220°/45°SE orientation. Dikes show a nearly vertical plunge, unlike most structures in the mine, indicating that the ore-zones only reflect an earlier structural control. Individual dikes are continuous for up to 2000 feet but are more often wedge-shaped both laterally and vertically. Contacts are always sharp, often irregular, and usually oblique to the fabric in the surrounding volcanics. A slight chill is occasionally apparent and some dikes appear to be compositionally zoned. The dikes are pale to dark grey in colour with a speckled appearance. Veins are observed within the dikes cross-cutting fabric, commonly along the contacts and also cutting contacts.

TIMING OF MINERALIZATION

Foliation strikes 070°NE, dipping 65° to 80°S, with a strong, penetrative, prolate stretching lineation plunging 60° to 81°E downdip in the plane of the foliation in both the volcanic rocks and the porphyries. Superimposed on this fabric, in some regions, is a subhorizontal crenulation cleavage striking 10° to 100°. Extension, as indicated by varioles in the V8 unit and breccia fragments from the Central Subgroup, is prolate, subvertical, and defines a strain ellipsoid with axes ~5:1:1. The volcanic flows and interflow sediments, where measured, uniformally strike 248° to 274°, dipping and younging 60°S/SE. Thus stratigraphy and intrusive porphyry contacts are cut by the higher angle foliation on this northern limb of the Porcupine Syncline.

MAIN Au-(W) SYSTEM

The Main Ore-zone in Hollinger, located between the western end of the Pearl Lake Porphyry (PLP), and the Millerton Porphyry (Figure 236.1), strikes 060°NE/67°S and plunges 55°S in the same sense as the porphyry intrusions. Quartz veins, stringers, and stockworks with associated pyritized wall rocks occur dominantly in the sheared volcanic rocks (breccias and pillow lavas) of the Central and Vipond Subgroups, and to a lesser extent, in the porphyries. Individual orebodies often dip more steeply, between 75°S and vertical. A continuum of orebody types was observed between the following end members:

1. Well defined tabular continuous veins which branch, pinch, and swell, and are often located in interflow positions.
2. Tabular vein zones with series of irregular but approximately parallel stringers.
3. *En echelon* quartz stringers in s- or z-shaped ductile shear-generated fractures. Individual veins are shallow and cross-cut the steep foliation, despite the attitude of the actual zones being parallel to the main structure.

The latter type is most prominent within the porphyries where veins are observed to result from local ductile shearing of a pre-existing fabric, while others result from brittle fracture within ductile shear zones to give the *en echelon* sets. Veins in general show evidence of rapid, pure extensional opening with growth of marginal carbonate and/or albite, followed by open space filling with quartz. Spurs and bifurcations extending from the main veins are indicative of high fluid pressure which produced hydraulic fracturing (Wood and Spooner 1984).

The larger vertically continuous tabular veins, which are found in the volcanic rocks and at interflow horizons, show a longer, more complex history, with features such as lamination and brecciation indicative of multiple stages of formation. Many are parallel to fabric and show a slight boudinage, although again, on a small scale, splays and spurs cut the sub-vertical foliation.

These observations suggest that the vein-filled fractures are superimposed upon a sequence of volcanic rocks deformed and folded during regional deformation and then, after porphyry intrusion, in more local shear zones. Thus the position of major "ore-zones" is controlled by pre-existing structure resulting in favourable regions with enhanced permeability. Fracturing developed in the late stages of the latter event. Fluid introduction may have reactivated deformation especially in the more brittle homogeneous porphyries, but, overall, post-vein strain is relatively limited.

Cu-(Au-Mo) System

Chalcopyrite dominated mineralization within the Pearl Lake Porphyry (PLP) below the 1100-foot level is concentrated in 2 main zones (Figure 236.2).

1. *Main*: This zone occupies a cylindrical east-west trending elongate zone, ~120 x 300 m, enclosed within the northeastern flank of the PLP, and comprises ~10 million tonnes at 0.8% Cu with a cut-off grade of 0.65%. Within the alteration zones, the grade falls off sharply to 0.1% and outside this, to less than 0.05% Cu, except for isolated values up to 0.2% related to irregular quartz veining. The Cu-Au mineralization examined on 5 levels comprises a central sericitic, quartz vein dominated, portion and a surrounding halo of disseminated mineralization associated with anhydrite-hematite alteration. Early "stockwork-type" veining is post-dated by veins formed during shearing and deformation of the PLP, while others cross-cut the shear-generated foliation at a high angle.

This region corresponds, on all levels, to an irregularity on the northern flank of the porphyry with tongues/apophyses of porphyry extending out off the contact in an intrusive manner oblique to the strike of the volcanic rocks, for example on the 3650-foot level.

2. *East*: The East Zone consists of disseminated and fine chalcopyrite stringers hosted in sericitized-carbonatized *metabasalt*, without quartz veining, at the eastern end of the PLP.

Mineralization comprises dominantly chalcopyrite with minor bornite (at higher levels) and (?)tetrahedrite associated with pyrite, anhydrite, carbonate, and hematite, both in quartz veins and as disseminated material. Molybdenite is observed, as finely disseminated flecks, on the 3125-foot and 3875-foot levels, especially in the volcanic-hosted East Zone. Gold values are extremely erratic and vary between trace and 2 g/tonne, but not consistently in relation to depth or mineral assemblage.

Two main alteration types are observed spatially related to the Cu-Au mineralization, with perhaps another minor one.

(a) Sericite (chlorite) Zone

(b) Anhydrite-hematite Zone

(c) Grey-albite Zone (?)

These alteration zones are lensoid and irregular in detail but are arranged crudely in a zonal fashion about the Main ore zone (Figure 236.2). Contacts between (a) and (b) are sharp, whereas others are gradational, as is the transition into unmineralized PLP. The grey-albite zone is apparently unmineralized and is transitional into "normal" PLP. It appears to be distinct from relict porphyritic portions of the porphyry, and albite laths may have grown in response to re-equilibration with the hydrothermal fluid.

One other assemblage was recognized on level 3875-foot only, in the region between the East and Main Zones, in which chlorite and carbonate are prominent. Anhydrite-quartz-chalcopyrite-molybdenite veins were present both parallel to fabric and cross-cutting at 196°/32°SE. On other levels the porphyry appears more chloritic close to the contact, but not on such a large scale.

Anhydrite-Hematite Alteration: This type of alteration consists of a fine- to medium-grained assemblage with a distinctive pink to orange-brown colour due to finely disseminated anhydrite and hematite, and salmon pink anhydrite stringers. Pyrite and chalcopyrite with minor molybdenite are finely disseminated. Zones are generally less than 5 m in width, except in the East Zone where the volcanic rocks show pervasive alteration of this type. Veining dominantly is parallel to and actually defines fabric. Quartz veining is distinctively absent and all mineralization is disseminated.

Sericite Zone: This central, pale green to cream fine-grained alteration type is distinctive in that the majority of the mineralization is hosted in large, irregular, late, quartz-carbonate veins. Anhydrite, barite, and K-feldspar are occasional minor vein components. Many of the veins are shear generated, whereas others are purely extensional. The surrounding porphyry is highly foliated and altered to a chlorite-talc and sericite assemblage. This zone hosts the higher grade Cu mineralization and appears to have been volumetrically more important at depth (Tony VanWeichen, Pamour Porcupine Mines Limited, personal communication, July/August, 1984). A complex veining history is most evident here with early chalcopyrite-pyrite (stockwork) stringers, large irregular veins and late, low angle discordant veins.

Many stringers of anhydrite and chalcopyrite cross-cut the fabric in the anhydrite-hematite zone. However, this alteration on the whole defines the fabric and is strike parallel. This relationship could be interpreted as indicating a pre-existing fabric along which mineralization was preferentially deposited in a similar stress regime. The boundaries between the anhydrite and sericite zones were *not* parallel to foliation, and, in places, truncated it at a shallow angle. Mineralization in the higher grade sericite zone is totally within quartz veins and not disseminated; the majority of these veins cross-cut the fabric at a high angle. The highly irregular nature of many of the quartz veins indicates emplacement into an already highly foliated porphyry. Likewise, veins parallel to the fabric are seen splaying or branching off perpendicular to the fabric, indicating hydraulic fracturing into a foliated rock.

On the other hand, it might be possible to view the anhydrite-hematite-hosted mineralization as pre-fabric and cross-cutting relationships (and therefore the whole of the sericite zone) as a later "remobilization" feature. However, for the reasons mentioned, this possibility appears to be unlikely.

In 3 dimensions, the Main Zone occupies a consistent position relative to the PLP and thus must have a pipe-like form gradually narrowing with depth. This structure follows the plunge of the PLP itself down to the northeast. Although mineralization extends as a belt of lower grade (~0.2% Cu) towards the eastern end, it is distinct from the higher grade, volcanic-hosted East Zone copper.

These observations are obviously in a degree of disagreement with some previous work, particularly that of Davies and Lutha (1978). The major zones of alteration recognized are the same except that we recognize the central sericitic core as distinct from the grey albite-quartz assemblage (Davies and Lutha 1978). However, extending their conclusions regarding the formation of textures within these alteration zones to the porphyry as a whole is unwarranted. Relict porphyritic textures and the discordant nature of the apophyses of the Pearl Lake Porphyry suggest a late magmatic intrusive body. Examination of other porphyries confirms this relationship. Samples of PLP collected show the plagioclase and quartz phenocrysts displaying variable degrees of strain, again consistent with their early formation.

Traverses away from these alteration zones, for example, on the 2375-foot, 3875-foot, and 3650-foot levels reveal a sharp contact striking east-west and dipping 50°to 70°SE. Ten metres inside the PLP, a relatively massive, unsheared dark porphyritic rock is commonly observed with "crowded" plagioclase and quartz phenocrysts 2 to 3 mm in size. Strain is relatively inhomogeneously distributed and the strong L-fabric plunging 65° southeast is variably developed. The fabric is intensified toward large irregular quartz-carbonate veins associated with increased silicification, white sericitization, and argillic alteration. However, this type of alteration and veining is nowhere seen to be significantly mineralized with respect to either gold or copper.

Outside the main contact is a region with variably oriented tongues and apophyses of PLP from 2 to 6 m in width. These show sharp basal and upper contacts, often slightly oblique to the fabric with a dip of 65°S parallel to the main contact. Such apophyses and lenses extending off the main east-west contact are not zones of "porphyritized" volcanic rocks, and are obviously intrusive in nature.

PRINCIPAL CONCLUSIONS

Despite the difficulty of recognizing different periods of vein generation, due to shearing, and the fact that new generations of material entered old vein channels rather than new fractures, some observations can be made pertinent to vein paragenesis:

1. Early, fabric-parallel quartz-carbonate-tourmaline veins on the 2750-foot level in Hollinger are cut by tourmaline stringers and then by main stage ("95 vein") quartz-carbonate veins. A similar relationship is observed on the 3875-foot level in McIntyre, where the early barren tourmaline set is spatially related to the PLP.
2. Quartz-carbonate-sphalerite veins are observed to cut shallow quartz-carbonate-chalcopyrite veins in the vicinity of the PLP on the 3150-foot level, while some quartz-chalcopyrite (± anhydrite ± K-feldspar) veins are seen to contain tourmaline. This observation suggests that the Cu-(Au) system was contemporaneous with an early barren period in the main Au-(W) system.
3. Late cross-cutting chalcopyrite-bearing quartz-carbonate veins, typical of the sericite zone bear obvious similarities in style, timing, and mineralogy to Au-bearing veins in the Main System. Anhydrite and chalcopyrite are common accessory phases in the Au-(W) veins (e.g. stope 310801), and pyritized selvages are common in both, suggesting some overlap spatially or temporally.
4. Cu-Mo-Au mineralization and the associated alteration haloes *post-date*, to varying degrees, the distinctive L-fabric ubiquitous throughout the central portions of the properties.
5. The main Au-(W) mineralization, although controlled by pre-existing structure, is later than almost all fabric development and earlier folding.

PART 2. CO_2–BEARING, LOW–MODERATE SALINITY FLUIDS IN ARCHEAN GOLD–QUARTZ–CARBONATE–PYRITE–(W–Mo) VEIN DEPOSITS AND MAGMATICALLY DERIVED Mo, W, Ta, AND Sn MINERALIZATION

by P.C. Wood, A.V. Thomas, D.R. Burrows, S.R. Noble, and E.T.C. Spooner

Fluid inclusions in Archean gold-quartz-carbonate-(W-Mo) vein deposits in the Yilgarn block (Australia; Groves *et al.* 1984) and the Superior Province (Canada), are characterized by significant CO_2 contents, low-moderate salinities (1-6 equivalent wt.% NaCl), and moderate total homogenization temperatures of 200° to 400°C. Selected *primary* inclusions in early scheelite, main stage scheelite, and quartz from the Hollinger Mine in the Porcupine Camp, Ontario, indicate the following: (a) CO_2-H_2O phase separation did occur; (b) liquid CO_2 is reasonably pure (CO_2 m.pt. = -56.7 ± 0.7°C, n = 100); (c) salinities determined from clathrate melting points for pure CO_2 vary from 0.4 to 7.7 equivalent wt.% NaCl (4.3 ± 1.8, n = 58); and (d) formation temperatures were equivalent to total homogenization temperatures of 271 ± 47°C (n = 33). The Archean gold data show close similarities in terms of CO_2 content, CO_2 composition, and H_2O salinity to data for fluid inclusions in 4 magmatic systems studied; Boss Mountain Mo, British Columbia; Logtung W-Mo, Yukon Territory; Mink Lake Mo, northwestern Ontario; and Tanco Ta-Sn, southeastern Manitoba. For example, salinities (equivalent wt.% NaCl) are moderate at 5.8 ± 2.3 (n = 98), 4.3 ± 1.4 (n = 95), 5.6 ± 1.2 (n = 48), and 7.5 ± 2.9 (n = 96), respectively. Hence, the properties of Archean gold-quartz-carbonate-(W-Mo) vein fluids are compatible with a magmatic derivation, as is the carbon isotopic composition (Burrows and Spooner 1984b). The similarity between the published ages for the Wawa domal tonalite gneiss granodiorite-quartz-monzonite terrain which intrudes the bases of supracrustal sequences (2707 to 2668 Ma), and the estimated age for late to post-tectonic pluton intrusion and gold mineralization (2700 to 2680 Ma), suggests that components of the former might be possible sources for Archean gold fluids.

(Modified slightly from: Geological Society of America, Abstracts with Programs, Volume 16, p.700, 1984).

PART 3. CARBONATE $\delta^{13}C$ VALUES FOR THE MAIN STAGE OF GOLD–QUARTZ–CARBONATE–PYRITE–SCHEELITE VEIN MINERALIZATION, HOLLINGER MINE

by D.R. Burrows, P.C. Wood, and E.T.C. Spooner

INTRODUCTION

Archean gold-quartz-Fe-carbonate-pyrite ± tourmaline ± tellurides ± W (scheelite) ± Mo vein systems constitute one of the most important types of gold ore deposit. However, their origin is controversial. Genetic hypotheses for the source of the hydrothermal fluid(s) which transported and deposited the gold and associated minerals include greenschist-amphibolite facies metamorphic dehydration and decarbonation reactions (Kerrich and Fyfe 1981; Groves *et al.* 1984), granulite facies metamorphic processes (Fyon *et al.* 1984), and igneous intrusions related to domal tonalite gneiss-granodiorite-quartz-monzonite-type material which intrudes the lower parts of Archean greenstone belts (Wood *et al.* 1984). We discuss here $\delta^{13}C$ (PDB) values for carbonate associated with Au mineralization in Hollinger, carbonate from 14 other Au mineralized locations in the Timmins area (Fyon *et al.* 1983), and magmatically derived carbonate associated with MoS_2 mineralization in the Mink Lake sodic granodiorite stock, northwestern Ontario (Burrows 1984) (Table 236.1).

SAMPLING

The carbon isotopic composition of carbonate in the Hollinger deposit has been determined as a source tracer by analysis of 14 samples for which the data are given in Table 236.1 and Figure 236.3. The samples are equally divided between vein and metasomatic wall rock carbonate, and were selected to be vertically and laterally representative of the

TABLE 236.1. δ^{13}C VALUES FOR CARBONATE ASSOCIATED WITH Au-QUARTZ-Fe-CARBONATE-PYRITE-SCHEELITE VEIN MINERALIZATION, HOLLINGER MINE, TIMMINS, N. ONTARIO.

Sample Number	Sample Description	δ^{13}C (‰; PDB)
33P-S342 (v)	Vein in volcanic fragmental unit. N.E. end of 33 pit. N. part of deposit.	−3.8
33P-S342 (w)	Wallrock; as above	−3.7; −3.6
55P-S330 (v)	Vein in mafic flow (no. 99). S.W. end of 55 pit. S. part of deposit.	−1.0
55P-2 (w)	Wallrock; as above	−0.9; −1.2
4-S124 (v)	Vein in strained Pearl Lake porphyritic intrusion. 425′ level. N.E. part of deposit.	−1.8; −2.0
4-S130 (w)	Wallrock in mafic volcanic (M1). 425′ level. S.W. part of deposit.	−4.1; −4.0
8-S310 (v)	Vein in mafic volcanic. 800′ level. S.W. part of deposit.	−0.1; −0.1
8-S310 (w)	Wallrock; as above	−2.2; −2.2
12-S166 (v)	Vein in strained Pearl Lake porphyritic intrusion. 1250′ level. N.E. part of deposit.	−3.3; −3.4
15-22 (w)	Wallrock in strained Millerton porphyritic intrusion. 1550′ level. S.W. part of deposit.	−4.3; −4.3
18-83-01 (v)	Vein in strained Millerton porphyritic intrusion. 1850′ level. S.W. part of deposit.	−5.0; −4.6
18-16 (w)	Wallrock; as above.	−4.6
27-S158 (v)	Vein in strained Millerton porphyritic intrusion. 2750′ level. Central part of deposit.	−4.5; −4.2
27-S155b (w)	Wallrock in strained Millerton porphyritic intrusion. 2700′ level. S.W. part of deposit.	−2.8; −2.7
$\bar{x}$		−3.0
s		±1.5

δ^{13}C analyses were carried out at the Isotope Lab., Department of Earth Sciences, University of Waterloo, Waterloo, Ontario, Canada N2L 3G1 by standard techniques. The estimated routine uncertainty is ± 0.2‰(1σ). Precision, as defined by the mean average deviation (Skoog and West 1962) for the 11 duplicates analysed in this study, is ± 0.1‰(=±3.1%). Samples from the high grade core zone of the Hollinger deposit were very difficult to collect because of inaccessible collapsed workings. One sample (27-S158-v) was obtained. Most samples come from the S.W., N.E., S., and N. parts of the deposit.

deposit. Hence, samples were obtained from the 33 and 55 pits at surface, and the 425-foot, 800-foot, 1250-foot, 1550-foot, 1850-foot, and 2750-foot levels underground. Sampling below the 2750-foot level was not possible since the lower levels, which extend down to 5450 feet, were no longer accessible. Lateral sample positions on the different levels were variable (Table 236.1). Host lithologies are either strained mafic flows or strained porphyritic intrusions (Table 236.1).

δ^{13}C VALUES FOR CARBONATE IN HOLLINGER AND OTHER Au MINERALIZED LOCATIONS IN THE TIMMINS AREA

The δ^{13}C values define a range of 4.7‰ from -4.8‰ to -0.1‰, and an arithmetic mean of -3.0 ± 1.5‰. Data for vein and wall-rock alteration carbonate are identical, according to a Kolmogorov-Smirnov statistical testing procedure discussed below (*see* Table 236.2), at -2.8 ± 1.8‰ and -3.2 ± 1.3‰, an observation consistent with the 2 being cogenetic. The histogram in Figure 236.3 shows that the Hollinger data are characterized by a marked positive skewness and, consequently, a mode of -4.3‰ significantly lower than the arithmetic mean. Thirty previous carbonate δ^{13}C determinations for the Hollinger system define a higher arithmetic mean of -0.6 ± 0.5‰ and a range from -1.5‰ to +0.3‰ (Fyon *et al.* 1983). The latter overlaps the top end of the range defined in this study. The samples were obtained from just 2 pits at surface (55 and 68) and have been described as coming from "stratabound pyritic 'flow-ore', and stratiform pyritic graphitic units" (Fyon *et al.* 1982), which are not the major ore types in the Hollinger

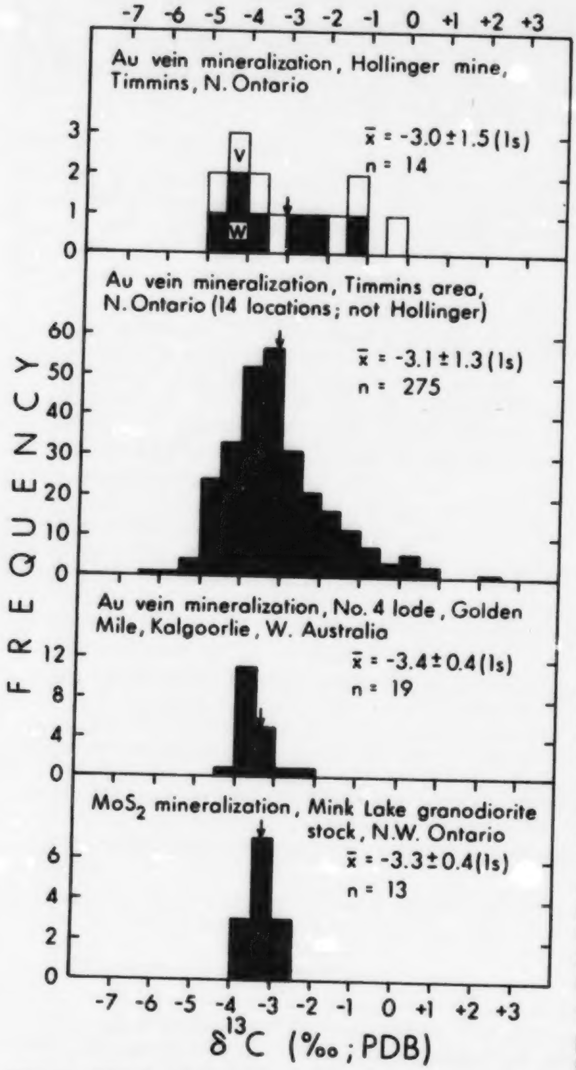

Figure 236.3. *Histograms of the carbonate $\delta^{13}C$ data. The histogram and statistics for the 14 Au mineralized locations in the Timmins area (Fyon et al. 1983) do not include the data for Hollinger or Hallnor because of the presence of graphitic interflow sediments in the sampled area. As suggested by Fyon et al. (1983) such material could modify $\delta^{13}C$ values. Data for the Number 4 lode, Golden Mile, Kalgoorlie, W. Australia are from Golding and Wilson (1983). 'v' denotes vein material and 'w' altered wallrock. Arrows denote arithmetic means.*

Deposit. This study contains data for 2 samples from the 55 pit (Table 236.1). They are relatively high at -1.1‰ and -1.0‰, and are thus quite consistent with the determinations in the previous study (Fyon *et al.* 1983). It appears, therefore, that the previous data were obtained from samples which were unrepresentative of the system as a whole. On the other hand, 275 values for a further 14 Au mineralized locations in the Timmins area (Fyon *et al.* 1983; e.g. Aunor, Buffalo Ankerite, and Delnite Mines, but data for Hallnor not included because of the presence of graphitic interflow sediments which could modify the $\delta^{13}C$ values) define a range and arithmetic mean which are very similar to the new Hollinger data: -6.1‰ to +0.8‰ with an outlier at +2.2‰ compare, -4.8‰ to -0.1‰ (Hollinger), and -3.1 ± 1.3‰ compare, -3.0 ± 1.5‰ (Hollinger). As the histogram in Figure 236.3 shows, the data for the 14 other Au mineralized localities in the Timmins area are also asymmetrically distributed with a distinct positive skewness. A χ^2 test confirms that the data are not normally distributed ($X^2_{calculated}$ (=64.3) $>\chi^2_{0.05;9}$ (=16.9)) and that, therefore, parametric statistical significance tests cannot be used. Hence, a two-tailed Kolmogorov-Smirnov test (Siegel 1956; Till 1974) was used to test the hypothesis that the new Hollinger sample and the sample for the 14 Timmins area Au locations are the same (*see* bottom of Table 236.2 for procedural details). A Kolmogorov-Smirnov test was chosen because it is sensitive to any kind of difference in the distributions from which 2 samples have been drawn. As the calculated and critical Kolmogorov-Smirnov D statistics given in Table 236.2 show, the above hypothesis can indeed be accepted at greater than the 5% significance level.

COMPARISON WITH $\delta^{13}C$ VALUES OF MAGMATICALLY DERIVED CARBONATE ASSOCIATED WITH MoS_2 MINERALIZATION, MINK LAKE GRANODIORITE INTRUSION, NORTHWESTERN ONTARIO

The $\delta^{13}C$ values for the pooled data (new Hollinger plus 14 selected Timmins area Au locations; arithmetic mean ± 1s = -3.1 ± 1.3‰, n = 289) may be compared with $\delta^{13}C$ values for magmatically derived carbonate associated with MoS_2 mineralization in the Mink Lake granodiorite stock, northwestern Ontario. This 1.5 by 3.25 km stock located 110 km northeast of Red Lake is an unmetamorphosed, completely post-tectonic intrusion in the Archean Uchi Belt (Burrows 1984). It is a sodic granodiorite in composition (SiO_2= 65 to 71%; Na_2O/K_2O = 1.6 to 3.2), and contains a 350 by 1000 m zone of MoS_2 mineralization and associated carbonate metasomatism completely enclosed within its southern end. Carbonate alteration zones occur as symmetrically developed selvages adjacent to aplite (SiO_2= 75 to 76%) and quartz-carbonate-K-feldspar-chlorite-pyrite veins, both of which contain MoS_2, and as larger, but localized, subhorizontal, tabular zones up to 3 m in width, also containing MoS_2, but lacking obvious internal veins. In the carbonate alteration zones biotite is completely replaced by Fe-chlorite ± talc, and then by calcite, Mg-chlorite, rutile, and pyrite. Plagioclase feldspar is replaced by albite, muscovite, and calcite (Burrows 1984). The MoS_2 mineralization and carbonate alter-

TABLE 236.2. CALCULATED AND CRITICAL KOLMOGOROV-SMIRNOV D STATISTICS.

Test	Calculated Kolmogorov-Smirnov D Statistic	Critical Kolmogorov-Smirnov D statistic for two-tailed tests at the 5% significance level.	Accept/reject hypothesis that there is no significant difference between the two samples.
Vein cf. wallrock carbonate $\delta^{13}C$, Hollinger mine Timmins, N. Ontario	0.28	0.86 (small sample value)	Accept
Pooled Hollinger cf. Timmins area carbonate $\delta^{13}C$	0.174	0.373 (large sample value)	Accept
Pooled Hollinger plus Timmins area carbonate cf. Mink Lake stock MoS_2 associated carbonate $\delta^{13}C$	0.267	0.386 (large sample value)	Accept
Pooled Hollinger plus Timmins area cf. No.4 lode Golden Mile, W. Australia carbonate $\delta^{13}C$	0.273	0.322 (large sample value)	Accept
No.4 lode, Golden Mile, W. Australia carbonate cf. Mink Lake stock MoS_2 associated carbonate $\delta^{13}C$	0.401	0.474 (small sample value)	Accept

The Kolmogorov-Smirnov D statistic is defined as the largest difference in relative frequency for a given class, between two samples. The hypothesis that there is no difference between two samples at a chosen level of significance is accepted if D calculated $<D_{critical}$. Two-tailed tests are used in this study since there is no reason to suppose that the mean of one sample should necessarily be greater than the mean of the other. For small samples (<40), Figure 7.3 of Till (1974) is used to obtain values for $D_{critical}$. The procedure for small samples is only valid if the numbers of determinations per sample are equal (Siegel 1956; Till 1974). For the comparison of vein and wallrock carbonate $\delta^{13}C$ from Hollinger this requirement does not present a problem (*see* Table 236.1). For the comparison of carbonate $\delta^{13}C$ values for No.4 lode, Golden Mile and the Mink Lake stock, however, the numbers of available values are unequal. Hence, the number of Mink Lake values was adjusted to the number of No.4 lode, Golden Mile values (19). For large samples, at the 5% significance level and for two-tailed tests, $D_{critical} = 1.36\ [(n_1 + n_2)/n_1 \cdot n_2]^{1/2}$, where n_1 and n_2 are the numbers of values in the two samples being compared.

ation are considered to be magmatically derived for the following reasons (Burrows 1984):

1. They are related directly to an observable silicate melt-hydrothermal fluid(s) transition since MoS_2 and carbonate occur in, and carbonate occurs adjacent to, aplite veins of granitic composition which represent late melt, as well as quartz-dominated hydrothermal veins.
2. Hydrothermal fluids trapped in 5 μm to 20 μm fluid inclusions are CO_2 rich, and show low aqueous phase salinities of 5.6 ± 1.2 equivalent wt.% NaCl (n = 48, Burrows and Spooner 1984a), which are characteristics of fluids shown to be magmatic in other cases (e.g. Boss Mountain Mo deposit, British Columbia, Macdonald 1983; Tanco Ta(-Sn) granitic pegmatite, southeastern Manitoba, Thomas 1985).
3. The δD and $\delta^{18}O$ characteristics measured and calculated for the hydrothermal fluid are consistent with a magmatic origin (Burrows 1984).
4. The mineralized zone occurs completely enclosed within the stock with no obvious external connections.
5. The mineralized zone developed marginal to an internal region of fractional crystallization, as shown by TiO_2, Zr, Li, Rb, and Sr variations for 47 samples from the stock.
6. The aplites, the compositions of which are compatible with derivation by fractional crystallization, are geochemically enriched in Mo, thus confirming a magmatic link with the MoS_2 mineralization (Burrows 1984).

Thirteen $\delta^{13}C$ determinations for Mink Lake carbonate from various associations define a very narrow range of 1.2‰ from -3.9‰ to -2.7‰, which is completely enclosed in the pooled Timmins area Au locality range of -6.1‰ to +0.8‰ with an outlier at +2.2‰. More importantly, the modal classes of the 2 data sets are exactly the same (-3.5‰ to -3.0‰, Figure 236.3) and the arithmetic means differ by only 0.2‰ (-3.3 ± 0.4‰ for Mink Lake, compare -3.1 ± 1.3‰). The latter is an unusual result since analytical uncertainty is estimated to be ± 0.2‰ (1σ). A two-tailed Kolmogorov-Smirnov test confirms that the pooled Timmins area Au location carbonate δ^{13}C sample, and the Mink Lake stock carbonate δ^{13}C sample, are drawn from the same population, at greater than the 5% significance level (Table 236.2). Therefore, since the carbonate in the Archean Mink Lake stock is magmatically derived, it can be concluded that the identical δ^{13}C values for the carbonate associated with the Archean Au mineralization in the Timmins area, are compatible with a magmatic derivation (Burrows and Spooner 1984b). At this stage it is important to use the word compatible, since it is possible that the carbon isotope ratios could also be compatible with as yet undefined carbonate δ^{13}C values characteristic of a different source, or sources; a possibility which is currently being investigated. However, for any other carbon isotope similarity to be relevant, it will have to show the same degree of statistical exactitude.

COMPARISON WITH δ^{13}C VALUES OF CARBONATE ASSOCIATED WITH Au MINERALIZATION, GOLDEN MILE, KALGOORLIE, WESTERN AUSTRALIA

This result may have broader applicability. The 1.2 by 3 km set of ~300 lodes, which constitutes the Golden Mile in the Norseman-Wiluna greenstone belt in the Archean Yilgarn block of Western Australia, is probably the largest known Archean gold-quartz-Fe-carbonate-pyrite ± tourmaline ± tellurides ± W (scheelite) ± Mo system in the world, since it has produced ~1200 tonnes Au (Travis *et al.* 1971; Lambert *et al.* 1984; compare total Hollinger system at 994.7 tonnes Au). Mineralization is similar to Hollinger in that it consists of quartz-Fe-carbonate-muscovite-pyrite altered wall rocks which post-date folding and regional metamorphism. The mineralization is related to narrow, siliceous shears and fractures (Golding and Wilson 1983). Of the gold, ~80% is associated with subhedral pyrite in altered wall rock, and ~20% occurs as tellurides. The important point is that the carbon isotopic composition of the associated Fe-carbonate of -3.4 ± 0.4‰(Figure 236.3), as defined by 19 determinations from 2 traverses of the Number 4 lode (DDH 5027 and DDH 5022; Golding and Wilson 1983), is closely similar to that of the pooled Timmins area Au locations (-3.1 ± 1.3‰), and exceptionally similar to the Mink Lake stock MoS_2 associated carbonate (-3.3 ± 0.4‰). Two-tailed Kolmogorov-Smirnov tests confirm that all the data are drawn from the same population at greater than the 5% significance level (Table 236.2). Hence, the Number 4 lode, Golden Mile δ^{13}C data are also compatible with a magmatic derivation.

PRINCIPAL CONCLUSION

The remarkable similarity in carbonate δ^{13}C values between Timmins area and Golden Mile Archean Au mineralization, on the one hand, and Mink Lake intrusion MoS_2 mineralization, on the other, as shown by a range in arithmetic means of only 0.3‰, suggests that Archean gold-quartz-Fe-carbonate-pyrite ± tourmaline ± tellurides ± W (scheelite) ± Mo vein mineralization could be magmatically derived.

This conclusion provides support for Wood's *et al.* (1984) hypothesis that the relevant fluids were derived from igneous intrusions related to domal tonalite gneiss-granodiorite-quartz-monzonite-type material which intrudes the lower parts of Archean greenstone belts.

PART 4. +3.5 ± 1.4‰ δ^{34}S (n = 33) FOR PYRITE ASSOCIATED WITH MAIN STAGE GOLD–QUARTZ–Fe–CARBONATE–PYRITE–SCHEELITE VEIN MINERALIZATION, HOLLINGER DEPOSIT

by P.C. Wood, D.R. Burrows, and E.T.C. Spooner

THE RELATIONSHIP BETWEEN Au AND PYRITE; PETROLOGICAL AND ANALYTICAL SCANNING ELECTRON MICROSCOPE OBSERVATIONS

Pyrite and gold are remarkably closely related in the Hollinger mineralization, as discussed below. Hence, any points which can be deduced from the properties of the pyrite would have a direct bearing on the gold. The first point to make is that it has been estimated from assay data that ~95% of the gold in the Hollinger Deposit occurred in mineralized wall rock, whereas only ~5% of the total gold is estimated to have occurred in the quartz-dominated vein system to which mineralized wall rock is spatially related. Hence, detailed petrological studies have been carried out on gold distribution in relatively high grade mineralized wall rock samples from the 1, 33, 55, and 400 pits at surface. The geometrical properties of a total of 342 separate gold particles have been determined using a scheme developed by D. Carson and J.E. Farr (Noranda Exploration Company Limited). As shown in Photo 236.1, the gold typically occurs as discrete particles, with rounded outlines, which vary from simple ellipsoidal to quite complicated shapes. Cross-sectional dimensions measured in two-dimensional polished sections, which are underestimates of the particle "diameters" in 3 dimensions, show a mode at ~7 μm, and a higher arithmetic mean of 12 ± 12 μm reflecting a strongly positively skewed distribution (Figure 236.4). The cross-sectional dimensions vary from < 1 μm to as much as ~250 μm. Very approximate *volume* % gold values have been calculated from the data for the 342 grains.

The most important point is that the figure for volume % of gold directly associated with pyrite is large at 97.1% (Figure 236.5). Of this figure, 80.5 volume % quite specifically occurs in the outer zones of pyrite grains, 11.1 volume % in the mid-zones, 2.9 volume % at the boundaries of pyrite grains, 2.3 volume % clearly filling fractures, and 0.3 volume % in pyrite core zones. Of the 2.9 volume % of gold which is not associated with pyrite in some way, only

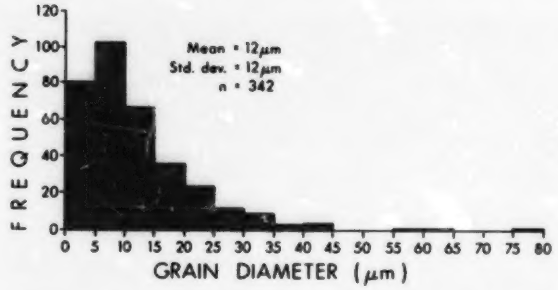

Figure 236.4. *Histogram of gold particle size distribution measured from grain "diameters" on polished sections.*

1.8 volume % occurs isolated in silicate and carbonate gangue minerals, and 1.1 volume % is associated with arsenopyrite.

The cogenetic nature of pyrite and gold is further emphasized by the discovery of submicron-sized pyrite particles within gold grains, by high resolution, back-scattered, electron imagery and energy dispersive electon probe microanalysis. For example, an ~6 µm by ~13 µm gold flake is shown in Photo 236.2, a back-scattered electron image taken on the JEOL JSM 840 in the Department of Geology, University of Toronto, in which intensity is related to mean atomic number. Within the gold flake can be seen at least 20 "dark" particles with cross-sectional dimensions of < 1 µm, and down to at least 0.1 µm. That these "dark" inclusions are predominantly pyrite is shown by the 2 energy dispersive probe spectra shown in Figure 236.6. One spectrum is derived from a gold-dominated area and shows subsidiary silver peaks, whereas the other is for a dark particle enclosed in gold. It shows an Fe peak (labelled) which is absent from the gold-only spectrum, thus confirming the presence of pyrite. The pyrite-sulphur peak cannot be distinguished from the Au peak.

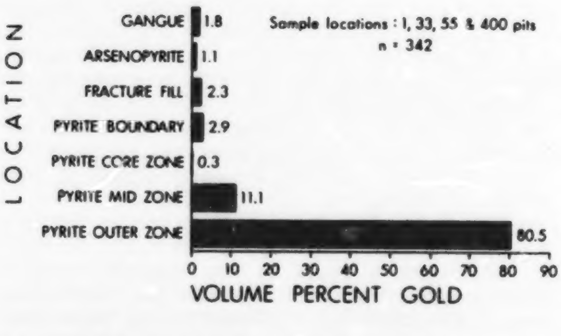

Figure 236.5. *Histogram indicating location and mode of occurrence of microscopic gold particles within altered wallrock material from 1, 33, 55, and 400 pits, Hollinger (Timmins) mine.*

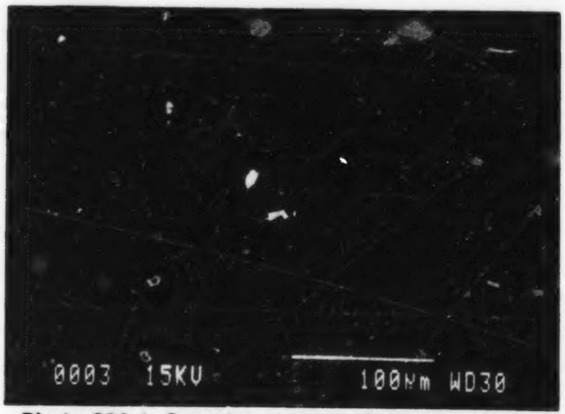

Photo 236.1. *Scanning electron photomicrograph in composition mode (back scattered electron image) indicating the occurrence of gold in altered wallrock pyrite grains. Chalcopyrite (Cp), pyrite (Py) and sphalerite (Sp) are also indicated.*

δ^{34}S VALUES FOR PYRITE IN THE HOLLINGER DEPOSIT

The sulphur isotopic composition of the pyrite associated with the gold in the Hollinger Deposit has been determined as a source tracer by analysis of 33 samples, 23 from mineralized wall rocks and 10 from veins. Data are given in Table 236.3 and Figure 236.7. The δ^{34}S values of mineralized wall rocks immediately adjacent to the 10 veins have been specifically determined and the differences between the vein/wall-rock pairs are tabulated (Table 236.3). The samples were selected to be vertically and laterally representative of the deposit. Hence, samples were chosen from the 1, 33, 55, and 400 pits at surface, and from the 425-foot, 800-foot, 1250-foot, 1550-foot, 1700-foot, 1850-foot, and 2750-foot levels underground. Sampling below the 2750-foot level was not possible since the lower levels, which extend down to 5450 feet, were no longer accessible. Lateral sample positions on the different levels relative to the main mineralized zone were variable (Table 236.3). Samples from the core zone of the Hollinger Deposit were very difficult to collect because of inaccessible collapsed workings. Data for 3 samples were obtained, however (12-S299 (W) and 17-S123 (V and W)). The other samples came from the southwestern, northern, northwestern, northeastern, and southern parts of the deposit. Host lithologies are strained mafic and ultramafic flows and fragmentals, and porphyritic intrusions (Table 236.3). Pyrite grains were separated from each sample under a microscope to ensure purity. Detailed reflected light petrography indicates that most pyrite grains contain minor (≤ 5%) amounts of sphalerite, chalcopyrite, pyrrhotite, galena, and rare arsenopyrite and, thus, that the analyses are for bulk sulphide sulphur. Sulphur isotope analyses were carried out at McMaster University on SO_2 gas obtained by direct burning of pyrite, as described by Thode and Rees

(1971) and Rees (1978). Analytical uncertainty is estimated to be ± 0.2‰.

The $\delta^{34}S$ values define a range of 7.7‰ from -0.7‰ to +7.0‰ and an arithmetic mean of +3.5 ± 1.4‰ (1s; Table 236.3). The histogram in Figure 236.7 shows that the data are more or less symmetrically distributed, with the arithmetic mean occurring in the principal modal class interval of +3.5‰ to +4.0‰. The data show a very strong central tendency with 64% of the values concentrated in the central 3 class intervals. However, the data also contain a small number of values with quite marked negative (-0.7‰) and positive (+7.0‰)deviations, which show no obvious correlations with host-rock lithology or spatial location (Table 236.3).

STATISTICAL SIGNIFICANCE TESTING OF VEIN COMPARED WITH WALL ROCK, AND DEEP COMPARED WITH SHALLOW $\delta^{34}S$ VALUES

Despite the approximate symmetry shown by the distribution of the values (Figure 236.7), a χ^2 test shows that the data are not normally distributed since $X^2_{calculated}$ (= 10.3) > $\chi^2_{0.05;2}$(= 6.0). Hence, parametric methods cannot be used in significance testing. In this study, Kolmogorov-Smirnov tests could not be used since the number of values in the samples to be compared were < 40 and significantly unequal (Till 1974). Hence, Mann-Whitney U tests, which depend on comparison of rank values, were applied. Mann-Whitney U tests compare the central tendencies of samples rather than the shapes of total distributions, as do Kolmogorov-Smirnov tests (Till 1974). The procedure for carrying out Mann-Whitney U tests is described by Siegel (1956).

Vein and wall rock $\delta^{34}S$ values can be compared to test whether or not they are drawn from the same population, since the arithmetic means are quite similar at +3.0 ± 1.9‰ (veins; n = 10) and +3.7 ± 1.2‰ (wall rocks; n = 23). Since the number of values in the larger sample is > 20, probability values are obtained from those of a normal distribution (Table A, *in* Siegel 1956). A two-tailed test was used since there is no reason to suppose that the bulk of one sample should necessarily be greater than the bulk of the other. The computed Mann-Whitney U statistic of 103.5 gives a high probability (62%) that the vein and wall rock $\delta^{34}S$ samples are the same; a result consistent with the two being cogenetic.

The $\delta^{34}S$ values for deep (17 and below) and shallow (12 and above) levels can also be compared to test whether or not there is a vertical trend, which appears to be unlikely since the arithmetic means are similar at +3.4 ± 1.1‰ (n = 12) and +4.1 ± 1.1‰ (n = 11), respectively. In this case, the number of values in the larger sample is between 9 and 20 and critical U values are obtained from Table K *in* Siegel (1956). The computed Mann-Whitney U statistic of 53.5 is greater than the critical U value of 38, confirming that there is no vertical difference at greater than the 10% significance level.

0007 15kV
1μm WD30

Photo 236.2. *Back scattered electron image of gold bleb containing numerous small inclusions, some of which have been identified as pyrite (see Figure 236.6).*

COMPARISON OF TOTAL $\delta^{34}S$ VARIANCE WITH VARIANCE BETWEEN VEIN AND ADJACENT WALL ROCK $\delta^{34}S$ VALUES

It can be seen from the data in Table 236.3 (column 4) that the differences between vein and immediately adjacent wall-rock pyrite $\delta^{34}S$ values are typically smaller than the total range of 7.7‰. For the 10 pairs, 4 differences are < ± 0.2‰, the estimated analytical uncertainty, and 5 more are ≤ 1.5‰. The tenth is large; at 4.8‰ it is 3 times greater than the next highest value. This qualitative observation raises the question of whether or not the variability between paired vein and wall-rock samples is less than the overall variability. The reason this question is important relates to the interpretation of fluid inclusion results. The problem is that the bulk of the gold (~95%) occurs in mineralized wall rock, as mentioned above, whereas fluid inclusion observations are only possible on vein materials. Definite linkage between vein fluid inclusion properties and the bulk of the gold is, therefore, difficult to prove unequivocally. General linkage of vein and wall-rock phenomena is obvious on the basis of geological observations and the significance testing described above between vein and wall-rock $\delta^{13}C$ and $\delta^{34}S$ values. However, one would like to be as sure as possible that the thermal and chemical properties determined for the fluid(s) trapped in the vein materials are precisely those of the hydrothermal fluid(s) which transported and deposited the large amount of gold which constitutes the Hollinger Deposit. Hence, if there were any line of evidence to link immediately adjacent vein and wall-rock properties, on the scale of centimetres, it would be very important since it would suggest that vein and wall-rock phenomena were quite specifically associated on a scale 5 orders of magnitude less than that of the deposit as a whole, and hence, that fluid inclusion properties determined for vein material might be applicable to immediately adjacent Au mineralization. The statistical procedure adopted is to calculate the ratio of the variance of the total data set (σ^2_T) to the average variance between paired vein and wall-rock values

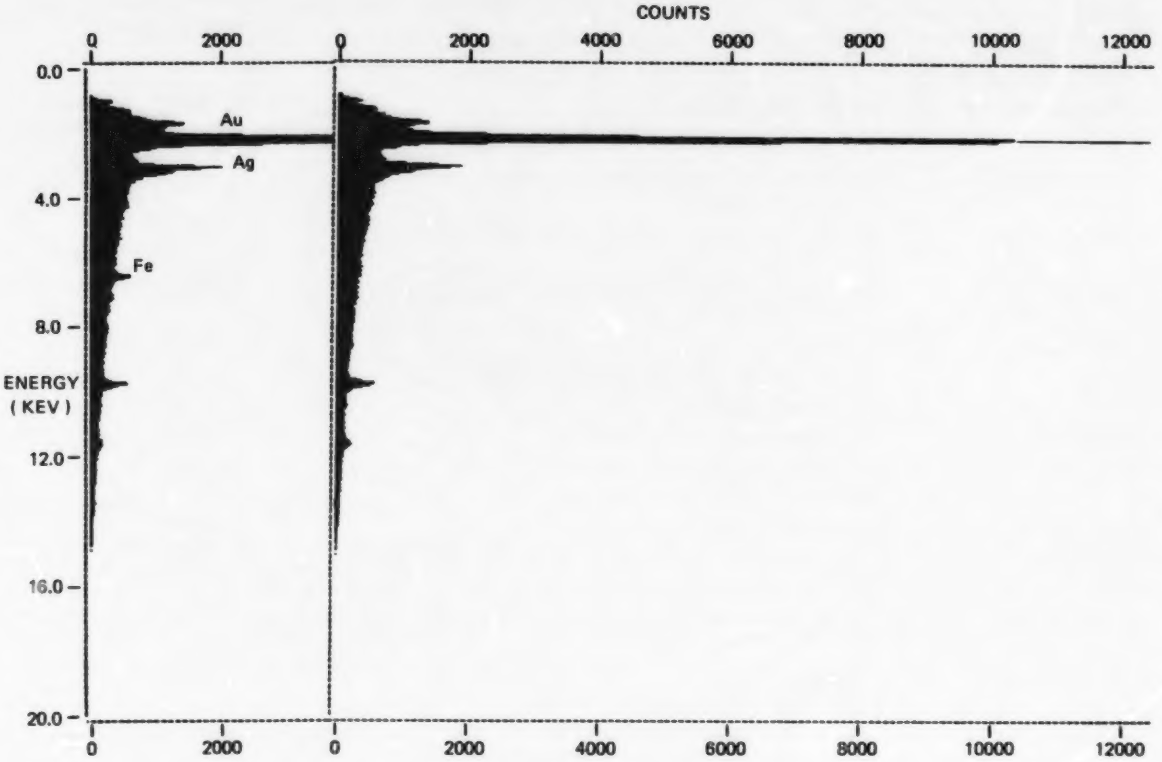

Figure 236.6. *Energy dispersive spectra from a pyrite inclusion in a gold bleb (on left) showing a small Fe peak (labelled) which is absent from the gold-only spectrum (on right). The peaks for Au and Ag are also indicated.*

(σ^2_{vw}), and to compare the ratio with the value for Fishers F statistic with N-1 and N degrees of freedom, where N is the number of pairs, at the 95% confidence level (modified from Garrett 1973). In strict terms, this form of test is not valid since the data cannot be assumed to be normally distributed. In fact, as discussed above, the complete data set does not conform to a normal distribution. However, there is apparently no non-parametric equivalent of this comparison of variances (Dr. A.P. Soms, Department of Statistics, University of Toronto, May, 1985, personal communication). Hence, the procedure used below can be used as an *assessment* of the problem rather than an exact test.

σ^2_T is simply the variance of the combined data for which vein/wall-rock pairs exist.

σ^2_{vw} is given by:

$$\sigma^2_{vw} = \frac{1}{2N} \sum_{i=1}^{N} \left(x_{vi} - x_{wi}\right)^2$$

where (x_{vi} - x_{wi}) is the difference between the ith δ^{34}S values for vein and adjacent wall-rock samples.

Fishers F statistic for 10 pairs at the 95% confidence level is 2.5, as derived from Figure 1 of Garrett (1973). Clearly, the larger the ratio of σ^2_T to σ^2_{vw}, the greater the variability of the total data set compared with the variability between pairs. Accordingly, if $\sigma^2_T/\sigma^2_{vw} > 2.5$, the hypothesis that the variability of the total data set is greater than the variability between vein/wall-rock pairs can be accepted at the 95% confidence level.

If all the pairs are considered, the result is $\sigma^2_T/\sigma^2_{vw} = 1.6$, which is close to but less than 2.5, and the hypothesis cannot be accepted at the 95% confidence level. However, the average variance between vein and wall-rock pairs (σ^2_{vw}) is very strongly influenced by a single value, the difference of -4.8‰ (pair 15-55, Table 236.3). In fact, the value of $(x_v - x_w)^2$ for this pair constitutes 80% of σ^2_{vw}. If this difference is then omitted as a statistical outlier, $\sigma^2_T/\sigma^2_{vw} = 5.20$, which is greater than twice the value of $F_{CRIT}(2.5)$, and the hypothesis can be accepted.

In geological terms, this finding means that in 9 cases out of 10 the variability between vein and adjacent wall rock δ^{34}S values is less than the total variability, at greater than the 95% confidence level, but that in 1 case out of 10 the relationship is perturbed. For natural processes a frequency of 9 out of 10 is high. An alternative is to consider all the data and to phrase the outcome at a reduced confidence level. Precise figures are not given in Garrett (1973). However, an approximate estimate for the confidence level to consider a σ^2_T/σ^2_{vw} value of 1.6 (all data; see above) to be significant would be the 80th.

TABLE 236.3. $\delta^{34}S$ VALUES FOR PYRITE ASSOCIATED WITH Au-QUARTZ-Fe-CARBONATE-PYRITE-SCHEELITE VEIN MINERALIZATION, HOLLINGER (TIMMINS) MINE, TIMMINS, N. ONTARIO.

Sample Number	Sample Description	$\delta^{34}S$ (‰;CDT)	$\delta^{34}S$ vein - $\delta^{34}S$ wallrock
1P-S 346 (w)	Mineralized wallrock in mafic volcanic: E. end of 1 pit; S.W. part of deposit	+3.7	
33P-S 342 (w)	Mineralized wallrock in flow top breccia; N.E. corner of 33 pit; N. part of deposit	+3.6	
55-1-W1	Mineralized wallrock in mafic flow (no.99); W. end of 55 pit; S. part of deposit	+3.4	
55-1-W2	As above	+3.6	
400-2-V	Vein in altered ultramafic flow; S.W. end of 400 pit; N.W. part of deposit	+3.6	0
400-2-W	Mineralized wallrock as above	+3.6	
4-S128(V)	Vein in Pearl Lake porphyritic intrusion; 425′ level-53E13; N.E. part of deposit	+3.0	-1.5
4-S128(W)	Mineralized wallrock as above	+4.5	
8-S305(W)	Mineralized wallrock in altered ultramafic flow; 800′ level-2W7; S.W. part of deposit	+7.0	
12-S133(w)	Mineralized wallrock in mafic volcanic; 1250′ level-7E10; N. part of deposit	+4.2	
12-S299(W)	Mineralized wallrock in mafic volcanic; 1250′ level-50E10; central part of deposit	+5.2	
15-26-V	Vein in Millerton porphyritic intrusion; 1550′ level-15-08-01 stope; S.W. part of deposit	+4.1	0
15-26-W	Mineralized wallrock as above	+4.1	
15-33-V	Vein as above	+4.2	+0.8
15-33-W	Mineralized wallrock as above	+3.4	
15-55-V	Vein as above	-0.7	-4.8
15-55-W	Mineralized wallrock as above	+4.1	
15-58-V	Vein as above	+4.7	+0.1
15-58-W	Mineralized wallrock as above	+4.6	
15-61-V	Vein as above	+0.7	-0.7
15-61-W	Mineralized wallrock as above	+1.4	
17-S012 (V)	Vein in Millerton porphyritic intrusion; 1700′ level-15 NHW7; S.W. part of deposit	+5.2	+1.5
17-S123 (V)	Vein in mafic volcanic; 1700′ level - 55AEM4; central part of deposit	+3.8	-0.2
17-S123 (W)	Mineralized wallrock as above	+4.0	

TABLE 236.3 cont'd

Sample Number	Sample Description	$\delta^{34}S$ (‰;CDT)	$\delta^{34}S$ vein - $\delta^{34}S$ wallrock
18-16-W	Mineralized wallrock in Millerton porphyritic intrusion; 1850' level- 18-83-01 stope; S.W. part of deposit	+4.3	
18-20-W	As above	+3.1	
18-23-W	As above	+1.4	
18-29-W	As above	+3.7	
18-100-W	As above	+3.7	
18-83-09a (V)	Vein in mafic volcanic; 1850' level-18-83-09 stope; S.W. part of deposit	+1.8	-0.3
18-83-09a (W)	Mineralized wallrock as above	+2.1	
27-8155a (W)	Mineralized wallrock in Millerton porphyritic intrusion; 2750' - M4XC just before central shaft; S.W. part of deposit	+3.4	
$\bar{x} \pm 1s$	All data (n = 33)	+3.5 ± 1.4	
$\bar{x} \pm 1s$	Vein data (n = 10)	+3.0 ± 1.9	
$\bar{x} \pm 1s$	Mineralized wallrock data (n = 23)	+3.7 ±1.2	

The conclusion that vein and adjacent wall rock $\delta^{34}S$ values are quite specifically linked in at least 9 cases out of 10, constitutes significant supporting evidence that the thermal and chemical properties of ore fluid(s), as derived from fluid inclusions in vein materials, are applicable to adjacent Au mineralized wall rocks.

COMPARISON OF HOLLINGER $\delta^{34}S$ VALUES

1. *Hunt, Morning Star, Mount Charlotte, and Watertank Hill Deposits, Yilgarn Block, Western Australia:*

The Hollinger data are very similar to data for these 4 deposits (Lambert *et al.* 1984) which show a range from +0.7 to +8.0‰ (compare, -0.7 to +7.0‰ for Hollinger), and an arithemtic mean of +3.0 ± 1.3‰ (n = 37), which compares with +3.5 ± 1.4‰ (n = 33) for Hollinger. These Australian deposits are also related to quartz-pyrite vein systems which cross-cut lithologies and fabrics. Hence, the similarity in $\delta^{34}S$ values is very satisfactory.

2. *Other Types of Archean Sulphur:*

Unfortunately, these $\delta^{34}S$ values for Archean gold deposits which cluster around +3.0 to +3.5‰ do not appear to be very obviously useful for distinguishing sulphur sources or depositional processes (Wood *et al.* 1985), since they are similar in a general sense to $\delta^{34}S$ values for various types of Archean sulphur in komatiites (e.g. -0.5 to +3.8‰ for Kambalda, n = 68; Seccombe *et al.* 1981), volcanic-hosted massive sulphide deposits (e.g. -0.1 to +2.3‰ for Quemont, n = 58; Lusk *et al.* 1975), and post-tectonic, granodiorite-hosted MoS_2 mineralization in the Mink Lake stock, northwestern Ontario (+0.4 to +2.9‰; n = 8; Burrows 1984). On the other hand, in detail, there may be a difference which requires further examination and testing, since the sulphur isotopic composition of the sulphur in the 3 examples listed immediately above shows a tendency to be lower than that of the Au associated sulphur. The arithmetic means for Kambalda, Quemont (pyrite), and Mink Lake are quite similar at +2.4 ± 0.8‰, +1.8 ± 0.4‰, and +1.6 ± 0.9‰, respectively, whereas the arithmetic mean for Hollinger is +3.5 ± 1.4‰. Magmatic $\delta^{34}S$ values defined from porphyry copper deposits are typically in the range from -3 to +1‰ (Ohmoto and Rye 1979), whereas $\delta^{34}S$ values for the Climax, Urad-Henderson, and Mount Emmons porphyry MoS_2 deposits in the Colorado mineral belt are quite high at +2.5 to +5.3‰ (Stein and Huebner 1984). Hence, there may be some meaning in these differences of a few per mil which requires further research to work out.

3. *Golden Mile, Kalgoorlie, Western Australia:*

In contrast to the $\delta^{34}S$ values for the Hunt, Morning Star, Mount Charlotte, and Watertank Hill Deposits, Lambert *et al.* (1984) found that $\delta^{34}S$ values for pyrite in the Golden Mile lodes was markedly lower, defining a range from -7.0 to -1.6‰ and an arithmetic

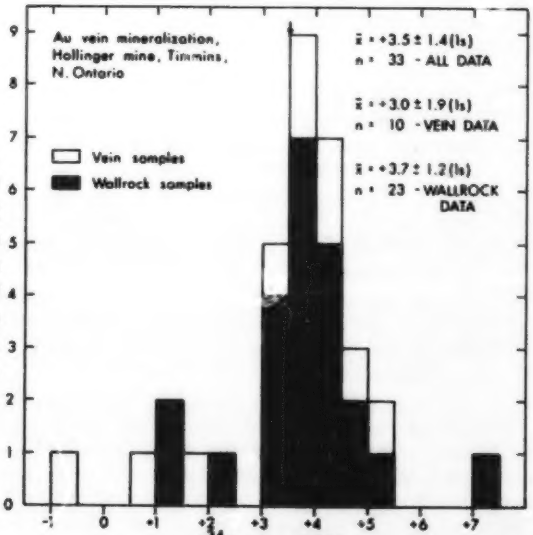

Figure 236.7. Histogram of sulphide $\delta^{34}S$ data for vein and altered wallrock material. Arrow denotes arithmetic mean.

mean of -4.3 ± 1.7‰ (n = 12). Since the Golden Mile is the largest example of Archean gold-quartz-Fe-carbonate-pyrite ± tourmaline ± tellurides ± W (scheelite) ± Mo mineralization known, with production of ~1200 tonnes Au (Lambert *et al.* 1984), they suggested that relatively negative pyrite $\delta^{34}S$ values might indicate potential for unusually large vein Au deposits. Interestingly, Hemlo, which appears to be a very different type of Au deposit than the Golden Mile and Hollinger, is also characterized by relatively negative pyrite $\delta^{34}S$ values down to -17.5‰ (Hattori and Cameron 1985). The Hollinger-McIntyre-Coniaurum-Vipond-Crown-Moneta system as a whole has produced an amount of Au comparable to that from the Golden Mile (end-1984 production = 994.7 tonnes Au, compared to 1200 tonnes). The fact that Hollinger pyrite $\delta^{34}S$ values average +3.5‰, therefore, indicates that Lambert's *et al.* (1984) suggestion is, unfortunately, unlikely to be valid (Wood *et al.* 1985). It is possible, however, that positive $\delta^{34}S$ values might be of no discriminatory use, whereas negative values might still indicate potential for a large Au vein deposit. This possibility is essentially disproved by Schwarcz and Rees' (1984) pyrite $\delta^{34}S$ data for the Canadian Arrow Deposit in the Timmins area, which are characterized by an arithmetic mean of -11.2 ± 1.0‰ (n = 18), since Canadian Arrow contains reserves of only 399 000 tonnes at 3.4 g/tonne Au (Canadian Mines Handbook, 1984-1985).

CONCLUSIONS

1. 97.1 volume % of gold in mineralized wall-rock material in Hollinger (= ~95% of total gold) is directly associated with pyrite.
2. The $\delta^{34}S$ value of the pyrite is +3.5 ± 1.4‰ (n = 33) and shows no vertical variation.
3. The $\delta^{34}S$ values of vein and wall-rock pyrite were drawn from the same population, with a high probability of 62% (Mann-Whitney U non-parametric test).
4. In 9 cases out of 10, the variance between vein and adjacent wall-rock pyrite $\delta^{34}S$ values is less than the total $\delta^{34}S$ variance at greater than the 95% confidence level.
5. Hence, from 4 above, thermal and chemical properties of ore fluid(s), derived from fluid inclusions in vein materials, are applicable to adjacent Au mineralized wall rocks.
6. $\delta^{34}S$ values of ~ +3.0 to +3.5‰ do not appear to be very useful for distinguishing sources or processes involved in the formation of Archean vein gold deposits.
7. The possibility that potential for unusually large Archean vein gold deposits might be recognizable from negative $\delta^{34}S$ values (Lambert *et al.* 1984) appears to be unlikely.

ACKNOWLEDGMENTS

We are extremely grateful to Pamour Porcupine Mines Limited, a member of the Noranda Group, for permission to work in the Hollinger (Timmins) and McIntyre (Schumacher) Mines. We would very much like to thank Mr. W.W. Holmes and Mr. W.M. Longworth for their very generous assistance and encouragement without which this work could not have been done. We would also like to thank Mike Cherry (Ontario Geological Survey), Brian O'Donovan (photographer), Subhash Shanbhag (draftsman) and, particularly, Anne Marie Cooperwhite (secretary) for their help, which we much appreciate. We acknowledge with gratitude the assistance of McMaster University, and the Isotope Laboratory, Department of Earth Sciences, University of Waterloo, where the isotope analyses were carried out. In addition to the Ontario Geoscience Research Fund, this research has been financially supported by the Ontario Geological Survey and the Natural Sciences and Engineering Research Council of Canada (NSERC) (Grant A6114 to E.T.C. Spooner). Finally, the work on the Mink Lake stock and its MoS_2 mineralization, which has turned out to be so important for interpreting the $\delta^{13}C$ and other data, was made possible logistically and financially by Noranda Exploration Company Limited, in particular Mr. W.A. Nash, whom we would like to thank very much indeed.

REFERENCES

Allen, C.C., and Folinsbee, R.E.
1944: Scheelite Related to Porphyry Intrusives, Hollinger Mine; Economic Geology, Volume 39, p.340-348.

Bertoni, C.H.
1983: Gold Production in the Superior Province of the Canadian Shield; Canadian Institute of Mining and Metallurgy, Bulletin, Volume 76, Number 857, p.62-69.

Burrows, D.R.
1984: Geology and Geochemistry of Molybdenite Mineralization within an Archean Granodiorite Intrusion, Mink Lake, N.W. Ontario; Unpublished M.Sc. Thesis, University of Toronto, 262p.

Burrows, D.R., and Spooner, E.T.C.
1984a: Fluid Inclusion Evidence for H_2O-CO_2 Phase Separation Associated with Magmatically Derived MoS_2 Mineralization Within a Post-Tectonic Archean Granodiorite/Trondhjemite Intrusion, Mink Lake, N.W. Ontario (Abstract); p.49 *in* Geological Association of Canada/Mineralogical Association of Canada, Program with Abstracts, May 14-16, 1984, Volume 9, 128p.
1984b: Low $\delta^{13}C$ Carbonate Alteration Associated with Magmatically Derived MoS_2 Mineralization Within a Post-Tectonic Archean Granodiorite/Trondhjemite Intrusion, Mink Lake, N.W. Ontario (Abstract); p.50 *in* Geological Association of Canada/Mineralogical Association of Canada, Program with Abstracts, May 14-16, 1984, Volume 9, 128p.

Davies, J.F., and Lutha, L.E.
1978: An Archean Porphyry Type Disseminated Cu Deposit, Timmins, Ontario; Economic Geology, Volume 73, p.383-396.

Ferguson, S.E.
1968: Geology and Ore Deposits of Tisdale Township; Ontario Department of Mines, Geological Report 58, 177p.

Fyon, J.A., Crocket, J.H., and Schwarcz, H.P.
1983: Ontario Geoscience Research Grant Program, Grant No. 49—Application of Stable Isotope Studies to Gold Metallogeny in the Timmins-Porcupine Camp; Ontario Geological Survey, Open File Report 5464, 182p.

Fyon, J.A., Schwarcz, H.P., and Crocket, J.H.
1984: Carbonatization and Gold Mineralization in the Timmins Area, Abitibi Greenstone Belt: Genetic Links with Archean Mantle CO$_2$—Degassing and Lower Crustal Granulitization; *in* Geological Association of Canada/Mineralogical Association of Canada, Program with Abstracts, London, May 14-16, 1984, Volume 9, 128p.

Fyon, J.A., Schwarcz, H.P., Crocket, J.H., and Knyf, M.
1982: Gold Exploration Potential Using Oxygen, Carbon, and Hydrogen Stable Isotope Systematics of Carbonatized Rock and Quartz Veins, Timmins Area; p.59-64 *in* Geoscience Research Grant Program, Summary of Research 1981-1982, edited by E.G. Pye, Ontario Geological Survey, Miscellaneous Paper 103, 219p.

Garrett, R.G.
1973: The Determination of Sampling and Analytical Errors in Exploration Geochemistry—a Reply; Economic Geology, Volume 68, p.282-283.

Golding, S.W., and Wilson, A.F.
1983: Geochemical and Stable Isotope Studies of the No. 4 Lode, Kalgoorlie, Western Australia; Economic Geology, Volume 78, p.438-450.

Groves, D.I., Phillips, G.N., Ho, S.E., Henderson, C.A., Clark, M.E., and Woad, G.M.
1984: Controls on Distribution of Archean Hydrothermal Gold Deposits in Western Australia; p.689-712 *in* Gold '82—Proceedings of the International Symposium, Zimbabwe, edited by R.P. Foster, A.A. Balkema Publishers, Rotterdam, 753p.

Hattori, K., and Cameron, E.M.
1985: Pyrite of Distinctive Isotopic Composition Associated with the Hemlo Gold Mineralization; p.61-62 *in* Association of Exploration Geochemists, 11th International Geochemical Exploration Symposium, Programme and Abstracts, April 29-May 2, 1985, 105p.

Kerrich, R., and Fyfe, W.S.
1981: The Gold Carbonate Association: Source of CO$_2$, and CO$_2$ Fixation Reactions in Archean Lode Deposits; Chemical Geology, Volume 33, p.265-299.

Lambert, I.B., Phillips, G.N., and Groves, D.I.
1984: Sulphur Isotope Compositions and Genesis of Archean Gold Mineralization, Australia and Zimbabwe; p.373-387 *in* Gold '82—Proceedings of the International Symposium, Zimbabwe, edited by R.P. Foster, A.A. Balkema Publishers, Rotterdam, 753p.

Lusk, J., Campbell, F.A., and Krouse, H.R.
1975: Application of Sphalerite Geobarometry and Sulfur Isotope Geothermometry to Ores of the Quemont Mine, Noranda, Quebec; Economic Geology, Volume 70, p.1073-1083.

Macdonald, A.J.
1983: Boss Mountain Molybdenite Deposit: Fluid Geochemistry and Hydrodynamic Considerations; Ph.D. Thesis, Unpublished, University of Toronto, 407p.

Ohmoto, H., and Rye, R.O.
1979: Isotopes of Sulfur and Carbon; p.509-567 *in* Geochemistry of Hydrothermal Ore Deposits, Second Edition, edited by H.L. Barnes, John Wiley and Sons Publishers, New York, 798p.

Pamour Porcupine Mines Limited
1983-1985: Annual Reports 1982-1984; Noranda Group, Toronto.

Rees, C.E.
1978: Sulphur Isotope Measurements Using SO$_2$ and SF$_6$; Geochimica et Cosmochimica Acta, Volume 42, p.383-389.

Schwarcz, H.P., and Rees, C.E.
1984: S-34 in Pyrite from Gold Deposits (Abstract); p.1 *in* Geoscience Research Seminar and Open House '84, December 4-5, 1984, Abstracts, Ontario Geological Survey, 23p.

Seccombe, P.K., Groves, D.I., Marston, R.J., and Barrett, F.M.
1981: Sulfide Paragenesis and Sulfur Mobility in Fe-Ni-Cu Sulfide Ores at Lunnon and Juan Main Shoots, Kambalda: Textural and Sulfur Isotopic Evidence; Economic Geology, Volume 76, p.1675-1685.

Siegel, S.
1956: Nonparametric Statistics for the Behavioral Sciences; McGraw-Hill Publishers, New York.

Skoog, D.A., and West, D.M.
1962: Fundamentals of Analytical Chemistry; Holt, Rinehart and Winston Publishers, New York.

Stein, H.J., and Huebner, M.
1984: A Heavy Isotope Enriched Sulfur Source for Climax-Type Porphyry Molybdenum Deposits: Molybdenite Compositions (Abstract); p.667 *in* Geological Society of America, Abstracts with Programs, November 5-8, 1984, Volume 16, Number 6, 371p.

Thode, H.G., and Rees, C.E.
1971: Measurement of Sulphur Concentrations and the Isotope Ratios $^{33}S/^{32}S$, $^{34}S/^{32}S$ and $^{36}S/^{32}S$ in Apollo 12 Samples; Earth and Planetary Science Letters, Volume 12, p.434-438.

Thomas, A.V.
1985: A Petrological and Fluid Inclusion Study of the Tanco Pegmatite, S.E. Manitoba; Unpublished M.Sc. Thesis, University of Toronto, 508p.

Till, R.
1974: Statistical Methods for the Earth Scientist; Macmillan Publishers, London.

Travis, G.A., Woodall, R., and Bartram, G.D.
1971: The Geology of the Kalgoorlie Goldfield; Special Publications, Geological Society of Australia, Volume 3, p.175-190.

Wood, P.C.
1983: Controls on Tungsten (Scheelite) Mineralization in the Hollinger-McIntyre Gold Vein System, Timmins; p.188-190 *in* Summary of Field Work, 1983, by the Ontario Geological Survey, edited by John Wood, Owen L. White, R.B. Barlow, and A.C. Colvine, Ontario Geological Survey, Miscellaneous Paper 116, 313p.

Wood, P.C., and Spooner, E.T.C.
1984: Post-Strain Gold-Quartz-Carbonate-Sulphide-Scheelite Vein Mineralization, Hollinger (Timmins) Mine, Porcupine Camp, Ontario (Abstract); p.700 *in* Geological Society of America, Abstracts with Programs, November 5-8, 1984, Volume 16, Number 6, 371p.

Wood, P.C., Burrows, D.R., and Spooner, E.T.C.
1985: +3.2 ± 1.5 per mil $\delta^{34}S$ for Pyrite in the Hollinger (Timmins) Gold Mine (Abstract); p.A69 *in* Geological Association of Canada/Mineralogical Association of Canada, Program with Abstracts, May 15-17, 1985, Volume 10, 123p.

Wood, P.C., Thomas, A.V., Burrows, D.R., Macdonald, A.J., Noble, S.R., and Spooner, E.T.C.
1984: CO_2-Bearing Low-Moderate Salinity Fluids in Archean Gold-Quartz-Carbonate-(W-Mo) Vein Deposits and Magmatically Derived Mo, W, Ta and Sn Mineralization (Abstract); p.700 *in* Geological Society of America, Abstracts with Programs, November 5-8, 1984, Volume 16, Number 6, 371p.